GEOLOGY AND GEOCHEMISTRY OF THE WARREGO Au–Cu–Bi MINE, TENNANT CREEK, NORTHERN TERRITORY, AUSTRALIA

by

M. Richard Wedekind

Submitted in partial fulfilment of the requirements for the degree of Doctor of Philosophy at the University of Tasmania.

University of Tasmania
Hobart
1990

This thesis contains no material which has been accepted for the award of any other higher degree or graduate diploma in any tertiary institution and that, to the best of the author's knowledge and belief, the thesis contains no material previously published or written by another person, except when due reference is made in the text of the thesis.

M.R. Wedekind
August 1990.

ACKNOWLEDGEMENTS

Thanks to my supervisor Ross Large for initiating this project and maintaining his enthusiasm and encouragement throughout the slow gestation of this thesis. Ross' keenness for applied research and ability to gain the support of the mining industry has been instrumental in the successful continuation of this study.

I would like to acknowledge the support provided by Peko-Wallsend Operations Limited (now North Broken Hill Peko) in providing unrestricted access to their Tennant Creek operations, logistic support in the form of transport, accommodation during field work, and some analytical costs. Brian Williams of Geopeko is largely responsible for this support and it is his unflagging interest in things 'academic' that has allowed this project to flourish and whose comments and criticisms kept me on the straight and narrow. Bob Love (the man at the scene) has been my toughest critic when it comes to the arm waving, as Senior Geologist in Tennant Creek with considerable underground experience at Warrego, he was able to defuse some of my wilder assertions.

John Walshe (A.N.U.) has shown considerable interest in the progress of this thesis, always ready to discuss a problem and suggest the unthinkable.

Staff and students of the Geology Department in the University of Tasmania are gratefully acknowledged for their assistance and friendship. Colleagues and friends who have directly provided help and assistance throughout this study include Ron Berry, Tony Crawford, Garry Davidson, Bruce Gemmell, Brian Gulson, Brian Harrold, Terry Hoschke, Dave Huston, Peter McGoldrick, Terry Quinlan, Mark Rattenbury, Joe Stoltz and Khin Zaw.

Superb technical assistance has been provided by Wis Jablonski (microprobe), Mike Power Snr. and Mike Power Jnr. (mass spectrometry), Phil Robinson (geo-chemical analyses) and Simon Stephens (polished thin sections).

June Pongratz has produced many of the diagrams, and is responsible for the final presentation and production of this thesis.

Special thanks go to my parents for their support and encouragement throughout the course of this study. The occasional R & R in Sydney was much appreciated.

Finally a debt is owed to Sharon, not only has she been prepared to endure this thesis, providing constant support and encouragement, she has actively helped through-

out with sample preparation and analysis, drafting, sample cataloguing, data input and proof reading.

Support for this work was provided by a Commonwealth Scholarship and a collaborative University of Tasmania-Industry research grant.

CONTENTS

Chapter Six — PETROGRAPHY AND PARAGENESIS

Chapter Seven — GEOCHEMISTRY AND ALTERATION

Chapter Eight — STABLE ISOTOPES

Chapter Nine — THERMODYNAMIC MODELLING OF THE FORMATION OF THE WARREGO OREBODY

Chapter Ten — SUMMARY AND MODEL OF FORMATION

List of Figures

List of Tables

List of Plates

ABSTRACT

The recently closed Warrego Au–Cu–Bi mine located 51 km west of the town of Tennant Creek in the Northern Territory, has produced in excess of 1.2 million ounces of gold, 80,000 tonnes of copper and 10,000 tonnes of bismuth to make it the largest producer of these three commodities in the Tennant Creek goldfield. As with all economic mineralisation in the goldfield, ore is hosted by magnetite-rich, ellipsoidal pipes (ironstone lodes) which also comprise variable proportions of quartz and chlorite. Economic mineralisation (chalcopyrite, bismuthinite and native gold) is located in fractures within the ironstone lode, and is clearly related to an event that post-dates ironstone formation.

The ironstone lodes are hosted by Lower Proterozoic turbidites of the Warramunga Group which comprise poorly sorted, immature sediments that retain the distinctive trace element compositions of two felsic source regions. The similarity in composition and age (~1870 Ma) of the sediments, a quartz porphyry which forms the immediate hangingwall to the ironstone lodes, and the Tennant Creek Granite, suggests that they are all consanguineous. The porphyry has been interpreted as a sill that was intruded prior to lithification and folding of the Warramunga Group (McPhie, 1990), and as such, preceded ironstone lode formation and mineralisation. The Warrego Granite outcrops less than 1 km from the Warrego mine, and the effect of contact metamorphism is strongly evident as the overprinting of cleavage and hydrothermal alteration associated with mineralisation by cordierite, biotite and andalusite porphyroblasts. Conditions of contact metamorphism are calculated to have been between 500° and 550°C and < 2.5 kbar. Extensive recrystallisation of quartz and sulphide minerals within the ironstone lodes has masked paragenetic relationships and destroyed fluid inclusion evidence of the conditions of mineralisation.

Compared to the typically uniform attitudes observed elsewhere in the goldfield, the Warrego ironstone lodes have an unusual plunging attitude, and the sediment and cleavage orientations in the Warrego area are highly anomalous. A simple 90° anticlockwise rotation about a horizontal axis of the block hosting the Warrego mine restores structural elements to typical goldfield attitudes, and the ironstone lode to a horizontal,

east-west alignment where alteration is now concentrated below the lode. Rotation of the block during intrusion of the Warrego Granite is suggested.

Ironstone lode formation is localised at the lower contact of the quartz porphyry which is believed to have acted as an impermeable barrier to the flow of hydrothermal fluids. Fluids appear to have been channelled to the site of deposition by a cleavage-parallel fault generated during folding of the relatively rigid porphyry, and then migrated laterally below the contact, progressively replacing the sediments with chlorite, magnetite and quartz. Textural and trace element data are consistent with a replacement model of lode formation, although some open space filling is likely. Reaction of hydrothermal fluids with cooler more oxidised waters appears to be the most likely method of promoting magnetite deposition, which was initially localised as a front against the relatively unaltered sediments. Continuous fracturing and infilling of this zone by quartz and magnetite during lode formation has resulted in the observed zonation from a magnetite core to an outer quartz-magnetite rim.

Evolution of the system through the tapping of deeper, hotter and more reduced fluids is associated with the subsequent introduction of economic mineralisation. This evolution of the system is possibly related to the intrusion of granite at depth and subsequent establishment of a convecting hydrothermal system. A direct magmatic contribution to the fluid in the form of fluids and/or metals cannot be ruled out.

Two styles of mineralisation are evident:

1. The copper orebodies are characterised by a sulphide-rich assemblage comprising chalcopyrite, pyrite, pyrite/marcasite (after pyrrhotite) and cobalt-rich phases localised within the brecciated core of the ironstone lode. An outer zone of relatively barren quartz-magnetite surrounds the mineralised core. This zonation and mineral assemblage is virtually identical to that reported for the Peko mine (Whittle, 1966).
2. Localised within two distinct zones on the footwall side of the ironstone lodes, a sulphide-poor, chlorite- and muscovite-rich mineral assemblage is characteristic of that described in the Juno mine (Large, 1974, 1975). Similarly there is a well developed zonation in metals (Au → Bi → Cu), bismuth sulphosalts (decreasing Se/Pb), and mineralogy (magnetite–chlorite–muscovite → magnetite sulphide → quartz–magnetite).

Both styles of mineralisation fill fractures without evidence of replacement or alteration of the ironstone lode.

The two styles of mineralisation are interpreted to result from the late-stage oveprinting of the copper-rich assemblage by the gold pods which is associated with the oxidation of pyrrhotite. Support for this interpretation is derived from the mixed sulphur isotope signature throughout the ironstone lode, and different chlorite chemistry in the two assemblages. Recrystallisation associated with the intrusion of the Warrego Granite has destroyed textural evidence which might support this interpretation.

Oxygen and hydrogen isotope results suggest that the fluid source for both ironstone lode formation and mineralisation was formation waters. A consistent difference in isotopic composition between barren and mineralised systems results from a 100°C temperature difference between the two stages which is in agreement with fluid inclusion evidence. Lead and sulphur isotopes, and trace element modelling indicate that although relatively localised leaching of the Warramunga Group is sufficient to produce the ironstone lodes, leaching of significantly larger volumes of rocks is required to produce the observed metal abundances.

Fluid inclusion evidence in other mineralised ironstone lodes consistently indicates phase separation occurred with economic mineralisation, and a model whereby pressure release associated with fracturing of the ironstone lode has resulted in destabilisation of metal complexes in solution to promote their rapid deposition is preferred.

Chapter One

INTRODUCTION

1.1 Mining History of Development of the Goldfield

The township of Tennant Creek lies virtually at the geographic centre of the Northern Territory on the Stuart Highway 1024 km south of Darwin and 507 km north of Alice Springs (Fig. 1.1). The town has a population in excess of 2000 people and while initially acting as a service town for the mining industry developed on the surrounding goldfield, is with declining production increasingly important in servicing the cattle industry and acting as a transport and tourist centre.

Gold was first discovered in the Tennant Creek region in 1926, and mining has since yielded in excess of 117 tonnes (4 million ounces) of gold, making it the sixth largest goldfield in Australia (K. Yates, unpublished report 1986). In excess of 130 mines in the field have recorded gold production[1], but only eleven (Table I) have accounted for 97 per cent of the total, and four (Warrego, Nobles Nob, Juno, and Peko) have accounted for over 75 per cent.

Gold mineralisation occurs with bismuth and copper in magnetite and hematite-rich lodes known locally as ironstones (see Terminology — Section 1.4). Two styles of mineralisation are observed in the goldfield, gold-rich orebodies with low copper (e.g. Juno mine; 0·4 Mt @ 56 g/t Au, 0·3% Cu)[2] and copper-rich orebodies with low gold (e.g. Gecko mine; 4·9 Mt @ 0·8 g/t Au, 3·8% Cu). Bismuth is commonly associated with both styles of mineralisation, but has only been extracted as an economic by-product from mines operated by Peko Mines Ltd. In several of the mines, locally significant amounts of lead, zinc, cobalt, selenium, and uranium also occur, but of these, only selenium from Juno mine has been recovered. Extraction of cobalt from the Peko mine tailings is currently under evaluation (Australian Development Annual Report, 1989).

The history of exploration and mine development in the Tennant Creek Goldfield can be divided into two stages: an initial period of small syndicate prospecting and

---

[1] Production figures include proven and probable reserves for mines still in operation.
[2] All units used in this thesis are metric.

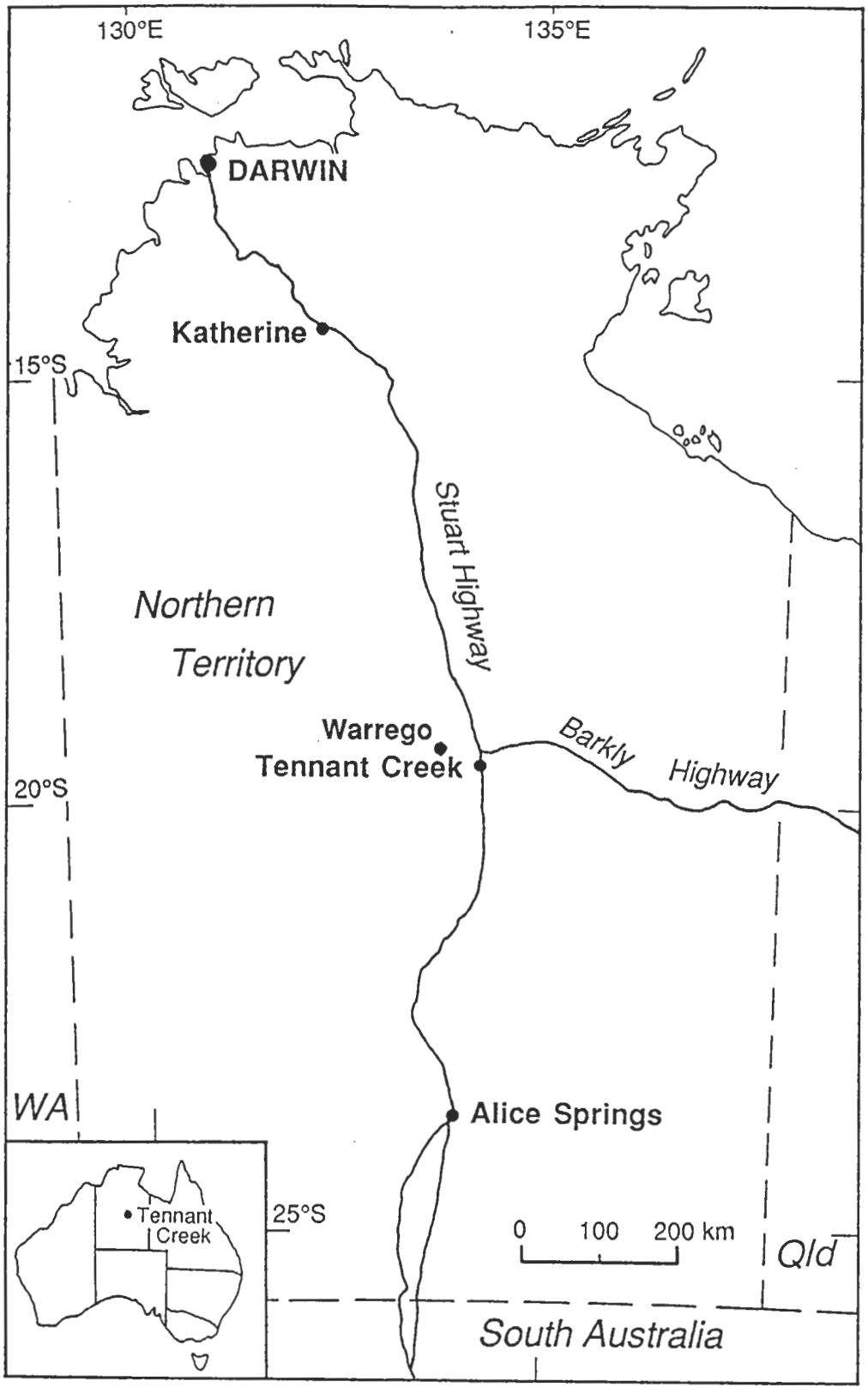

Figure 1.1 — Location map.

Table I — Tonnage and Grade of the Major Gold-Producing Mines in the Tennant Creek Goldfield.

Mines	Million metric tonnes	Grades Au (g/t)	Cu (%)	Bi (%)	Contained gold (kg)
Warrego*	6.95	6.6	2	0.32	46020
Nobles Nob	2	19.5			39000
Juno	0.45	56.1	0.33	0.57	25344
Peko	3.7	3.5	4.01	0.2	12870
White Devil*	0.28	22			6160
Orlando	0.68	8.8	4.01	0.1	5997
Argo	0.3	13.6	0.8	0.6	4080
Gecko*	4.9	0.8	3.8	~0.15	3920
Eldorado	0.15	22.7			3314
TC8	0.04	67	1.2	0.5	2345

* Mines in production

mining lasting up to the start of the Second World War, and a period of company sponsored exploration which has continued to the present day. Initial prospecting resulted in the discovery of most of the mines in the region, although the majority were small-tonnage, near-surface deposits associated with outcropping ironstone lodes (Ivanac, 1954). Three of the largest mines in the Goldfield (Nobles Nob, Peko, and Eldorado) were discovered during this period, although in the case of Nobles Nob and Peko, the full significance of the resources was not realised until the second phase of exploration was commenced. The second phase of exploration came with the formation of two mining companies to develop the Peko and Nobles Nob mines; Peko Gold Mines NL (later Peko-Wallsend Ltd, and now North Broken Hill Peko) and Australian Development NL respectively. The spectacular gold mineralisation encountered in the development of the Nobles Nob mine and considerable copper resource discovered at Peko provided the cash flow for further exploration in the goldfield. These two companies have dominated the scene ever since.

The potential of magnetic techniques to define extensions to known ironstone lodes and discover non-outcropping lodes was recognised relatively early (Rayner and Nye, 1936; Richardson et al., 1936; Richardson and Rayner, 1937), but it was not until BMR aeromagnetic surveys came available in 1956 that geophysics was routinely used in exploration. The characteristic bulls-eye magnetic anomalies presented by the magnetite lodes provided drill targets that were relatively easily modelled (Farrar, 1979), and testing of these anomalies resulted in a spectacular succession of discoveries for Peko:

Orlando, 1962[1]; Ivanhoe, 1965; Juno, 1968; Warrego, 1972; Gecko, 1973. Although there is no direct correlation between the size of an ironstone lode and amount of ore contained, there is a tendency for the larger lodes to contain significant mineralisation, and hence the spectacular string of discoveries as the best targets were tested.

Over 650 ironstone lodes crop out or have been intersected in drill hole throughout the Goldfield (Le Messurier et al., in press), but fewer than 200 are known to be mineralised to any extent, and only 30 have produced greater than 30 kg of gold. Following the heady exploration days of the 1960s and early 1970s, lesser magnetic anomalies have been tested and consequently discoveries have been smaller relatively small short-lived deposits e.g. Argo (1985), and TC8 (1986). Exploration is further complicated by the fact that economic mineralisation may represent only a small portion of the total ironstone lode and raises uncertainty on the part of the explorer as to just what is effective testing of a target.

The recently opened White Devil mine (1987) is based on a deposit that was tested by Geopeko (exploration arm of Peko-Wallsend Ltd) with eight diamond drill holes before being sold to Australian Development Ltd. The subsequent development of a mine which is likely to become the fifth largest gold producer in the goldfield highlights the present dilemma facing explorers and the need for a third 'clever' phase of exploration in the Goldfield. Current research carried out at the University of Tasmania (of which this thesis is part) is designed to give a better understanding of the mineralisation in the Tennant Creek Goldfield and develop exploration techniques in which prospects may be evaluated from a single drillhole through the use of one or a combination of techniques, e.g. lead isotopes, stable isotopes, fluid inclusions, or geochemistry.

1.2 Warrego Mine — Discovery and Development

The Warrego mine is located on a broad 'bulldust' covered alluvial plain some 51 km west of the town of Tennant Creek (Fig. 1.1). The ironstone lode on which the mine is developed does not crop out, and the closest exposure of host rocks is 5 km to the east. The Warrego Granite was observed to crop out in gravel pits 800 m west of the mine site (Le Messurier, unpublished company report, 1976), but its contact relationship with the host rocks to the lode is masked by cover.

The Explorer 5 prospect was pegged in 1958 by Peko Mines NL following identification of a 2200 nT magnetic anomaly on the Bureau of Mineral Resources 1956 airborne magnetic survey. Serious problems were encountered in initial drill testing of the anomaly because of an anomalous cleavage orientation in the area — the first two diamond drill holes were abandoned after excessive deviation (DDH 1 strayed 60° from

---

[1] Opening date of mine.

its planned course even after wedging six times). It was not until 1962 that the first lode intersection was made made in DDH 3. A total of 29 surface holes were subsequently drilled to prove a resource leading to the development of the Warrego mine.

Shaft sinking commenced late in 1967 on what was essentially a copper resource with indicated reserves of 3·17 Mt @ 2·2% Cu and 1·7 g/t Au. Limited production of copper-rich ore began in late 1972, and full scale production commenced in 1973. The discovery of a gold- and bismuth-rich zone during routine ore blocking on 8 level in early 1972, brought about a change in status of the Warrego mine. Now a significant gold mine, shaft sinking was re-commenced to provide access to the lower levels of the orebody so that this new resource could be defined.

Two pods (see Terminology) of high-grade gold ore centred approximately on 10 and 13 levels were defined, and total reserves were improved to 5 Mt @ 7·0 g/t Au, 2·6% Cu, and 0.3% Bi. Full production of the high-grade gold-bismuth ore was achieved in mid 1974. The fortuitous discovery of significant gold at Warrego prevented premature closure of the mine following the decline in world copper prices in 1974, although ore outlines were amended to maximise gold production.

After nearly a decade in the top five gold, and top ten copper mines in Australia, the Warrego mine has gradually declined in production. The recent improvement in the price of copper in the last few years has allowed the mine to remain in production following exhaustion of gold ore. The mine was finally closed in late 1989 after pillar extraction resulted in ground stability problems.

1.3 General Statement of Aims and Methods

This thesis was undertaken as part of a wider project with Geopeko, initiated by Ross Large at the University of Tasmania, to study the enigmatic mineralisation found in the Tennant Creek Goldfield. Through a better understanding of the orebodies and processes controlling mineralisation, it was hoped that more efficient exploration techniques could be developed to assist in the discovery of further resources in the area. The Warrego mine was selected for this study because with dwindling reserves and imminent mine closure, this would be the last opportunity to study the most significant producer of gold (35,000 kg) and copper (80,000 metric tonnes) in the goldfield. The study complements earlier work on the Juno mine (Large, 1974, 1975), and hopes to elucidate major differences in the mineralogy and metal ratios in these two deposits.

The program of research undertaken in this study has involved three aspects:

1. Extensive logging of diamond drill core — four mine sections were selected as representative of the range of mineralisation styles observed in the Warrego ironstone lode. This typically involved detailed logging and sampling of drillcore (in excess of 3800 m). Because much of the orebody had been removed through mining

operations, underground services were restricted to only a few levels, and drives are encrusted with dust and grime, drillcore offered the best exposure throughout the mine area, and therefore only limited underground checking of rock relationships was undertaken.

2. To examine alteration around the ironstone lodes, underground mapping and sampling was undertaken on 14 level where the main ore haulageway and its extension as a deep drill drive offered the most extensive section available through the mine sequence. Surface drillholes were no longer available.
3. Laboratory studies involving, examination of samples in polished thin section and polished slab, stable isotopic studies (S, O, H), XRF analyses of major and trace elements/constituents, and microprobe analysis of mineral phases.

To complement this work, drillcore from a large barren ironstone lode (Explorer 28) was also examined and sampled to evaluate differences between barren and mineralised systems. Although only limited petrographic work was undertaken on this deposit, detailed examination of the chemistry and stable isotope composition of chlorites is reported. A brief description of the deposit is given in Appendix H.

The results and interpretation of this work are presented in the following chapters. Although topics developed throughout this thesis are often inter-related, it is hoped they are presented in a format that provides a logical development of the study and its findings, with minimal need to cross-reference between chapters.

Chapter Two summarises previous regional studies of the Tennant Creek Inlier. It describes in detail the local geology of the Warrego area as interpreted from previous work on the deposit (Duncan, 1970), and mapping and sampling undertaken during this study. The local geology is correlated with the Inlier as a whole, and interpretations as to the regional setting of sedimentation of the Warramunga Group are suggested.

Chapter Three describes the macro features of the Warrego ironstone lode, its overall geometry, and relationship to the host rocks. Mineralogy of the ironstone lode is discussed, and a generally consistent pattern of mineral zonation is established.

Chapter Four examines the unusual attitude of both the ironstone lode and host rocks compared to other deposits in the goldfield. A simple structural model is developed to restore the attitude of the lode and host rocks to an orientation consistent with the rest of the Goldfield.

Chapter Five looks at metal zonation within the lode through contouring of assay data and detailed analysis of the chemistry of a single drill hole passing through the main mineral assemblages. A model is suggested to explain the relationships of economic mineralisation to the ironstone lode.

Chapter Six describes the petrography of the lodes and the chemistry of the mineral phases. A general paragenetic sequence is established and the implications of observations are generally discussed in terms of ironstone lode formation and mineralisation.

Chapter Seven examines the chemistry of the host sediment, porphyry and ironstone lode, primarily to better understand surrounding alteration and the process of lode formation. This work also has implications for a genetic relationship between the porphyry and sediments, and the tectonic setting during sediment deposition.

Chapter Eight looks at the chemistry of the mineralisation and lode formation through the use of stable isotopes. Extensive sulphur isotopic evidence is presented which has significant implication for the conditions of ore formation. Oxygen and hydrogen isotope results from the lode and altered sediments provide evidence that further constrains the processes of lode formation, and has implications for the source of fluids.

Chapter Nine combines the constraints provided by previous chapters with thermodynamic modelling of ore deposition. A model of lode formation and mineral deposition is suggested, and probable sources of metals and fluids are discussed.

1.4 Terminology

Before further discussion of the geology of the Warrego orebodies it is necessary to clarify the meaning of some potentially confusing local terms used in the Tennant Creek area.

Ironstone lode: refers to discrete bodies comprised predominantly of magnetite (or hematite above the base of oxidation), observed throughout the Tennant Creek area. Although clearly epigenetic, all terms referring to mineralisation are related to economic mineralisation, i.e. gold, copper, and bismuth. Thus ironstone lodes may be mineralised or unmineralised.

Gold pod: Often individual ironstone lodes contain discrete zones within, or immediately adjacent to them which are characterised by the occurrence of exceedingly rich gold mineralisation, a general lack of sulphide minerals, and a distinctive gangue assemblage comprising magnetite, chlorite and muscovite. These 'gold pods' may comprise discrete zones within an otherwise barren system, e.g. Skipper Extended (Ivanac, 1954), almost the entire lode, e.g. Juno mine (Large, 1974, 1975), or may be gradational into sulphide-rich copper orebodies, e.g. Peko (Whittle, 1966) and Warrego.

Sediments and volcanics: Because rocks within the Warramunga Group are lithified and metamorphosed, the terms *sediment* and *volcanic* used throughout this thesis imply metasedimentary and metavolcanic rocks.

Chapter Two

LOCAL GEOLOGY

2.1 Introduction

The Tennant Creek goldfield has had a long history of investigation by geologists from company, federal and state government, and university backgrounds. Despite important contributions from many workers, advances in the understanding of the mode of formation of the ironstone bodies, their associated mineralisation, and the controls thereof are still problematic and often contentious. The first detailed description of the goldfield and its deposits (Ivanac, 1954) today remains an important reference as many of the small early mines are now inaccessible. Crohn and Oldershaw (1965), carried out the first regional mapping for the Tennant Creek 1-Mile Sheet area, and this was followed by mapping of the Mount Woodcock 1-Mile Sheet area immediately to the north by Dunnet and Harding (1967). This work was combined and improved in the new Tennant Creek 1:250,000 Sheet mapping of Mendum and Tonkin (1976), and was updated by Dodson and Gardener (1978). The most up-to-date compilation of the geology of the Tennant Creek Inlier by Le Messurier et al., (in press) contains much of the recent work by company geologists (mainly Geopeko) using state-of-the-art remote sensing techniques including high resolution aeromagnetic data processing, radiometrics, and air photographic interpretation. This has been backed up by extensive on-the-ground mapping by company geologists.

Advances in the understanding of the ore deposits comes largely from university-based studies in co-operation with the mining companies. Whittle (1966) studied two of the most significant mines in the field (Nobles Nob, and Peko), documenting important relationships between the orebodies and the host rocks. Large (1974, 1975), first described gangue and metal zonation in his study of the Juno deposit and presented a model for the formation of the ore bodies. This work remains the key reference in understanding Tennant Creek gold mineralisation.

The purpose of this chapter is to document the local geology in the immediate environs of the Warrego orebody, and provides only a brief summary of the regional Tennant Creek geology. It is not proposed to reproduce work that is already well presented in Le Messurier et al. (in press).

2.2 Regional Geology

The early Proterozoic Warramunga Group occupies the central part of the Tennant Creek Inlier — a window through extensive early Phanerozoic platform sediments in the centre of the Northern Territory (Fig. 2.1). The Warramunga Group rests unconformably on amphibolite-facies rocks to the south of the field (Whittle, 1966), and on interbedded sediments and volcanics to the east and southwest (Le Messurier et al., in press). The high grade metamorphic basement rocks have Sm-Nd model ages of between 2300 and 2500 Ma (Black and McCulloch, 1984), and the basement sequences to the east and southwest have been correlated with Arunta Division 1 rocks (Le Messurier et al., in press) which have been dated elsewhere at 1980±190 Ma (Black and McCulloch, 1984). To the north and west, the Warramunga Group is unconformably overlain by the Tomkinson Creek Beds, a Middle Proterozoic shallow-water sedimentary sequence correlated with the Hatches Creek Group to the south of the field (Blake, 1984). Dating of felsic volcanics in the lower part of the Hatches Creek Group yield a probable crystallisation age between 1820 and 1810 Ma (Blake and Page, 1988). The Warramunga Group rocks were folded, cleaved, metamorphosed to sub-greenschist facies, and eroded before the Tomkinson Creek Beds and Hatches Creek Group was deposited (Blake, 1984; Le Messurier et al., in press). All units are unconformably overlain to the east and west by flat lying Middle Cambrian sediments.

The turbiditic greywacke, shale, siltstone, and volcanics of the Warramunga Group have a probable maximum thickness of 6000 m (Mendum and Tonkin, 1976), and are subdivided into the Bernborough and Carraman Formations. The Bernborough Formation (Large, 1975) forms the basal section of the Warramunga Group and comprises siltstone and shale interbedded with acid volcanics and tuffs. Zircons extracted from the volcanics have been dated by U-Pb at 1870±15 Ma, which is interpreted as the age of volcanism and sedimentation (Black, 1984), and the age has subsequently been reinterpreted at 1875±33 Ma (Page, 1988) because there is evidence of recent Pb loss and/or the presence of older inherited components.

The Carraman Formation (Large, 1975) consists of felsic greywacke and shales that apparently overlie the Bernborough Formation, and crop out over most of the field. A distinctive magnetic horizon within the Carraman Formation has been named the Black Eye Member (Le Messurier et al., in press), and consists of siltstone, tuffaceous greywacke, and shale with an anomalously high iron oxide content of up to 15%. The iron oxides, of probable diagenetic/metamorphic origin, consist of disseminated magnetite euhedra that have been variably oxidised to hematite. Several argillaceous banded iron formations (BIF) up to several metres thick (Rattenbury, 1990a), and what appear to be continuous horizons of quartz ± feldspar porphyry of uncertain origin, i.e.

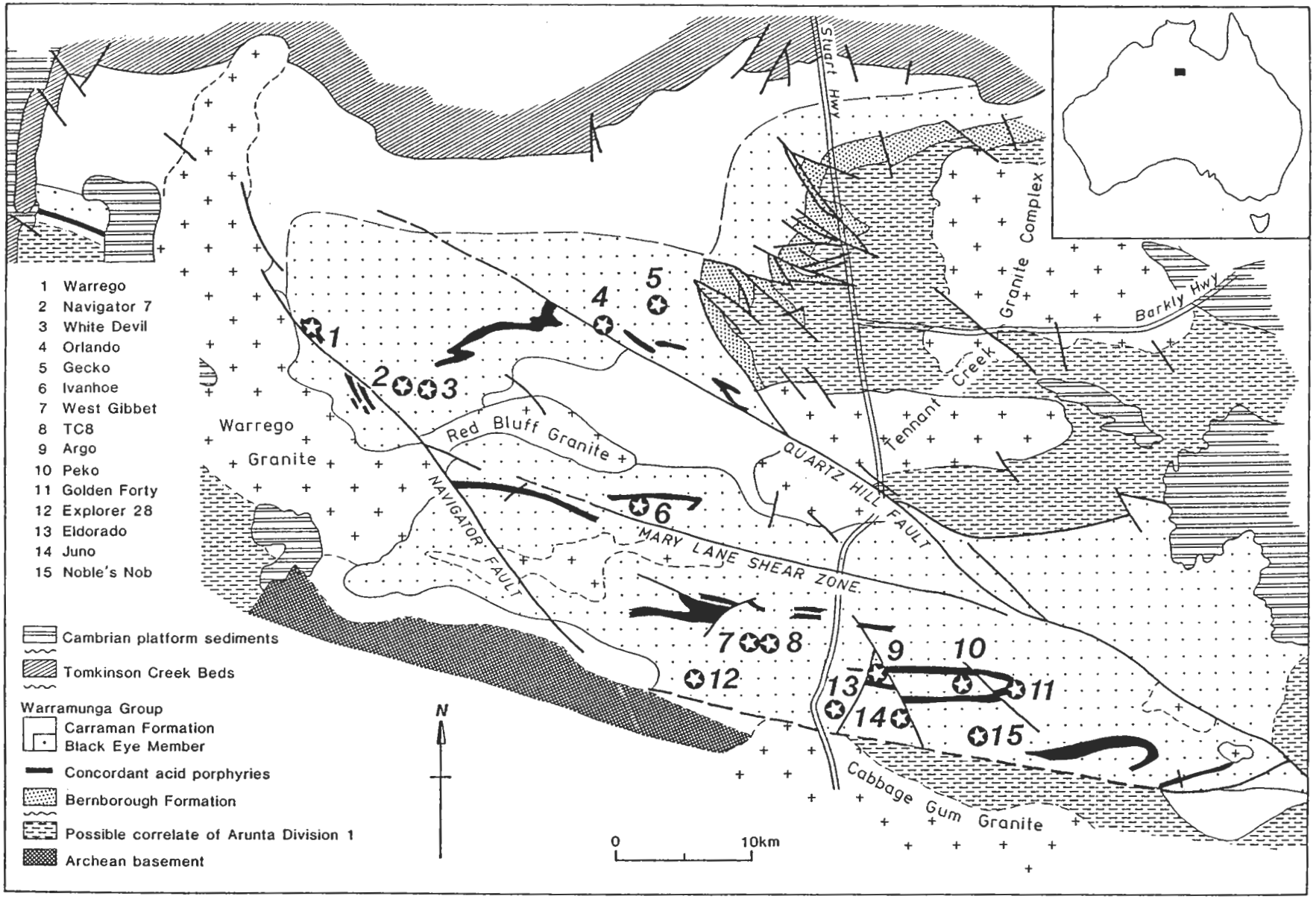

Figure 2.1 — Regional geology of the Tennant Creek Goldfield and location of the major mines and prospects discussed in this thesis (adapted from Le Messurier et al., in press).

of ash flow/pyroclastic derivation (Duncan, 1970; Large, 1975) or a syn-sedimentary sill (McPhie, 1990) occur within the Black Eye member. These units have been used as stratigraphic markers within the otherwise monotonous lithologies of the Carraman Formation, and have assisted in interpreting the regional structure.

Intrusive Rocks

Two periods of granite intrusion of pre- and post-folding age were recognized in the field based U-Pb zircon, and Rb-Sr whole rock ages (Black, 1977, 1984). The northern mass of the Tennant Creek Granite complex (Fig. 2.1), and the Cabbage Gum Granite have U-Pb zircon ages of 1870±20 Ma and 1846±8 Ma respectively. Page (1988) has reinterpreted the Tennant Creek Granite age 1864±7 Ma and because the Cabbage Gum Granite is gneissic queries that the age determined is related to igneous crystallisation. A single Rb-Sr whole rock age of 1796 Ma from the southern mass of the Tennant Creek Granite Complex has been interpreted as a reset metamorphic age (Black, 1984).

The contact relationships of the Cabbage Gum Granite are masked by extensive cover, but parts of the Tennant Creek Granite are well exposed and it can be divided into two separate masses (Fig. 2.1). The northern mass from which the U-Pb zircon age was determined has a 20 km diameter circular outcrop pattern, and intrusion through the basement is believed to have caused doming of the overlying Warramunga sediments to form a broad anticline defined by flexures in the Bernborough Formation (Dunnet and Harding, 1967). The close agreement in age between the northern granite mass and volcanics within the Bernborough Formation led Black (1984) to suggests a coeval relationship. Textural, mineralogical and chemical similarities (Duncan, 1970) support this interpretation.

The southern mass of the Tennant Creek Granite complex is elongated in an east-west direction, and the intruded Warramunga sediments again define a broad domal shape with contacts sub-parallel to the bedding strike, but is locally transgressive (Crohn and Oldershaw, 1965). The southern mass offers the best exposure of granite in the field, comprising a succession of intrusive phases of which the main and oldest is a porphyritic granite that is in places strongly foliated parallel to the regional Warramunga Group cleavage (Crohn and Oldershaw, 1965). The non-foliated nature of the later phases may indicate that at least some intrusive activity was late- or post-folding.

The Warrego and Red Bluff granites have given Rb-Sr whole rock isochrons indicating a 1650–1660 Ma crystallization age (Black, 1984), and therefore are suggested as belonging to a younger period of intrusion. Although it is possible that these are reset metamorphic ages (Page, 1988), the intrusion of the Warrego Granite into the overlying Tomkinson Creek Beds, the observation of contact metamorphic assemblages related to the Warrego Granite overprinting mineralisation, and the

similarity of reset of Rb-Sr (Black, 1977) and Pb-Pb (Dean et al., 1988) mineralisation ages to those recorded for the granite support the premise that these ages are real.

Although they are rarely recognised at the surface due to the deep weathering, mafic intrusives are commonly intersected in drillcore where they are typically fresh and undeformed. Dolerite and diorite dykes, stocks and plugs, intrude the Warramunga Group rocks, overlying Tomkinson Creek Beds, and the Archean basement, and although there has been no successful dating of these rocks, sills near the base of the Tompkinson Creek Beds are intruded by the Warrego Granite (Le Messurier et al., in press) indicating an age that is post-folding of the Warramunga Group, but pre-intrusion of the Warrego Granite. Lamprophyre dykes are also relatively common and appear to be localised in northwest striking fault and shear zones. A Rb-Sr whole rock isochron on two lamprophyre dykes yielded an age of 1664±16 Ma, suggesting an association with the later phase of granite intrusion (Black, 1977), and the lamprophyres are therefore younger than the dolerite and diorite intrusives.

Structure

The structural picture in the Tennant Creek area is relatively simple; the Warramunga Group has undergone one major east-west folding episode that has produced upright cylindrical folds with a well defined, steeply north dipping axial plane cleavage (Rattenbury, 1990a). This interpretation concurs with that of Mendum and Tonkin (1976) who discounted the early folding episode proposed by Dunnet and Harding (1967). Thus the variation in the plunge of fold axes observed throughout the goldfield is interpreted to result from local non-cylindrical folding rather than interference with earlier (or later) deformation (Rattenbury, 1990a).

Four orders of folding are recognised in the field (B. Williams, written comm., 1988), ranging from first order folds with wavelengths from 10–20 km, to fourth order folds with wavelengths of several metres. Fold limbs generally dip between 50° and 80° north and south, and are rarely overturned (Mendum and Tonkin, 1976). Asymmetric chevron folds and crenulation cleavage is locally associated with a deformation of the regional cleavage adjacent to granites, and where east-west fold structures are truncated by northwest and northeast trending faults of which the Quartz Hill and Navigator faults are the best examples (Rattenbury, 1990a).

Folding of the Warramunga Group is suggested to be related to a northern Australia-wide metamorphic/deformational event, the Barramundi Orogeny (Etheridge et al., 1987). Constraints provided by the metamorphic age of the Archean basement, and the probable age of volcanics in the Hatches Creek Group place the Orogeny between 1920 and 1870 Ma (Page, 1988).

Ironstone Lodes

Virtually all mineralisation in the Tennant Creek area is closely associated with replacement bodies known locally as ironstone lodes which range in size from a few hundred tons to over 14 Mt. The ironstone lodes form flattened, pipe-like to ellipsoidal bodies composed of magnetite (50–80%), quartz (0–60%), and chlorite (0–40%), with variable amounts of hematite, pyrite, talc, dolomite, muscovite, and calcite. Gold mineralisation may be extremely rich, and is usually associated in a zonal relationship with a variety of bismuth sulphosalts and chalcopyrite. Anomalous trace element contents for cobalt, uranium, selenium, molybdenum, tungsten, lead and zinc are also reported. Above the water table (approximately 100 m below the surface) the lodes are typically oxidised to an assemblage of hematite, quartz, goethite, and clay minerals.

Control on the location of individual lodes appears to be related to structural features generated during folding. The lodes are frequently located in the cores of third order folds with their long and intermediate axes orientated in the plane of the east-west cleavage; typically the long axis is vertical. This relationship of ironstone lode with the structural elements has generally been taken to indicate ironstone lode formation occurred contemporaneously with folding of the Warramunga Group sediments (Ivanac, 1954; Whittle, 1966; Large, 1975, Wall and Valenta, 1990, Rattenbury, 1990b). The similarity in composition and setting of ironstone lodes (both mineralised and unmineralised) throughout the goldfield suggest that they were all formed by similar processes under essentially the same conditions.

Rb-Sr ages of hydrothermal muscovite associated with gold mineralisation from Warrego, Juno, TC8, Nobles Nob, and Golden Forty mines yield consistent ages around 1810 Ma, which is similar to the ~1796Ma reset Rb-Sr age recorded from the foliated Tennant Creek Granite (Black, 1977). Although ages determined for mineralisation across the goldfield are consistent, the similarity of fluid compositions involved in mineralisation and ironstone lode formation suggest there was not a significant time break between the two stages (Chapters Eight and Ten). Therefore the 1810 Ma age is suggested to represent a reset metamorphic age which is consistent with an intense tectonothermal event recorded throughout northern Australia (Black, 1977).

Synthesis

The relative timing of events in the Tennant Creek Inlier is reasonably constrained, and some general conclusions about the rock relationships and mineralisation can be suggested (Fig. 2.2). Deposition of the Warramunga Group (Bernborough Formation) appears to be consanguineous (and coeval?) with the Tennant Creek Granite and was accompanied or closely followed by folding associated with the Barramundi Orogeny. The implied relationship between ironstone lode formation and folding of the Warramunga Group is belied by a consistent mineralisation age that post-dates the

Barramnundi Orogeny by some 50 Ma. Similarly, there is an absence of any obvious evidence for tectonic and/or thermal events which, between the end of the Barramundi Orogeny and the intrusion of the Warrego and Red Bluff granites, may have reset the mineralisation age. However, folding of the Hatches Creek Group was apparently decoupled from the Warramunga Group (Wall and Valenta, 1990), and it is likely that much of this deformation was taken up in pre-existing structures which had localised mineralisation.

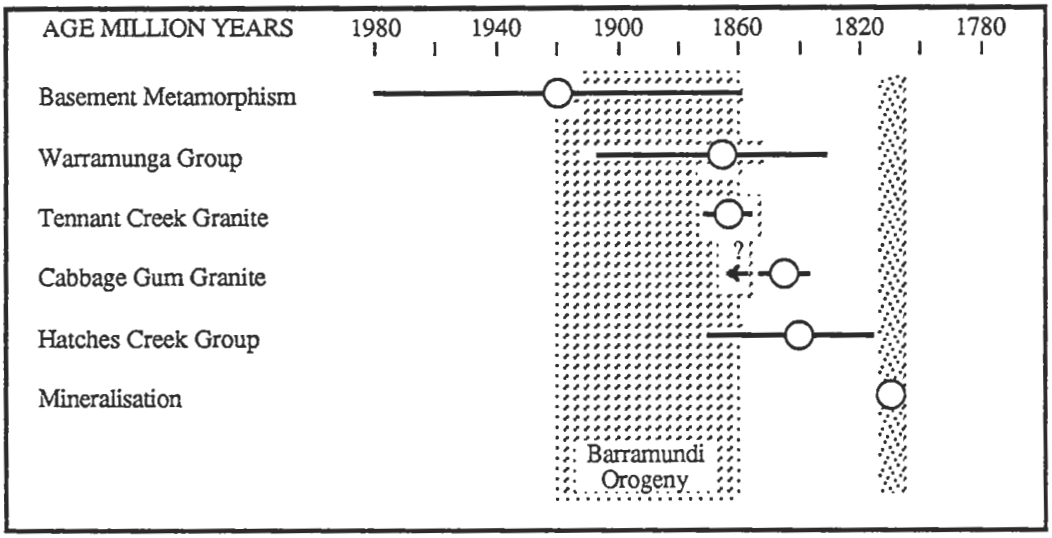

Figure 2.2 — Age relationships of rocks within the Tennant Creek Inlier illustrating an apparent time gap between ironstone lode formation and the introduction of economic mineralisation. The young ages determined for the Warrego and Red Bluff Granites do not fit on this time scale. (Source Page, 1988).

2.3 Warrego Geology

The lack of outcrop in the immediate Warrego area has meant that all information regarding the sediments and volcanics within the mine environs has been derived from surface drilling and augering, underground development, and ore blocking. Most of the data presented in this section comes from mapping and petrographic examination of geochemical samples collected at regular intervals along the main 14 level ore haulageway, and its continuation as the FEX deep drilling exploration drive. This level was selected because it provides the widest available section (>300m stratigraphic thickness) through the immediate host rocks to the ironstone lodes. The general relationships of local geological features discussed in this section are illustrated in Figure 2.3.

The most important feature within the mine sequence is the steeply dipping, northwest trending Footwall Fault which separates contact metamorphosed sediments adjacent to the Warrego Granite, from the variably contact metamorphosed and hydrothermally altered sediments and volcanics that host the Warrego ironstone lode to the east. The fault appears to be a branch of the major Navigator Fault system which extends from northwest of Warrego some 30 km southeast into the Cabbage Gum Basin (Mendum and Tonkin, 1976) (Fig. 2.1).

The extent of movement on the Footwall Fault is unknown, but the contrasting alteration assemblages on either side (see below) suggest that vertical movement has been at least 1 km. The fault appears to truncate the the Warrego ironstone lode between 2 and 4 levels, but because of their different orientations, they diverge with depth (Fig. 2.3). As there is no mineralisation or hydrothermal alteration associated with the fault, it is likely to be a post-mineralisation feature that has played no role in the mineralisation process either as a trap or fluid channelway.

Sequence West of the Footwall Fault

The sediments between the Footwall Fault and the Warrego Granite form a sequence of metasediments that are known in mine terminology as 'pink sediments' because of the pink colouration imparted by abundant K-feldspar alteration, (not hematite as suggested by Goulevitch (1975)). The well bedded, south-dipping sediments are often finely laminated and typically individual units are less than 1 m in thickness. They show good grading consistent with turbidity current deposition, and facing evidence indicates they are overturned (Goulevitch, 1975).

The metagreywacke and metapelite (Plate I) comprise quartz (30–40%), and K-feldspar (20–30%), in a strongly foliated sericitic matrix (40–50%) that gives the sediments a pervasive schistose fabric. Clots and individual blades of chlorite and muscovite that occur throughout the sediments (<5%) are typically without a preferred

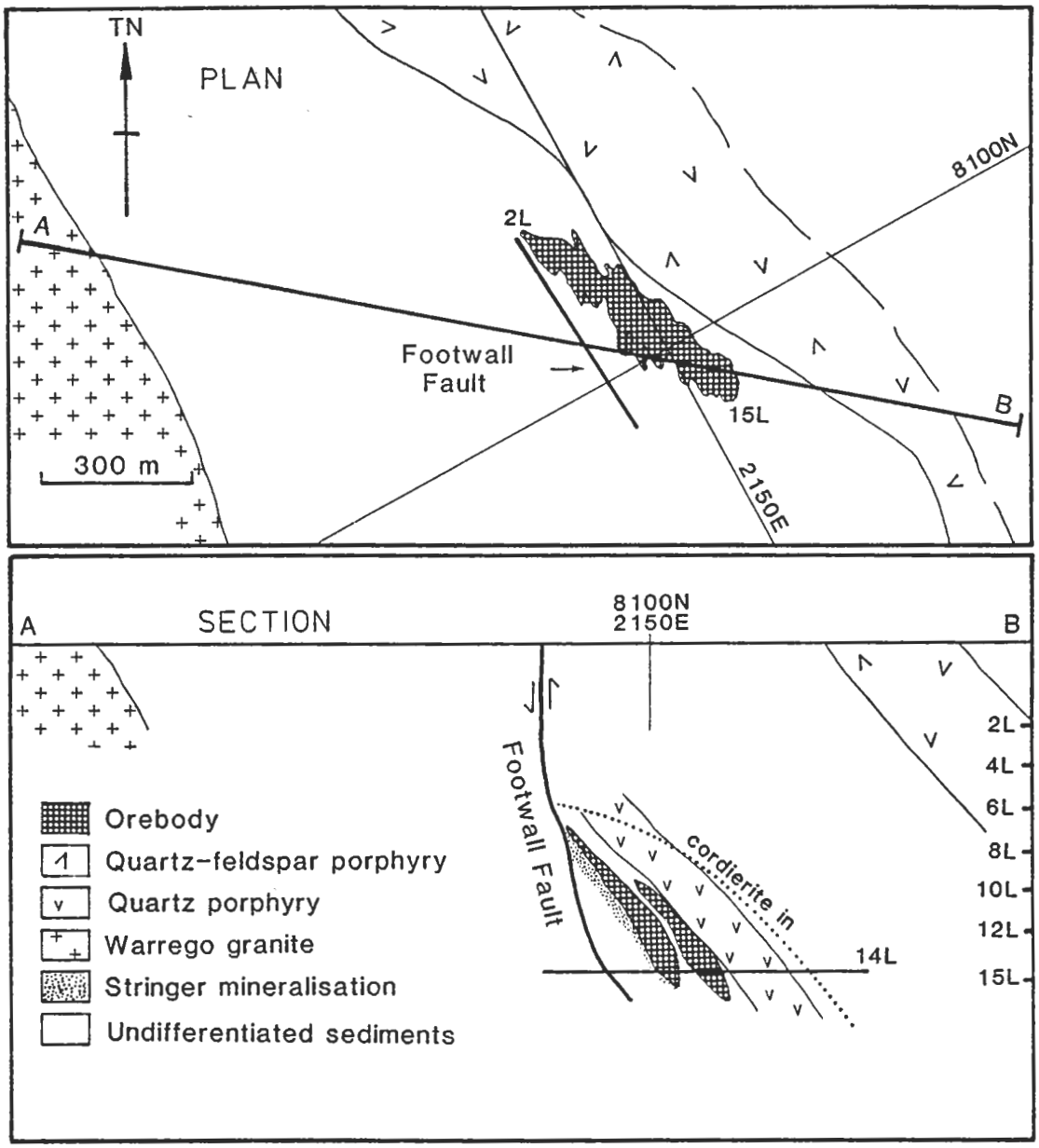

Figure 2.3 — Generalised plan and section of the Warrego area illustrating the relationship of the ironstone lodes to the quartz porphyry, faulting, contact metamorphism, and the Warrego Granite. The outline of the Warrego ironstone lode in the plan comprises level plans projected to the surface.

orientation, and clearly overprint the dominant foliation. Chlorite also occurs in veins that are commonly offset by movement along cleavage surfaces. Idiomorphic crystals of hematite are evenly disseminated through the sediments (<2%), and it is evident from their octahedral shape and rare relic cores, that original magnetite has been pseudomorphed by hematite. The hematite euhedra also exhibit pressure shadows of quartz and chlorite indicating they are pre-tectonic in origin. A diagenetic/metamorphic origin for the magnetite is suggested because its even distribution throughout the sediments shows no correlation with grainsize, as would be expected if they were sedimentary in origin. Other minor phases within these rocks include abundant fine bladed rutile that is aligned parallel to the foliation along sericite grain boundaries or cleavage planes, and rare crystals of zircon, and apatite.

Contact metamorphism associated with the intrusion of the Warrego Granite is evident as the recrystallisation of the sedimentary sequence, and intrusion of pegmatite dykes, and a pervasive zones of potassic alteration throughout the sediments. Quartz has been recrystallised to form clear inclusion-free grains that are often elongate parallel to the cleavage. Where in contact with each other, quartz grain boundaries are typically straight and 120° triple junctions are common. The presence of 'static' chlorite poikiloblasts overgrowing the foliation suggest that peak thermal metamorphism post-dated deformation.

Pegmatite dykes comprising variable proportions of quartz, albite, K-feldspar (microcline), and muscovite are common below 12 level west of the Footwall Fault. That similar dykes have been recognised within 100 m of the Warrego Granite on the surface some 1–2 km south of the mine (Le Messurier, unpublished company report, 1976), may indicate the close proximity of the Warrego Granite in the lower levels of the mine and/or a shallow dipping contact for the granite. Potassic alteration of the sediments occurs both as discrete turbid inclusion filled grains of K-feldspar in the sediments (possibly after plagioclase), and as areas of pervasive alteration where the sediments have been completely altered to K-feldspar, hematite, and muscovite. Late-stage K-feldspar veins crosscut the foliation and often have margins of potassic alteration that replace the adjacent sedimentary rocks. Mineralisation west of the Footwall Fault is extremely rare; isolated blebs of sulphides (principally chalcopyrite altering to bornite) are observed within chlorite veins in the sediments, and within the pegmatite veins.

The relationship of the pervasive potassic alteration west of the Footwall Fault to the mineralisation to the east is uncertain. The association of the potassic alteration with oxidation of magnetite and chalcopyrite to hematite and bornite respectively, suggests that this is an overprint restricted west of the Footwall Fault, that post-dates mineralisation and is possibly related to granite and pegmatite dyke intrusion. However, elsewhere the effects of contact metamorphism appear to be isochemical and are without

indications of extensive metasomatic alteration. Therefore is is possible that this assemblage represents an outer alteration envelope that is associated with mineralisation. Support for this premise is seen beyond the immediate area of mineralisation east of the orebody where similar potassic alteration is also observed (see below). Such outer potassic alteration aureoles are observed extending several kilometres beyond gold skarn ores (L.D. Meinert, written comm., 1991).

Sequence East of the Footwall Fault

The sequence east of the Footwall Fault hosts the Warrego orebody, and has a markedly different character from that observed west of the fault. The rocks show pervasive chlorite alteration associated with orebody formation, have a different contact metamorphic mineral assemblage, and contain two major porphyritic units that are conformable with the bedding.

Sediments

Bedding in the fine to medium grained sediments east of the Footwall Fault is rarely observed underground, although it is relatively common in non-orientated drill core. Contributing to its lack of definition underground, is the well developed continuous cleavage in these rocks, the strong chloritic alteration associated with mineralisation, and the pervasive recrystallisation resulting from the contact metamorphic overprint of the Warrego Granite. It is clear from mapping and core logging that bedding is uniformly right-way-up, and that on a mine scale, folding is not evident (Chapter 4). Massive units of fine grained sandstone and siltstone are the dominant components in the sequence; the coarser greywackes observed on the western side of the Footwall Fault appear to be absent.

Hangingwall sediments overlying the quartz porphyry in the FEX drive are similar to those observed west of the Footwall Fault. Shaley units have a distinctive pink colouration due to potassic alteration, muscovite is the dominant phyllosilicate, and magnetite is extensively altered to hematite, although not as pervasively as occurs west of the Footwall Fault. Stratigraphically below the porphyry, chloritised metasediments form the immediate host rocks to the ironstone lodes (Plates I and II), consisting of clear inclusion-free recrystallised quartz (30–70% depending on the degree of alteration), in a strongly foliated matrix of chlorite ± sericite (40–70%). Magnetite euhedra (rarely exhibiting hematite alteration) are disseminated through the metasediments, and with chlorite, increase in abundance toward the footwall of the ironstone lodes (<5% to >50%). Accessory minerals include apatite and zircon, and fine blades of rutile. The intensity of contact metamorphism increases both towards the Footwall Fault on 14 level and with depth. Poikiloblastic dark green biotite (variably altered to chlorite) and diffuse chlorite clots (after cordierite) that crosscut the foliation, first appear near the upper

Plate I

A: Typical 'pink sediments' from west of the Footwall Fault, comprising predominantly quartz and minor K-feldspar (after plagioclase?) in a strongly foliated sericitic matrix. Disseminated opaques are hematite which has pseudomorphously replaced original magnetite euhedra. Thin section (PPL), sample 107019.

B: Poikiloblastic muscovite grain in a patch of strong K-feldspar and chlorite alteration associated with K-metasomatism of the sediments associated with intrusion of the Warrego Granite. Relict sedimentary quartz grains are preserved, but the matrix has been completely replaced. West of the Footwall Fault. Thin section (PPL), sample 107022.

C: Chlorite clot surrounded by variable potassic alteration. Note the abundant opaques comprising hematite euhedra (after magnetite) and fine blades of rutile. West of the Footwall Fault.Thin section (PPL), sample 107022.

D: Typical sediments from east of the Footwall Fault, showing minor effects of hydrothermal alteration, but significant recrystallisation associated with the intrusion of the Warrego Granite. The sample predominantly comprises recrystallised, inclusion-free quartz in a chloritic matrix Abundant disseminated magnetite euhedra are clearly evident. Thin section (PPL), sample 106981.

E: Poikiloblastic biotite related to contact metamorphism of the Warrego Granite overprints the foliated Warramunga Group metasediments. Thin section (PPL), sample 106980.

F: Sharp contact between sediments (left) and quartz porphyry (right). A cross-cutting tourmaline vein in the sediments becomes a diffuse zone of intense chlorite, biotite, and tourmaline within the porphyry. Thin section (PPL), sample 106977.

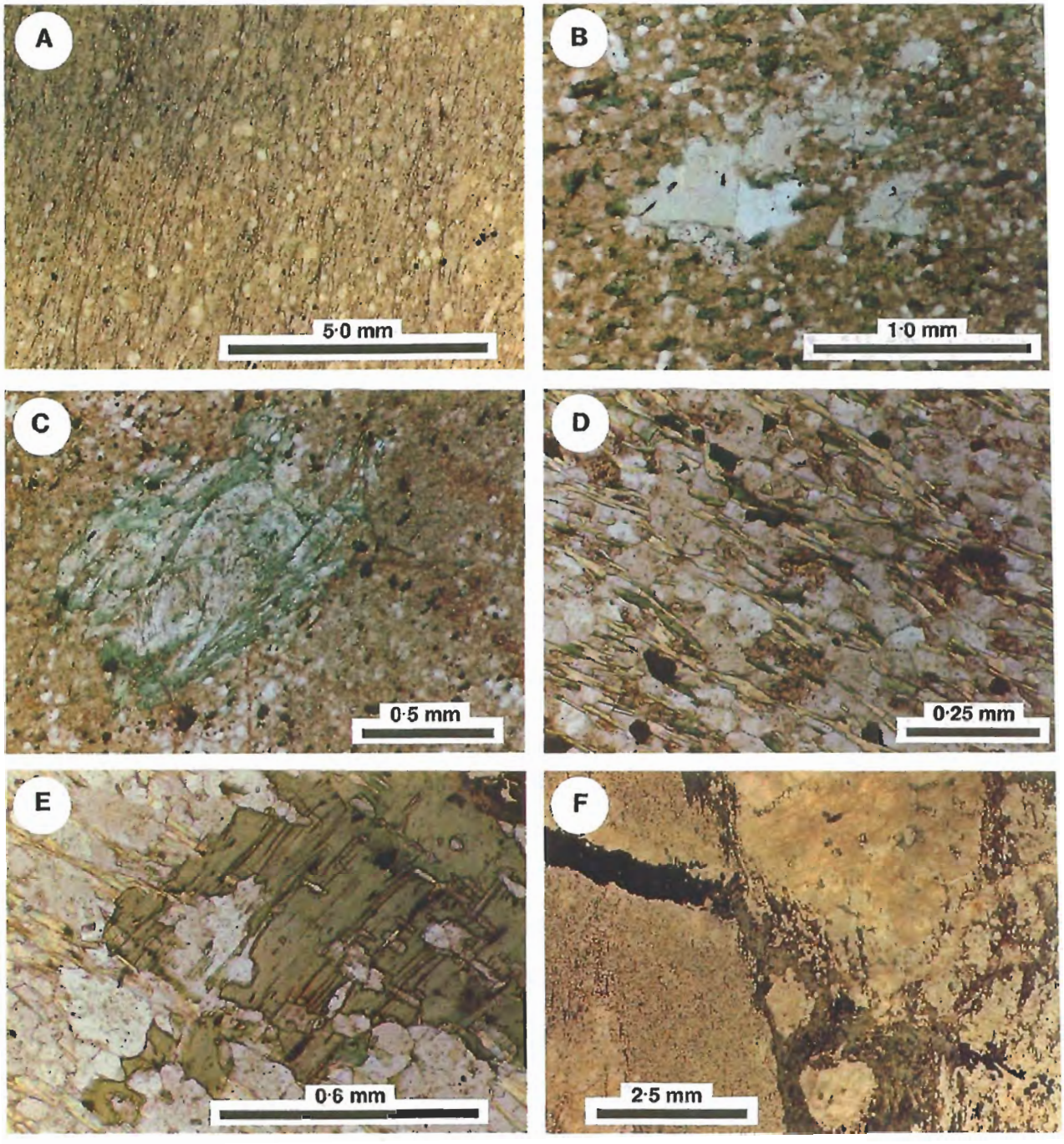
A
5·0 mm
B
1·0 mm
C
0·5 mm
D
0·25 mm
E
0·6 mm
F
2·5 mm

Plate II

A: Strong hydrothermal alteration of the quartz porphyry matrix illustrates the strong foliation and replacement of quartz by chlorite. A biotite porphyroblast overprints the dominant mineral foliation. Opaques are hematite/rutile intergrowths after ilmenite. Thin Section (PPL), sample 106981.

B: Intense hydrothermal alteration of sediments in the immediate footwall of the ironstone lode has completely replaced the sedimentary assemblage with chlorite (chl) and magnetite (mt). This rock is still recognisable as a sediment because of the preservation of zircons (surrounded by yellow-brown alteration haloes) and rutile blades (rt). Thin section (PPL), sample 107000.

C: Aggregates of hydrothermal monazite $(Ce,La,Th)PO_4$ associated with strong hydrothermal alteration of the porphyry. Thin section (PPL), sample 106980.

D: Drill core examples of 'dalmatianite' contact metamorphic assemblage observed in the Warrego sedimentary sequence. Left: rounded irregular spots (Sample 109096). Centre: Strongly deformed clots overprinted by a finer biotite spotting (Sample 109147). Right: Relatively undeformed spots cut by late quartz veins (Sample 107131). The coin is 2·5 cm in diameter.

E: Diffuse, undeformed chlorite spots in thin section illustrate their often annular appearance, poikilitic rims, and common overprint of dark green biotite. Thin section (PPL), sample 107034.

F: Post-metamorphic deformation of chlorite spots evident as cleavage parallel shearing and pressure shadows developed around disseminated magnetite. Thin section (PPL), Sample 108888.

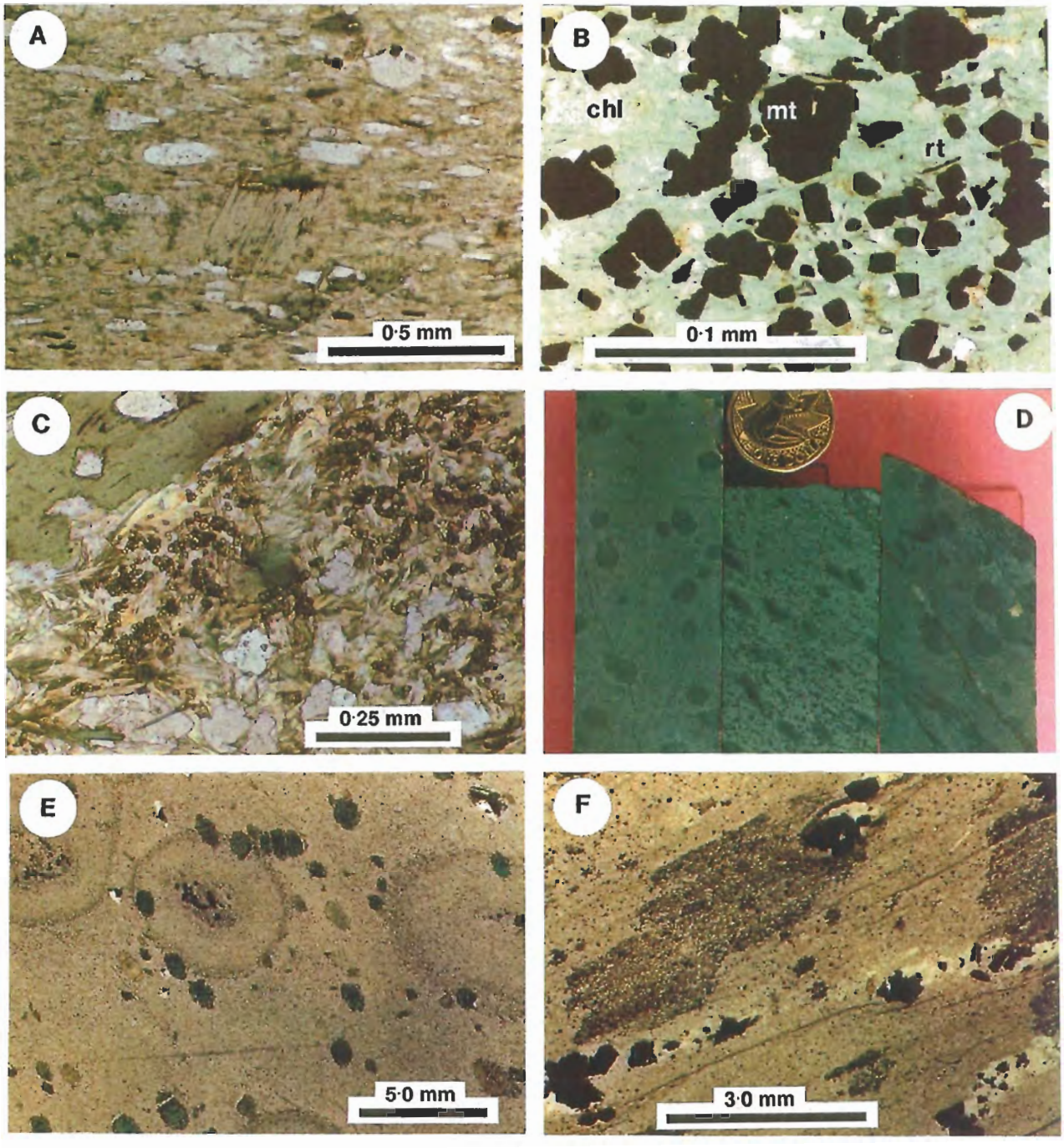
A
0·5 mm
B
chl
mt
rt
0·1 mm
C
0·25 mm
D
E
5·0 mm
F
3·0 mm

contact of the quartz porphyry in 14 level and are only observed below 5 level (Plates I and II). The boundary marking the first appearance of these assemblages is taken as the cordierite-in isograd (Fig. 2.3) marking the transition from low- to medium-grade contact metamorphism (Winkler, 1979). Abundant quartz-muscovite-tourmaline (schorl) veining at the contact of the porphyry is similar to the pegmatite veins attributed to localised fluid ingress associated with the intrusion of the Warrego Granite (see Chapter Eight).

The poikiloblastic chlorite spots may be up to 1 cm across, are generally oval in shape, and are occasionally annular in appearance with darker rims and/or cores (Plate II). The cleavage within the sediments can be traced uninterruptedly through the spots which are frequently deformed by movement along cleavage planes and kink bands.

These spots are interpreted to represent retrogressed cordierite related to the peak thermal metamorphism. Large rhombohedral andalusite porphyroblasts (Plate III), up to 2 cm across are restricted to the most extensively chlorite-muscovite altered sediments in the immediate footwall to the magnetite lodes. Although now largely altered to felted muscovite, cores of andalusite have been identified both optically and by XRD.

The strong correlation between the occurrence of the contact metamorphic minerals and hydrothermal alteration assemblages, indicate that the presence of a pre-existing iron-, magnesium-, and aluminium-rich assemblage that was generated during hydrothermal alteration has provided rocks of favourable chemistry for the development of this contact metamorphic mineral assemblage. The Warrego spotted sediments are very similar to the dalmatianite rocks reported in altered zones at Millenbach mine, Quebec, where a similar relationship between altered rocks and later contact metamorphism is suggested (Simmons et al., 1973). The implication of this relationship is that contact metamorphism has been an isochemical heating process in which the relatively minor fluid flows that were generated (devolatilisation of the granite and marginal hydrothermal cells), have been restricted to specific fractures (see veins below) and contacts.

However, despite the restriction of contact metamorphic assemblages to zones of hydrothermal alteration, the intensity of contact metamorphism is observed to diminish with decreasing depth and distance from the Footwall Fault. The fine grained sediments in the upper levels of the mine show fine vitroclastic textures suggesting they are vitric tuffs (Duncan, 1970), and the coarser sediments contain angular quartz and rock fragments similar to the tuffaceous greywacke elsewhere in the field.

Quartz Porphyry

The 'quartz porphyry' forms a unit up to 50 m in thickness that appears to be broadly conformable within the Warrego stratigraphic sequence. The porphyry contains intercalated lenses of siltstone and shale that may be tens of metres in thickness, but because they are of limited lateral extent correlation between drillholes is extremely difficult. On

Plate III

A: Hand specimen and drill core examples of porphyries from the Warrego mine. From left to right, strongly foliated quartz porphyry (sample 106980), relatively unaltered sediment clast within matrix-rich quartz porphyry (sample 109125), quartz-feldspar porphyry dyke (sample 108800), and strongly altered quartz porphyry in which the matrix has been completely replaced by chlorite (sample 108831). Coin diameter is 2·5cm.

B: Hand specimen and drill core examples of andalusite porphyroblasts in strongly hydrothermally altered sediments. From left to right, zoned andalusite rhombs (sericitic rims) in massive chlorite alteration (sample 108655), rectangular andalusites restricted to a chlorite-chalcopyrite vein in spotted sediment (sample 109146), and massive chlorite-magnetite rock from the footwall of the ironstone lode showing abundant development of diffuse andalusites (sample 107000).

C: Thin section (PPL) of relatively unaltered quartz-feldspar porphyry containing large oval, embayed quartz crystals and strongly sericitised euhedral plagioclase. Sample 107028.

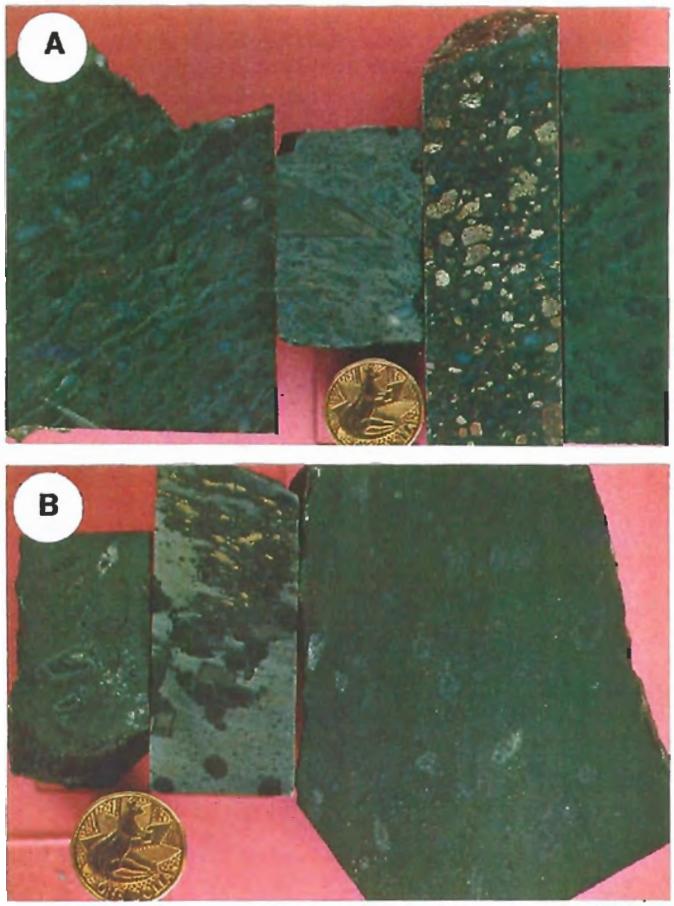
A
B
C
10·0 mm

14 level the porphyry is quite massive, but between 2 and 4 levels (Fig. 2.4) thick wedges of sediments are observed in drillcore. Rare lenses of quartz porphyry, as little as 1cm in thickness (i.e. one quartz phenocryst wide), are observed marginal to the porphyry contact, yet are compositionally indistinguishable from the main porphyry.

Contacts with the adjacent sediments although sharp are frequently irregular showing evidence of apparent soft sediment deformation, and transposition along cleavage planes. For the purposes of mapping, the contact of the quartz porphyry is taken as the last occurrence of quartz porphyry in the sequence, and this (the lower contact of the quartz porphyry is the best constrained by drilling and development), forms a well defined boundary that is apparently conformable with the enclosing sediments (Chapter 3 and 4).

The porphyry is variably foliated parallel to the cleavage in the sediments, and comprises 10–30% ellipsoidal blue quartz phenocrysts (5–7 mm in length) that are characterised by radial narrow embayments, broken, fractured, and sericitised plagioclase (albite) crystals, and angular lithic fragments of volcanic derivation (Plates II and III). Plagioclase phenocrysts were only recognised in samples from the upper 20 m of the porphyry, suggesting that it comprises several individual units that were not recognised during underground mapping. The quartz phenocrysts are evenly distributed throughout the porphyry, and there is no grading in size or abundance toward the sediment contacts. Angular clasts of sediment up to several centimetres long are commonly observed, and these (as do the major contacts) show no evidence of chill margins.

The matrix of the porphyry is typically strongly altered to chlorite and muscovite and the well developed foliation exhibited by these minerals wraps around the quartz phenocrysts. Clots of coarse biotite (variably altered to chlorite) are commonly observed to have overgrown the mineral foliation and as with the sediments are related to the contact metamorphic overprint of the Warrego Granite.

The porphyry is distinctive within the Warrego mine sequence for its total absence of magnetite (and hematite after magnetite); opaques (with the exception of minor sulphides), exclusively comprise disseminated idiomorphic crystals of intergrown hematite and rutile that are interpreted as the alteration product of original magmatic ilmenite. This observation is consistent with the relatively non-magnetic signature of porphyries in regional aeromagnetic compilations (B.T. Williams, pers. comm., 1988).

Intricate primary textures within the matrix of the porphyry consisting of complex arcuate shapes have been described in surface drillhole samples from the upper levels of the mine by Duncan (1970); these were suggested to indicate the former presence of glass shards and indicated a pyroclastic origin for the unit. Subsequent examination of the same samples by McPhie (1990) has failed to confirm textural evidence of glass shards, although the presence of relict perlitic cracks was confirmed.

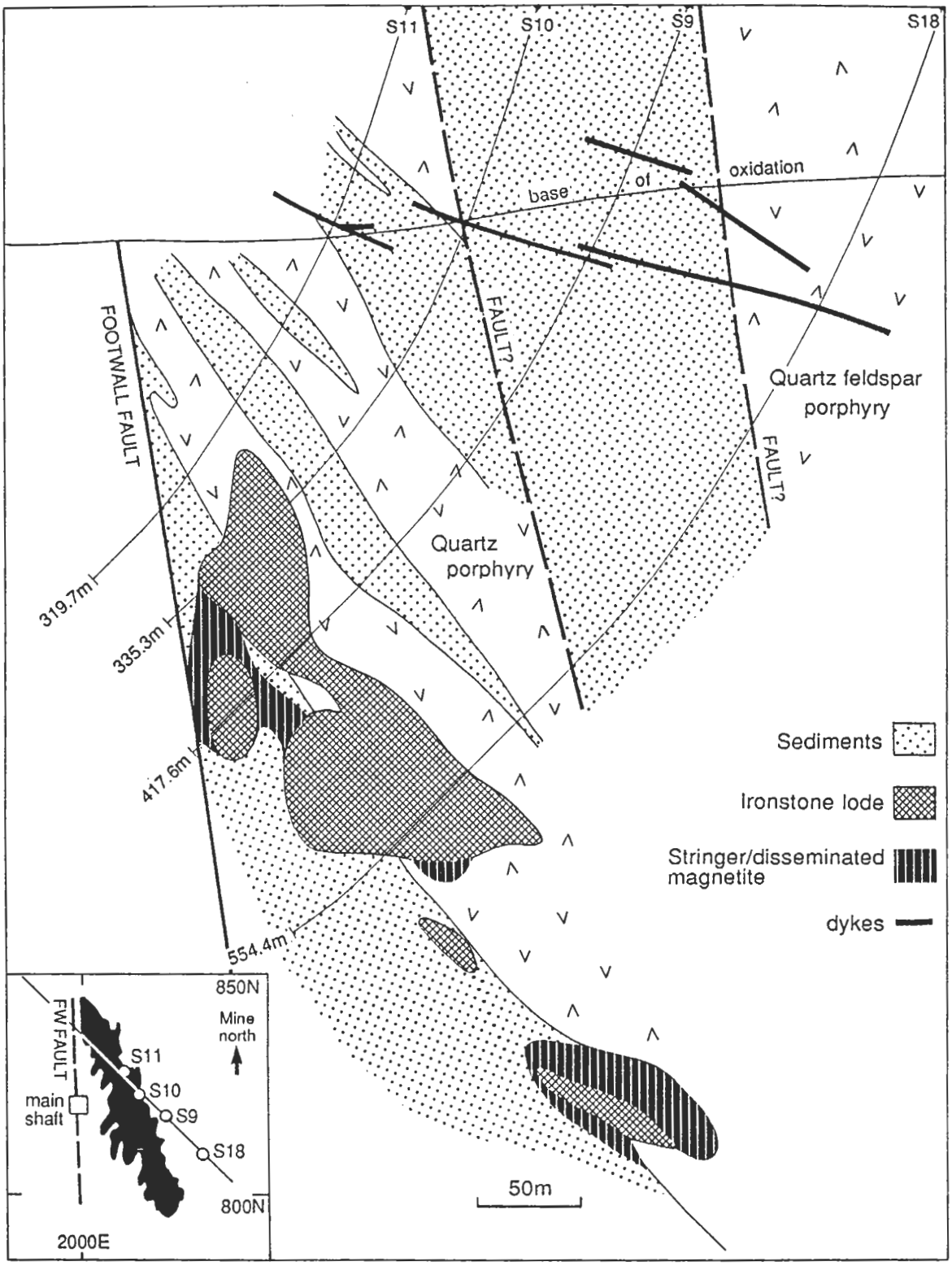

Figure 2.4 — Oblique section through the Warrego ironstone lode and adjacent host rocks as defined by surface drilling and underground mapping (compiled from unpublished Geopeko data). Note the intercalation of quartz porphyry and sediments, and the discordant attitude of the quartz-feldspar porphyry. Also note the extremely irregular outline of the ironstone lode and its localisation at the quartz porphyry-sediment contact.

Quartz Feldspar Porphyry

Overlying the quartz porphyry but separated by some 150 m of sediment, is a thick unit of quartz feldspar porphyry that has only been intersected in surface drillholes. Because this material is no longer available, it has not been examined in this study and details presented here are summarised from the work of Duncan (1970), and logging by company geologists.

The unit has a thickness ~250m (Goulevitch, 1975), and appears to be broadly conformable, but unlike the quartz porphyry, the quartz-feldspar porphyry forms a massive unit without intercalations of sediment. Drill logs record a succession of units differing in phenocryst size, composition, and concentration which suggests that it is a composite body. No attempt has been made to correlate individual units between drillholes, and it seems unlikely that this would be possible.

The quartz feldspar porphyry comprises prominent phenocrysts of quartz (9–17%), K-feldspar (12–20%), and plagioclase (3–14%) that together constitute between 28 and 41% of the rock volume. Blocky euhedral to rounded elongate microcline phenocrysts range in size between 1–2.5 cm and invariably display sieved or honeycombed patterns of internal cavities and embayments. Plagioclase may completely pseudomorph the original K-feldspar phenocrysts. Rectangular albitised plagioclase phenocrysts up to 7 mm in length, are commonly altered to sericite, and quartz phenocrysts are identical to those in the quartz porphyries.

The matrix comprises a crystalline mosaic of quartz and K-feldspar with variable quantities of plagioclase, biotite, chlorite, and muscovite with the phyllosilicates generally defining a distinct foliation that wraps around the phenocrysts. Again relict textures within the groundmass are reminiscent of perlitic cracking and arcuate fragmental patterns are described as typical of volcanic ash (Spry, 1963, Duncan, 1970). McPhie's (1990) comments as to the interpretation of these textures are similar to those for the quartz porphyry.

The general relationship of the quartz porphyry and quartz feldspar porphyry is illustrated in Figure 2.4 and it is evident that either, the quartz-feldspar porphyry is discordant to the stratigraphy i.e. intrusive, or it is fault bounded. The interpretation of relict textures is therefore critical in making this distinction (see below).

Dykes

Lamprophyric and mafic to intermediate dykes ranging from approximately 1–10m in thickness have been intersected in surface drillholes (Duncan, 1970) and have been mapped underground by various mine geologists. Even in drillcore, mafic-intermediate dykes are extremely difficult to distinguish from zones of strong hydrothermal alteration due to pervasive chloritisation, and destruction of virtually all crystal textures. Examples were only recognised during mapping on 14 level because they were intruded into a

texturally different rock type i.e. fine grained dyke into quartz porphyry. However in thin section, dykes are readily recognised by their relatively undeformed character, the presence of highly altered sericitic clots suggesting the former presence of phenocrysts, and the occurrence of euhedra of iron-titanium oxide suggesting the former presence of ilmenite.

An unusual rock type has been mapped in the immediate footwall of the No. 3 orebody (see Chapter Four) which comprises coarse randomly orientated muscovite crystals up to 2 mm long associated with strong chlorite and carbonate alteration. The unusual mineralogy and presence of sericite clots suggesting the former presence of phenocrysts appear to indicate an intrusive origin although this rock is indistinguishable from the sediments on the basis of trace element chemistry (Chapter Seven).

The generally undeformed nature of the dykes indicates these are related to a post-mineralisation intrusive episode, and the difficulty in recognising dykes during mapping suggests that their presence is likely to have been underestimated.

Veins

In addition to the pegmatite dykes and minor tourmaline veining along the contacts of the quartz porphyry, prominent quartz veins are also related to the intrusion of the Warrego Granite. The veins are typically less than 10 cm in width, are oriented parallel to the cleavage and are observed cross-cutting the ironstone lodes and associated mineralisation. The veins are predominantly composed of buck quartz with minor pockets of coarse muscovite and/or tourmaline.

The distinctive mineralogy, cross-cutting relationship with the lode, and stable isotopic signature of the quartz and muscovite (Chapter Eight) suggest that that the veins post-date mineralisation and have a magmatic signature indicating a probable association with the Warrego Granite.

2.4 Conditions of Contact Metamorphism

Previous investigations of the Warrego mine had noted the presence of chlorite spotting in the sediments and andalusite in the immediate footwall of the ironstone lode (Large, 1974; Goulevitch, 1975), however no genetic interpretation was suggested to explain their presence. Subsequent dating of the nearby Warrego Granite, and the apparent resetting of some Warrego mineralisation ages (Black, 1977, 1984) suggested a post-mineralisation age for granite intrusion and provided a link between the unusual mineral assemblage in Warrego mine and the granite.

Consequently, at the time this study was undertaken, the possibility of a contact metamorphic overprint on the orebody and adjacent host rocks was recognised, but the true extent and possible effects on mineralogy, geochemistry, and stable isotopic relationships was unknown. Obviously to correctly interpret the results presented in this

study, the possible influence of contact metamorphism must be constrained. Assuming the metamorphic mineralogy observed in the footwall of the ironstone lode on 14 level represents the peak equilibrium metamorphic mineral assemblage, i.e. biotite, chlorite, andalusite, cordierite, and quartz, it is possible to estimate temperature and pressure conditions.

Using the thermodynamic database of Berman et al. (1985) and phase diagram program of Perkins et al. (1986) a temperature between 500° to 550°C, and pressure less than 2.5 kbar is indicated for the reaction:

$$11 \text{ quartz} + 2 \text{ clinochlore} + 8 \text{ andalusite} \Leftrightarrow 5 \text{ cordierite} + 8H_2O$$

illustrated in Figure 2.5. Although the assumption of equilibrium between the mineral phases is clearly simplistic (biotite is observed to have overprinted cordierite (Plate II) and the relationship of andalusite to biotite and cordierite is uncertain because of its restricted distribution), experimental calibration of the cordierite-in isograd for pelitic rocks suggest that similar temperatures are observed under the low pressure (<2.5 kbar) conditions expected during contact metamorphism (Winkler, 1979).

The high temperatures indicated during contact metamorphism will clearly have affected the mineral assemblages in the ironstone lode and surrounding host rocks as is evident in the recrystallisation of quartz in the sediments. However indications that primary mineralogical and chemical zonation in the orebody has been preserved (Chapters Five to Eight) support an interpretation that metamorphism was isochemical. The decreasing intensity of contact metamorphism at shallower levels in the mine may also mean that primary mineralisation characteristics such as temperature indicators are preserved at these lower levels (Chapter Eight).

2.5 Origin of the Porphyries

There was considerable debate as to the origin of the Tennant Creek porphyries during the 1960's and early 1970's in response to the hypothesis that they were not volcanic, but diagenetic in origin. Elliston (1963) proposed that the formation of colloidal accretions within wet sediments prior to dewatering, gave rise to the "igneous-looking" rocks on crystallisation. Subsequent workers have been unanimous in their rejection of this hypothesis; all suggest that the porphyries are clearly volcanic in origin, being variously described as lava flows, pyroclastics, or shallow intrusions (Spry, 1963; Crohn and Oldershaw, 1965; Whittle, 1966; Dunnet and Harding,1967; Duncan, 1970; Large, 1974, 1975; Mendum and Tonkin, 1976; and McPhie, 1990).

However, some consideration must be given to the mode of emplacement of the porphyries within the moderate to deep water succession of turbiditic sediments. Although a small proportion of the porphyries cross-cut the stratigraphy and are clearly intrusive, e.g. Creek Bed Porphyry (Duncan, 1970), and those at White Devil mine (Nguyen, 1987, 1990; Rattenbury, 1988), the majority are conformable with bedding

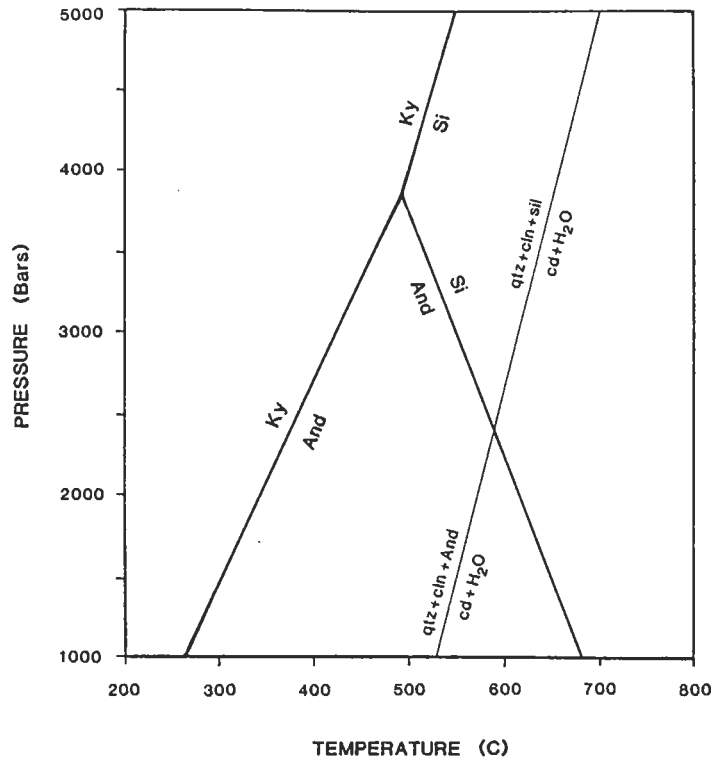

Figure 2.5 — Experimentally determined stability diagram for the contact metamorphic mineral assemblage observed in the footwall of the Warrego ironstone lode.

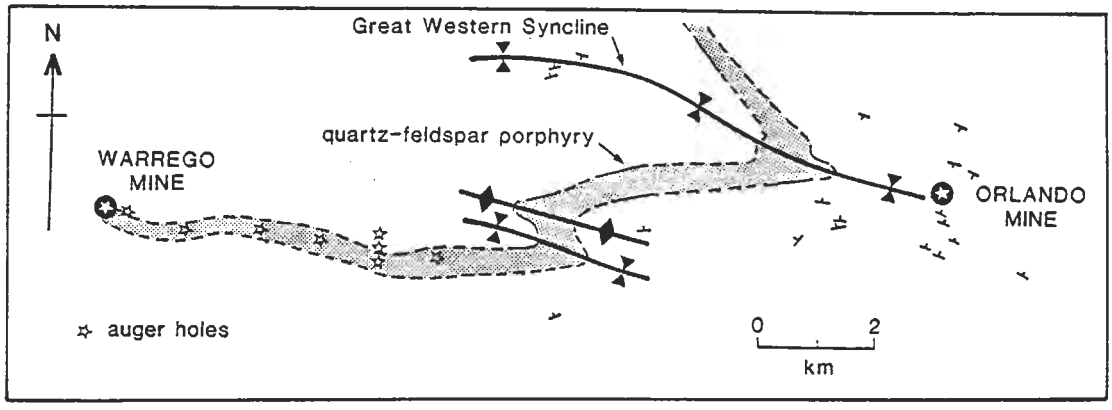

Figure 2.6 — Relationship of the Warrego porphyry to the Great Western Porphyry illustrating the location of shallow auger holes used to link the two units (adapted from Duncan, 1970).

and apparently form a continuous unit covering a wide area (Duncan, 1970; Large, 1974). This broadly conformable nature combined with petrographic features such as the interpreted presence of glass shards and perlitic cracking patterns within the matrix, and the occurrence of embayed and broken phenocrysts, volcanic lithic fragments, and sediment clasts have been interpreted as indicative of a pyroclastic origin for the porphyry (e.g. Spry, 1963; Duncan, 1970; Large, 1974).

Although Burnham (1983) calculated that submarine pyroclastic flows may be generated from H_2O-bearing silicic melts at water depths of at least 10,000 m, there seems to be little record of their actual occurrence other than where generated at extremely shallow water depths, or where subaerial flows have entered shallowly shelving water (Fiske, 1963; McBirney, 1971; Cas, 1978; Howells et al., 1979; Sparkes et al., 1980a, 1980b; Orton, 1990). An alternative model involving the redeposition of subaerially derived pyroclastic debris by subaqueous turbidity current seems more favourable. Fisher and Schmincke (1984) and Cas and Wright (1987) suggest that such processes produce internally massive and structureless deposits resembling those produced by pyroclastic flows, and include the preservation of fragile shard fragments, with little or no abrasion. Carey and Sigurdsson (1980) describe a 14,000 km^2 submarine pyroclastic debris flow in the Grenada Basin where delicate shards of vesiculated glass are preserved in a massive poorly sorted deposit that is some 0.3 m thick 250 km from source. Such deposits are suggested to have derived from subaerial pyroclastic flows that on entering the sea, continue down slope as debris flows (Carey and Sigurdsson, 1980), or by the mass slumping of pyroclastic debris accumulating on the flanks of volcanic islands (Cas and Wright, 1987).

The homogeneous, coarse, crystal-rich character of the Tennant Creek porphyries, without significant grainsize variation, or intercalation of sediment is however at odds with such a derivation or setting. Recently McPhie (1990) has suggested that the porphyry represents a coherent, phenocryst-rich magma that was intruded conformably into unconsolidated wet sediments. The salient features of her model are that textural features (perlitic cracks, massive character, lack of other than sedimentary foreign rock fragments, and local development of columnar-like jointing) support the interpretation that the porphyry represents an originally coherent, phenocryst-rich magma. Fluidal and globular intermixing of porphyry and sediment at both the upper and lower porphyry contacts is inconsistent with the rapid quenching expected of submarine lava flow tops, but more consistent with peperite textures developed through the intrusion of a magma into wet, unlithified sediments. The presence of indurated sediments adjacent to the porphyry margins is cited as evidence of premature dewatering associated with intrusion.

Certainly the expression of doubt upon the interpretation of glass shards in the porphyry matrix (McPhie, 1990) undermines the key argument for a pyroclastic origin.

Similarly the intermixing of the porphyry with sediments at both the lower *and* upper contacts is difficult to reconcile with a pyroclastic or sediment slumping model; a pyroclastic or debris flow might be expected to entrain large blocks of the substrate during deposition, but for subsequent turbidity currents to achieve similar erosion of the underlying porphyry is extremely unlikely.

In view of its relative attractiveness, features observed in the Warrego porphyries are considered in the light of the sill model. Although the lower contact of the quartz porphyry is well defined in underground development and diamond drilling, the upper contact is less well exposed. Certainly the upper contact of the quartz porphyry on 14 level is marked by the incorporation of clasts of one within the other. However, in contrast to McPhie's (1990) mainly outcrop observation of a massive homogeneous porphyry core, Figure 2.4 illustrates large scale interbanding of quartz porphyry and sediment parallel to the main footwall contact and bedding in the sediments. Similarly the main quartz-feldspar porphyry is far from homogeneous, containing multiple units that are defined by variations in crystal size and relative proportion of matrix. The relationship of the two porphyries at Warrego separated by in excess of 100 m of sediment also questions a simple, single, coherent intrusive event.

No evidence has been noted in underground mapping and core logging of any obvious contact effects at the porphyry margins. The expected recrystallisation of sediments adjacent to porphyry margins has not been reported by McPhie (1990), but possibly accounts for the more indurated character of these sediments. Unfortunately the metamorphic overprint of the Warrego Granite is likely to have masked any primary differences in the sediments immediately adjacent to the porphyry.

The apparent discordance of the quartz-feldspar porphyry relative to the sediments and quartz porphyry illustrated in Figure 2.4 is not understood. Certainly the general parallelism of its lower contact with the Footwall Fault may indicate this is a faulted contact; an interpretation which is not inconsistent with its likely behaviour as massive, relatively rigid body during tilting of the sequence during granite intrusion (Chapter Four). The possibility that the quartz-feldspar porphyry is a large dyke, and therefore similar to the White Devil porphyries, cannot be ruled out.

Despite these obvious differences between the general model and the specific Warrego setting, the sill model is, in the author's opinion, the most credible in terms of explaining the porphyry relationships at Warrego and the Tennant Creek field in general. Modification to the model to incorporate multiple intrusions of magma would appear to be the main requirement to account for the specific relationships observed at Warrego.

2.6 Correlation within the Warramunga Group

The monotonous nature of the sediments and poor outcrop has made correlation within the Warramunga Group difficult. The two commonly used marker horizons are the hematite shales, and the conformable porphyries, both of which can be traced discontinuously over much of the field (Fig. 2.1). The porphyries intersected in the Warrego mine are essentially the same (texturally, mineralogically, and chemically) as other porphyries, and the volcanics within the Bernborough Formation (Spry, 1963; Duncan, 1970) and together appear to represent a period of extensive plutonism/ volcanism within the Warramunga Group.

Although there have been no attempts to link the porphyries through trace element geochemistry or age dating, there is a general correlation between outcrop and drillhole intersections of the porphyries across the Warramunga Group. The sequence observed in the Warrego area consisting of a thick (~250 m) quartz-feldspar porphyry underlain by an irregular intermixed sequence of quartz porphyry and sediments (~50 m) is also observed in the Peko syncline in the vicinity of the Golden Forty mine (Pontifex, 1964). In other areas there is either insufficient outcrop, or contacts are masked (e.g. Great Western Porphyry (Duncan, 1970), to establish if the relationship of the quartz-feldspar porphyry and quartz porphyry is common in all situations.

The Warrego porphyries are directly along strike (~10 km) from the Great Western Porphyry, a continuous horizon that extends a further 10 km in apparent conformity with the enclosing sediments reproducing the fold pattern of the Great Western Syncline (Fig. 2.6). Cleavage recorded in the porphyry is parallel to that of the regional cleavage in the enclosing sediments, and is axial planar to the Great Western Syncline (Duncan, 1970). Elliston (1963) suggested a correlation between the Warrego and Great Western porphyries, and support for this link was obtained from eight shallow auger holes (Duncan, 1970), that penetrated the overburden and sampled underlying weathered rock (Fig. 2.6). Duncan (1970) supported this correlation based on petrographic, chemical, and mineralogical criteria.

The sediments in the Warrego area generally appear finer grained than those in the southeast of the goldfield, and it has been suggested by various workers (Crohn and Oldershaw, 1965; Norris, 1980) that the original environment of deposition for the Warramunga Group was a northwest-southeast orientated elongate basin that deepened to the west. Mendum and Tonkin (1976) considered sandstone outcropping in the east and northeast of the field represent the margins of the marine basin into which the Warramunga Group sediments were deposited. Sedimentological studies in the Eldorado area (Norris, 1980), and current directions recorded in the southeast (Norris, 1980; Rattenbury, 1990b), and in the north of the goldfield (Edwards, 1987) suggest that prograding submarine fans, and current directions were from the east to the northwest.

2.7 Environment of Deposition of the Warramunga Group

From the above discussions a model for the environment of deposition of the Warramunga Group is proposed. Conventionally the Carraman Formation is considered to overlie the Bernborough Formation, but it is suggested here that they may in fact represent facies variations of equivalent age rocks. A comparison of the distribution of sedimentary, volcanic, and intrusive rocks in a modern arc setting (Lesser Antilles) with those of the Warramunga Group show obvious similarities, i.e. a central igneous complex surrounded by a rim of subaerial and shallow marine sediments and volcanics that grades laterally into deeper water volcaniclastic sediments (Fig. 2.7). Such a model applied to the Warramunga Group would successfully explain the compositional similarity, and association in space and time of the granite and the porphyries, and also provides an eastern source for the sediments and the apparent deepening of the basin to the west

The following model is suggested to describe the deposition of the Warramunga Group.

1. Intrusion of (or part of) the Tennant Creek Granite Complex into the basement of volcanic sediments correlated with Arunta Division 1, and commencement of active 'island arc-style' volcanism.
2. Rapid build-up of a volcanic apron comprising proximal well sorted sandstones interbedded with lava flows, and intruded by stocks and plugs (Bernborough Formation). Distal sediments comprise turbiditic volcanic greywacke-shale sequences (Carraman Formation). Abundant disseminated iron oxides and the occurrence of argillaceous banded-iron-formation suggest a chemical component to the sediments, possibly indicating fumarolic activity on the seafloor around the volcanic ediface.
3. Shallow intrusion of the porphyry as a sill in a series of magma pulses into the wet unlithified Warramunga Group sediments.
4. Continued deposition of turbiditic volcanic sediments related to erosion and uplift of the volcanic complex. Fumarolic activity appears to have waned and died resulting in sediments above the Black Eye Member being free of iron oxides.
5. Regional metamorphism and folding of the Warramunga Group associated with ironstone development and Au-Cu-Bi mineralisation. This period was possibly associated with intrusion of the Tennant Creek Granite higher into its own volcanic framework.
6. Uplift and erosion.
7. Deposition of the Hatches Creek Group and Tompkinson Creek Beds.

8. Intrusion of the Warrego and Red Bluff Granites, associated with refolding of the sediments and porphyries in the immediate vicinity of the Warrego mine and contact metamorphism of the Warrego orebody and associated sediments.

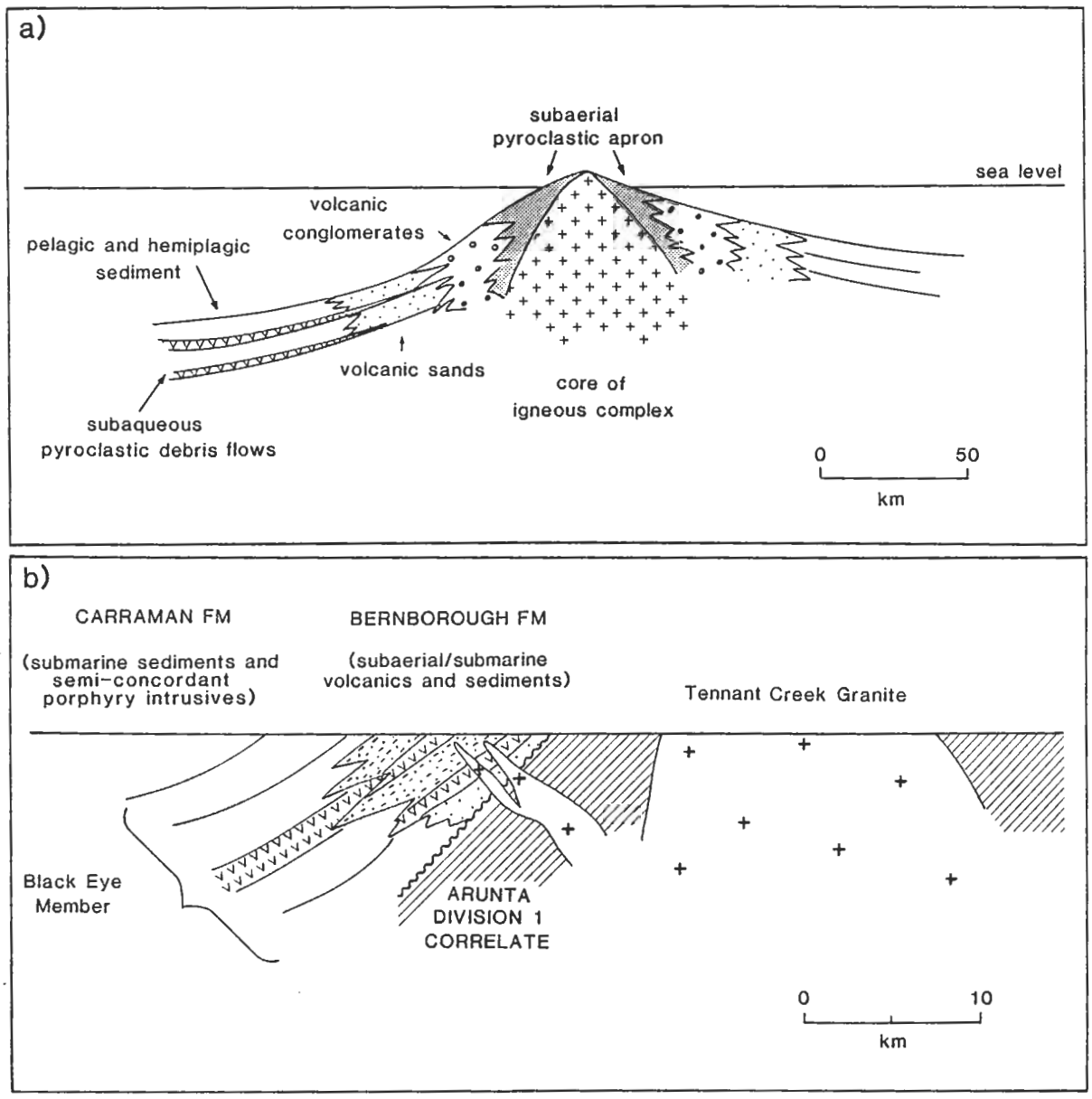

Figure 2.7 — Comparison of the geology of (a) the Lesser Antilles volcanic arc (after Sigurdsson et al., 1979) with (b) the Warramunga Group.

Chapter Three

WARREGO OREBODY

3.1 Introduction

The Warrego mineralised system[1] consists of two major and several smaller oblate lenses of magnetite ± quartz (0 to 60 modal %) ± chlorite (0 to 40 modal %) ± sulphides (0 to 30 modal %), that plunge ~45° to the southeast (Fig. 3.1). The larger of the two lenses, the 'No. 1 orebody', extends from 140 m to 790 m below the surface, giving an overall length in excess of 900 m when the plunge of the lode is taken into consideration. On 9 level (see Table II relating mine levels to depth below surface), the No. 1 orebody reaches its maximum dimensions of 200 m by 75 m, and is aligned sub-parallel to bedding as defined by the quartz porphyry contact.

The smaller lens, the 'No. 3 orebody', lies less than 50 m stratigraphically above the No. 1 orebody to which it is connected by a narrow neck of ironstone lode between 12 and 14 levels. The No. 3 orebody extends from 440 m to 735 m below the surface, and although on 13 level its maximum dimensions are similar to those of the No. 1 orebody, it rapidly tapers above and below this level.

Table II: Depth Below Surface (m) of Main Warrego Mine Levels.

Surface	0	8 Level	413	
2 Level	160	9 Level	450	
3 Level	203	10 Level	490	*
4 Level	244	12 Level	568	
5 Level	282	13 Level	610	
6 Level	322	14 Level	650	
7 Level	366	15 Level	672	

* There is no development on 11 Level

[1] The Warrego mineralised system refers to the collection of ironstone lodes and the associated alteration envelope as defined by underground development and drilling of the Warrego mine.

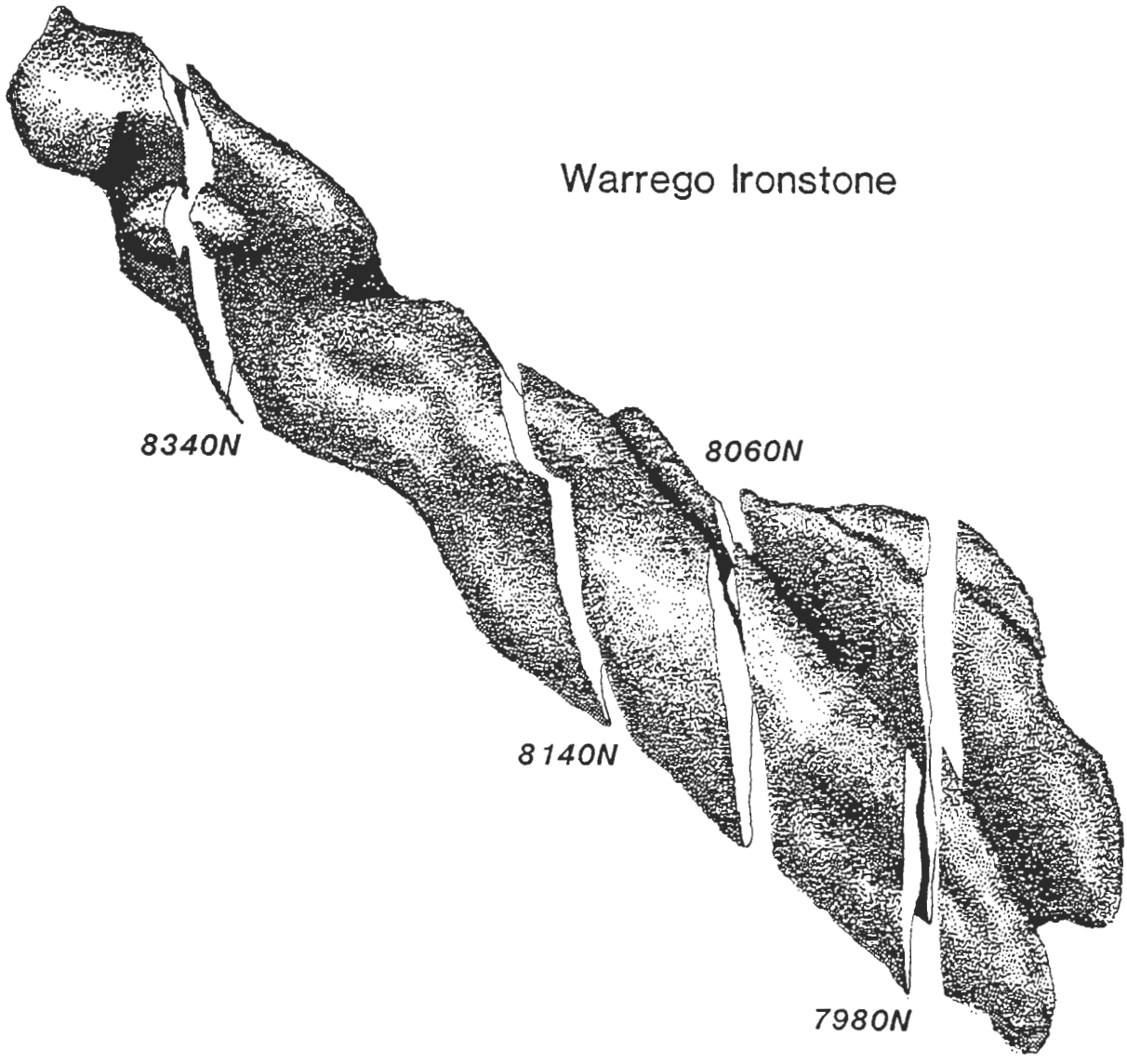

Figure 3.1 — Isometric diagram of the Warrego ironstone lode illustrating its overall shape, geometry, and the relationship of the four sections selected for detailed examination in this study.

The combined ironstone lodes in the Warrego system have a mass in excess of 14 Mt and the No. 1 orebody is probably the largest ironstone lode in the Tennant Creek goldfield (T. Hoschke, pers. comm., 1988). A breakdown of the mass of individual ironstone lodes is given in Table III, and illustrates the relatively insignificant contribution of the smaller lodes to the overall mass. The two small pods (North East and Footwall) are located near the top of the No. 1 orebody where the lode outline becomes very irregular with deeply embayed margins (e.g. Figure 2.4).

Table III: Mass of the Warrego Ironstone Lodes (Mt)

No. 1 Orebody	12.38
No. 3 Orebody	1.40
North East Pod	0.17
Footwall Pod	0.09
Total	**14.04**

The plunging attitude of the ironstone lodes means their orientation is skewed with respect to the mine sections[1], which not only makes it difficult to visualise the continuity of geology between sections, but also impairs the identification of overall patterns in mineralogy, geochemistry, and metal zonation. Therefore, documentation of the Warrego system has been approached on two scales:

1. Locally, the composition and zonation of the ironstone lodes has been examined on the mine section scale. Four representative mine sections were selected for detailed documentation through the re-logging of drillcore and scrutiny of selected samples in polished thin section. The four mine sections used in this study were; 8340N (copper orebody between 3 and 8 levels), 8140N (gold pod between 8 and 12 levels), 8060N gold-rich copper orebody between 10 and 14 levels), and 7980N (gold pod between 13 and 15 levels). The relationship of these sections to the overall system is illustrated in Figure 3.1, and their geology in Figures 3.2 to 3.5. Further work describing metal zonation, stable isotope analysis, and rock and mineral chemistry based on these sections is described in following chapters.
2. To relate trends in mineralogy and metal distribution observed on the mine section scale to the orebody as a whole, a series of 'true' composite sections through the ironstone lodes were constructed utilising existing mapping and logging by company geologists, and computer generated metal contour plots (Fig. 3.6). Because these are true sections through the ironstone lodes, correlation between them is simplified and easier to follow (Figure 3.7).

[1] Mine sections (east-west) are labelled by their northing on the mine grid in which Mine North is 59° west of True North.

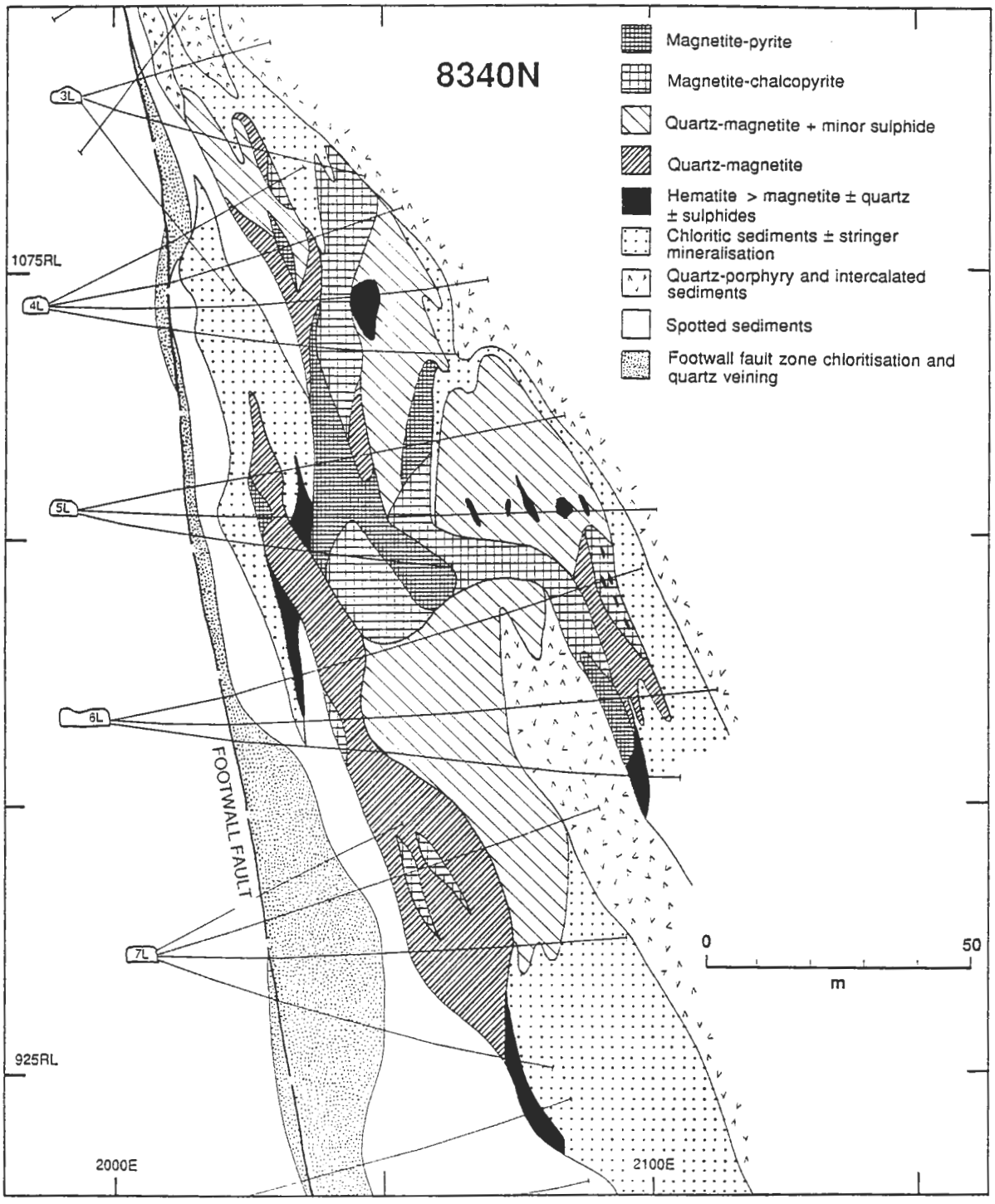

Figure 3.2 — Geological cross-section: 8340N.

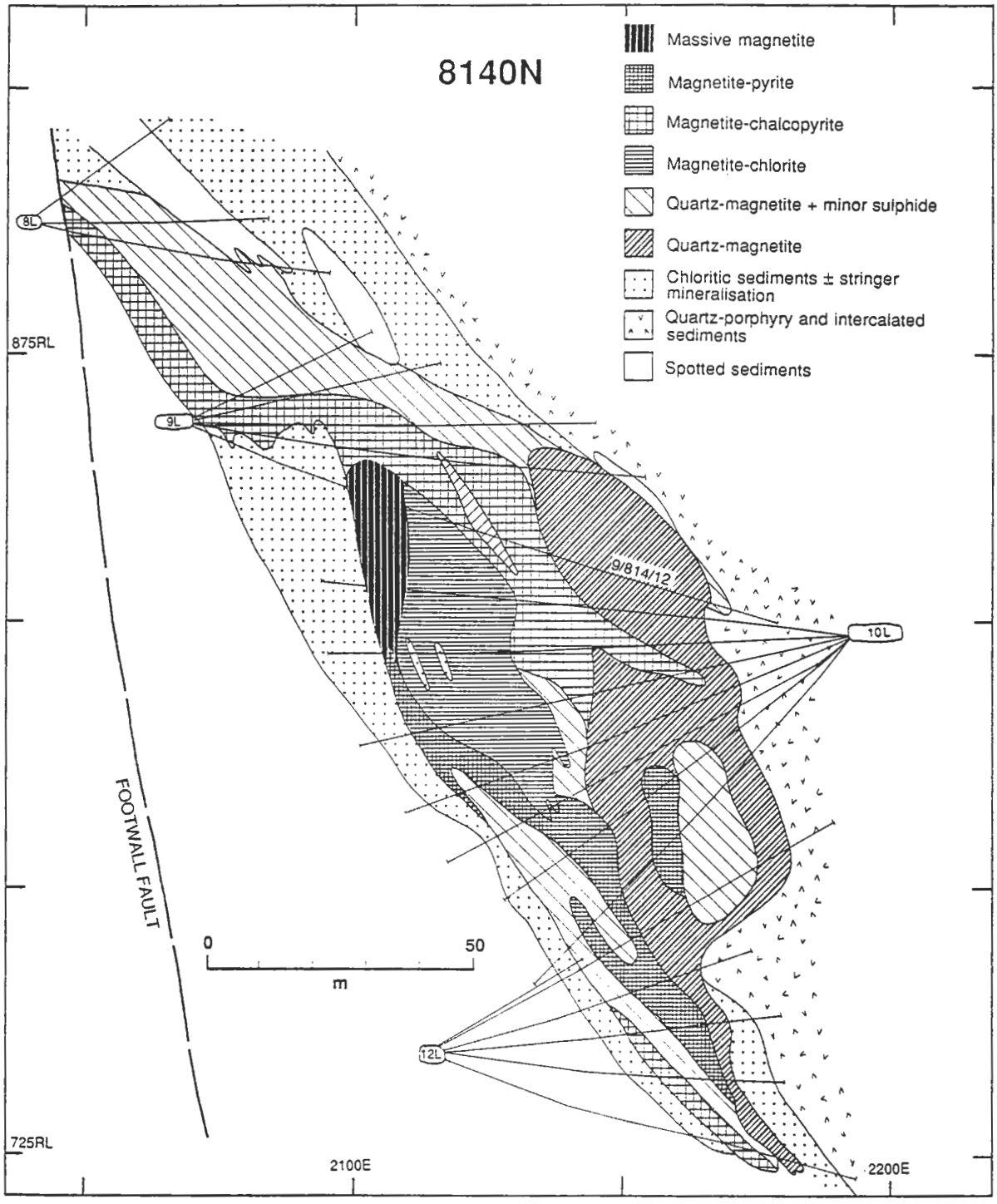

Figure 3.3 — Geological cross-section: 8140N.

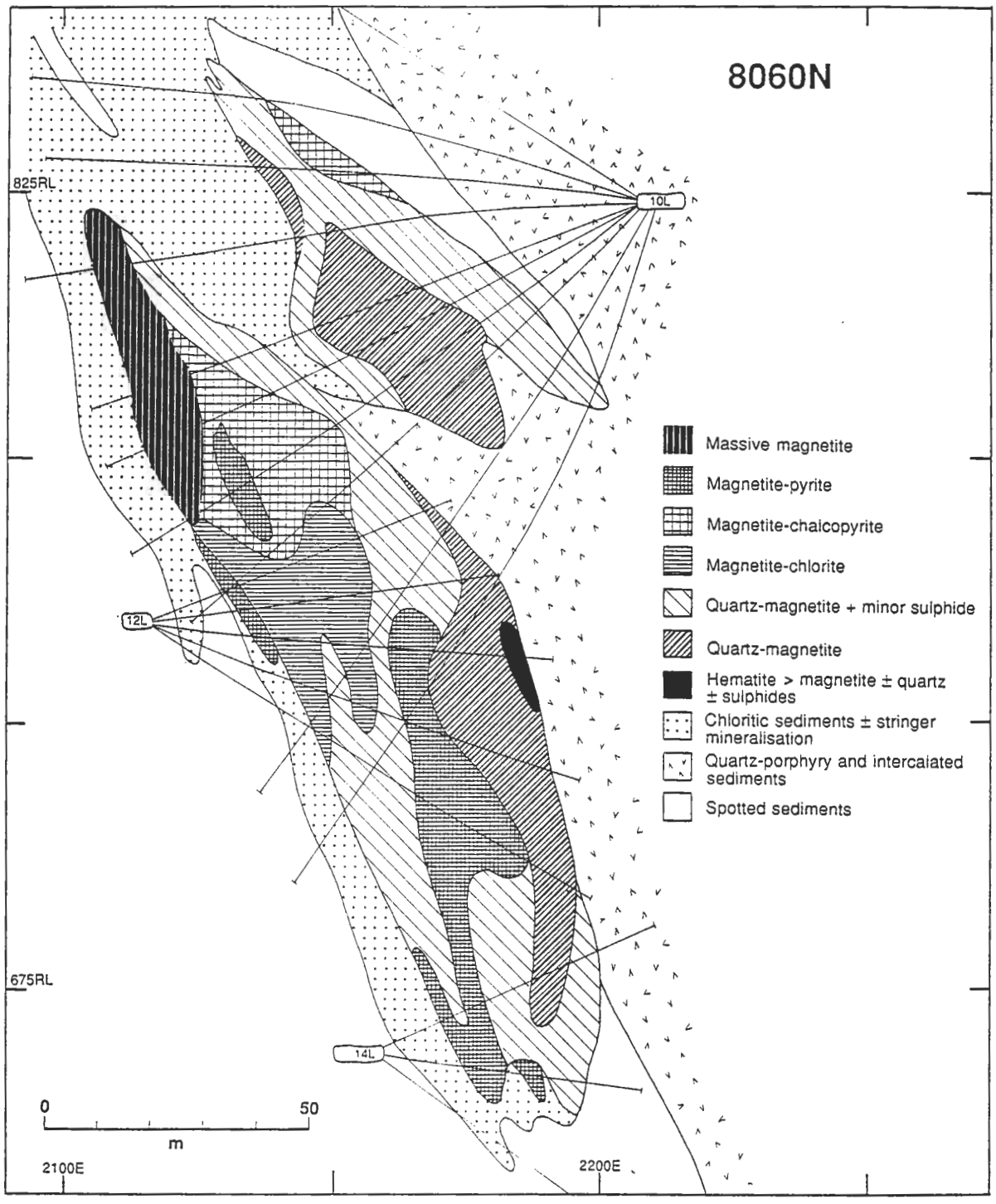

Figure 3.4 — Geological cross-section: 8060N.

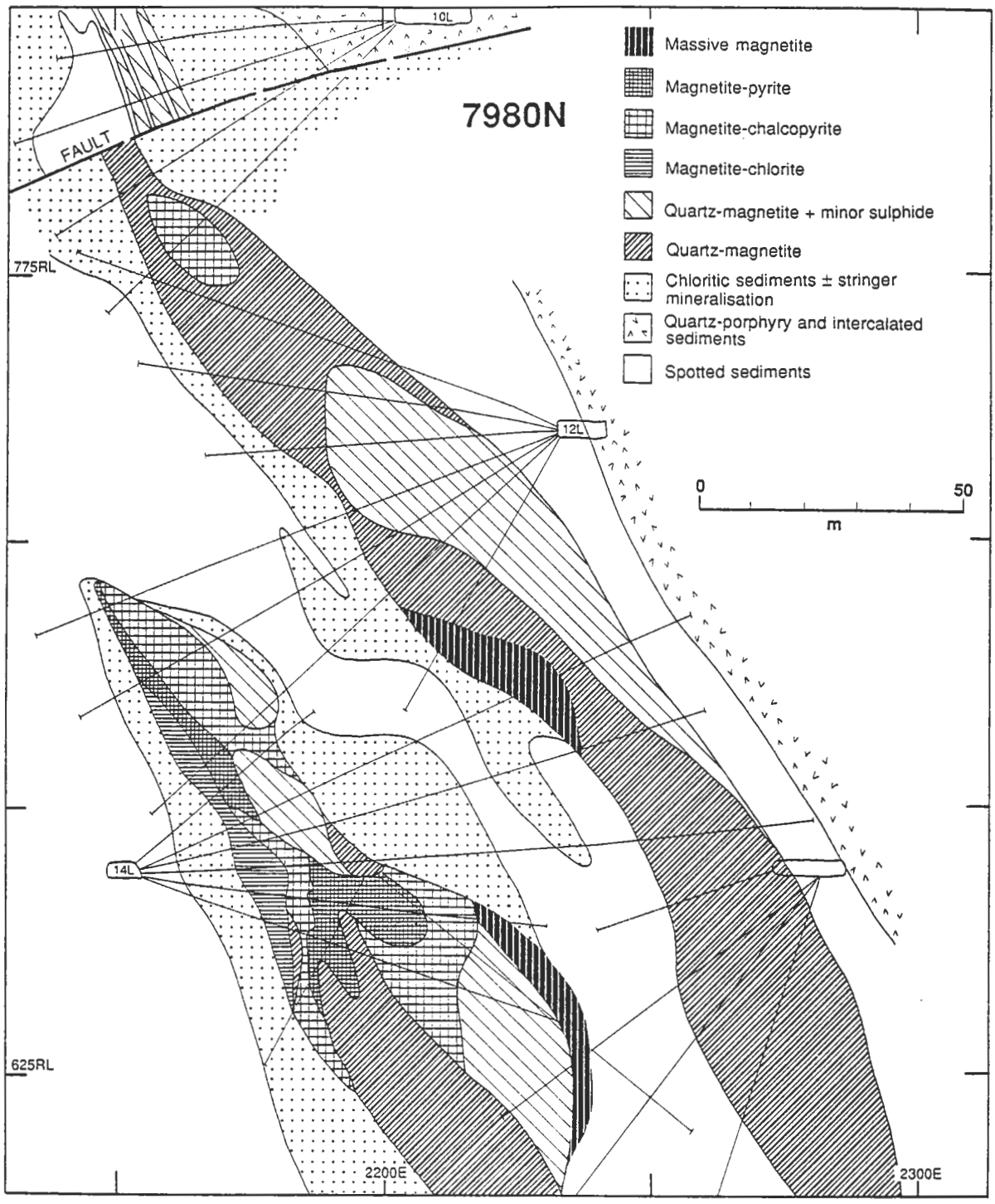

Figure 3.5 — Geological cross-section: 7980N.

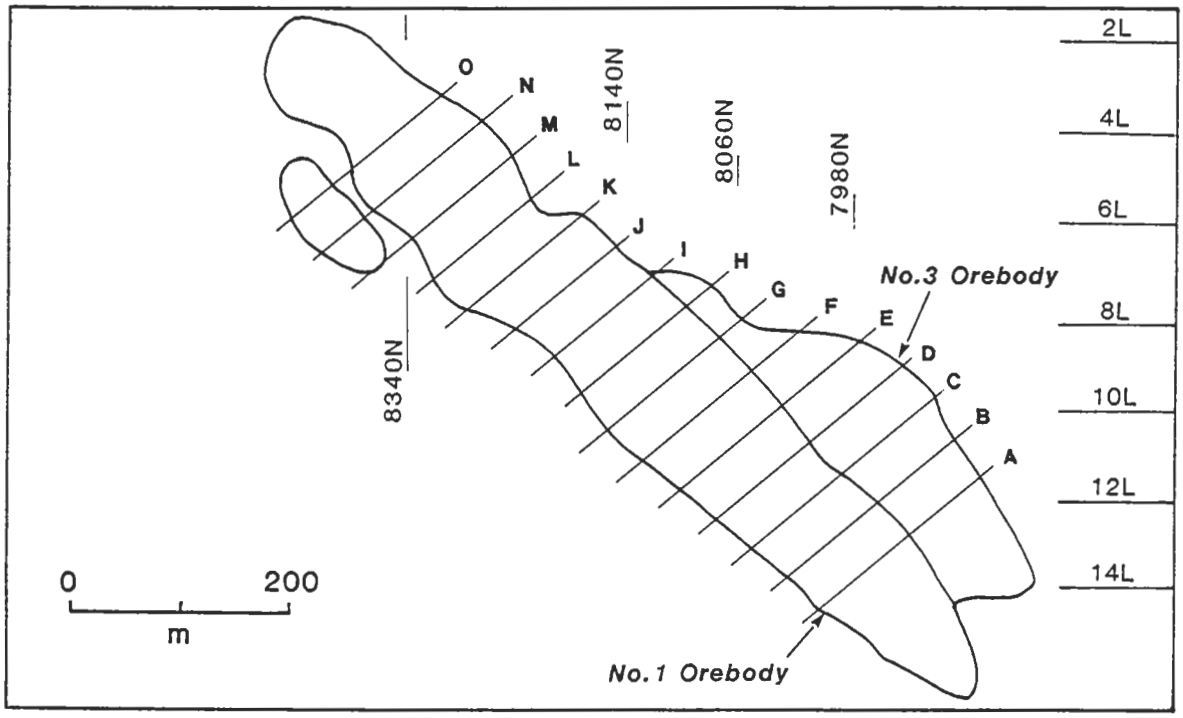

Figure 3.6 — Longitudinal projection of the Warrego ironstone lodes illustrating the location and orientation of true sections in Figure 3.7.

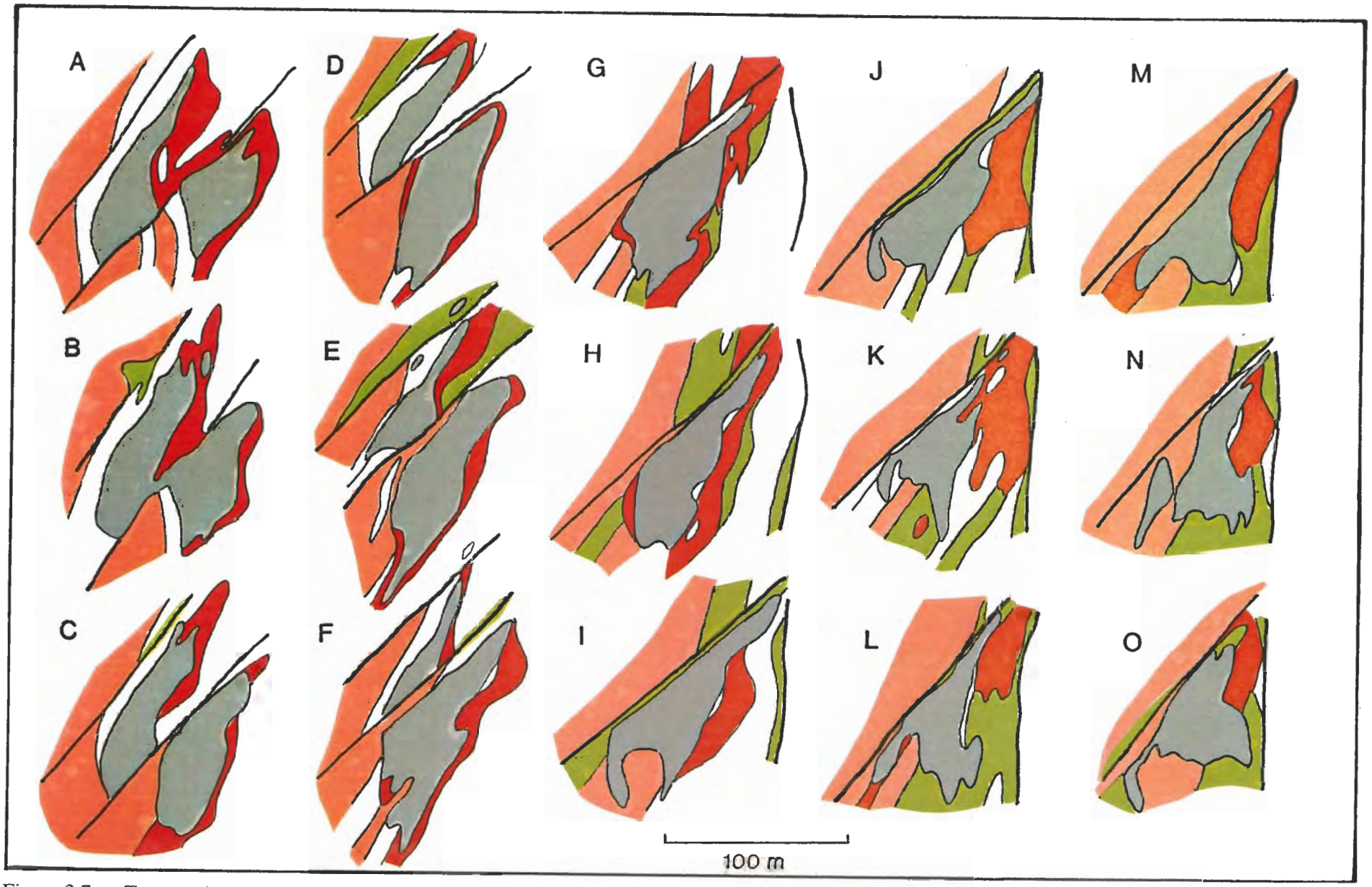

Figure 3.7 — True section through the Warrego ironstone lodes illustrating the general relationship of the lodes (grey) to alteration (intense stringer — red,and chloritic sediments — green), and the quartz porphyry (pink). White areas correspond to relatively unaltered spotted sediments. The proposed orebody fault displacing the No. 1 and No. 2 orebodies and following the hangingwall contact of the upper No. 1 orebody is also illustrated. The relationship of the sections to the ironstone lode is illustrated in Figure 3.6.

3.2 Shape and Attitude of the Lodes

The long axes of the ironstone lodes plunge 47° to 147[1] paralleling to the orientation of fold axes determined in the host rocks (Chapter Four), and the plane containing the long and intermediate axes of the lodes dips 66° to 066, sub-parallel to the bedding attitude as defined by the lower contact of the quartz-porphyry. Although the lodes are broadly stratiform, the No. 1 orebody is broadly transgressive of the quartz porphyry/ sediment contact, such that above approximately 6 level, the No. 1 orebody is at least partially hosted by porphyry, while below this level it is hosted by sediments, and may be up to 50 m below the contact (Figs 2.4, 3.2 to 3.5 & 3.7).

In contrast to the generally smooth outline of the ironstone lode below 6 Level, the lode is highly irregular in shape and associated with smaller satellite pods above this level (Figs 3.2 to 3.5 & 3.7). In the upper mine levels, the ironstone lode appears to constitute a series of coalesced pods, which are spatially related to the occurrence of discrete lenses (or a lens) of sediment within the porphyry that has preferentially localised ironstone lode formation. The highly irregular lode outline in section 8340N (Fig. 3.2), well illustrates this point, with lenses of ironstone lode localised in sediment intercalations within the porphyry.

Typically alteration in the form of strong chloritisation of the sediments and associated stringer mineralisation is restricted to the footwall of the lodes, and is observed to have its' widest development towards the present top of the lode (e.g. Fig. 3.7). It is also evident that even within the sediments, certain horizons are more prone to alteration and replacement. Wedges and lenses of unaltered chlorite spotted shales are often observed immediately adjacent to the ironstone contacts (e.g. Fig. 3.7 H to N), and alteration fronts are observed to inter-digitate within the sedimentary units parallel to the stratigraphy (Fig. 3.7 J & K). Although the relative susceptibility of some sedimentary units to alteration compared to others, has not been investigated in this study, the preferential location of ironstone lodes within argillaceous rather than siltstone and sandstone units has been described elsewhere in the goldfield (Ivanac, 1954; Whittle, 1966; Wyborn, 1971). It seems likely that sediment composition has also been a controlling factor in the localisation of the Warrego ironstone lodes.

3.3 Relationship of the No. 1 and No. 3 Orebodies

The relationship of the No. 1 and No. 3 orebodies has been considered by previous mine geologists, and models involving either a simple, stacked series of stratiform lenses, or a single folded lens have been suggested (B. Love, pers. comm., 1985). However, to the author's knowledge there has been no consensus of opinion as to their probable relationship, nor has any one model been documented and justified. In constructing the

---

[1] All bearings are given as plunge and trend relative to True North.

series of 'true' sections for the Warrego ironstone lodes, it became apparent that the relationship of the quartz porphyry to the two lodes could not easily be accommodated in a simple model involving a stacked series of lenses. The consistent offset observed between both the porphyry and the ironstone lode in mine plans and true sections below approximately 10 level suggests that either folding or faulting has produced this relationship (Fig. 3.7). The area of probable folding or faulting corresponds to the linear alignment of the northern and southern margins of the No. 3 and No. 1 orebodies respectively, and examination of this zone in the true sections reveals a uniformly dipping plane that extends beyond the immediate area of the No. 3 orebody, following the hangingwall contact of the No. 1 orebody for nearly its entire length (Fig 3.7). The orientation of this plane is virtually identical to that of cleavage measured within the host sediments (Chapter Four).

On a mine scale, folding of the quartz porphyry is restricted to minor flexuring (Chapter Four) which is incompatible with the tight folding that would be required to produce the present relationship. Because the massive porphyry is likely to have behaved as a relatively rigid block within the Warramunga Group sediments, deformation by faulting rather than folding is probable, and it is suggested that the porphyry deformed by cleavage parallel reverse faulting during folding of the Warramunga Group. The relationship of the ironstone lode to the faulting of the porphyry is less well constrained, either faulting of the porphyry has generated a suitable environment for lode formation, and the apparent offset of the ironstone lodes is simply a function of the pre-existing relationship of the porphyry contact, or both the porphyry and ironstone lode have been displaced by the same event.

Striations measured on the hangingwall contact of the No. 1 orebody on 5 Level suggest a reverse sense of movement that is compatible with the apparent offset in the porphyry and post-ironstone faulting. However, deformation associated with the intrusion of the Warrego Granite was accompanied by flattening and tightening of folds (Chapter Four), and it is likely faults were reactivated, especially at the contact zone between the rigid ironstone lode and the more ductile sediments. Support for a post-faulting origin to the ironstone lode is provided by the fact that the two lodes are connected by a narrow neck between sections 8040N and 8000N (Fig. 3.7B) which must clearly overprint the fault position in either model, and the absence of obvious deformation or fragmentation of the ironstone lode in the vicinity of the fault position. The presence of stringer mineralisation in the hangingwall of the No. 1 orebody in the position of the proposed fault also suggests that economic mineralisation was introduced post-faulting (see below).

Apart from indications of faulting along the hangingwall contact of the No. 1 orebody on 5, 6, and 7 levels, and the apparent offset in the lodes and porphyry, there is little documented evidence elsewhere of faulting. Key areas for the recognition of this

fault between the two orebodies are now frequently inaccessible due to loss of exposure through mining operations, but in the majority of cases original mapping by company geologists does not identify faulting in this position. In drillcore the contact area is frequently strongly chloritised with a well developed fabric, and it is likely that in underground mapping, mine geologists have been unable to distinguish faulting within the strongly foliated and hydrothermally altered rocks commonly found in this position. The lack of observed evidence for faulting may also result from dyke intrusion along this zone of weakness. On 14 Level, in the position of the proposed fault, an unusual rock, type that was not recognised in previous mapping, has been interpreted as a dyke (Chapter Two).

3.4 Mineral Assemblages and Zonation

For the purposes of logging and construction of geological sections (Figs 3.2 to 3.6), the mineralogy of the ironstone lodes has been divided into four readily identifiable mineral associations. These reflect the relatively simple mineral assemblages observed in the Warrego mine and define a general zonation pattern from footwall to hangingwall of the ironstone lode (Fig. 3.8).

Stringer Mineralisation/Chlorite Alteration

Although an envelope of pervasive chloritisation surrounds the ironstone lodes, it is asymmetrical in its distribution being more strongly developed on the footwall side. The hangingwall contacts of the ironstone lodes are typically knife-sharp, with an adjacent alteration zone of coarsely crystalline chlorite, disseminated euhedral magnetite, ±muscovite, ±sulphides that is invariably less than 1 m in width (Plate IVB). Within this zone of intense alteration all sedimentary features have been obliterated. The footwall alteration zone, although mineralogically similar is significantly wider, typically being in the order of 1 to 5 m in width (Figs 3.2 to 3.5). Beyond this zone, the intensity of the alteration decreases with distance from the lode. Strongly cleaved and recrystallised sediments are veined by discrete chlorite-rich veins and stringers with magnetite or chalcopyrite that are sub-parallel to cleavage (Plate IVA). A pervasive chloritisation of the sediments (2–5 modal % chlorite) is common of all sediments and porphyries east of the footwall fault.

Exceptions to this alteration pattern occur in the immediate footwall of the two gold pods, where not only is the alteration zone considerably wider (widths in excess of 30 m), but also the pattern of alteration is quite distinct. Magnetite stringers associated with chlorite and muscovite alteration form an anastomosing set of veins, commonly without preferred orientation that impart a fragmented and brecciated appearance to the sediment.

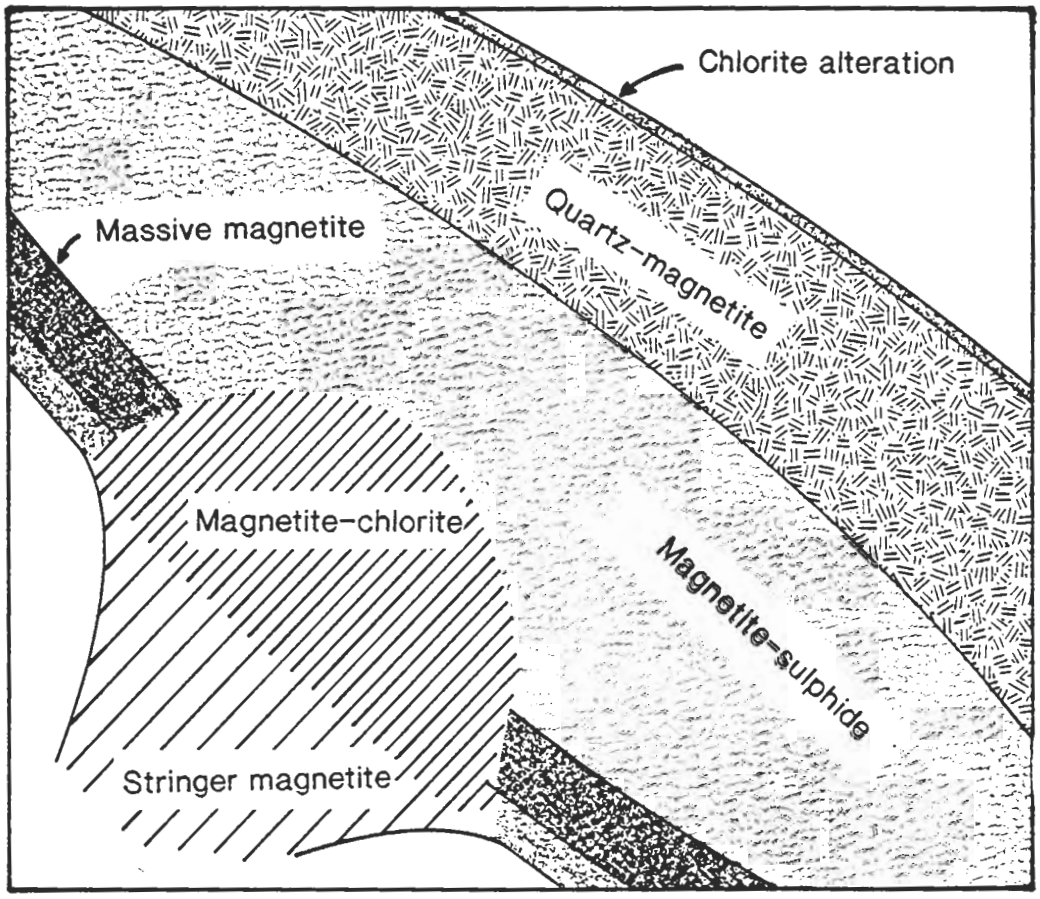

Figure 3.8 — Idealised section through the upper gold pod illustrating the relationship of the mineral assemblages described in the text.

Plate IV

A: Relatively unaltered sediment cut by a chlorite vein in the weakly altered outer zone surrounding the ironstone lodes. Thin section (PPL), sample 107003.

B: Intensely altered inner zone immediately adjacent to the ironstone lode. Sediment has been completely replaced by chlorite and magnetite. This rock is only recognisable as once being sediment by its trace element ratios. Large sericitic porphyroblasts (after andalustite) are restricted to this assemblage. Thin section (PPL), sample 107000.

C: Drill core samples of intense stringer veining of the footwall sediments adjacent to the gold pods. Two styles of veining are exhibited, top (sample 109312) and bottom left (sample 108681) show intense breccia-type magnetite-chlorite veining without significant alteration of the adjacent sediment. In contrast the bottom right (Sample 109314) shows the partial replacement of a sediment clast by chlorite and muscovite. The coin is 2·5 cm in diameter.

D: Hand specimen samples of stringer veins. The sample on the left (sample 109310) shows no internal zonation to the virtually massive magnetite vein and a relatively narrow chloritic margin that contains abundant finely disseminated magnetite. The sample on the right (sample 109311) is virtually magnetite-chlorite lode, but contains clasts of highly altered sediment that are being replaced by magnetite along the cleavage.

E: Hand specimen (sample 109304) of magnetite-chlorite ore from the upper gold pod. Veinlets and clots of magnetite occur in a matrix of chlorite and muscovite. This sample contains minor pyrite and abundant visible gold.

F: Drill core and hand specimen samples of magnetite-sulphide. The sample on the left (sample 108474) is virtually massive chalcopyrite replaced by late quartz-hematite veinlets. The sample on the right (sample 109309) comprises strongly breccciated magnetite lode veined and infilled by chalcopyrite. Although this texture appears replacive, under the microscope the magnetite clasts are un-replaced.

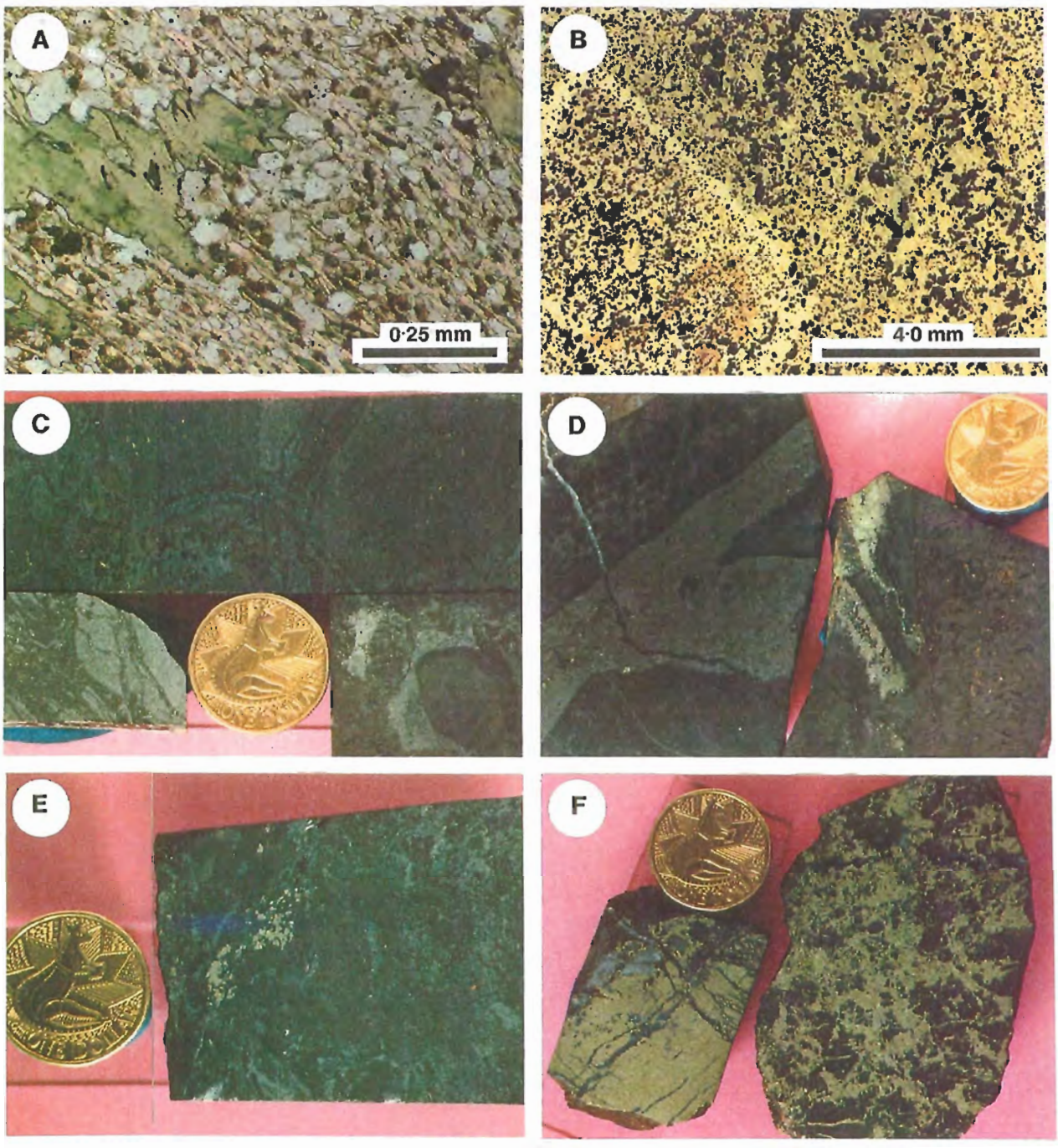
A
0·25 mm
B
4·0 mm
C
D
E
F

The intensity of veining reduces from 20 to 50 veins (up to 4 cm wide) per metre in the immediate footwall, to 1 or 2 (less than 5 mm wide) per metre 10 to 20 m from the contact. Textures within the ironstone lode immediately above the stringer zone indicate that at least in part, the lode has formed through the coalescence of individual stringer veins with the rare preservation of highly altered sediment clasts (Plate IVD).

Textures in this zone are far from definitive as to the mode of stringer emplacement, in many samples stringer veins appear to brecciate and disrupt the host rocks without significant peripheral alteration (Plate IVC), while in others, the stringers have diffuse margins and enclose extremely altered to totally replaced sediment clasts (Plate IVC). These relationships suggest, that although stringer veins are likely to be controlled by discrete planes of weakness within the rock, replacement adjacent to the fractures has also been an important mechanism of lode formation. It is this latter style of alteration which can be traced with increasing intensity into the magnetite-chlorite assemblage of the lode proper, and appears to be representative of the mechanism of ironstone lode formation. Examples of unequivocal replacement textures from Warrego and two barren ironstone lode systems are illustrated in Plate V. These examples clearly assist in the interpretation of how the colloform clots and ribbon textures observed within the ironstone lodes form. (see Chapter Five).

Extremely rich gold and bismuth grades may be associated with stringer veining, but generally economic mineralisation is restricted to within the margins of the ironstone lodes. Sulphides with the exception of bismuthinite are typically absent from the stringer zone; pyrite has not been observed but chalcopyrite occurs in occasional remobilised veinlets or discrete blebs within both the magnetite stringers and adjacent sediments.

Exploratory diamond drilling for the down plunge extension of the No. 1 orebody has indicated that not only does the ironstone lode close off with depth, but also that there is a general reduction of alteration in this direction. This observation differs from other Tennant Creek orebodies (e.g. Juno mine, Large, 1974, 1975) where well developed alteration pipes extend below the ironstone lodes. At Warrego intense alteration may occur both stratigraphically above and below the lodes (Fig. 3.2 to 3.5 and 3.7), but in sections 8140N, 8060N, and the majority of the true sections, alteration is observed to be most intense vertically above the lodes. This 'overturned' relationship of the alteration assemblage to the ironstone lodes is in keeping with the structural interpretation that the Warrego ironstone lodes have been overturned during intrusion of the Warrego Granite (see Chapter Four).

Magnetite-Chlorite

Localised in relatively restricted 'pods' on the footwall side of the No. 1 orebody, the magnetite-chlorite assemblage is characterised by the presence of up to 40 modal %

Plate V

A: Thin section (PPL) example of intense chlorite-magnetite alteration of sediments. Zones of more intense alteration are marked by bands containing high concentrations of disseminated magnetite. The magnetite coalesces to form ribbons perpendicular to the band margins and is suggested as a precursor to some of the irregular colloform bands of magnetite and chlorite observed in the ironstone lodes. Sample 107000.

B: An example of stringer veining from a well defined alteration pipe below the West Gibbet prospect located 5 km west of Tennant Creek. What is interpreted as an original fracture (horizontal in this plate) has tapped fluids from an area of intense alteration (qtz-mt-chl). Alteration marginal to the fracture is observed as the irregular formation of magnetite-chlorite fronts replacing the sediment parallel to the cleavage (vertical). DDH WG9 212·9 m.

C: Atolls of hematite developed in chloritic sediments adjacent to the stringer zone at West Gibbet. Although rare, these textures are identical to colloform clots observed in Warrego and other ironstone lodes and their formation within chloritic sediments has important implications for ironstone lode formation. Although the true 3-D dimensions of these clots could not be established in this drillcore sample, the clots are elongate in the third dimension and the possibility that they are tubes cannot be eliminated. DDH WG9 260·7 m.

D: Hematite-chlorite-quartz stringer from the Explorer 28 Prospect. Note the advancing chlorite alteration front between cleavage parallel quartz veins; the sharp alteration front is marked by a thin film of hematite. Bedding is evident in the unaltered sediment. DDH 5, 263.35 m.

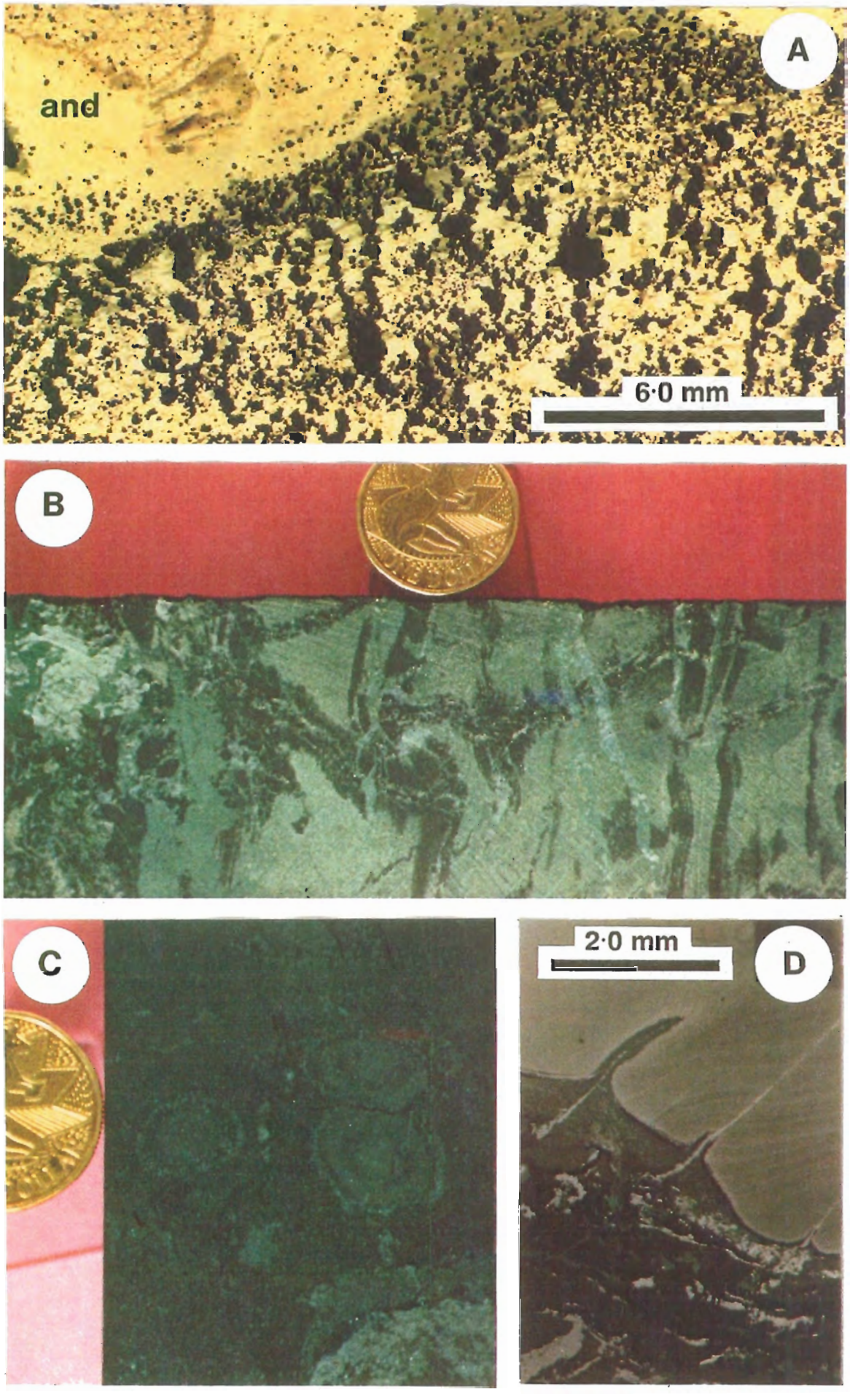
A
and
6·0 mm
B
C
2·0 mm
D

chlorite and muscovite, and an almost total absence of sulphides with the exception of bismuthinite and occasional pyrite (Plate IV E). This assemblage is characteristic of gold- and bismuth-rich ore in not only Warrego mine, but other gold-rich deposits in the Tennant Creek district e.g. Nobles Nob mine (Whittle, 1966) and Juno mine (Large, 1974, 1975). However, the Warrego mine is something of an exception as there is not one, but two discrete gold pods centred on 10 and 13 levels. Although these pods have relatively small total masses (0.5 to 1 Mt), their significance in terms of economic mineralisation far outweighs their modest size.

As described above, the close association between the occurrence of the magnetite-chlorite gold pods and areas of intense footwall stringer veining means that rather than the typical knife-sharp ironstone lode boundaries, the contact is diffuse and gradational. In three dimensions the form of the two gold pods (as approximated by the distribution of magnetite-chlorite) differ, the larger central pod is oval in section (Fig. 3.3), extending laterally into the core of the lode where it grades into the magnetite-sulphide assemblage. The smaller, lower pod is restricted to a relatively narrow zone along the footwall contact (Fig. 3.5).

The magnetite-chlorite zone is characterised by diffuse clots and irregular bands of magnetite intergrown with chlorite and muscovite (Plate IV E). Occasional phyllosilicate-rich patches within the magnetite-chlorite zone may represent relict clasts of the original host rocks. The textures and mineral relationships in this zone are comparable with a formation involving replacement processes similar to those illustrated in Plate V.

Moving laterally away from the core of the gold pod, chlorite rapidly becomes the dominant phyllosilicate and is increasingly confined to fractures within massive magnetite. This assemblage grades into either relatively massive magnetite, or chlorite veins give way to an increasingly sulphide-rich assemblage dominated by chalcopyrite. The contact with the magnetite-sulphide mineral assemblage is taken as the first appearance of significant sulphide mineralisation (>5%), but the chlorite content may still remain relatively high (up to 5%) several metres beyond this point.

Magnetite-Sulphide and Quartz-Magnetite-Sulphide

The magnetite-sulphide zones contain a mineral assemblage comprising magnetite and chalcopyrite with variable proportions of pyrite, bismuthinite, and gold. All economic copper mineralisation in both the No. 1 and No. 3 orebodies was contained within this assemblage, as was a considerable proportion of the total gold content of the Warrego mine. As with the magnetite-chlorite assemblage, the sulphides may constitute up to 40 modal % of the lode, filling irregular networks of fractures, which in high-grade copper ore may best be described as a magnetite breccia in a matrix of chalcopyrite (Plate IV F).

The highest grade copper mineralisation tends to occur within a brecciated core to the ironstone lode, with sulphide abundances decreasing into both the hangingwall and footwall as the transition is made to the quartz-magnetite and magnetite-chlorite assemblages respectively. This core of magnetite-sulphide extends into the upper portions in the No. 1 orebody where large sections of the lode constitutes economic copper ore (Fig. 3.2). The boundary between magnetite-sulphide and quartz-magnetite-sulphide is taken as the first appearance of quartz veining (>5 modal %), and although locally this assemblage is quite copper-rich, values are discontinuous, and average chalcopyrite contents drop from around 15 modal % to less than 5 modal %. Quartz veins within this zone may carry significant mineralisation, and drillhole intersections of 2 to 3 cm wide quartz veins which have sections of massive chalcopyrite are relatively common.

Banded pyrite-magnetite is locally significant, especially marginal to the gold pods on the footwall side of the No. 1 orebody where tourmaline is a common accessory, and also in the cores of the lodes associated with the magnetite-sulphide ore (Figs 3.2 to 3.5). Locally the bands are up to 1 m across and may comprise 80 to 90 modal % pyrite. Textural relationships suggest that the bands formed through the replacement of magnetite along shears within and marginal to the ironstone lodes (Plate VI A). Only minor chalcopyrite is associated with these bands, and boundaries between the pyrite-magnetite and chalcopyrite-magnetite zones are difficult to decipher due to the almost ubiquitous recrystallisation of both sulphides. The relationship illustrated in Plate VI A suggests that chalcopyrite veining is crosscutting and has displaced the banded magnetite-pyrite lode, however, possible remobilisation of chalcopyrite makes this interpretation equivocal.

Quartz-Magnetite

Commonly occurring towards the hangingwall of the lodes, quartz-magnetite may be gradational from the magnetite-sulphide, but often the boundary is abrupt. The assemblage typically comprises ragged and irregular fragments of magnetite flooded by quartz that may constitute up to 60 modal % of the lode (Plate VI B). After magnetite, quartz is the most abundant mineral in the ironstone lodes and overall, barren quartz-magnetite probably constitutes 30 to 40 modal % of the total ironstone lode. Quartz and magnetite are virtually the only components in this assemblage although rare clots of chlorite and sulphides are observed.

Quartz occurs both intimately intergrown with the ragged magnetite, and as sharp boundaried massive, buck quartz veins crosscutting the lode. Several parageneses of quartz veining may be identified from their crosscutting relationships, but because there is no economic mineralisation associated with these veins, there is little information that

Plate VI

A: Hand specimen sample (sample 109308) of magnetite-sulphide lode. Brecciated ironstone lode shows both chalcopyrite veining, and banded pyrite assemblages. The pyrite and chalcopyrite show ambiguous paragenetic relationships. Re-crystallisation of the sulphide make definitive interpretation impossible.

B: Drill core sample (sample 108832) from the quartz-magnetite assemblage. Magnetite occurs as diffuse quartz flooded clots and quartz is the dominant mineral present. Minor late chalcopyrite-hematite veinlets cut the assemblage.

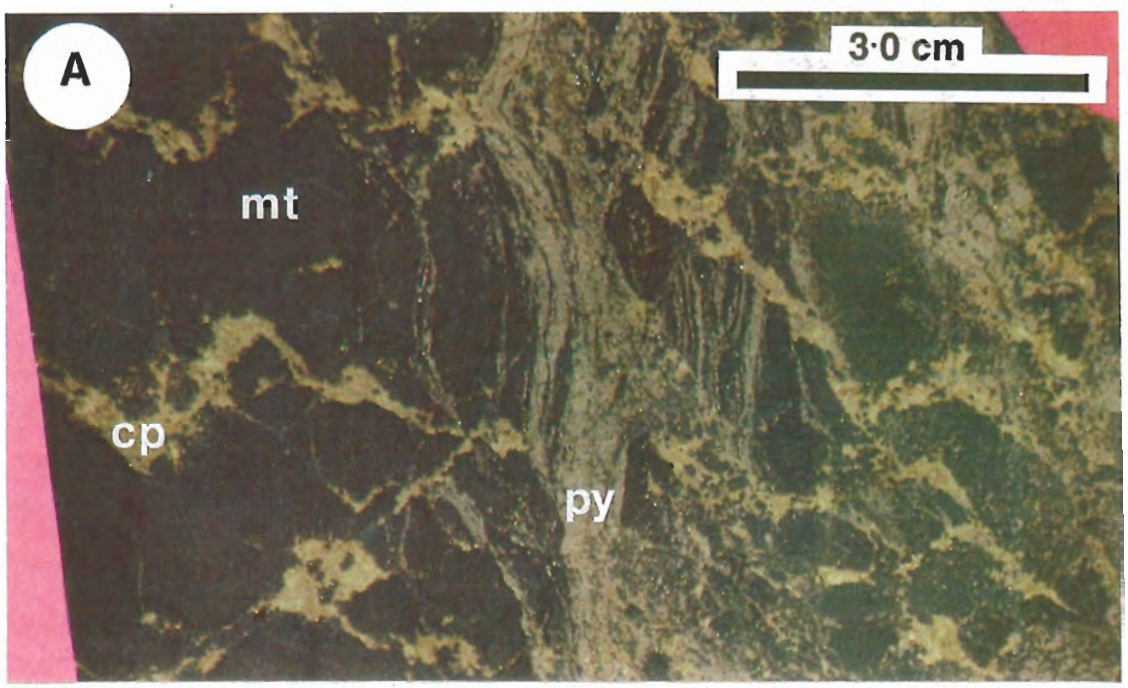
A
3·0 cm
mt
cp
py

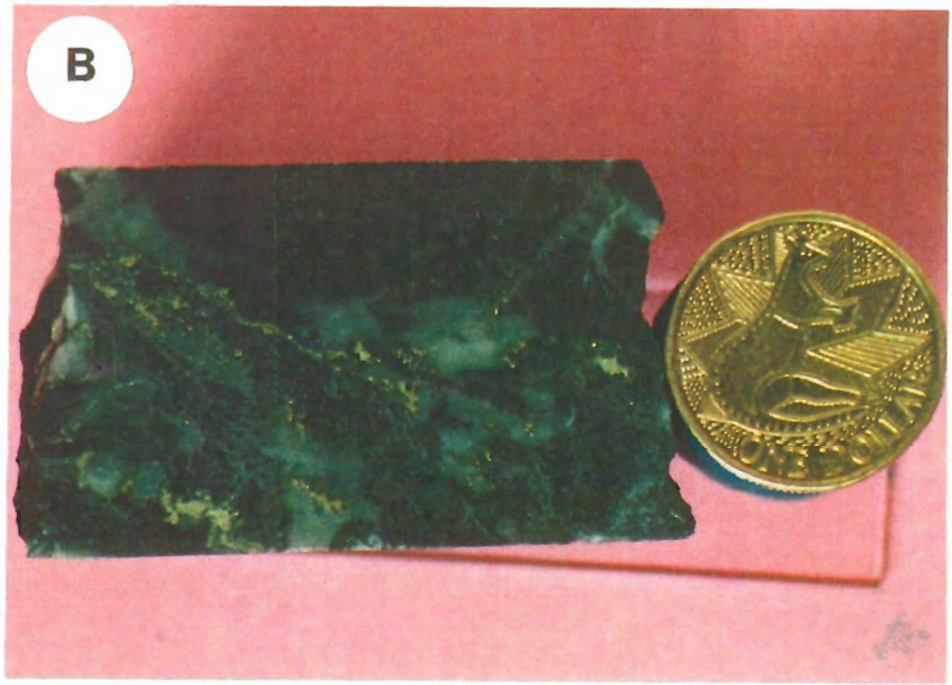
B

can be obtained on their timing relative to it. Brecciated fragments of magnetite-sulphide within quartz veins indicate that at least some of the veining was late- or post-mineralisation in age. Late-stage vuggy quartz veins containing minor carbonate, hematite and chalcopyrite are relatively common it the quartz magnetite and magnetite-sulphide assemblages (Plate IV F and VI B).

Quartz veining stops abruptly at the hangingwall contact of the ironstone lode which may be related to the relative behaviour of the ironstone lode and adjacent sediments to deformation.

Massive Magnetite

The occurrence of massive, monomineralic magnetite without significant associated chlorite/muscovite, sulphide or quartz is relatively common, although generally only a minor constituent of the overall ironstone lode (Figs 3.3 to 3.5). On a hand specimen scale, the transition to massive magnetite from any of the mineral assemblages described above, is observed as a decreasing intensity of fracturing in the lode such that the chlorite/muscovite, chalcopyrite or quartz is restricted to discrete cracks and fractures (compare Plate IV F with Plate VI A). No attempt has been made to document the overall intensity of fracturing within the ironstone lodes, other than to note that dilution of the magnetite content by other phases is most significant in the quartz-magnetite assemblage which is usually observed at the lode margins (particularly on the hangingwall side of the lode).

3.5 Discussion

Controls on Lode Localisation

Because of their generally stratiform character, at or close to the contact between sediments and a stratiform quartz porphyry, and the asymmetric footwall only alteration pattern, the Warrego ironstone lodes are at first appearance candidates for classification as the oxide equivalents of volcanogenic massive sulphide deposits. However, on closer inspection the lodes are transgressive of the stratigraphy, and appear to be localised within specific sediment horizons which were particularly amenable to alteration and ironstone lode formation. An epigenetic origin can also be argued by analogy with other, same aged, Tennant Creek ironstone deposits where the ironstone lode cross-cuts the stratigraphy and an epigenetic origin is more easily demonstrated, e.g. Juno mine (Large, 1974, 1975) and TC8 mine (Wedekind et al., 1990).

This lithological control on ironstone lode formation has not been definitively tested, but the location of the lodes at or close to the lower porphyry contact is significant, as is the shape of the lode when hosted by porphyry compared to sediment.

Two possible relationships may be implied from the close association between the ironstone lodes and the porphyry. Either the lode is genetically related to the porphyry, i.e. fluids released from, or mobilised in response to the intrusion of the porphyry were responsible for lode formation, or the porphyry has acted as a barrier to hydrothermal fluid flow and has localised mineralisation at or close to its' contact. Evidence elsewhere in the goldfield for the recrystallisation of sediments adjacent to the porphyry contact (McPhie, 1990), is supportive of the latter model whereby lower permeability of re-crystallised sediment adjacent to the porphyry has acted as a barrier to fluid flow and helped localise the ironstone lodes in their observed position. This model is further supported by two observations of the geometry of the Warrego ironstone lodes:

1. For the most part the ironstone lodes are not located at the sediment-porphyry contact, but anything up to 30 m below it; typically where the ironstone lode is thickest, it is in direct contact with the porphyry, but tapers away from the contact as the lode thins, e.g. Figs 3.3 and 3.7. While it is apparent that the porphyry is not a favourable host to ironstone lode formation, it is difficult to argue that it has acted as a barrier to fluid flow. However, an underplating of contact metamorphosed and relatively impervious sediments could explain the tapering of the lode from the contact. Thus while the core of most intense fluid flow and alteration eventually alters and replaces the sediment right to the contact, less intense alteration peripheral to this zone is less able to penetrate the hornfels contact zone and hence the ironstone tapers back from the contact.
2. In the upper part of the mine the lode outline is highly irregular and seems to a large extent controlled by the occurrence of sedimentary units within the porphyry. Here, for the most part the ironstone lode abuts the porphyry and while the observation of preferential sediment replacement relative to porphyry holds, there is no evidence of a welded buffer. However, consideration of the thickness of the porphyry may have an important bearing on this relationship. Figure 2.4 illustrates that in the upper levels of the mine, rather than forming a massive unit as it does on 14 level, the porphyry is intercalated with thick wedges of sediment. This reduction in the overall thickness of the porphyry may indicate a weakly developed hornfels zone in the adjacent sedimentary rocks and therefore fluid flow could have penetrated to the porphyry contact.

Further support for the barrier model is evident in the lack of evidence for a genetic relationship between the porphyry and the ironstone lodes. Typically intrusives that have been genetically linked to mineralisation display significant hydrothermal overprinting as the intrusion cools and the hydrothermal cell contracts e.g. porphyry copper-style skarn replacement of adjacent sedimentary rocks (Einaudi et al., 1985). There is only relatively minor hydrothermal alteration of the porphyry and significantly, the porphyry is devoid of magnetite.

Relationship of ironstone lode formation and economic mineralisation

Textural relationships observed within the lode support a two-stage process in which the ironstone lode has been overprinted by later economic mineralisation. However it is impossible to confirm the relative time frame over which these events occurred; an evolving hydrothermal system is just as compatible as a distinct two-stage model. Extensive fracturing of the ironstone lode to allow incursion of mineralising fluids is evident and mineralisation was clearly accompanied or preceded by deformation.

The magnetite in the ironstone lodes shows two associations with the gangue and ore mineralogy; there are the quartz-magnetite and magnetite-sulphide associations where there is clear evidence that once massive magnetite lode has been fractured and infilled with later mineral phases. Typically the fractures are clean breaks suggesting that mineral deposition has filled open space rather than through the pervasive replacement of magnetite. The second association is that observed in the gold pods where gold and bismuth mineralisation are intimately associated with chlorite, muscovite and magnetite that is without the obvious fracture control observed elsewhere in the lode. Because the outline of the ironstone lodes in the vicinity of the gold pods does not differ markedly from elsewhere, i.e. there is no thickening of the lode that would indicate that the gold pods formed via replacement of the sediment in the footwall of the lode, and it is therefore likely that this style of mineralisation also represents the infilling fractures in a pre-existing ironstone lode. It is suggested that the gold pod mineralisation assemblage of magnetite, chlorite and muscovite infills fractures within the ironstone lode and that overgrowth and infilling by magnetite masks the original fractured character of the lode (see also Chapters Five and Seven).

Chapter Four

STRUCTURE

4.1 Introduction

A large block of Warramunga Group sediments located within 5 km of the eastern contact of the Warrego Granite has an anomalous cleavage orientation compared to most of the goldfield. The steeply dipping, north-west trending cleavage orientation parallels the Navigator Fault, and Le Messurier et al. (in press) have described this area as a mega-kink (Fig. 4.1). They suggest that typical Warramunga Group structures have been rotated into their present orientation through movement on this late fault. This is not the only area within the Warramunga Group where abnormal cleavage orientations are observed; in the vicinity of the Quartz Hill Fault, anomalous bedding and cleavage orientations also indicate block rotation of sediments through movements on this fault (Rattenbury, 1990b).

However in the immediate environs of the Warrego mine, a quite distinct cleavage orientation and fold attitude has been recognised. Bedding measurements from west of the Footwall Fault (Goulevitch, 1975), define reclined folds with a well developed axial plane cleavage, that plunge 45° to the southeast. The long axis of the Warrego orebody plunges southeast at 40°–50° sub-parallel to this calculated fold axis orientation, and in plan the lode strikes north-south approximately parallel to the quartz porphyry (Fig. 3.2). This attitude is distinct from the typical orientation of Tennant Creek ironstone lodes which characteristically have long axes aligned either near vertical or horizontal, and virtually all have an east-west elongation in plan parallel to the regional cleavage (Ivanac, 1954; Crohn and Oldershaw, 1965; Whittle, 1966).

Thus the immediate Warrego area is clearly anomalous with respect to both the regional and mega-kink structural styles, and the general attitude of the ironstone lodes. Two models have been proposed to account for these differences:

1. Goulevitch (1975), citing the close agreement between the plunge of the Warrego ironstone lode and the fold axis defined by bedding and cleavage intersections, and the broad antiform defined by the contact of the hangingwall quartz porphyry with

the ironstone, proposed that there was a strong structural control on lode localisation. This model was further refined by Large (1974), based on broad scale mineral zonation observed in Warrego that appeared analogous with the well documented Juno deposit. In this model the orientation of the lode and sediments were considered unchanged from the time of mineralisation, and that favourable structural orientation of the strata resulted in an orebody that was an exception to the rule for Tennant Creek.

2. Le Messurier et al. (in press), ascribe the unusual orientation of the lode and host rocks to rotation in the 'mega-kink'. In this model the Warrego lodes and adjacent sediments have been rotated in the kink from an original orientation similar to other Tennant Creek ironstones into their present position.

4.2 Aims and Methods of this Study

The purpose of this study was to determine the relationship of structure to the orebody, and to derive a model that was consistent with the shape, attitude, mineral and metal zonation, and geochemistry within the Warrego ironstone lode, *and* with other ironstone in the Tennant Creek goldfield. Because of physical (past and present mining activities), logistical (lack of ventilation and water services to many levels), and practical (grime encrusted walls in underground development) factors, mapping on anything other than a reconnaissance scale was impractical, and consequently original mapping carried out by previous mine geologists has been used extensively for this analysis. Additional data has been collected by check mapping on 7, 8, 12, 14, and 15 levels.

As part of a detailed geochemical sampling programme, openings on 14 level were mapped, and a suite of 28 orientated samples were collected to document the relationship between the various structural elements within the mine. 14 level was selected for this study as it provides the longest section through the sediments hosting the Warrego ironstone. As well as the immediate host rocks to the lodes, some 60–70 m of footwall sediments are exposed east of the Footwall Fault, and an exploration drill drive (FEX drive) exposes nearly 200 m of the hangingwall sequence (Fig. 4.2).

Because magnetite is commonly disseminated in the sediments, and comprises the bulk of the ironstone lodes, measurements of structural information are recorded relative to the surveyed drive orientation rather than by compass. It is therefore likely that readings are accurate to only ±10°, accounting for much of the scatter in the data collected.

4.3 Structural Elements in the Warrego Mine

The Footwall Fault

The main structural feature within the Warrego mine environs is the steeply dipping Footwall Fault (80° to 061)[1], that forms a well defined 10–15 m wide, highly chloritic shear zone with minor associated quartz veining. The fault appears to truncate the ironstone lode between 2 and 4 levels, but because of the less steeply plunging nature of the lode they diverge with depth (Fig. 2.3). On 15 level the fault occurs some 60–70 m from the footwall of the lode and is clearly unrelated to the mineralisation process.

The extent of movement on the Footwall Fault is unknown, but based on the different contact metamorphic mineral assemblages observed on either side, a vertical component of at least 1 km seems likely. Timing of movement on the fault is uncertain, but the apparent variation in metamorphic grade across it, truncation of the upper portion of the ironstone lode, and apparent offset of the Warrego Granite (Fig. 4.1), indicates the fault has been active since mineralisation and granite intrusion.

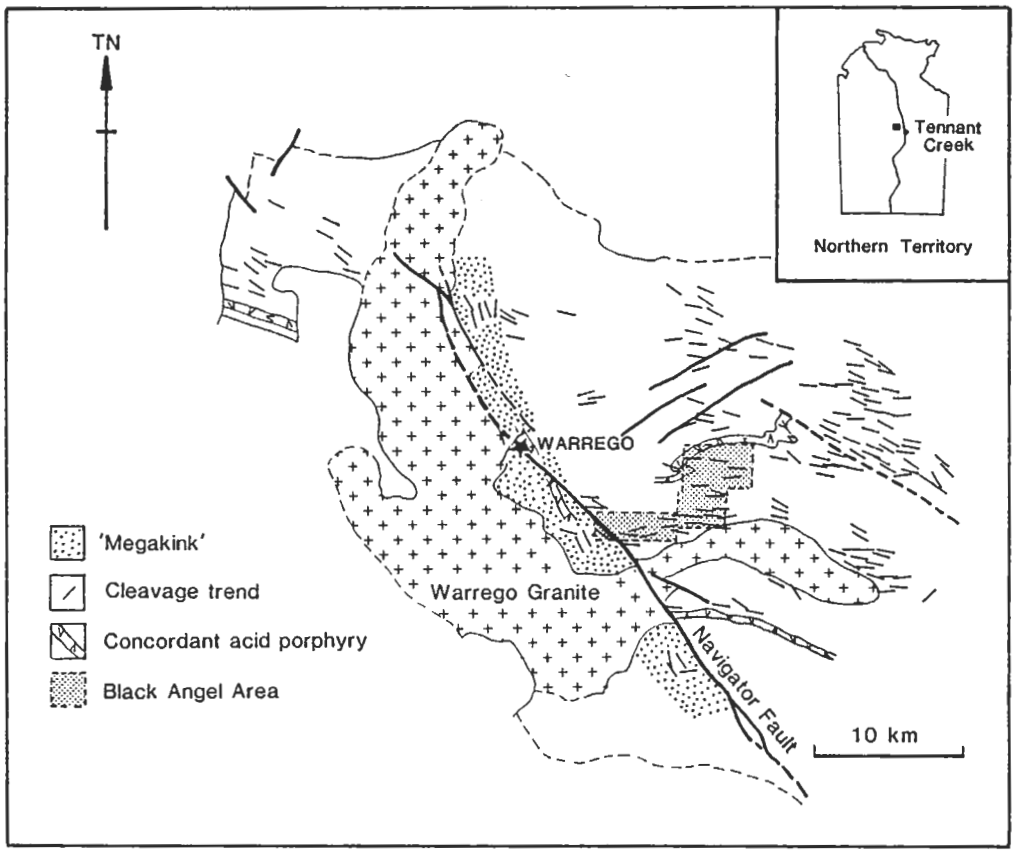

Figure 4.1 — Regional sketch map of the Warrego area illustrating the location of the 'mega-kink', defined by the northwest strike of cleavage. (Adapted from B. Williams, unpublished data).

[1] Orientation of structural elements are quoted as the plunge and trend relative to True North.

Bedding

West of the Footwall Fault, bedding is well exposed underground in variably potassium-metasomatised and recrystallised greywacke-shales. Bedding orientations can be used to define reclined folds plunging 33° to 128 (Fig. 4.3a). Due to the lack of marker horizons within the sedimentary sequence, it has not been possible to map out individual folds, but trend lines of bedding strike suggest fold wavelengths of the order of 50 m. Facing defined by graded bedding indicates that the sequence is largely overturned (Goulevitch, 1975).

East of the Footwall Fault, bedding is difficult to recognise in the chloritic, recrystallised and strongly cleaved sediments hosting the ironstone lodes, and less than 20 measurements of bedding have been made on all levels of the mine, (Geopeko unpublished data). Nearly all coincide with the cleavage orientation and as isoclinal folding has not been recognised within the Warrego mine, nor the Warramunga Group as a whole, it is likely that some cleavage planes have been misidentified as bedding. In this study, bedding has only been observed in non-oriented drill core, and slates in the 'FEX' drive furthest from the ironstone lode (Fig. 4.2).

The most obvious lithological marker in the mine sequence is a quartz porphyry that forms the immediate hangingwall for much of the ironstone lodes. The lower contact of the porphyry is well defined from drive mapping and diamond drilling below 4 level, and structural contours of this contact suggest a uniformly dipping plane (50° to 058). This constant attitude is supported by an interpretation of structure based on the attitude of bedding relative to the non-oriented drill core using the method of Laing (1977). Thus on the mine scale, folding east of the Footwall Fault is probably restricted to minor flexuring. The orientation of the porphyry agrees with bedding recorded in the FEX drive (average of three samples 69° to 052), and the generally conformable attitude of the porphyry elsewhere in the goldfield further supports this relationship (Fig. 4.3a). Graded bedding observed in drillcore, and oriented samples collected from the FEX drive shows that the sediments east of the Footwall Fault are right way up.

Cleavage

A well developed cleavage within the sediments and quartz porphyry is typically defined by the alignment of chlorite and muscovite in the matrix, and dimensional preferred orientation of recrystallised quartz in the sediments and phenocrysts in the porphyry. The orientation of the cleavage (44° to 106), although showing a broad scatter (Fig. 4.3b), is essentially identical on either side of the fault and is axial planar to the folding defined by the bedding orientation.

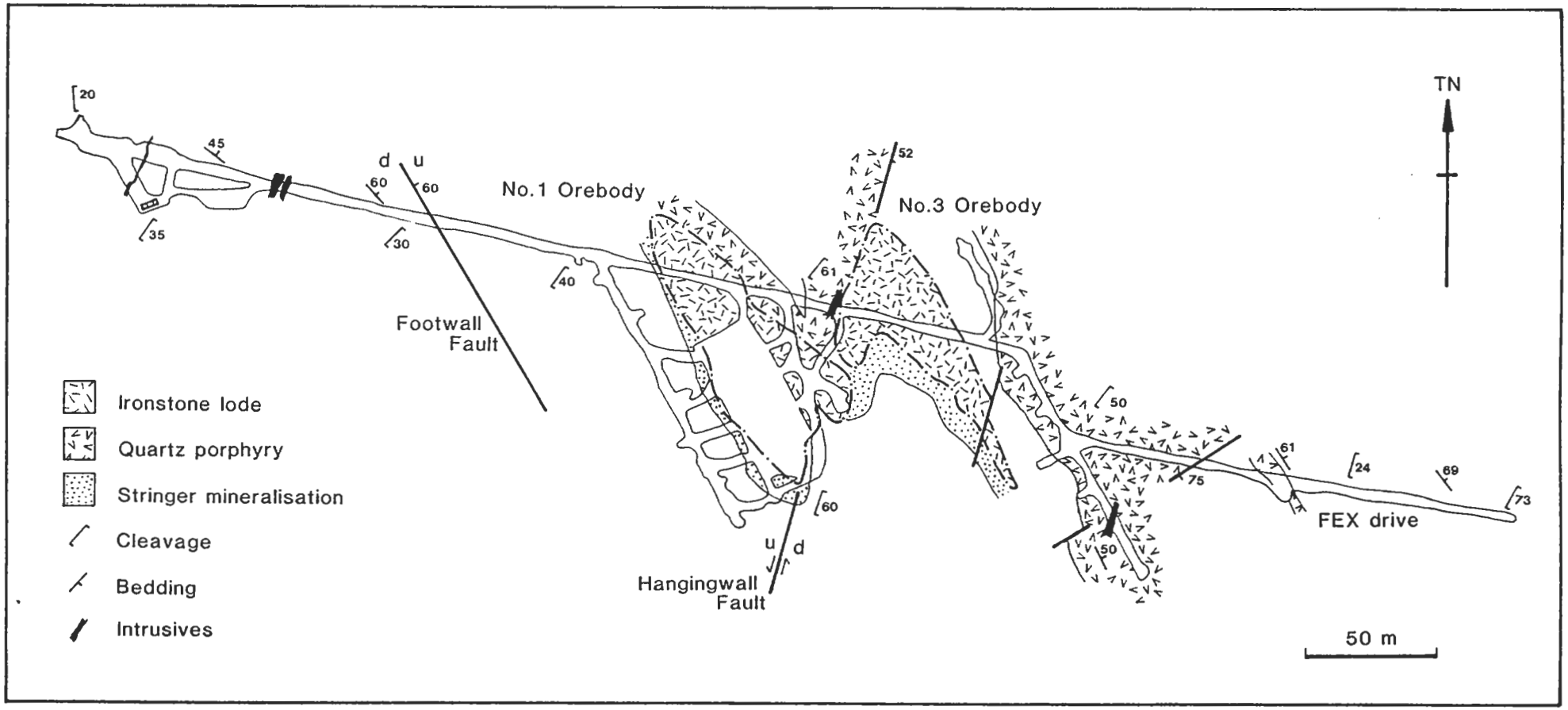

Figure 4.2 — 14 level geological plan of the Warrego mine illustrating the relationship of the various structural elements, and proposed fault between the No. 1 and No. 3 orebodies.

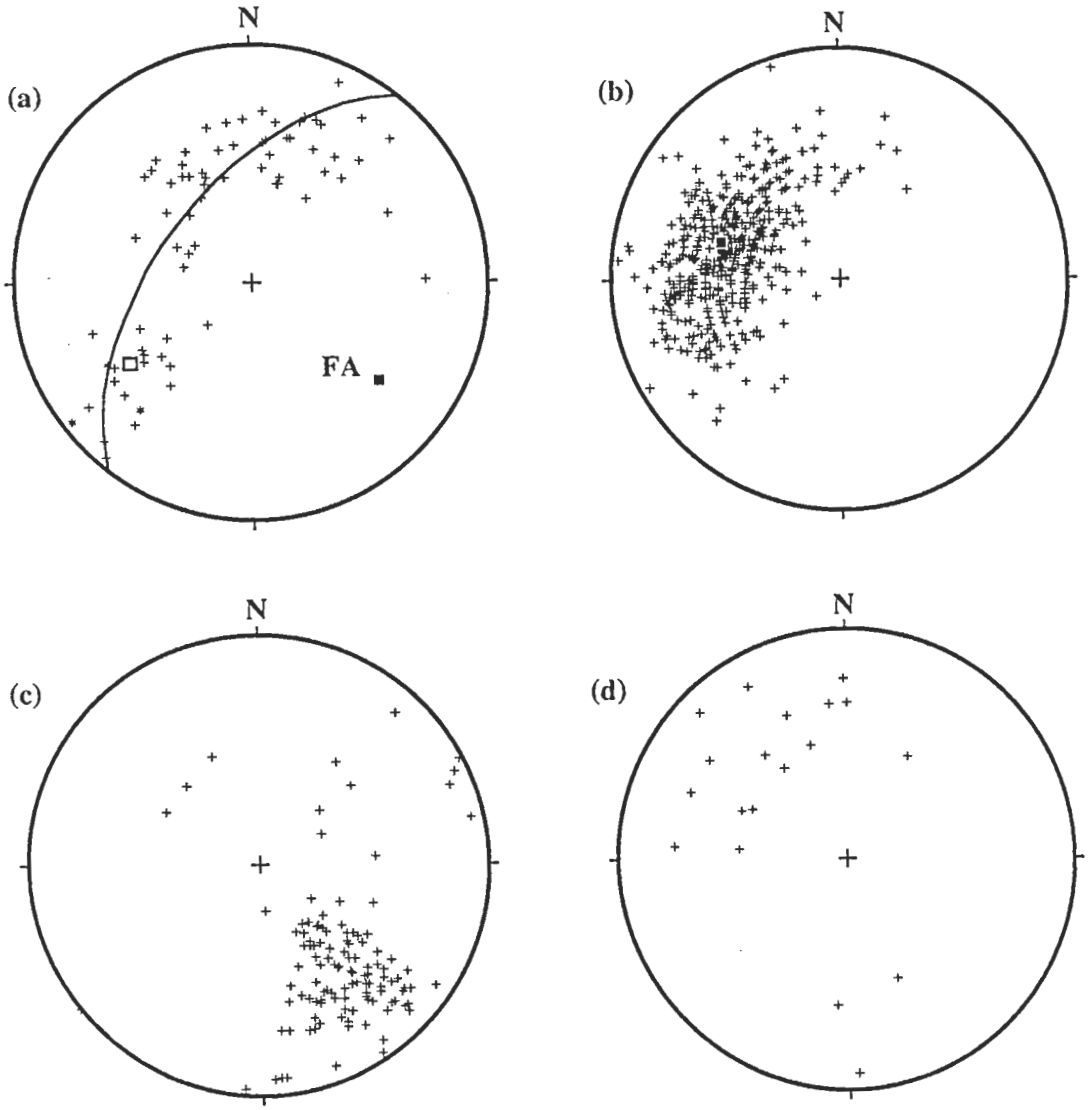

Figure 4.3 — Equal area, lower hemisphere, stereonet projections illustrating the main structural elements recorded within the Warrego mine. (a) 72 poles to bedding west of the Footwall Fault (+), pole to the attitude of the quartz porphyry lower contact (□), and 3 poles to bedding east of the Footwall Fault in the FEX drive (*). (b) 478 poles to cleavage measured on both sides of the Footwall Fault, the mean attitude (■) is essentially the same on both sides of the fault. (c) 124 poles to kink bands measured on both sides of the Footwall Fault. (d) 19 poles to sulphide bands within the Warrego ironstone lode. (Data compiled from unpublished Geopeko data and this study.)

Poikiloblastic chlorite spots (after cordierite) formed during contact metamorphism are commonly deformed into ellipsoidal shapes that are elongate parallel to the cleavage, while biotite and andalusite porphyroblasts commonly grow across the mineral foliation. These apparent conflicting timing relationships between the contact metamorphic mineral assemblage and the cleavage suggest that the cleavage producing deformation (and hence folding) was coincident with granite intrusion. However the chlorite poikiloblasts grow across the cleavage often preserving the mineral foliation in inclusions within them. The aligned quartz and chlorite in the sediment abut against the chlorite spots, and there is only minor wrapping of the spots by the foliation. These observations are consistent with the growth of the contact metamorphic assemblage during flattening of a pre-existing mineral foliation. There is no evidence from mine mapping or in oriented thin section of another foliation in these rocks, and it appears the cleavage measured in the Warrego Mine represents the original regional cleavage that has been modified through flattening during the intrusion of the Warrego Granite.

Kink Bands

1–2 cm wide kink bands are a common feature on both sides of the Footwall Fault, forming discontinuous and anastomosing bands that have a general orientation perpendicular to cleavage (Fig. 4.3c) with a reverse sense of displacement. Although overprinting the well developed cleavage, their orientation perpendicular to it suggest that the kink bands may be related to this deformation.

Sulphide Banding

Banding of sulphides (mainly pyrite) is a common feature both within the ironstone lode and at the contact with altered footwall sediments. Zones of almost massive pyrite typically less than 5 m across are regularly logged in drill core, especially towards the footwall of the lode. Although the banding measured in drives shows a wide scatter in orientation, it is generally sub-parallel to the cleavage in the sediments (Fig. 4.3d). Stringer mineralisation in the footwall of the lode also displays an orientation sub-parallel to the cleavage orientation.

Faults

Minor faulting and shearing is a common feature within the Warrego mine, especially in the chloritic sediments adjacent to the ironstone lodes. Typically the extent of movement is unknown unless a displacement can be observed on sediment-ironstone, or sediment-porphyry contacts. Where recognised displacement is usually less than 10 m.

The relationship of the No. 1 and No. 3 orebodies has been discussed in Chapter Three where it was suggested that their apparent offset is related to the localisation of ironstone lode formation at the lower contact of the quartz porphyry where reverse

faulting has provided a conduit for mineralising solutions, and the impermeable porphyry has forced lateral migration of fluids. The consistent orientation of the fault trace (here called the Orebody Fault) as defined by the ironstone lodes, and the hangingwall contact of the No. 1 orebody in the upper levels of the mine (38° to 095), is sub-parallel to the cleavage. Fibre lineations and slickensides on the surface of this fault measured on 7 and 12 levels indicate it is a reverse fault which is consistent with both cleavage parallel faulting of the porphyry during folding, and late-stage reactivation associated with movement of the Footwall Fault. The remarkably linear nature of the south-east contact of the No. 1 orebody in mine plans has been recognised by previous workers e.g. Davies, (unpublished company report, 1982), but no sense of movement or possible connection between the No. 1 and No. 3 orebodies was suggested.

Dykes and Granite Related Veins

Mafic-intermediate dykes and quartz-muscovite±tourmaline±K-feldspar veins are common on both sides of the Footwall Fault. They typically have two orientations either parallel to cleavage or the Footwall Fault. Granite-related veins are common on 14 level with a general attitude sub-parallel to the cleavage orientation (Fig. 4.2). An intrusive quartz feldspar porphyry dyke has been mapped on 14 level which is clearly crosscutting of the quartz porphyry, and is also orientated sub-parallel to the cleavage.

4.4 Original orientation of the Warrego orebody

Any model of the structural evolution of the Warrego area must be consistent with the following observations:

1. The attitude of bedding and fold axial planes on both sides of the Footwall Fault are different to those observed elsewhere in the Warramunga Group.
2. The Warrego cleavage has a markedly different attitude to that of the region, and that associated with the Navigator Fault. The cleavage has also been modified by flattening associated with the the intrusion of the Warrego Granite.
3. The cleavage orientation is paralleled by granite-related veining and faulting that displaces the ironstone lode.
4. Kink bands and cleavage have a constant orientation across the Footwall Fault.
5. Bedding west of the Footwall Fault is largely overturned, while that to the east is right-way-up.
6. The plunge of the Warrego lode is approximately parallel to the fold axis defined by the bedding attitudes west of the Footwall Fault.
7. The footwall contact of the Warrego lode is sub-parallel to the attitude of the quartz porphyry-sediment contact, and the extensive alteration and stringer mineralisation along the footwall of the lode indicate that although the lode is right way up, alteration is strongest at the upper or leading edge of the lode.

8. Sulphide banding within and marginal to the ironstone lode, and stringer mineralisation in the footwall have an orientation sub-parallel to the cleavage.

These observations have important implications for the structural models previously proposed for the formation of the orebody. The model for the emplacement of the ironstone lode being controlled by a plunging fold (Goulevitch, 1975) was based on the assumption that the present attitude of the structural elements was the control on lode formation. This is clearly an over simplification of the situation as lode formation pre-dated granite intrusion and its associated deformation. Apparent folding of the quartz porphyry-ironstone lode contact suggested by Goulevitch (1975) is in fact due to faulting of the quartz porphyry by the Orebody Fault and subsequent ironstone lode formation against the faulted porphyry contact. This model does not explain the unusual structural orientation and orebody attitude in the Warrego mine compared to the rest of the Tennant Creek goldfield.

Similarly the mega-kink model (Le Messurier et al., in press) is also inconsistent with the above observations. Although probably representing reorientation of the original regional cleavage, the moderate dip of the cleavage in the Warrego area cannot be explained by simple rotation of the regional steeply dipping east-west cleavage attitude about the vertical fold axis implicit in the mega-kink model. The ~120° clockwise rotation required to rotate the cleavage from an original east-west to the present northeast strike is excessive compared to the typical maximum rotation of structural trends in mega-kinks of 20° to 30° (Powell et al., 1985).

The following reconstruction attempts to restore the structural elements of the Warrego area to a regional attitude via a deformation that is consistent with the above observations. This model assumes the rotation of the Warrego ironstone lode and adjacent sediments occurred during intrusion of the Warrego Granite and has been achieved by a body rotation (i.e. buckling with no flattening component). As an example of the regional structure to model the original attitude of the Warrego structural elements, bedding and cleavage attitudes in the Black Angel area some 8 km southeast of the Warrego mine (Fig. 4.4a and 4.4b respectively) were selected (Rattenbury, 1990b). The upright east-west trending folds with regular plunges (~25° to 277) recorded in this area are typical of the Warramunga Group as a whole (M. Rattenbury, pers. comm., 1988).

The rotation axis required to restore the Warrego structural elements to the regional attitude can be approximated by the intersection of respective fold limbs at Warrego Mine with those in the Black Angel area. Therefore the fold axis must occur within the shaded area in Figure 4.4c, and the fold axis used in Figure 4.4d (3° to 130) was selected

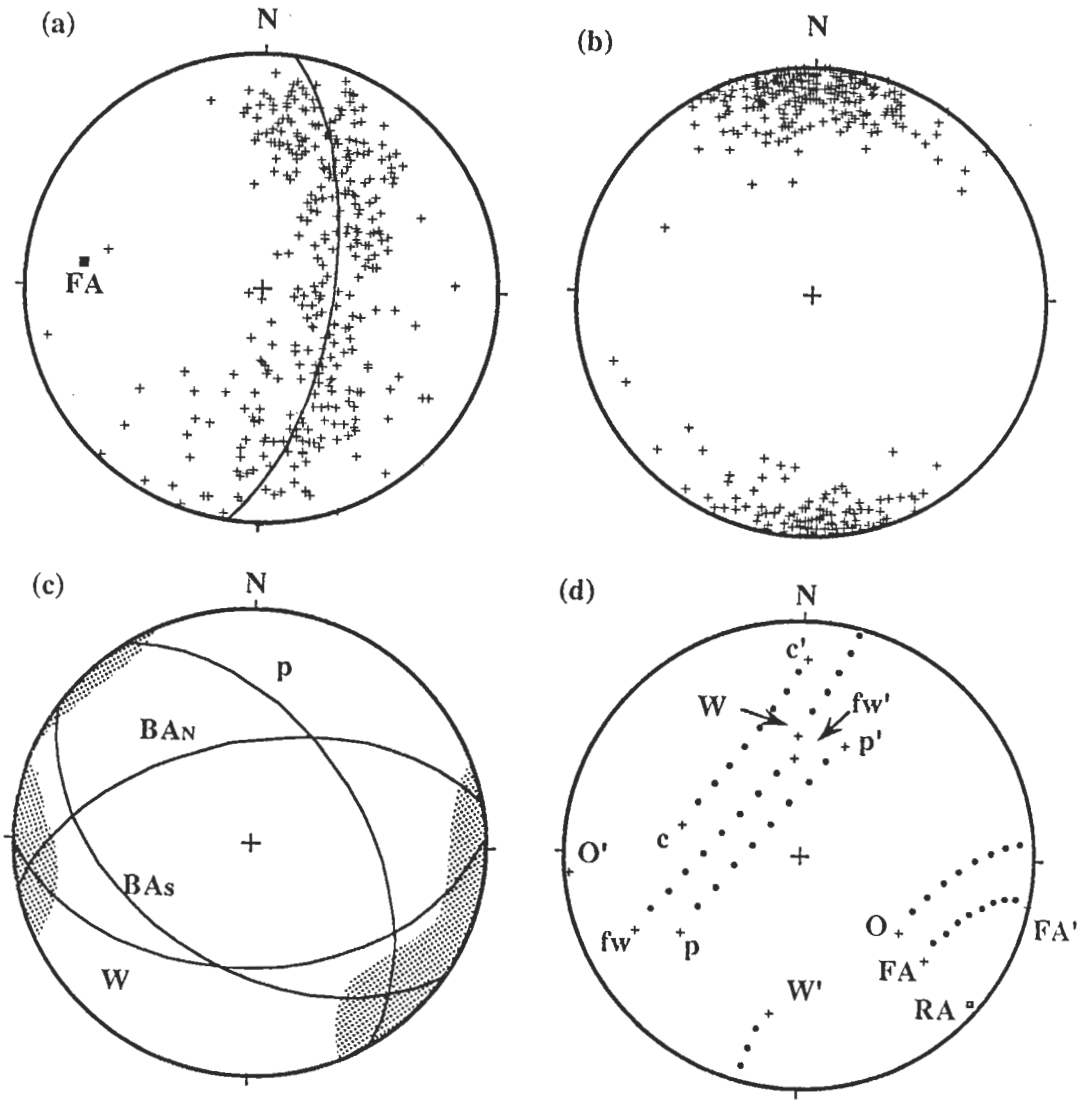

Figure 4.4 — Equal area, lower hemisphere, stereonet projections illustrating regional structure and the proposed model for the present attitude of the Warrego ironstone lode and adjacent sediments. (a) 246 poles to bedding from the Black Angel area. (b) 421 poles to cleavage in the Black Angel area. (c) Representative bedding planes from the Warrego and Black Angel areas. The intersection of the porphyry (p) with the south dipping Black Angel bedding planes (BAS), and the bedding planes west of the Footwall Fault (W) with the north dipping Black Angel bedding planes (BAN) constrain possible locations of the fold axis which rotated the Warrego bedding (stippled area). (d) The rotation model in which the Warrego structural elements are rotated 90° about a subhorizontal rotation axis (3° to 130) back into pre-Warrego Granite orientations . O = plunge of the orebody, O' = plunge of the orebody restored, FA/FA' = fold axis defined by bedding west of the Footwall Fault, RA = rotation axis, p/p' = pole to porphyry attitude (equivalent to poles to bedding east of the Footwall Fault), W/W' = poles to bedding west of the Footwall Fault , fw/fw' = pole to footwall contact of the ironstone.

because by trial and error, it gives the best overall 'match' to the regional attitude via a 90° clockwise rotation. The western bedding can be restored to an upright north dipping attitude (57° to 011), the stratiform porphyry to an upright south dipping attitude (43° to 200), the fold axis and ironstone lode plunge is restored to a horizontal east-west attitude, and the lode dips to to the north (36° to 175). A 90° angle of rotation also restores the cleavage orientation to that of the regional field cleavage in the Black Angel area.

4.5 Discussion

The proposed model results in a near perfect restoration of the Warrego structural elements to a regional Tennant Creek attitude. The reorientation of the Warrego ironstone lode to a horizontal east-west attitude is consistent with the majority of ironstones in the field where lode orientation parallel to the fold axis is observed as their localisation in the cores of folds parallel to cleavage, e.g. Juno mine (Large, 1974). However the Warrego ironstone lode does not lie in the plane of cleavage, but has an orientation similar to that of the immediately overlying quartz porphyry. This relationship implies a stratigraphic as well as structural control on lode formation as has been suggested in Chapter Three. Another consequence of the rotation model is that the top or leading edge of an originally horizontal Warrego ironstone lode would form the lower plunging edge in the present orientation of the lode. This relationship is consistent with the absence of a stringer alteration zone down plunge of the orebody, and the concentration of stringer mineralisation at the present top of the lode.

The deformation has not occurred by simple body rotation alone, as the contact metamorphic assemblage has been slightly deformed, but the close match of the Warrego and Black Angel structural elements imply the effects of flattening have not been major. Slight flattening may account for the observed spread of the poles to cleavage (Fig. 4.3b) and possible tightening of the folds as suggested by the imperfect girdle distribution of poles to bedding (Fig. 4.3a). Reactivation of cleavage parallel faults e.g. the Orebody Fault, may either be related to flattening associated with the intrusion of the Warrego Granite, or to movement on the Footwall Fault as both faults have a similar sense of movement (Fig. 4.2). Rotation of the Warrego area possibly occurred along northeast trending faults, examples of which displace the Great Western syncline to the northeast (Fig. 4.1)

The relationship of the mega-kink (Le Messurier et al., in press) to the rotation proposed for the Warrego area is unknown. The lack of outcrop in the Warrego area has meant it is not possible to establish the boundaries between the Warrego 'block' and the mega-kink. It is possible that the Warrego area has acted independently from the mega-kink zone during intrusion of the Warrego Granite. The increasing contact metamorphic

grade with depth in the Warrego Mine may indicate the Warrego block is underlain by granite, and is possibly bounded by faults to the east.

4.6 Summary

The orientations of the Warrego ironstone lode and associated sediments and porphyry are anomalous when compared with the typical orientations observed throughout the remainder of the Tennant Creek goldfield. A simple model is suggested and illustrated (Fig. 4.5), in which the Warrego area has been rotated from a regional attitude into its present orientation during the intrusion of the Warrego Granite. The relationship between the contact metamorphic assemblage and the cleavage suggest the rotation may not have been by a simple body rotation, but included a flattening component perpendicular to cleavage.

Removal of the granite-related rotation restores the Warrego ironstone lode to a horizontal attitude with its long axis aligned east-west parallel to the regional fold axes, similar to virtually all other ironstone lodes in the Tennant Creek area. The moderate south dip of the intermediate axis sub-parallel to the porphyry contact is consistent with geological and zoning constraints and suggests a stratigraphic as well as structural control on lode formation.

1. ~ 1875 Ma
Deposition of the Warramunga Group and intrusion of the conformable porphyry.

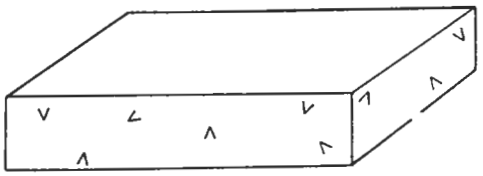

2. ~ 1870 Ma
Barramundi Orogeny: Folding about E-W axes, formation of ironstone lodes, and mineralisation.

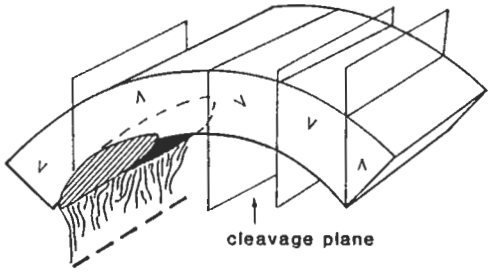

3. ~1810 Ma
Tectonothermal event (volcanism and deformation of Hatches Creek Group?) resets mineralisation age — not illustrated.

4. 1650-1660 Ma
Intrusion of the Warrego Granite causes localised upending of folds in the Warrego area. Original fold axes now plunge to the southeast. Movement along, and faulting parallel to the cleavage tightens folds.

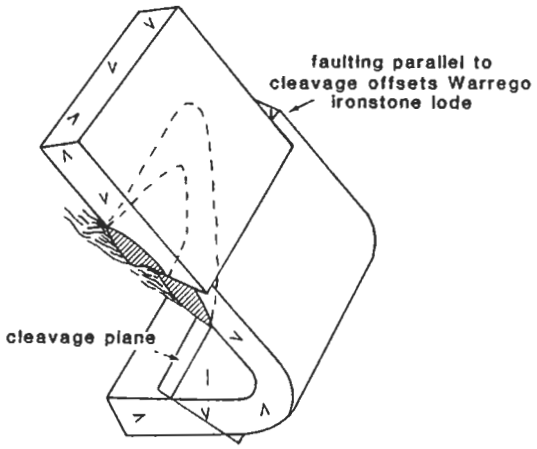

5. Present
The Footwall Fault juxtaposes overturned sediments to the west and upright host rocks and the Warrego ironstone lode to the east.

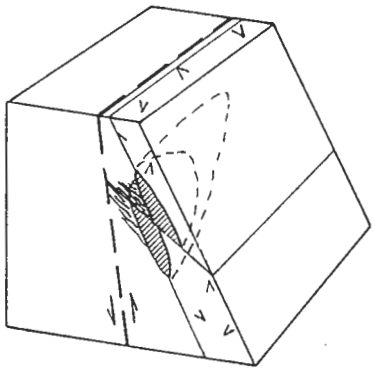

Figure 4.5 — Cartoon depicting the proposed structural model for the present attitude of structural elements in the Warrego area.

Chapter Five

METAL ZONATION

5.1 Introduction

Patterns of metal zonation in Tennant Creek orebodies were first documented for the Juno mine (Large, 1974, 1975), and similar though less perfect examples have since been observed or can be inferred from earlier studies e.g. Peko mine (Whittle, 1966), Golden Forty mine (Wyborn, 1971), TC8 (unpublished company data), and White Devil mine (Nguyen, 1987, Nguyen et al., 1990). However, other deposits in the field show no recognisable zonation patterns e.g. Argo mine (Meade, 1986) which has possibly been complicated by subsequent remobilisation of the ore, or Gecko mine (Large, 1974, Huston, 1989, 1990; Main et al., unpublished manuscript) which appears to show a reverse zonation pattern.

In the Juno mine, gold, bismuth, and copper show a well developed zonation of successive envelopes from a gold-rich core to a thin rim of copper mineralisation at the outer margin of the ironstone lode (Fig. 5.1). Each metal shows a marked concentration in successive enveloping zones that are typically discrete and without overlap. Large (1974) made a comparison between the metal zonation observed in the Juno mine and the apparent zonation in the Warrego mine with the then recent discovery of the gold-rich mineralisation at depth. He suggested Warrego followed a similar pattern to Juno with gold at depth overlain by copper although there was a general asymmetry to the zonation because of the orebodies plunging attitude (Fig. 5.2).

This chapter examines metal zonation within the Warrego orebody in a manner similar to the approach taken in Chapter Three. Metal zonation is described for the four studied mine sections (8340N, 8140N, 8060N, and 7980N), and is then related to the orebody as a whole in the composite true sections. Metal grade contours were generated on 10 m sections through the mine using the TORRES® ore reserve computer system at the Geopeko Head Office in Gordon.

The grades of gold, bismuth, and copper within the the Warrego orebody are quite variable, and rapid variations ranging from the detection limit to maximum values of 1,218·7 g/t gold, 18·0% copper, and 18·6% bismuth in 1m core splits, may occur over

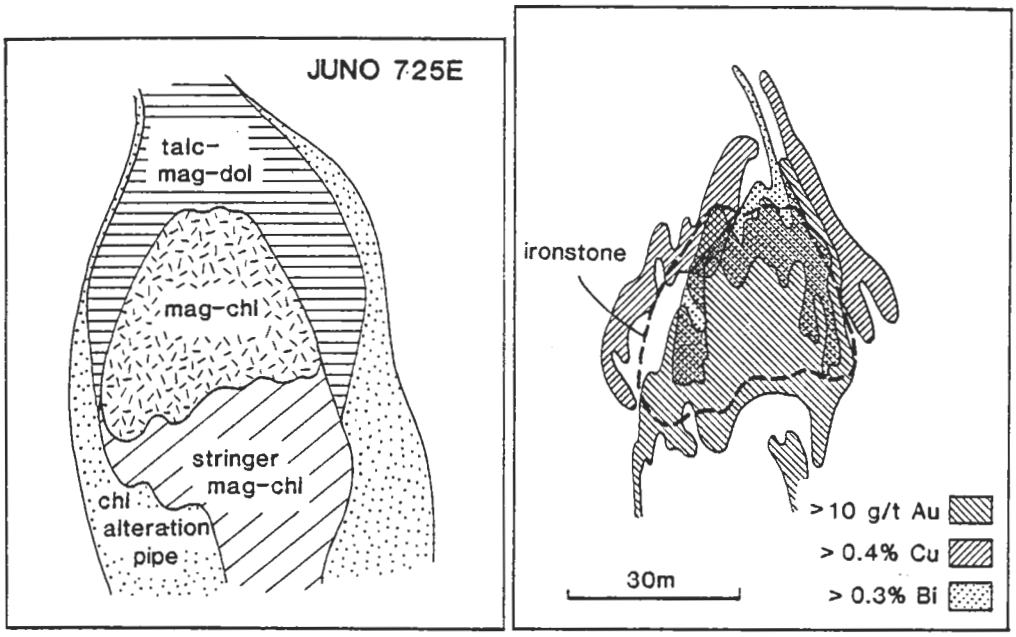

Figure 5.1 — Mineral and metal zonation in the Juno ironstone lode (adapted from Large, 1974). mag = magnetite, dol = dolomite, and chl = chlorite.

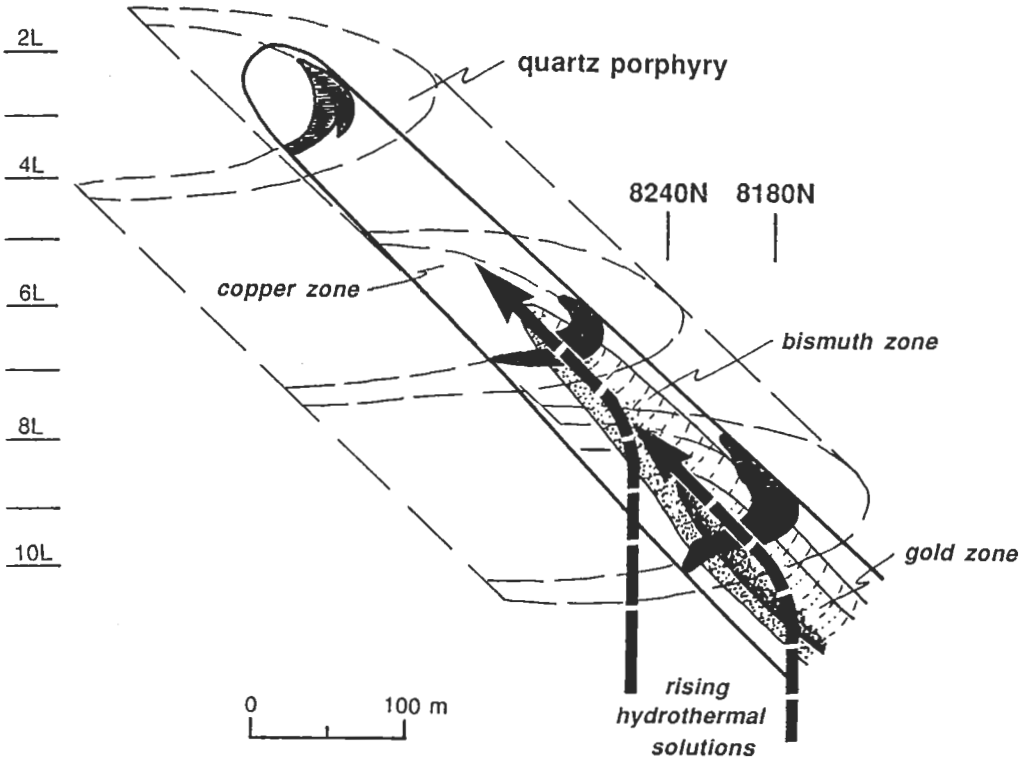

Figure 5.2 — The relationship of depth to the distribution of gold, bismuth, and copper zonation in the Warrego orebody, as suggested by Large (1974).

only a few metres. However there is a general pattern of overlapping zones that conform to the pattern gold-bismuth-copper identified in the Juno mine. The relative concentration of metals and strength of zonation patterns observed within the ironstone lode varies with the particular 'style' of mineralisation under consideration i.e. gold pod or copper orebody. Metal zonation in the four mine sections is illustrated in Figures 5.3 to 5.6, showing the distribution of gold, bismuth, and copper relative to the ironstone lodes and each other.

5.2 Section 8340N — Copper Orebody

The 8340N section is representative of the copper orebody in the upper levels of the mine and is characterised by consistent copper grades of 1·5 to 5% over all but the lowermost part of the ironstone lode. Gold and bismuth are present in sufficient quantities (~1·5 to 3 g/t and ~0·1 %) to be a significant credit in the copper concentrates produced from this ore. Figure 5.3 illustrates the metal distribution patterns observed in this section.

Gold

Gold mineralisation in this section is restricted to the upper half of the ironstone lode with the 1.5 g/t contour closely corresponding to the lode outline. Localised areas where grades exceed 3 g/t occur within this area, but are without an obvious pattern of distribution other than for a slightly greater concentration of gold at the top and centre of the lode.

Copper

Copper mineralisation shows a similar distribution pattern to gold, although mineralisation extends to the bottom of the lode. The 1.5% copper contour closely follows the ironstone outline with the mineralisation concentrated towards the hangingwall leaving barren quartz-magnetite in the lower footwall. As expected the 3% copper contour closely follows the magnetite-sulphide mineral assemblage and two main concentrations of high-grade copper mineralisation are defined at the top of, and in the core of the lode.

Bismuth

Bismuth concentration in the copper orebodies are typically low and values greater than 0.2% are rare. The 0.1% bismuth contour for section 8340N illustrate a marked localisation of bismuth mineralisation in the hangingwall of the upper part of the ironstone lode.

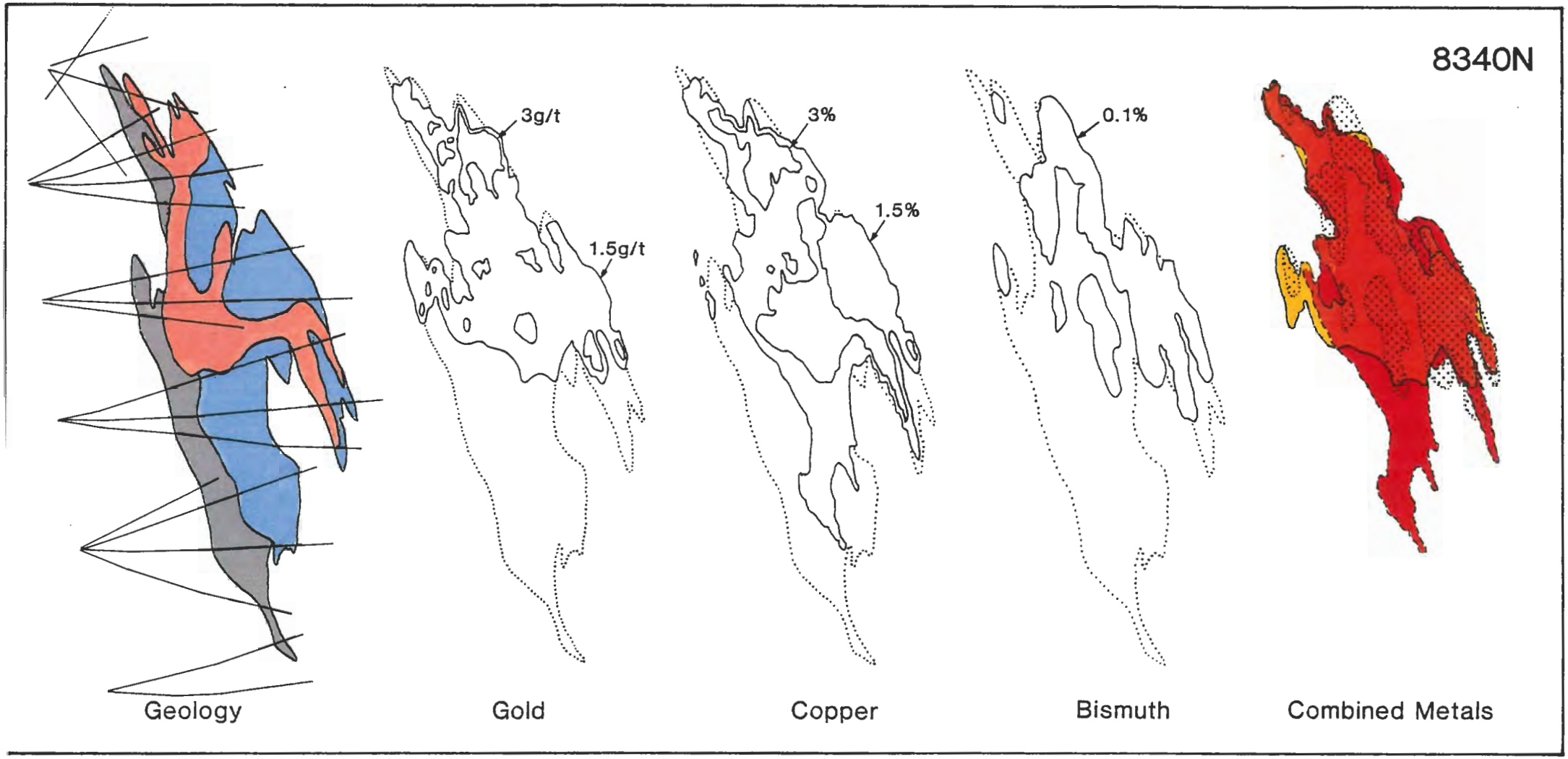

Figure 5.3 — Metal zonation: 8340N.

Key to Figures 5.3 to 5.6

- Chlorite magnetite/massive magnetite
- Magnetite sulphide
- Quartz-magnetite-sulphide
- Barren quartz magnetite

Combined metals:

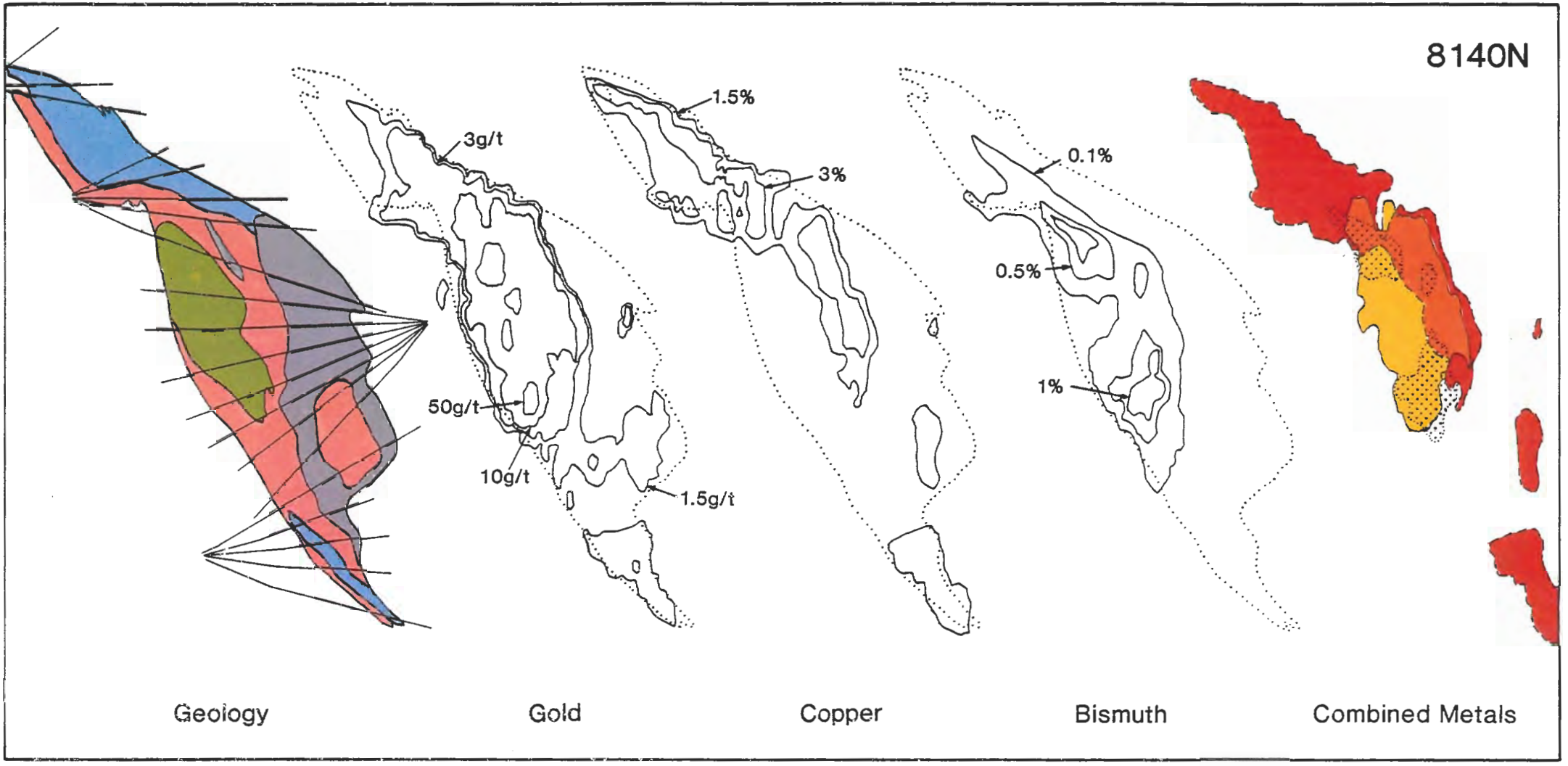

Figure 5.4 — Metal zonation: 8140N.

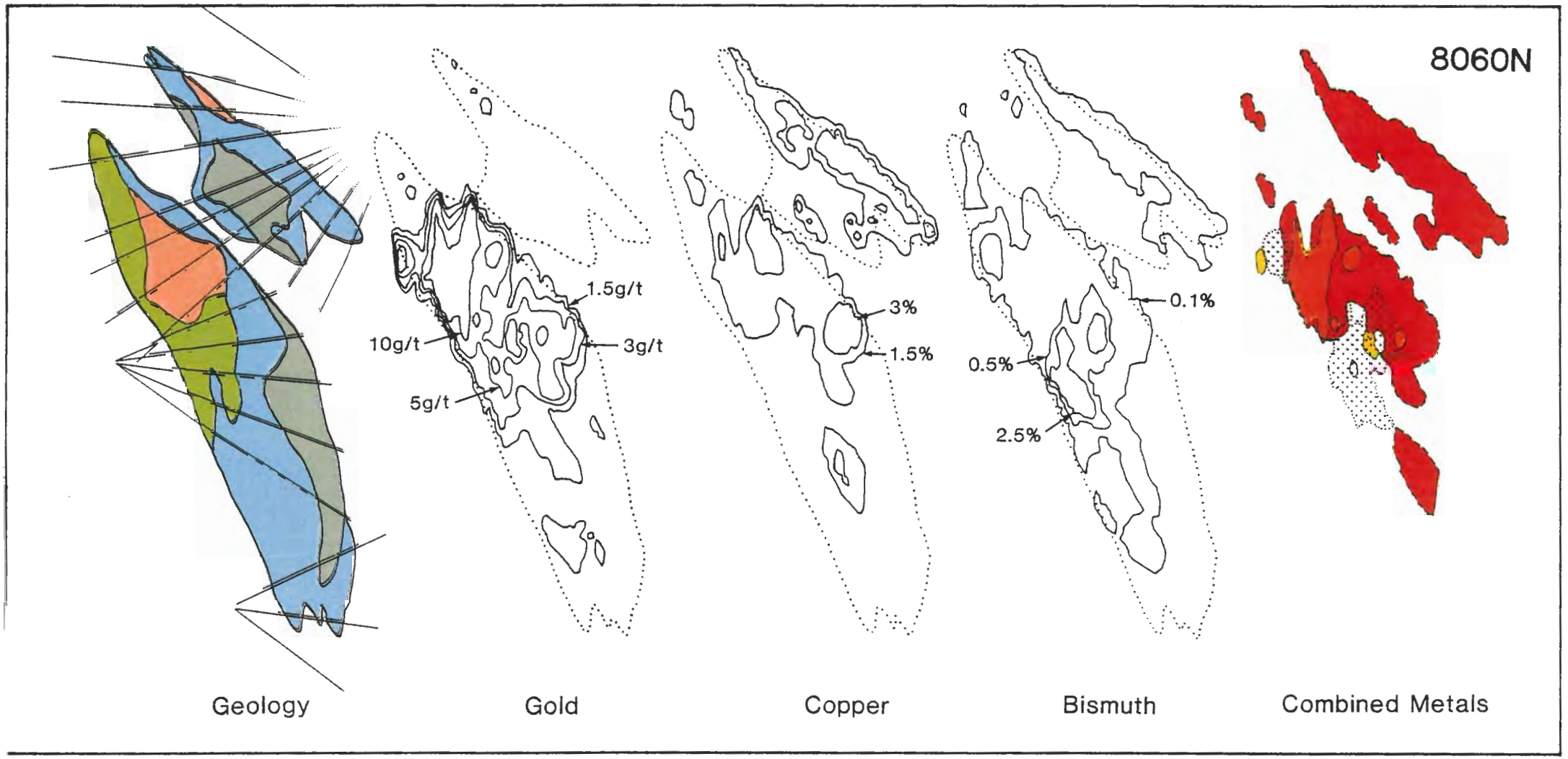

Figure 5.5 — Metal zonation: 8060N.

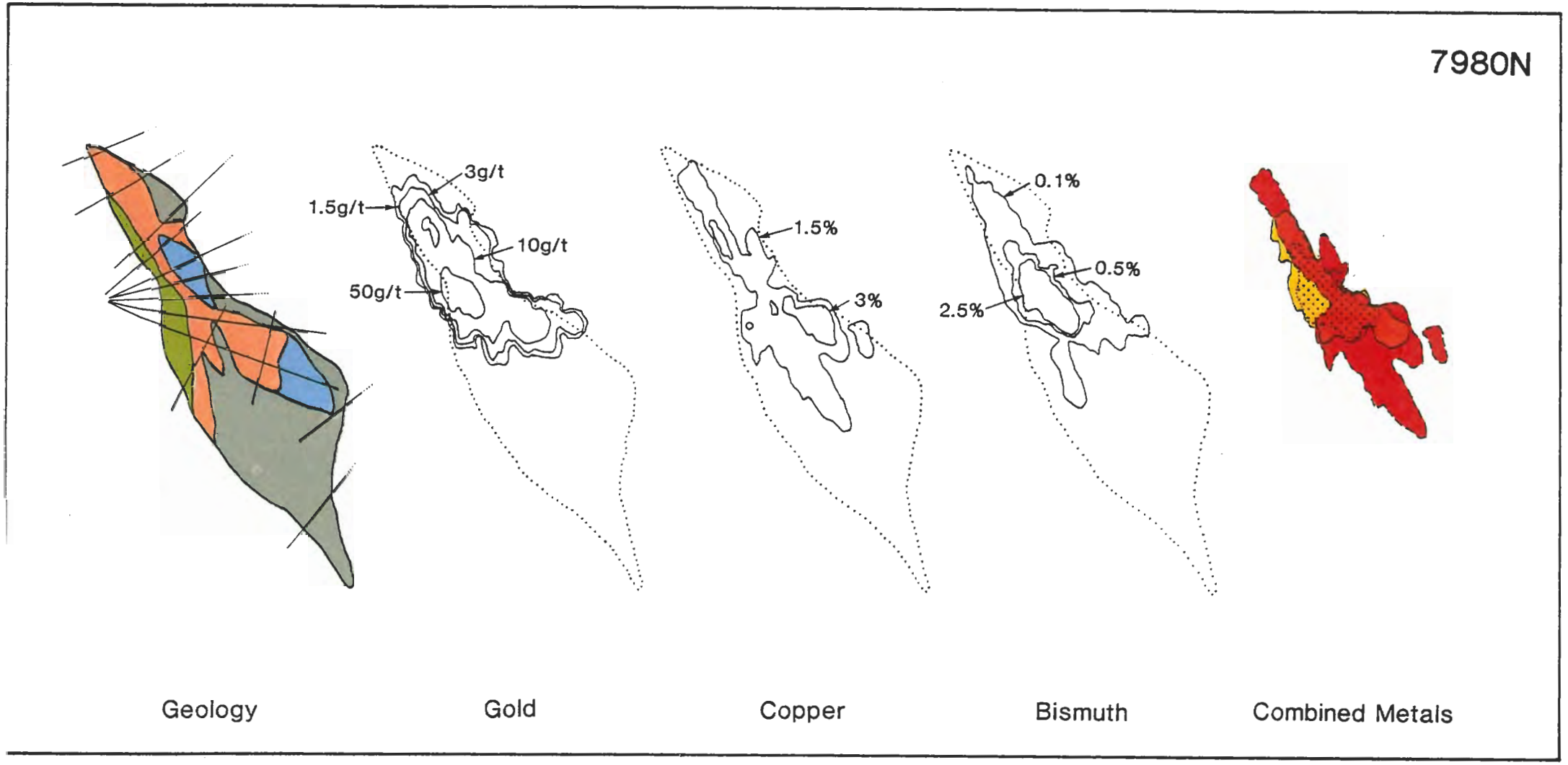

Figure 5.6 — Metal zonation: 7980N.

Zonation

The distribution patterns of gold, copper, and bismuth show a broadly overlapping relationship that is restricted within the boundaries of the ironstone lode. There is no obvious zonation apart from a general concentration of metals in the upper half of the lode that is possibly constrained by an increasing abundance of quartz with depth. Highest grades of gold, copper and bismuth mineralisation overlap suggesting a common paragenesis, although bismuth is also concentrated at the upper hangingwall contact. The concentration of mineralisation in the upper half of this section is consistent with the structural model which suggests the Warrego ironstone lode has been overturned (Chapter Four).

5.3 Section 8140N — Gold Pod

This section through the large central gold pod in the Warrego orebody shows the classic features of gold pod style mineralisation that is characteristic of mineralisation in the Tennant Creek goldfield. There is an extensive zone of stringer mineralisation in the footwall of the ironstone lode immediately adjacent to the gold pod, and mineral zonation within the lode ranges from a core of magnetite-chlorite in the footwall through magnetite-sulphide to barren quartz-magnetite in the hangingwall (Chapter Three). Metal distribution and zonation within this section is illustrated in Figure 5.4.

Gold

Gold mineralisation is widely distributed in this section, but the footwall and hangingwall boundaries are sharply constrained as indicated by the close spacing of contours against the footwall stringer zone and the overlying quartz-magnetite. Lateral variation in the gold grade is less sharply constrained, gradually decreasing with distance from the core of the gold pod. The large oval described by the 10 g/t contour (77 m × 36 m) approximately defines the boundary of the gold mineralisation in mining terms, but overlaps with the magnetite-sulphide adjacent to the gold pod proper. This enrichment of gold in the copper ore marginal to the pods is a common feature of the metal distribution in the Warrego orebody and is discussed more fully in section 5.6.

The highest gold grades are restricted to within the magnetite-chlorite assemblage where values may be extremely rich. An irregular band of such ore is defined by the 50 g/t contour in section 8140N where a maximum 1 metre drillcore assay of 811 g/t was recorded. This band of high grade gold ore is aligned sub-parallel to the footwall contact of the lode from which it is separated by some 5 to 10 m of relatively low grade ore. This differs from many of the ironstone lodes in the Tennant Creek area where gold is concentrated at the immediate footwall contact, e.g TC8 mine (Wedekind et al., 1990), but is similar to the Juno mine where gold is concentrated through the core of the lode (Large, 1974, 1975).

Copper

The 1.5% copper contour defines a discontinuous concave-towards-the-footwall outline corresponding to the magnetite-sulphide mineral assemblage wrapping around the gold pod. The maximum copper grades are similar to those in the upper copper orebodies (generally less than 5 %), but the distribution of copper is much more localised being bounded in footwall and hangingwall by magnetite-chlorite and quartz-magnetite assemblages respectively. As in section 8340N, the highest copper grades occur in the upper part of the lode either along the hangingwall contact or through the core of the lode.

Bismuth

Bismuth shows the same concave-towards-the-footwall distribution pattern as copper, but the mineralisation is not as widely developed through the lode being restricted to the immediate vicinity of the gold pod. The highest bismuth grades are concentrated at the contact between the magnetite-chlorite and magnetite-sulphide mineral assemblages although there is considerable overlap of bismuth in both the magnetite-chlorite and magnetite-sulphide mineral assemblages.

Zonation

Section 8140N displays the best development of a 'Juno-style' zonation pattern of all the sections studied, but differs in there being a broad overlap in metal distribution rather than the distinct and separate shells. High-grade gold mineralisation is restricted within the magnetite-chlorite assemblage, but high values extend into the copper-rich zones where the 10 g/t gold contour is almost coincident with the 1.5% copper contour in the area adjacent to the gold pod. Bismuth overlaps with gold and copper mineralisation, but highest grades coincide with the chlorite-magnetite and magnetite-sulphide contact between the highest gold and copper grades.

Thus despite the broad overlap in metal concentrations, a footwall to hangingwall zonation of gold-bismuth-copper is shown by the high grade distribution of each metal. Laterally removed from the gold pod, the mineralisation shows a distribution pattern that is similar to that observed in section 8340N where the 1.5 g/t gold and 1.5 % copper contours are coincident. Mineralisation is concentrated towards the upper part and footwall of the lode with quartz extensively developed in the hangingwall and towards the bottom of the lode showing a similar distribution pattern to that observed in section 8340N.

5.4 Section 8060N — Copper/Gold Orebody

Section 8060N is equidistant between the two gold pods in the Warrego orebody, and is characterised by an association of gold-rich copper ore rather than gold pod style mineralisation. As in the previous sections, mineralisation is restricted to the upper part of the No. 1 orebody and in the hangingwall of the rapidly tapering No. 3 orebody. Metal distribution and zonation in this section is illustrated in Figure 5.5.

Gold

The distribution of gold in this section encompasses the upper and central portions of the ironstone lode, with mineralisation broadly confined within its boundaries and sharp contacts at both the hangingwall and footwall contacts. Contours define two centres of gold concentration, an upper zone where the contours are closely spaced and apparently comprising two coalesced vertical bands, and a more diffuse zone where contours are more widely spaced. The two centres are elongated at an angle to the ironstone lode boundary in an en échelon arrangement, and appear to be the up- and down-plunge extensions of the two gold pods. Apart from minor isolated patches, gold mineralisation is absent from the No. 3 orebody.

Copper

Copper mineralisation as defined by the 1.5 % contour is localised in the core and towards the hangingwall of the No. 1 orebody. Copper grades are not high, reflecting the generally minor occurrence of magnetite-sulphide in this section. The highest copper values occur in two centres at or near the hangingwall contact. In the No. 3 orebody, copper forms an extensive but narrow zone that is largely restricted to the hangingwall contact.

Bismuth

Bismuth mineralisation extends along the footwall of the No. 1 orebody and fills the entire central portion of the lode. Two separate zones of higher grade bismuth mineralisation are concentrated at the footwall of the lode. Bismuth is also localised along the hangingwall contact of the No. 3 orebody.

Zonation

Although weak and not as well defined as in section 8140N, there is a general zonation pattern in this section with gold and bismuth concentrated towards the footwall of the lode, and copper in the hangingwall. There is no clear zonal relationship of gold and bismuth from footwall to hangingwall with these metals either overlapping or adjacent.

The distribution of all three metals may be resolved into two centres of concentration that have a broadly en échelon pattern of distribution. The upper centre forms a sharply bounded zone of gold mineralisation which correlates with the distribution of copper, although the highest copper values are offset toward the hanging-wall of the ironstone lode. Bismuth overlaps the gold and copper but is concentrated on the footwall side of the gold. The lower mineralisation centre forms a diffuse zone of gold mineralisation that is again overlapped by copper which is displaced toward the hangingwall. Bismuth overlaps the gold with the higher grade area having a more extensive distribution than the gold.

The two centres of mineralisation appear to represent the lower and upper extensions of the gold pods centred on 8140N and 7980N respectively. The two pods have different characters in their distal extensions with the central gold pod (8140N) forming a larger, sharp boundaried copper-gold association, while the lower pod (7980N) appears to be at the end of its up-plunge extension with gold grades diffuse and irregular although the high bismuth grades associated with this pod is still evident.

5.5 Section 7980N — Gold Pod

The lower gold pod in the No. 1 orebody is approximately centred on section 7980N, and although smaller in size than the main pod, it is notable in that it has the highest recorded grades of both bismuth and gold for the Warrego mine. The No. 3 orebody has been omitted from Figure 5.6 as only restricted copper mineralisation occurs in the hangingwall of the upper part of the lode.

Gold

Gold in section 7980N overprints a narrow neck in the upper part of the ironstone lode, and there is a significant overlap of mineralisation into both the hangingwall and footwall of the lode. Closely spaced contour intervals again reflecting the sharp cut-off in gold grade to within the immediate ironstone lode environment. As with the 8140N gold pod, the highest gold grades occur within the the magnetite-chlorite assemblage towards and into the footwall of the lode, but these values continue into the surrounding magnetite-sulphide.

Copper

Copper ore is concentrated within an elongate zone in the core of the ironstone lode that is sub-parallel to its' margins. The marked thickening of the mineralised zone adjacent to the magnetite-chlorite is characterised by higher copper values towards the hangingwall contact of the lode.

Bismuth

Bismuth mineralisation occurs through the upper part of the No. 1 orebody extending into both the footwall and hangingwall in a manner similar to gold. The distribution of bismuth generally follows the pattern of gold although the highest grades occur in the core of the ironstone lode. The lower gold pod is characterised by higher bismuth grades than the upper gold pod.

Zonation

Because of the relatively narrow width of the ironstone lode in this section, metal zonation appears to be telescoped and is not as well developed as in the larger central pod. The highest gold grades occur at the immediate footwall contact, with bismuth overlapping and extending laterally into the core of the lode. The high-grade copper occurs at the hangingwall contact or lateral to the gold and bismuth.

There appears to be two trends to the mineralisation in this section, not only the footwall to hangingwall pattern typical of sections 8140N and 8060N, but there is also an elongation to the mineralisation through the core of the lode. This pattern is also observed in sections 8340N and 8060N, and is discussed below.

5.6 Metal Zonation on an Orebody Scale

To understand the metal distribution, possible controls thereon, and to correlate trends observed in individual sections within the orebody as a whole, metal contours have been constructed for the true sections described in Chapter Three and illustrated in Figure 3.6 and 3.7. The true sections have been contoured for gold (≥10 g/t) and copper (≥1.5%) as these values appear to define natural boundaries within the lode (Fig. 5.7). Grades above 10 g/t gold are restricted to the gold pods and gold-enriched copper ore immediately adjacent to them, and the 1.5% copper contour marks the sharp cut-off of copper mineralisation which often corresponds to the ironstone lode boundary.

The most obvious feature in these sections is the duality of the ironstone lode, which may be divided into an upper gold-poor (sections K to O), and a lower gold-rich (sections A to J) lode. Concomitant with the decreasing abundance of gold in the upper levels of the mine, the lode is more pervasively mineralised and signifies a decrease in the relative abundance of barren quartz-magnetite in the upper levels of the mine. Where distinct pods of gold-rich mineralisation become apparent, increasingly large proportions of the two ironstone lodes contain quartz-magnetite that is devoid of mineralisation.

The lower gold pod extends from sections A to E, and the larger central pod from D to K. The area of overlap between the two pods corresponds to the area represented in section 8060N where an en échelon arrangement of two distinct metal concentrations was observed (Fig. 5.4). Quinlan and Leahey (1979) describe the central gold pod as

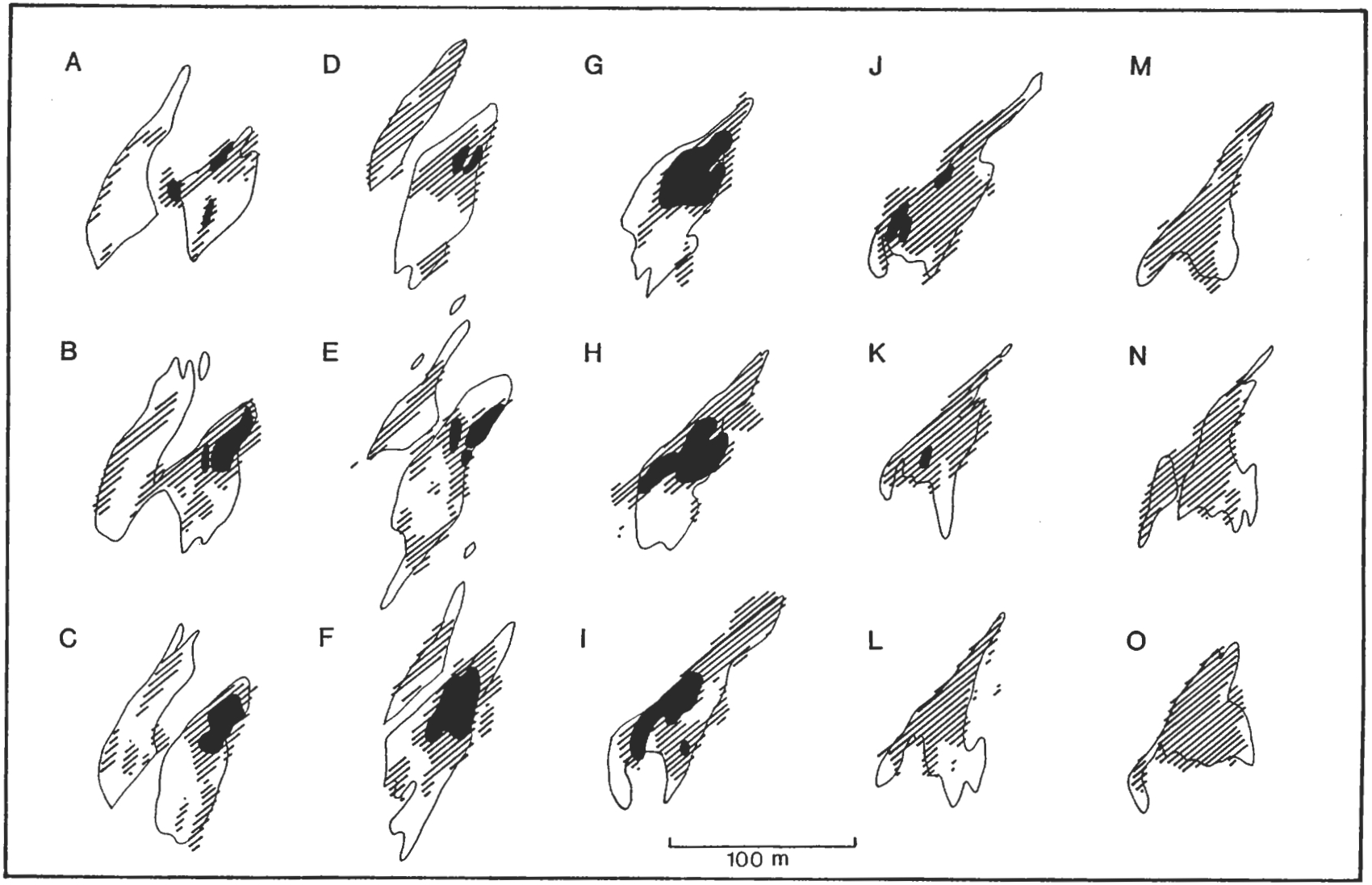

Figure 5.7 — True sections through the Warrego ironstone lodes illustrating metal distribution. Solid = ≥10 g/t Au, hatched = ≥1.5% Cu. See Figure 3.6 for the relationship of these sections to the ironstone lode.

comprising a series of lenticular en échelon pods of high-grade gold ore, suggesting that the relationship between the two gold pods is repeated on a smaller within-pod scale (see below).

As has been illustrated in sections 8140N, 8060N, and 7980N (Figs 5.4, 5.5, and 5.6), the copper ore peripheral to the gold pods is enriched in gold. The gold pods proper (high-grade gold associated with magnetite-chlorite) are much smaller in extent than that defined by the 10 g/t gold contour in the true sections, and the gradient of decreasing gold grade from footwall into the lode is likely to represent the path followed by the mineralising fluids through the ironstone lode. In both pods their lateral extension as gold-rich copper ore does not follow the footwall contact, but spreads laterally through the core of the ironstone lode. The implication is that the overprinting economic mineralisation was focused at specific sites (the gold pods), and having penetrated the lode, the fluid was able to move laterally through its core. Such movement was possibly facilitated by breccia or shear zones within the ironstone lode itself. Figure 5.8 illustrates the relative distribution of the two gold pods in long section and the lateral up- and down-plunge extension of the pods through the core of the lode rather than along the footwall contact.

Although gold-rich mineralisation is typically restricted to the footwall or core of the ironstone lode, the lower gold pod is a notable exception as gold and copper mineralisation also occurs in the hangingwall of the lode (Figs 5.6 and 5.7A). This occurrence of stringer mineralisation 'wrapping around' the lower ironstone lode is taken as evidence that the No. 1 and No. 3 orebodies were separate entities at the time of mineralisation, and support the model of ironstone lode localisation via fluid concentration in the Orebody Fault which offset the quartz porphyry.

5.7 Trace Element Zonation

The concentration of trace elements other than gold, bismuth and copper in Tennant Creek ironstone lodes have been examined by various workers Wyborn, 1971 (Mo, Ag, Se), Large, 1974, 1975 (Se, U, Pb, S), Smith, 1980 (Pb, Zn, Co, Mo), Large and Robinson, 1987 (Pb, U, Th, Mo, Zn, As, Sb, Ag, low level Au), Edwards, 1987 (Zr, Y, Ga, Th, Rb, Sr), and Horvath, 1988 (Sr, Rb, U, Cd, As, Sb, Ag, low level Au, Pb, Zn, Co, Mo, W, REE). However, the only systematic examination of trace element variation through an orebody has been of the Juno mine by Large (1974, 1975).

The Juno study indicated trace elements and their ratios exhibit similar zonation patterns to the gangue minerals and metals. Uranium shows the same umbrella-shaped distribution of the other metals, with the 80 ppm contour closely correlated with the boundary between the high grade gold and bismuth contours. Copper and sulphur show a complementary steady increase from the gold to copper zones, as do the ratios Bi/Se,

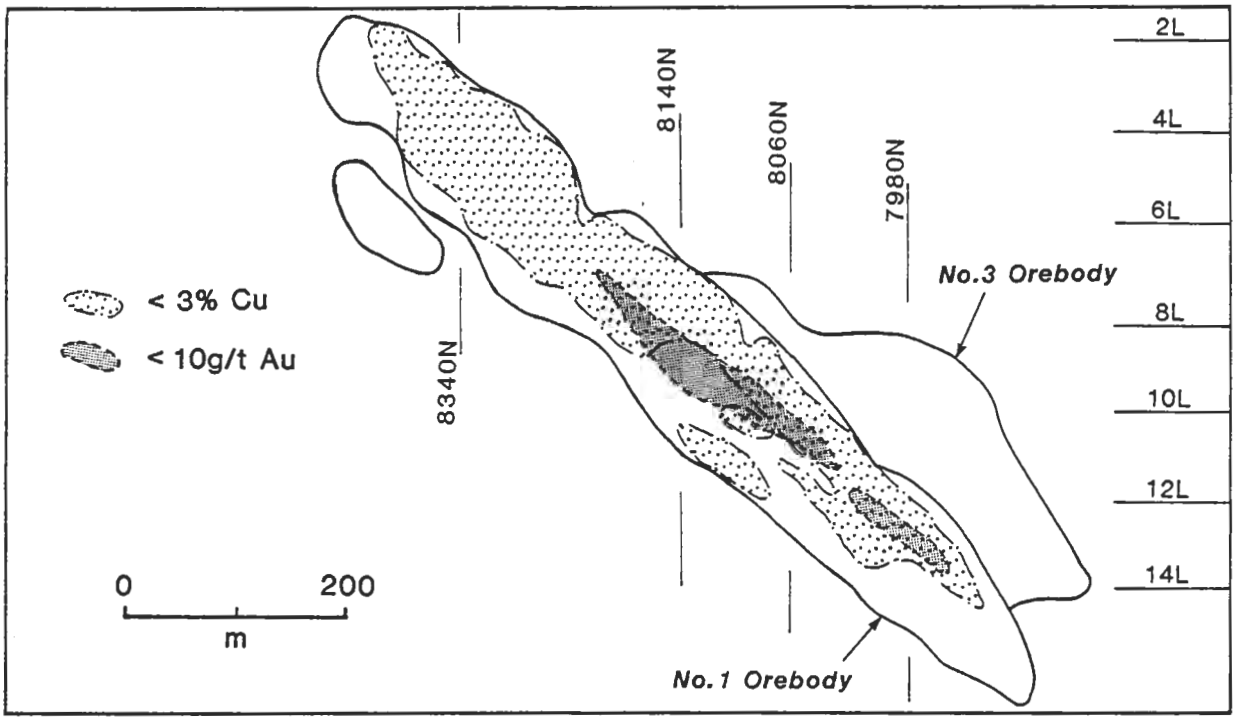

Figure 5.8 — Long section through the No. 1 orebody illustrating the metal distribution and relationship of the gold pods to the four section examined in this study.

S/Se, and Bi/Pb. The variation in bismuth, lead, and selenium reflects the changing chemistry of bismuth sulphosalts across the bismuth zone.

To determine whether similar trace element zonation patterns exist in the Warrego ironstone lode, drillhole 9/814/12[1] was selected for detailed examination. This drillhole probably affords the most complete section through the various zones in the Warrego orebody; starting in relatively unaltered sediment, the hole passes through the footwall stringer, magnetite-chlorite, magnetite-sulphide, and quartz-magnetite zones of the ironstone lode and into the hangingwall quartz porphyry. One hundred and three, one metre core splits were analysed for a suite of trace elements that have previously been identified as anomalous, or likely to be anomalous (Edwards, 1955, Fander, 1966; Large, 1974, Smith, 1980). Raw data values, method of analysis, and a detailed log of drillhole 9/814/12 are presented in Appendix B, and a series of plots of trace element content (in ppm) versus depth down the drillhole are illustrated in Figure 5.9 to 5.23. Before plotting, the element values were 'smoothed' i.e the one metre assay values were composited to give average values over a three metre interval — a statistically more appropriate interval to reflect variance within the orebody (Quinlan, 1976).

Several of the trace elements analysed in drillhole 9/814/12 show coherent behaviour with one or more of the others, and it has been possible to group these and describe their distribution together. The possible relationship of these groupings is discussed in terms of mineral zonation and their possible genetic implication.

Iron

As is to be expected, the geology of drillhole 9/814/12 is broadly reflected in the abundance of iron in the samples. The sediment-ironstone contact is marked by a dramatic increase in iron content from ~10 to ~70 weight % (Fig.5.9). The massive magnetite and magnetite-chlorite zones maintain a relatively constant iron content before values show an erratic decrease in abundance corresponding to dilution from quartz and chalcopyrite. The contrast between highly altered sediments at the start of the drillhole and relatively unaltered sediments at the immediate lode contact is also apparent (Appendix B).

Gold

Two distinct populations of gold are observed in the drillhole; a 9 m wide interval through the gold pod that is strongly enriched in gold (40–48m), is separated by a relatively barren zone from 16m of much lower, but still high grade gold mineralisation that is associated with sulphides (52–78 m). The drop in grade between these two populations is attributed to the nugget effect because visible gold was observed in this

[1] Drillhole 12 on 9 level, in section 8140N.

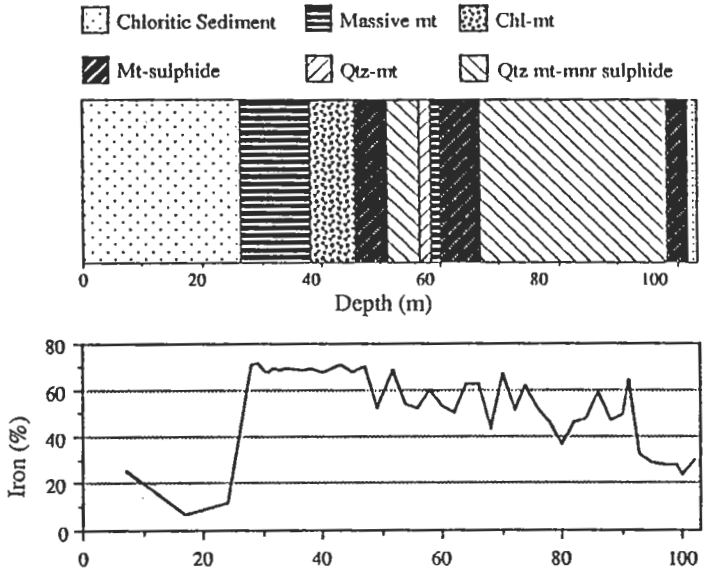

Figure 5.9 — Element variation and geology in drillhole 9/814/12: Fe.

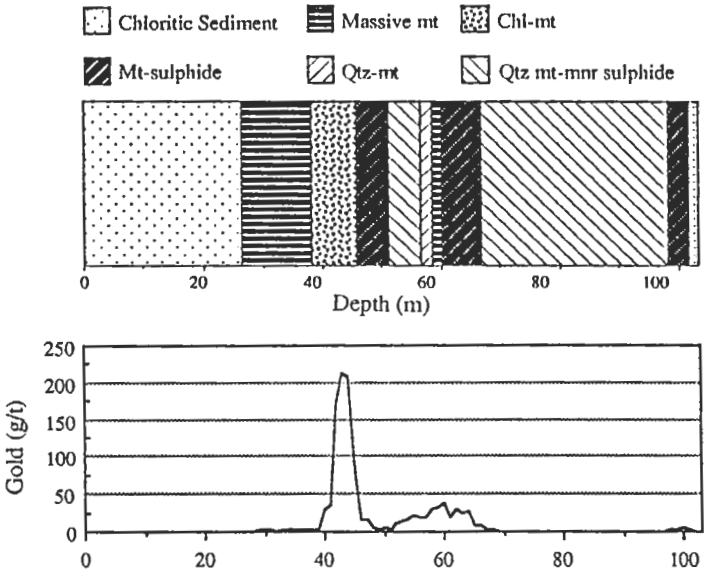

Figure 5.10 — Element variation and geology in drillhole 9/814/12: Au.

interval, and original company assays indicate values similar to the sulphide-hosted gold of ~10g/t. These two association correspond to the gold pod and gold-rich copper ore associations described previously.

The most significant points observed in the distribution of gold in the drillhole are:

1. The very sharp boundaries to the gold pod without any tailing off of grade into the sulphide-rich ore, and the 10 m wide zone between the footwall of the ironstone lode and the gold pod where grades are relatively low (1 to 3g/t). These observation indicate that high-grade gold mineralisation was localised, and because the barren footwall of the ironstone lode comprises relatively massive magnetite, suggests that the distribution of mineralisation is related to the degree of fracturing in the lode. The abrupt drop in grade into the magnetite-sulphide assemblage indicates either a physico-chemical control resulting in 'bonanza' gold deposition or that the gold pod mineral assemblage represents a different paragenesis. The difference between the gold pod and sulphide ore is illustrated by the strong correlation between gold and copper in drillhole 9/814/12 at gold values ≤10 g/t, and the deterioration of the relationship above this value (Fig. 5.11).
2. Gold grades in the quartz-magnetite zone drop off to levels that are lower than in the chloritic sediments of the footwall and reflects either a sealing of the lode by quartz that has prevented access by hydrothermal fluids, or fluid undersaturation with respect to gold.

Copper and Sulphur

Copper and sulphur constitute major elements for much of the length of the drillhole and their correlation is related to the abundance of chalcopyrite especially in the magnetite-sulphide zones. Compared to chalcopyrite, the other sulphides (pyrite and bismuthinite) are minor and their variation in the drillhole is insufficient to dramatically alter the ratio of sulphur to copper (Fig. 5.12).

The distribution of these elements in the hole indicate variable chalcopyrite in the footwall sediments with lower values in the immediate footwall of the lode. Within the lode the general absence of sulphides in the magnetite-chlorite is evident, as is their marked concentration in the magnetite-sulphide zones. The concentration of copper and sulphur (chalcopyrite) does not form a single copper zone as observed at Juno mine, but rather there are several bands of copper-rich ore separated by relatively barren intervals. Similar to the gold, values in the quartz-magnetite zone are lower than those recorded in the footwall sediments.

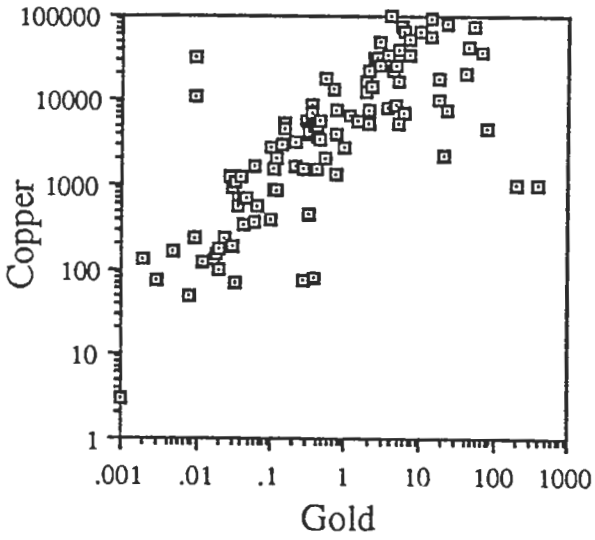

Figure 5.11 — Co-variation of Cu with Au in drillhole 9/814/12.

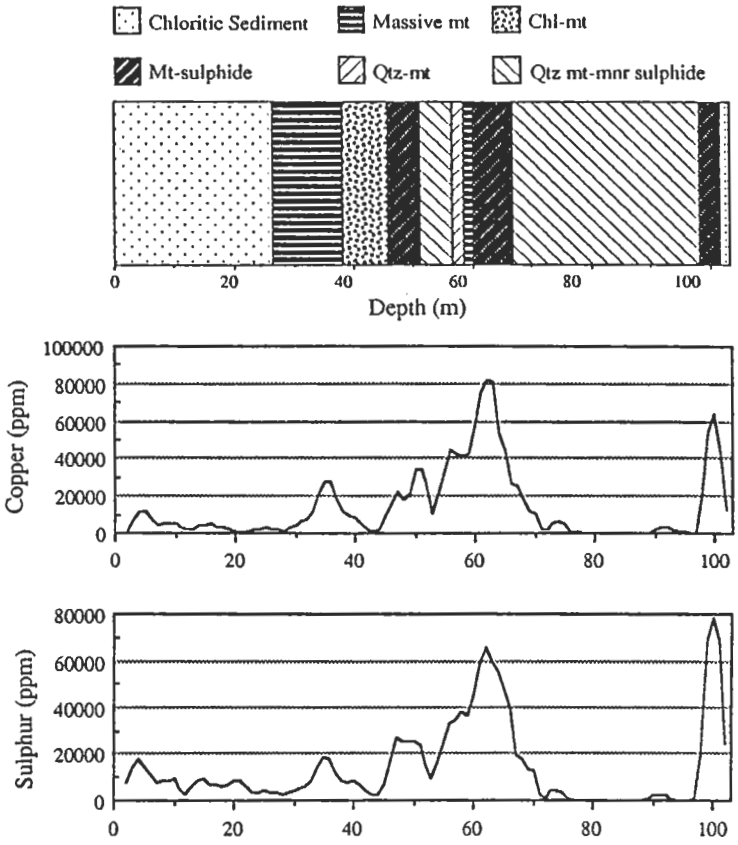

Figure 5.12 — Element variation and geology in drillhole 9/814/12: Cu & S.

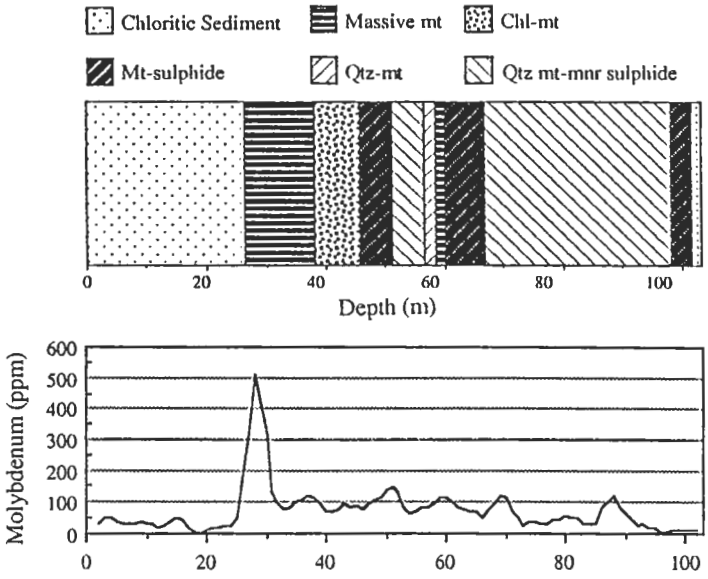

Figure 5.13 — Element variation and geology in drillhole 9/814/12: Mo.

Molybdenum

Smith (1980) identified molybdenum as an anomalous element (≥50 ppm) in *both* barren and mineralised ironstone lodes in the Tennant Creek goldfield. Within the ironstone lode intersected by the drillhole, molybdenum is certainly anomalous at a level that is remarkably constant (50–100 ppm), and although the concentration drops off in the quartz-magnetite zone, values do not fall below values in the footwall sediments (Fig. 5.13). This relationship suggests that molybdenum was probably concentrated in the ironstone lode during its formation rather than introduced with late-stage economic mineralisation. However, the strong enrichment in molybdenum at the immediate footwall of the ironstone lode may imply some later concentration or introduction of molybdenum. Molybdenum and to a lesser extent uranium, are the only elements in this study which show a footwall enrichment and possibly indicate a different paragenesis. Molybdenite is observed in the footwall of the lower gold pod intimately associated with gold (Chapter Six) but this paragenesis is not evident in this drillhole.

Bismuth, Lead, and Antimony

The presence of native bismuth, and bismuth oxides and carbonates in the ironstone lodes above the water table was recognised early in the mining history of the Tennant Creek goldfield (Stillwall and Edwards, 1942), and was used by prospectors as a guide to gold-rich ore (McKeown, 1942). Below the water table a complex range of bismuth sulphosalts including copper-, lead-, silver-, and selenium-rich varieties have been identified and described by Stillwell and Edwards (1942), Edwards (1955), Fander (1966), Large (1974, 1975), Large and Mumme (1975), Mumme (1975a, 1975b, 1976), and Mumme and Watts (1976).

Lead mineralisation has been reported in several Tennant Creek mines notably Peko (Whittle, 1966) and Orlando (McNeil, 1966), where discrete zones of (non-economic) galena mineralisation were delineated. In Peko mine lead-zinc mineralisation is localised marginal to the ironstone lode disseminated in sericitic schists, while in Orlando a body of massive to banded galena and sphalerite ore is localised marginal to a dolomitic breccia. However in the majority of mineralised ironstone lodes, lead occurs as a trace element localised within bismuth sulphosalts as in the Juno mine (Large, 1974,1975).

The antimony content of ironstone lodes has been examined for samples from several Tennant Creek mines and prospects by Large and Robinson (1987), but no discrete antimony minerals have been described. Large and Robinson (1987) showed mineralised deposits typically have antimony values above 12 ppm but no interpretation was made as to the possible mineral host.

The close correlation of bismuth, lead, and antimony in drillhole 9/814/12 which all display a characteristic treble peak pattern of enrichment suggests these elements are related (Fig. 5.14). Their close correlation is further demonstrated in the lead-bismuth and antimony-bismuth plots of Figure 5.15 where there is a strong linear correlation between these elements at values above 100 to 1000 ppm bismuth. Below this level correlation becomes erratic or non-existent which is largely because lead and antimony are at their detection limit. These relationships strongly suggest lead and antimony are trace constituents in bismuth minerals; an observation which is supported by the identification of antimoniferous bismuth sulphosalts in the copper orebodies (Chapter Six).

The bismuth grade through the ironstone lode has a fairly constant background of approximately 1000 ppm, until the quartz-magnetite zone where again values drop to below those in the footwall sediments. The highest values occur on the footwall sides of the magnetite-chlorite and magnetite-sulphide assemblages, with lesser enrichment in the central magnetite-sulphide zone. This pattern is closely followed by that for antimony, but lead only shows a marked concentration in the main magnetite-sulphide zone and is relatively low in the other assemblages.

Following the identification of a well developed zonation in the chemistry of bismuth minerals at Juno mine (relatively lead- and selenium-rich in the core of the lode to copper-rich at its margins), Large (1974) also examined bismuth minerals in the Warrego mine where a similar pattern was observed. Copper-rich bismuth sulphosalts were identified above 7 level, selenium-poor, lead-copper bismuth sulphosalts between 7 and 8 levels, and seleniferous bismuth sulphosalts marginal to the gold pods on 8 level. Similar trends were sought in drillhole 9/814/12 through the variation of the Bi/Pb and Bi/Sb values through the gold pod (Fig. 5.16). There is an irregular, but generally consistent trend of increasing lead content relative to bismuth across the lode towards both footwall and hangingwall from the central gold pod. A much weaker trend of increasing antimony relative to bismuth is also apparent, but this relationship may simply reflect the increasing lead content of bismuth minerals.

Selenium

High contents of selenium in bismuth sulphosalts from the Tennant Creek mines was first reported in the Juno mine by Fander (1966), and subsequently Large (1974), Large and Mumme (1975), and Mumme (1975b) described a complex range of seleniferous bismuth sulphosalts in the Juno mine from which selenium was actually extracted on a commercial basis. Although programs were undertaken to evaluate the resource of selenium in the copper orebodies of Warrego mine (Johnson, 1972, unpublished

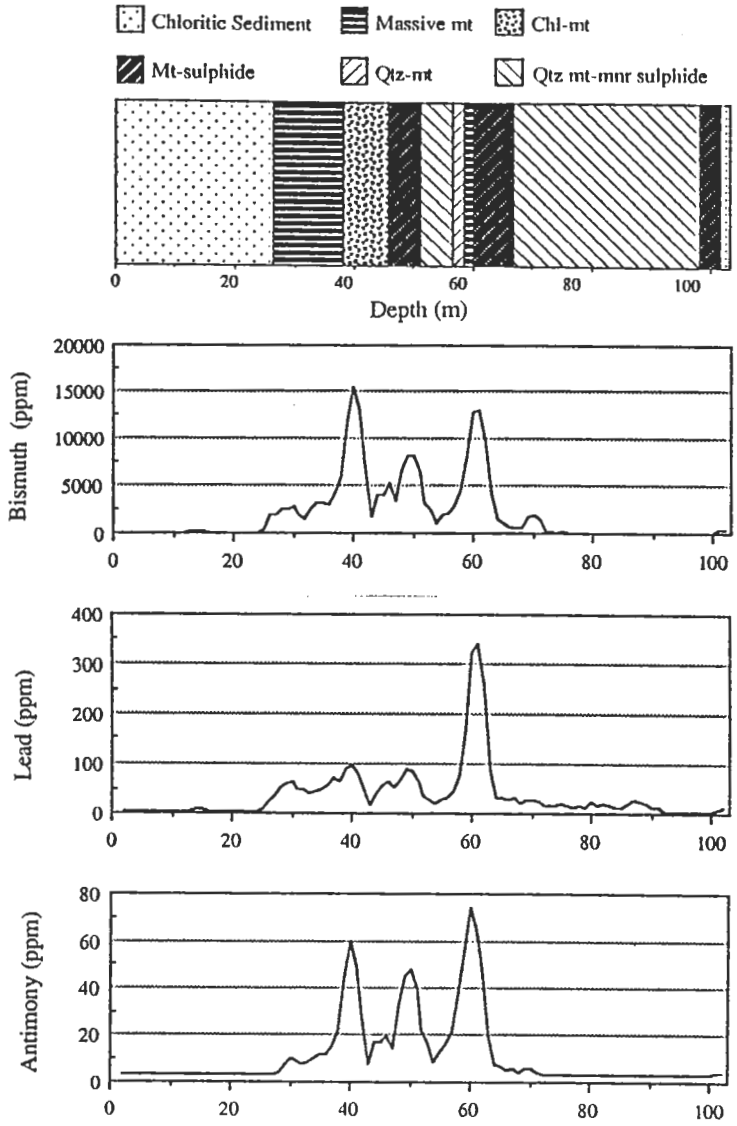

Figure 5.14 — Element variation and geology in drillhole 9/814/12: Bi, Pb, & Sb.

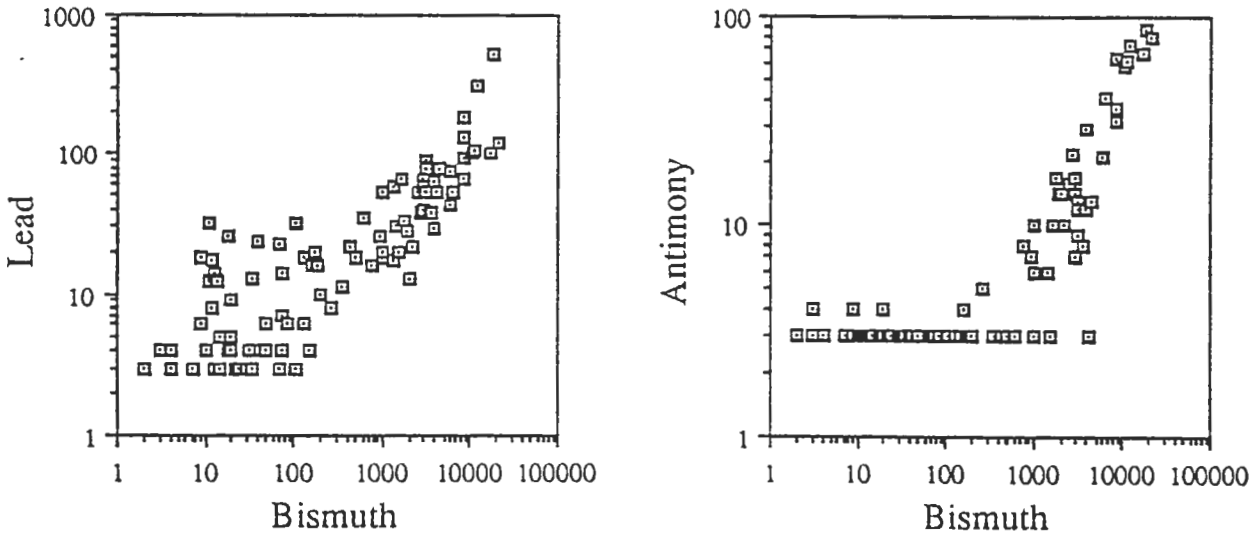

Figure 5.15 — Co-variation of Pb and Sb with Bi in drillhole 9/814/12.

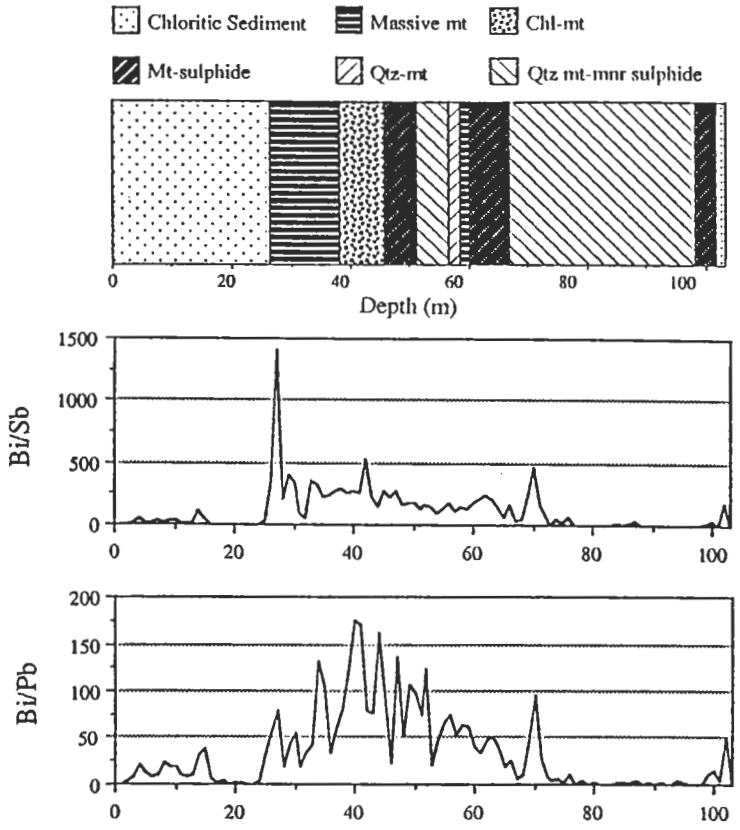

Figure 5.16 — Element variation and geology in drillhole 9/814/12: Bi/Pb and Bi/Sb.

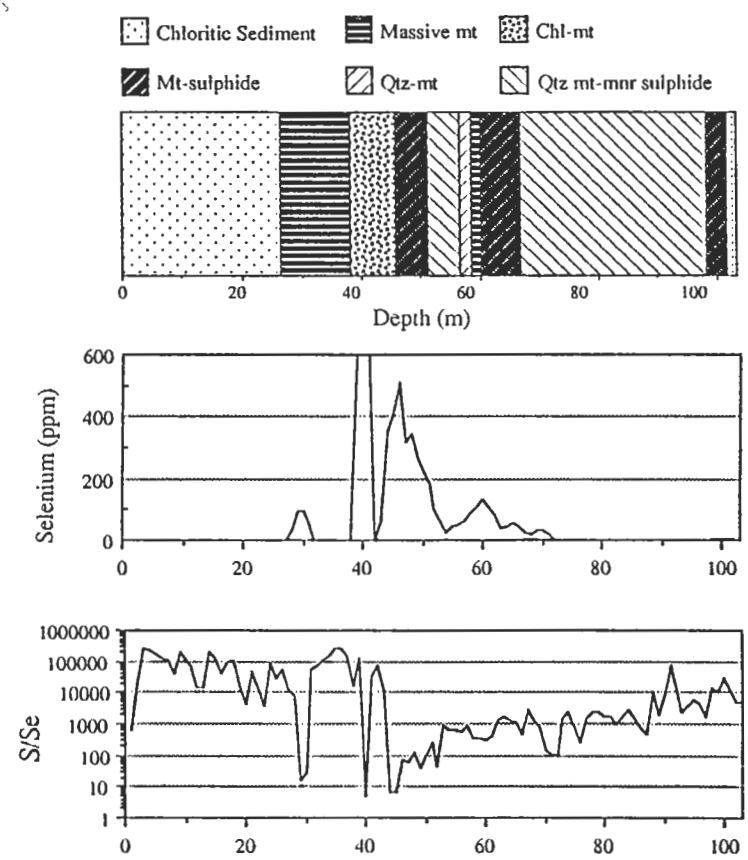

Figure 5.17 — Element variation and geology in drillhole 9/814/12: Se and S/Se.

company report), the results appear to have been insufficient to warrant its' extraction from the ore.

In drillhole 9/814/12, selenium is enriched in the magnetite-chlorite and magnetite-sulphide assemblages, and although there is a marked decrease in its' abundance across the lode, there is a similarity to the pattern of enrichment exhibited by the bismuth group of elements (Fig. 5.17). The dramatic decrease in selenium abundance (41–44 m) matches similar falls in the bismuth group of elements and corresponds to the zone of extreme gold enrichment. The good correlation between selenium and bismuth (Fig. 5.18) suggest bismuth sulphosalts are the main host for selenium, although there is a population of relatively high bismuth samples from the massive magnetite zone, where selenium values at or near the detection limit.

The decreasing abundance of selenium across the lode is similar to the pattern observed in the composition of bismuth sulphosalts in the Juno mine (Large, 1974. 1975). A plot of S/Se values in drillhole 9/814/12 (Fig. 5.17) shows a marked increase across the lode with the exception of the gold-rich zone and the massive magnetite footwall where values are close to those in the footwall sediments. Selenium also shows a weak enrichment in the footwall of the lode similar to molybdenum and uranium.

Uranium

Uraninite has been identified in Juno (K.Wright, 1969, unpublished company report), and Warrego (S. Whitehead, 1969, unpublished AMDEL report) mines, and anomalous uranium contents have also been identified in several mines and prospects in the Tennant Creek area (Large and Robinson, 1987). Uranium in drillhole 9/814/12 shows the same treble peak distribution of bismuth, lead, and antimony, although there is not the same dramatic drop in abundance corresponding to the gold-rich zone (Fig. 5.19). There is also minor enrichment in the footwall of the lode.

The good correlation of uranium with bismuth (Fig. 5.20), suggests an association between the two, although rather than representing a trace element in bismuth sulphosalts, the relationship may simply indicate a close paragenetic relationship. This relationship is supported by the observed intimate association of rich uraninite mineralisation (1–2 volume %) with bismuthinite and hematite (S. Whitehead, 1969, unpublished AMDEL report).

Zinc

Zinc mineralisation (as sphalerite) accompanies lead in several of the Tennant Creek mines as described above, and has also been recorded in the Argo mine (Meade, 1986), but in all cases concentrations are insufficient to warrant extraction. Sphalerite has been

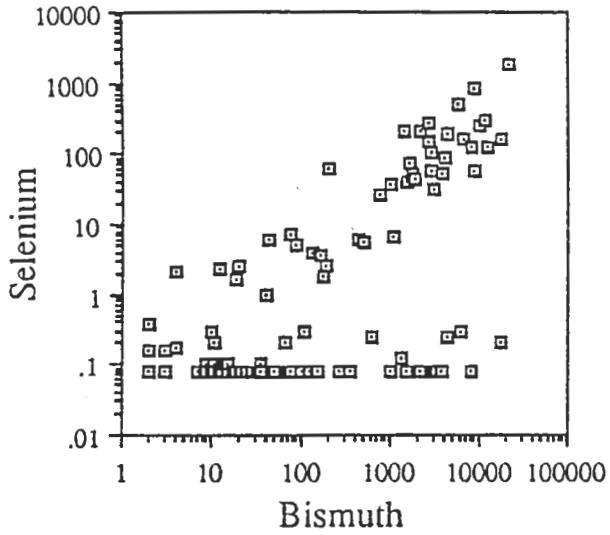

Figure 5.18 — Co-variation of Se with Bi in drillhole 9/814/12.

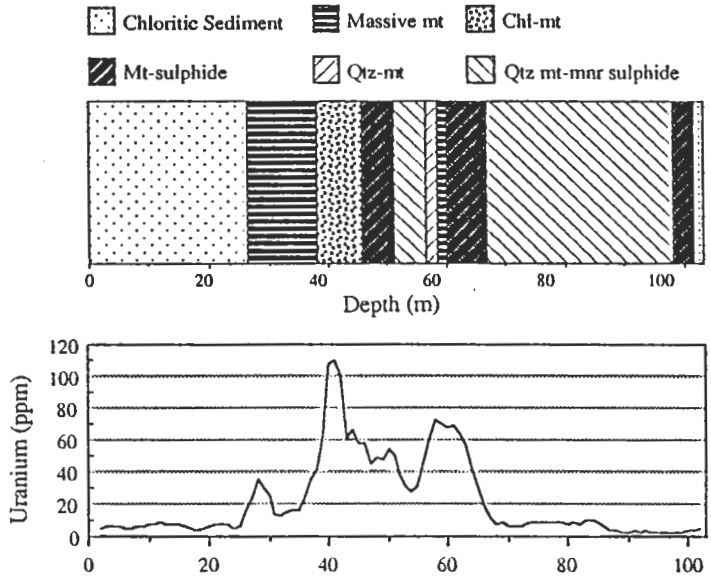

Figure 5.19 — Element variation and geology in drillhole 9/814/12: U.

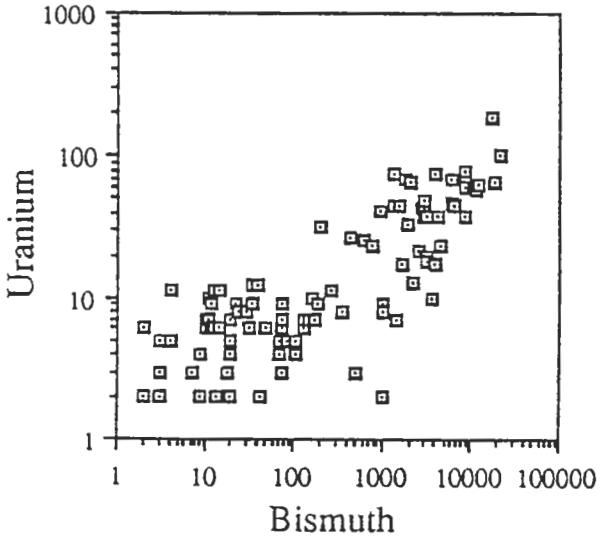

Figure 5.20 — Co-variation of U with Bi in drillhole 9/814/12.

observed as microscopic inclusions in chalcopyrite in the copper orebodies in the Warrego mine (Chapter Six), but has not been observed in lower levels.

In drillhole 9/814/12, zinc shows a distribution pattern similar to that of copper, with the highest values concentrated toward the hangingwall side of the main magnetite-sulphide zone (Fig. 5.21). In the ironstone lode zinc levels are generally elevated relative to the sediments although values in the main quartz-magnetite approach these low levels. The highest zinc values are slightly displaced (1–2 m) form the peak copper values in the main magnetite-sulphide zone and a general zonation in this assemblage of bismuth-copper-zinc is apparent from footwall to hangingwall.

Rubidium

Rubidium typically substitutes for potassium in feldspar, biotite and muscovite, and as such its abundance in the drillhole is likely to reflect the changing proportion of these minerals. Because muscovite is the dominant potassic mineral in the Warrego sediments and lode, it is likely to be the major host of rubidium. However, rubidium is also mobile under conditions of hydrothermal alteration, and is generally depleted in the sediments surrounding the Warrego lode (Chapter Seven).

The abundance of rubidium in drillhole 9/814/12 appears to reflect this relative mobility during alteration (Fig. 5.22). The less intensely altered sediments immediately adjacent to the ironstone lode contact (Appendix B), are relatively enriched compared to stringer mineralisation at the start of the drillhole (0–15 m), and within the lode itself. Rubidium contents in sediments adjacent to the lode are still depleted relative to unaltered sediments remote from the ironstone lode (200–300 ppm). Within the ironstone lode the low levels of rubidium reflect the treble peak concentration pattern of the bismuth mineralisation indicating an association of muscovite with economic mineralisation.

Strontium

Like rubidium, strontium rarely forms its own minerals and typically substitutes for calcium or potassium in plagioclase, muscovite, and biotite. Strontium is therefore expected to be concentrated in muscovite and display a distribution pattern similar to that of rubidium. While mirroring the enrichment of rubidium in the unaltered relative to the altered sediment, abundances within the lode are quite different displaying a distribution pattern identical to the bismuth group of elements (Fig. 5.22). Similar to antimony there is an excellent correlation between bismuth and strontium above bismuth values of between 100 and 1000 ppm (Fig. 5.23). This strong correlation with bismuth, and lack of an appropriate calcic host phase suggests that strontium may occur as a trace constituent in the bismuth sulphosalts.

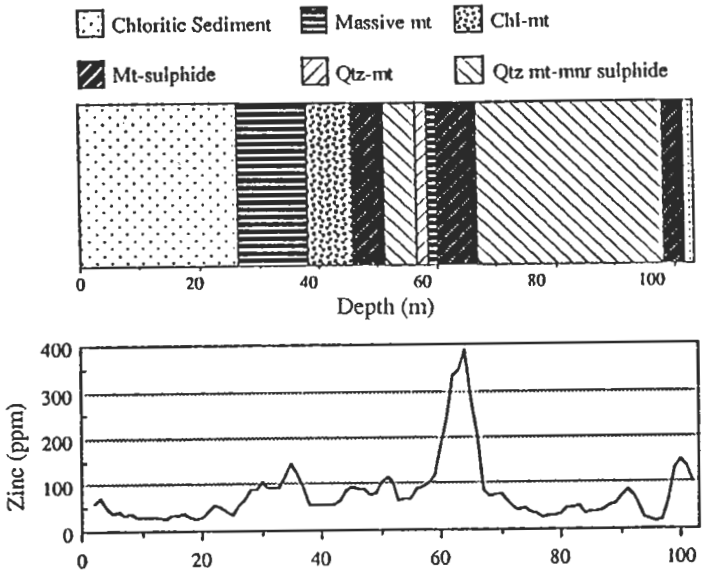

Figure 5.21 — Element variation and geology in drillhole 9/814/12: Zn.

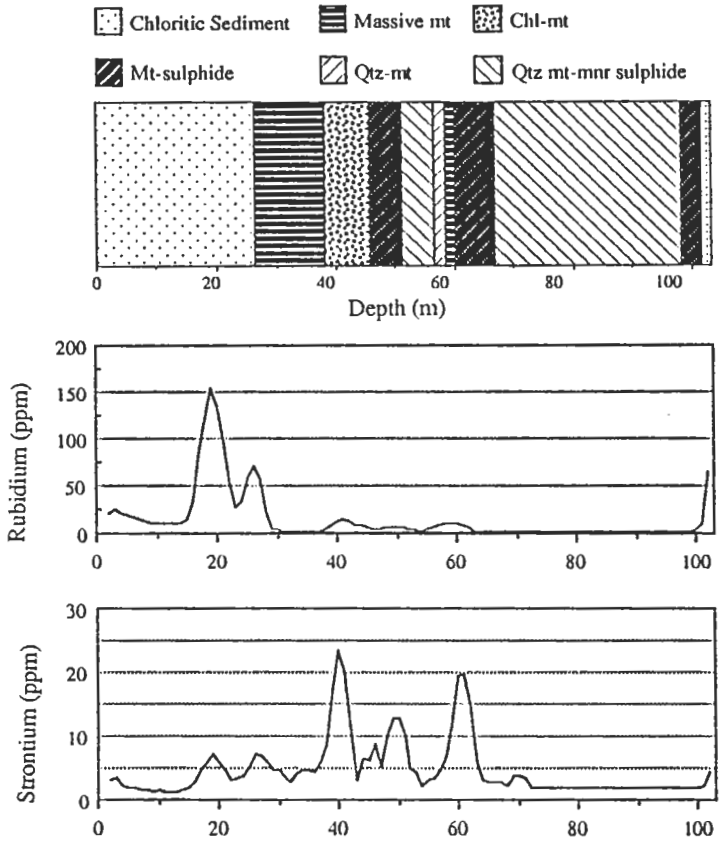

Figure 5.22 — Element variation and geology in drillhole 9/814/12: Rb & Sr.

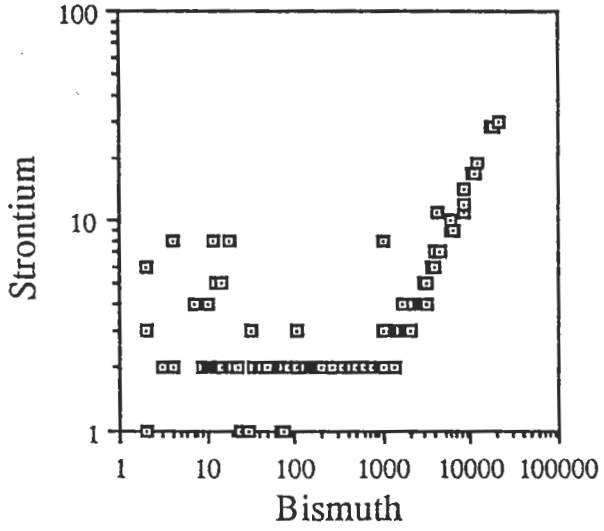

Figure 5.23 — Co-variation of Sr with Bi in drillhole 9/814/12.

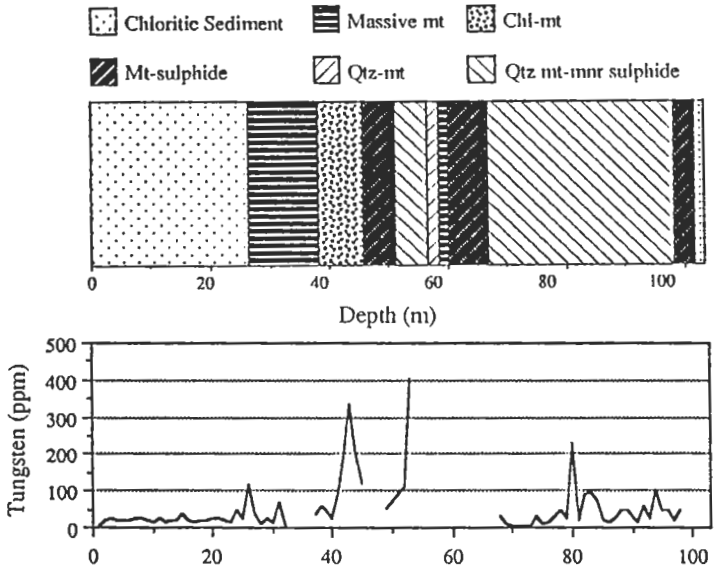

Figure 5.24 — Element variation and geology in drillhole 9/814/12: W

Tungsten

Although rare, tungsten mineralisation has been reported in the Tennant Creek Goldfield. Ivanac (1954) recorded grains of 'wolfram' at the Olive Wood prospect, and significant, but localised quantities of scheelite have been reported in Argo mine (R. Baxter, pers. comm., 1985). Horvath (1988) identified significant enrichment of tungsten in samples from the Eldorado mine with values in the massive magnetite/ hematite lode and adjacent stringer zone of between 30 and 1400 ppm.

Because of strong bismuth interference, it was not possible to analyse tungsten for the full length of drillhole 9/814/12, but localised enrichment up to 400 ppm was identified (Fig. 5.24). Although there is insufficient information to allow correlation with most of the other elements, there is an overlap of high-grade gold and tungsten.

5.8 Summary and Discussion

On a cross-section scale it is possible to identify a relatively simple overlapping zonation of gold, bismuth, and copper for section 8140N (Fig. 5.4), but on a smaller scale the situation is more complex. Extreme gold enrichment with low associated bismuth and copper is observed in the centre of the magnetite-chlorite zone in drillhole 9/814/12. On the footwall side of this zone the expected metal zonation is reversed i.e. gold-bismuth-copper towards the footwall, and as at Juno mine (Large, 1974), there is a relatively well defined concentration of uranium between the zones of maximum gold and bismuth enrichment. Zonation on the hangingwall side of the gold pod is less well defined, and although zones of maximum bismuth and copper mineralisation generally overlap, copper is marginally displaced toward the hangingwall to produce the expected gold-bismuth-copper zonation sequence.

Separated from the gold pod by a zone of relatively barren quartz-magnetite the main magnetite-sulphide zone shows a different zonation pattern. Copper and gold are strongly correlated, both increasing in content through the massive-magnetite to the centre of the magnetite-sulphide zone before dropping markedly into the quartz-magnetite. Bismuth is concentrated on the footwall side of the magnetite-sulphide zone and rapidly declines into into the copper-gold association. Zinc is concentrated in the centre of the magnetite-sulphide zone where copper begins to decline.

Concentrations of all trace elements in the quartz-magnetite zone are significantly reduced, often to levels below those recorded in the relatively unaltered sediments of the footwall. It seems likely that the drop in grade of the quartz-magnetite zone is the result of a combination of factors which might include:

1. A change in the physico-chemical conditions promoting metal deposition,
2. Dilution caused by the deposition of barren quartz, and/or
3. An inability of mineralising solutions to penetrate a pre-existing quartz magnetite assemblage.

Because quartz appears to be an integral part of the mineral zonation pattern in Warrego and other ironstone lodes, and overprinting by later quartz veins is not observed in magnetite-chlorite and magnetite-sulphide assemblages, the first option is preferred.

These observations are consistent with a simple footwall to hangingwall physico-chemical gradient across the lode very similar to that described at Juno mine (Large, 1974, 1975), with the exception that the zonation has been modified by a strong lateral component to the fluid flow through the ironstone lode. It is suggested that mineralising fluids penetrated the ironstone lodes at the site of the gold pods and were then able to migrate laterally through the core of the lode (Fig. 5.25). From the above observations it appears that the mineralisation overprint in section 8140N has been incomplete, and that fluid flow was restricted to two relatively permeable zones. The result has been the repetition of metal zonation patterns such that the gold pod is zoned from a gold-rich core through bismuth and copper towards *both* the hangingwall and footwall. The second permeable zone contains copper-rich mineralisation with bismuth concentrated toward the footwall. Thus the gross features of the expected zonation pattern are observed, but in detail the patterns are more complex. This result is compatible with the computer modelling of ore reserves by Quinlan and Leahey (1979) which suggested the gold pods were composed of several discrete gold-rich zones.

An implication of this detailed zonation study is that the core of the gold pod is not intersected in section 8140N. Gold pod mineralisation is separated from the footwall by some 10 m of relatively barren massive magnetite, and the flow of mineralising solutions appears to be controlled by permeable zones within the lode. Also the footwall alteration is less intense in the immediate footwall of the lode. Up section from 8140N, the gold pod rapidly diminishes, and gold-rich copper ore extends through the core towards the hangingwall (Fig. 5.8). However, down section in 8120N and 8100N, high-grade gold mineralisation ($\geq$ 50 g/t) is concentrated at the contact between the ironstone lode and footwall stringer zone, and is surrounded by well developed bismuth and copper zones (Fig. 5.26). It therefore seems likely that mineralising fluids were concentrated in the vicinity of 8100N to 8120N, where they penetrated the ironstone lode via permeable zones. Lateral fluid flow through multiple fracture systems resulted in the modified zonation observed in section 8140N.

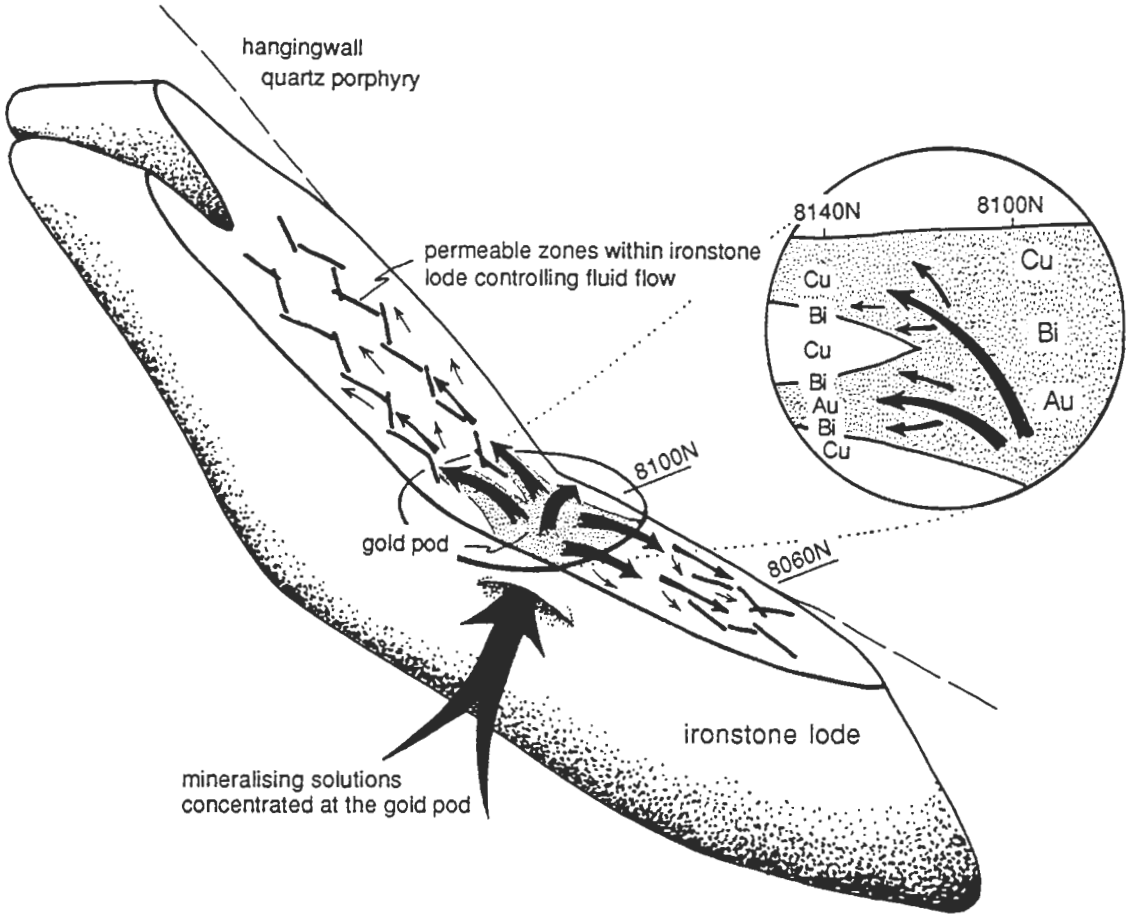

Figure 5.25 — Proposed model for the formation of mineral zonation observed in drillhole 9/814/12. Fluid flow is concentrated in the region of the gold pod between 8100N and 8120N and then follows fractures laterally through the lode. Two main fluid fluid conduits are recognised from perturbations in the expected metal zonation.

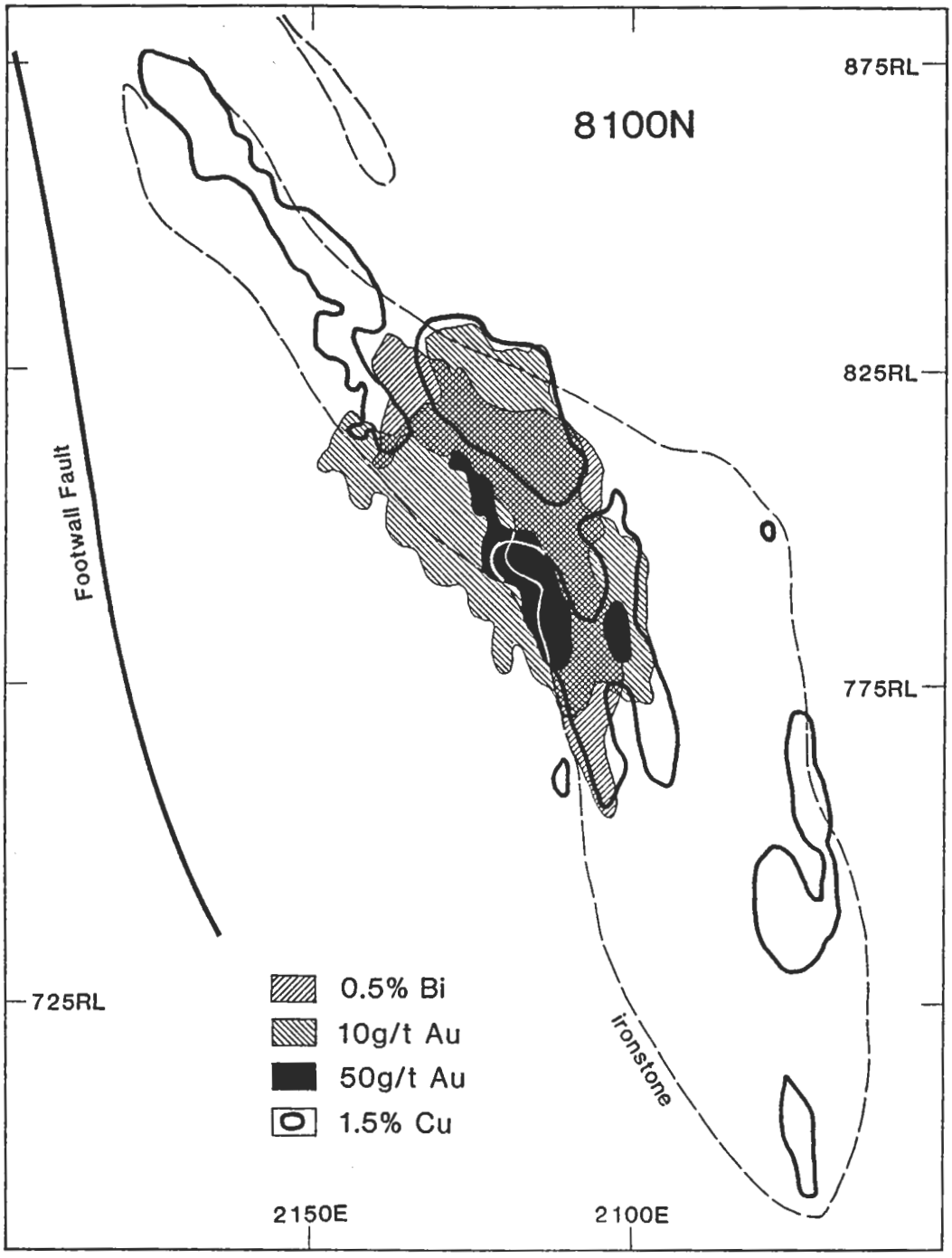

Figure 5.26 — Metal distribution in section 8100N. The well developed zonation pattern and concentration of gold right on the footwall contact of the ironstone lode suggest that this is the site of fluid access to the lode during mineralisation.

Chapter Six

PETROGRAPHY AND PARAGENESIS

6.1 Introduction

The mineral associations observed within and adjacent to the Warrego ironstone lodes (stringer-mineralisation, magnetite-chlorite, magnetite-sulphide, and quartz magnetite) have been described on a hand specimen scale in Chapter Three. This chapter documents in detail the petrography of these mineral associations based on careful examination of drillcore specimens in polished thin section. Once again the majority of samples were collected from the four mine sections already discussed (i.e. 8340N, 8140N, 8060N, and 7980N); comparisons are made with other Tennant Creek ironstone lodes where information or samples were available.

Rather than simply document the mineral associations observed, this chapter will include a description of the paragenetic relationships and probable controls on mineral formation that may be inferred from the textural relationships. Minerals observed in the Warrego ironstone lodes are described individually rather than their occurrence in a particular association because characteristic textures are often common to several associations. Where available, details on the chemical composition and general chemistry of the phase will also be discussed.

6.2 Magnetite

Magnetite is the most abundant constituent in the ironstone lodes, but its proportions are quite variable depending on the mineral assemblage with which it is associated. Magnetite may comprise almost 100% of the lode in the irregular lenses of massive magnetite that occur without any apparent pattern of distribution throughout the lodes, or as little as 40 volume % within the quartz-magnetite assemblage which is commonly restricted to the lode margins.

Petrography

Three forms of magnetite are recognised in polished thin section on the basis of crystal morphology, and the characteristic associations of these polymorphs provide insights

into the conditions associated with ironstone lode formation, and separate the process into two distinct phases. The characteristic polymorphs of magnetite are:

Type I: The bulk of the magnetite in the lodes comprises a mass of equigranular magnetite crystals ranging in size from 20–100 microns that have curved, sutured grain boundaries. This texture is best observed after etching with HI for up to one minute, but is readily recognised as the areas of massive, finely pitted magnetite common of all lode mineral associations.

On a thin section scale, zones of Type I magnetite are essentially massive and monomineralic, and where associated with other minerals, these invariably occur in fractures that overprint the Type I magnetite. Minor chlorite is observed at magnetite grain boundaries, but as this may be related to either the deposition of magnetite, or subsequent fluid infiltration along grain boundaries from nearby fractures, its paragenetic position is ambiguous. The granoblastic texture characteristic of Type I magnetite suggests possible recrystallisation, but if so, it is not related to contact metamorphism associated with the intrusion of the Warrego Granite. Identical textures have been described in most of the Tennant Creek ironstone lodes, the majority of which are well removed from the known occurrence of post-mineralisation granite intrusion, e.g Ivanhoe and Orlando, (Toole, 1966, unpublished report to Mount Isa Mines Ltd.), Juno (Large, 1974), Eldorado (Norris, 1980; Horvath, 1987), and White Devil (Nguyen, 1987; Nguyen et al., 1990).

Type IA: Intimately associated with Type I magnetite, but subordinate to it, Type IA stands out as it forms radiating aggregates of bladed magnetite crystals and colloform clots which show concentric zoning that may be up to 2 mm in diameter (Plate VII A-C). These textures are observed in thin section throughout the ironstone lodes, always within massive Type I magnetite, but without any apparent pattern to their distribution. Rare macro-colloform banding of magnetite and chlorite is observed in the magnetite-chlorite mineral assemblage (Plate VII A), but because the magnetite is texturally different (Type II) and chlorite is a major constituent of the assemblage, this is considered to be unrelated to the paragenesis of magnetite Types I and IA.

Spherulitic and bladed magnetite has been documented in nearly all Tennant Creek deposits; including Peko (Edwards, 1955, Wright, 1969), Golden Forty (Wyborn, 1971), Juno (Large, 1974, 1975), Gecko (Large, 1974), Eldorado (Norris, 1980, Horvath, 1987), and Argo (Meade, 1986). Such textures appear to be more abundant in these deposits compared to Warrego, and frequently show delicate colloform textures or internal grain shapes that are not observed at Warrego (e.g. Large, 1975, Fig. 12). Large (1974, 1975), also describes macro-colloform textures in the magnetite-chlorite zone of Juno mine where inter-banded magnetite and chlorite

Plate VII

A: Example of the variable textures observed in the magnetite chlorite assemblage ranging from relatively massive magnetite to finely banded colloform textures. Gold and bismuthinite mineralisation is restricted to cracks and fractures in the magnetite. Sample 109304 is 11cm across.

B: Colloform clots of Type IA magnetite cut by later chalcopyrite veins. Sample 106958.

C: Clot of Type IA magnetite showing preferential replacement of hematite around its margin. Sample 108683a.

D: Skeletal Type II magnetite lining and partially filling a fracture in massive Type I magnetite. Sample 108879. Coin is 2·5cm across.

E: Photomicrograph illustrating the relationship of Type II magnetite overgrowths on Type I magnetite in chalcopyrite-filled fractures. Sample 109178.

F: Bands of coalesced Type II magnetite impart a 'colloform-like' texture with the chlorite-muscovite matrix. Sample 109304.

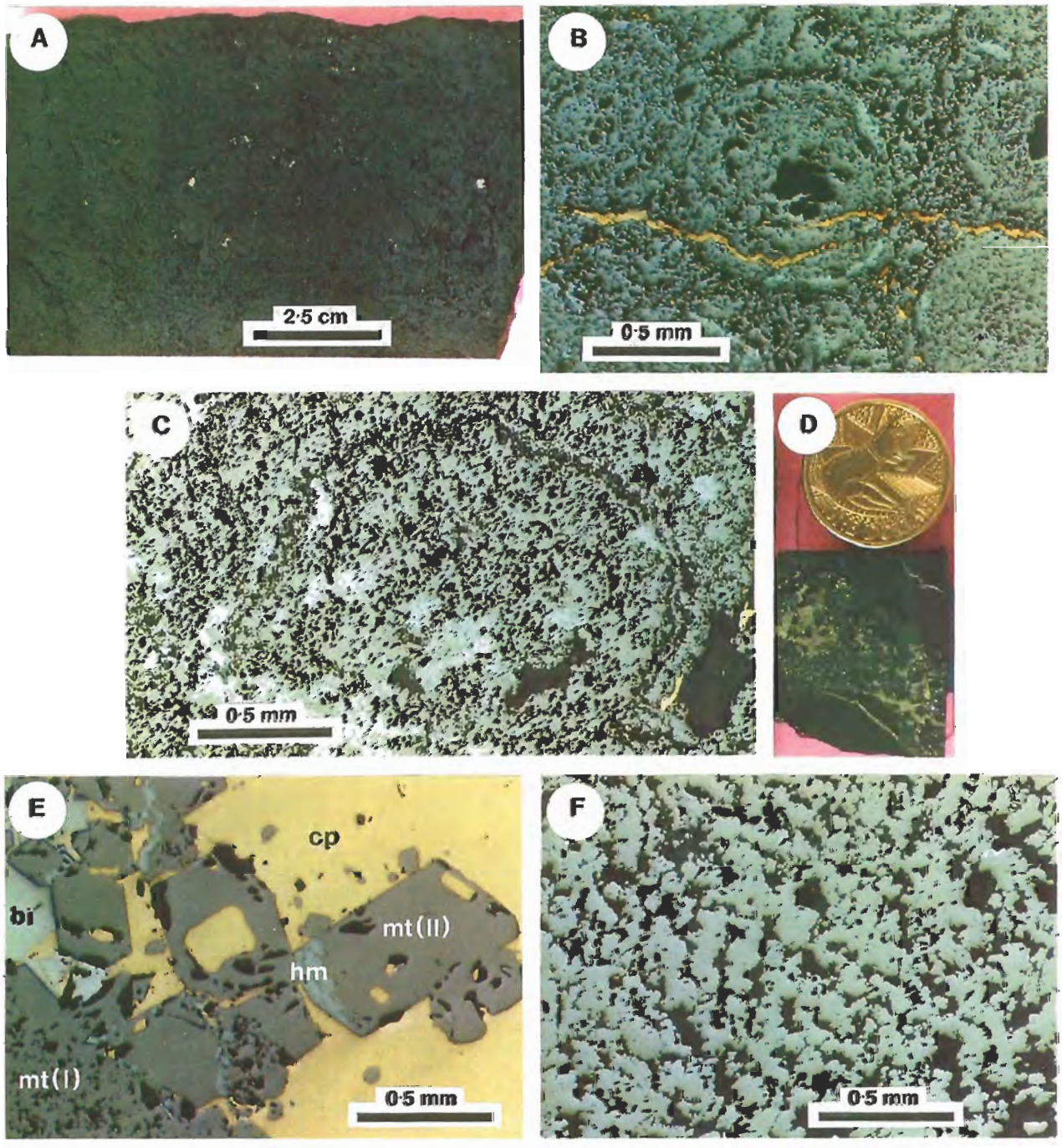
A
2·5 cm
B
0·5 mm
C
0·5 mm
D
E
cp
bi
mt(II)
hm
mt(I)
0·5 mm
F
0·5 mm

form fist-size botryoidal clumps that are possibly analogous to the macro colloform textures observed at Warrego.

The spherulitic and bladed magnetite textures are considered to be primary textures and are directly related to the precipitation of magnetite at the time of ironstone lode formation. While it is uncertain if Type I magnetite represents an unmodified crystallisation texture, both it and Type IA clearly related to ironstone lode formation, preceding the introduction of economic mineralisation, and are therefore termed primary magnetite.

Type II: Lining virtually all cracks and fractures in the massive primary magnetite is a selvedge of coarsely crystalline euhedral magnetite in which individual crystals may be up to 2 mm across (Plate VII D), but are more typically are in the range of 0.1–0.5 mm (Plate VII E). The crystals are often skeletal with large cavities that are typically infilled with chalcopyrite (Plate VII D & E). The degree to which Type II magnetite fills the fractures is quite variable; complete filling of fractures by Type II magnetite may be distinguished by the better polish taken by this form of magnetite, and the euhedral grain boundaries often delineated by minor interstitial sulphides or chlorite. These Type II magnetite-filled veins are characteristic of narrowing terminations to wide chalcopyrite-filled fractures. Fractures with only minor Type II overgrowths are also common where only a thin selvedge can only be resolved at high powers of magnification under the microscope. Type II magnetite is associated with economic mineralisation, and again this relationship has been described in other Tennant Creek ironstone lodes e.g Juno (Large, 1974, 1975), Golden Forty (Wyborn, 1971), and Gecko (Large, 1974).

A variant of the Type II magnetite is the abundant, fine grained (less than 0.2 mm), euhedral magnetite which, disseminated through the Black Eye Member becomes increasingly concentrated in the chloritic sediments adjacent to the ironstone lodes. There is an almost complete transition from chloritic sediment with disseminated magnetite to massive magnetite lode in the magnetite-chlorite gold pods in the footwall of the No. 1 orebody. Magnetite euhedra become so abundant they begin to coalesce to form an open aggregate in a matrix of chlorite (Plate VII F). However, while this area clearly represents an area of lode construction, it is unrelated to the formation of the primary lode. The magnetite-chlorite zone is intimately associated with gold mineralisation, and peripheral to this footwall lode constructional area, the gold pod mineral assemblage is restricted to fractures within the primary lode typical of the majority of economic mineralisation within the lode.

Magnetite stringers in the footwall of the gold pods vary from trains of coarse euhedral magnetite which may be only one crystal wide in a chlorite-muscovite matrix, to 1–2 cm wide zoned veins with a semi-massive core of coalesced magnetite surrounded by narrow margins of finer grained magnetite that grade laterally into

chloritic sediments and disseminated fine magnetite (Plate IV D). These stringers may carry significant gold mineralisation, or be totally barren of economic mineralisation which is to be expected of footwall zones where alteration associated with both ironstone lode formation has been pervasively overprinted by that associated with economic mineralisation. The limited extent of the footwall stringer system exposed in the Warrego mine make meaningful interpretation of this zone virtually impossible.

Paragenesis and Formation of the Magnetite Lode

The Type IA magnetite textures preserved within Warrego and other ironstone lodes are not restricted to the Tennant Creek environment; similar textures have been recognised in a variety of ore forming environments including banded-iron-formations (Han, 1978a, 1978b), volcanogenic massive sulphide deposits (Frater, 1983, Huston, 1988), skarns (Stevenson and Jeffery, 1964, Norris, 1985), and the magnetite flows of El Laco, Chile (Henriquez and Martin, 1978). The acicular, bladed and colloform textures are not a characteristic crystal form of magnetite, and it is likely they reflect the replacement of a hematite or hydrated iron oxide precursor (Ramdohr, 1969; Large, 1974; Han, 1978a, 1978b). Alternatively conditions of extremely rapid precipitation of iron as it is dumped from a supersaturated solution in response to changing physico-chemical conditions might result in the direct precipitation of magnetite in these uncharacteristic crystal forms. Hildebrand (1986) has suggested similar textures in the El Laco magnetite may result from direct sublimation of magnetite from an iron enriched supercritical fluid.

Much debate has centred on the origin of the colloform textures observed in the Tennant Creek ironstone lodes, and generally parageneses involving a colloidal precursor have been favoured in the past, e.g. Wright (1969), and Large (1974, 1975). Large proposed a metasomatic process of ironstone lode formation at Juno mine, suggesting that total chlorite replacement of the sediments preceded the bulk precipitation of amorphous iron-oxide hydroxides which in turn replaced chlorite. However, conditions favouring the formation of colloidal iron-oxide hydroxides appear to be restricted to relatively low temperature and pressure environments. The currently forming metalliferous sediments containing iron oxide hydroxides described in the Red Sea (Bischoff, 1969a, 1969b; Zierenberg and Shanks, 1983; Singer and Stoffers, 1987), and at mid ocean ridges (Alt et al., 1987), are forming on the seafloor under low pressure and at temperatures that are less than 100°C. Similarly the genesis of banded-iron-formations has also been attributed to colloidal processes (Han, 1978a, 1978b; Ewers and Morris, 1981) at, or near the seafloor, under low temperature conditions.

Bischoff (1969b) describes the goethite-amorphous facies of the Atlantis II Deep as comprising spherules of poorly crystalline goethite and amorphous "limonite" that are less than 50 μm in diameter, and experimental studies on the aging of iron oxide gels produce particles of similar or smaller diameter (Collepardi et al., 1972, 1973; Murray, 1979). This size range is significantly smaller than the microscopic textures observed within the ironstone lodes and is incompatible with macro-colloform textures observed in Juno mine (Large, 1974, 1975). Another feature of the experimental studies and descriptions of the currently forming deposits is the relatively low temperatures (less than 100°C) at which these apparently metastable materials were converted to hematite (Bischoff, 1969a; Collepardi et al., 1972,1973; Murray, 1979) and magnetite (Hackett and Bischoff, 1973).

Based on the probable thickness of Carraman formation overlying the Black Eye Member (Le Messurier et al., in press), the ironstone lodes must have formed at depths of at least 2 km below the surface, and assuming the geothermal gradient is the sole heat source for the hydrothermal fluids, minimum temperatures in the vicinity of 100°C are indicated. This temperature is likely to be a gross under-estimation in view of the unknown true thickness of sediment originally overlying the the Black Eye Member, and the probability that significantly higher geothermal gradients were present during a tectonically active period that was associated with granite intrusion and volcanism. It is therefore suggested that under these conditions the ironstone lodes were formed via direct precipitation of hematite rather than via some gel or colloidal precursor.

Type I magnetite probably represents modified primary magnetite lode resulting from heating and recrystallisation although not necessarily implying a Type IA precursor. This process may have been accompanied by the introduction of economic mineralisation. In the Warrego mine, Type IA magnetite appears to be less common and is without the delicate internal textures observed in other ironstone lodes possibly suggesting that the intrusion of the Warrego Granite is responsible for the complete or partial destruction of these textures through recrystallisation. Han (1978b) in his examination of microstructures in magnetite through induced oxidation of samples from banded-iron-formations has noted the obliteration of pre-existing hematite crystal textures at moderate metamorphic grades. Regardless of the initial state of the magnetite, a relatively simple relationship between the magnetite polymorphs is interpreted. Type I and IA represent the primary ironstone lode paragenesis, while Type II is related to the overprint of economic mineralisation.

Recently Edwards (1987), and Wall and Valenta (1990) have suggested that ironstone lode formation is likely to have occurred through open space filling of reverse fault/shear zones generated during folding of the Warramunga Group, and therefore the

observed colloidal textures are related to rapid crystallisation in open spaces in a manner similar to many vein deposits (e.g. Roedder, 1968). However, this observation belies textural evidence of at least a partial replacement paragenesis for the ironstone lodes, e.g. Plate V. The formation of hematite clots in chloritised sediment as illustrated in Plate V C, clearly demonstrates the viability of generating such textures via replacement.

The evidence in the zones of intense stringer mineralisation underlying the gold pods indicate processes of both replacement and open open space veining have operated. Two stringers varieties are recognised in the footwall:

1. Diffuse magnetite stringers with intense chlorite-magnetite alteration of the adjacent sediments (Plate IV D). Typically mineralisation is not associated with these veins; and
2. Sharp bordered breccia veins which frequently contain significant economic mineralisation (Plate IV C, and Plate VIII).

Plate VIII illustrates in hand specimen and thin section the relationship of gold-bearing stringers to the sedimentary host rocks. Clasts of sedimentary rock show no evidence of replacement by chlorite or magnetite associated with veining, but rather show strong contact recrystallisation of quartz suggesting that although hot, the mineralising fluids were in equilibrium with the sediment. Therefore the deposition of magnetite, chlorite, and muscovite mineralisation between the sediment clasts must have occurred largely through the infilling of open spaces.

The similarity in mineralogy (chlorite-muscovite-magnetite), and presence of abundant gold and bismuth mineralisation in the stringers, indicates they are related to the gold pod mineralisation. However, their relationship to the other mineral assemblages (magnetite-sulphide and quartz-magnetite) is less obvious. While the chlorite-muscovite assemblage is intimately intergrown with magnetite and there is no obvious fracturing of the lode, the magnetite-sulphide and quartz-magnetite assemblages are characterised by the filling of cracks and fractures in massive magnetite by chalcopyrite and quartz respectively.

Therefore, either the gold pod mineral assemblage differs from the others and has formed through the coalescence of stringers at the base of the ironstone lode, or similar to the other assemblages, fills open spaces within the fractured ironstone through the deposition of magnetite, chlorite and muscovite. The deposition of magnetite as overgrowths on pre-existing ironstone lode and infilling between fragments has created the semblance of relatively massive lode. Specimens from this assemblage (Plate VIII A, Plate VIII D), comprise relatively massive areas of magnetite surrounded by diffuse intergrowths of magnetite, chlorite, and muscovite which is compatible with this interpretation. Similarly, the outline of the footwall contact does not change in the

Plate VIII

A: Magnetite stringers associated with gold mineralisation illustrating the relatively unaltered nature of sediment clasts between stringers.

B: Photomicrograph of the area outlined in Plate VIIIA, illustrating the relatively unaltered nature of the sediment clasts between stringer veins. PPL.

C: Further enlargement of the edge of the clast outlined in Plate VIIIB. Recrystallisation of the clast margins indicate mineralising solutions were significantly hotter than the host rocks, but were compositionally in equilibrium.

D: Gold- and bismuth-rich magnetite-chlorite assemblage illustrating the complex parageneses of magnetite mineralisation. Patches of massive Type I magnetite are overgrown and infilled by diffuse banded magnetite-chlorite-muscovite mineralisation. Deformation associated with the intrusion of the Warrego Granite has remobilised bismuthinite into the fractures sub-parallel to cleavage.

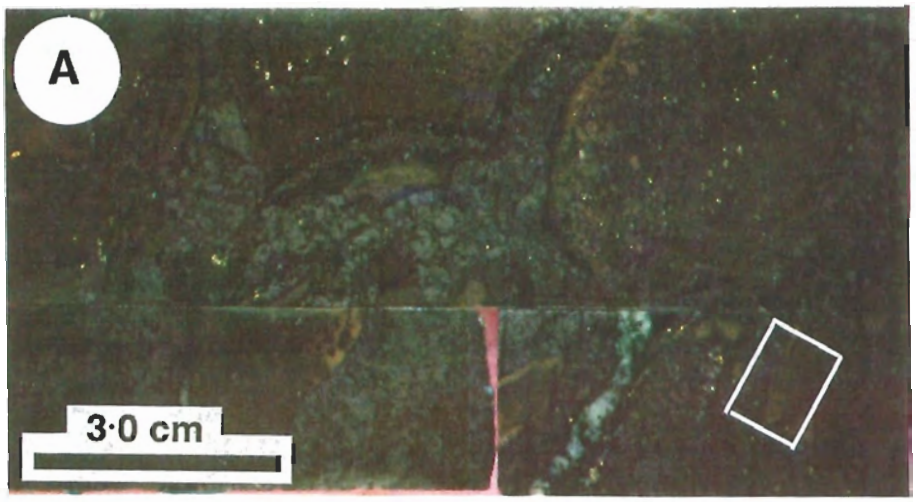
A
3·0 cm

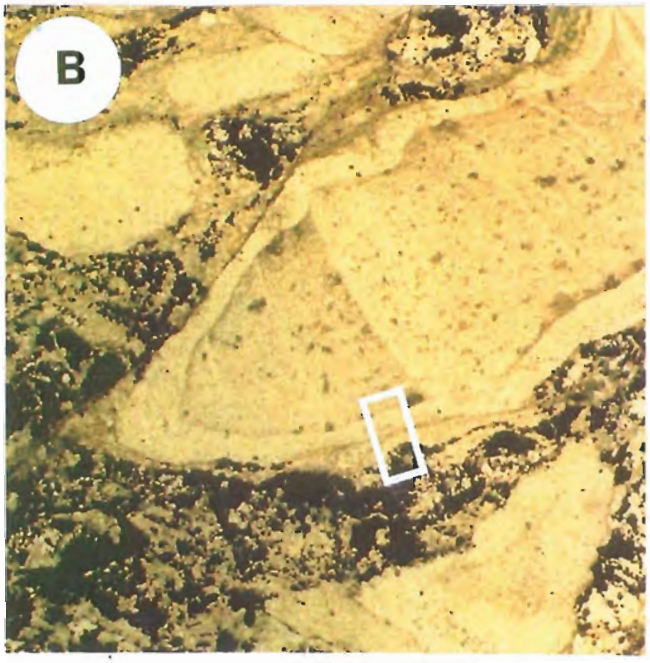
B

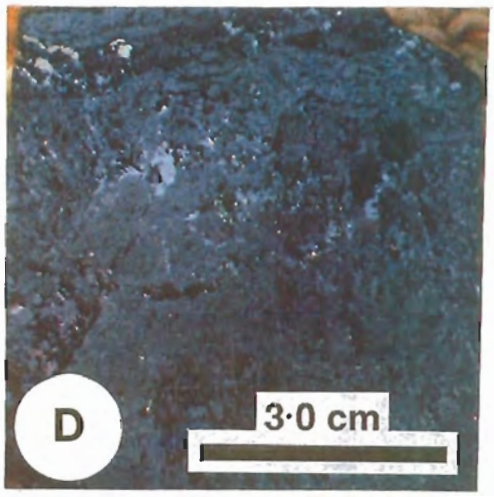
D
3·0 cm

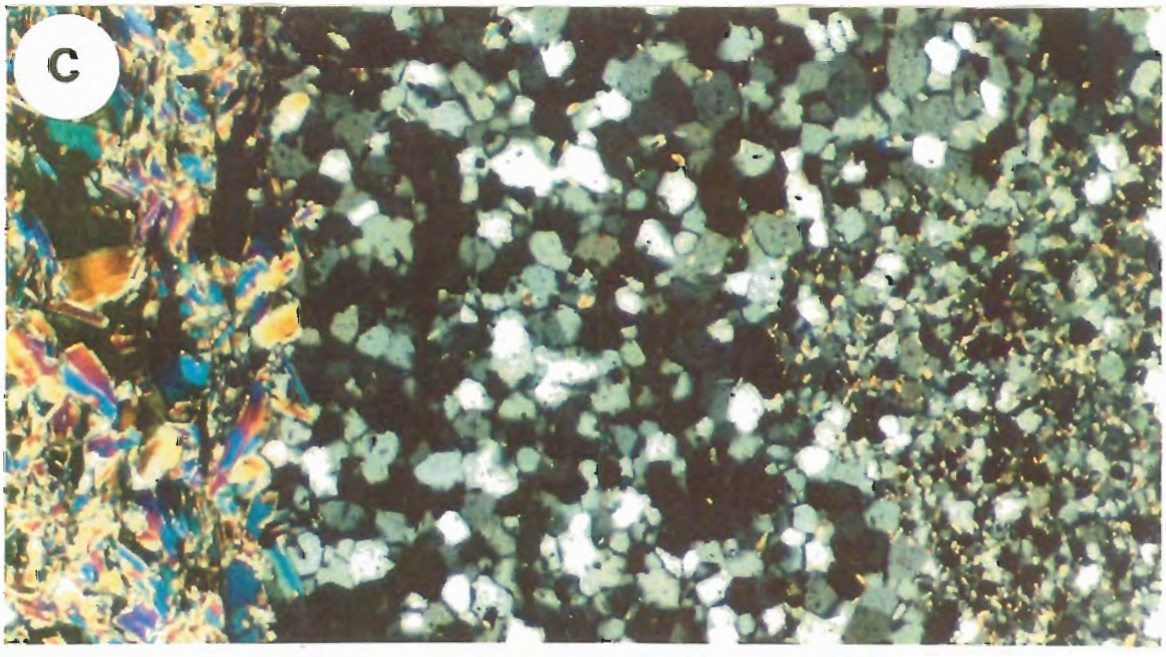
C

vicinity of the goldpods as would be expected if they were accreted onto the base of the lode (see Figs 5.4, 5.6 and 5.26). Therefore the latter option of infilling of fractured lode by a compositionally similar matrix is preferred.

In contrast, the Type 1 stringers are surrounded by diffuse haloes of chlorite and magnetite alteration which together with a decreasing magnetite grainsize from the core to vein edge strongly indicate at least, partial replacement of the sediment during their formation. These veins are also comprised predominantly of magnetite, suggesting that magnetite growth in the alteration assemblage occurs via chlorite replacement. Although cross-cutting relationships have not been observed, the two types of stringer veins are paragenetically distinct and appear unrelated. Type 2 stringers are clearly related to economic mineralisation, while Type 1 appear to be related to ironstone lode formation.

The abundance of textures that are indicative of replacement of sediment by chlorite and magnetite on a hand specimen and thin section scale supports the replacement model of ironstone lode formation proposed by previous workers, e.g. Large, 1974, 1975. However the cogent argument put forward by Edwards (1987), and Wall and Valenta (1990), requires further examination. The 'open-space' model is based largely on the low contents of immobile trace elements within the ironstone lode (Chapter Seven). Structural evidence of reverse faulting in the lode environment is contentious, stratigraphy may often be correlated on either side of the lode without displacement, e.g. Nobles Nob (Whittle, 1966; Rattenbury, 1989), Juno (Large, 1974, 1975), and TC8 (Wedekind et al., 1990) being notable examples. Detailed mapping of the Nobles Nob open pit also revealed there is no fault control on the emplacement of the lode (Rattenbury, 1989).

The extent of the trace element 'dilemma' for a replacement model is presented in detail in Chapter Seven, but is graphically illustrated in Plate IX. Typical polished thin section examples of sedimentary rock that has been completely altered to chlorite and magnetite adjacent to the ironstone lode are illustrated. Almost without exception these contain abundant, finely disseminated needles of rutile and occasional euhedral, zoned zircons of undoubted magmatic origin. These minerals clearly illustrate the expected immobility of at least Zr and Ti in this environment. Yet in the immediately adjacent ironstone lode, rutile and/or zircon has *never* been observed. Either zircon has been completely removed, or the lodes represent open space filling.

Some textural evidence of zircon mobility is observed as delicate zircon overgrowths on most of the magmatic zircons (Plate IX C), and zircon has been identified within two of the Tennant Creek ironstone lodes. Horvath (1988) identified a solitary zircon associated with quartz-magnetite lode at Eldorado mine, and more significantly Whittle (1966) has documented *"abundant zircon where it* (chalcopyrite)

Plate IX

A: Highly altered sediment in the immediate footwall of the No.1 orebody with abundant disseminated magnetite and chalcopyrite mineralisation. The sedimentary origin of the rock is recognised by the presence of blades of rutile and euhedral magmatic zircons. Sample 109058.

B: As in A (PPL). Note the presence of hydrothermal monazite and xenotime surrounding the zircon crystal.

C: Back-scattered electron image of a zircon from the footwall alteration zone illustrating the zircon overgrowth on the original crystal. The common observation of such overgrowths of inferred hydrothermal origin attest to at least some Zr mobility during alteration and mineralisation. Sample 109058.

D: Typical chloritic sediments in the footwall of the ironstone lode contain abundant disseminated magnetite and bladed rutile. Sample 108924.

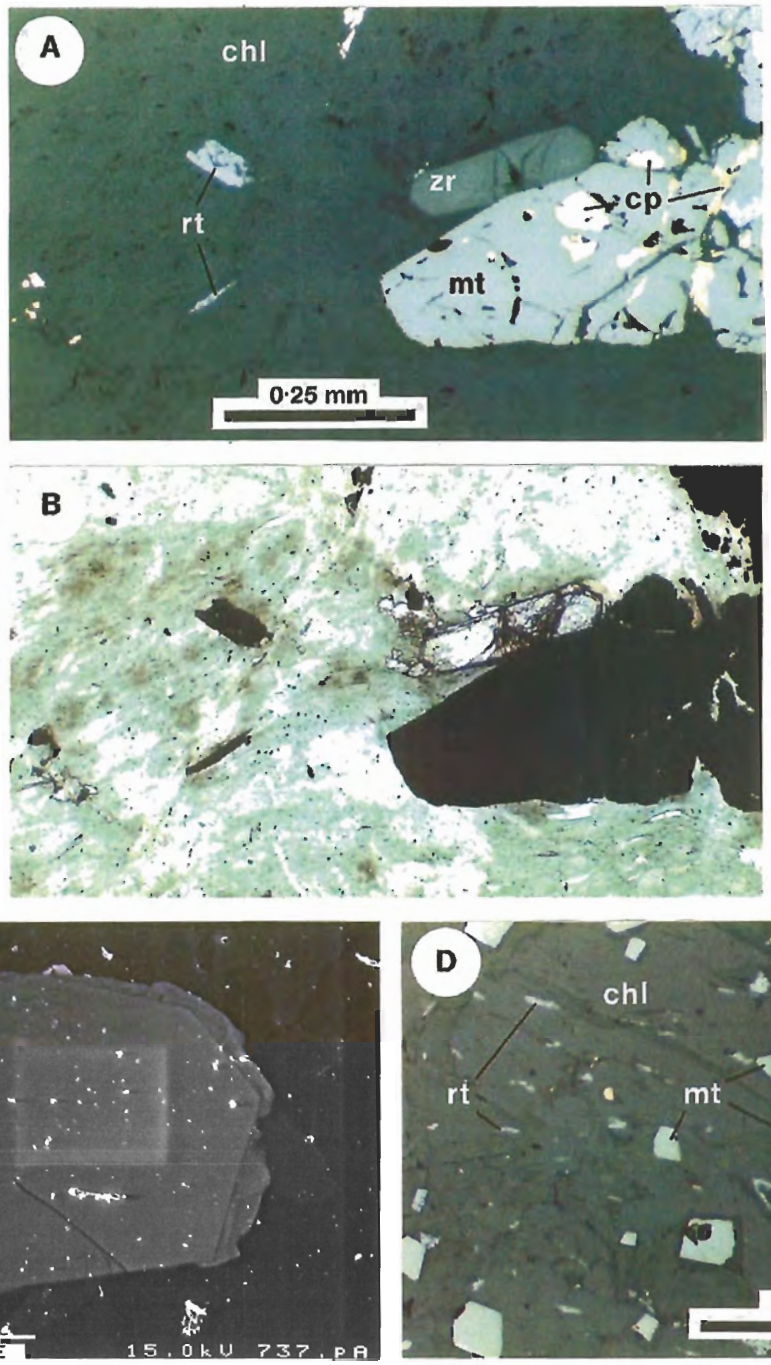
A
chl
rt
zr
cp
mt
0·25 mm
B
C
r20.00μ SE
15.0kV 737.pA
D
chl
rt
mt
0·2 mm

transgressed the talcose magnetite and pyrite-bearing lode material". Unfortunately this assemblage is not illustrated or discussed further, but it appears zircon has been mobile in the system and has been concentrated at a mineralogical contact that is possibly indicative of a physico-chemical boundary where zircon complexes in the fluid became unstable. Further evidence of immobile element 'mobility' is discussed in Chapter Seven, but it is apparent that given fluids of appropriate composition almost any element is mobile.

By way of explanation of Plate IX the mineral assemblage is characteristic of economic mineralisation, i.e. Type II magnetite associated with chalcopyrite mineralisation suggesting possible alteration of the lode margins via fluid migration during mineralisation. By implication, fluid flow associated with ironstone lode formation must have been considerably more intense, or was compositionally different and more corrosive.

Initial fluid flow associated with ironstone lode formation must have been localised by some pre-existing feature in the rocks, be it the propagation of fluid flow from blind thrusts localised in the cores of anticlines (Rattenbury, 1989), or concentration at the boundaries of apparently impermeable units (porphyry at Warrego, hematite shale at Gecko (An. 3), or sedimentary breccia at Gecko (K-44)). A process of alteration along this discontinuity is proposed that is in many respects similar to the relationship illustrated on a thin section scale in Plate V D. The cleavage-parallel quartz vein represents the channelised fluid flow, and the zone of chlorite alteration (much like a roll front uranium deposit) the envelope of sediment-fluid reaction. Wedekind et al. (1990) proposed actual lode formation is promoted by a redox barrier defined by hematitic sedimentary units within the stratigraphy and although obvious evidence of a more oxidised sediment package (i.e. hematite BIF) is lacking at Warrego, such a chemical control is not improbable (Chapter Nine).

Two other features of Plate V D, especially important to understanding ironstone lode formation, are: the sharp boundary to the alteration and the outer shell of hematite developed close to the contact. Knife-sharp lode boundaries are characteristic of the Tennant Creek orebodies where there is no development of an outer shell of partial replaced and fragmented host rock as are observed in other replacement deposits hosted by sediments or volcanics, e.g. de Roo (1989), and Beams and Hartley (1990). Similarly the initial precipitation of magnetite/hematite at the outer fluid interface might explain the common localisation of mineralisation within a brecciated ironstone core, e.g. Warrego, Peko (Elliston, 1966, Whittle, 1966), and possibly also Gecko (Huston, 1989). Formation of the lode from rim to core would maintain a plane of weakness within the lode that would be susceptible to subsequent deformation, whereas incremental growth of a lode from a core is likely to behave as a rigid block in which all subsequent deformation is localised at the lode margins. Support for this style of lode

formation is observed at Peko where near the base of the ironstone lode, the core comprises brecciated chloritic sediments. The development of an rigid outer zone would also have implications for the formation of the quartz-magnetite zones (see below).

It is suggested that pervasive chloritisation of the sediments through alteration and veining along the fluid conduit allows the growth of Type IA magnetite, transforming irregular stringer systems into massive lode. The formation of a homogeneous chloritic medium would permit crystal growth much as it would occur in, say, a magma. Random nucleation on pre-existing magnetite (or other phases) and rapid growth of crystals via fluid diffusion through the chlorite seems the most likely mechanism to produce the spherulitic textures.

Barton et al. (1977) attribute fibrous crystal growth and "gel" precipitates to very high degrees of supersaturation of a particular phase in the solution, which is not unlike the mechanism proposed to explain the spherulitic textures at El Laco where supersaturation in magnetite was achieved through degassing or rapid quenching of the melt, and crystal growth exceeded the rate of diffusion (Henriquez and Martin, 1978). Under such conditions it may be possible to directly crystallise magnetite in a bladed or colloform habit that is not typical of 'normal' equilibrium conditions.

Frater (1983) records the occurrence of spherical and nodular structures consisting of annular aggregates of fine quartz, chlorite, magnetite, and pyrite that are superimposed on tuffs and chlorite altered rocks up to 1 km away from the Golden Grove orebody. Their origin was similarly attributed to initially restricted crystal nucleation followed by supersaturated precipitation and rapid crystal growth in an isotropic medium.

6.3 Quartz

Quartz is an important component in most of the Tennant Creek ironstone lodes where it is typically observed in the form of cross-cutting buck quartz veins. Both the mineralised and unmineralised ironstone lodes contain significant quartz; typically its distribution through the lode is erratic, and some lodes are more strongly veined than others. Generally there is an antipathetic relationship between the occurrence of quartz and economic mineralisation, and therefore understanding its distribution within the lode is important to constraining the mineralisation process.

Petrography

The quartz-magnetite assemblage observed in the Warrego ironstone lode is dominated by quartz and magnetite (typically greater than 90 volume %), and generally other minerals such as chlorite or sulphide are a minor or insignificant proportion of the total. Quartz may constitute up to 60 volume % of the lode, occurring both as numerous

veins (less than 1 to 2 cm wide) and as pervasive flooding of the magnetite. Cross-cutting relationships between the veins imply this mineralisation was accompanied by intensive brecciation and fracturing of the lode, but typically it is impossible to directly determine the paragenesis of quartz relative to the economic mineralisation. Rare examples of mineralised ironstone occurring as fragments within the veins are observed suggesting that at least some of the veins are late- or post-mineralisation.

In some samples, delicate colloform textures between quartz and magnetite are preserved and appear to suggest that they were co-precipitated (Plate X A). An alternative paragenesis involving either the partial replacement of magnetite, or complete replacement of another phase (chlorite?) seems unlikely, and therefore at least some quartz was associated with the initial formation of the ironstone lode. Similar textures between magnetite and quartz have been observed in other mines in the Tennant Creek area, e.g. Juno (Wright, 1969; Large, 1974), Peko (Wright, 1969), and Gecko (Huston, 1990a).

Contact metamorphism associated with the intrusion of the Warrego Granite has totally recrystallised quartz within the Warrego ironstone lode, and has destroyed much of the information regarding the paragenesis and initial depositional state of the quartz. Recrystallisation also means all fluid inclusion evidence relating to the conditions of lode formation and mineralisation have been destroyed (Chapter Nine).

Paragenesis

Although quartz is not a major component in all of the ironstone lodes, e.g. Juno mine is characterised by relatively minor quartz-magnetite zones (Large, 1974, 1975), quartz often forms part of the overall mineral zonation pattern observed, e.g. Warrego, Peko (Elliston, 1966), Juno (Large, 1974,1975), and TC8 (Wedekind et al., 1990). To better constrain the paragenesis of silica deposition, the overall relationship of quartz to the zonation of the Warrego lode requires examination. Typically quartz is concentrated at the outer margins of the lode surrounding the quartz-free and often mineralised core. Quartz is virtually absent from the zones of stringer mineralisation and intense chlorite alteration in the footwall of the ironstone lode, and is an insignificant phase associated with gold pod mineralisation. However, in the magnetite-sulphide assemblage surrounding the gold pods, quartz increases in abundance towards the hangingwall (<20 volume %), to become the dominant mineral in the quartz-magnetite assemblage (~60 volume %). In the copper orebodies in the upper part of the mine, a core of magnetite-sulphide is generally surrounded by quartz-magnetite-sulphide, with quartz-magnetite zones generally restricted to the margins of the ironstone lodes (both footwall and hangingwall).

Plate X

A: Colloform magnetite textures preserved in the quartz-magnetite assemblage indicating their probable contemporaneous deposition as part of the original formation of the ironstone lode. Sample 109015.

B: Randomly oriented intergrowth of chlorite and muscovite characteristic of gold pod mineralisation. Sample 109306.

C: Common association of discrete chlorite blades in copper ore. Irregular pools of bismuthinite are a common accessory. Sample 109072.

D: Chlorite-muscovite intergrown with bismuthinite infilling fractured Type I magnetite from the central gold pod. Sample 109073.

E: Typical deformation textures in chlorite within the ironstone lode illustrating the kinking of crystals and infiltration of bismuthinite along cleavage planes. Sample 109305.

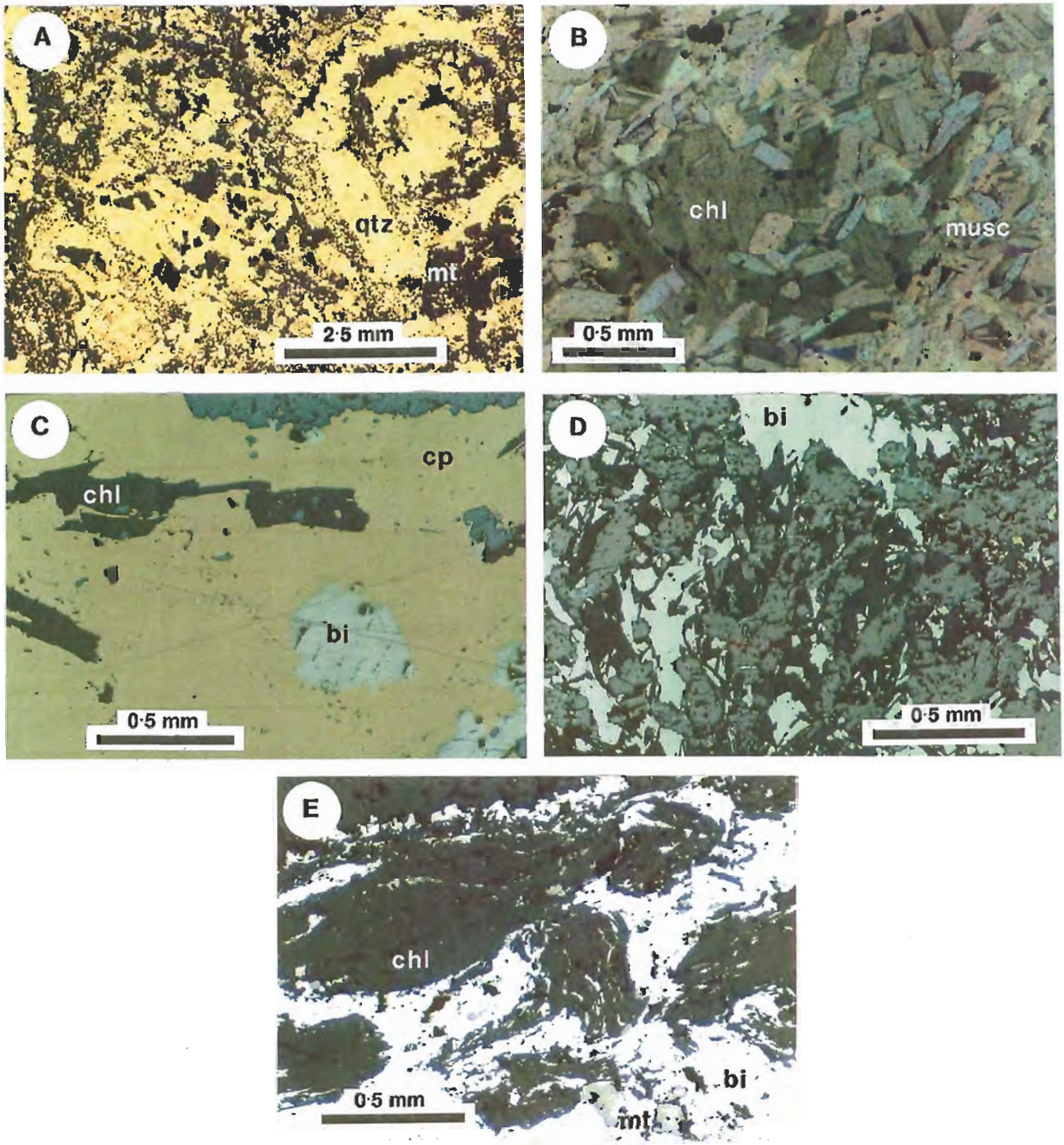
A
qtz
mt
2·5 mm
B
chl
musc
0·5 mm
C
cp
chl
bi
0·5 mm
D
bi
0·5 mm
E
chl
bi
0·5 mm
mt

The increasing proportion of quartz through the magnetite-sulphide assemblage toward the lode margins, together with the transition from mineralised to barren veins suggest that the deposition of quartz is part of the zonation associated with economic mineralisation and was deposited in response to the same physico-chemical conditions that promoted ore deposition. However, the barren character of the quartz-magnetite may in part reflect the presence of primary quartz-magnetite lode assemblage which has effectively sealed these zones from later mineralising fluids. The prevalence of barren quartz zones surrounding the gold pods in the lower levels of the mine (Chapters Three & Five) apparently reflect a difference in the intensity, or timing, of mineralisation in the gold pod compared to the copper orebodies.

Although the quartz magnetite zones are characterised by cross-cutting quartz veins, the ironstone fragments between the veins are similarly veined on a smaller scale and also contain complex intergrowths of quartz and magnetite. It is therefore concluded that an outer quartz-rich zone was intrinsic to the ironstone lode prior to economic mineralisation, and therefore related to the process of ironstone lode formation. In the model of ironstone lode formation developed in Section 6.2, an early formation of massive lode at the outer margins of the chlorite alteration zone is implied, and as such would tend to respond differently to deformation than the relatively chloritic core. Fracturing of this outer ironstone during continuing deformation and/or fluid overpressuring might be expected to promote both quartz and magnetite deposition through the associated pressure release as fluids are drawn into the fractures, e.g. Fournier, 1986. Thus the development of a quartz-magnetite outer margin would result as part of the process of ironstone lode formation and might effect the later deposition of economic mineralisation.

6.4 Chlorite

Chlorite is an important constituent both within, and adjacent to, the Warrego, and other Tennant Creek ironstone lodes. It is the dominant mineral associated with hydrothermal alteration of the host sediments, and is an important accessory mineral accompanying economic mineralisation. There is an increasing abundance in chlorite toward the ironstone lode margins, where together with disseminated magnetite it replaces the original sediment. Although the width of intense alteration at the ironstone lode contact maintains a fairly uniform 10 cm along the hangingwall, in the footwall it varies from several metres, to up to forty metres in the vicinity of the gold pods. Sediments surrounding this zone of intense alteration generally show extensive chloritisation of the matrix and occasional cleavage-parallel chlorite ± magnetite ± sulphide veining. The intensity of alteration generally diminishes with distance, but because of the limited access and overprint of contact metamorphism it has not been possible to define the transition from the hydrothermal alteration to a regional

greenschist assemblage. Generally, visible signs of chloritisation associated with hydrothermal alteration are not apparent beyond 50 m from the lode margins.

Chlorite is also abundant within the ironstone lodes where it is the dominant silicate mineral associated with economic mineralisation. Chlorite occurs with muscovite in the gold pods (up to 40 volume %), and is the predominant, often only, silicate in the magnetite sulphide zone (≤ 5 volume %). At the outer margins of the magnetite sulphide zone, an increasing abundance of quartz corresponds to decreasing chlorite and sulphide contents, before complete transition to the quartz-magnetite zone which is largely devoid of chlorite.

Petrography

Chlorite shows limited textural variation within and surrounding the Warrego ironstone lodes. Three varieties are identified which are related to their host (sediment or ironstone lode), and their paragenesis. In the sediments, with the exception of retrograde chlorite after biotite and cordierite, matrix chlorite shows a strong preferred orientation parallel to the cleavage. Individual crystals form thin, discrete blades that are generally less than 0.1 mm in length, and they are pleochroic (straw-yellow to green), showing anomalous purple-blue interference colours (Plate I D). Pseudomorphous retrograde chlorite after biotite and cordierite preserves cross-foliation orientations and poikilitic textures respectively. Chlorite after biotite is typically a darker green (in plain polarised light) than that associated with the sediment matrix (Plate II E), but the diffuse chlorite after cordierite does not appear to differ from the that of the matrix.

Intensification of hydrothermal alteration toward the ironstone lodes occurs with an increasing proportion of matrix chlorite (through quartz dissolution), and the occurrence of stringers of chlorite ± magnetite ± chalcopyrite. In the matrix, masses of fine chlorite with a strong preferred orientation predominate, while in the sub-parallel to cleavage stringers, chlorite is coarser (≤0.5mm in length), and tabular in outline (Plate IV A). This coarse, massive style of chlorite that is directly associated with mineralisation forms the second chlorite association. Deformation of both stringer and matrix chlorite occurs in cleavage parallel shears, and the development of chlorite pressure shadows around the rigid magnetite crystals is common (Plate II F).

Within and immediately adjacent to the gold pods chlorite loses its preferred orientation, and occurs in randomly oriented masses of tabular crystals, often intergrown with muscovite, magnetite, bismuthinite, and gold (Plate X B & D). Moving from the footwall into the magnetite-chlorite zone, magnetite becomes more massive with the chlorite and economic mineralisation restricted to cracks and fractures. Although the abundance of chlorite reduces with increasing sulphides (predominantly chalcopyrite), chlorite maintains both its size and tabular shape, with crystals occurring either discretely or in clusters within the sulphide (Plate X C). Although not as strong

as that observed in the sediments, deformation of the chlorite within the ironstone lode is commonly observed as kinked crystals, with remobilisation of sulphides along cleavage traces (Plate X E). It is evident that chlorite within the ironstone lode has been protected from much of the post-mineralisation deformation associated with granite intrusion.

Chlorite directly associated with economic mineralisation generally shows the same straw-yellow to pale green pleochroism of the host rock chlorite, and has anomalous purple-blue to brown interference colours. However, within the gold pods, dark-green to yellow-brown pleochroic chlorite with dark blue-grey interference colours is also observed. Although texturally similar to other chlorites in this zone, their frequent association with paragenetically late, quartz-filled fractures, hematite alteration, and the remobilisation of gold and bismuthinite mineralisation suggest they may be related to localised, post mineralisation alteration and recrystallisation of the ironstone lode. Further evidence of late-stage alteration of the magnetite-chlorite is the apparent zonation in some chlorites when observed under crossed polars. Rimming, and along cleavage traces, the replacement of purple-blue by brown birefringent chlorite is relatively common in the gold pods especially in kinked and deformed crystals suggesting alteration to a less iron-rich composition (e.g. Laird, 1988). This alteration is clearly post-mineralisation, and may be associated with either the waning stages of mineralisation or the intrusion of the Warrego Granite.

The third chlorite association occurs in distinct veinlets ($\leq$ 0.5 mm wide) of fine, radiating, yellow to emerald-green chlorite. The veinlets are observed in all mineral assemblages throughout the ironstone lodes; the veinlets cross-cut all other parageneses of chlorite, and clearly represent very late-stage hydrothermal alteration.

Chemistry

In excess of 500 microprobe analyses of chlorite have been made from samples collected from the Warrego mine (Appendix D). Before compilation, the chlorite data were first 'cleaned' in the manner of Foster (1962), such that analyses suggesting admixture of mica through intergrowth or beam overlap (i.e. Na_2O, K_2O, or CaO $\geq$0.5 wt.%), and/or giving totals indicating significantly high or low water contents (>91 wt.% and <86 wt.% respectively) were rejected. Chemical formulae were calculated on the basis of 28 oxygen atoms, and the assumption that all iron is ferrous following the method outlined by Deer et al. (1966). Although there are typically many analyses from a single thin section, no attempt has been made to 'average' compositions because, significant scatter between petrographically indistinguishable chlorites occurs on the scale of a single thin section.

To examine the variability of chlorite composition within, and surrounding the Warrego ironstone lode, samples have been divided into lode: magnetite-chlorite (mt-

chl), magnetite-sulphide (mt-side), and quartz-magnetite (qtz-mt), and host rocks: altered sediment (altd sed), sediment (sed), and porphyry. In order to examine the compositional variation of chlorite within the goldfield additional samples from Juno mine (including analyses from Large, 1974), Explorer 28 prospect and TC8 mine are included.

Following Bayliss' (1975) proposal to simplify the overly complex nomenclature of chlorites, they are subdivided into iron- and magnesium-rich end members only (chamosite and clinochlore respectively), with the adoption of compositional modifiers as suggested by McLeod and Stanton (1984), (Figure 6.1). Chlorite variation within the sample set is illustrated by plotting analyses on a $Fe^{\#1}$ versus Si diagram which illustrates both tetrahedral substitution of Al^{IV} for Si, and octahedral solid solution of Fe^{2+} and Mg^{2+} in the chlorite structure (Fig. 6.2).

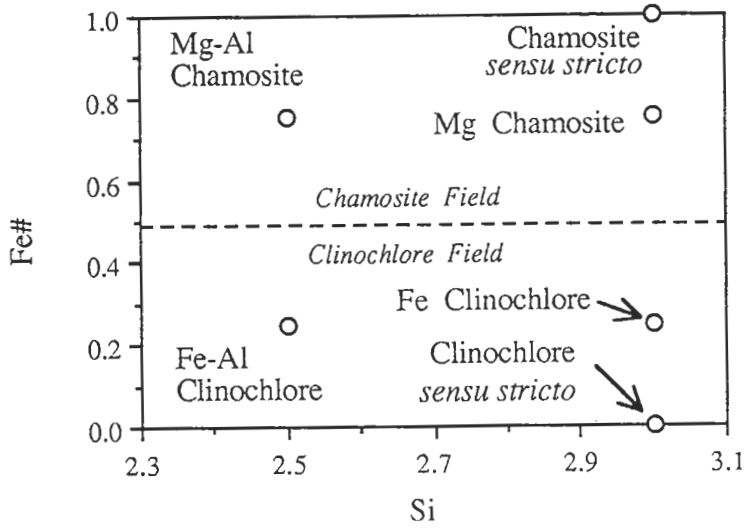

Figure 6.1 — Chlorite classification scheme following the recommendations of Bayliss (1975) and McLeod and Stanton (1984).
Chamosite *sensu stricto* = $(Fe_5Al)(Si_3Al)O_{10}(OH)_8$;
Clinochlore *sensu stricto* = $(Mg_5Al)(Si_3Al)O_{10}(OH)_8$;
Mg-Al Chamosite = $(Fe_{3.75}Mg_{1.25}Al)(Si_{2.5}Al_{1.5})O_{10}\ OH)_8$;
Mg Chamosite = $(Fe_{3.75}\ Mg_{1.25}Al)(Si_3Al)O_{10}(OH)_8$;
Fe-Al Clinochlore = $(Mg_{3.75}Fe_{1.25}Al)(Si_{2.5}Al_{1.5})O_{10}(OH)_8$; and
Fe Clinochlore = $(Mg_{3.75}Fe_{1.25}Al)\ (Si_3Al)O_{10}(OH)_8$.
$Fe^{\#}$ = Fe/(Fe+Mg).
(Adapted from McLeod and Stanton, 1984).

[1] $Fe^{\#}$ = Fe/(Fe + Mg)

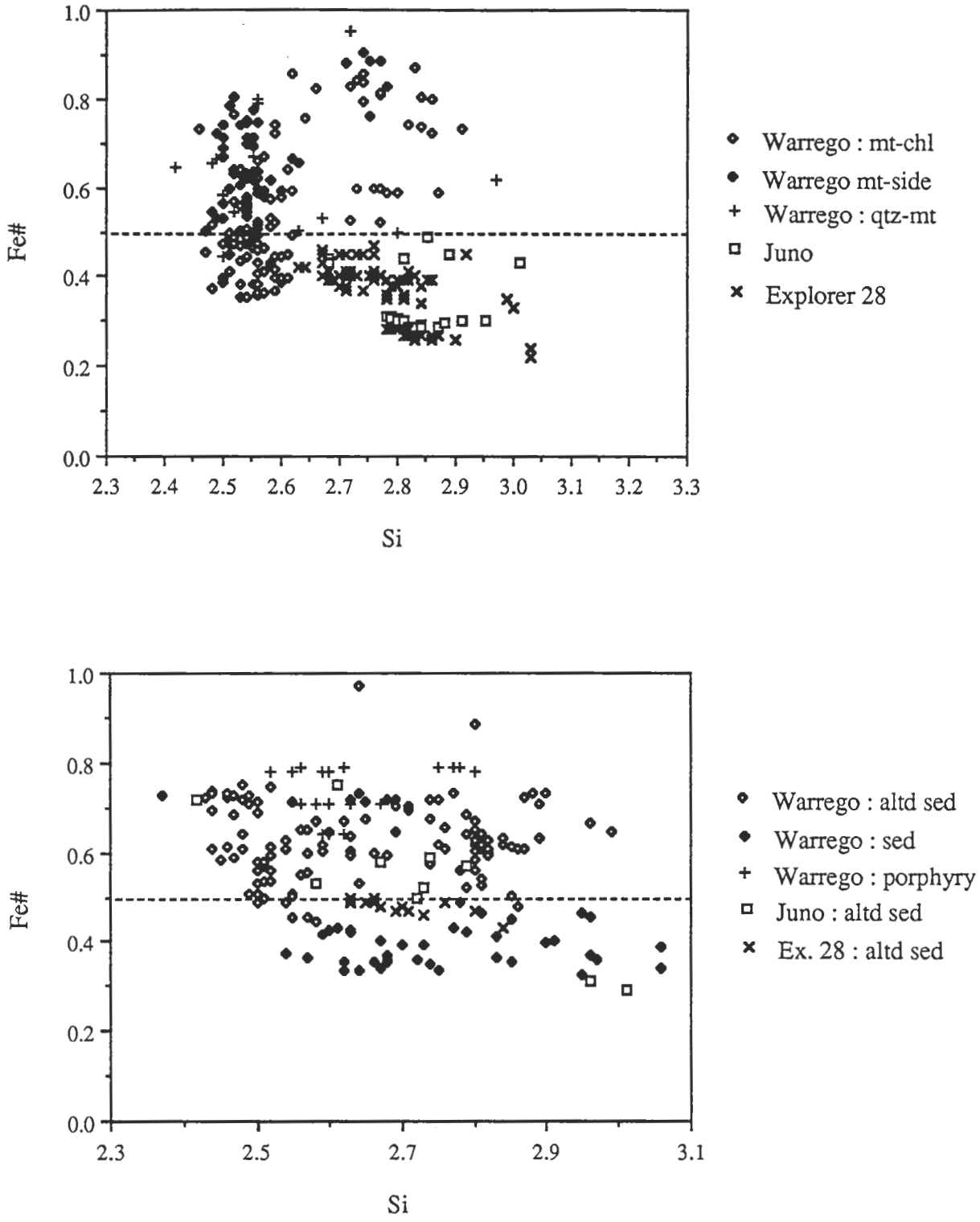

Figure 6.2 — Composition of chlorites from the Warrego ironstone lode and adjacent sediments. Chlorites from Juno mine and Explorer 28 prospect are included for comparison.

Within the ironstone lode two general groupings are evident, the majority of chlorites are aluminous varying between iron-rich clinochlore (Fe-Al clinochlore) and Mg-rich chamosite (Mg-Al chamosite), while the remainder are iron-rich and less aluminous. This second grouping corresponds to the late-stage, yellow-emerald green chlorites described above, and confirms their different paragenesis from the main mineralisation event.

Although the composition of chlorites from the three lode assemblages broadly overlap, those from the magnetite-chlorite show a trend to magnesium-rich compositions with a significant proportion (44%) of the analyses falling in the clinochlore field. Chlorites from the magnetite-sulphide assemblage, fall predominantly within the chamosite field. To examine this compositional variation in greater detail, magnetite-chlorite samples containing visible gold, and gold-rich magnetite-sulphide samples have been plotted individually in Figure 6.3. Excluding late emerald green chlorite analyses, the gold-rich, magnetite-chlorite samples are relatively homogeneous compositionally, and are in large part responsible for the magnesian-rich trend in the data set. In contrast, within sample variation in the magnetite-sulphide samples is greater, and they are more iron-rich in composition.

The compositional range of chlorites from the quartz-magnetite and magnetite-sulphide assemblages are indistinguishable. Because quartz-magnetite proper is generally devoid of chlorite, and these chlorites are associated with minor sulphide mineralisation, they are interpreted to represent magnetite-sulphide mineralisation localised within the quartz-magnetite assemblage.

In comparison to the bulk of the Warrego ironstone lode data, chlorites from Explorer 28 prospect, and Juno mine are magnesium rich, and broadly overlap the range in $Fe^{\#}$ of the gold-rich samples from the magnetite-chlorite zone in Warrego. However, unlike the Warrego analyses, they show significant variation in their Si content, and in both Explorer 28 and Juno, the full spectrum is observed within a single thin section. Although several chlorite parageneses are evident in the Explorer 28 samples (Appendix H), chlorites from Juno are petrographically identical (Large, 1974).

Analyses of the chlorite composition of sediments within the Warrego mine sequence were obtained from the suite of samples collected on 14 level (Chapter Seven), and altered sediments were sampled adjacent to the lode on several mine sections. The sediment chlorites are readily distinguished from hydrothermal chlorites on the basis of their composition. Chlorites from the sediments show a wide range in Si that is similar to the ironstone lode samples from Juno and Explorer 28, but show a relatively restricted range in $Fe^{\#}$ falling within the clinochlore field. In contrast, the altered sediments are variable both in terms of Si and $Fe^{\#}$ falling predominantly within

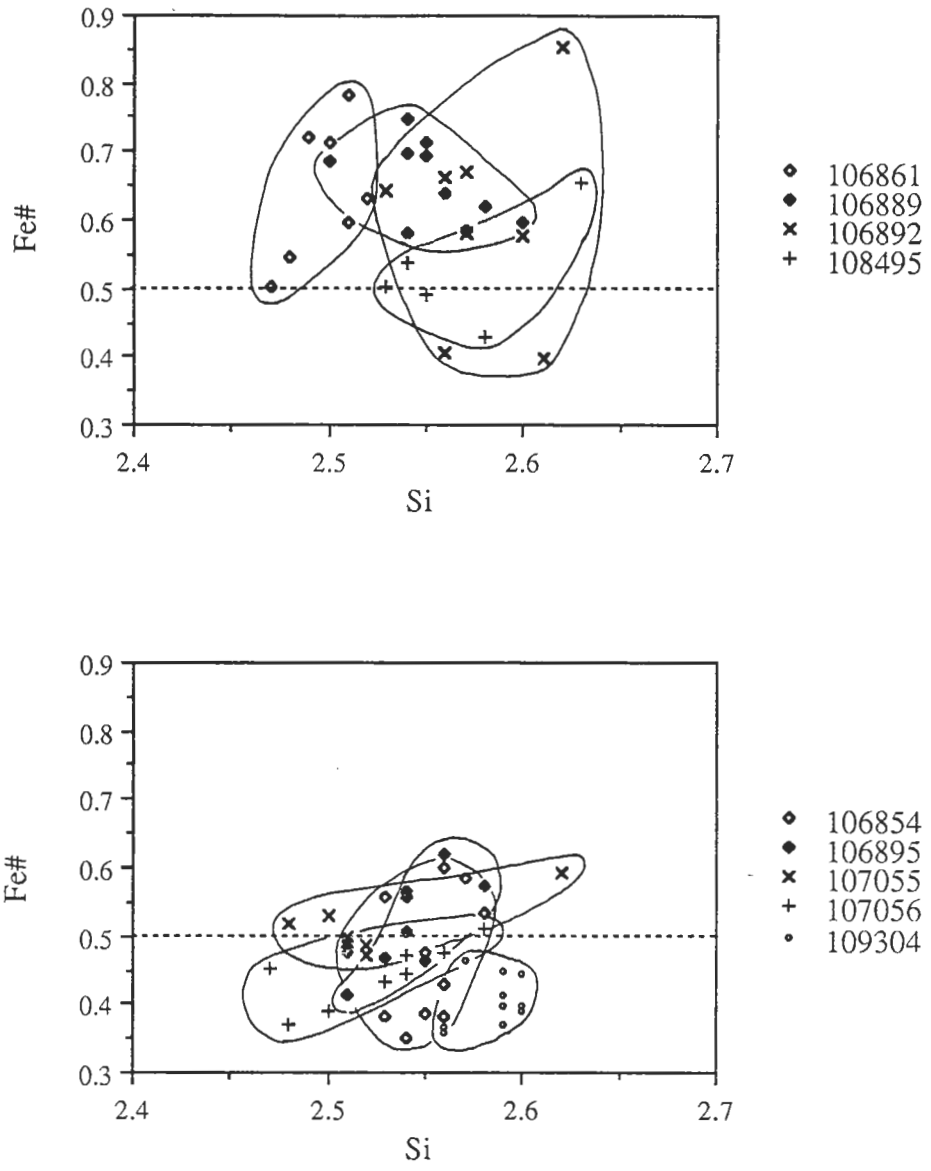

Figure 6.3 — Within sample compositional variation of chlorites from the Warrego ironstone lode. Top: Samples from the magnetite-sulphide zone are predominantly chamositic in composition. 106861 (11·0 g/t Au), 106889 (7·3 g/t Au), 106892 (51·1 g/t Au), and 108495 (0·6 g/t Au). Bottom: Samples from the magnetite-chlorite zone are more restricted in composition and tend to clinochlore compositions. 106854 (811·5 g/t Au), 106895 (3·4 g/t Au), 107055 (292·0 g/t Au), 107056 (570·0 g/t Au), and 109304 (~1000 g/t Au).

the chamosite field. The small cluster of 'unaltered' analyses plotting well within the chamosite field are from the dyke in the immediate footwall of the No. 3 orebody, again emphasising its different chemistry relative to the adjacent sediments (Chapter Seven).

Chlorites in hydrothermally altered sediments and stringer mineralisation from Explorer 28 (single sample), and Juno (seven samples), show a compositional range that is similar to those from Warrego, however the trend to increasingly magnesian compositions from the footwall altered sediments to the outer talc-magnetite zone observed at Juno (Large, 1974, 1975), and possibly indicated for Explorer 28, is apparently reversed at Warrego.

Variation in the proportion of octahedrally and tetrahedrally coordinated Al in the chlorite again highlights the difference between relatively unaltered sediment and the hydrothermal alteration (Fig. 6.4). Unaltered sediment analyses plot at or above the $Al^{IV} = Al^{VI}$ line, while altered sediment and lode samples fall below this line. This is the reverse of trends noted in chlorite alteration in the Alligator River uranium deposits (Ewers et al., 1983; Nutt, 1989), and is therefore likely to reflect different chemical conditions of ore formation.

Discussion

Chlorite compositions in the Warrego environment show several features that are significant in terms understanding the process of ore formation. The ironstone lode is surrounded by two alteration zones that may be distinguished by their chlorite composition. While chlorites from both zones show wide, overlapping ranges in Si (and hence Al) content, they are easily distinguished in terms of $Fe^{\#}$. The outer zone of chloritic, but relatively unaltered sediments is characterised by the presence of Fe-clinochlore, while the inner strongly altered zone surrounding the ironstone lode is characterised by Mg-chamosite. Following the well established pattern identified by Albee (1962), both zones show relatively good correlation between the $Fe^{\#}$ of chlorite and FeO/(FeO+MgO) in the the rock (Fig. 6.5). This relationship suggests that the boundary between them reflects the the dimensions of the hydrothermal system. The outer zone is rock dominated with chlorite compositions directly reflecting the bulk composition of the sediments, while the inner zone in which hydrothermal chlorite is the dominant mineral, is fluid dominated with chlorite (and bulk rock) compositions reflecting the conditions of hydrothermal alteration i.e. temperature, fO_2, fH_2S, pH, and fluid chemistry (e.g. Albee (1962), Walshe and Solomon (1981), McLeod and Stanton (1984), Cathelineau and Nieva (1985), Walshe (1986), Bryndzia and Scott (1987), Kranidiotis and MacLean (1987), Neall and Phillips (1987), and Shikazono and Kawahata (1987)).

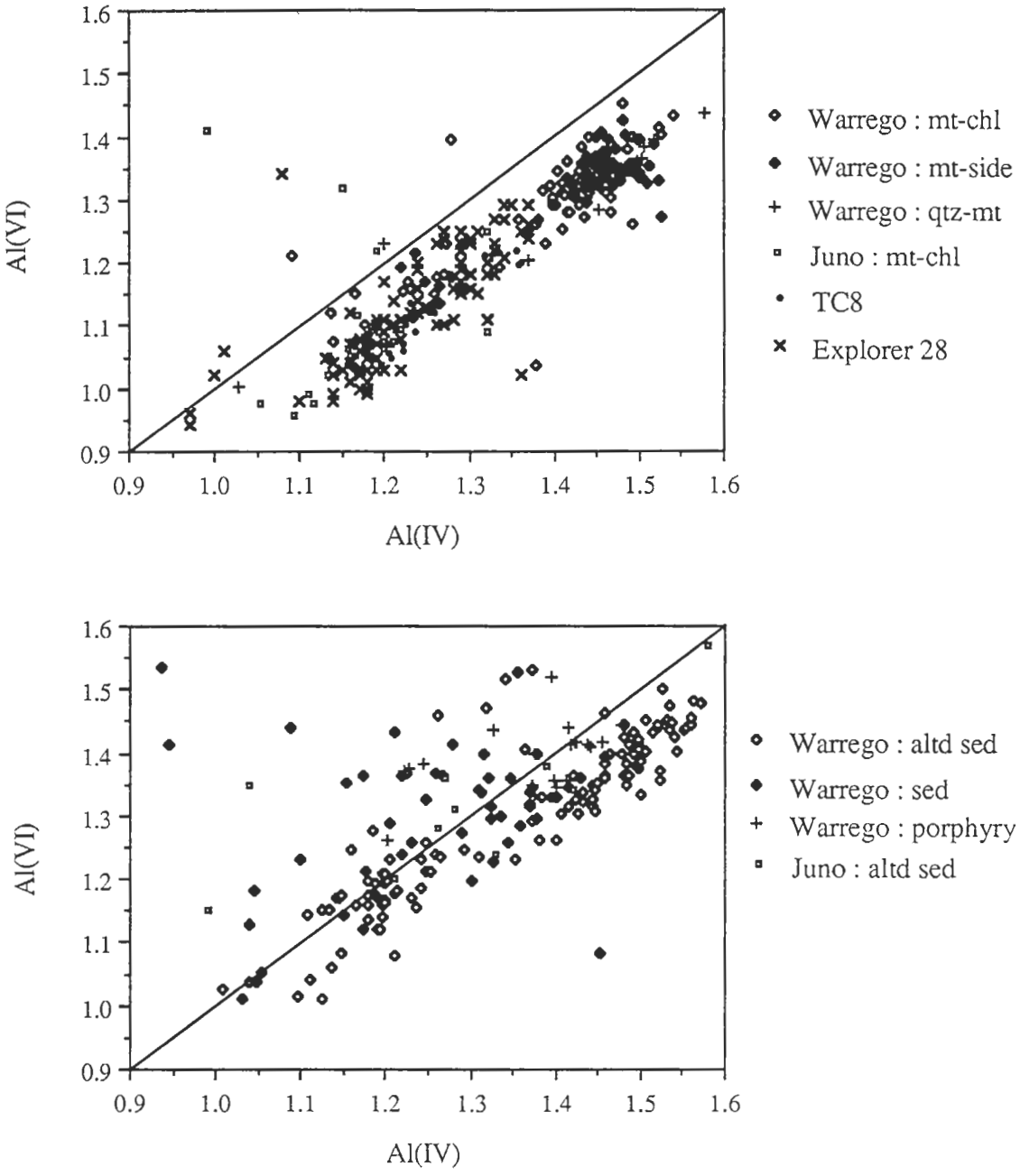

Figure 6.4 — Relationship between tetrahedral (Al(IV)) and octahedral (Al(VI)) aluminium in chlorites from Warrego ironstone lode and adjacent sediments. Chlorites from Juno and TC8 mines and Explorer 28 prospect are included for comparison.

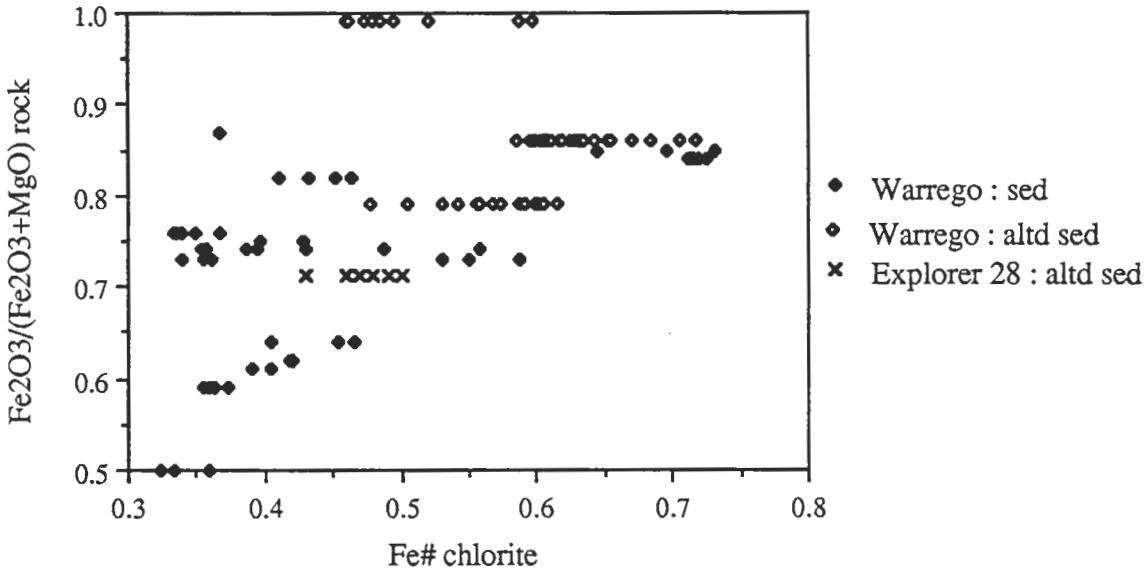

Figure 6.5 — The composition of chlorites from the altered and relatively unaltered sediments surrounding the Warrego ironstone lode show a general dependence on the bulk rock composition.

The variable Si contents of chlorites from both zones is not unusual, with similar ranges reported for chlorites in a variety of studies on both hydrothermal alteration, and regional metamorphism, e.g. Hendry (1981), Ewers et al. (1983), Cathelineau and Nieva (1985), Shikazono and Kawahata (1987), Kalogeropoulos and Scott (1988), Laird (1988), Slack and Coad (1989). In contrast, chlorites associated with intense hydrothermal alteration have been shown to have relatively restricted Si contents (e.g. Larson, 1984). It therefore seems likely the variability in Si for the chlorites from the sediments is typical, probably reflecting the relatively low initial metamorphic grade (Laird, 1988). Prograde and retrograde metamorphism associated with the Warrego Granite is therefore likely to have been isochemical.

The tendency to a narrower and relatively low Si range in chlorite composition in the altered sediments and ironstone lode is interpreted to reflect a decreasing rock, and increasing fluid influence on the chemistry of the chlorite. Chlorite within the ironstone lode is associated with economic mineralisation in the fractured massive magnetite and as such must have been deposited directly from solution. Therefore the narrow range in Si for these chlorites directly reflects the hydrothermal conditions, and influence from the sediment composition is negligible.

The depletion in Al^{VI} relative to Al^{IV} in the altered host rock and ore compared to the sediments may have implications for the chemistry of the ore formation process. Because Al^{3+} substitutes for Si^{4+} in tetrahedral layers of the chlorite structure, the resulting charge imbalance must be compensated for by the substitution of an equivalent amount of R^{3+} (typically Al^{3+}) for R^{2+} (Fe^{2+} and Mg^{2+}) in the octahedral layers (Foster, 1962). In general, relatively few chlorite compositions plot on this line (Foster, 1962) suggesting either octahedral site vacancies (above the $Al^{VI} = Al^{IV}$ line), or ferric iron substitution for Al^{3+} (below the line). Because ferric iron contents cannot be determined by the microprobe, a 'rough' approximation may be obtained from the excess of Al^{IV} over Al^{VI}. The proportion of Fe^{3+} as a percentage of the total iron in the samples has been calculated assuming $Al^{IV} = Al^{VI} + Fe^{3+}$. Recalculation of the structural formulae to maintain 28 oxygen ions (Walshe, 1986) does not significantly alter the results, and therefore this correction has not been applied. The results are illustrated in Figure 6.6 and suggest that similar to chlorites where ferric iron contents were directly measured (Foster, 1962; Deer et al., 1962), the bulk of the Warrego chlorites have ferric iron contents less than 5% of total iron. However, the magnetite-chlorite analyses exhibit generally higher percentages of ferric iron compared to the remainder of the Warrego data, and overlap the range observed for Juno, TC8 and Explorer 28 samples. The ferric iron content determined by this method underestimates those calculated for the Juno samples by Walshe (1986), but the general relation-

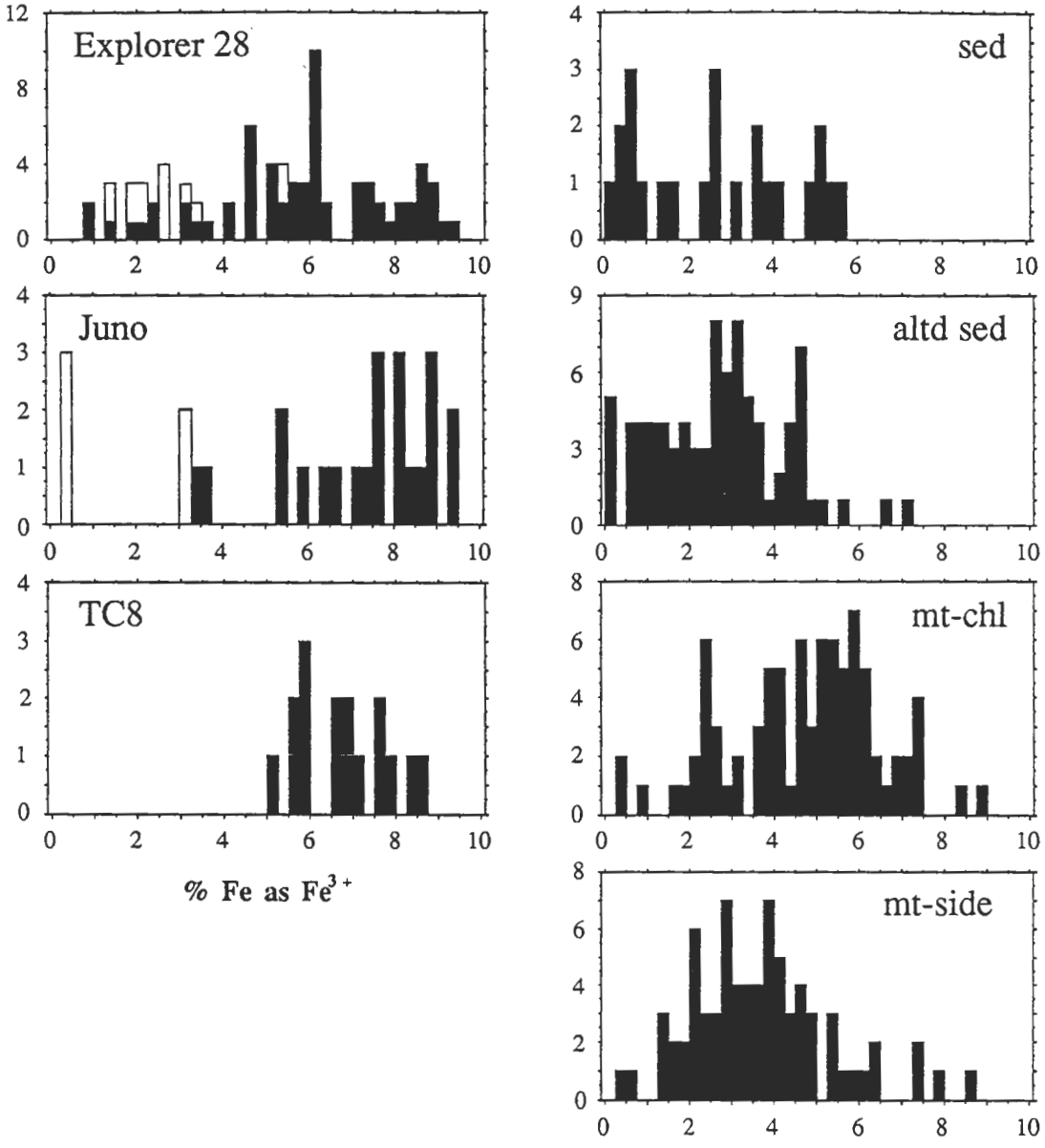

Figure 6.6 — Frequency distribution plots of the calculated ferric iron content of chlorite as a percentage of total iron. Open bars in charts for Juno mine and Explorer 28 prospect are altered sediments adjacent to the ironstone lodes.

ships indicate a similarity between Juno, TC8, Explorer 28, and the Warrego gold pod that may indicate a relatively oxidised fluid compared to that associated with magnetite-sulphide assemblage.

A model relating the observed variation in chlorite composition to the formation of the ironstone lode is suggested as follows: regional greenschist facies metamorphism, or low intensity (rock dominated) hydrothermal alteration lateral to the main fluid conduit, has resulted in chloritisation of the sediment in which chlorite compositions reflect the initial bulk rock variation. With increasing chloritisation of the rocks proximal to the forming ironstone lode, in association with high water/rock ratios, chlorite compositions become relatively iron-rich reflecting a fluid control. Despite the high inferred water/rock ratios, the chlorite preserves variable Si contents characteristic of the unaltered sediments. However within the ironstone lode, chlorite deposition directly from solution produces a relatively iron-rich and Si-poor compositional range. Variation in $Fe^{\#}$ and possibly Fe^{3+} for chlorites in the ironstone lode suggests either the gold pod represents a separate paragenesis to the sulphide ore, or an evolution of chemical composition as fluids interact with the lode. The former model is preferred by the author (Chapter Nine and Ten).

The relatively simple model proposed here is, however, clearly inappropriate in the case of both Explorer 28 and Juno. In both there is a trend to more magnesian and siliceous chlorite compositions from altered sediment, through stringer mineralisation (Juno), to the magnetite-chlorite of the lode (Large, 1974, 1975), and this is the reverse of the Warrego pattern. Also Si does not show the narrowing of compositional range with increasing intensity of alteration. It seems likely that chlorite variation reflects variability of the original sediments, and possibly these systems have lower water/rock ratios.

6.5 Muscovite

Muscovite in the Warrego ironstone lode is restricted to a relatively small area incorporating the gold pods and the stringer mineralisation in their immediate footwall. Unlike the fine sericite of the sediments, the muscovite shows no preferred orientation and typically occurs as discrete, randomly orientated blades up to 0.5 mm in length. Muscovite is always associated with chlorite (Plate IX B) in what appear to be equilibrium assemblages, although late-stage, incipient chlorite alteration along cleavage planes is frequently observed.

As described in section 6.4, the chlorite-muscovite mineral assemblage is characteristic of the gold pod and the stringer zone immediately below it. The direct correlation between the occurrence of muscovite and gold mineralisation helps constrain the conditions of ore formation because its presence is generally indicative of relatively acid fluid conditions (e.g. Crerar and Barnes, 1976). The restriction of the

muscovite to the gold pod again suggests either a chemical evolution or different parageneses for the gold and copper mineralisation.

There has been no attempt to correlate muscovite composition within the ironstone lode other than to note that they are phengitic in composition (i.e. between muscovite and celadonite in composition).

6.6 Gold

Gold in the Warrego ironstone lodes occurs almost exclusively as free gold allowing the use of relatively simple gravity separation and concentration. However, the fine grain size of gold in copper ore means that most is reported in the copper concentrates.

Petrography

There are three distinct populations of gold in the Warrego ironstone lode that are related to their location in the lode and associated mineralogy.

Gold Pod: Here gold is characteristically coarse grained and frequently visible to the naked eye in an assemblage of magnetite, muscovite, chlorite and bismuthinite. The coarsest individual gold grain observed from the mine was approximately 3 mm in diameter, but grains in the range from 0.5–1 mm are commonly dispersed through the pod in an apparently random manner. In polished section the gold has sharp straight edged margins where hosted by coarse bladed muscovite and chlorite, but these margins are more irregular when the gold mantles and invades fractures in magnetite. Gold commonly shares grain boundaries with bismuthinite but observations of gold with chalcopyrite are rare (Plate XI A).

Although there is some evidence of gold remobilisation into cracks in magnetite (Plate XI B), movement appears to have been on the scale of millimetres, and the presently observed mineral relationships are not likely to have been modified significantly by the intrusion of the Warrego Granite. Therefore, the observed association of gold and bismuthinite with chlorite, muscovite and magnetite filling fractures and overprinting the massive magnetite represents a primary texture associated with the overprint of economic mineralisation on the lode.

Gold-rich Copper Ore: Marginal to the gold pods, relatively high grades of gold occur in the copper ore, which is evidenced by the abundance of small gold grains hosted by chalcopyrite. Gold is only rarely visible (with the naked eye), typically forming in the gold-rich copper ore discrete, rounded grains ranging from a few μm to approximately 100 μm in size. The majority of gold grains occur in clusters often associated with bismuthinite and are invariably hosted by chalcopyrite (Plate XI C). Less commonly, gold may occur with bismuthinite and chalcopyrite as inclusions and

Plate XI

A: Gold pod-style mineralisation from the central gold pod. Large irregular gold grains are associated with bismuthinite and minor chalcopyrite in a matrix of chlorite and muscovite. Irregular magnetite textures result from the overgrowth of primary Type I by Type II magnetite. Sample 109304.

B: Coarse gold remobilised into cracks and fractures in the massive Type I magnetite. Sample 106893.

C: Gold mineralisation associated with copper ore commonly occurs as clusters of rounded grains, often in associated with bismuthinite. Sample 109066.

D: Concentration of gold in fractures and as inclusions within pyrite. Replacement of magnetite is also evident as numerous relict fragments. Sample 108461a.

E: Hematite alteration where not only has there been extensive replacement of magnetite but also dissolution to allow the growth of bladed hematite in the porous lode. Note magnetite seems to be preserved from hematite alteration within and adjacent to the chalcopyrite. Sample 108902.

F: Extensive hematite alteration as the replacement of original magnetite and chalcopyrite. Note pyrite is largely unaffected. Sample 108983a.

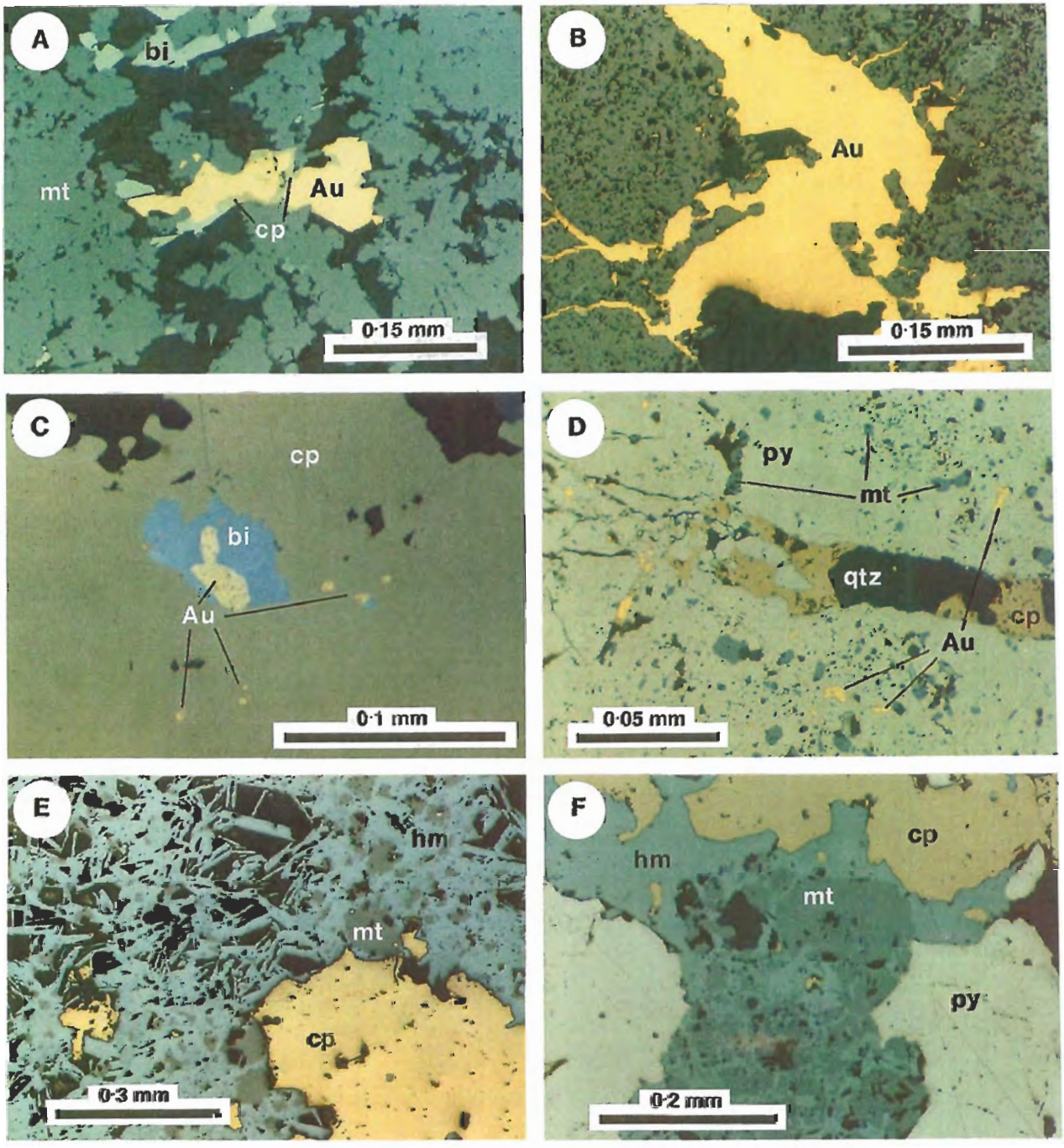
A
bi
mt
Au
cp
0·15 mm
B
Au
0·15 mm
C
cp
bi
Au
0·1 mm
D
py
mt
qtz
cp
Au
0·05 mm
E
hm
mt
cp
0·3 mm
F
cp
hm
mt
py
0·2 mm

veinlets within pyrite (Plate XI D), or within chalcopyrite filled lamellar bands of pyrite and marcasite. Gold is very rarely associated with the quartz in the sulphide veins, and has not been observed in association with chlorite or magnetite.

The constant association of gold and chalcopyrite suggests they are genetically related and identical chalcopyrite-gold associations are observed in Peko, Orlando, and Ivanhoe mines (Edwards, 1955; Whittle, 1966). The correlation observed between gold and copper grades throughout the copper orebodies in the Warrego mine (Chapter Five) suggest contemporaneous deposition of gold and chalcopyrite in a relatively constant ratio that has not been modified by subsequent metamorphism.

Copper Orebody: The copper orebodies in the upper levels of the mine have an average gold grade of 2 to 3 g/t, and rarely exceed 5 g/t in 1 metre drillcore assays. However most polished thin sections from this ore contain one or two minute (1 to 3 μm) gold grains that are often associated with chalcopyrite in cracks and fractures in pyrite.

This common association of gold in fractured pyrite within the copper orebodies and to a lesser extent in gold-rich copper ore marginal to the gold pods, suggests that gold has been remobilised and concentrated during deformation and metamorphism. Boyle (1979) has indicated that gold occurring in solid solution, or as atomic layers in pyrite, may subsequently be concentrated through diffusion to zones of low chemical potential such as fractures and grain boundaries. Experimental work by Jean and Bancroft (1985), provides supporting evidence for the formation of layers of gold on sulphides from relatively low gold solution concentration through its rapid deposition at defect sites through a process of adsorption and reduction.

In other Tennant Creek orebodies, a similar association of gold localised as inclusions and within fractures in pyrite has also been recorded, e.g. Golden Forty (Wyborn, 1971) and Orlando (Whittle, 1962 — unpublished AMDEL Report) mines. However, in the Peko mine no pyrite association with gold has been recorded (Edwards, 1955). In many respects the Peko mine appears to represent an undeformed equivalent of the copper orebodies in the Warrego mine (Chapter Ten); a comparison of the relative gold recoveries of the two mines may indicate if gold at Warrego has been concentrated during deformation and contact metamorphism to make it more amenable to recovery. White (1962) reports the recovery of gold from Peko mine at 67% which is similar to an estimate of 74% based on the average grade of gold in copper concentrate produced from Peko (3.5 g/t — Peko Mines unpublished data), compared to the average gold grade of Peko tailings (1.2 g/t — Australian Development Ltd 1986, Annual Report).

A similar estimate of the gold recovery from Warrego ore is not valid, as most gold production has come from gold pod, or gold-rich copper ore marginal to them, where gold is relatively coarse and easily recovered. However, the year by year

variation of head grade and gold production (Peko Mines unpublished data) suggest recoveries were constant (>90%) for most of the mine life which includes a period of copper ore extraction (1980–81). The initial period of copper ore production before discovery and development of the gold pods (1974–75) was marked by lower recoveries (84% in 1974), but this is still significantly higher than the recoveries reported at Peko mine. It is therefore suggested that a significant proportion of gold in the Peko mine may have been locked up in sulphides (pyrite?) and was not recovered, whereas the metamorphic overprint of the Warrego Granite at Warrego mine has concentrated gold in the copper orebodies making it more amenable to extraction.

Gold Fineness

A brief examination of the variability of gold fineness within the Warrego ironstone lodes has highlighted what appears to be a consistent increase in the silver content of gold, with distance form the gold pods. Details of the individual samples are provided in Appendix D and are summarised in Figure 6.7.

There appears to be a distinct separation of the different styles of gold mineralisation based on average gold fineness of individual samples (Fig. 6.7a), but consideration of individual analyses (Fig. 6.7b), suggests that there is a continuum of values ranging from approximately 700 to 1000 fine. Samples from within the core of the two gold pods show compositions greater than 950 fine, whereas samples from section 8140N though still high are somewhat lower between 900 and 950 fine. In view of the apparent fineness zonation, these lower values in the gold pod assemblage of section 8140N corroborate evidence presented in the Chapter Five that section 8140N is peripheral to the core of the gold pod.

Individual gold grains were routinely checked for within grain fineness variation and without exception maintained a homogeneous composition from rim to core. Annealing studies on gold grains by Czamanske et al. (1973) suggest that primary fineness variation within individual gold grains will be homogenised during metamorphism, and it is therefore likely gold grains at Warrego have been homogenised by the intrusion of the Warrego Granite. However the within orebody variation identified in this study is considered a primary depositional feature related to changes in the physico-chemical conditions during deposition of the gold (see below).

Gold fineness data from Tennant Creek mines is relatively scarce. Edwards (1955) estimated the fineness of Peko gold by colour at between 800 and 850, and high fineness has been reported for many of the near surface (above water table) deposits (Ivanac, 1954) where supergene enrichment is likely to have leached silver. The high fineness reported for Eldorado mine (905 to 963), is likely to result from similar

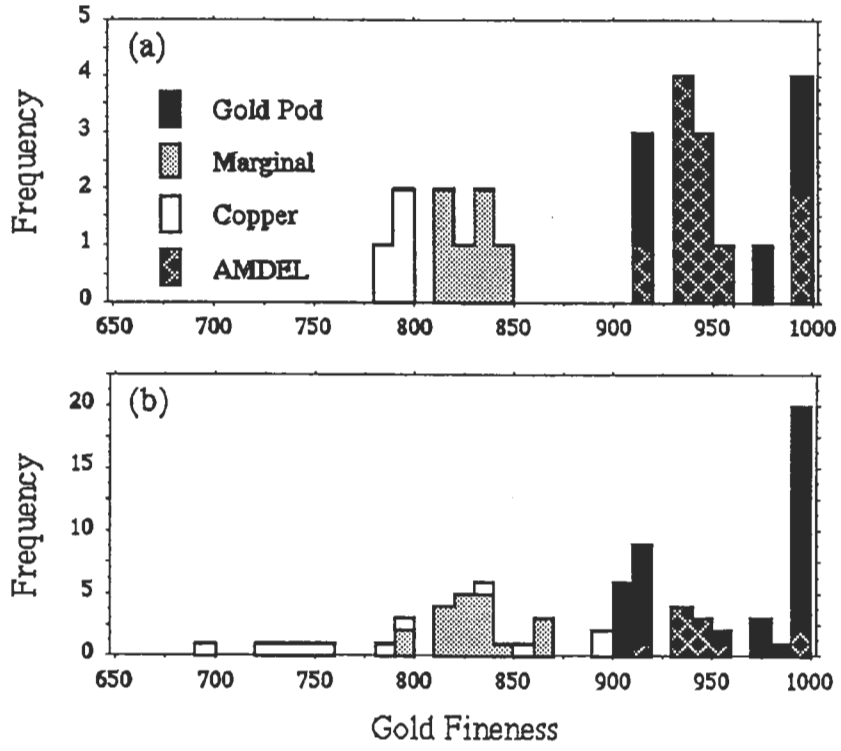

Figure 6.7 — (a) Averaged gold fineness for selected samples from the Warrego orebodies including gold pod, copper orebody and gold-rich copper ore. (b) All gold fineness analyses for individual gold grains in samples in (a). Gold Pod are samples from the magnetite-chlorite gold pods, Marginal are those from gold-rich copper ore marginal to the gold pods, and Copper samples are from copper ore in the upper levels of the mine. The AMDEL analyses come from an unpublished report by The Australian Mineral Development Laboratories (1975), on gold benefaction from the then newly discovered gold pod in Warrego mine.

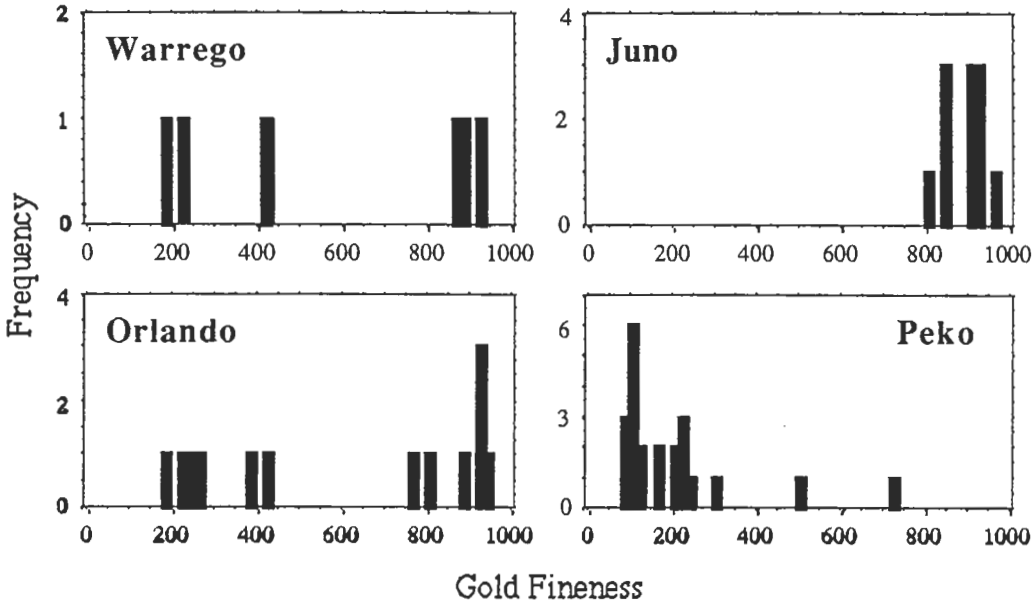

Figure 6.8 — Gold fineness from Tennant Creek mines based on the yearly silver and gold production figures where available. (a) Warrego mine (n = 6), (b) Juno mine (n = 11), (c) Orlando mine (n = 13), (d) Peko Mine (n = 22).

enrichment (Horvath, 1988). Fineness ranging from 820 to 890 are reported from the Gecko mine (Huston, 1990a) and 'high' fineness is also reported at White Devil (Huston, 1990b). Fineness has also been calculated for the Warrego, Juno, Orlando, and Peko mines from yearly gold and silver production where data are available (Fig. 6.8). Although far from satisfactory, the overall results are consistent with those observed in the Warrego mine.

Warrego mine shows two populations, the low fineness values correspond to the early production of copper ore (1973–75), and high fineness is correlated with gold pod production (1976–78). This pattern of higher silver contents in copper ore is in accord with the direct measurement of gold fineness. In contrast Juno mine shows uniformly high fineness values (1967–74), with a slight decrease to less than 900 fine corresponding to the last three years of mine life (1975–77) which is probably related to production of lower grade and increasingly copper-rich ore.

Orlando mine shows a pattern similar to Warrego, which may correspond to the two gold associations observed in this mine; high-grade, gold-chlorite, and lower grade, chalcopyrite-pyrite assemblages (McNeil, 1966; Whittle, 1962 — unpublished AMDEL report). The lower fineness values correspond to the last six years of production (1970–75) where gold production fell sharply but copper production remained relatively constant.

Peko mine differs from the above mines with the bulk of production showing a single concentration at unrealistically low fineness values. This corresponds to the dominant copper-gold association observed in this mine. Anomalous high fineness years correspond to the first and last years of production (1955 and 1976 respectively) and is probably related to preferential extraction of gold-rich ore.

A significant feature of Figure 6.8 is that while the fineness of individual gold grains associated with gold pod-style mineralisation correlate well with the ratio of gold and silver recovered from the ore (> 800 fine), the copper ore is enriched in silver giving an estimated fineness that is much lower than the minimum measured in gold grains from Warrego mine. Because no silver minerals have been observed in any of the Tennant Creek mines, silver in the copper orebodies probably occurs in solid solution, or as submicroscopic inclusions within the sulphides. Whittle (1966) suggested tetrahedrite and galena host silver in Peko mine, but galena from Orlando mine was specifically analysed for silver and proved negative (Watmuf, 1973 — unpublished AMDEL Report).

Assuming gold fineness of Tennant Creek orebodies fall within the range observed in Warrego mine (700 to 1000 fine) and chalcopyrite is the dominant host of silver (being the most abundant sulphide in all mines), its silver content must fall in the range of 200 to 600 ppm (average ~270 ppm). This range is consistent with the

measured silver content of chalcopyrite from a range of mines (Boyle, 1979; Nishiyama and Kusakabe, 1986) and it is therefore seems likely that the bulk of the silver in Tennant Creek copper orebodies is hosted by chalcopyrite.

A model involving the diffusion of silver from chalcopyrite to gold during metamorphism and deformation, as a possible cause of lower gold fineness in the copper orebodies is unlikely. The general observation of low fineness gold with copper ore at Tennant Creek, and the lack of distinction between the fineness of gold grains hosted by pyrite compared to chalcopyrite in the copper orebodies at Warrego, suggest gold fineness variation in the Warrego mine is a primary feature related to ore deposition.

6.7 Chalcopyrite

Chalcopyrite forms the bulk of the sulphide mineralisation in the Warrego ironstone lodes, and is the host mineral for all of the copper mineralisation. Very rare bornite (after chalcopyrite) is observed in stringer mineralisation well removed from the ironstone lodes proper, and is the only other copper mineral observed in or adjacent to the deposit.

Petrography

The distribution of chalcopyrite within the ironstone lodes is strongly zoned in the lower gold-rich part of the ironstone lode where the zonation: magnetite-chlorite, magnetite-sulphide and quartz-magnetite from footwall to hangingwall is well established. In the upper copper orebodies, chalcopyrite mineralisation is more pervasive throughout the lode, but as with the gold-rich mineralisation highest grades tend to occur in the core and towards the top of the lode (Chapter Five).

Although rare, chalcopyrite occurs in the gold pods typically as minor blebs and irregular aggregates dispersed through the chlorite-muscovite matrix, and as rounded inclusions in massive bismuth mineralisation. Chalcopyrite has also been observed forming very fine (<5 μm) rims around large gold grains (Plate XI A), suggesting chalcopyrite and gold were deposited together. Similarly chalcopyrite is rare in the quartz-magnetite zone, there being a gradual decrease in abundance with the increasing intensity of quartz veining. This is not the result of quartz overprinting the magnetite-sulphide assemblage, but rather a complementary increase in quartz with decreasing chalcopyrite abundance across the ironstone lode from footwall to hangingwall.

Typically chalcopyrite is the main vein mineral in the magnetite-sulphide zone, completely filling cracks and fractures in the massive magnetite lode. Chalcopyrite has been recrystallised during contact metamorphism (evident in the early stages of polishing as annealed equant grains with 120° triple junctions), and is remobilised into cracks and fractures in pyrite and magnetite. Thus there is little information on the paragenetic

relationships of the minerals in the vein assemblage. Fortunately mineral phases are few, and contemporaneous deposition seems likely.

Evidence for deformation post-dating the peak thermal metamorphism of the Warrego Granite is seen as the kinking of, and formation of, deformation twins in chapcopyrite grains, together with the occurrence of open brittle fractures throughout all forms of mineralisation (Plate IV F). These fractures may be lined, or filled with a quartz and hematite mineral assemblage and are possibly related to the hematite alteration of massive magnetite lode (see below).

Paragenesis

Despite annealing and local remobilisation of the chalcopyrite, a general paragenetic relationship of the chalcopyrite mineralisation can be surmised. Clearly mineralisation has overprinted the ironstone lode and is therefore related to a late-stage episode of deformation and mineralisation that involved fracturing and deformation of the lode. A consanguineous formation of ironstone lode with disseminated copper mineralisation, that was remobilisation and concentration into cracks and fractures at a later date can be discounted by the total absence of chalcopyrite in the areas of massive magnetite. Complete remobilisation of the chalcopyrite from such a paragenesis is untenable.

The relationship of chalcopyrite with other ore minerals is less obvious. Although chalcopyrite fills cracks and fractures in magnetite and pyrite, there is no evidence of replacement and it is likely the minerals represent an original equilibrium assemblage. The common concentration of Type II magnetite, and to a lesser extent pyrite at the vein margins may imply a slightly earlier paragenesis. The good correlation between gold and copper observed in Figure 5.11 suggests recrystallisation has not effected primary relationships.

6.8 Hematite

Hematite is only a minor constituent of the ironstone lodes, where it generally occurs as irregular patches within the massive magnetite, and as the partial replacement of individual magnetite crystals in the vein assemblages (Plate VI C & E). The hematite alteration is without any systematic pattern of development and there is no indication why one crystal is replaced in preference to another. In addition to pseudomorphous replacement, fine overgrowths on the edges of magnetite crystals against chalcopyrite are observed, especially in the copper orebodies. Such alteration is minor, and typically hematite makes up significantly less than 1% of the mineral assemblage.

However, hematite may be locally abundant and two associations are recognised. Within the magnetite-sulphide assemblage, late-stage possibly granite related deformation has resulted in open space fracturing which is associated with bladed specular hematite and strong alteration of magnetite (Plate XI F). Locally total replacement of

magnetite occurs and large hematite blades up to several millimetres across may develop. Hematite in this association may constitute 10–20% of the rock, and these zones appear to be more prevalent in the upper copper orebodies.

The second association of strong hematite alteration occurs in massive magnetite zones where there has been virtually total replacement of the magnetite leaving a porous open space network of interlocking bladed hematite which contain relict patches of magnetite (Plate XI E). Sulphide mineralisation associated with these zones appears to be largely unaffected by the reaction occurring as irregular zones within the hematite and may even preserve unaltered or weakly altered magnetite crystals. These zones of alteration may be quite extensive and are apparently related to post-mineralisation, deformation and oxidation of the lode. Their localisation in the core of parts of the No. 1 orebody may suggest reactivation of the same structures which localised ore mineralisation.

Paragenesis

Local concentrations of hematite appear to be related to post-mineralisation alteration that is probably associated with syn- to late syn-granite intrusion based on the overprinting of annealed chalcopyrite by hematite veinlets.

6.9 Pyrite

Pyrite mineralisation occurs throughout the ironstone lodes in a variety of styles ranging from almost massive bands that may be up to a metre wide, to individual idiomorphic crystals occurring in both the massive magnetite, and chalcopyrite filled fractures cutting through it.

Petrography

Three distinct forms of pyrite are recognised within the ironstone lodes, each it is suggested belongs to a different paragenesis, or fluctuating conditions during the mineralisation event. The three forms of pyrite are described in terms of their associations and distribution through the lode.

Euhedral Pyrite: The most abundant form of pyrite consists of relatively large euhedral crystals (up to 5 mm across) that occur in almost massive bands constituting between 5 and 10 % of the total ironstone lode, and as individual crystals or aggregates in both the massive magnetite and chalcopyrite-filled veins.

1. *Vein-hosted pyrite*: Pyrite hosted by chalcopyrite veins occurs as discrete euhedra that may be up to 5 mm across, although aggregates of these crystals are also common. Typically the pyrite displays idiomorphic outlines against the hosting chalcopyrite or magnetite (Plate XII), and commonly shows the effects of brittle deformation with fractures healed by chalcopyrite or more rarely bismuthinite,

hematite, and gold. Rounded inclusions within the pyrite may comprise magnetite, chalcopyrite, bismuthinite, and pyrrhotite.

Rounded magnetite grains are common within the cores of large pyrite crystals and pyrite aggregates. Pyrite often mantles both Type I and II magnetite at vein boundaries, indicating overgrowth and replacement of magnetite (Plate XI F, XII C). However rounded pyrite grains are also observed within Type II magnetite suggesting pyrite deposition continued throughout the mineralisation history in the Warrego mine.

Zonation within the pyrite crystals is evident as the selective replacement of particular zones at the outer margins by of pyrite crystals, and by alternating growth zones of pink and normal pyrite (Plate XII F). Microprobe analysis indicate that the pink pyrite is cobalt-rich. The apparent disruption of growth zoning in pyrite in Plate XII F suggests that pyrite euhedra were fragmented prior to overgrowth and replacement by cobalt-rich pyrite. Cobalt-rich pyrite is restricted to the copper orebodies at the top of the mine.

2. *Massive pyrite*: On a microscopic scale, textures within the massive banded pyrite suggest an equilibrium assemblage of pyrite, magnetite and chalcopyrite. However hand specimen textures indicate deformation of the ironstone lode through fracturing and shearing, and replacement by pyrite (Plate XII B & VI A). The massive pyrite consists of intergrown euhedral crystals that typically constitute between 80 and 90 % of the bands, with minor relict magnetite oriented parallel to the pyrite banding. Chalcopyrite commonly fills the interstices between pyrite and and magnetite.

   The relationship of the banded pyrite to the chalcopyrite ore is difficult to constrain because recrystallisation and remobilisation have masked original depositional textures. However the sharp boundaries between vein-style chalcopyrite and massive pyrite bands, and general absence of chalcopyrite veining in the pyrite, suggest that pyrite bands post-date chalcopyrite. Pyrite banding is observed within the core of the lodes and at the footwall contact, where deformation appears to have been concentrated. Sulphur isotopes fail to distinguish between any of the styles of pyrite observed in the Warrego ironstone lodes (Chapter Eight) and therefore the pyrite overprint is considered part of the main mineralisation process rather than a post mineralisation effect.

Plate XII

A: Characteristic magnetite-sulphide mineralisation. Fractured Type I magnetite is overgrown by euhedral Type II magnetite and infilled by chalcopyrite, chlorite and euhedral pyrite. Sample 109072.

B: Massive banded pyrite comprising largely of recrystallised pyrite. Banding is defined by trains of relict magnetite and variation of the size of pyrite crystals. Sample 108790.

C: Pitted Type I magnetite is overgrown by relatively smooth Type II magnetite. Pyrite has overgrown and replaced magnetite. Sample 108983a.

D: Pyrite euhedra in massive Type I magnetite. These crystals are removed from obvious fractures which might suggest a replacement origin. Sample 109072.

E: Growth zoning in a pyrite porphyroblast is defined by relict magnetite inclusions that suggest contemporaneous growth of the two phases. Sample 108528.

F: Pyrite euhedra in chalcopyrite showing evidence of replacement and overgrowth by cobalt-rich pyrite (co). The apparent termination of growth zones in the pyrite on the right suggests possible deformation of crystals. Sample 108468.

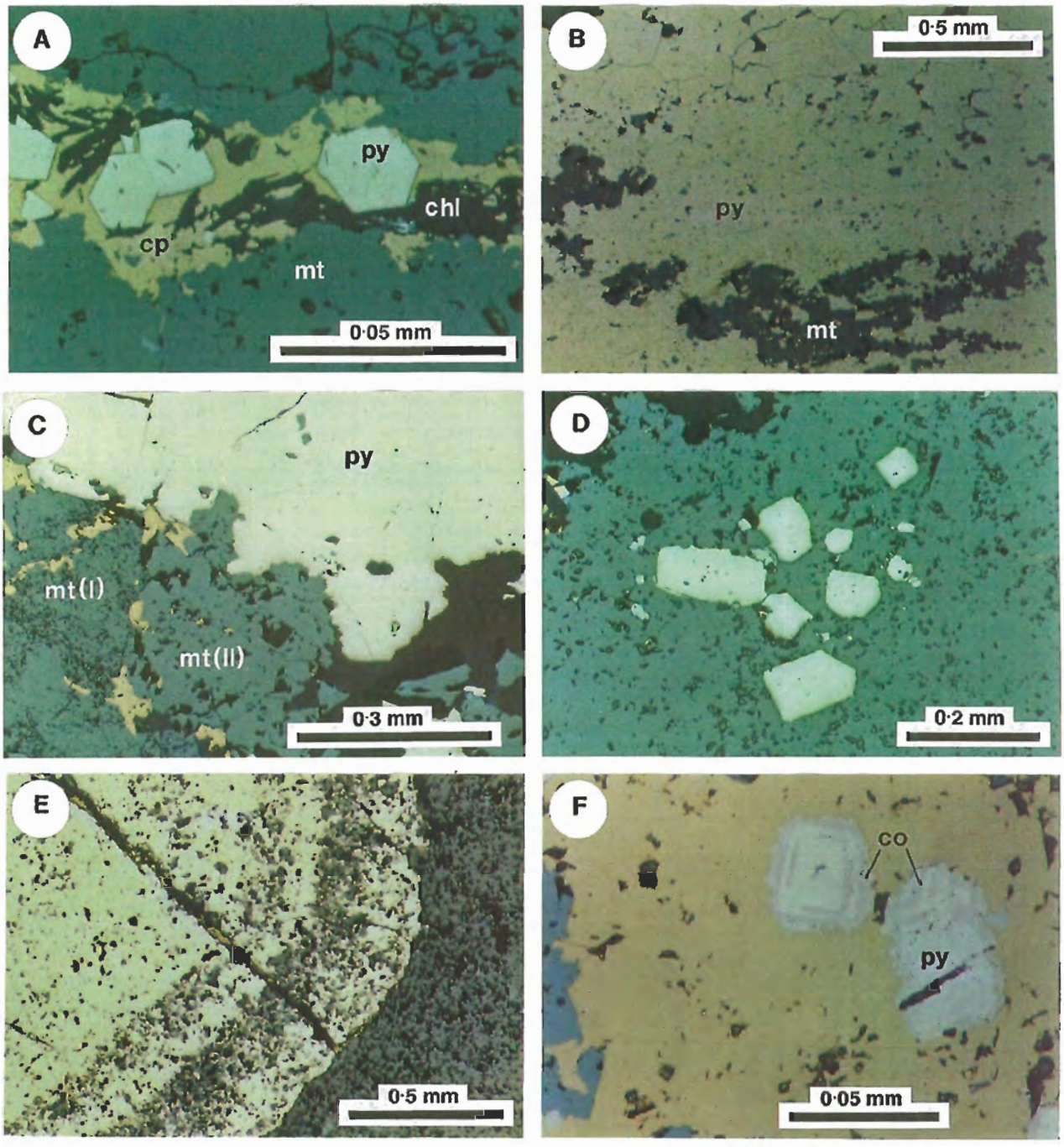
A
py
chl
cp
mt
0·05 mm
B
0·5 mm
py
mt
C
py
mt(I)
mt(II)
0·3 mm
D
0·2 mm
E
0·5 mm
F
co
py
0·05 mm

3. *Pyrite in massive magnetite*: Idiomorphic pyrite occurs within massive magnetite as occasional discrete crystals which are often removed from obvious fluid channelways (Plate XII D). The observation of growth zoning defined by magnetite inclusions may indicate some pyrite mineralisation accompanied ironstone lode formation (Plate XII E).

Porous Pyrite: This polymorph of pyrite is named for its porous looking inclusion filled habit. Its distribution is restricted to forming overgrowths on, and infilling between euhedral pyrite. However, there appears to be a gradation from porous pitted material to massive smooth pyrite. Close inspection of large euhedral pyrite crystals reveal many are composed of an aggregate of euhedral pyrite crystals that has been overgrown and infilled by porous pyrite to form the single crystal (Plate XIII A). The overgrowths of porous pyrite are cracked and infilled by remobilised chalcopyrite indicating that the growth and formation of this form of pyrite is associated with mineralisation rather than some contact metamorphic growth of pyrite.

Although porous pyrite appears quite distinct from the euhedral variety, clearly representing nucleation and growth on pre-existing pyrite, it probably reflects the mechanism by which the host pyrite itself was formed and therefore reflects the continuum between semi-random nucleation and growth of pyrite in the vein which eventually merge and are infilled to form large euhedral pyrite crystals.

Lacy Pyrite: This is an unusual form of pyrite that although common within the Warrego mine does not appear to be described elsewhere in the literature. Consisting of what appear to be random and irregular patches of an extremely fine lacework of pyrite that is infilled by chalcopyrite. Similar to the porous pyrite, there appears to be a continuum between the lacy pyrite and small euhedral pyrite crystals.

Patches of lacy pyrite are characterised by a narrow outer rim that although only a few microns wide appears to have regular crystal terminations against the chalcopyrite. Within these rims, extremely fine (almost at the limit of resolution of the microscope) colloform bands display a generally concentric arrangement within the inclusion. The extremely fine grained character of this mineral preclude positive identification although a pyrite-marcasite intergrowth seems likely.

It is suggested that the preservation of such delicate textures in the recrystallised chalcopyrite preclude a pre-contact metamorphic origin for the lacy pyrite. Similarly the delicate colloform structures are not compatible with dissolution or replacement of pyrite, and they are therefore attributed to crystallisation during or after intrusion of the Warrego Granite.

Plate XIII

A: Pyrite aggregate showing overgrowth of porous pyrite. Sample 108983a.

B: Lacy pyrite comprising an outer rim of crystalline pyrite infilled by an extremely finely lacework of pyrite and chalcopyrite. Sample 108541.

C: Inclusion in pyrite containing pyrrhotite (po) and chalcopyrite (cp). Sample 108983a.

D: Banded pyrite-marcasite (py-mc) after pyrrhotite. The decrease in volume associated with this reaction is evident as the now quartz-filled cracks defining the bands. Pyrite overgrowth of pyrite-marcasite is evident. Sample 109066.

E: ' Clast' of banded pyrite-marcasite that may reflect the original outline of the original pyrrhotite crystal. Strong remobilisation of chalcopyrite into cracks and rimming and replacement by pyrite is also evident. Sample 108555.

F: Relict pyrite-marcasite banding that shows extensive overgrowth and replacement by pyrite. Sample 108555.

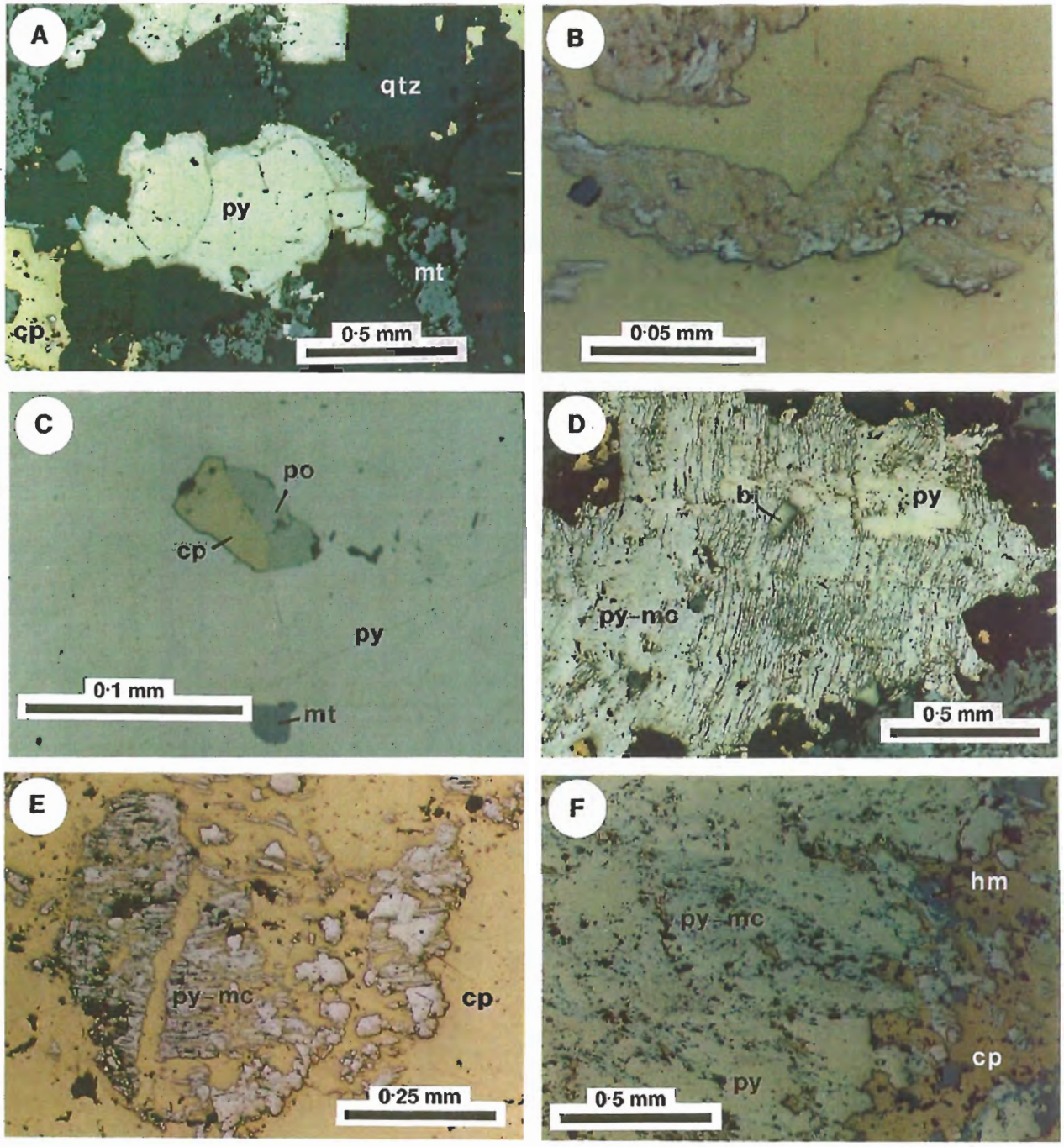
A
qtz
py
mt
cp
0·5 mm
B
0·05 mm
C
po
cp
py
0·1 mm
mt
D
b
py
py–mc
0·5 mm
E
py–mc
cp
0·25 mm
F
hm
py–mc
cp
py
0·5 mm

Paragenesis

Pyrite exhibits a wide paragenesis covering the entire period of economic mineralisation in the Warrego ironstone lode and possibly also ironstone lode formation itself. Pyrite appears to have preceded copper mineralisation accompanying the formation of Type II magnetite to form euhedral crystals that typically occur at vein margins. Pyrite forms part of the overall zonation sequence being rare in the gold pods, and concentrated with other sulphides in the magnetite-sulphide zone.

Pyrite euhedra appear to have grown through the overgrowth and amalgamation of smaller crystals — a process that probably continued throughout the life of the hydrothermal system. Typically pyrite aggregate overgrow and mantle magnetite vein margin although there is evidence of some replacement. During the later stages of mineralisation conditions must have changed sufficiently to promote the replacement of magnetite by massive pyrite in major shear zones through the core and at the footwall margin of the lode.

Deformation associated with the intrusion of the Warrego Granite and rotation of the Warrego ironstone lodes has resulted in deformation of the pyrite and remobilisation of the more mobile sulphides (chalcopyrite and bismuthinite) together with the deposition of hematite and gold into fractures. This event was probably associated with the apparent exsolution or crystallisation of very fine colloform intergrowth of pyrite/marcasite and chalcopyrite, the significance of which is not understood.

6.10 Marcasite–Pyrrhotite

Although pyrrhotite is a rare constituent in the Warrego ironstone lode, the common occurrence of marcasite and marcasite-pyrite intergrowth throughout the magnetite-sulphide ore suggests pyrrhotite was once an important constituent in the mineral assemblage.

Petrography

Pyrrhotite: Throughout the sulphide assemblage of the Warrego ironstone lode pyrrhotite occurs either within rounded inclusions in pyrite crystals commonly associated with chalcopyrite (Plate XIII C), or more rarely as ragged relicts within masses of intergrown marcasite-pyrite. Despite the rarity of their occurrence, the presence of pyrrhotite is an important indicator of the physico-chemical conditions at the time of ore formation. Similarly its recognition lends credence to the assumption that abundant marcasite-pyrite throughout the copper orebodies represents a pyrrhotite precursor.

Pyrite/Marcasite: Throughout the copper orebodies in the Warrego ironstone lodes, fine lamellar intergrowths of pyrite and marcasite are common. Although typically occurring as irregular clots and patches (Plate XIII D), rare examples are observed that

suggest an original euhedral crystal outline (Plate XIII E). Typically the bands of pyrite and marcasite that are only a few microns in width, and alternate with quartz, chalcopyrite, bismuthinite, or hematite that has apparently been mobilised into spaces between the bands. Minor gold and bismuthinite may also be associated or intergrown with the bands.

Pyrite is commonly observed rimming and/or overgrowing the pyrite-marcasite assemblage and may mask the true original extent of the this assemblage (Plate XIII D & F). Generally subordinate to the pyrite, the pyrite/marcasite assemblage probably constitutes less than 5% of the lode in the copper orebodies.

Paragenesis

The occurrence of inter-banded pyrite and marcasite has long been recognised as an alteration product related to the oxidation of pyrrhotite (Ramdohr, 1969). Alteration of pyrrhotite may occur through either:

1. The leaching of iron and partial oxidation of the sulphide in situ (Fleet, 1978), or
2. Local solution of pyrrhotite, and partial oxidation of sulphur followed by the precipitation by pyrite or marcasite (Murrowchick and Barnes, 1986).

Differentiation between these mechanisms is important because mechanism 2 may provide information of the pH conditions at the time of alteration. Murrowchick and Barnes (1986) list several criteria that may distinguish the reaction products of these two processes. Mechanism 1 involves a volume decrease of greater than 26% and results in a porous pseudomorph of the original pyrrhotite where marcasite forms in three orientations related by 120° rotations about the pyrrhotite c-axis. Mechanism 2 is more likely to produce well developed crystals that are randomly oriented with respect to the original pyrrhotite.

The common observation of chalcopyrite, hematite, and/or quartz mobilised between the pyrite/marcasite lamellae at Warrego suggest an originally porous crystal, and suggest pyrrhotite has been oxidised to pyrite/marcasite by the first mechanism. A regular zig-zag orientation is also observed in the pyrite-marcasite lamellae suggesting crystal structure of the original pyrrhotite. It is difficult to constrain the precise timing of the alteration event, but the common observation of pyrite overgrowths on the pyrite/marcasite suggest this event occurred during the main mineralisation stage.

Pyrrhotite is a relatively common constituent of the sulphide-rich orebodies in the Tennant Creek goldfield and its occurrence has been described in Peko (Edwards, 1954; Whittle, 1966), Orlando (Mc'Neil, 1966; Whittle, 1966), and Ivanhoe (Whittle, 1966) mines. In Peko mine a well developed zonation was recognised within the lode with chalcopyrite giving way to pyrrhotite with depth in the lode (Edwards, 1954; Whittle, 1966). Marcasite lamellae (often associated with pyrrhotite) are also a common constituent of the chalcopyrite-rich ore (Whittle, 1966). The West Peko prospect

contains significant pyrrhotite mineralisation and similar to the banded pyrite mineralisation at Warrego appears to replace the magnetite lode.

Pyrite/marcasite is restricted to the magnetite-sulphide mineral assemblage at Warrego and although no attempt has been made to document its distribution on a mine scale, it appears to be most abundant in the upper copper orebodies. The original pyrrhotite appears to have been restricted to the chalcopyrite mineralisation and had an abundance roughly equivalent to or slightly less than the euhedral pyrite.

6.11 Bismuth Sulphosalts

Tennant Creek mines are characterised by the ubiquitous occurrence of bismuth sulphosalts associated with gold and copper mineralisation in the ironstone lodes. Native bismuth, wittichenite, bismite, and bismutite were recognised in the oxidised surface mineralisation (Stillwell and Edwards, 1942) and their presence was used by early prospectors as an indication of the often extremely fine grained gold mineralisation (McKeown, 1942). Subsequently a wide range of bismuth sulphosalts of lead, copper, and selenium have been identified in ores from below the water table, including the identification and naming of three new bismuth sulphosalts junoite, pekoite, and proudite from the Juno mine (Large and Mumme, 1975; Mumme, 1975b, 1976; Mumme and Watts, 1976). The rarity of these minerals on a world-wide scale is probably related to the requirement of high selenium contents to stabilise the structure of these minerals (Mumme, 1976).

The Warrego mine is no exception to the pattern observed elsewhere in the field, with the occurrence of a variety of bismuth sulphosalts occurring as minor constituents within the ore. Bismuthinite is the dominant bismuth mineral with wittichenite, ?emplectite, guanajuatite, and tetradymite recognised as trace constituents in the ore. The identification of the bismuth telluride tetradymite is significant as it is the first verified occurrence of tellurides in the Tennant Creek goldfield.

A compilation of bismuth minerals identified in the Tennant Creek Goldfield with their chemical formulae and reference where they first reported is presented in Table IV.

Table IV: Bismuth Minerals Recognised in the Tennant Creek Goldfield.

Native bismuth	Bi	Stillwell & Edwards, 1942
Bismite	Bi_2O_3	Stillwell & Edwards, 1942
Bismutite	$Bi_2CO_5.H_2O$	Stillwell & Edwards, 1942
Wittichenite*	Cu_3BiS_3	Stillwell & Edwards, 1942
Lillianite	$Pb_3Bi_2S_6$	Stillwell & Edwards, 1942
Bismuthinite*	Bi_2S_3	Edwards, 1955
Matildite	$AgBiS_2$	Edwards, 1955
Emplectite*?	$CuBiS_2$	Edwards, 1955
Guanajuatite*	$Bi_2(Se,S)_3$	Fander, 1966
Junoite	$Bi_8Pb_3Cu_2(S,Se)_{16}$	Large, 1974
Proudite	$Bi_{10}Pb_8(S,Se)_{23}$	Large, 1974; Mumme, 1976
Heyrovskyite	$6(Pb,Bi)Bi_2(S,Se)_4$	Large, 1974
Aikinite	$Bi_6Pb_2Cu_2(S,Se)_{12}$	Large, 1974
Weibullite	$Bi_6Pb_4(Se,S)_{13}$	Henley et al., 1975
Krupkaite	Bi_3PbCuS_6	Henley et al., 1975
Pekoite	$CuPbBi_{11}S_{18}$	Mumme & Watts, 1976
Hodrushite	$Cu_8Bi_{12}S_{22}$	Huston, 1990a
Hammarite	$Cu_2Pb_2Bi_4S_9$	Huston, 1990a
Tetradymite*	$Bi_2Te_2(S,Se)$	This study

* Bismuth sulphosalts recognised in the Warrego mine.

Petrography

Two bismuth associations are observed within the Warrego mine:

The first association, of bismuthinite[1] occurring marginal to and within the gold pods, occurs both as massive veins (generally less than 5 mm wide) and disseminated through the chlorite-muscovite matrix in the gold pod. In the lower gold pod, bismuth mineralisation is considerably stronger than that observed elsewhere in the mine and stringers of bismuthinite-magnetite extend into the footwall of the lode (Plate X E). Massive bismuthinite veins and veinlets penetrate cracks and fractures in the massive

[1] Although containing significant proportions of selenium, for simplicity seleniferous bismuthinite is referred to in the text as bismuthinite.

magnetite of the lode, and while some is clearly remobilised and recrystallised, bismuthinite is clearly introduced after primary magnetite deposition.

Within the gold pods the more typical association of bismuthinite is as isolated jagged grains intergrown with the phyllosilicate gangue minerals in the matrix to the magnetite lode (Plate X D). Bismuthinite is the dominant sulphide within the gold pods with chalcopyrite only occurring as a rare constituent forming occasional isolated grains in the chlorite-muscovite matrix. Towards the margins of the gold pods, chalcopyrite content increases at the expense of bismuthinite and phyllosilicates, and bismuthinite tends to form discontinuous pools within the veins and is often concentrated in veinlets off the main chalcopyrite-filled veins. This association may indicate bismuthinite is more easily remobilised than chalcopyrite, although contradictory evidence is provided by the common occurrence of chalcopyrite filled cracks within patches of massive bismuthinite.

The second association of bismuth mineralisation is that of the magnetite-sulphide assemblage marginal to the gold pods, and in the copper orebodies. Here bismuthinite generally occurs as isolated rounded inclusions less than 50 μm across within the massive chalcopyrite (Plate X C). Bismuthinite may occur in clusters (often associated with gold), or occasionally as aggregates within the chalcopyrite. Bismuth minerals are rarely visible in fresh ore, but once drillcore has been exposed to the air for several months, bismuthinite tarnishes a characteristic blue indicating its presence.

The distinction between the various bismuth sulphosalts is subtle and often very difficult to detect. Bismuthinite is typically strongly pleochroic (white to pale blue-grey) and anisotropic making the identification of the often small associated phases difficult. Tetradymite occurs as small 10 to 20 μm inclusions within bismuthinite that are distinguished by their slightly higher reflectance and lower polishing hardness (Plate XIV C). These inclusions were indistinguishable from bismuthinite on the microprobe and could only be analysed (and identified) by very careful mapping of the thin section under reflected light conditions before analysis.

Identification of emplecite and wittichenite was similarly difficult as colour variation between these minerals and bismuthinite is similarly subtle especially as these minerals are hosted by chalcopyrite which imparts a slight colour variation. The presence of these phases was only recognised through routine microprobe analysis of bismuth sulphosalts, and it is therefore likely that other bismuth sulphosalts remain to be identified in the Warrego orebody.

Plate XIV

A: Bismuthinite and tourmaline (tm) vein in the footwall of the lower gold pod. Sample 109305.

B: Banded pyrite veins in the footwall of the central gold pod (opaque). Euhedral tourmaline appears to have nucleated of and replaced pyrite. The undeformed and unaltered character of the tourmaline (perfect preservation of growth zoning) suggest the tourmaline is associated with the Warrego Granite. Sample 106949.

C: Tetradymite inclusion in bismuthinite. These inclusions are recognised by their higher reflectance than bismuthinite and its poorer polish. Note the triple junction grain boundary between bismuthinite grains. Sample 109304.

D: Carrolite (ln) overgrow of porous pyrite aggregates which already have cobalt-rich pyrite overgrowths (co). Sample 108475.

E: Kinked blade of molybdenite (mo) within a gold-rich vein. Sample 107056.

F: Irregular sphalerite inclusion (sp) within massive chalcopyrite in the copper orebodies. Sample 108465.

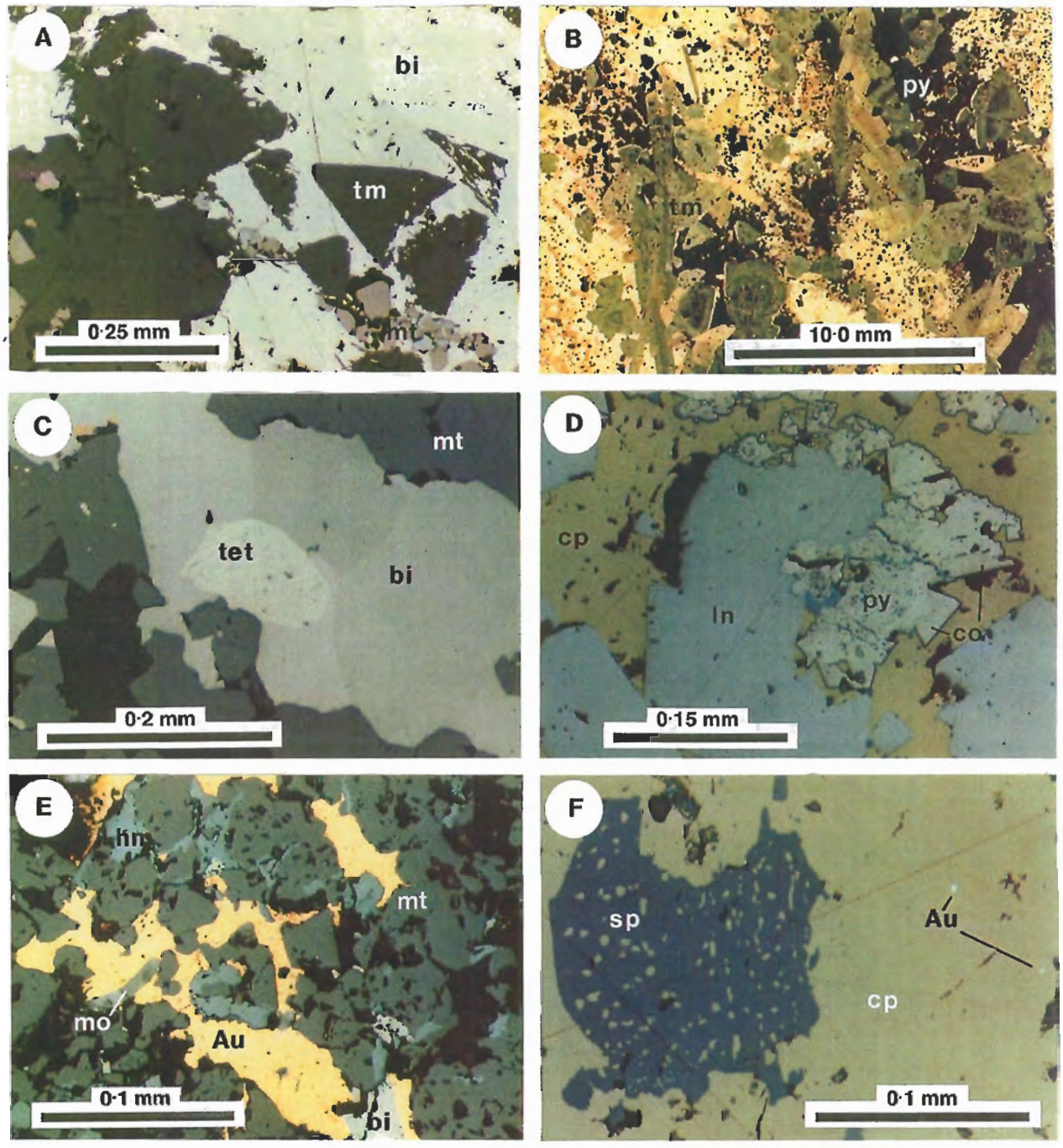
A
bi
tm
mt
0·25 mm
B
py
tm
10·0 mm
C
mt
tet
bi
0·2 mm
D
cp
py
ln
co
0·15 mm
E
hm
mt
mo
Au
0·1 mm
bi
F
sp
Au
cp
0·1 mm

Chemistry of Bismuth Sulphosalts

The compositional range of bismuth sulphosalts from the Warrego mine is illustrated in Figure 6.9 for the system Bi-S-Se-Te-Cu and detailed analyses are presented in Appendix D. Despite the inability to analyse for lead on the microprobe due to the close overlap of the x-ray peaks for bismuth, sulphur, and lead, it appears that unlike Juno mine, lead bearing bismuth sulphosalts are rare or absent in the Warrego mine. Although indications of lead were suggested in the spectra of individual samples during probing, and measurements of 2–12 wt.% lead in bismuth minerals from Warrego by Large (1974), the Warrego lode generally has low lead contents (Chapter Five), and members of the bismuthinite-aikinite series are likely to form only a minor constituent of the ore.

The main features of Figure 6.9 are summarised in terms of the main mineral components in the Bi-Cu-S-Se-Te system.

Bismuthinite: The strong clustering of analyses at the bismuthinite apex of the tetrahedron show it to be the dominant bismuth mineral in the Warrego mine (cf. Juno mine where junoite ($Bi_8Pb_3Cu_2(S,Se)_{16}$) is the dominant bismuth sulphosalt). Selenium is a common trace constituent of sulphide minerals especially of lead and bismuth (Sindeeva, 1964), and the solid solution of sulphur and selenium up to a ratio of 1:1 reported for the bismuthinite structure by Early (1950), matches the maximum selenium contents observed in the Warrego bismuthinite of approximately 20 wt.% selenium (i.e. $Bi_2Se_{1.5}S_{1.5}$). The clustering of analyses between Bi_2SeS_2 and Bi_2SSe_2 apparently represent a separate Se-rich bismuthinite population that came from two samples. One was collected from the immediate footwall of the main gold pod on section 8100N, and the other from extremely rich gold ore (~1000 g/t) collected from broken ore from the central gold pod. Both samples come from the area thought to represent the main focus of mineralising solutions (Chapter Five).

This observation of high selenium contents in bismuthinite from the footwall correlates well with the chemical zonation observed in drillhole 9/814/12 of a footwall to hangingwall decrease in selenium content (Chapter Five). The break in the solid solution series between the bulk of the Warrego samples and the gold pod samples may reflect a sampling gap rather than a real compositional break, as there is a relatively smooth and continuous variation in the bismuth-selenium ratio in drillhole 9/914/12 (Chapter Five).

Separation of the analyses into their respective mineral associations i.e gold pod, gold-rich copper ore adjacent to the gold pod, and copper ore in the upper levels of the mine, shows the variation in selenium content of bismuth sulphosalts observed in drillhole 9/814/12 also occurs on an orebody scale (Fig. 6.10). The selenium content of bismuthinite is generally low in the copper orebodies, variable in copper ore marginal

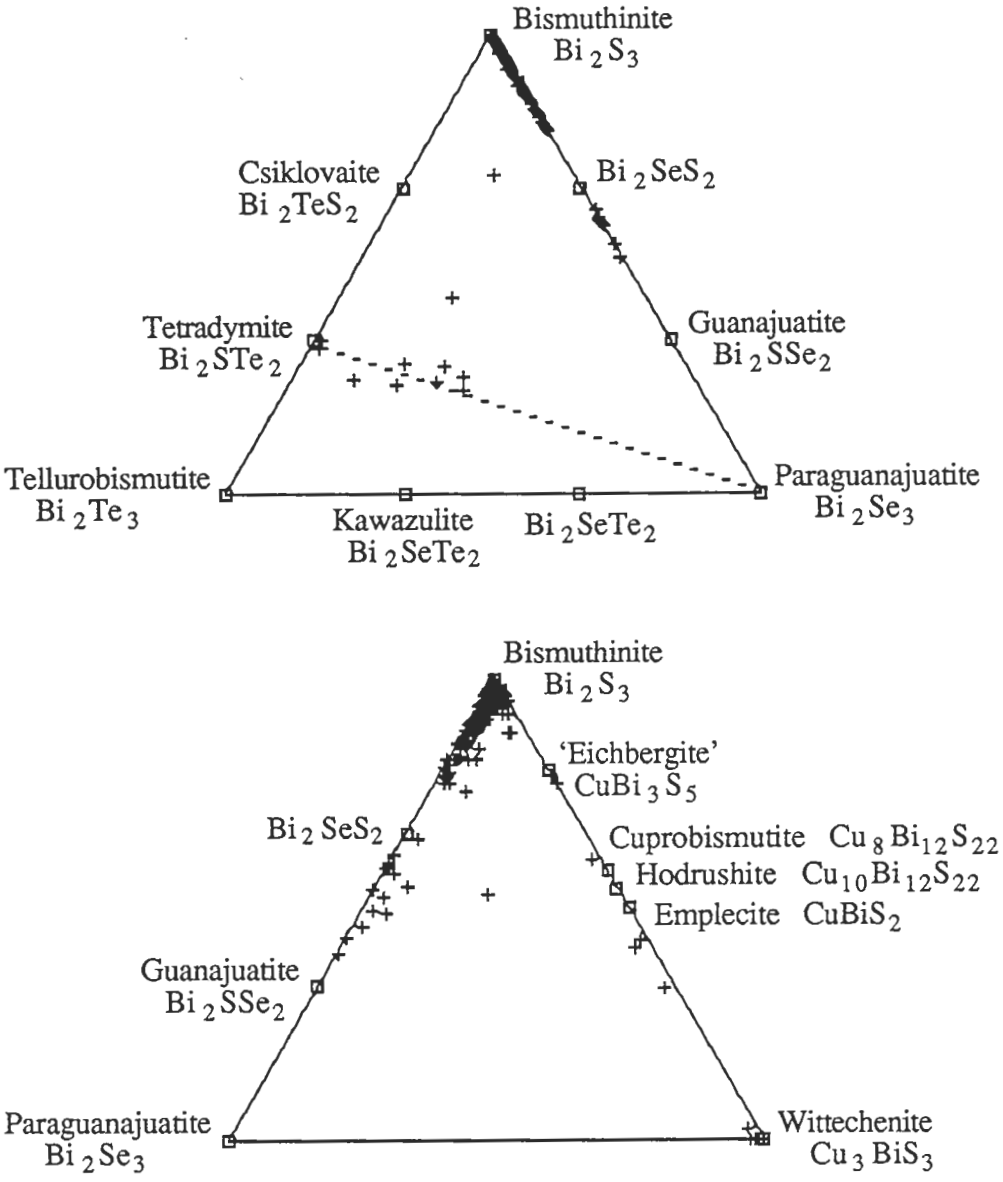

Figure 6.9 — Composition of bismuth minerals from the Warrego mine illustrating their compositional range in the Bi-Cu-S-Se-Te system. Analyses are projected onto the bismuthinite–tellurobismutite–guanajuatite and bismuthinite–guanajuatite–wittichenite faces of the bismuthinite–tellurobismutite–guanajuatite–wittichenite tetradedron. Analyses of individual points are provided in Appendix D. n = 243.

to the gold pods, and generally high in the gold pod. Low selenium contents in the gold pod samples (inset), correspond to the bismuthinite in the lower gold pod where remobilisation and contact metamorphism has possibly altered their selenium content.

Tetradymite: The system Bi_2S_3–Bi_2Te_3 contains four main phases (bismuthinite, csiklovaite, tetradymite and tellurobismutite), with solid solution reported between these phases, but in the system Bi_2Te_3–Bi_2Se_3 the occurrence of exolved Bi_2TeSe_2 within paraguanajuatite suggests the possibility of miscibility gaps in this system (Miller, 1981).

The range in composition of tellurium-rich bismuth minerals from Warrego mine show a linear trend between ideal tetradymite and paraguanajuatite suggesting a mixing array between these two compositions. This mixing may be the result of solid solution, beam overlap with adjacent phases, or submicroscopic inclusions within the tetradymite grain. As this array trends toward the paraguanajuatite composition rather than the composition of the hosting bismuthinite, it seems more likely that the mixing results from paraguanajuatite inclusions within the tetradymite possibly exolved during cooling of the mineral assemblage. Two analyses show compositions that might be expected from mixing of tetradymite and the hosting bismuthinite, which are quite different to the linear trend.

Wittichenite: Copper-bismuth sulphosalts in the Warrego mine appear to be concentrated in the copper orebodies in the upper levels of the mine, but identification of the phases present has proved difficult. Several analyses correspond to the ideal wittichenite composition, but the bulk fall on the Bi_2S_3–Cu_3BiS_3 tie line in positions that do not correspond to the composition of known minerals. A possible explanation for this observation is that these minerals are members of the bismuthinite-aikinite series (Bi_2S_3–$CuPbBiS_3$) which were not successfully detected because of the inability to analyse for lead.

Paragenesis

Despite some recrystallisation and remobilisation of the bismuth minerals, their relationships are not dissimilar to other Tennant Creek mines, and a paragenesis of bismuth mineralisation introduced coincidentally with gold and copper overprinting the massive magnetite lode is consistent in all these deposits. The pattern of a decreasing selenium content in bismuthinite with distance from the gold pods, and an associated increase in copper and possibly also lead-rich bismuth sulphosalts is similar to that observed in the Juno mine (Large, 1974, 1975), and is thought to result from physico-chemical gradients through the orebody (Chapter Nine).

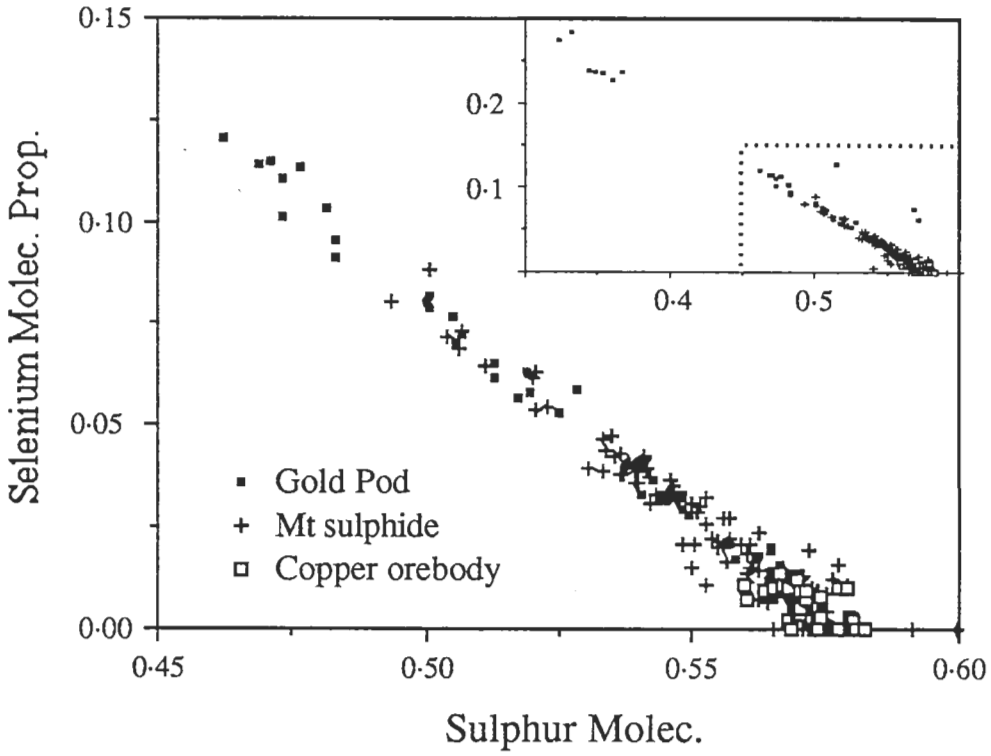

Figure 6.10 — Variation of the molecular proportion of sulphur and selenium in bismuth sulphosalts from the Warrego mine illustrating the general trend of lower selenium content in the copper ore. n = 243.

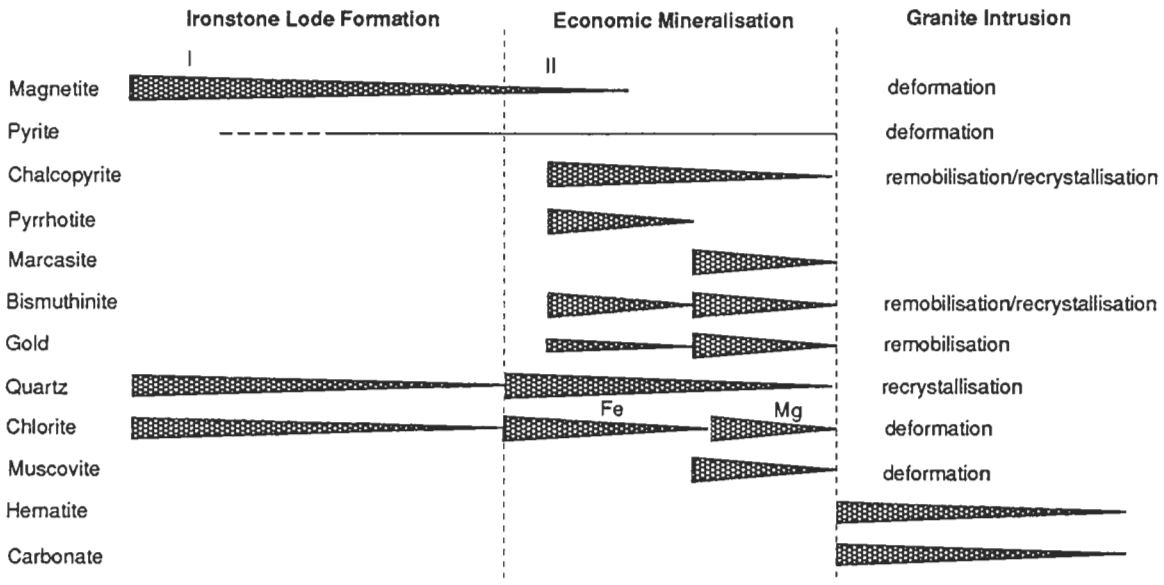

Figure 6.11 — Mineral paragenesis as observed in the Warrego Mine.

Bismuth minerals with their variable chemistry, low melting points, complex solid solution and miscibility gaps between phases makes them useful indicators of the conditions prevailing during mineralisation. Mumme (1976) considers the stability of the complex lead-rich bismuth sulphosalts discovered in the Juno mine is largely due to significant selenium in the mineralising fluid available to stabilise the crystal structure. He therefore considered slow cooling after deposition was important in ordering the minerals, and deposition was from relatively low temperature hydrothermal fluids consistent with other selenium-rich minerals. Sindeeva (1964), Large (1974,1975), Mumme, (1976), and Miller (1981) have all suggested that an abundance of selenium-rich minerals may indicate the solutions that deposited them were sulphur poor. Other possible controls on selenium content are likely to include temperature (Auclair et al., 1987), pH (Yamamoto, 1976), and fO_2 (Thorpe et al., 1976; Shikazono, 1978; Pringle and Thorpe, 1980; Schønwandt, 1983). For further discussion see Chapter Nine.

Blebs of gladite ($CuPbBi_5S_9$) resembling exsolution textures within pekoite ($CuPbBi_{11}S_{18}$) from Juno mine were described by Large (1974), and unsuccessful attempts by Mumme and Watts (1976) to synthesize this phase at temperatures below 400°C led them to suggested it formed when slow cooling to temperatures below 300°C resulted in its segregation from an original solid solution with pekoite. Assemblages useful in constraining the conditions of ore deposition in the Warrego mine include chalcopyrite-wittichenite which has a maximum stability temperature of 395°C (Sugaki et al., 1981), and the occurrence of tellurides which generally suggests temperatures of less than 350°C (Afifi et al., 1988a, 1988b).

6.12 Carrollite

Restricted to the copper orebodies in the upper part of the Warrego mine, a distinctive mineral has been identified that appears to correspond to carrollite. This phase may constitute up to 10% of the lode in the copper-rich ore occurring as euhedral crystals very similar in form and distribution to pyrite but distinguished by its pink colour, perfect crystal outline that is rarely cracked or fractured, and better polish. Crystals may be up to 0.5 mm across and may form large intergrowths with pyrite and their associated cobalt-rich overgrowths. (Plate XIV D). The perfect crystal outlines suggest they have undergone recrystallisation similar to the chalcopyrite during granite intrusion rather than the brittle fracturing of pyrite.

Analyses of several grains from different samples give a constant microprobe composition of $Co_{2.9}Fe_{0.1}CuS_{5.7}$ which approximates the proportions of carrollite $CuCo_2S_4$. A similar cobalt mineral (linnaeite — Co_3S_4) has been reported in the Peko mine (unpublished AMDEL report, 1960), but arsenic cobalt minerals appear to be more abundant. Abundant cobaltite and minor safflorite is reported in Peko (Edwards,

1955; Whittle, 1966), Orlando and Ivanhoe (Whittle, 1966), and Gecko (Huston, 1990a) mines. Peko mine tailings report high cobalt contents (4 Mt @ 0.09% — Australian Development Annual Report, 1986) attesting to the high cobalt content of this ore. Cobalt has been analysed in the copper orebodies from the Warrego mine as part of a geochemical study carried out on 200 one-metre core splits sampled randomly between 2 and 8 levels the early 1970's. A geometric mean of this population of 0.04 % (maximum 0.41%) indicates that although levels are lower than those observed in the Peko mine, cobalt values are still relatively high. There is no information on the cobalt content of the gold pods and copper ore marginal to the pods, but it is likely to be insignificant due to the absence of cobalt minerals from this ore.

6.13 Minor Minerals of Restricted Association

Molybdenite

Although molybdenum is an elevated trace element in many ironstone lodes in the Tennant Creek area (Smith, 1980; Large and Robinson, 1987), discrete molybdenum minerals are rarely observed. Molybdenite has been recorded in the lower levels of Peko (Whittle, 1966), and in White Devil (Nguyen, 1987) mines and its occurrence in the Warrego mine appears to be the only other documented instance.

Molybdenite in the Warrego mine has been observed in association with a mineral assemblage that is restricted to the immediate footwall of the gold pods. Here stringers of magnetite with abundant gold and bismuthinite mineralisation, is found associated with muscovite, chlorite, tetradymite and molybdenite. Individual or clusters of two or three molybdenite laths typically in the order of 40 × 15 μm are hosted by bismuthinite and have been observed wholly within single gold grains (Plate XIV E). In both of the gold pods molybdenite is intimately associated with gold grains; either immediately adjacent to, or within them suggesting a close paragenetic association.

Tourmaline

Tourmaline is a relatively common constituent of the rocks hosting the Warrego ironstone lodes typically occurring in quartz-muscovite veins, but is also observed disseminated through the sediments as euhedral crystals overprinting the foliation of the recrystallised sediments. Tourmaline occurs within the ironstone lodes or alteration assemblages adjacent to them in three associations.

1. Veins of essentially the same composition as those containing tourmaline in the sediments and porphyries have been observed within the ironstone lode on 14 level. These veins overprint mineralisation within the lode, and are consistent with the interpretation of a Warrego Granite related origin of those in the sediments.

2. In the hangingwall of the No. 1 orebody between 7 and 8 levels, a 3–5 m wide zone some 10 m above the ironstone lode contact, an assemblage of tourmaline-chlorite has been logged by company geologists. Although the writer has not examined these rocks, Large (1974) indicated the assemblage is transitional with the chlorite-muscovite-magnetite alteration at the ironstone lode margin. The position of this lens appears to correspond in position and orientation to that expected for the Orebody Fault.
3. At the footwall contact of the No. 1 orebody, discontinuous zones of massive pyrite up to 2 m in width are observed, and in at least one instance tourmaline has been part of the assemblage. Here, euhedral tourmaline appears to have nucleated on and replace pyrite and magnetite crystals (Plate XIV B). In the immediate footwall of the lower gold pod, large euhedral tourmalines also occur disseminated through remobilised bismuthinite in the stringer mineralisation, and in the contact metamorphosed sediments adjacent to them. The tourmaline crystals are often cracked and broken, especially in the vicinity of the lower gold pod where bismuthinite has been remobilised into cracks (Plate XIV A).

The conflicting paragenetic relationships of tourmaline and economic mineralisation make it impossible to categorically assign the tourmaline to a particular paragenesis i.e. economic mineralisation, or granite intrusion and contact metamorphism. However, a granite related paragenesis is preferred because in all cases, tourmaline overgrows and replaces the host assemblage be it magnetite, pyrite, or host rocks, and the tourmaline is typically fresh and unaltered with a random orientation in what is often a strongly foliated host. Tourmaline-pyrite veins are also recorded in the deepest levels of the Peko mine where they overprint the chlorite-anthophyllite-talc alteration assemblage (Whittle, 1966). However, Whittle proposed that this assemblage was a late-stage alteration assemblage related to, or preceding economic mineralisation. There are no young granites (i.e. of Warrego Granite age), recognised in the south eastern part of the goldfield, although there appears to be a contact metamorphic overprint on the sediments hosting the Eldorado ironstone lode which may indicate the presence of granite at relatively shallow depths beneath the Warramunga Group sediments in this area.

Costibite–Famatinite

Within bismuth-rich portions of the copper orebodies in the upper levels of the mine, a rare assemblage is observed. Irregular pools (typically less than 50 μm across, of a white mineral with a higher reflectance than bismuthinite, has been identified by microprobe analysis as costibite (CoSbS). A narrow rim of a grey mineral surrounding the costibite is tentatively identified as famatinite (Cu_3SbS_4). Because this rim is only a few microns wide it has been difficult to obtain a clean analysis, but the mineral

contains copper, antimony, and sulphur in the general proportions of famatinite. These antimony sulphosalts are frequently associated with late-stage quartz-carbonate-hematite veins which cross-cut and replace chalcopyrite veins (Plate XV A &B). This veining is considered post-peak thermal metamorphism associated with the intrusion of the Warrego Granite, and as such probably represents remobilisation of cobalt- and antimony-rich phases during veining.

Phase relations of these antimony-rich minerals provide no useful controls on the condition of mineral formation as they are both stable to temperatures in excess of 800°C (Cabri et al. 1970a, 1970b; Skinner et al., 1972).

Sphalerite

Minute blebs of sphalerite are disseminated throughout the upper copper orebodies, typically occurring as rounded inclusions ~2 μm across within chalcopyrite (Plate XIV F), although it is also observed as inclusions within pyrite. Trains of sphalerite and bismuthinite inclusions are observed along the grain boundaries of chalcopyrite suggesting concentration during recrystallisation.

6.14 Discussion

Despite the relatively simple mineral assemblage observed within the Warrego ironstone lodes, the effects of contact metamorphism have complicated the interpretation of the parageneses especially between the relatively mobile and ductile sulphide phases. However, apart from recrystallisation and localised remobilisation into cracks and fractures, the intrusion of the Warrego Granite and deformation associated with ironstone lode rotation is not believed to have significantly changed the distribution or composition of phases over distances greater than a few centimetres. This is evident in the preservation of well developed zonation in mineralogy, chemistry, and sulphur isotopes (Chapter Eight).

A general paragenesis of ironstone lode formation followed by the introduction of economic mineralisation is indicated for the Warrego and other Tennant Creek mines. This subdivision of the mineralisation into distinct events is summarised in the paragenetic sequence illustrated in Figure 6.11.

The massive magnetite of the ironstone lode retains colloform textures within the magnetite and quartz-magnetite mineral assemblages which suggest rapid precipitation of magnetite or a hematite precursor from solutions supersaturated with iron. Quartz-magnetite intergrowths appear to have been restricted to the outer margins of the lode, and textures within the stringer zone below the gold pods indicate that a significant proportion of the lode formed via direct replacement of the host sediments.

Minor pyrite may have accompanied ironstone lode formation, but the bulk of sulphide and economic mineralisation overprints the ironstone lode and is associated

Plate XV

A: Late-stage hematite(hm)–quartz(qtz)–carbonate(CC) vein in the copper orebody with associated pools of paracostibite (pc) rimmed by famatinite (fm).

B: Extensive veining and replacement of chalcopyrite by late-stage hematite–quartz–carbonate veins. Sample 108476.

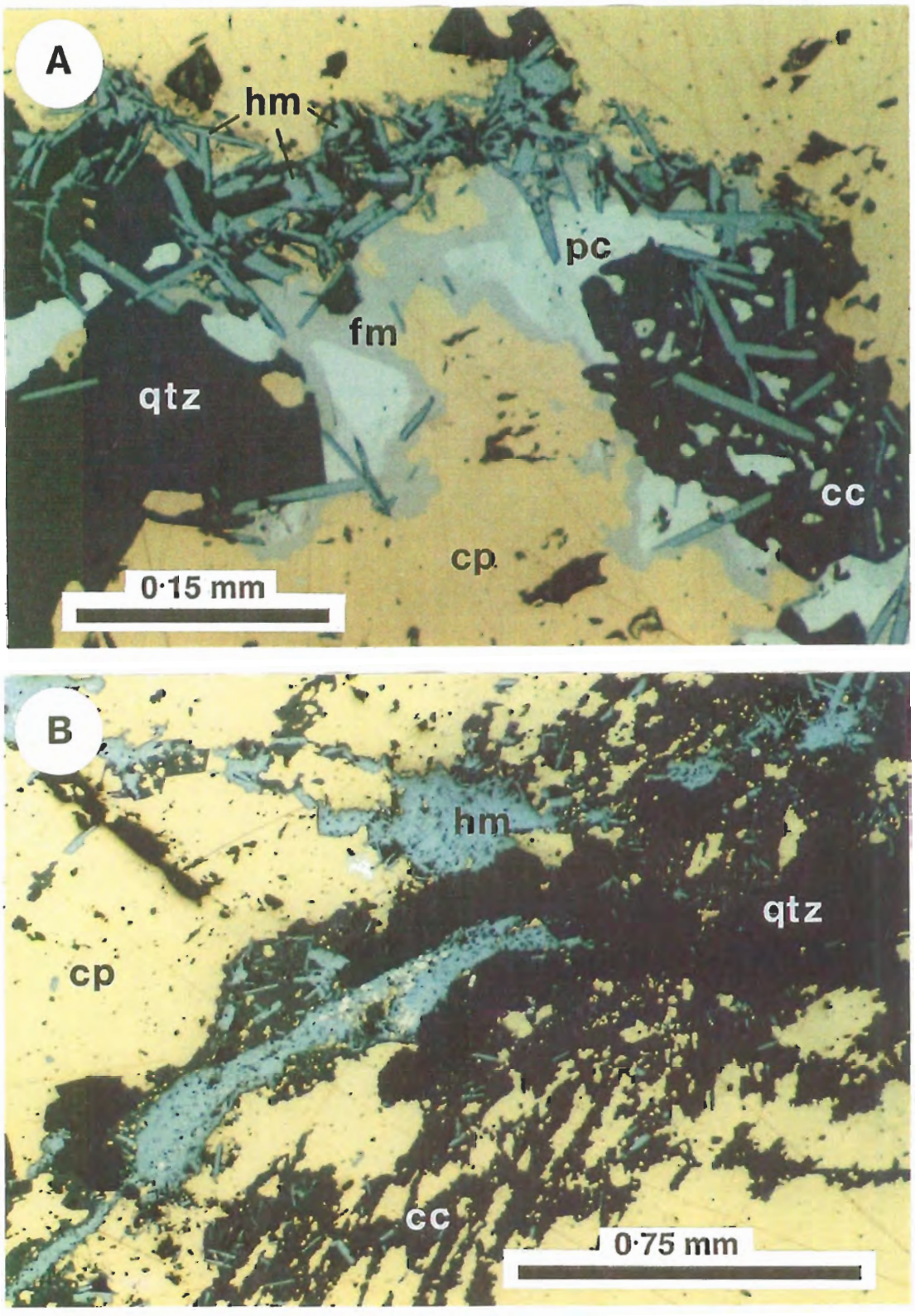
A
hm
pc
fm
qtz
cc
cp
0·15 mm
B
hm
qtz
cp
cc
0·75 mm

with extensive brecciation. The sharp breaks in the massive magnetite and typical overgrowth of euhedral Type II magnetite suggest quartz and sulphide mineralisation has infilled fractures without alteration or replacement, and suggest that there has been a considerable increase in the overall volume of the lode. The relationship of the gold pods to the lode are less obvious because clean breaks in the lode are not evident, and the assemblage appears to comprise a homogeneous intergrowth of magnetite, chlorite and muscovite. However, it is suggested that the outline of the fractures has been smoothed by the overgrowth and infilling of magnetite associated with the magnetite-chlorite-muscovite gold pod mineral assemblage.

Two styles of mineralisation are observed in the Warrego mine, which in many respects characterise mineralisation in the goldfield. Gold-rich, gold pod-style mineralisation is typically copper-poor and associated with considerable bismuth mineralisation (i.e. Juno), whereas copper lodes generally have low gold grades, contain pyrrhotite, and may be associated with cobalt, zinc and lead (i.e. Peko). That the two mineralisation styles are observed within a single ironstone lode suggest that either:

1. Mineralisation is related to a single event in which the changing physico-chemical conditions of the ore fluid resulted in the observed zonation from gold- to copper-rich mineralisation styles, or
2. Copper-rich mineralisation was initially deposited throughout the ironstone lode and a late-stage event associated with changing chemistry of the hydrothermal system as it matured and/or the ingress of solutions with a different chemistry resulted in a gold-rich overprint in the vicinity of the gold pods.

While many of the mineralogical and chemical differences between the two styles of mineralisation are compatible with physical or chemical gradients within the mineralising system, e.g. decreasing gold fineness and changing bismuth chemistry, other differences are not compatible with a single stage model. Notable is the abundant evidence throughout the copper orebodies of the former presence of pyrrhotite which indicates relatively reduced conditions at the time of mineralisation. This contrasts with the ferric iron-rich magnesian chlorites of the gold pod which apparently indicate relatively oxidised conditions. A fluid evolution model involving the reduction of oxidised solutions in equilibrium with magnetite in the gold pod to (at least) the magnetite-pyrrhotite stability boundary in the copper orebody is to say the least improbable. Whereas the early introduction of relatively reduced copper-rich solutions followed by more oxidised gold-rich solutions which overprinted the lode and oxidised the pyrrhotite to a pyrite/marcasite assemblage is consistent with observations.

Chapter Seven

GEOCHEMISTRY AND ALTERATION

7.1 Introduction

In an attempt to further constrain the mechanism of formation of the Warrego orebody, a programme of geochemical sampling of the sediments and porphyries hosting the Warrego ironstone lode was undertaken. 14 level was selected for this study because the main ore haulageway and its extension as a deep exploration drill drive (FEX drive), provides the most extensive exposure of the host rocks in both the footwall and hangingwall. Samples were collected at 20 m intervals along the drives and at closer intervals in the immediate footwall and hangingwall of the two ironstone lodes (Figure 7.1). Additional samples were collected from drillhole 3 in the FEX drive, and the gold pod and its immediate footwall on 14 level. A total of 72 samples were analysed for major and trace elements by XRF spectrometry and are reported in Appendix C.

The samples have been divided into five general groupings: sediments (40), ironstone lode (11), porphyry (10), dykes (6), and veins (5), and these are first discussed in terms of their general character and chemical variability.

7.2 Sediments and Porphyries

Petrographically the sediments vary from coarse, poorly sorted, immature greywackes to finely laminated shales. All are well cleaved, and show variable effects of contact metamorphism and hydrothermal alteration. The porphyries exhibit similar variability, with samples that are quartz or quartz-feldspar phyric, typically with a strongly chloritised matrix. Both the sediments and porphyries show a range in their major and trace element chemistry that reflects their composition and alteration, and as such are chemically indistinguishable from each other. Because of the modification of the primary element chemistry of these rocks through alteration, attempts to characterise their source and possible tectonic setting at the time of deposition rely on the use of immobile trace elements.

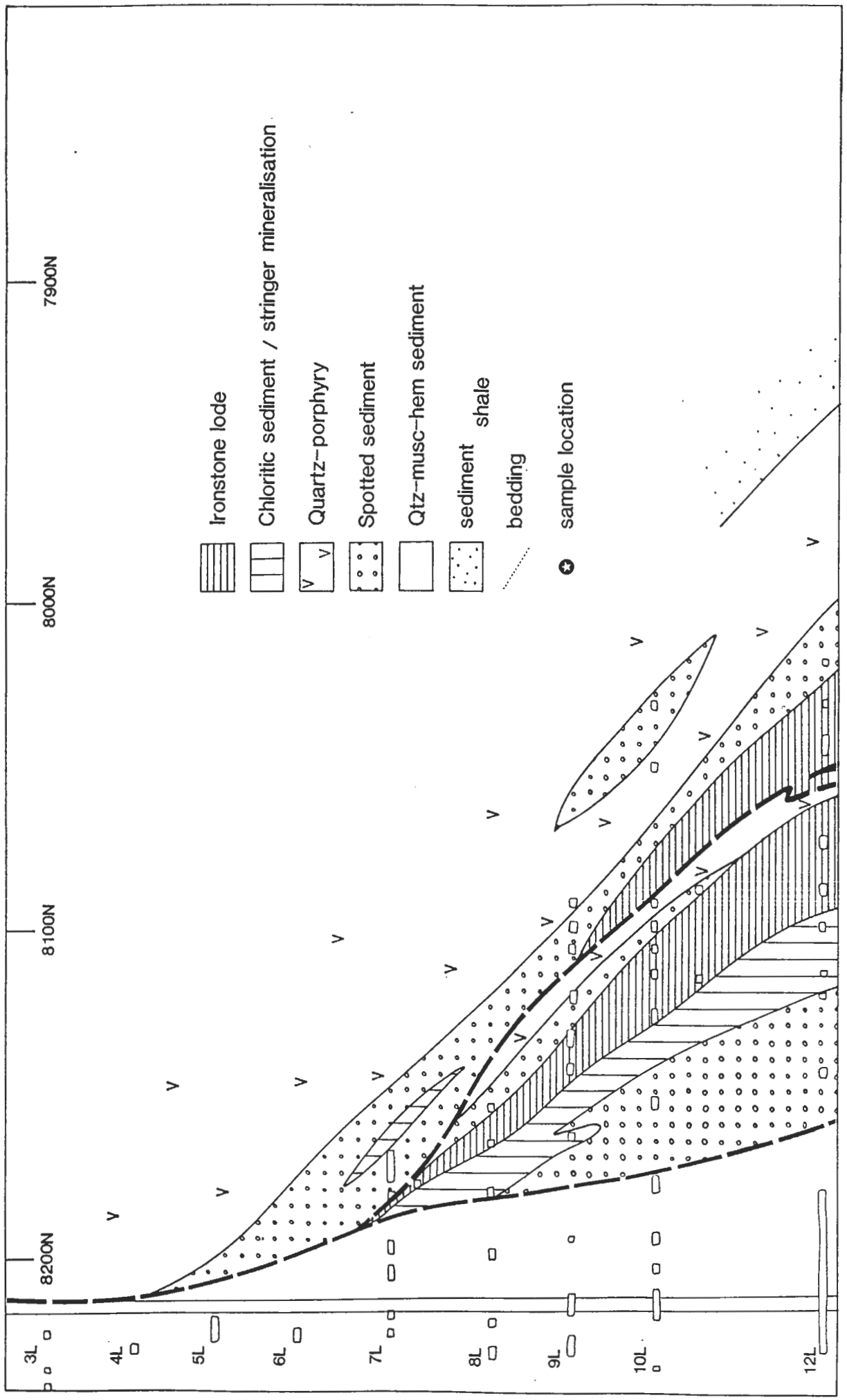
Ironstone lode
Chloritic sediment / stringer mineralisation
Quartz-porphyry
Spotted sediment
Qtz-musc-hem sediment
sediment
shale
bedding
sample location
7900N
8000N
8100N
8200N
3L
4L
5L
6L
7L
8L
9L
10L
12L

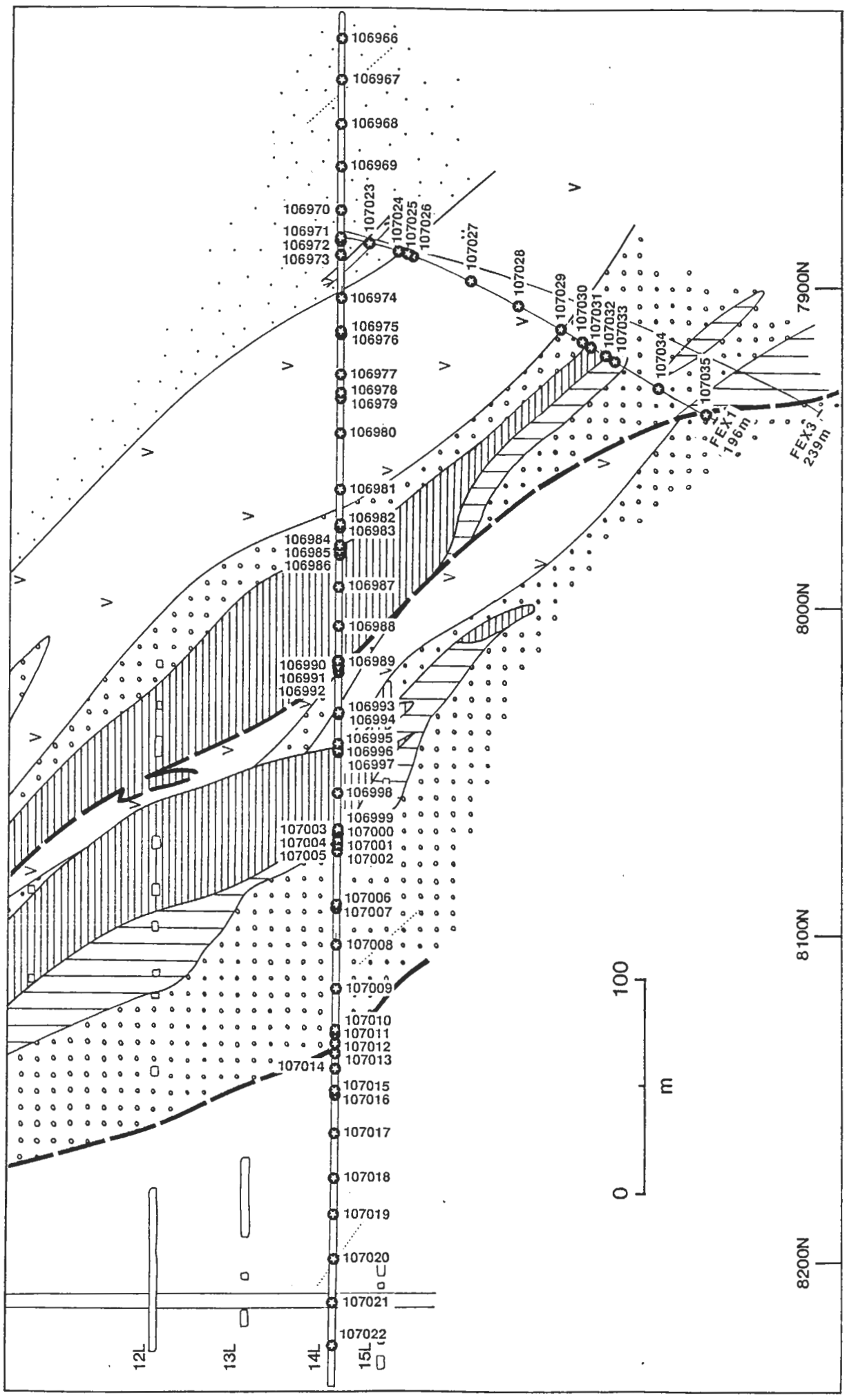

Figure 7.1 — Oblique section through the Warrego ironstone lodes along the line of the 14 level and the FEX drives (Fig. 4.2) illustrating the location of samples discussed in this chapter.

Elements with a high charge/ionic radius (e.g. Ti, Zr, Y, Nb, Ce, Ga, and Sc) are minor and trace constituents of rocks, and because of their predictable partitioning into restricted mineral species, they may be used to characterise the degree of magmatic differentiation in volcanic rocks (Pearce and Cann, 1973; Winchester and Floyd, 1977). These elements are also considered inert during secondary processes and therefore ratios of these 'immobile elements' have been used to characterise tectonic settings of volcanic (Pearce and Cann, 1973) and sedimentary (Bhatia and Crook, 1986; Morris, 1988) rocks, as well as to define the original character of altered volcanics (Floyd and Winchester, 1978). The most commonly used index of differentiation and alteration is the ratio of Ti and Zr (e.g Winchester and Floyd, 1977; Floyd and Winchester, 1978; Petersen, 1983; Bhatia and Crook, 1986; MacLean and Kranidiotis, 1987).

A frequency histogram of Ti/Zr for the sediments and porphyries of the Warrego mine sequence (Figure 7.2) shows their separation into two distinct populations with mean values of 12.4 and 19.4 and standard deviations of 1.4 and 1.5 respectively. The sediments are equally divided between the two populations, but the porphyries define a tight grouping that overlaps with the highest concentration of sediment samples within the lower Ti/Zr population. Although the high Ti/Zr population shows a slight negative skewness, the well defined separation and low standard deviations of the two populations indicate that mixing between the two has been minimal.

To test the assumption of Ti and Zr immobility in the Warrego host rocks, correlation coefficients of commonly suggested immobile elements have been calculated (Table V). High degrees of correlation between particular elements result because, either they have been added or removed in constant proportions with alteration (e.g. K, Pb, Rb, and Sr show relatively high correlation coefficients as they are removed during breakdown and dissolution of feldspar and muscovite), or, because they have been resistant to alteration (e.g. Ti and Zr), they maintain their primary ratio despite dilution or enrichment resulting from the addition or removal of other phases respectively. With the exception of Ce, the porphyries show a high degree of correlation between the immobile elements, whereas the sediments (divided into the high and low Ti/Zr populations), show decidedly weaker correlations. However in all three groups, Ti and Zr are strongly correlated, attesting to their immobility, the validity of separating the samples into the two populations, and the potential use of Ti/Zr as an index against which mobility of other elements may be measured. The general lack of correlation between the other 'immobile' elements is attributed to the inherent compositional variability within the sediments that results from sorting during deposition, and the mobility of several of these elements during alteration (see below).

There is no recognisable pattern in terms of alteration, grainsize, sorting, or spatial distribution in the sequence to account for the two populations defined by Ti/Zr. Both

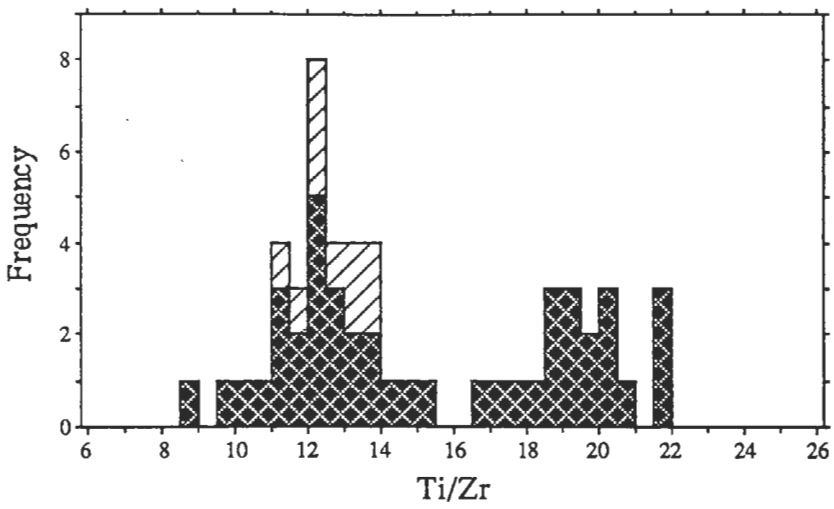

Figure 7.2 — Frequency distribution of Ti/Zr for sediments (cross-hatched) and porphyries (diagonal lines) of the Warrego sequence illustrating their separation into two, essentially non-mixed populations.

TABLE V: Correlation between Immobile Elements

Porphyry (Low Ti/Zr)

	TiO2	Al2O3	P2O5	Ce	Ga	Nb	Sc	Th	Y	Zr
TiO2	1									
Al2O3	0.982	1								
P2O5	0.917	0.959	1							
Ce	0.763	0.677	0.638	1						
Ga	0.857	0.926	0.925	0.499	1					
Nb	0.953	0.966	0.914	0.628	0.895	1				
Sc	0.972	0.981	0.949	0.708	0.885	0.930	1			
Th	0.944	0.947	0.933	0.706	0.918	0.957	0.922	1		
Y	0.933	0.899	0.881	0.832	0.718	0.852	0.942	0.847	1	
Zr	0.982	0.969	0.929	0.807	0.858	0.943	0.956	0.945	0.942	1

Sediment (Low Ti/Zr)

	TiO2	Al2O3	P2O5	Ce	Ga	Nb	Sc	Th	Y	Zr
TiO2	1									
Al2O3	0.296	1								
P2O5	0.444	0.426	1							
Ce	0.377	-0.013	0.271	1						
Ga	0.022	0.725	0.165	-0.228	1					
Nb	0.680	0.718	0.483	0.331	0.338	1				
Sc	0.457	0.644	0.487	0.543	0.206	0.840	1			
Th	0.634	0.532	0.583	0.612	0.330	0.779	0.748	1		
Y	0.447	0.459	0.444	0.609	0.215	0.602	0.675	0.683	1	
Zr	0.826	0.007	0.270	0.417	-0.280	0.537	0.337	0.472	0.348	1

Sediment (High Ti/Zr)

	TiO2	Al2O3	P2O5	Ce	Ga	Nb	Sc	Th	Y	Zr
TiO2	1									
Al2O3	0.928	1								
P2O5	0.760	0.627	1							
Ce	0.245	0.308	0.129	1						
Ga	0.390	0.304	0.075	0.439	1					
Nb	0.846	0.876	0.581	0.048	0.289	1				
Sc	0.325	0.623	-0.037	0.253	0.061	0.583	1			
Th	0.895	0.832	0.803	0.116	0.214	0.830	0.314	1		
Y	0.339	0.348	0.604	0.390	-0.045	0.265	0.147	0.497	1	
Zr	0.958	0.864	0.818	0.110	0.219	0.859	0.259	0.899	0.327	1

populations show varying degrees of alteration, with the sediments in each ranging from coarse, poorly sorted greywacke to finely laminated shales. Samples 107006 and 107007, are poorly sorted medium and fine-grained sandstones respectively, they were collected from within a single sedimentary unit, and despite their variable chemistry, belong the same Ti/Zr population. On 14 level the distribution of samples between the two populations is apparently random, with abrupt changes from one to the other throughout the sequence (Figure 7.3). Ti/Zr is therefore considered to represent a primary 'signature' that is related to the source of the sediments and porphyries rather than to a secondary sorting or alteration processes. The abrupt variation from one population to the other, and their distinct non-mixed character strongly suggests that there are two fluctuating 'sources' for the sediments and that they were deposited as discrete events without mixing.

To examine in greater detail the differences in chemistry of the three populations within the Warrego mine sequence, selected major element oxides and trace and minor elements have been plotted against Ti/Zr in Figure 7.4. To help distinguish primary variation in the composition of the sediments and porphyries from alteration, samples that are obviously altered (containing significant chlorite) are distinguished in the plots (open symbols) from those that are relatively unaltered (filled symbols). Because Ti/Zr is relatively constant within each population, it may be used as a standard against which the mobility of other elements is assessed.

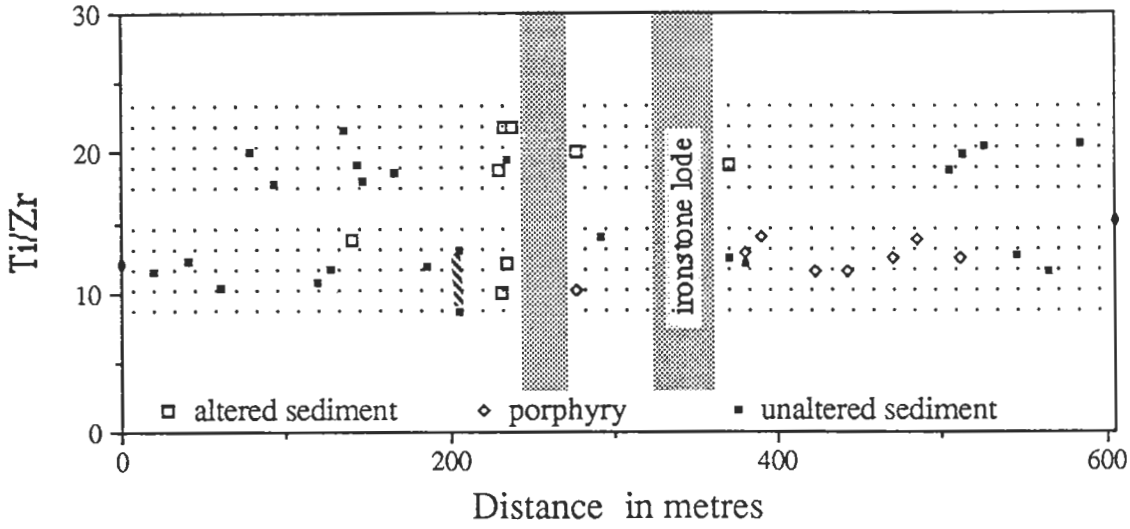

Figure 7.3 — Variation of Ti/Zr for sediments and porphyries on 14 level of the Warrego mine. Note the lack of correlation of the two populations with either alteration or sediment grain size. Samples 107006 and 107007 (medium and fine sandstone samples collected from a single graded bed) are joined by the striped tie-line.

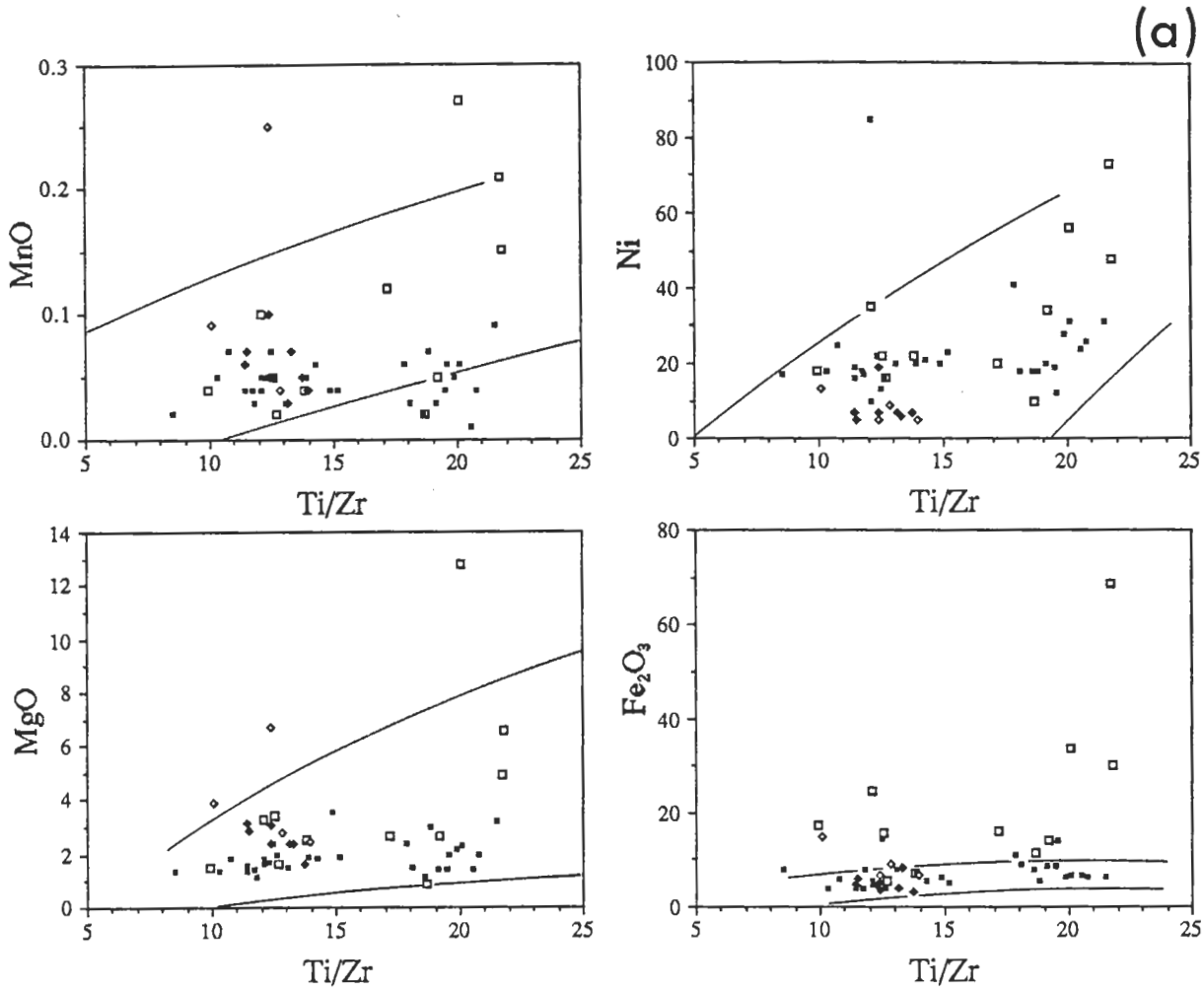

Figure 7.4 — Variation of elements with Ti/Zr illustrating patterns of (a) enrichment (Fe_2O_3, MnO, MgO, and Ni), (b) depletion (SiO_2, Al_2O_3, K_2O, and Sc), and (c) relative immobility (TiO_2, Ga, V, and Zr) with alteration. Also indicated are typical igneous fractionation trends illustrating the relative conformity of much of the sediment chemical variation with probable source rock chemistry. Symbol: diamond = porphyry; square = sediment; filled and open symbols represent unaltered and altered samples respectively.

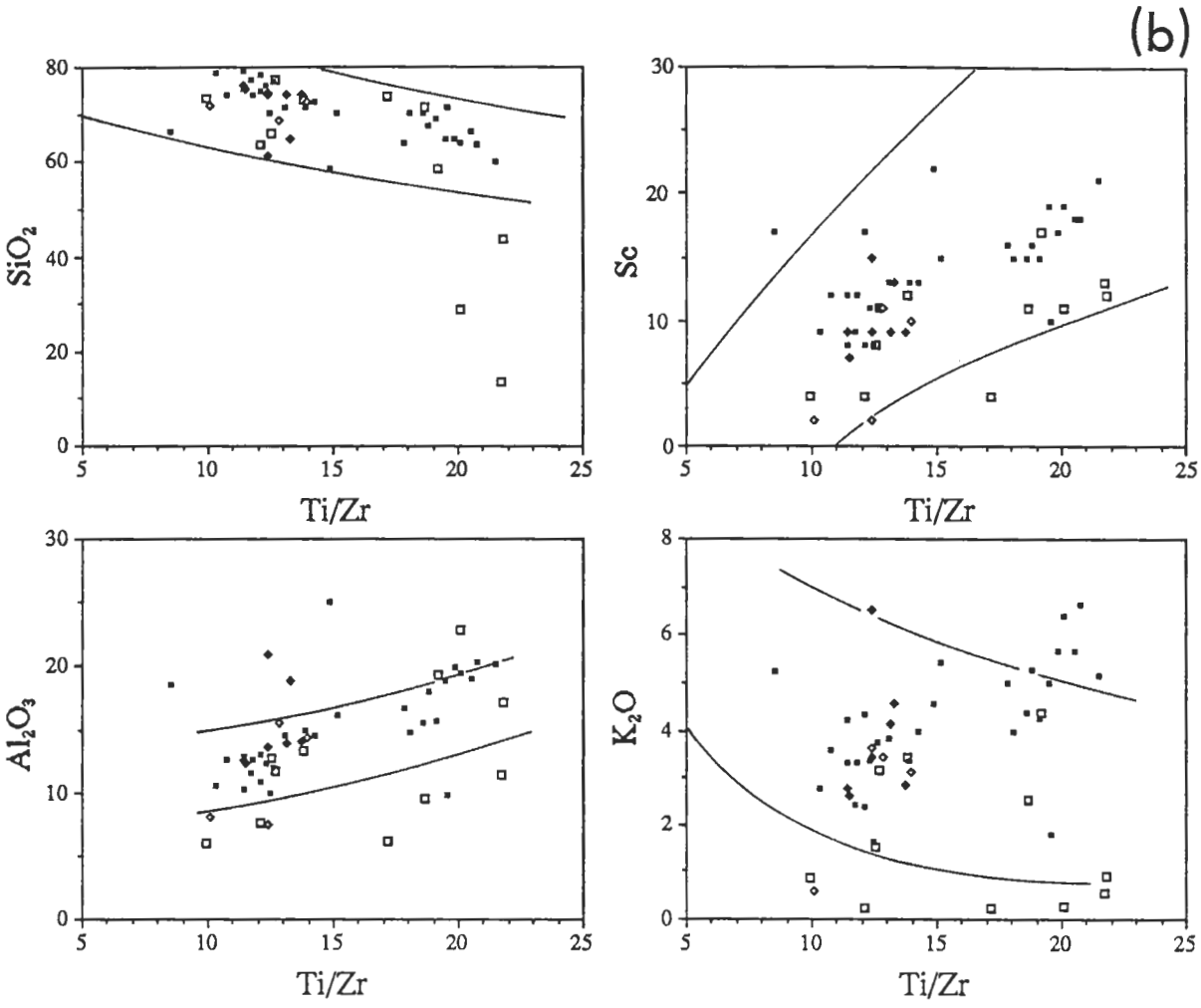

Figure 7.4 — cont.

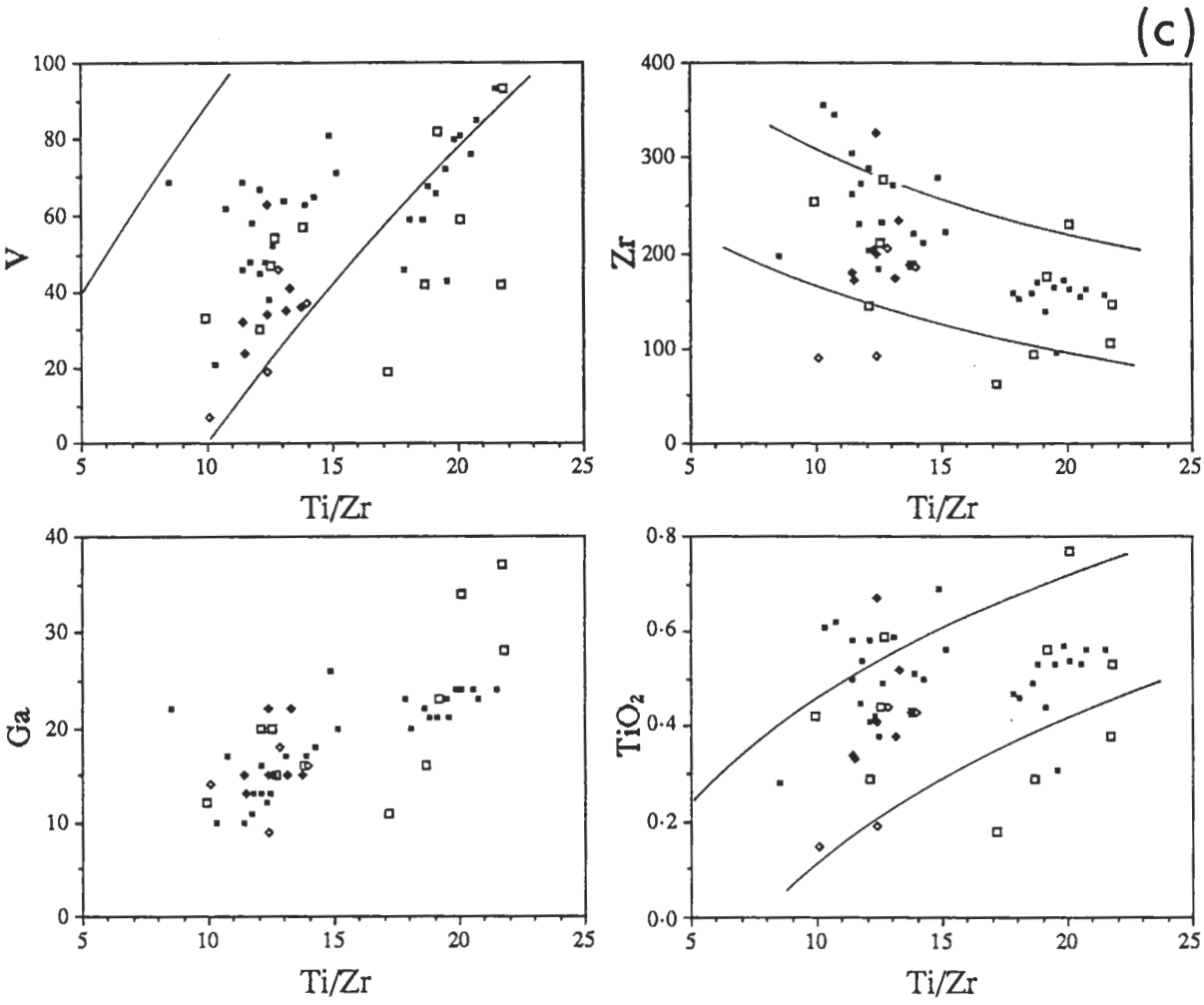

Figure 7.4 — cont.

Three patterns are evident in the relationship of altered to non-altered rocks in Figure 7.4: relative enrichment (e.g. Fe_2O_3, MnO, MgO, Bi, Cu, Mo?, Nb?, Ni and Zn), depletion (e.g. SiO_2, Al_2O_3, CaO, Na_2O, K_2O, Ba, Cr, Pb, Rb, Sc, and Sr), and constancy (e.g. TiO_2, P_2O_5, Ce, Ga, La, Nd, Th, U, V, and Zr). The patterns of element enrichment and depletion conform with observed mineralogical changes observed in hand specimen and thin section. That is, enrichment in Fe_2O_3 and MnO (magnetite), MgO (chlorite), and 'ore' elements (Bi, Cu, Mo, Ni, and Zn), accompanied by depletion of SiO_2 (quartz), Al_2O_3, CaO, Na_2O, K_2O, Ba, Pb, Rb, and Sr (feldspar and muscovite). Elements that are relatively immobile under the alteration (i.e. showing greater variability in the unaltered sediment than between the unaltered and altered sediments) are constituents of minerals such as apatite, rutile, monazite, and zircon which are the most resistant in hydrothermal and metamorphic alteration.

Another characteristic of the unaltered sediments highlighted in Figure 7.4 is the often coherent behaviour of elements and element oxides with Ti/Zr (i.e. SiO_2, TiO_2, Al_2O_3, K_2O, Cr, Ga, Ni, Rb, Sc, V, and Zr). Because Ti/Zr is a good index of magmatic differentiation (decreasing with more siliceous compositions), this coherent behaviour may reflect primary magmatic variation in the source rocks. Typical magmatic differentiation trends (defined for the Cambrian Mt Read Volcanic Belt of western Tasmania — A.J. Crawford, unpublished data) have been superimposed on the Warrego Ti/Zr plots, and although trends are often so broad as to encompass the entire range of Warrego samples, there is often a good correlation, e.g SiO_2, Fe_2O_3, Cr, Sc, Ni, V, and Zr against Ti/Zr.

However other plots (notably Al_2O_3 and K_2O), define trends that differ significantly from those expected of magmatic differentiation. Because these elements are representative of the argillaceous components within the sediments, it would appear that the high Ti/Zr population is slightly more argillaceous (less well sorted) than the low Ti/Zr population. The relatively minor variations in the proportion of matrix required to produce this variation (5–10%), were not visually detected in thin section, and is probably attributable to the variable alteration and metamorphism observed in the sediments. Therefore the major element chemistry of the sediments reflect the bulk composition of the source material, although modified by sedimentary processes such as sorting. The trace elements appear to preserve primary magmatic differentiation trends.

As would be expected for an intrusion, the quartz±feldspar porphyry analyses are relatively tightly grouped and do not show the same degree of variation exhibited by the sediments. A single sample (107023), which shows anomalous major and trace element enrichment (CaO, K_2O, Na_2O, Ce, La, Nb, Nd, Pb, Rb, Sr, Th, U, V, Y) relative to the other porphyry samples, is from a narrow porphyry dyke intersected in the FEX drillhole. Enrichment in this suite of elements is characteristic of the Warrego Granite

(Wyborn et al., 1987; Stoltz, 1990), and this dyke is therefore correlated with the intrusion of this body.

Sorting in the unaltered sediments is likely to be recorded by SiO_2/Al_2O_3 which will reflect the ratio of arenaceous to argillaceous components in the sediments. Because K-feldspar is only a very minor or non-existent constituent of the sediments, K_2O content should therefore be largely a function of the argillaceous component and be correlated with SiO_2/Al_2O_3. Thus a plot of SiO_2/Al_2O_3 against K_2O should result in the data points falling on a mixing curve that defines the sorting between the argillaceous and arenaceous end-members (Lickley et al., 1987). Figure 7.5a illustrates that the Warrego sediments generally behave in the predicted manner, with the unaltered sediments defining a hyperbolic mixing line. Separation of the sediments into their two Ti/Zr populations (Figure 7.5b), reveals there is considerable overlap, and therefore rather than representing two end members of an unmixing or sorting process, both populations show essentially the same sorting range. Therefore the distribution of Ti/Zr values has not been generated by sorting, but has been preserved in spite of it.

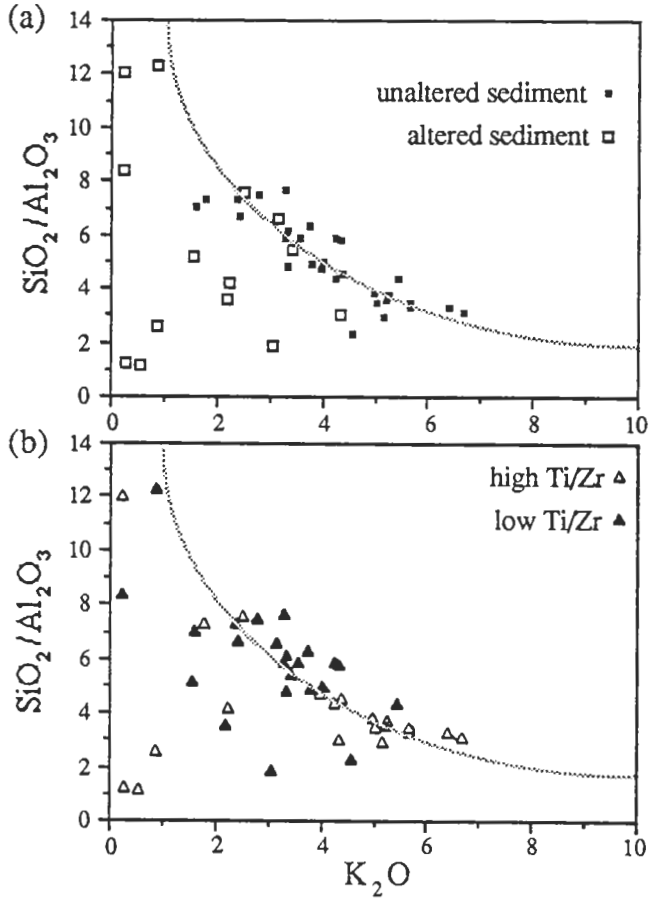

Figure 7.5 — Sorting plots for sediments from the Warrego sequence. SiO_2/Al_2O_3 is a function of the ratio of argillaceous and arenaceous components of the rocks, and because K_2O is also a function of this ratio, the plot defines a mixing curve between argillaceous and arenaceous end-members. The mixing curve represents sorting of end-members of an originally homogeneous sedimentary material. Figure a) illustrates the general conformity of unaltered sediments to the hyperbolic mixing line, while b) illustrates a broad overlap of the two Ti/Zr populations indicating that Ti/Zr has been preserved during sorting and that the two populations cannot represent some sorting of an originally homogeneous source material.

7.3 Tectonic Setting

Previous authors have suggested that because the volcanic derived Warramunga Group sediments are often coarse, poorly sorted, and immature in character, they are derived from a relatively proximal volcanic source (e.g. Ivanac, 1954; Large, 1974, 1975). Although many of the primary sedimentary features in the Warrego mine have been modified through alteration and recrystallisation, there is a strong volcaniclastic component to these sediments evidenced in their petrography in the upper parts of the mine less affected by contact metamorphism (Duncan, 1970; this study). In addition, the similar major and trace element chemistry of the porphyries and sediments suggest that they are derived from similar sources. The preservation of two distinct populations based on Ti/Zr values suggest very rapid erosion and redeposition of freshly erupted material into an adjacent sedimentary basin.

Floyd and Winchester (1978) suggested that fingerprinting of the original character of altered volcanic rocks through the use of immobile element ratios can also be extended to volcanogenic sediments, provided they do not contain much non-volcanogenic material. Because the Warramunga Group sediments appear to fit this criteria, it is suggested that the high and low Ti/Zr populations observed in the Warrego sequence are derived from volcanics with compositions at the dacite-andesite and rhyolite-rhyodacite transitions respectively. Thus the Ti/Zr values appear to be related to slight differences in the degree of fractionation of the two source regions. The apparently random fluctuations between these two sources observed through the stratigraphy of the mine sequence is interpreted as representing slumping and turbidity current deposition triggered by localised tectonic or volcanic activity in their respective source areas.

The porphyries in the Tennant Creek Inlier have been linked to the Tennant Creek Granite on the basis of their similar petrography and major element chemistry (Duncan, 1970), and the similarity in age of volcanics within the Bernborough Formation (suggested in Chapter Two to be coeval with the porphyries of the Carraman Formation) and the Tennant Creek Granite (Black, 1984). With the exception of this study and analyses of porphyries within the Warramunga Group more than 50 km south of Tennant Creek in the Davenport province (Blake et al., 1987), there are no published trace element data on the composition of porphyries within the Warramunga Group. However comparison of this limited and widely separated data with the Tennant Creek Granite (Wyborn et al., 1987) on primordial mantle-normalised element variation diagrams (Fig. 7.6) further supports the co-magmatic nature of their association. The Warrego unaltered sediments and porphyries, and the Davenport province porphyries show patterns that are essentially identical to those of the Tennant Creek Granite; differing only where alteration is assumed to have removed relatively mobile elements (i.e. Ba and Sr).

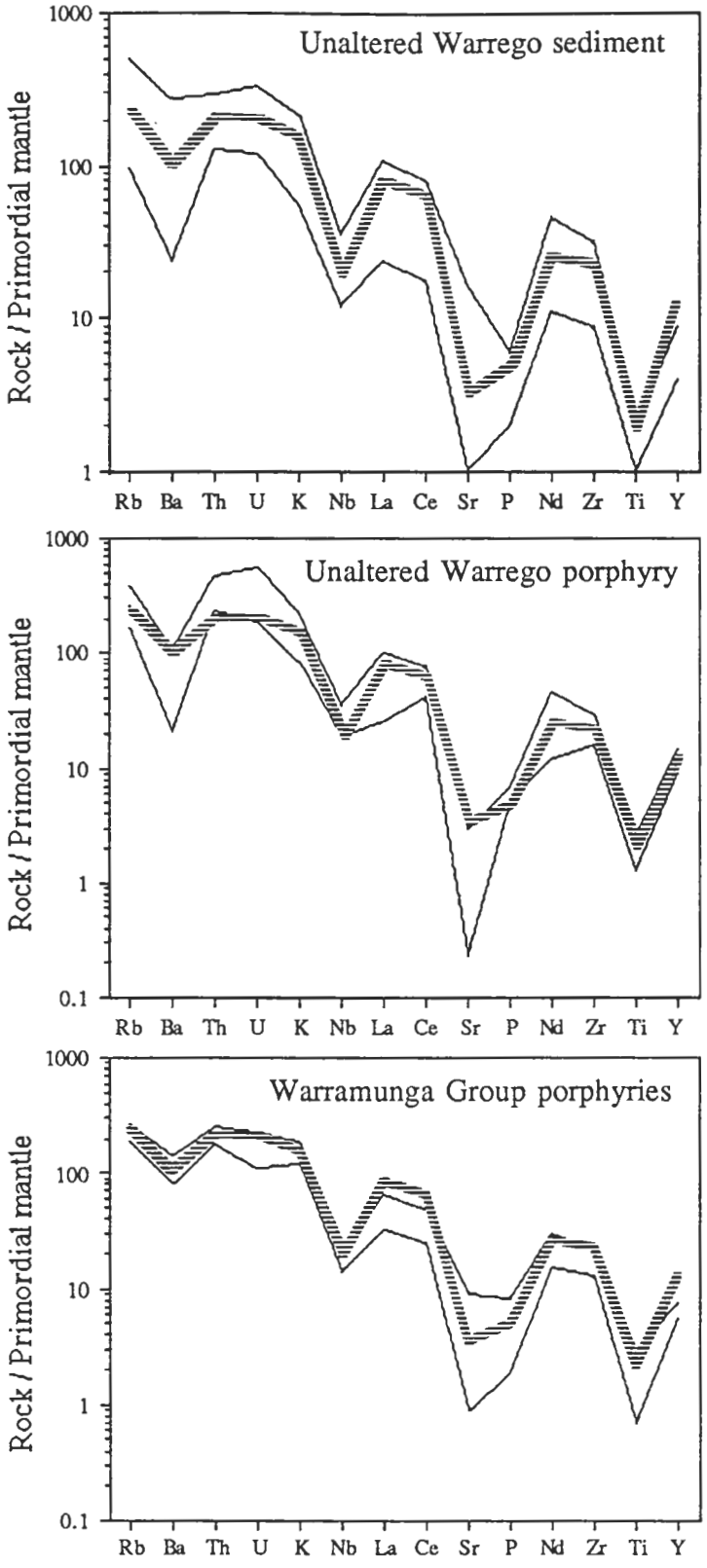

Figure 7.6 — Primordial mantle normalised geochemical diagrams illustrating the compositional range of unaltered Warrego sediments, porphyry, and the Davenport porphyries (Blake et al., 1987) compared to the Tennant Creek Granite - striped line (Wyborn et al., 1987). Excellent correlation between these rocks is evident with the exception of Ba and Sr which are which were likely to have been mobile during alteration.

Bhatia (1983) and Bhatia and Crook (1986), have suggested that it is possible to geochemically characterise the tectonic setting of turbidites through a comparison of the chemistry of the sediment and the presumed source rocks i.e. oceanic island arc (andesitic), continental island arc (dacitic), active continental margin (granite-gneiss and siliceous volcanics) and passive margin (older sedimentary and metamorphic rocks). However, comparison of the averaged compositions of greywacke samples thought representative of these tectonic settings (Bhatia, 1983; Bhatia and Crook, 1986), with the Warrego Granite (Wyborn et al., 1987) on a primordial mantle-normalised element variation diagram, indicates that three of the four tectonic settings are indistinguishable from the range observed for the Warrego sediments and porphyries (Fig. 7.7). It therefore seems likely that while the sediments and porphyries were probably derived from a source of similar composition to the Warrego Granite, it is not possible to determine a direct genetic link between the two. The compositional similarity of similar aged intrusions and volcanics in the Mount Isa, Pine Creek, and Tennant Creek Inliers (within the range observed in the Warrego sediments and porphyries — Wyborn et al., 1987) further illustrates this point.

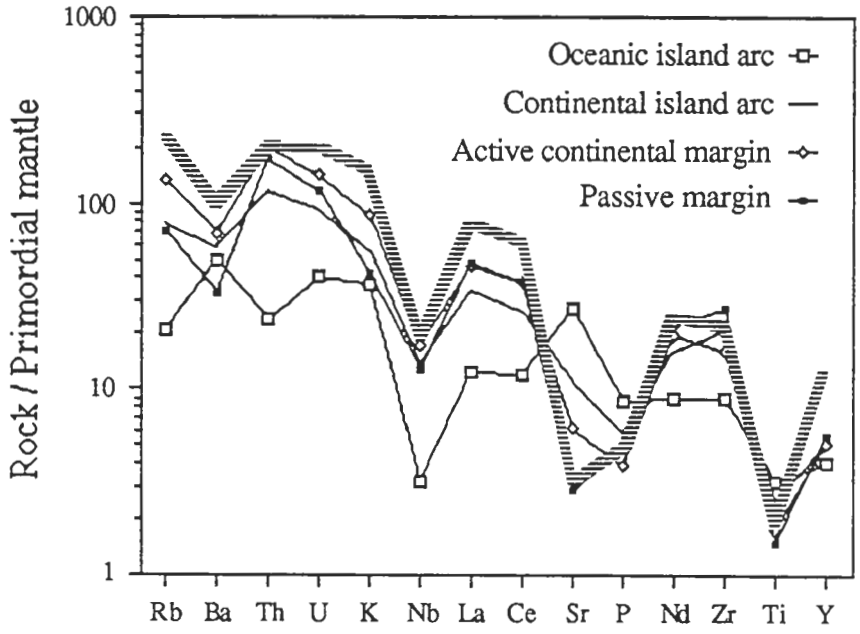

Figure 7.7 — Primordial mantle normalised geochemical diagram of averaged Paleozoic greywacke compositions from diverse tectonic settings in eastern Australia compared to the Warrego Granite (striped line from Figure 7.6). Note: with the exception of the Oceanic Island Arc setting these diagrams are virtually indistinguishable from the range observed in the Warrego sediments.

7.4 Dykes

Dykes within the Warrego sequence are difficult to distinguish underground unless there is a marked contrast between the lithologies (e.g. fine-grained dyke hosted by quartz porphyry), and therefore their proportion within the sequence has probably been underestimated. Two dykes analysed in this study are massive, dark green, and are characterised by abundant disseminated Ti-oxides. In thin section relict ferromagnesian minerals are pseudomorphed by chlorite in a recrystallised carbonate- and muscovite-rich matrix. Chemically, the dykes are quite distinctive from the sediments with relatively low SiO_2 and Th, and high TiO_2, MgO, P_2O_5, Cr, Ni, Sc, V, and Zn. High Ti/Zr (64 and 73) suggest a basaltic primary composition for the dykes but little other information is discernible due to their extensive alteration. There is no evidence of contact alteration, and there are no sulphides associated with the dykes or elevated abundances of ore elements.

Highly altered rocks at the footwall of the No. 3 orebody (106990–106992), and overlying the No. 1 orebody (106995), have a markedly different chemistry to that of the altered rocks in the footwall of the the No. 1 orebody, and therefore an origin other than alteration of sediment associated with ironstone lode formation is suggested. The samples from both localities contain abundant finely disseminated anatase/rutile, but no magnetite or hematite, similar to the hangingwall porphyries and the mafic dykes. They also exhibit isolated sericitic patches preserved within the altered matrix, suggesting the pseudomorphous replacement of phenocrysts, but as there are no 'quartz eyes' evident in these rocks they clearly do not represent thin units of quartz porphyry. The matrix of sample 106995 comprises a randomly oriented mass of felted chlorite, but samples 106990 to 106992 are quite distinct, comprising coarse, randomly oriented blades of muscovite (altering to a fine sericite) in a carbonate and chlorite matrix. Ti/Zr values overlap with the low Ti/Zr sediment population and the porphyries.

While it does not appear possible to definitively establish the affinity of these samples, the content of Ti-oxides rather than Fe-oxides, together with the presence of altered phenocrysts and a distinctive alteration assemblages suggest these rocks are igneous in origin. Their location in the immediate footwall and hangingwall of the No. 3 and No. 1 orebodies respectively corresponds to the location of the proposed Orebody Fault and it is possible that a dyke or dykes were intruded along this plane of weakness. The coarse, randomly orientated textures observed in these samples are distinct from the typically strongly foliated character of the ironstone lode contacts suggesting a post-Warrego Granite age to these rocks again supporting an intrusive origin.

7.5 Granite-Related Veins

Four samples from quartz veins and one from a pegmatite vein were analysed as a comparative study of what are considered granite-related features. Although somewhat tenuous, the linking of the pegmatites and quartz-muscovite-tourmaline veins to the Warrego Granite is based on the observation of similar veins in the vicinity of the Warrego Granite on the surface (Le Messurier, unpublished company report, 1976), and their distinction from the characteristic chlorite alteration associated with the ironstone lodes and mineralisation. Also the veins are observed on both sides of the Footwall Fault, well removed from the alteration associated with the ironstone lodes, supporting a non-mineralisation vintage. Quartz-tourmaline veins are also observed cross-cutting the ironstone lode and the elevated rare earth elements in sample 106988 are attributed to such veining (see below).

The veins vary from massive buck quartz to those carrying a significant proportion of coarse bladed muscovite and fibrous radiating tourmaline crystals. Despite the pink colouration and presence of orthoclase within the the pegmatite vein, the dominant feldspar appears to be albite (supported by the whole rock chemistry, 5 wt. % Na_2O versus 1.5 wt. % K_2O). The pink colouration is probably imparted by the finely disseminated hematite in the typically turbid feldspars.

The chemistry of the non-pegmatite veins is dominated by SiO_2, Al_2O_3, and K_2O (quartz and muscovite), which differs from the typically pervasive chlorite-dominated alteration associated with the mineralisation. Elevated contents of some trace elements in the vein samples suggest there has been some mobilisation of Cu (maximum value 193 ppm), Bi (103 ppm), Mo (38 ppm), La (78 ppm), Ce (165 ppm), Nd (65), and Zr (175 ppm), although elevated values of many of these elements in granite-related veins and pegmatites is not uncommon (e.g. Guilbert and Park, 1986).

7.6 Ironstone Lode

The main drive passes through the ironstone lode marginal to the lower gold pod, thus samples collected along this drive comprise either quartz-magnetite or quartz-magnetite-sulphide assemblages. Both the No. 1 and No. 3 orebodies were sampled, with the hangingwall to footwall sequence represented by samples 106986 to 196989 and 106997 to 106999 respectively. Sample 107000 has been included in the discussion of ironstone geochemistry as an example of the most altered sediment, being collected 1 metre from the footwall contact of the No. 1 orebody. Because access to much of the ironstone lode on this level was restricted because the bulk of the ore had been extracted (Fig. 4.2), two additional samples from the gold pod were collected from drillcore (107055 and 107056) to cover the spectrum of mineral assemblages observed on this level. Samples 107031 and 107032 are also from drill core and were sampled from a narrow intersection of

ironstone lode from FEX 3, the deepest intersection of the Warrego ironstone lode (Fig. 7.1).

Compared to the host sediments, Fe_2O_3 and MnO are enriched in the ironstone lode, while SiO_2 and to a lesser extent Al_2O_3, MgO, K_2O, TiO_2, and Na_2O show varying degrees of depletion. CaO and P_2O_5 (apatite) appear to be the exception among the major elements, remaining relatively constant. The simple chemistry of the ironstone lode samples is reflected in the calculated normative mineralogy of the samples (quartz, magnetite, chlorite, muscovite, and sulphides) which is illustrated in Figure 7.8. Magnetite is the dominant mineral (including 107000) ranging from slightly over 50 weight % to approximately 90 weight %. The variability in the proportion of the other minerals reflects to a certain extent the gangue mineral zonation discussed in Chapter Three. The No. 3 orebody shows a gradation from quartz-magnetite to a magnetite-chlorite assemblage from hangingwall to footwall (106986 to 106989); however the No. 1 orebody the zonation is reversed (106997 to 106999). There is an abrupt transition from the altered footwall sediments to the quartz-magnetite lode rather than the gradation apparent in the gold pods (e.g. 107055 to 107056). Muscovite (K_2O) is generally only a minor constituent within the lode, but shows enrichment at or near the footwall contact to the gold pod.

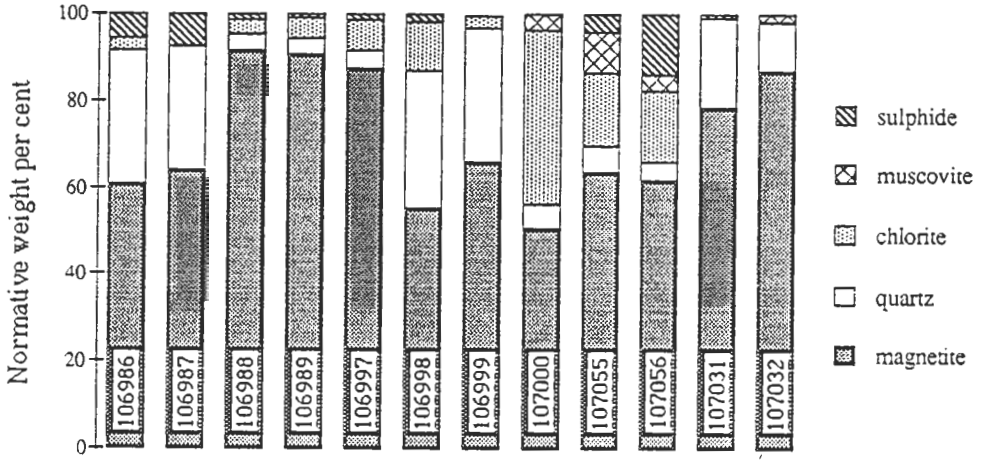

Figure 7.8 — Normative mineralogy calculated for the ironstone samples illustrate the variable proportions on the four main mineral constituents. Samples 106986 to 106989 and 106997 to 107000 represent the hangingwall to footwall sequence for the No. 3 and No. 1 orebodies respectively.

The variability of trace elements within the ironstone lodes has been discussed in Chapter Five, and samples from 14 level exhibit similar ranges in abundance. Typically the ironstone lodes show extreme to anomalously high enrichment in elements associated with mineralisation (Au, Cu, Bi, Mo, Pb, Sb, U, Zn), but similar to the pattern of major elements, is depleted in most others. The Ti/Zr values which remained so consistent within the sediments and porphyries are quite variable, ranging from 6 to 200 reflecting the low abundance of Zr relative to TiO_2 (although both are depleted within the ironstone lode). Unfortunately, the high bismuth contents of the two gold pod samples interfered with the detection of Zr and it was not possible to follow the transition from altered sediment to magnetite-chlorite lode. One sample (106988) with low Ti/Zr (6.7) is associated with elevated LREE and quartz-tourmaline veining, and it is suggested this value results from the introduction of 'immobile' phases rather than reflecting preserved primary sedimentary ratios.

7.7 Alteration

Although an epigenetic model is generally accepted for the formation of the ironstone lodes, recent debate has centred on how this process occurs. Large (1974, 1975) favoured a process of isovolumetric replacement whereby sediments were initially altered to chlorite and then replaced by magnetite, but recently Edwards (1987), and Wall and Valenta (1990) have questioned this interpretation suggesting that the lodes form through a process of open space filling of dilatant fault zones. Examination of mineral textures in hand specimen and polished thin section suggest that both replacement and open space filling mechanisms are likely to have contributed to lode formation (Chapter Six), yet it is virtually impossible to quantify the extent to which the two processes have acted. Chemical modelling of the alteration surrounding the lode, and of the lode itself are critical in constraining the exact process of lode formation.

Host Rocks

Typically studies of alteration surrounding ore deposits involve comparison of the chemistry of the alteration assemblages to a reference 'least altered' rock, following the method of Gresens (1967), or techniques derived from it (e.g. Grant, 1986). Gains and losses of major and trace elements, together with volume changes within the rock may be calculated to provide important insight into fluid flow, mineral transport, and controls on ore deposition. Many of these studies have been carried out on deposits hosted by volcanics, where the host rock composition can apparently be accepted as constant within the immediate orebody environs (e.g Beaty and Taylor, 1982; Andrews et al., 1986). However, as has been illustrated in Figure 7.4, the host rocks in the Warrego sequence are derived from two source populations and show a range in chemistry that results from the variable proportions of arenaceous and argillaceous components. This

background compositional variation lowers the sensitivity of modelling to define effects of alteration, especially where variation of an element within the sediments is greater than the change induced by alteration.

Lickley et al. (1987) demonstrated the use of sorting curves (Fig. 7.5) to determine real gains and losses of K_2O (and hence alteration haloes) in altered sediments of variable primary composition. However, despite the well defined sorting curve displayed for the Warrego sediments, this technique cannot be applied to them, as the alteration associated with mineralisation and ironstone lode formation involves chlorite replacement of both quartz and muscovite. Therefore SiO_2/Al_2O_3 does not remain constant, and rather than the gains and losses of K_2O occurring as a simple horizontal displacement from the sorting curve, a vertical component of 'shift' is introduced which varies with the intensity of alteration, and is impossible to predict.

It has therefore been necessary to assume a 'standard' least altered rock composition for the sediments with its inherent loss of sensitivity to alteration-induced changes. To minimise the variability within the Warrego sequence, a least altered standard was selected for both the high and low Ti/Zr populations which were compared independently of each other. In each case the standard was selected from the FEX drive after careful examination for homogeneity and minimum effects of alteration or contact metamorphism. Because of the small number of samples collected from the porphyry and their variable chemistry resulting from compositional differences (i.e. quartz- and quartz-feldspar phyric porphyries), rather than being considered separately, they have been included in the low-Ti/Zr sediment population.

Using the isocon method of Grant (1986), the relative gains and losses of major and trace elements relative to the least altered composition were calculated for the Warrego sediments and porphyries using equation (6) of Grant (1986),

$$(\Delta C_i/C_i^O) = (M^A/M^O)\cdot(C_i^A/C_i^O) - 1$$

where ΔC_i is the gain or loss in concentration of component i relative to the least altered equivalent, C_i^O and C_i^A are the concentrations of component i in the least altered and altered samples respectively, and M^A and M^O are the reference masses of the sample under consideration and least altered sample respectively. The ratio M^A/M^O is a constant for each sample, and is defined by either the slope of a best fit line passing through the origin and several immobile elements on an isocon diagram i.e. a line joining points of equal geochemical concentration (Fig. 7.9), or the ratio of a particular element that is deemed immobile in the altered sample relative to the least altered sample. Because TiO_2 and Zr have been demonstrated as immobile within the sediments and porphyries, the

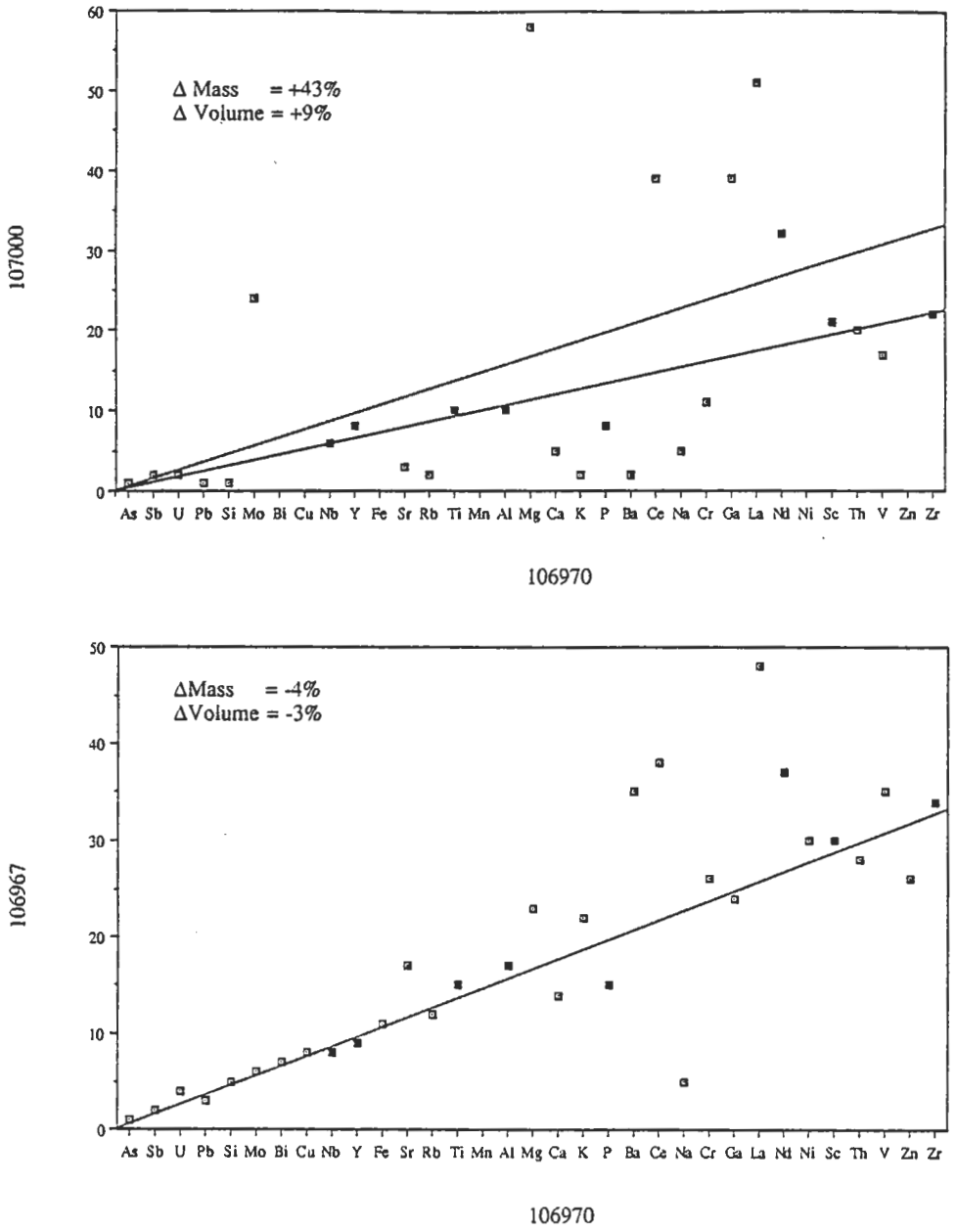

Figure 7.9 — Isocon diagrams illustrating the definition of isocon lines (lines of equal geochemical concentration) for the most altered sediment (107000) and an unaltered sediment (106967). The upper line is the constant mass line and the lower line is the best fit line matching immobile elements (filled symbols). Enrichment and depletion in a particular element is defined by displacement above and below the isocon respectively. The wide scatter of some elements in sample 106967 is interpreted as original sedimentary variability. The values of individual points are the ratio of the concentration of the element or element oxide in the altered sample to the standard unaltered sample (106970) multiplied in the manner As = $(C_{As}^{A}/C_{As}^{O}) \times 1$, Sb = $(C_{Sb}^{A}/C_{Sb}^{O}) \times 2$ .... to maintain a consistent sequence and remove the need to scale data (after Huston, 1988).

value of M^O/M^A used to calculate gains and losses has been taken as the ratio of TiO_2 and Zr in the altered rock relative to the least altered rock.

The geometry of the isocon diagram is illustrated in Figure 7.9 in which the most altered sediment (107000) is compared to the least altered (106970). A line of equal geochemical concentration passing through the origin and a group of elements (Nb, Y, TiO_2, Al_2O_3, Sc, Zr), signifies these elements have been immobile during alteration and have retained their relative ratios in spite of significant addition and subtraction of other elements (observed as displacement above and below the isocon respectively). In this illustration, iron (off scale) and MgO show enrichment of 1426% and 390% respectively, while Ba shows almost total removal (–89%). A comparison with an unaltered sample (106966 and 106970), is also illustrated in which elements fall along the constant mass isocon, i.e. a slope of 1. The scatter of points about the isocon reflects the variable primary composition of the sediments.

The isocon diagrams presented here incorporate modifications suggested by Huston (1988) in which elements are ordered sequentially (i.e. As = $(C^A/C^O) \times 1$, Sb = $(C^A/C^O) \times 2$ ...) so the sequence remains constant from diagram to diagram and there is no necessity to scale data to conform to a particular range in composition (Grant, 1986; Osterberg et. al., 1987). The order of elements is arbitrary, but typically elements of low abundance (a few ppm) that show large enrichment (e.g. Cu and Bi) are placed at the beginning of the sequence to minimise offset from the isocon, and immobile elements (Nb, Y, TiO_2, Al_2O_3, P_2O_5, Nd, Sc, and Zr) are evenly spaced through the sequence to allow better definition of isocon lines.

Within the sediments, elements that show irregular patterns of enrichment or depletion (e.g. TiO_2, Al_2O_3, P_2O_5, Ce, Ga, La, Nb, Nd, Rb, Sc, Th, V, Y, and Zr) are interpreted (by virtue of their relative immobility during alteration), to reflect the original compositional variation within the sediments. Only relatively minor enrichment or depletion of these elements is observed, even in the most altered samples immediately adjacent to the ironstone lodes. Patterns of enrichment (e.g. Fe_2O_3, MnO, MgO, K_2O, Bi, Mo, Ni, Rb, and Zn) and depletion (e.g. CaO, Na_2O, Ba, Pb, Sr) which exceed background variation are attributed to the effects of hydrothermal alteration. Plots of the calculated gains and losses for Fe_2O_3, Ba, and Zr relative to unaltered sediment along the 14 level drive are used to illustrate the patterns of enrichment, depletion, and constancy respectively (Fig. 7.10). While enrichment is typically restricted to the immediate margins of the ironstone lode, patterns of depletion are more extensive, extending into the quartz porphyry in the hangingwall, and to the Footwall Fault on the footwall side of the ironstone lodes. The preservation of feldspar in the upper porphyry suggest alteration of the porphyry has not been pervasive with the strongest alteration being observed at the contacts to leave a relatively unaltered core.

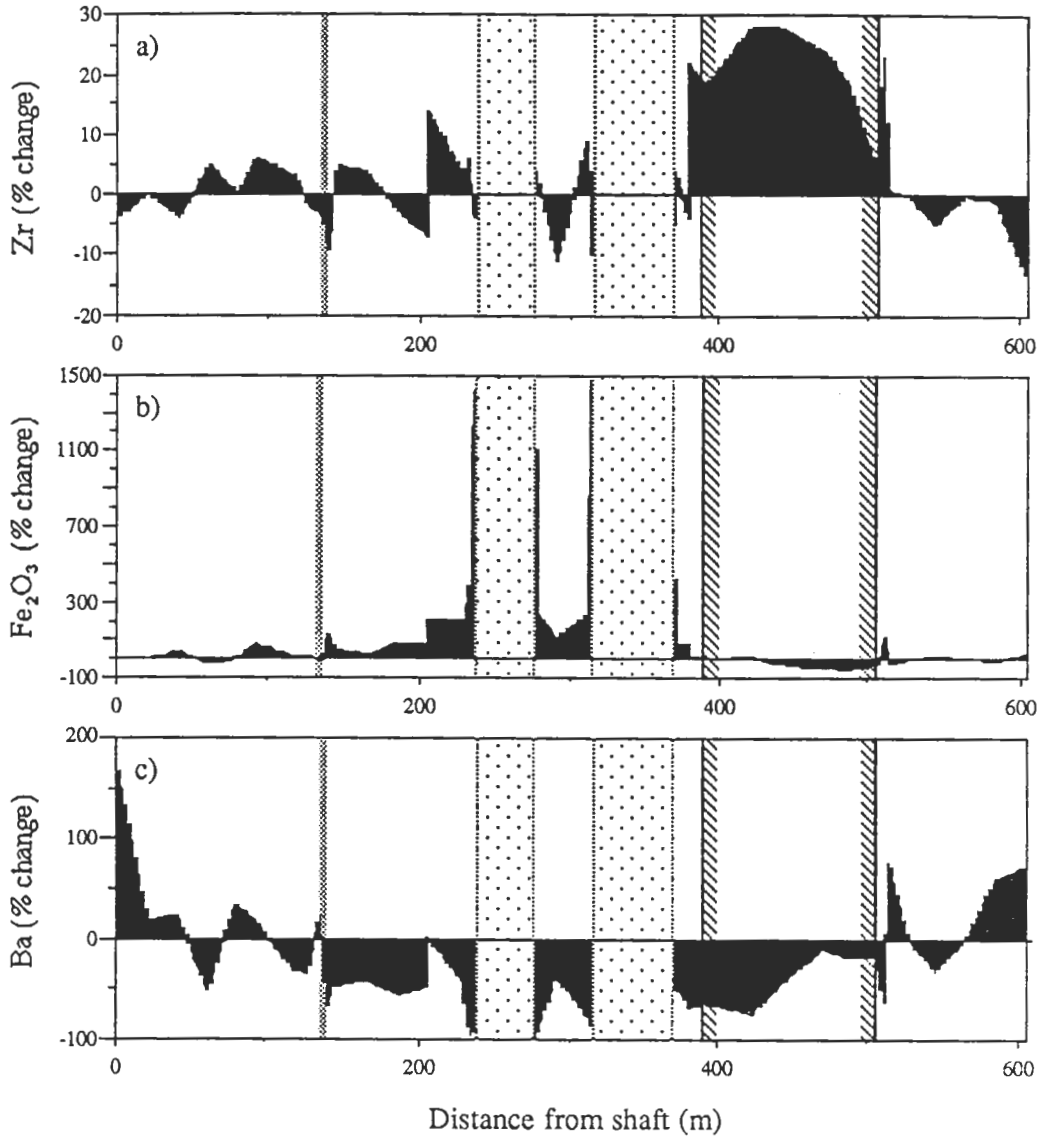

Figure 7.10 — Calculated gains and losses for selected trace and major elements along the 14 level drive to illustrate patterns of relative immobility (Zr), depletion, (Ba), and enrichment (Fe_2O_3). The location of the the Footwall Fault, ironstone lodes, and porphyry are marked by fine stipple, open stipple and hatchured boundary lines respectively.

The intensity of alteration shows a marked increase immediately adjacent to the ironstone lodes, and is most intense in the footwall of the No. 1 orebody where alteration extends some 40m from the lode contact. Iron is the only element which shows a consistent pattern of enrichment toward the ironstone lode contact (Fig. 7.10), with other elements showing irregular patterns of enrichment (MgO, MnO, Bi, Ce, Cu, Ga, La, Mo, U, and Zn), and depletion (SiO_2, Al_2O_3, K_2O, Cr, Nb, Ni, Rb, Sc, and V). The overall irregularity to the pattern of alteration reflects the preservation of relatively unaltered sediments (e.g. 107002) within the altered zone, and is consistent with observations in core logging of isolated, relatively unaltered wedges of sediment adjacent to the ironstone lode, or wholly enclosed by altered sediment (Chapter Three).

Using Grant's (1986) adaptation of Gresens' (1967) equation, it is a simple matter to calculate mass and volume changes associated with alteration. The mass change relative to the unaltered sample is the inverse to the slope of the isocon i.e a decrease in slope is related to an increase in mass, and changes in mass are related to changes in volume and specific gravity such that

$$M^A/M^O = (V^A/V^O)\cdot(\rho^A/\rho^O)$$

where V^A and V^O, and ρ^A and ρ^O are the volumes and specific gravities of the altered and least altered samples respectively.

The changes in the mass and volume of the altered sediments along the 14 level profile (Fig. 7.11) for the most part show the irregular pattern of enrichment and depletion observed for the immobile elements and are probably related to original compositional variation in the sediments and porphyry[1]. Corresponding to the major changes in the sediment chemistry associated with alteration at the ironstone lode margins, there is an increase in both the mass and volume of the sediments, indicating that the change in mineralogy from quartz and muscovite in the sediments, to the chlorite and magnetite of the alteration assemblage is not achieved by direct replacement alone but involves volume changes as well. In thin section, these altered rocks exhibit cleavage-parallel chlorite-magnetite, quartz, and quartz-sulphide veining which shows evidence of open space filling supporting calculated volume increases.

However, the most intensely altered sediment immediately adjacent to the footwall of the No. 1 orebody (107000) shows a calculated volume change of only 9% compared to the 50–60% increase observed for less altered samples. This level of volume change is indistinguishable from the background volume variation of the unaltered sediments. The total absence of veining in the massive chlorite-magnetite assemblage suggests that a

---

[1]Calculated gains and losses for all samples are listed together with mass and volume changes in Appendix E.

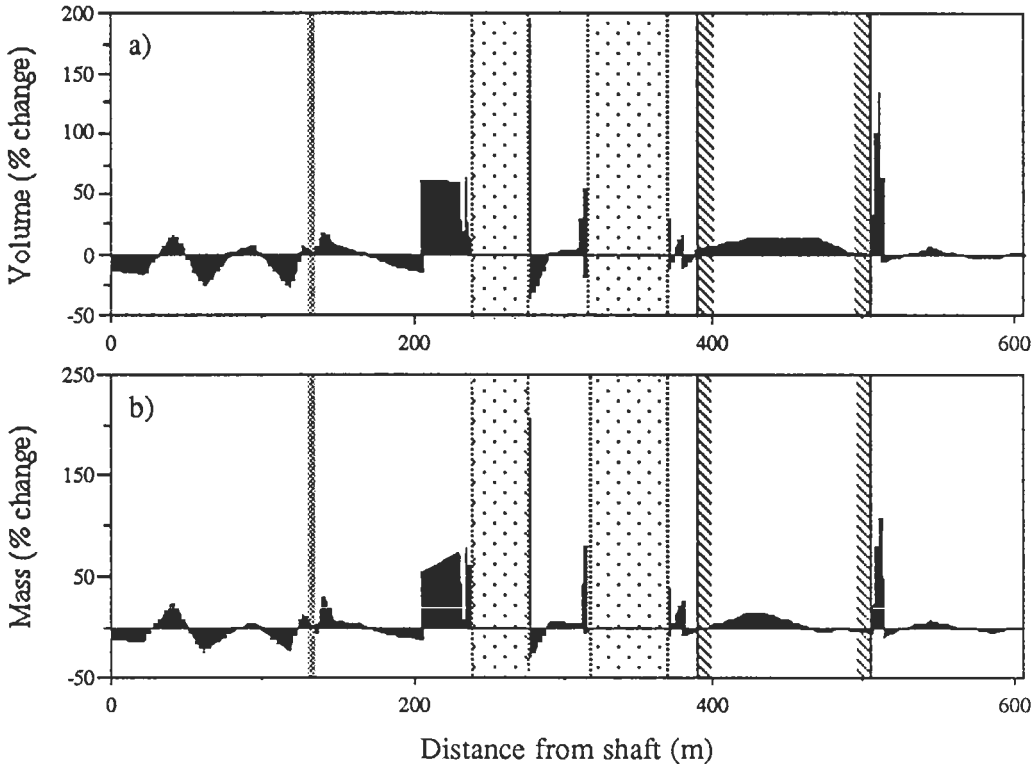

Figure 7.11 — Calculated changes of mass and volume relative to the least altered sediment sample. Symbols representing geological boundaries are as for Fig. 7.10.

second alteration style involving replacement of the sediment without significant variation in volume.

Ironstone Lodes

Because the Warramunga Group consists entirely of turbiditic greywacke-argillite and porphyries without evidence for other sedimentary units that might be more favourable to replacement (e.g limestones), any modelling of mass, composition or volume changes under a replacement model of ironstone lode formation, must include the least altered sediment as the original unreplaced precursor. If however the lodes formed by open space filling, calculations based on the relative enrichment or depletion of samples to unaltered sediment become meaningless. Provided some component of the original material remains with unchanged ratios of immobile elements, and dilution has not lowered trace elements abundances to levels that are at or below their detection limits, the changes in composition, mass, and volume may be accurately estimated for either (or combinations) of the two processes.

Ironstone samples show strong enrichment of Fe_2O_3, MnO, Bi, Cu, and Mo while other elements are depleted to varying degrees. All recognised immobile elements, with the exception of P_2O_5, are depleted to virtual background levels and attempts to fit an isocon result in near horizontal lines (Fig. 7.12). Calculated changes in element concentrations based on the large values of M^A/M^O defined by the low slope of the isocons give values of either near complete depletion or extreme enrichment. Several elements consistently show anomalous enrichment relative to the near horizontal isocon which may be real or artificial. Although close to their levels of detection, the proportions of CaO and P_2O_5 approximate those of apatite (i.e. 3·33 : 1) indicating it is probably present as a trace mineral within the ironstone lode. Similarly, consistent enrichment in Ni and MnO within the ironstone lode suggest they are possibly present trace elements within magnetite. Na_2O appears anomalous because it is found in amounts that are at, or near to its detection limit by the XRF technique, which is further compounded by the reduction of detection limits in ironstone samples due to the high x-ray absorbence of the magnetite.

Despite the relatively wide alteration zone in the footwall of the No. 1 orebody, the actual contact between the altered sediments and the massive ironstone lode is abrupt and there is a marked mineralogical contrast on either side. In addition to the obvious differences between the massive magnetite of the lode and massive chlorite of the sediment, minor but significant trace element differences are observed that are consistent with observations regarding the distribution of trace minerals made in Chapter Six. Accessory minerals other than zircon do not appear to be restricted to one or other population as is illustrated by the relative enrichment in La, Ce, and Nd within the ironstone lode samples. This contrast in the abundance of 'insoluble' minerals between

the lodes and the sediments is marked and attests to a fundamental difference between the lode and the host sediments as identified in the 14 level drive.

The gold pods mark the only place where the sharp outline of the lodes is softened and there is a gradation between the sediments and lode proper. The transition from altered sediment with disseminated and stringer magnetite to ironstone lode is observed as the gradual increase in the proportion of both disseminated and stringer magnetite which forms at the expense of phyllosilicates. Here the mineralogical distinction based on the presence of rutile and zircon in the chlorite-magnetite of the altered sediment and magnetite-chlorite of the gold pod is less marked. Sample 107055, collected from the contact zone between stringer magnetite and the relatively massive magnetite-chlorite of the lower gold pod is significant among the ironstone lode samples because it is the only one for which the majority of trace elements are well above their detection limits. Importantly the immobile elements (TiO_2, Al_2O_3, P_2O_5, Nb, Sc, V, and possibly Zr[1]) show coherent behaviour when compared to the least altered sediment on an isocon diagram, and the slope of the isocon is intermediate between that of the altered sediments and the flat patterns of the other ironstone lode samples (Fig. 7.12).

Calculation of the mass and volume changes involved in the transformation of unaltered sediment to gold pod compositions yield changes in mass and volume of 104%, and 22–28% respectively[2]. The low calculated volume change is consistent with that of the most altered sediment in the footwall, and supports a model for the direct replacement of the sediment with minimal open space filling. Sample 107056 is from within the lower gold pod on 14 level, some 6 metres from the footwall contact, and although it contains relatively low trace element contents, it is possible to construct an isocon using V[1] as an immobile element; V consistently falls on or near the isocon line in all samples suggesting that it has been immobile (Fig. 7.12). Calculations suggest mass and volume changes of the order of 192–194% and 68–76% respectively are again not unrealistic in view of the nearly 40 volume % of this sample comprising sulphides, chlorite, and muscovite (Fig. 7.8) which are suggested as having been introduced during mineralisation (Chapter Six).

An example of an isocon for a quartz-magnetite sample (106999) illustrates the typical pattern of ironstone samples where low trace element contents (often at their detection limits) are observed, correlation between immobile elements is weak, and unrealistic mass and volume changes are calculated (Fig. 7.12). Although significant trace element dilution will result from the the obvious volume changes associated with

---

[1]Zircon could not be analysed in this sample because of the high Bi content.

[2]Because Ti/Zr ratios of the ironstone samples are variable and do not characterise one or other of the source populations, changes in mass and volume are quoted for both possible precursor populations.

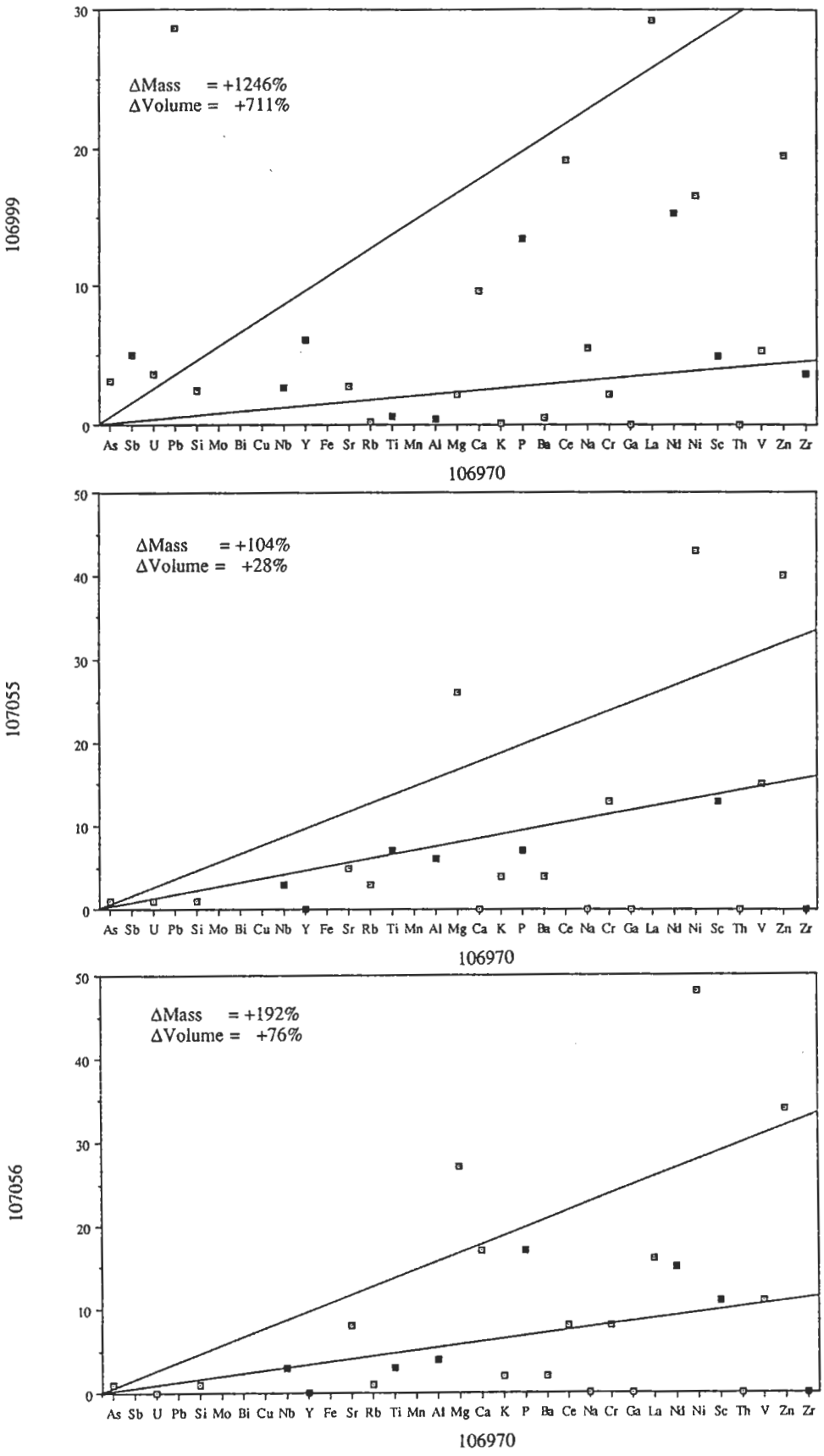

Figure 7.12 — Isocon diagrams for samples 107055 (immediate footwall to the gold pod), 107056 (gold pod), and 106999 (quartz-magnetite) indicating the preservation of sedimentary immobile trace element ratios in the gold pod samples, but a complete lack of coherence in the quartz-magnetite samples which generate unrealistic estimates of volume and mass change.

subsequent mineralisation of the lode, some trace element mobility or open space filling is still required to explain the extreme dilution. Figure 7.13 illustrates isocon diagrams for a theoretical complete replacement of sediment by magnetite, followed by dilution by 60 volume % quartz, and an open space model of dilution of sediment with magnetite. These examples illustrate the difficulty in generating the low trace element abundances observed in sample 106999 (Fig. 7.12) without resorting to either immobile element mobility of open space filling by magnetite.

7.8 Rare Earth Elements

The rare earth elements (REE) are a group of elements (La, Ce, Pr, Nd, Pm, Sm, Eu, Gd, Tb, Dy, Ho, Er, Tm, Yb, and Lu) that have found wide application in petrology because, in spite of the overall similarity of their chemical and physical properties, they may fractionate relative to each other under processes of partial melting or fractional crystallisation (Henderson, 1984). Because of their relatively large ionic radii, the REE are typically concentrated in accessory minerals where they substitute for similar sized elements (e.g. Ca^{2+}, Y^{3+}, Th^{4+}, U^{4+}, Mn^{2+}, and Zr^{4+}), but their variable size means they may fractionate relative to each other into particular minerals e.g. zircon and apatite favour the HREE (heavy REE, Gd to Lu), and MREE (medium REE, Pm to Ho) respectively (Henderson, 1984). Thus the chondrite normalised REE pattern of an igneous rock depends to a large extent upon the degree of fractionation or partial melting it has undergone during melt evolution. In contrast, sedimentary rocks have very uniform patterns regardless of their source material, showing a characteristic LREE (light REE, La to Nd) enrichment, small negative Eu anomalies, and fairly constant HREE abundances relative to chondrites. These patterns have remained constant with time since the Archean, although the absolute abundances of REE appear to be increasing with the age of the earth (Nance and Taylor, 1976).

Studies of the mobility of REE, and modification of their primary signature in igneous rocks has subsequently highlighted their possible use in quantifying conditions of hydrothermal alteration (e.g. Graf, 1977; Floyd, 1977; McLennan and Taylor, 1979; Finlow-Bates and Stumpfl, 1981; Campbell et al. 1984; Cullers and Graf, 1984; Ludden et al., 1984; Bartley, 1986; Vance and Condie, 1987; MacLean, 1988; and Michard, 1989).

The REE contents for a selection of Warrego 14 level sediment and ironstone samples were determined (Appendix C), and are illustrated on Post-Archean Australian Sediment (PAAS) normalised plots in Figure 7.14. An approximation of the REE behaviour in all samples was obtained from the XRF analyses of La, Ce, Nd, and Y[1]

---

[1]Because of its' similar ionic radius and $3+$ oxidation state, Y can be used to model the behaviour of Ho (Ludden et al., 1982; Henderson, 1984).

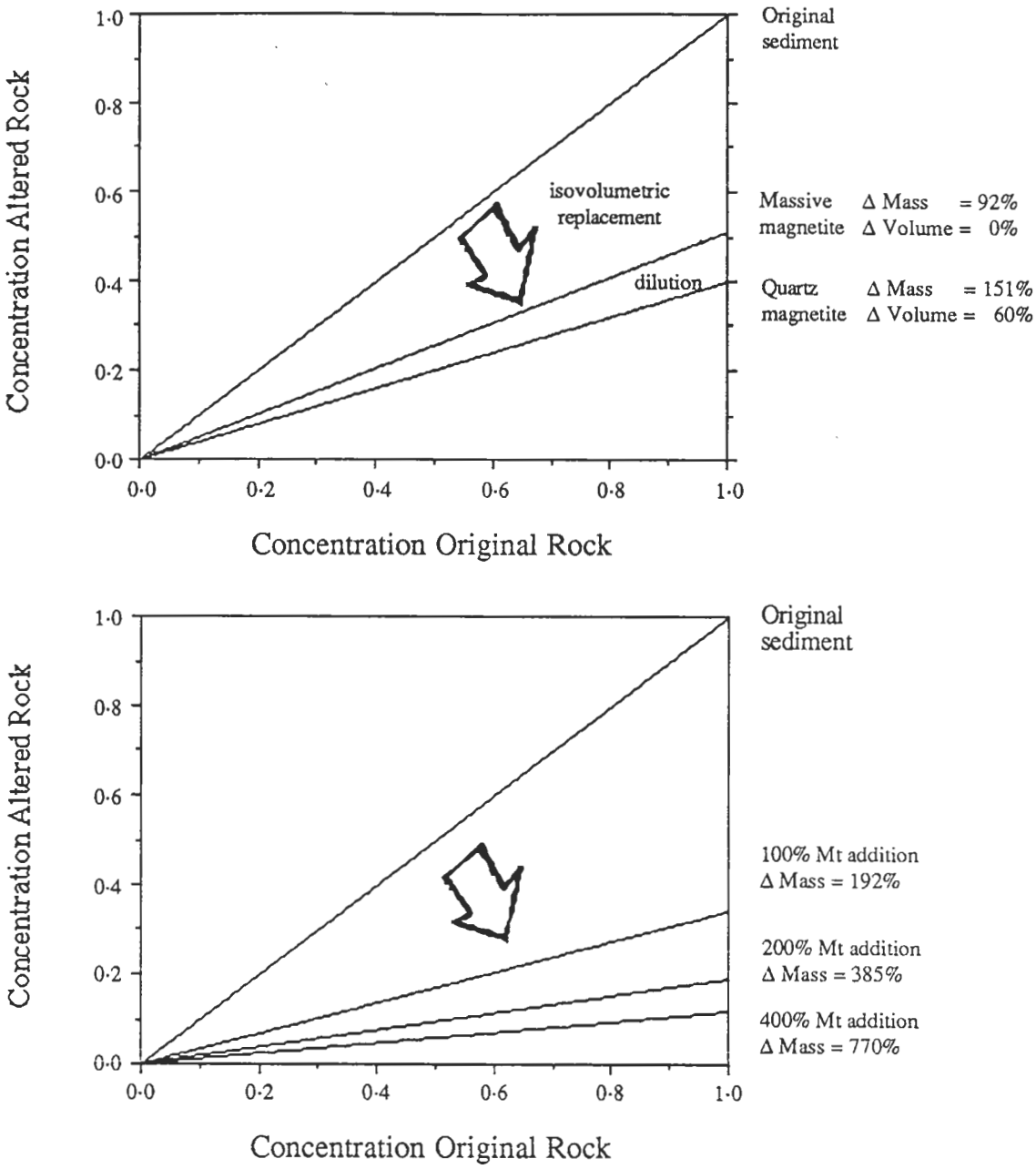

Figure 7.13 — Isocon models providing examples of hypothetical ironstone lode formation models. The upper diagram illustrates expected depression of an isocon resulting from complete isovolumetric replacement of sediment by magnetite, followed by 60% dilution by by quartz veining. The lower diagram illustrates depression of an isocon accompanying dilution of sediment by magnetite. These figures illustrate the relative difficulty in generating the flat isocons observed in ironstone lode samples without either mobility of immobile elements, or dilution.

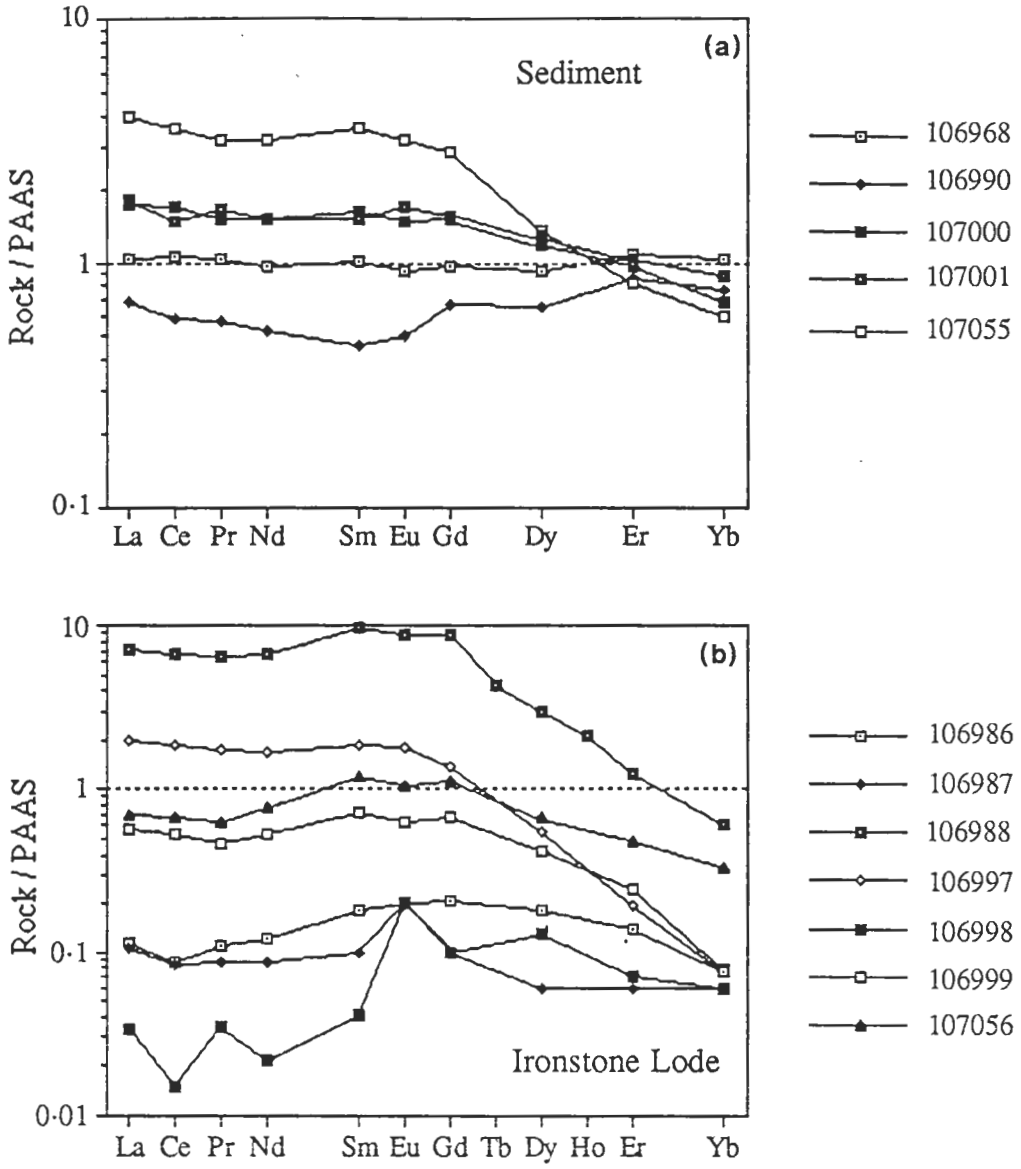

Figure 7.14 — a) PAAS (Nance and Taylor, 1976) normalised REE plots for altered (107000, 107001, and 107055) and unaltered (106968) sediments from 14 level in Warrego mine. Samples 107000 and 107001 are altered sediments in the immediate footwall of the No. 1 orebody; 107055 from the immediate footwall of the gold pod; and 106990 the unusual carbonate altered rock in the footwall of the No. 3 orebody. Note sample 106968 is virtually identical in REE content to PAAS. b) PAAS normalised REE plots for ironstone lode samples from 14 level, Warrego mine. Samples 106986 to 106988 are from the No. 3 orebody, 106997 to 106999 from the No. 1 orebody. Samples 107056 also from the No. 1 orebody is from the lower gold pod on 14 level.

from pressed powder pills, which (similar to sample 106968), all show the flat PAAS signatures typical of sediments. There is no difference in either the pattern, or abundances of REE within the sediments of differing Ti/Zr values or with the porphyry. Because the unaltered sediments in the Warrego sequence show virtually identical REE patterns and abundances relative to PAAS, the mobility of REE in the altered sediments and ironstone lode is discussed in terms of the PAAS normalised plots rather than the more commonly used chondrite normalised plots.

The altered sediments in the footwall of the No. 1 orebody (107000, 107001, and 107055) show patterns of LREE and MREE enrichment, and HREE (Er and Yb) depletion relative to PAAS. This apparent mobility of LREE is supported by petrographic evidence of clusters of non-detrital monazite ($(La,Ce,Nd)PO_4$) associated with chlorite veining, and evidence of zircon immobility in these rocks suggests that HREE abundances probably reflect primary abundances reduced through the increasing mass associated with alteration. The unusually altered rocks in the footwall of the No. 3 orebody (106990) show depleted REE patterns relative to PAAS which is probably related to the strong carbonate alteration. There is little evidence remaining that might characterise the original affinity of this rock.

Although the REE patterns of the ironstone lode samples generally show the same MREE enriched profile, actual abundances range from background to significant enrichment relative to PAAS. The correlation between quartz-rich samples (106986, 106987, 106998, and 106999), and low REE abundances suggest they have been diluted through the addition of quartz; the irregular REE patterns of samples 106998 and 106987 result because REE are at their detection limits. Further support for the REE abundances representing a pre-mineralisation signature is seen as the similarity in abundance and shape of the profiles for samples 107056 (magnetite-chlorite) and 106999 (quartz magnetite); both have similar magnetite contents but distinctly different proportions of other minerals (Fig. 7.8).

In addition to MREE enrichment, several samples show similar levels of LREE enrichment (106988, 106997, and 107055). This pattern appears to be transitional between the MREE enriched pattern of the ironstone lode, and the LREE and MREE enriched pattern of the altered sediment, which is in accord with the location of sample 107055 at the footwall contact of the central gold pod However, the other two samples comprise relatively massive ironstone lode although sample 106988 which shows the highest REE enrichment of all the samples contains cross-cutting quartz-tourmaline veins.

The modelling of REE mobility and deposition in hydrothermal solutions is significantly complicated by the lack of information on REE partitioning between hydrothermal fluids and the accessory minerals which commonly host the REE. Their relative insolubility, the differential mobility of REE under different physical and

chemical conditions, variable stability of REE complexes in solution, and relative fractionation of REE into minerals on precipitation from solution make it difficult to model or predict their behaviour. However, certain constraints can be placed upon the conditions of mineralisation during the formation of the Warrego ironstone lode. Fluid conditions for the Warrego system are likely to be of low pH and high salinity (Chapter Nine), favouring the solubility of LREE relative to HREE which are typically most resistant to mobilisation except under conditions of high fluid F^- or CO_3^{2-} (McLennan and Taylor, 1979; Hynes, 1980; Taylor and Fryer, 1982; Humphris, 1984). Studies of REE mobility in alteration pipes beneath volcanogenic massive sulphides are in accordance with this observation showing LREE and MREE mobility while HREE remain immobile (e.g. Finlow-Bates and Stumpfl, 1981; Campbell et al., 1984; Palacois et al., 1986; MacLean, 1988). Although an alteration pipe beneath the Warrego ironstone lode has not been defined, alteration in the immediate footwall shows a pattern of LREE enrichment consistent with volcanogenic massive sulphides (Campbell et al., 1984; Vance and Condie, 1987) and suggests that LREE have been mobilised during alteration remote from the ironstone lode and deposited with chlorite alteration in the footwall to the lode.

The marked relative enrichment in MREE in the ironstone lode is not consistent with REE impurities in magnetite, which typically has low REE contents (Cullers and Graf, 1984), but is more compatible with the presence of a phase, or phases that is preferentially enriched in REE, e.g. apatite (Fig. 7.15). Although not observed in the ironstone mineral assemblage, the relative enrichment, and proportions of CaO and P_2O_5 in many of the ironstone samples suggest that apatite is a minor phase within the lode assemblage. The extreme REE enrichment in sample 106988 is not understood, King et al. (1988) measured quite variable, but generally low REE abundances in tourmalines from gold-bearing vein deposits, but the coincidence of extreme REE enrichment and tourmaline-rich veins may suggest some form of remobilisation or magmatic enrichment.

Calculation of correlation coefficients for the REE from all samples (Table VI) indicate a consistent pattern REE of behaviour in all samples. LREE and MREE are strongly correlated suggesting they have behaved coherently, while the HREE are correlated with Ti and Zr suggesting they have been immobile during alteration and are probably hosted within zircon. Because quartz appears to dilute total REE abundances while retaining the same overall pattern of relative enrichment and depletion, it is suggested REE were introduced during formation of the magnetite lode and that for these

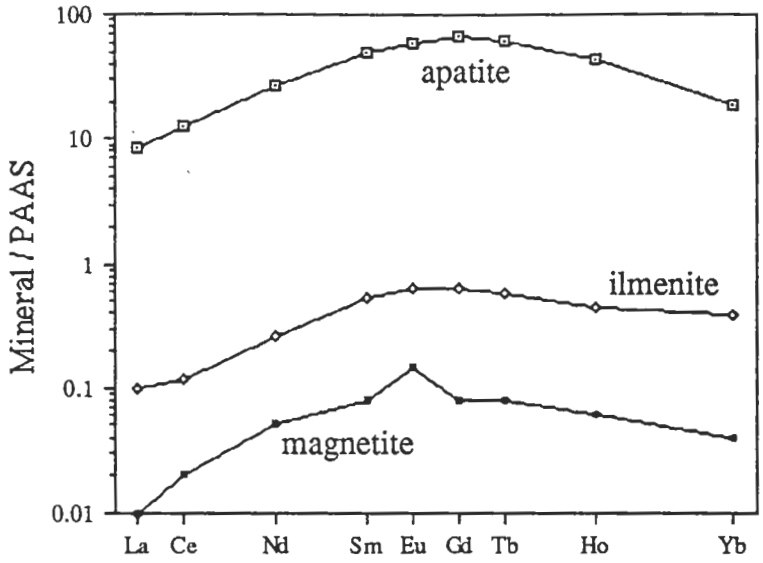

Figure 7.15 — PAAS normalised REE content of accessory mineral phases in the Skaergaard intrusion (Paster et al., 1974), illustrating the strong MREE enriched pattern shown by apatite, and relatively low REE content of oxide phases.

TABLE VI: Correlation coefficients for REE from all samples.

	La	Ce	Pr	Nd	Sm	Eu	Gd	Dy	Er	Yb	Y	Ti	Zr	Nb
La	1													
Ce	1.00	1												
Pr	1.00	1.00	1											
Nd	1.00	1.00	1.00	1										
Sm	0.99	0.99	0.99	0.99	1									
Eu	0.99	0.99	0.99	0.99	1.00	1								
Gd	0.99	0.99	0.99	0.99	1.00	1.00	1							
Dy	0.95	0.95	0.96	0.95	0.92	0.92	0.93	1						
Er	0.58	0.59	0.60	0.58	0.51	0.50	0.53	0.78	1					
Yb	0.30	0.31	0.33	0.30	0.21	0.21	0.23	0.54	0.94	1				
Y	0.82	0.82	0.81	0.82	0.85	0.84	0.84	0.75	0.30	-0.02	1			
Ti	0.12	0.13	0.15	0.12	0.03	0.01	0.03	0.35	0.83	0.95	1.12	1		
Zr	0.26	0.27	0.29	0.27	0.20	0.19	0.20	0.44	0.82	0.91	-0.19	0.86	1	
Nb	0.08	0.10	0.10	0.08	0.01	-0.16	-0.01	0.22	0.53	0.57	0.14	0.71	0.39	1

samples at least, quartz overprinting has not been associated with significant REE mobility.

Two interpretations of the REE abundances in the ironstone lode are possible:

1. They directly reflect the REE levels of the fluid which, because of the high resistance of zircon to alteration and dissolution, was enriched in LREE and MREE relative to HREE, or
2. REE abundances within the ironstone lode were controlled by the mineral assemblage with LREE and MREE enrichment resulting because apatite and monazite are accessory phases in the mineral assemblage. Other REE in solution (HREE), were not deposited simply because a suitable host phase was not available. Once formed, HREE complexes appear to be more stable and may have been carried further in the overall system (Henderson, 1984).

It seems likely the observed REE patterns result from a combination of the two models. Although the strong evidence of Zr immobility in the altered sediments adjacent to the lode suggests that similar to presently active high salinity and low pH geothermal systems, fluids were likely to be enriched in LREE and MREE relative to HREE (Michard and Albaréde, 1986; Sturchio et al., 1986; McLennan, 1989; Michard, 1989), it is unlikely the considerable enrichment of REE in the ironstone lode could accumulate without the synchronous deposition of a favourable host phase. Studies of the REE content of massive ore in volcanogenic massive sulphide deposits (Graf, 1977; Whitford et al., 1988) show levels of REE nearly two orders of magnitude lower than those observed in the Warrego samples suggesting that apatite precipitation coincident with ironstone lode formation is probably an important control on the REE levels observed.

Eu anomalies in the ironstone samples are typically small and negative with an average value for Eu/Eu* of 0.68 (excluding the two anomalous ironstone samples at the limit of detection). This value is little different from that determined for the altered sediments in the footwall (Eu/Eu* = 0.71), and contrasts significantly from the typical pattern of strong Eu depletion observed in hydrothermally altered rocks (Taylor and Fryer, 1982; Campbell et al., 1984; Sturchio et al. 1986; MacLean, 1988; Whitford et al., 1988). This relatively coherent behaviour of Eu relative to the other REE during alteration suggests conditions of relatively high fO_2 during ironstone lode formation, where Eu^{3+} dominated over the more mobile Eu^{2+} (hematite stable — Graf, 1978). The ironstone lode samples also differ from chemical sediments associated with volcanic activity (both exhalative massive sulphide deposits and iron formations), which are characterised by positive Eu anomalies throughout geological history (Fryer, 1977; Graf, 1977, 1978; Cullers and Graf, 1984; Whitford et al., 1988).

7.9 Discussion

Two patterns of alteration are observed in the footwall of the No. 1 orebody:

1. The immediate contact of the ironstone lode is marked by a zone of extreme alteration comprising almost exclusively chlorite and disseminated magnetite. This alteration style appears to entirely envelope the ironstone lode, although widths of alteration in the hangingwall are considerably narrower than those observed in the footwall. Despite the strong alteration, the preservation of primary immobile element ratios indicate these rocks were derived from the alteration of Warramunga Group sediments. Modelling of the mass and volume changes attending alteration suggest the increase in mass associated with the introduction of magnetite has not been accompanied by an increase in volume supporting an isovolumetric replacement model for alteration.
2. Beyond the 2 or 3 metre wide inner zone, alteration is less pervasive, typically occurring as cleavage parallel veinlets of chlorite-magnetite, quartz, and chalcopyrite in chloritised sediments. Although diffuse chlorite-magnetite veinlets may largely result from replacement marginal to cleavage controlled microfractures, the quartz and chalcopyrite veins have sharp boundaries and are clearly dilational. This observation is supported by mass balance calculations which suggest that volume increases in these rocks are in the the order of 50%.

In spite of the increasing alteration intensity toward the ironstone lode, the actual contact is remarkably abrupt and marked mineralogical and chemical changes are observed across it (cf. samples 106999 and 107000 in Figure 7.8). The only exception to this pattern is the gold pods where there is a significant increase in the width of alteration adjacent to the ironstone lode and a gradational contact from chlorite-magnetite to the magnetite-chlorite of the lode proper is observed. In sample 107055 from the contact zone, the coherent retention of sedimentary immobile trace element ratios is consistent with a model of ironstone formation via direct replacement without significant volume changes. Within the gold pod, sample 107056 similarly appears to preserve sedimentary trace element ratios although, as suggested in Chapter Six, volume increases are indicated associated with fracturing of the lode and introduction of chlorite, muscovite and magnetite mineralisation. That the two most strongly altered samples and a lode sample preserve sedimentary trace element ratios suggest isovolumetric replacement of the sediment by chlorite and magnetite, and dilute trace element abundances through the increased mass of the rock. Subsequent introduction of mineralisation has further reduced abundances and is interpreted as responsible for calculated volume changes in samples 107055 and 107056.

However, it is apparent from modelling that the low levels of trace elements (Fig. 7.13) cannot be realistically generated without open space filling during ironstone lode

formation and/or zircon mobility. Other studies of the often intense hydrothermal alteration associated with ore deposition (principally volcanogenic massive sulphides) stress the immobility of, and constant relative proportions of the high field strength elements especially Ti and Zr, e.g. Davies et al. 1979; Finlow-Bates and Stumpfl, 1981; Ludden et al. 1982; Costa et al., 1983; Date et al., 1983; Kerrich and Watson, 1984; Larson, 1984; Kishida and Kerrich, 1987; MacLean and Kranidiotis, 1987; Grenne, 1989. Examples where mobility of TiO_2 has been documented include the studies Riverin and Hodgson, 1980; Gibson et al. 1983; and Larson, 1984, but their key assumption of constant volume during alteration are based on the the preservation of delicate volcanic textures. This inference has been questioned by Costa et al. (1983) who warn that small undetected variation between the linear dimensions of petrographic features in altered and unaltered rocks may lead to gross errors in the estimation of the volume changes, and that tacit assumption of isovolumetric behaviour is invalid.

However examples of high field strength element mobility have been demonstrated. Campbell et al. (1984) showed mobility of U, Th, Hf, and Zr in the most intensely altered zones of the Kidd Creek mine, Ontario and suggested that the degree of mobility may be related to the size of the overall system (at greater than 100 Mt, Kidd Creek is the world's largest massive sulphide deposit). This observation is supported by evidence from Michard and Albaréde (1986) and Michard (1989) that extremely high water/rock ratios are necessary to cause changes in water/rock REE abundances. TiO_2 mobility has been demonstrated for the gold-bearing quartz veins of the Sigma mine, Quebec (Robert and Brown, 1986), and TiO_2, Y, and Zr were mobile during the carbonation of metabasalts (Hynes, 1980). Hynes found a high degree of correlation between the the abundance of TiO_2, Y, and Zr, with the degree of carbonation of basalts and suggested the overall mobility of these typically immobile elements was attributable to the high levels of CO_2 in the fluid phase. In the Sigma mine the noncoherent behaviour of TiO_2 and Al_2O_3 within the carbonate alteration zone adjacent to the mineralised quartz veins, and the presence of ilmenite and rutile within the vein assemblage indicates that TiO_2 leaching from the wallrock and redeposition within the vein has occurred. The carbonate alteration observed in this deposit may also indicate TiO_2 was mobilised by fluids that were of high CO_2 content. Mobility of TiO_2 and Zr during alteration has also been suggested in the vicinity of the Headway-Coulee prospect, Ontario (Osterberg et al., 1987), where the non-coherent behaviour of, and concentration changes in these elements of up to 30% relative to least altered rocks have been calculated. However, Whitford et al. (1989), have suggested mobility in this case may be the result of inappropriate selection of a parental composition. Jack (1989) suggests that some mobility of TiO_2, Nb, Y, and Zr has occurred in the core of the stringer zone of the Hellyer massive sulphide deposit in western Tasmania, and Whitford et al. (1989) indicate that although immobile elements may have been sparingly mobile,

there is an overall areal immobility in the nearby Que River deposit. In the intensely chloritised ore zone at the Jabiluka U deposit (Nutt, 1989), major elements of the most and least altered samples suggest significant mobility of Ti (isocon defined by Al_2O_3, FeO, Fe_2O_3, P_2O_5, and Th) although further trace element analyses would be required to confirm this observation.

Hydrothermal zircons have been documented (Clout, 1989; Rubin et al., 1989) where Zr mobility has been attributed to high F and CO_2 contents in the fluid respectively. Although the origin of the zircons described form the Peko mine is uncertain, their location within the ironstone lode at a compositional boundary suggest that these are also examples of hydrothermal zircons. Although carbonate alteration is associated with many ironstone lodes at Tennant Creek, Peko and Warrego contain insignificant amounts and high CO_2 contents in the fluid cannot be invoked to explain possibly mobility.

It thus appears that in general, the high field strength elements and HREE are immobile under most conditions of hydrothermal alteration although under specific conditions i.e. high fluid CO_2 or F content, or extreme conditions of water/rock ratios, some relative mobility of these elements may occur. However, in no example has the removal of elements occurred on a scale required to reduce trace element abundance to those observed in Warrego or other Tennant Creek ironstone lodes through dissolution alone. Although an extensive alteration pipe proper has not been defined beneath the Warrego ironstone lodes, the general style of alteration observed in the footwall of the lode, especially beneath the gold pods, is very similar to the massive chlorite alteration extending beneath volcanogenic massive sulphide deposits as summarised by Franklin et al. (1981); Urabe et al. (1983); and Lydon (1984, 1988). The pipe beneath the Bruce deposit, Arizona, appears to be typical, being well zoned with a sericitic outer halo and a chlorite-rich core in which massive foliated to felted laths of chlorite may make up over 50% of the rock volume with subordinate quartz, and accessory sodic plagioclase, epidote, magnetite, and rutile (Larson, 1984).

The observation of high field strength element immobility in the Warrego alteration zone is similar for the majority of investigated deposits and despite evidence of within thin section scale mobility of TiO_2, observed as fine rutile blades paralleling cleavage and chlorite grain boundaries (probably derived through the breakdown of ilmenite), this is not considered significant on a hand specimen scale. The preservation of the high field strength element ratios from the unaltered sediments into the most altered suggest that these are primary values modified by an increase in the mass of the bulk rock, but not mobilisation.

A possible explanation for these observations again draws on a model of ironstone lode formation invoking the early formation of a relatively rigid outer ironstone shell. With continued deformation during formation, deposition of magnetite within open

fractures would significantly dilute trace element abundances. The significance of this model as opposed to one of total open space filling is that in the area of the gold pod, sedimentary trace element patterns are preserved in what were massive magnetite rocks prior to the introduction of economic mineralisation. In the shell model, these rock would be among the last replaced and being less rigid for much of the formation period would be less diluted. The core of chloritic sediments in the Peko mine provides a good example of an incompletely replaced core (see Fig. 10.2).

7.10 Summary

Consideration of the chemistry of the ironstone lodes, host sediments and porphyries has provided an important insight into not only the processes of ironstone lode formation, but also the tectonic setting and regime under which the Warramunga Group was deposited. Based on distinctive Ti/Zr values, it is suggested that:

1. The approximately 400m stratigraphic thickness exposed in the Warrego mine on 14 level was derived from two sources of rhyodacitic and dacitic composition; and
2. Deposition was rapid without mixing or reworking (the coarse and poorly sorted character of the sediments indicate that the source was relatively close).

The overlap of the porphyry Ti/Zr values with one of the sediment populations, and the general similarity in both major and trace element chemistry, suggest that they were derived from the same ultimate source; the sediments probably representing the rapid reworking and slumping of subaerial volcanic material into an adjacent, relatively deep water sedimentary basin, and the porphyries, subvolcanic equivalents. The combination of similar chemistry, close spatial association and similar ages indicate that the Tennant Creek Granite may be equivalent to the porphyry and ultimately the parent of all components within the Warramunga Group.

In spite of the variable chemistry of the sediments resulting from sorting during deposition, the consistent Ti/Zr of the two populations has permitted an evaluation of the alteration surrounding the Warrego ironstone lodes. Relative to the unaltered sediments furthest from the lodes, patterns of major and trace element enrichment and depletion indicate most alteration is restricted between the Footwall Fault and the hangingwall of the porphyry, although the core of the porphyry appears to be relatively unaltered. A pervasive background alteration throughout this interval resulted from the breakdown of feldspars to sericite and is observed as a halo depleted in Na_2O, Ba, Pb, Rb and Sr. Closer to the ironstone lodes chloritisation and increasing abundance of magnetite are the main features of alteration directly associated with lode formation. In the footwall of the No. 1 orebody, alteration extends some 40 to 50 m from the lode, but in the footwall of the No.3 orebody and the hangingwall of both, alteration is restricted to only a few metres.

Characterisation of changes (particularly volume) associated with the formation of the Warrego ironstone lodes has been achieved through the use of immobile element ratios in both the altered sediments and ironstone lode itself. Similar to patterns observed in other ore deposits (particularly volcanogenic massive sulphides), the high field strength elements have remained immobile within the alteration system and retain their primary ratios relative to unaltered sediments. Volume changes as high as 60% are recorded in the footwall altered sediments where stringer quartz and sulphide veining occurs, but minimal changes are suggested for the massive chlorite alteration in the immediate footwall to the lode.

The transition from the altered sediments in the footwall, to the massive magnetite ± quartz, ± sulphide lode is typically knife sharp despite the increasing degree of alteration toward the lode contact, and although the envelope of altered sediments in the footwall is wider, there is little difference between the footwall and hangingwall contacts. The gold pods are the exception, where the contact appears gradational from chlorite-magnetite to magnetite-chlorite although differences in the accessory mineral assemblage are the same at all contacts. At the transition zone between lode and altered sediment in the footwall of the gold pod, and in the gold pod itself, immobile elements have maintained their ratios relative to the least altered sediment but have been diluted. Calculated volume changes in this sample support the model of ironstone lode formation proposed by Large (1974, 1975) in which the lode has formed through the isovolumetric replacement of the sediments by the magnetite. However, ironstone samples from elsewhere in the lodes have trace element ratios below detection, suggesting dilution as well as isovolumetric replacement is required to explain trace element patterns.

An alternative model of open space filling, as suggested by Edwards (1987), and Wall and Valenta (1990) is inconsistent with observed replacement textures and the preservation of sedimentary trace element ratios in the gold pod samples (included clasts or sediment fragments are extremely rare). However some open space filling of the lode is required to explain the extreme depletion of trace elements observed in lode samples removed from the gold pod. It is suggested that fracturing and open space filling of fractured ironstone lode during replacement is sufficient to produce observed trace element abundances.

Chapter Eight

STABLE ISOTOPES

8.1 Introduction

The use of stable isotopes in modelling the genesis of mineral deposits has found wide use in the past twenty years, largely through the development of fast and efficient techniques of sample preparation and analysis, and the development of the theoretical and experimental basis to understand and model variations observed in isotopic ratios. Isotopes of sulphur, carbon, oxygen, and hydrogen are routinely analysed from individual minerals and whole rock samples to define temperatures of mineral deposition, fluid composition and evolution, and the likely source of these elements. Detailed isotopic studies of mineral deposits have enabled the development of models of formation and evolution when used in conjunction with other geological techniques including mapping, petrography, fluid inclusions and thermodynamic modelling.

Sulphur isotopes form the basis of this study with an intensive examination of the isotopic composition of sulphide minerals and its zonation within the four sections through the Warrego orebody examined in this study. Limited oxygen and hydrogen isotope analyses have also been made of chlorite mineral separates from the sample suite collected on 14 level as part of the alteration study.

8.2 Sulphur Isotopes

A total of 278 analyses of mineral separates of pyrite, chalcopyrite and bismuthinite have been analysed from the Warrego mine, principally from the four mine sections examined in this study, i.e. 8340N, 8140N, 8060N, and 7980N. Methods of sample selection, preparation and analysis are described in Appendix F together with sample locations and values. Additional samples from other than the four main sections were the bismuthinite-chalcopyrite pairs collected for geothermometry. Sample selection was constrained to localities where sufficient bismuthinite and chalcopyrite could be extracted for analysis. All analyses are quoted as per mil deviation of the $^{34}S/^{32}S$ ratio of the sulphide relative to the troilite phase of the Cañon Diablo meteorite (Ault and Jensen, 1963).

Frequency diagrams for the results of this study are illustrated in Figure 8.1 and show a remarkably narrow range in values (0‰ to 4‰) over the 500 m strike length

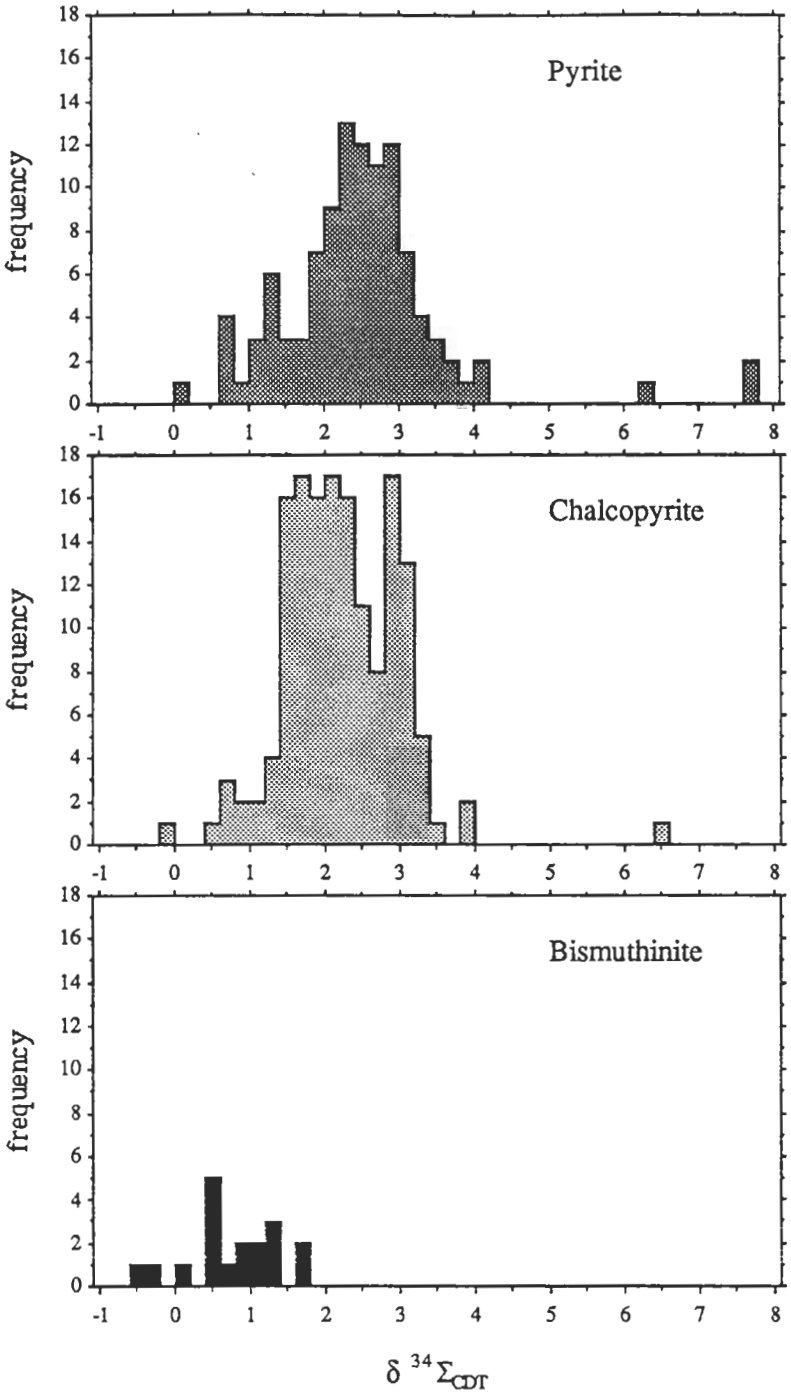

Figure 8.1 — Frequency distribution of $\delta^{34}S_{CDT}$ for pyrite (n=107, mean = 2·6, std. dev. = 1·1), chalcopyrite (n = 153, mean = 2.3, std. dev. = 0·9), and bismuthinite (n = 18, mean = 0·8, std. dev. = 0·6) in the Warrego mine.

between sections 8340N and 7980N. Outliers in the pyrite and chalcopyrite populations correspond to minerals analysed from the hangingwall sediments and porphyry. The individual populations for each mineral show displacement to higher $\delta^{34}S$ in the order bismuthinite < chalcopyrite < pyrite in accordance with the expected fractionation between these sulphide minerals (Ohmoto, 1972; Bente, 1982). The bimodality observed in the distribution of $\delta^{34}S$ for chalcopyrite appears to reflect a sampling bias rather than two paragenses of copper mineralisation (see below).

Because it was impracticable to obtain pure separates of the lacy pyrite (Chapter Six), it has not been possible to determine if this form of pyrite conforms to the overall $\delta^{34}S$ pattern of the mine. However, examples of porous, massive banded, euhedral, and tourmaline associated pyrite and a single marcasite sample show neither anomalous $\delta^{34}S$ values relative to the total population of pyrite, nor to the zonation patterns in individual sections. It therefore seems likely that the source and chemical conditions under which these various forms were originally precipitated were essentially the same.

Zonation

There is a well developed pattern of zonation of sulphur isotopes on the four sections studied that matches well with the patterns already observed in the mineralogy and metal zonation in the Warrego orebody. Although the frequency distribution of pyrite and chalcopyrite is related to their relative fractionation factors, the difference between the two is generally small and it has been possible to use the values of both to define a single contoured diagram for each of the four sections (Fig. 8.2 to 8.5).

8340N: A core of $\delta^{34}S$ < 2‰ is defined in the upper part of the ironstone lode and extends into the footwall of this section. The lower part of the ironstone lode is characterised by $\delta^{34}S$ > 3‰ whereas sediments in the footwall and hangingwall to the lode have lower values. The position of the $\delta^{34}S$ = 3‰ approximates the 1·5 g/t gold contour line in Figure 5.3 and the highest gold and copper grades in this section overlap with the lowest values for $\delta^{34}S$.

8140N: This section shows a relatively simple footwall to hangingwall zonation for the length of the ironstone lode. The $\delta^{34}S$ < 2‰ contours define a core of lower values on the footwall side of the lode that do not extend into the footwall proper while the 3‰ contour follows the hangingwall contact. The lowest $\delta^{34}S$ values overlap with the highest grades of gold, bismuth and copper mineralisation, while values > 2‰ are restricted to the assemblages containing quartz as a major constituent or the hangingwall porphyry or sediments.

8060N: A core of $\delta^{34}S$ < 2‰ corresponding to the mineralised portions of the lode occupies the lower two thirds of the No. 1 orebody with lowest values corresponding to the gold-rich zone between 10 and 12 levels. The copper- and bismuth-rich ore in the

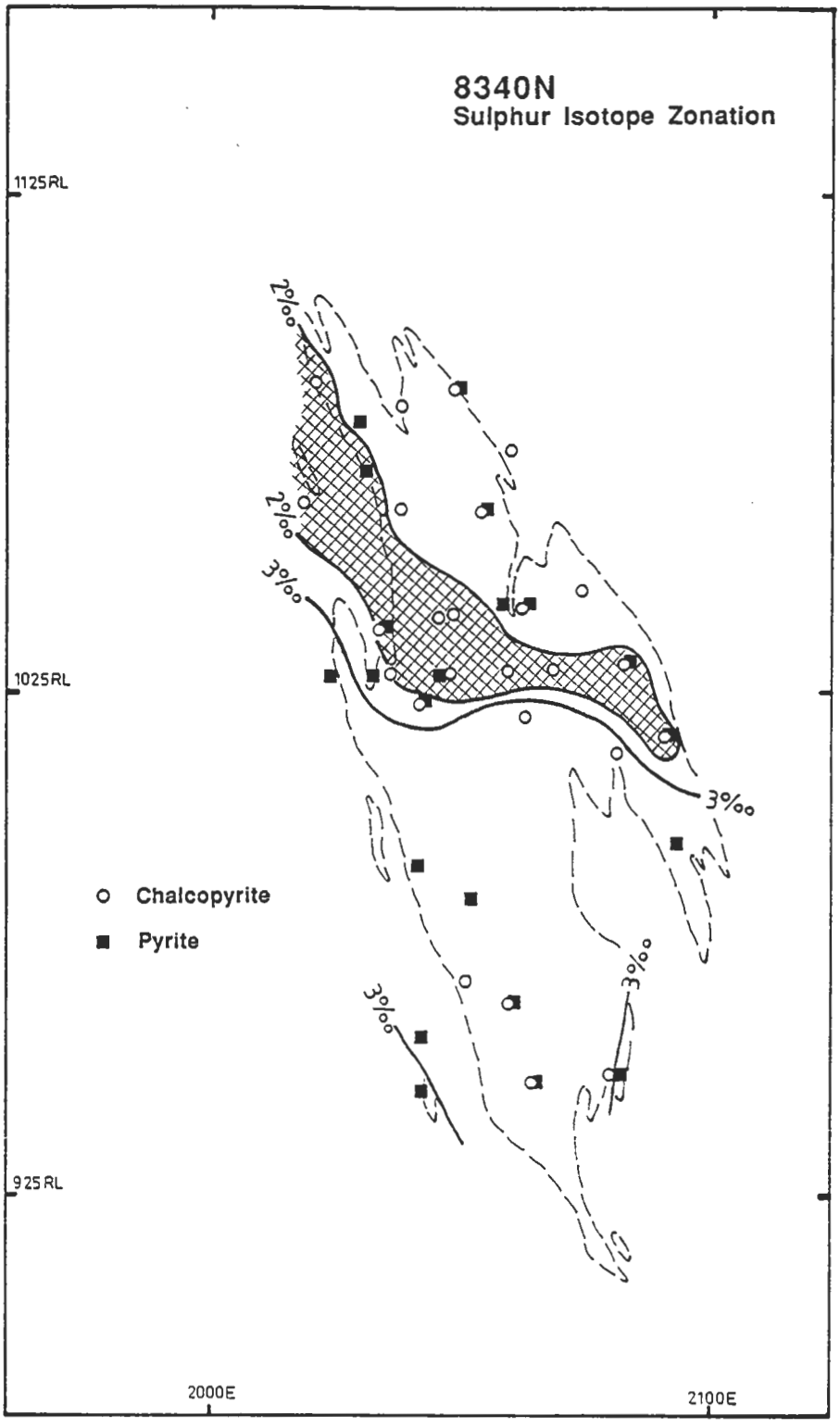

Figure 8.2 — Sulphur isotope zonation and sample location in section 8340N of the Warrego mine. Stippled area highlights values <2‰. Actual sample values are presented in Appendix F.

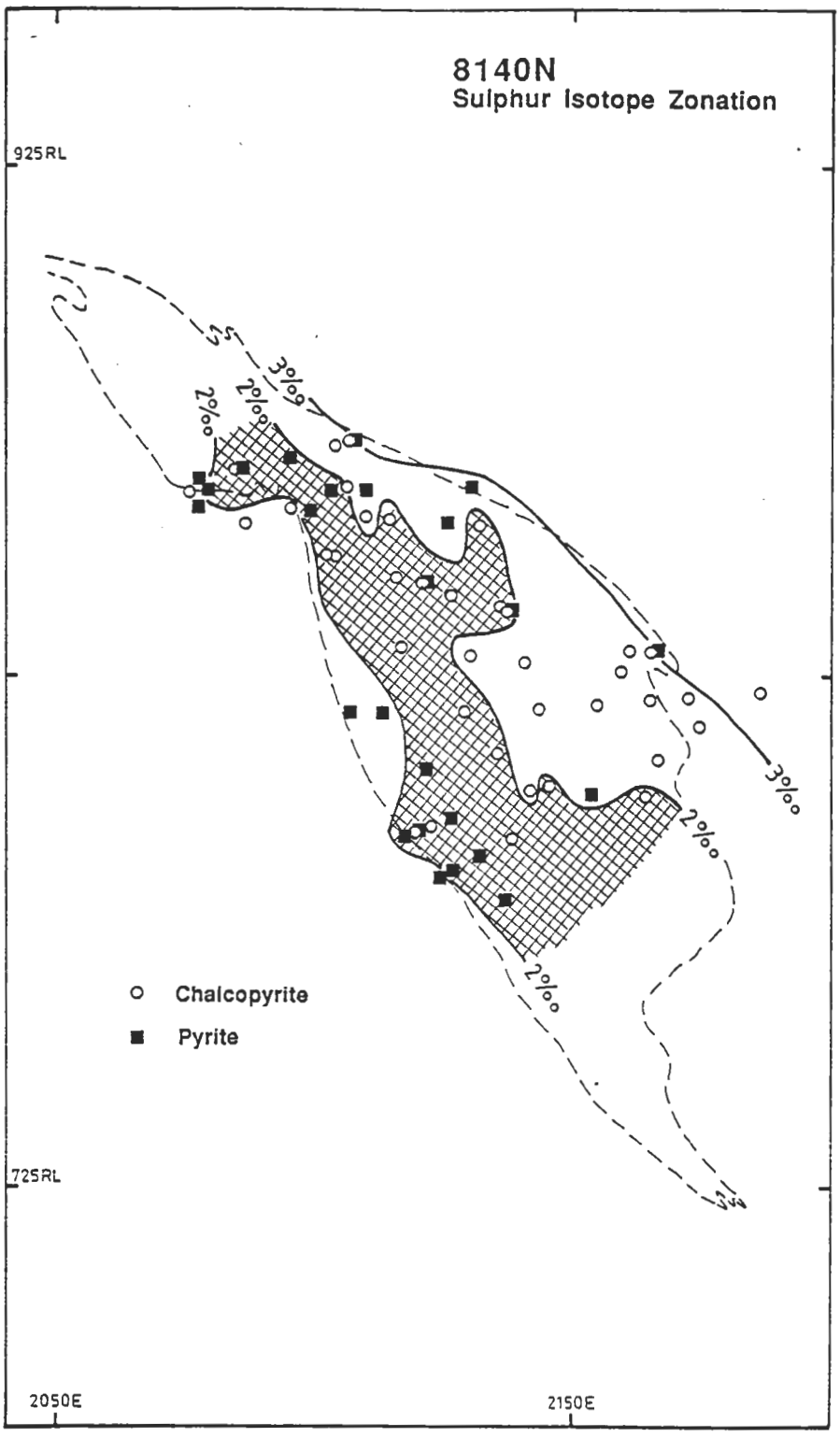

Figure 8.3 — Sulphur isotope zonation and sample location in section 8140N of the Warrego mine. Stippled area highlights values <2‰. Actual sample values are presented in Appendix F.

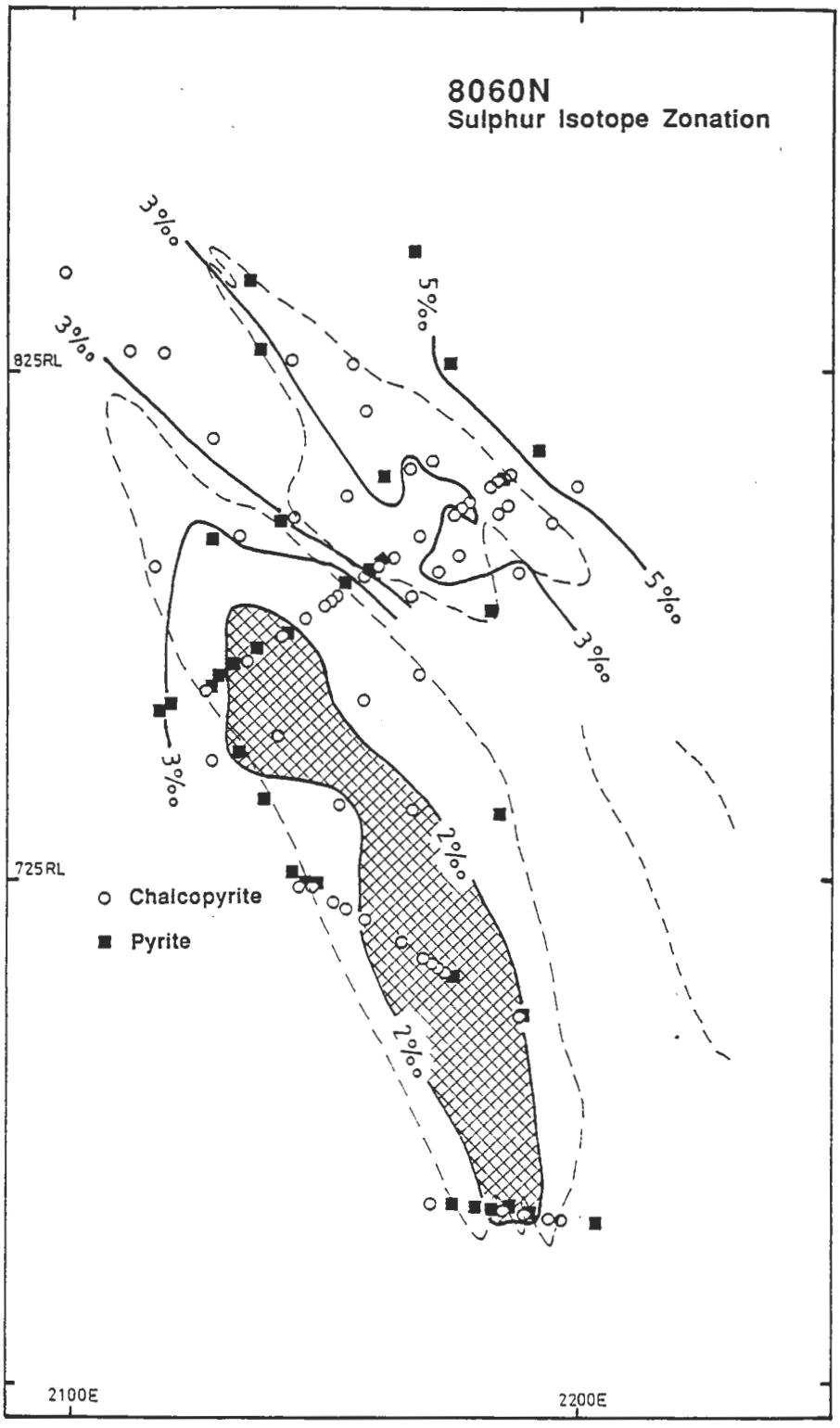

Figure 8.4 — Sulphur isotope zonation and sample location in section 8060N of the Warrego mine. Stippled area highlights values <2‰. Actual sample values are presented in Appendix F.

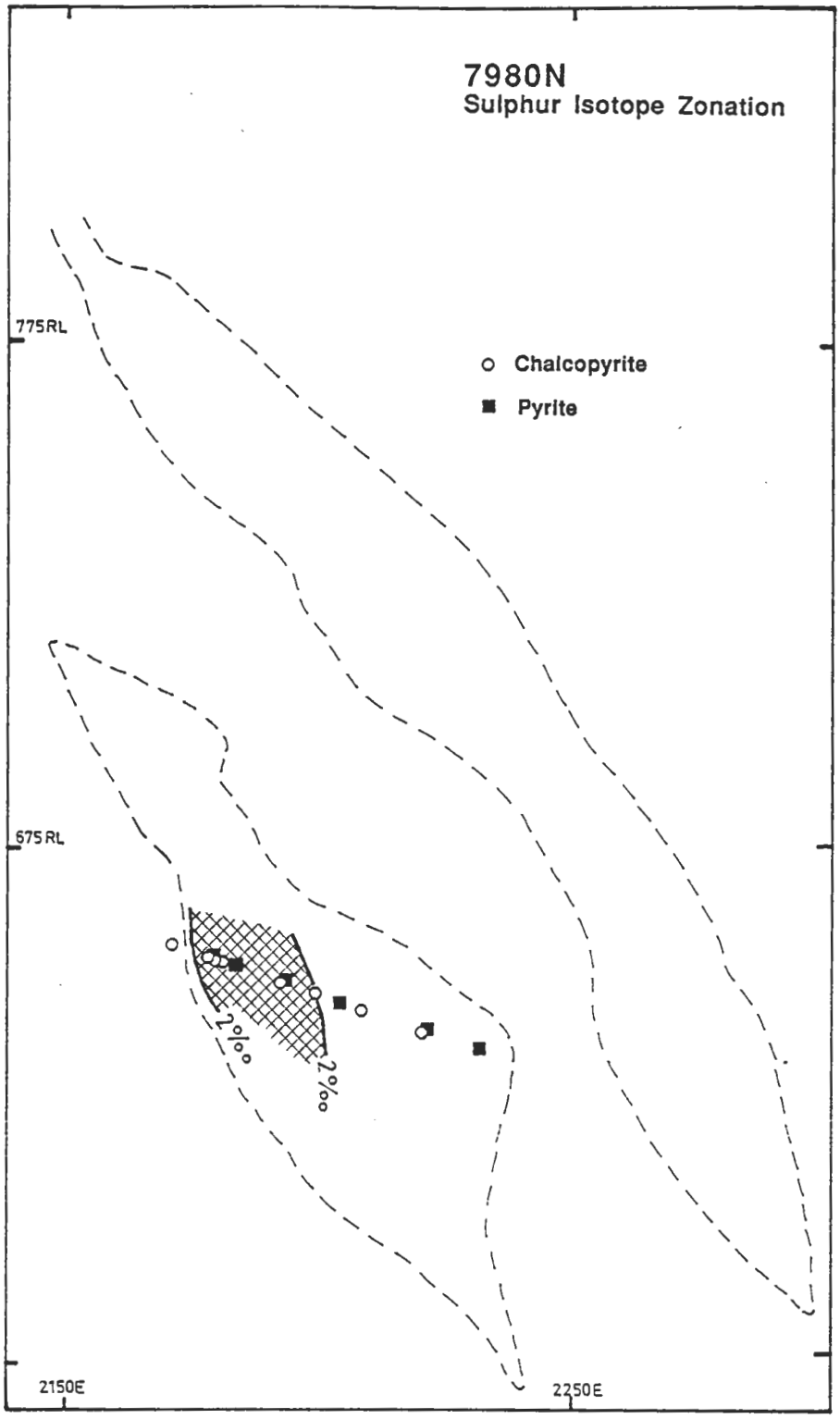

Figure 8.5 — Sulphur isotope zonation and sample location in section 7980N of the Warrego mine. Stippled area highlights values <2‰. Actual sample values are presented in Appendix F.

hangingwall of the No.3 orebody is characterised by values > 3‰ while lower grade quartz-magnetite-sulphide ore on the footwall side of the No. 3 orebody has values similar to the outer footwall and hangingwall zones in the No. 1 orebody. The highest isotope values analysed from the Warrego mine are found in the hangingwall of the No. 3 orebody at the lower contact of the quartz porphyry, marking a steep isotopic gradient from the hangingwall of the No. 3 orebody into the overlying host rocks. A wedge of altered sediments between the No. 1 and No. 3 orebodies at the top of the lodes has lower values than the over- and underlying ironstone lode and correlates well with the suggested position of the Orebody Fault.

7980N: Limited sampling on the 7980N section suggests that similar to the other sections, the lowest isotope values are correlated with areas of highest grade mineralisation. A core of lower $\delta^{34}S$ values is located on the footwall side of the ironstone lode overlapping with the gold-rich ore.

From these sections, an overall impression of the variation of $\delta^{34}S$ in the Warrego ironstone lode and adjacent rocks can be inferred. There is a well preserved isotopic zonation pattern within the lodes which to a large extent mimics the pattern of mineralisation. Cores of low $\delta^{34}S$ values are localised within the ironstone lode, and overlap with the highest grade mineralisation. The lowest $\delta^{34}S$ values tend to occur on the footwall side of the ironstone lode, and although there are relatively few samples from the host rocks, and their paragenetic relationship to the lodes is unconstrained, there seems to be a general concordance to the overall pattern with highest values found in the hangingwall sediments and porphyry.

Because it does not seem unreasonable to assume the highest grades of mineralisation within a given mine section indicate the zone of most intense hydrothermal alteration, the correlation of low $\delta^{34}S$ values with the highest grades of mineralisation suggest that the sulphur isotopic composition may be used to indicate the geometry of the mineralising system and fluid pathways. In sections 8060N and 8340N, low $\delta^{34}S$ values extend into the footwall in the upper part of the ironstone lode indicating that fluids were derived from this direction; an interpretation that is consistent with the structural model suggesting the lodes have been overturned (Chapter Four). Similarly the localisation of low $\delta^{34}S$ values within the core of the lode is compatible with the interpretation that fluid flow has been channelled along structures within the lode.

Detailed examination of individual drillholes confirms the correlation between low $\delta^{34}S$ and mineralisation. Figure 8.6 illustrates two well-defined patterns of high-grade gold intersections associated with low $\delta^{34}S$ from drillholes from sections 8140N and 8060N. Although the isotopic composition of sulphides in the gold pods is difficult to characterise because of their low abundances in these areas, section 8140N shows an overall pattern of decreasing $\delta^{34}S$ values toward the highest gold values. Where it has

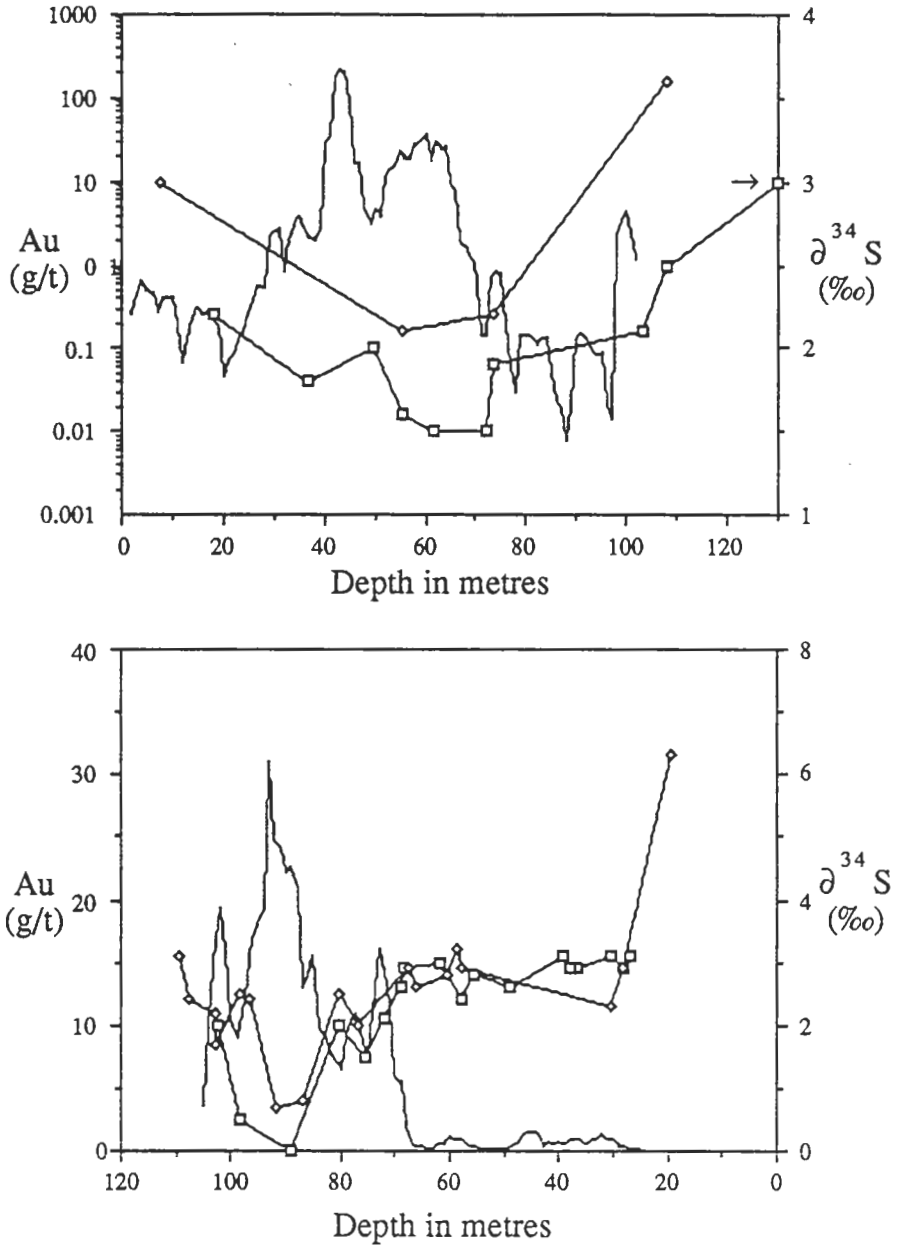

Figure 8.6 — Plots illustrating the co-variation of $\delta^{34}S$ of chalcopyrite and pyrite (squares and diamonds respectively) with gold grade in selected drillholes from the Warrego mine. Top: drillhole 9/814/12 through the central gold pod in section 8140N. Note the indicated analysis (→) is from drillhole 10/814/11, and the log scale for gold values. Bottom: drillhole 10/806/68 through gold-rich copper ore between the two gold pods on section 8060N.

been possible to achieve a high sample density as in the gold-rich copper ore marginal to the gold pods (drillhole 10/806/68), there is an almost perfect reverse correlation between gold grade and $\delta^{34}S$.

As in the gold pods, the outer zone of the ironstone lodes is characterised by a sulphide poor mineral assemblage (quartz-magnetite), where suitable samples containing sufficient sulphide minerals for isotopic analysis are typically rare. This may result in the apparent bimodality of the chalcopyrite $\delta^{34}S$ frequency diagram (Fig. 8.1); values less than ~2·5‰ and greater than ~3‰ occur in the magnetite-sulphide assemblage and the hangingwall contact zone respectively. Therefore, it is suggested that the under-representation of the quartz-magnetite assemblage in the sampling is reflected in the overall frequency of $\delta^{34}S$ between values of 2·5‰ and 3·0‰.

A feature of this study is that regardless of the gold grade, both the range and minimum values of $\delta^{34}S$ in each section is approximately the same. Thus the lowest $\delta^{34}S$ values associated with low-grade gold in section 8340N, are not significantly different from the lowest $\delta^{34}S$ values from high-grade gold mineralisation in sections 8140N or 7980N. This observation has significant implications for the modelling of ore deposition (see below).

Geothermometry

The relative fractionation of sulphur isotopes between the fluid and different sulphide minerals is temperature dependant, and therefore pairs of sulphide minerals that were deposited in equilibrium, may be used to determine the temperature of mineral deposition. The simple sulphide mineral assemblage of the Warrego ironstone lodes means that there are only two mineral pairs available for geothermometry i.e. pyrite-chalcopyrite and bismuthinite-chalcopyrite. The latter is severely restricted in its application by the generally low abundance of bismuth within the lode (~0·2%).

Because of the small difference in the relative isotopic fractionation between the fluid and pyrite and chalcopyrite (Ohmoto and Rye, 1979), the accuracy of temperatures determined by the pyrite-chalcopyrite pair is typically poor and these minerals provide an unreliable geothermometer. Also, because pyrite is commonly deposited over a wide range of chemical and physical conditions, it is likely to have preceded or post-dated chalcopyrite deposition and therefore may not represent an equilibrium assemblage (Rye and Ohmoto, 1974). In contrast, bismuthinite-chalcopyrite pairs are significantly more reliable because of the relatively large difference in fraction factors (bismuthinite is approximately the same as galena). Temperature estimates provided by this geo-thermometer correlate well with paragenetic, petrological and fluid inclusion data (Bente, 1982). Bismuthinite-pyrite pairs generally appear to be less reliable because these two phases are not normally found in isotopic equilibrium (Bente, 1982).

Of possible significance in the determination and application of the sulphur isotopic composition of bismuthinite from the Warrego mine is the possible effect of high selenium contents on isotopic fractionation. An assumption that selenium content has little or no effect on the relative fractionation of ^{32}S and ^{34}S into the bismuthinite mineral appears to be borne out by the homogeneity of $\delta^{34}S$ values from samples that are likely to be of variable Se content, and the generally reasonable temperature estimates provided by the bismuthinite-chalcopyrite geothermometer (see below).

Pyrite-Chalcopyrite: Pyrite and chalcopyrite are common constituents within the ironstone lodes often coexisting in apparent equilibrium. However recrystallisation of the chalcopyrite tends to mask the true paragenetic relationship of these two minerals, and therefore temperatures determined from these minerals must be viewed with caution. A total of 29 pairs of coexisting pyrite and chalcopyrite were analysed for $\delta^{34}S$ from samples collected from the four sections and the FEX 1 drillhole. Of these, ten could not be used for geothermometry because values of $\Delta^{34}S$ were negative, and a further ten gave temperatures that were considered geologically unreasonable, i.e. greater than 600°C. The remaining nine samples gave temperatures in the range 201° to 528°C illustrated in Figure 8.7.

Bismuthinite-Chalcopyrite: Because of the relative scarcity of co-existing high grade bismuth and copper ore, assay logs for all underground drilling in the Warrego mine were examined to identify potential samples for sulphur isotope geothermometry on this mineral pair. A total of 17 bismuthinite-chalcopyrite pairs and a single pyrite-bismuthinite pair were collected and analysed to yield a relatively coherent range of temperatures from 319° to 609°C.

Overall, the temperatures determined from sulphur isotope pairs in the Warrego mine span a wide range, with the upper limit much higher than those commonly observed in hydrothermal ore deposits. Typically precious and base metal deposits of vein, replacement, and seafloor style form in the temperature range of 150°C to 350°C (Ohmoto, 1986), and while porphyry and skarn deposits may form at significantly higher temperatures, there is little evidence that the Tennant Creek ironstone lodes are analogous with these deposit types (see Chapter 9). Therefore it seems more likely that at least the higher temperatures indicate that either the minerals represent a disequilibrium assemblage, or they have re-equilibrated during contact metamorphism.

Figure 8.8 illustrates the relationship of temperature determined from sulphur isotope pairs plotted against depth below the present surface. There is a general pattern of increasing temperature with depth that is consistent with a re-equilibration model and suggests a temperature gradient of between 400°C km^{-1} and 800°C km^{-1}. The upper limit of chlorite spotting (after cordierite) within the Warrego mine occurs at approximately 5 level (–282 m) and as all samples used for temperature determinations were collected below this level, they may be expected to have suffered the effects of contact

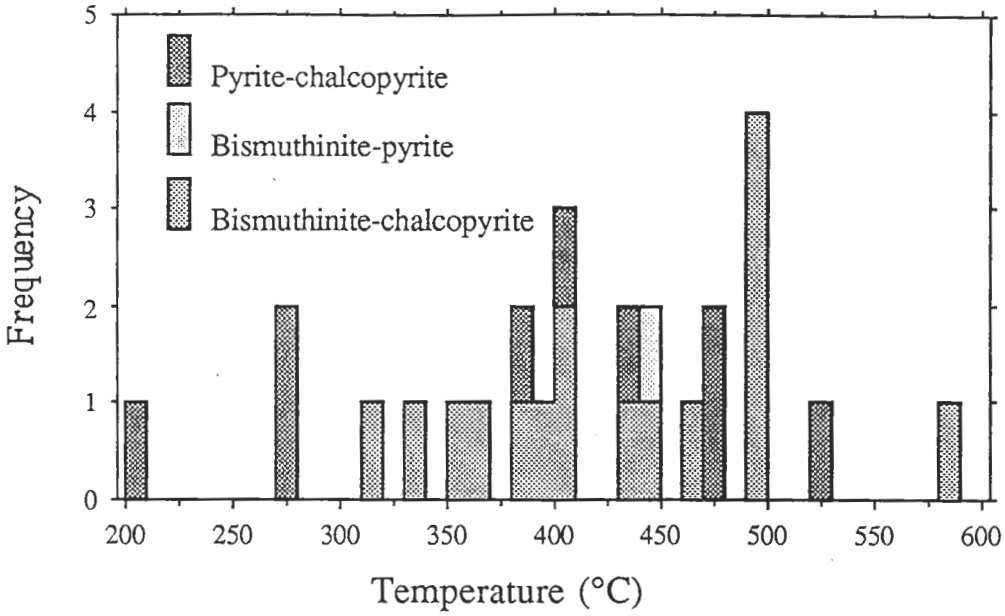

Figure 8.7 — Frequency distribution of temperatures determined from the pyrite-chalcopyrite, bismuthinite-chalcopyrite and bismuthinite-pyrite sulphur isotope geothermometers for samples from the Warrego mine.

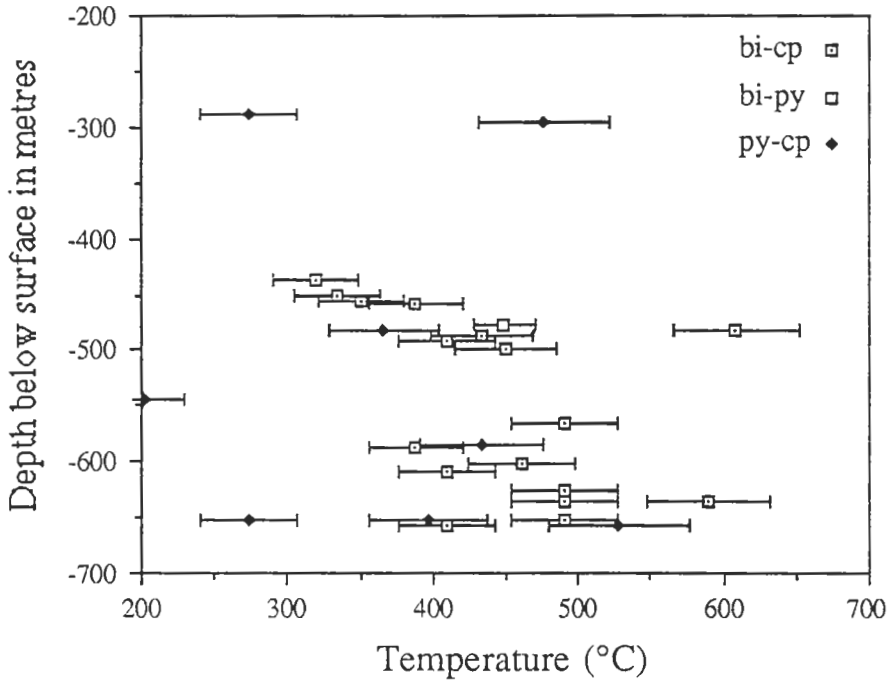

Figure 8.8 — Variation of temperatures determined by sulphur isotope geothermometry with depth in the Warrego mine illustrating the relatively erratic temperatures from the pyrite-chalcopyrite pair, and more consistent values for bismuthinite-pyrite and bismuthinite-chalcopyrite.

metamorphism to some degree. Certainly such high geothermal gradients support this premise.

Below –500 m temperatures determined by the sulphur isotope geothermometry are quite erratic but tend to cluster between 400°C and 500°C and it is suggested these temperatures represent re-equilibration temperatures associated with the intrusion of the Warrego Granite. However, the relatively coherent grouping of samples between -400 m and –500 m depth may be indicative of primary temperatures of deposition and thus their spatial distribution has been investigated in greater detail. These samples all come from the central gold pod and their relationship relative to the overall geometry of the ironstone lode is illustrated in Figure 8.9. The considerable thickening of stringer mineralisation in the footwall is characteristic of the gold pods, and indicates the zone of most intense alteration and probably also the highest temperatures. Although there is a general decrease in temperature from footwall to hangingwall (excluding the geologically unreasonable temperature of 609°C) there is also a strong vertical temperature gradient which again suggests the effect of contact metamorphism.

Other Mines

Studies of the sulphur isotope composition of other mines in the Tennant Creek goldfield compiled from various studies is illustrated in Figure 8.10. Although the database is rather limited, it provides an interesting comparison to the distribution observed for the Warrego mine (stippled range in Figure 8.10). Generally the other lodes show a wider overall range in the data and are shifted to more negative values of $\delta^{34}S$. Most deposits show relative fractionation between the sulphide minerals in the order pyrite > chalcopyrite > galena/bismuthinite in accordance with experimentally determined values as summarised by Ohmoto and Rye (1979), and Bente (1982), although disequilibrium is implied by geologically unreasonable temperatures for pyrite–chalcopyrite pairs in the White Devil mine (Nguyen, 1987) similar to that observed in Warrego mine.

Discussion

The contact metamorphic mineral assemblage in the Warrego mine suggests that the orebody has been heated to temperatures in the range 500° to 550°C (Chapter Two), resulting in extensive recrystallisation of the sulphide mineral assemblage. The possible modification of primary sulphur isotopic compositions attending such metamorphism must be considered before modelling of the systematics of ore deposition can be attempted. The extensive analyses of the sulphur isotopic composition of pyrite, chalcopyrite and bismuthinite throughout the orebody provide an excellent data base to evaluate any such effects.

Examples detailing the effects of contact or regional metamorphism on sulphur isotope systematics in ore deposits are extensively covered in the literature, dealing with

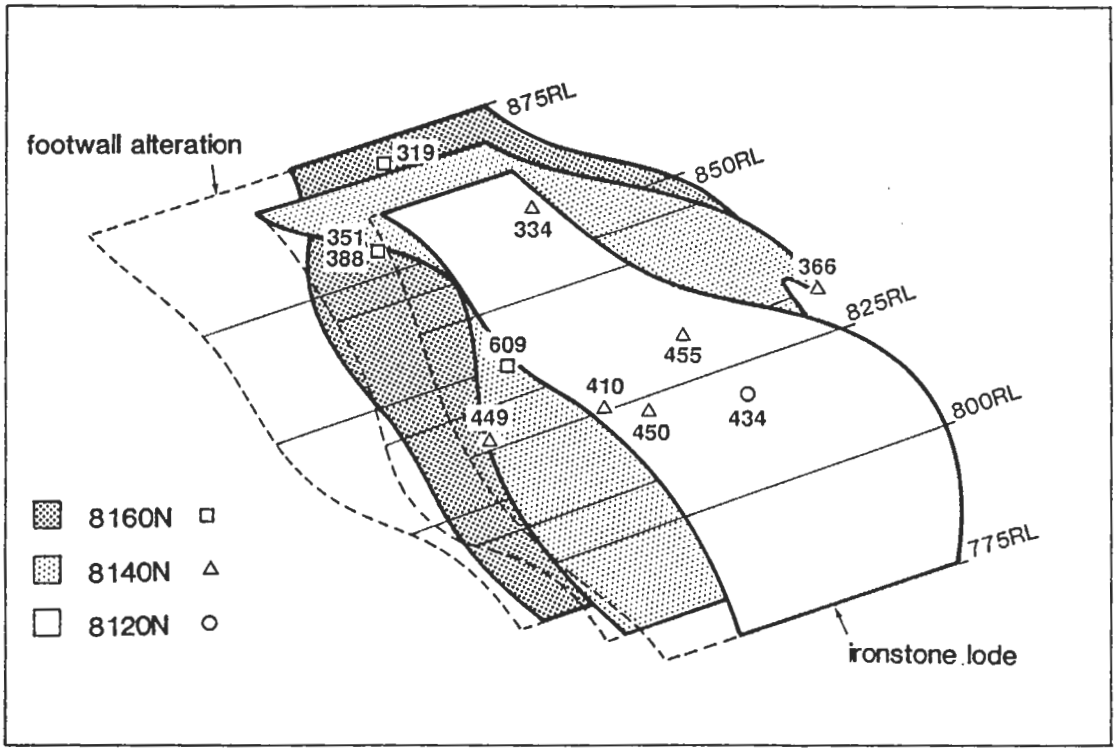

Figure 8.9 — Isometric view of the mine sections comprising the central gold pod illustrating temperature variation as defined by bismuthinite-chalcopyrite pairs. The clear relationship of increasing temperature with depth support a metamorphic re-equilibration of these minerals.

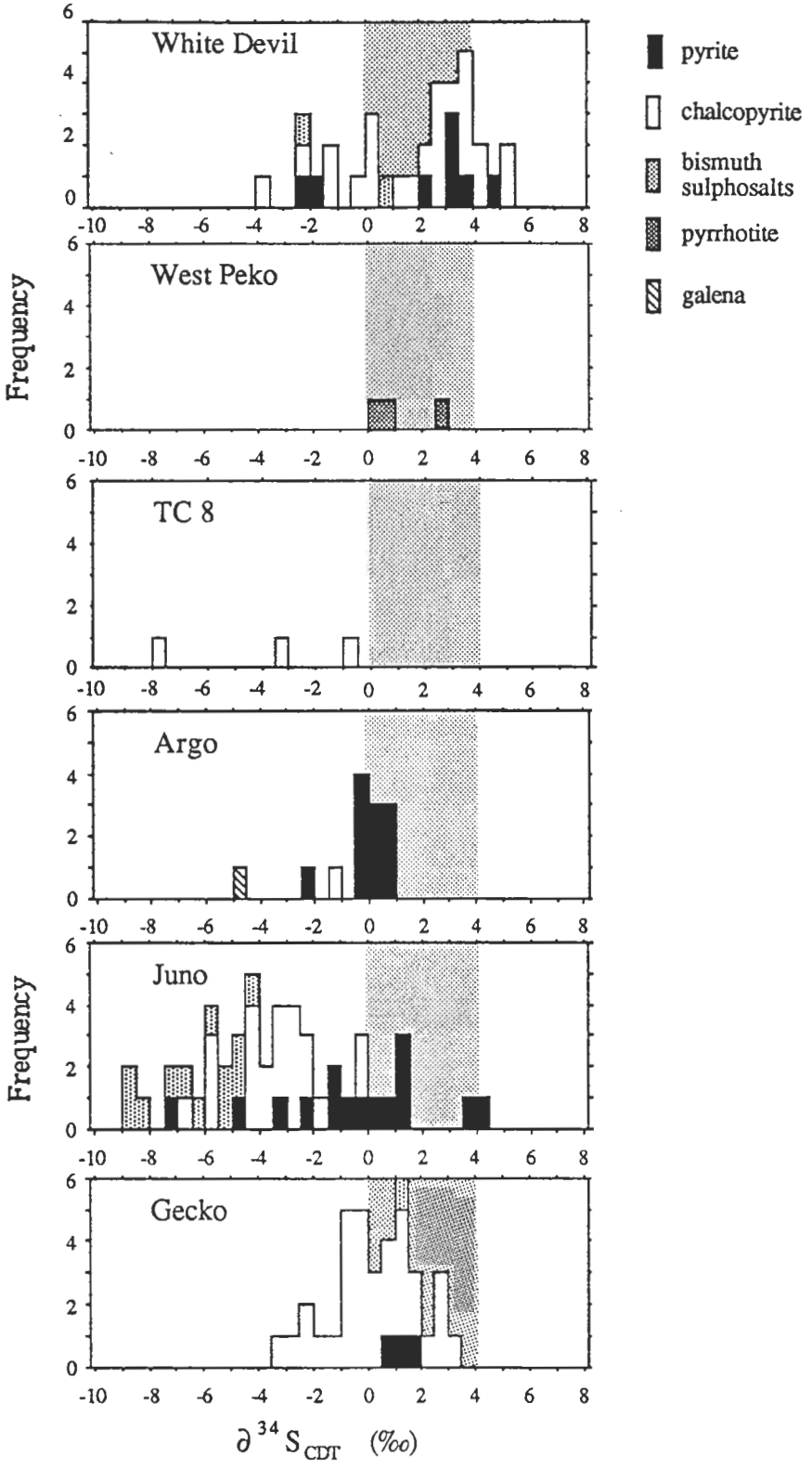

Figure 8.10 — Variation in the sulphur isotopic composition of selected mines in the Tennant Creek Goldfield compared to the range observed in the Warrego mine (stippled). Source of data is as follows: White Devil (Nguyen, 1987; Nguyen et al., 1990; Huston, 1989), West Peko (this study), TC8 (Wedekind and Adrichem, 1987), Argo (Wedekind and Adrichem, 1987), Juno (Large, 1974), and Gecko (Huston, 1989).

conditions that range from the fairly typical greenschist facies metamorphism where there has been no apparent disruption to primary isotope systematics (e.g. Green et al., 1981; South and Taylor, 1985), to extreme conditions involving multiple events of amphibolite-granulite facies metamorphism where there has been complete re-equilibration of the sulphide mineral assemblage (Both and Smith, 1975). Previous studies on a variety of ore deposit types that have undergone contact or regional metamorphism similar to the conditions observed at Warrego (300°C to 600°C), all exhibit disequilibrium relationships between sulphide- and sulphate-sulphide mineral pairs. These results suggest that the primary isotopic values and relationships are preserved (Rye and Rye, 1974; Bachinski, 1977, 1978; Ripley and Ohmoto, 1977; Rickard et al., 1979; Willan and Coleman, 1983; Seccombe et al., 1985).

Bachinski (1978) studied massive sulphide deposits in Newfoundland, and noted that despite conspicuous changes in the gangue mineral assemblage and fabric of the ore resulting from amphibolite facies contact metamorphism, the isotopic composition of sulphides still reflected ratios related to the ore formation process. Similarly, despite evidence of at least partial re-equilibration during garnet-amphibolite metamorphism of the Aberfeldy barite-zinc-lead deposit (530–580°C), Willan and Coleman (1983) suggested re-equilibration had not occurred over distances greater than 1cm, and that variation along and across the strike of the orebody reflected primary processes during deposition. Ohmoto and Rye (1979) in their review of sulphur isotope systematics, suggest that metamorphism of coexisting sulphide minerals below upper-amphibolite grade have usually undergone incomplete isotopic re-equilibration unless there has been a change in mineralogy. Partial re-equilibration between the mineral pairs may be observed on a local scale, but overall the composition and zonation of an orebody is unaffected.

The rate-limiting step in re-equilibration is probably related to the strength with which sulphur is bonded in minerals, and therefore ranges from very sluggish for pyrite to relatively rapid for sphalerite and galena (Bachinski, 1977). This relationship has been confirmed experimentally (Salomons, 1971) where it was observed that pyrite had a tendency to retain its isotopic composition while other sulphides readily re-equilibrated, and hence sphalerite and galena may record the temperature of metamorphism, while pyrite retains its primary composition (Ohmoto and Rye, 1979). Bachinski (1977) suggests the failure of pyrite and chalcopyrite to re-equilibrate in the Notre Dame Bay massive sulphide deposits may be related to the different responses of these two minerals to deformation; while pyrite remains rigid undergoing brittle deformation, chalcopyrite is recrystallised and remobilised around it, and exchange between the two minerals is limited.

The Warrego orebody shows a very narrow range in sulphur isotope values similar to the distribution commonly observed in porphyry copper and skarn deposits (Ohmoto, 1986), and pre-1.7 Ga volcanogenic massive sulphide (VMS) deposits (Franklin et al., 1981; Eastoe et al., 1990). Archean and Early Proterozoic VMS deposits typically display the same narrow range in sulphur isotope values, but their distribution is invariably centred on 0‰ (Eastoe et al., 1990), distinct from the ~2‰ value observed for the Warrego mine (Eastoe et al., 1990). Despite this narrow range, there is also a well developed zonation in the sulphur isotopes typically showing a footwall to hangingwall increase in $\delta^{34}S$, that mirrors patterns of both mineral and metal zonation. Because similar patterns of mineral and metal zonation are observed in other unmetamorphosed Tennant Creek orebodies (Chapter Five), both the range and zonation in the sulphur isotopes observed in the Warrego mine are considered to be primary and therefore reflect the changing physico-chemical conditions during mineralisation.

The core of low $\delta^{34}S$ values is likely to represent the zone of most intense interaction between the fluid and the lode and therefore lateral variation from the core reflects the changing physico-chemical conditions of the fluid as it interacts with the lode, temporal variations in the isotopic composition of the fluid, or a metamorphic overprint. Rye and Rye (1974) describe isotopic zonation in the Homestake gold mine, which they attribute to metamorphic processes. Systematic variation in sulphur isotopes from ~9‰ in the stretched limbs to ~6‰ in the dilatent zone is attributed to the breakdown of pyrite during metamorphism to form pyrrhotite while excess sulphur has migrated into dilatent zones reacting with wallrocks to produce sulphide zones of lighter $\partial^{34}S$. However, with the exception of pyrrhotite, sulphide minerals within the Warrego lode have remained stable and appear to have undergone relatively static metamorphism. The conversion of pyrrhotite to marcasite and pyrite is likely to have occurred without exchange or movement of sulphur, e.g.

$$2FeS + H^{+} + {}^{1}/_{2}O_2 \Leftrightarrow FeS_2 + Fe^{2+} + H_2O$$

and because there does not appear to be a complimentary mineral reduction, oxidant appears to be supplied by the moving fluid.

Textural changes in sulphide minerals resulting from metamorphism are clearly evident within the Warrego mine, with chalcopyrite and bismuthinite invariably recrystallised and locally remobilised. This appears to have been accompanied by isotopic re-equilibration, evident as the trend of increasing temperature with depth observed in Figure 8.8. The similar fractionation factors of galena and bismuthinite relative to H_2S suggests they have similar sulphur-metal bond strengths and therefore bismuthinite-chalcopyrite re-equilibration is consistent with observations for the re-equilibration of sphalerite-galena pairs in other metamorphosed orebodies (e.g. Lusk and Crocket, 1969). Similar to observations at Notre Dame Bay (Bachinski, 1977), pyrite

appears to have retained its primary form within the deformed chalcopyrite matrix and has not re-equilibrated texturally or isotopically. As pyrite-chalcopyrite pairs show disequilibrium relationships throughout the mine and thus probably retain their primary composition.

Re-equilibration of bismuthinite and chalcopyrite at a higher temperature means there is a reduction of $\Delta^{34}S$ between the two minerals (–1·1‰ for a temperature change from 300°C to 550°C). Considering this relatively small change in $\Delta^{34}S$ and the minor proportion of the overall sulphide assemblage bismuthinite constitutes, the change in $\delta^{34}S$ for chalcopyrite is likely to be minimal. This is born out by the co-variation of $\delta^{34}S$ for pyrite and chalcopyrite observed in the mine sections (Fig. 8.6), and the complete lack of correlation between bismuth grade and $\delta^{34}S$ for chalcopyrite (Fig. 8.11).

The steep temperature gradient within the mine (as defined by chalcopyrite-bismuthinite pairs) is consistent with modelled gradients developed adjacent to igneous intrusions (e.g. Cathles, 1977). That the temperature gradient is apparently vertical lends credence to the model relating rotation of the ironstone lode with intrusion of the Warrego Granite. A similar vertical temperature gradient is inferred from the distribution of contact metamorphic mineral assemblages (Chapter Two).

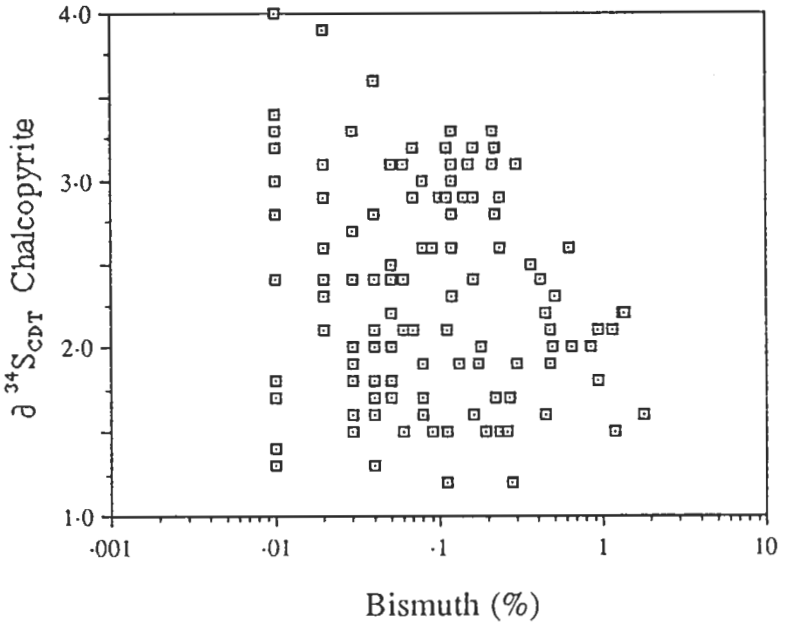

Figure 8.11 — Plot of measured $\delta^{34}S_{chalcopyrite}$ versus bismuth assay of the metre length of core from which the sample was taken. The lack of correlation between these two parameters suggests that re-equilibration of bismuthinite and chalcopyrite under higher temperature conditions have not significantly modified the primary sulphur isotope composition of the chalcopyrite.

It is uncertain if any of the sulphur isotope temperatures record mineralisation conditions, clearly chalcopyrite-pyrite pairs indicate disequilibrium relationships and the calculation of geologically reasonable temperatures from these may be more to do with chance than reality. Because isotopic re-equilibration follows mineral equilibration (Salomons, 1971) it is possible that recrystallisation of bismuthinite and chalcopyrite throughout the mine has not necessarily re-equilibrated the isotopic composition of these phases. Therefore any preservation of primary temperatures by recrystallised bismuthinite-chalcopyrite pairs might be recorded as a transition from metamorphic to mineralisation temperatures away from the intrusion. A change in the temperature profile with depth in the Warrego mine occurs at approximately –450 m (Fig. 8.8) where geologically reasonable temperatures (300–350°C — Chapter Nine) are determined from bismuthinite-chalcopyrite pairs and coincidentally (?) a pyrite-chalcopyrite temperature of 366°C also occurs.

8.3 Hydrogen and Oxygen Isotopes

The aims of this reconnaissance program of the hydrogen and oxygen isotope systematics of the Warrego mine were two-fold. Firstly it was hoped to determine something of the fluid history relating to the formation of the deposit through the fingerprinting of a source fluid, and secondly it was hoped that it would be possible to delineate either a target signature or enhanced alteration halo about the mineralised ironstone lodes that would be of use in exploration for further deposits. By way of a comparison, the barren Explorer 28 prospect was also examined.

A total of 25 hydrogen and 19 oxygen isotope analyses of chlorite, quartz, muscovite and biotite were carried out on samples selected from the suite collected on 14 level (Fig. 7.1). Because the silicate oxygen isotope line has only recently come into production after a complete overhaul and reconstruction of the vacuum lines, high temperature digestion of magnetite samples was not attempted. It proved virtually impossible to separate the finely intergrown magnetite and chlorite in the Warrego ironstone samples, so therefore no analysis of lode samples was attempted for fear of contaminating the reaction vessels with unreacted magnetite. A further nine hydrogen and five oxygen isotope analyses of chlorite separates, and a single quartz oxygen isotope analysis were made from the Explorer 28 prospect (Appendix H). All analyses are quoted as per mil deviation of the D/H and $^{18}O/^{16}O$ ratios of the sample relative to that of Standard Mean Ocean Water (Craig, 1961). Analytical techniques and results are presented in Appendix F.

Zonation

The interaction of hydrothermal fluids with the host rocks surrounding an orebody typically result in a shift in their respective isotopic compositions as they equilibrate

through the exchange of D/H and $^{18}O/^{16}O$ under the prevailing physico-chemical conditions. Typically, because hydrogen forms only a minor proportion of the total rock composition (0·11 wt % of a rock containing 1 wt % H_2O) the D/H ratio of the rock (unless water/rock ratios are very low), is controlled by the composition of the water. Conversely because oxygen is the major constituent of most rocks (~50 wt %), exchange between the fluid and rock will be controlled by the temperature and the relative fractionation factors between specific minerals and the fluid phase. Thus geothermal waters of meteoric or seawater origin typically show a shift to higher $\delta^{18}O$ as they react with sediments or volcanics of comparatively high $\delta^{18}O$ compositions, while maintaining a relatively constant δD (e.g. Taylor, 1979; Sheppard, 1986; Criss and Taylor, 1986). Samples of geothermal waters typically display $\delta^{18}O$ shifts with the largest changes generally associated with the hottest and most saline fluids (Craig, 1966), while shifts to higher D/H are both less common, and of lower magnitude. Shifts in D/H are possibly related to processes of evaporation and long term contact with hydrogen-rich shales (Craig, 1963; Clayton et al., 1966; Hitchon and Friedman, 1969). The progressive enrichment of ^{18}O in waters is balanced by ^{18}O depletion in the rocks with which the hot fluids have interacted, and may lead to the formation of well developed bulls-eye halos of ^{18}O depletion surrounding the zones of most intense water-rock interaction (e.g. Green et al., 1983; Criss et al., 1985).

Because the limited amount of data available for the Warrego mine comes from separates of a variety of minerals (chlorite, quartz, muscovite, and biotite), the $\delta^{18}O$ values for each sample have been normalised by calculating the composition of a fluid in equilibrium with the sample at a constant temperature (using fractionation factors referenced in Table VII), so that the different minerals may be directly compared. The selection of 350°C as the standard temperature is based on geothermometry using mineral oxygen isotope pairs — see below. Figure 8.12 illustrates the 14 level $\delta^{18}O$ profile resulting from this correction, and shows what appears to be a relatively well defined $\delta^{18}O$ anomaly about the ironstone lodes that is bounded by the Footwall Fault and the footwall contact of the quartz-porphyry. Although this pattern appears to match the geochemical alteration halo (e.g. Fig. 7.10), its identification as a halo must be considered speculative because of the lack of samples from either the sediments west of the Footwall Fault, or the porphyry and overlying sediments. It could equally be argued that the high $\delta^{18}O$ value at the Footwall Fault is related to late-stage/present day low temperature alteration through water migration along the fault zone. However, the contrast between the sediments and porphyry is probably related to the lower degree of alteration observed in the porphyry (as has been suggested by geochemistry in Chapter

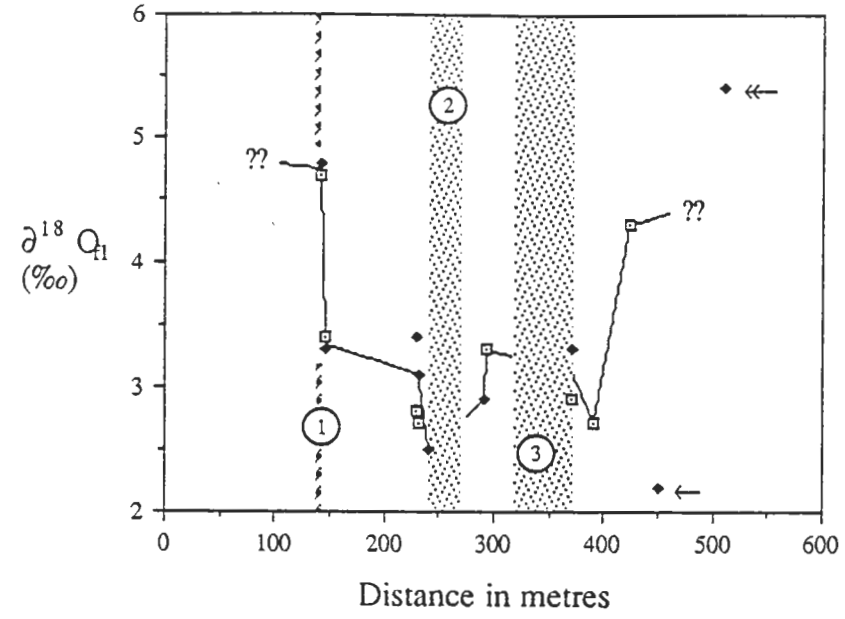

Figure 8.12 — Variation in $\delta^{18}O_{fl}$ with distance along the main and FEX drives on 14 level of the Warrego mine. $\delta^{18}O_{fl}$ represents the calculated ^{18}O value of the fluid in equilibrium with chlorite (boxes), and quartz, muscovite and biotite (filled diamonds) at 350°C to allow direct comparison between these different minerals. The anomalous points indicated by arrows are sample 106972 (double headed arrow) — a biotite separate from tourmaline veined sediment/porphyry, and 106977 (single headed arrow) — chlorite separate from the altered mafic dyke within the quartz porphyry. (1) Footwall Fault, (2) No. 1 orebody, (3) No. 3 orebody. The close overlap of quartz-chlorite pairs adjacent to the Footwall Fault indicate isotope geothermometer temperatures close to the 350°C used in to normalise the data. Wider separation of pairs adjacent to the lodes reflect lower geothermometer temperatures — see Table VIII.

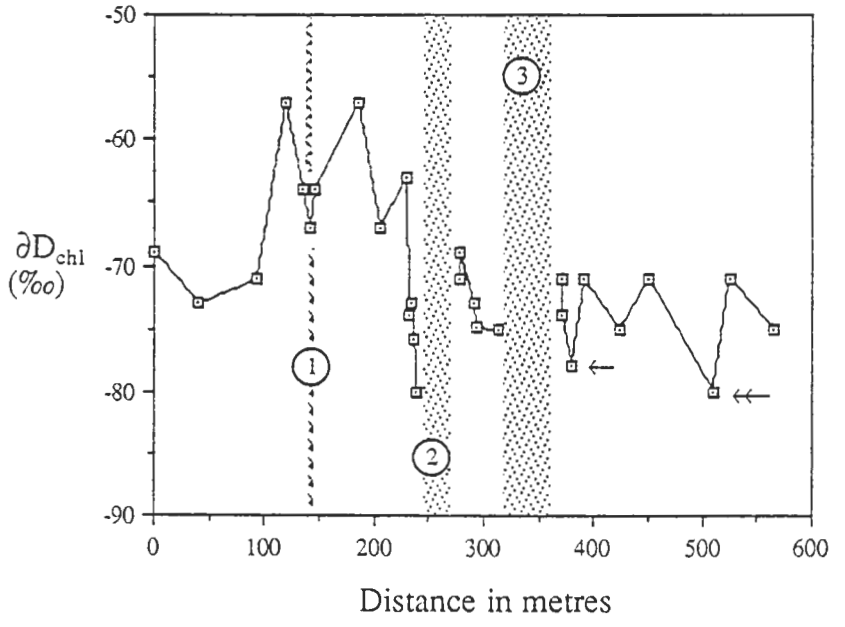

Figure 8.13 — Variation of $\delta D_{chlorite}$ along the main and FEX drives on 14 level in the Warrego mine. Symbols are as for Figure 8.12.

Seven), and may be attributed to permeability differences in the two rock types. Also evident in Figure 8.12 is a significant difference in the $\delta^{18}O$ composition of the alteration associated with the ironstone lode, and the tourmaline-biotite alteration associated with contact metamorphism.

Coverage of the 14 level section by hydrogen isotope analyses is more complete than for oxygen, and the profile for this section is illustrated in Figure 8.13. The D/H values are quite variable and may be divided into a relatively constant hangingwall composition, a depleted immediate footwall to the No. 1 orebody, and an enriched footwall sequence. The narrow zone of low D/H values determined in samples from the immediate footwall of the ironstone lode correlates with the zone of intense hydrothermal alteration observed in this position, and therefore low δD values appear to be related to mineralisation. This signature is distinct from hangingwall alteration, and implies different fluids.

The isotopic composition of the sediments between the footwall alteration zone and the Footwall Fault, differ from the hangingwall sediments and porphyry, but because these values extend across the Footwall Fault, any significance attributed to this feature must be related to an event that post-dated granite intrusion and the last movement on the fault. As noted in Chapter Two, the sediments on either side of the Footwall Fault are quite distinct, and there is no obvious petrographic explanation for the elevated values in this location.

Geothermometry

Similar to the use of the temperature dependence of isotopic fractionation in sulphur isotopes, the oxygen isotope composition of mineral pairs may be used to calculate temperatures, provided the variation in the fractionation factor of the mineral species with temperature is known, and that the minerals to which the technique is applied are in isotopic equilibrium. Triplicate isotope temperature concordancy is typically required to establish the reliability of temperature determinations (e.g. Bottinga and Javoy, 1973a, 1973b), but the separation of three silicate or oxide minerals from single specimens is often difficult to achieve. Such is the case for Warrego; because of the relatively simple mineralogy of the host rocks, and the present inability to analyse $\delta^{18}O$ of magnetite at the University of Tasmania, temperatures could only be determined by a single mineral pair. The most common mineral pair analysed for oxygen isotopes from the Warrego mine (and Tennant Creek ironstone lodes in general) is quartz-chlorite, and because of their widely different equilibrium fractionation factors (i.e large $\Delta^{18}O$ — Matsuhisa et al., 1979; Wenner and Taylor, 1971), they are particularly sensitive to temperature changes and hence they make useful geothermometers.

Mineral pairs for six samples were separated for $\delta^{18}O$ analysis from the Warrego sequence, of which five are quartz-chlorite pairs from the sediments, and the other a

single quartz-muscovite pair from a quartz-muscovite vein between the two orebodies. Although it has not been possible to extract pairs from the ironstone lodes themselves, samples 107004 and 107005 come from strongly chloritised sediments with associated stringer magnetite and sulphide mineralisation in the footwall to the No. 1 orebody, and samples 106985 and 106986 are adjacent samples on either side of the ironstone contact where chlorite has been extracted from the chloritic sediments, and quartz from the lode itself. Temperatures determined using equations cited in Table VII, with the exception of the quartz-muscovite pair, fall in the temperature range 300° to 350°C, suggesting that they represent samples that have equilibrated isotopically (Table VIII). The higher temperature determined for the quartz-muscovite vein, although overlapping the range of the altered sediments by virtue of its wide error bars, is believed to represent high temperature hydrothermal veining associated with the intrusion of the Warrego Granite.

Table VII — Fractionation equations for mineral-mineral and mineral-water oxygen and hydrogen isotope exchange.

Pair	1000 lnα	Reference
Hydrogen		
chlorite-water	~–35	Graham et al., 1987
biotite-water	$-22{\cdot}4(10^6/T^2)-4$	Suzuoki and Epstein, 1976
muscovite-water	$-22{\cdot}1(10^6/T^2)+19{\cdot}1$	Suzuoki and Epstein, 1976
Oxygen		
chlorite-water	$1{\cdot}56(10^6/T^2)-4{\cdot}7$	Wenner and Taylor, 1971
biotite-water	$0{\cdot}41(10^6/T^2)-3{\cdot}1$	Bottinga and Javoy, 1973 and Javoy, 1977
muscovite-water	$2{\cdot}38(10^6/T^2)-3{\cdot}89$	Friedman and O'Neil, 1977
quartz-water	$3{\cdot}34(10^6/T^2)-3{\cdot}31$	Matsuhisa et al., 1979
chlorite-quartz	$1.78(10^6/T^2)+1{\cdot}39$	Wenner and Taylor, 1979 and Matsuhisa et al., 1979
quartz-muscovite	$0{\cdot}96(10^6/T^2)+0{\cdot}58$	Friedman and O'Neil, 1977 and Matsuhisa et al., 1979

Recalculation (using the equation given in Table VII) of five quartz-chlorite $\delta^{18}O$ temperature pairs from the Eldorado mine (Horvath, 1988), yield a relatively consistent group of temperatures between 238° and 410°C (average 335°C, std. dev. 57°C) that overlaps with the range measured in Warrego. However, despite this similarity, it is possible that the Warrego temperatures are probably related to the contact metamorphism associated with the intrusion of the Warrego Granite. Extensive recrystallisation of the sediments, and the high temperatures of metamorphism during this event are likely to have resulted in isotopic re-equilibration. That the temperatures are relatively low compared to the probable temperatures of peak metamorphism (500–550°C), suggests that they result from retrograde resetting following peak contact metamorphism (possibly related to the retrogressive chloritisation of the biotite and cordierite in the peak mineral assemblage) rather than primary mineralisation. There being no such overprinting in the Eldorado area, the temperatures calculated there are probably those associated with mineralisation. A single quartz-chlorite pair from the Explorer 28 prospect yields an unrealistically high temperature of 632°C suggesting disequilibrium between quartz and chlorite.

Table VIII — Temperatures determined by oxygen isotope geothermometry

Sample No.	Mineral Pair	Temperature
106985 & 106986	qtz-chl	321^{+23}_{-21} °C
106994	qtz-musc	397^{+74}_{-56} °C
107004	qtz-chl	324^{+25}_{-22} °C
107005	qtz-chl	309^{+24}_{-21} °C
107010	qtz-chl	354^{+30}_{-26} °C
107012	qtz-chl	341^{+28}_{-25} °C

Explorer 28

By way of a comparison to the Warrego system, the δD and $\delta^{18}O$ of the lode and adjacent sediments to the Explorer 28 ironstone lode have also been examined (Appendix H). DDH 5 provides a 226 m intersection of relatively unaltered sediments followed by 191 m of alternating strongly chloritised zones with disseminated and stringer magnetite/hematite, magnetite/hematite ± talc ± chlorite ± quartz lode, and relatively unaltered

sediment. The drillhole was sampled at regular intervals and chlorite mineral separates were extracted for isotopic analysis.

Figure 8.14 illustrates the pattern of relative δD and $\delta^{18}O$ enrichment and depletion in this drillhole, with both δD and $\delta^{18}O$ showing coherent behaviour and a pronounced depletion in both occurring within and immediately adjacent to the lode. The pattern of abrupt variations in isotopic signature between relatively enriched sediment and depleted lode is maintained within the 'lode interval' where intervals of largely unaltered sediment preserve their isotopic signature.

The depleted δD value furthest from the alteration and ironstone lode development is attributed to surface weathering effects as this sample is was collected from just above the base of oxidation and shows visible effects of oxidation.

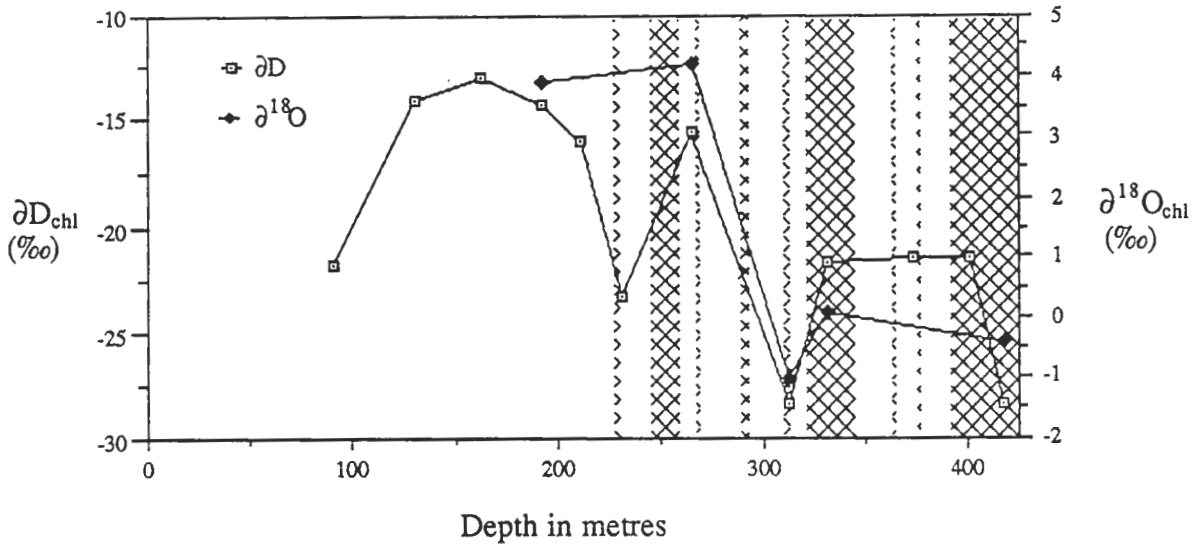

Figure 8.14 — Profile through the Explorer 28 ironstone lode along DDH 5 illustrating the variation of $\delta D_{chlorite}$ and $\delta^{18}O_{chlorite}$. The stippled area represents intervals of relatively massive magnetite/hematite in a sequence of alternating stringer and disseminated magnetite-hematite associated with strong chlorite alteration, and relatively unaltered sediments. Note the preservation of relatively unaltered sediment isotopic compositions within the alteration sequence.

Discussion

The δD and $\delta^{18}O$ composition of the Warrego host rocks appears to show some of the features observed in studies of oxygen and hydrogen isotope systematics in other ore deposits. An apparent halo of $\delta^{18}O$ depletion surrounds the Warrego orebody, extending from the Footwall Fault to the lower contact of the quartz porphyry, mirroring patterns observed in the more mobile major and trace elements (e.g. Ba, Cu, K_2O, Na_2O, and Sr — Chapter Seven). Such patterns of ^{18}O depletion have been described for other ore deposits, particularly VMS (e.g. Taylor, 1974; Beaty and Taylor, 1982; Green et al, 1983; Criss et al., 1985), and are interpreted to be the result of isotopic exchange between hot fluids and the host rocks beneath, and surrounding the ore deposits. Because there are no analyses of relatively unaltered rocks from the Warrego sequence west of the Footwall Fault or above the quartz porphyry, it is difficult to evaluate the extent of the $\delta^{18}O$ halo about the Warrego ironstone lodes. The halo may be restricted to the immediate footwall zone of the No. 1 orebody corresponding to the most intense alteration, or extend for some unknown distance. The probable similarity in the primary isotopic composition of the sediments and porphyry may indicate the presence of a restricted, intense halo immediately adjacent to the lode, with a broader, less intense, zone surrounding it. However, because the fractionation of δD in chlorite does not appear to be temperature dependant (Graham et al., 1987) and δD determinations have been made on pure chlorite separates, it is possible to interpret that variation observed in the profiles is related to fluids of different composition.

Although the fractionation of $\delta^{18}O$ is dependant on temperature and water/rock ratios, a general similarity between the oxygen and hydrogen isotope patterns is observed in both the Warrego and Explorer 28 data which also supports the interpretation of a multi-fluid signature.

The narrow zone of strongly depleted $\delta^{18}O$ and δD in the immediate footwall of the No. 1 orebody and throughout the Explorer 28 lode is distinctive. This pattern of lower δD and $\delta^{18}O$ contrasts with classic VMS alteration patterns of increasing δD with temperature, e.g. Sheppard (1986) and Beaty and Taylor (1982) and it is suggested that he different isotopic composition of the chlorite separates from these two locations is indicative of two hydrothermal fluids. A similar pattern of a distinct alteration signature was also observed in whole rock $\delta 18O$ analyses of sediments adjacent to the Argo ironstone lode (Large and Wedekind, 1987). Not only do these results imply strongly channelised flow of hydrothermal fluids, they also imply there has been minimal mixing between the two fluids; at least in the immediate vicinity of the lodes.

Fluid Source

The characterisation of the hydrothermal fluid source may be achieved through the measurement of δD and $\delta^{18}O$ either directly from the fluid (fluid inclusions and presently

active systems), or through calculation of the composition of water in isotopic equilibrium with alteration minerals within the rock. Complex modelling of the isotopic evolution of a particular system that may involve mixing of different fluids and reaction with a variety of host rocks are common in the literature, especially for currently active epithermal and submarine systems where the isotopic composition of the possible source fluids is well constrained (e.g. Sheppard, 1977; Zierenberg and Shanks, 1988). However with increasing age, the uncertainty of the composition of source fluids is also increased; debate as to whether the isotopic composition of seawater has remained unchanged with time continues. Muehlenbachs (1986) suggests $\delta^{18}O$ has remained constant for at least the last 3500 Ma, while Sheppard (1986) and Ohmoto (1986) indicate there may have been significant variation in both $\delta^{18}O$ and δD in ancient seawater. Because the isotopic composition of meteoric waters in part depends on that of seawater it is likely this has also varied with time if the variable composition model is accepted (Ohmoto, 1986).

Another factor that could further enhance the variability of the isotopic compositions of the source fluid is its salinity. Truesdell (1974) reported that ^{18}O is enriched in highly saline fluids at intermediate temperatures, and because Tennant Creek ore fluids are thought to to have been highly saline (Chapter Nine), this effect has possibly been of significance. Figure 8.15 illustrates the possible range of the four main generic water types that are considered important in ore forming processes (Taylor, 1974). The seawater and metamorphic water boxes cover the ranges suggested by Ohmoto (1986) and Sheppard (1986) respectively, but include a 5‰ expansion to higher $\delta^{18}O$ to accommodate the possible effects of high fluid salinity. As indicated above, the uncertainty of seawater composition with time will also be reflected in the composition of meteoric waters which are defined as a field rather than the typically linear meteoric water line (Ohmoto, 1986). The field of magmatic water is from Sheppard (1986).

Uncertainty in the measured isotopic composition of the hydrous minerals from the Warrego mine must also be considered. Despite the relatively tight clustering of $\delta^{18}O$ and δD, the effects of the contact metamorphism and probable high salinity of the ore fluids significantly enhances the range of possible equilibrium fluid compositions as is illustrated in Figure 8.15. Volatilisation, infiltration, and the disequilibrium effects associated with contact metamorphism during intrusion of the Warrego Granite, are likely to have depleted the $\delta^{18}O$ content of the rocks by values of up to 10‰ as are reported in halos surrounding other intrusive bodies (Valley, 1986). It is therefore likely the original fluid composition at Warrego was heavier (Path A) than that indicated by the calculated composition in equilibrium with the measured chlorite. Processes of

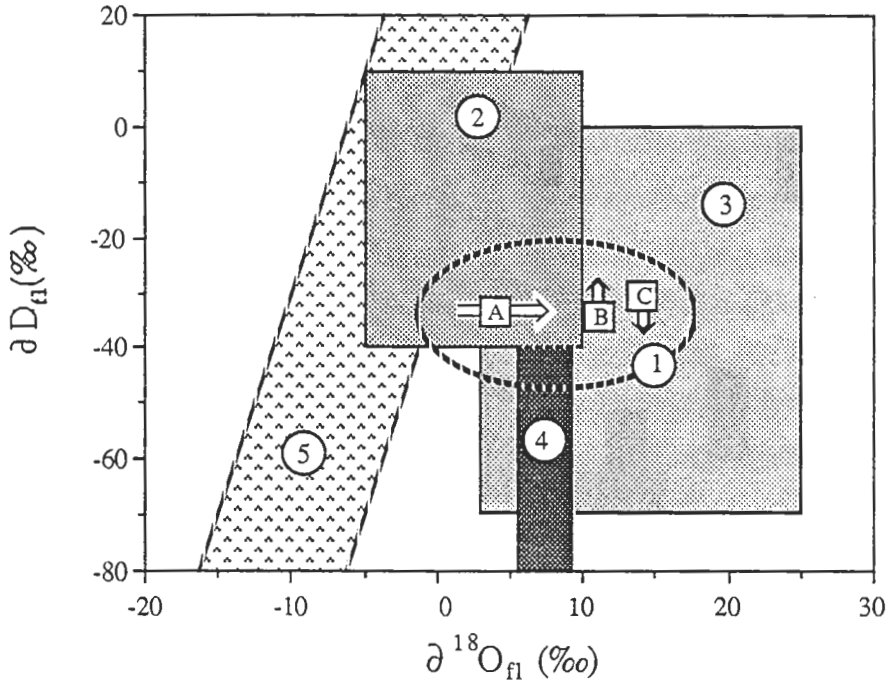

Figure 8.15 — Possible variation in the $\delta^{18}O$ and δD composition of fluids in equilibrium with primary chlorites from the Warrego mine (1) resulting from — A: depletion in $\delta^{18}O$ through volatilisation, infiltration, and disequilibrium effects associated with contact metamorphism, B&C: enrichment and depletion in δD during re-equilibration associated with contact metamorphism and disequilibrium effects associated with fluid salinity. 'Fluid boxes' are (2) probable range of seawater compositions for the last 3000 Ma; (3) metamorphic waters calculated as the composition of fluids in isotopic equilibrium with the range observed for metasediments and metabasalts; (4) range of magmatic waters calculated from the compositions of fresh igneous rocks; (5) probable range of meteoric waters during the last 3000 Ma. Fields (2) and (5) are from Ohmoto, (1986), fields (3) and (4) are from Sheppard (1986), and the slope of the meteoric water line ($\delta D = 8 \times \delta^{18}O + 10$) is from Craig (1961).

devolatilisation and chloritisation during contact metamorphism and retrograde alteration evident in the Warrego mine are also likely to result in enrichment and depletion in δD relative to the primary composition depending on the source of introduced fluids, water/rock ratios, distance of migration and whether the system is open or closed (paths B and C in Fig. 8.15). The salinity of the original fluid is also an important control on isotopic composition of the equilibrium hydrous mineral; Graham and Sheppard (1980) have shown that the δD composition of hydrous minerals in 4 M NaCl fluids may be depleted by up to 12 ‰ relative to pure water. Therefore saline fluids involved in the formation of the Warrego ironstone lode may have had significantly higher δD than would be predicted from the measured δD of chlorites (path B in Fig. 8.15).

The overall effect of the uncertainty in the isotopic compositions of the possible source fluids, and of the fluid in equilibrium with the chlorites from the Warrego mine is an inability to make any predictions as to the nature of the fluids responsible for the mineralisation. Meteoric, sea, metamorphic, connate, and magmatic waters or mixtures thereof could all potentially represent the composition of the source fluid, and based on the Warrego data alone there is little likelihood of forming any conclusions as to its probable source and evolution. However there is additional data available in the form of chlorite δD and $\delta^{18}O$ analyses from Juno and TC8 mines (Large, unpublished data), Eldorado mine (Horvath, 1988; Large, unpublished data), and the apparently barren One-oh-two prospect (Large, unpublished data). Together these deposits define a field with a relatively narrow range in $\delta^{18}O$ (0 to 7‰), but somewhat wider variation in δD (–5 to –45‰) (Fig. 8.16). Assuming that all of the ironstone lodes were formed under essentially the same conditions — which seems reasonable in view of the similarity in their mineralogy, apparent controls on their formation, and localised distribution; this combined data should better constrain the evolution of the fluid and its probable source. This discussion of δD and $\delta^{18}O$ variation within the ironstone lodes excludes the two outlying Warrego samples (106972 and 106994) which are respectively biotite and muscovite separates from veins that are considered late-stage, and are probably related to the Warrego Granite (Chapter Six). This interpretation is supported by the distinct fluid signature of these samples relative to other analyses and their close proximity of the compositional range of magmatic fluids in Figure 8.16.

Enlargement of the area of interest in Figure 8.16 and consideration of only chlorite samples from within or immediately adjacent to the ironstone lodes reveals a general coherence between deposit types that has implications both for fluid evolution and potentially also for exploration. Figure 8.17 illustrates a clear separation between barren (Explorer 28 and One-oh-two) and mineralised deposits (Warrego, Eldorado,

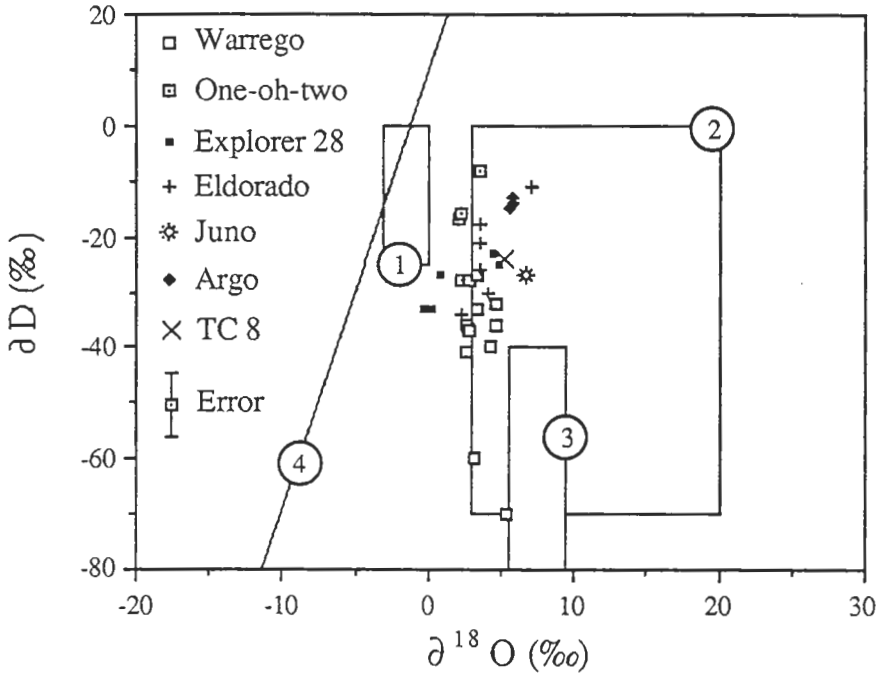

Figure 8.16 — δD–$\delta^{18}O$ diagram illustrating the calculated composition of fluids in equilibrium with chlorite at 350°C from several Tennant Creek mines and prospects compared to (1) probable range of seawater compositions for the last 2500 Ma; (2) range of metamorphic waters; (3) range of magmatic waters; (4) meteoric water line ($\delta D = 8 \times \delta^{18}O + 10$). Compositional ranges of waters are from Sheppard (1986), and meteoric water line is from Craig (1961). Error symbol represents the analytical uncertainty in the data points (±0.3‰ for oxygen and ±5‰ for hydrogen). Data from Tennant Creek deposits are as follows, Eldorado mine — Horvath, 1988; Warrego mine and Explorer 28 — this study; Juno, Argo, and TC8 mines, and One-oh-two prospect — Large (unpublished data).

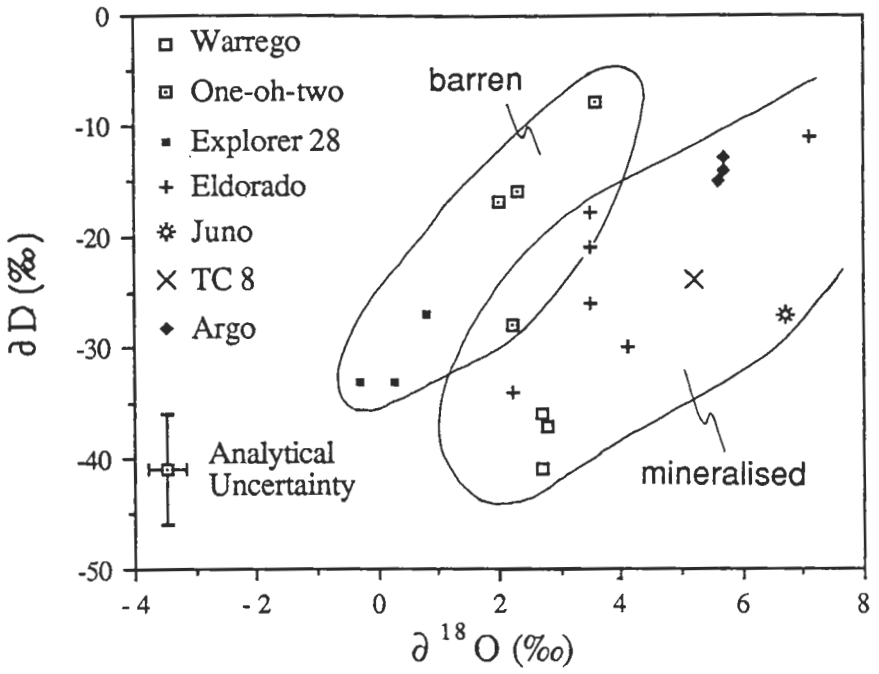

Figure 8.17 — Enlargement of Figure 8.16 illustrating the compositional range of fluids in equilibrium with chlorite at 350°C for samples from within or immediately adjacent to ironstone lodes only.

Juno, TC8, and Argo). It is also significant that Warrego and Juno (two of the top three richest mines in the goldfield) plot to the bottom of the mineralised field (low δD and high $\delta^{18}O$), while smaller and less significant producers plot between these and the barren deposits.

Typically five fluid sources are considered important in the formation of ore deposits (Taylor, 1974, 1979; Ohmoto, 1986), meteoric waters which include geothermal systems; seawater which is often associated with mid-ocean ridge hydrothermal venting and interpreted as important in most VMS deposits; metamorphic waters are those generated during dehydration during metamorphic reactions; formational waters which are transitional between meteoric water and seawater on one hand and metamorphic waters on the other; and magmatic waters derived either directly from the melt or fluids that have equilibrated with it.

Similar isotopic trends to those defined by the Tennant Creek ironstone lodes are observed in natural waters. The interaction of meteoric derived geothermal waters with country rocks typically produces shifts to higher $\delta^{18}O$ with increasing salinity, and relatively low temperature evaporation in acid hot spring environments may produce isotopic trends with positive slopes ~3 (Craig, 1963). However, these waters are typically of low salinity (<2 wt % NaCl equiv.) and unless direct interaction with

evaporitic sequences has occurred (Henley, 1985), it would be extremely difficult to produce the high salinities observed in the Tennant Creek fluid inclusion data (Chapter Nine). The absence of evaporitic sequences in the deep marine Warramunga Group sediments suggests that meteoric water was not a component in the Tennant Creek systems.

Seawater is apparently the most significant fluid component in VMS deposits (e.g. Pisutha-Arnond and Ohmoto, 1983; Urabe, 1987), and the field of possible seawater variation during the past 3500 Ma overlaps with most of the compositions suggested for the Tennant Creek deposits. The similarity in range of δD and $\delta^{18}O$ of Kuroko ore fluids to that of the Tennant Creek deposits (0 to –40‰ δD and 0 to 5‰ $\delta^{18}O$) suggests that a comparison between these two deposit types is warranted. Much debate over the origin of the Kuroko fluids has centred on the relative proportions of seawater and magmatic water required to explain the salinity and negative δD composition of fluids from these deposits (Ohmoto and Rye, 1974; Pisutha-Arnond and Ohmoto, 1983; Bryndzia et al., 1983; Urabe, 1987). Pisutha-Arnond and Ohmoto model diagenetic changes in the seawater to generate the high (for VMS deposits) salinities (~6 equiv. wt % NaCl) of the Kuroko ore fluids. Continued heating of these fluids to hydrothermal temperatures together with isotopic exchange with country rocks are then thought to have driven fluid compositions to higher $\delta^{18}O$ and lower δD while maintaining fluid salinity. However, Urabe (1983) states that the trend to lower δD is contrary to the observed increases in δD in other deposits (e.g. Beaty and Taylor, 1982) and suggests with other geological evidence that the negative δD values can only be achieved through the mixing of a significant magmatic component into the system. Although the salinities generated in this model are well below those indicated for Tennant Creek ore fluids, a seawater component with an increasing admixture of magmatic fluid might produce the trend to negative δD values from barren to mineralised ironstone lodes.

The place of metamorphic waters in the formation of ore deposits is uncertain due to their general overlap with formation waters and the diverse possible compositions of parent rocks and temperatures involved. Models involving metamorphic fluids in the formation of Archean gold deposits are gaining popularity (e.g. Golding and Wilson, 1987) although it is difficult to be categorical as to a specific source, or distinguish mixing between two or more fluids, and consequently these deposits are the subject of several interpretations. Rao (1976) suggests that greenschist facies metamorphism accompanied folding of the Warramunga Group, and modelling by Etheridge et al. (1983) indicate that fluid evolution under such conditions should be continuously derived through dehydration reactions under such conditions. However, abundant fluid inclusion evidence indicates that metamorphic fluids are of low salinity and therefore involvement of these fluids in the formation of the Tennant Creek ironstone lodes is unlikely.

Formation waters may represent original seawater trapped in the sediment pile at the time of formation although it appears that the majority of investigated are dominated by meteoric water (Clayton et al., 1966). The isotopic composition of the waters within a particular sedimentary basin is characteristic of it, and analyses typically display well defined isotopic fields showing positive correlation between δD, $\delta^{18}O$, temperature (30–100°C) and salinity (10 to 40 wt % dissolved solids) (Clayton et al., 1966). Most of the reservoir rocks are of a marine origin ranging back to at least Ordovician in age with fluid samples collected from between 500 and 3700 m (Sheppard, 1986). The high salinity of these waters, general coherent isotopic behaviour with low positive slopes of 2 to 3 on δD–$\delta^{18}O$ diagrams makes them likely candidates as source fluids for the ironstone lode mineralisation.

The apparent shift of the hydrothermal fluid composition to lower δD and higher $\delta^{18}O$ values from barren to mineralised ironstone lodes may be interpreted to indicate the mixing of formation waters with either magmatic or metamorphic fluids. However, because the magnitude of isotopic fractionation between fluid and a mineral is a function of temperature, an additional explanation for the shift is that the barren and mineralised lodes formed at different temperatures. Fluid inclusion evidence (Huston, 1990b) suggests that ironstone lode formation occurred at ~250°C, whereas economic mineralisation was associated with higher temperatures at ~350°C. Recalculation of the isotopic composition of the fluid in equilibrium with chlorite from barren ironstone lodes at 250°C would shift $\delta^{18}O$ by +1·7‰, and then the barren and mineralised fields would broadly overlap. However, to obtain a direct overlap of barren ironstone lode field with the Warrego and Juno mines, a temperature differential in excess of 150°C is required.

It is suggested that the positive slope to the field defined by the isotopic data from individual mines and prospects is related to a common fluid source that shows similarities to formation waters. However, shifts to lower δD with increasing temperature and salinity (Chapter Nine) in the mineralised deposits could also suggest the introduction of a different fluid at the time of economic mineralisation for which the most likely source would be magmatic fluids.

It is therefore concluded that while a magmatic component cannot be excluded from the model, it is most likely that the difference between the isotopic composition of chlorite in barren and mineralised ironstone lodes is related to the temperature of formation. Thus both had essentially the same source, i.e. formation waters.

Chapter Nine

THERMODYNAMIC MODELLING OF THE FORMATION OF THE WARREGO OREBODY

9.1 Introduction

As an important adjunct to reporting the physical and chemical characteristics of the Warrego ironstone lode and its associated mineralisation, modelling of lode formation and mineralisation is attempted using the available thermodynamic data on the stability of various mineral phases. It is largely through such modelling that an understanding of the probable processes controlling lode formation can be evaluated, and although relevant thermodynamic data is frequently scarce or may be conjectural, it is usually sufficient to constrain possible interpretations and enable the definition of a model that is consistent with observed geological relationships. It is stressed however, that interpretations of physicochemical conditions based on thermodynamic calculations can only approximate the actual conditions at the time of mineralisation

Before the physicochemical modelling of the evolution of the lodes and their mineralisation is attempted, the characteristics of the fluids as they are presently known is summarised, and because much of the primary character of the Warrego lode has been modified or completely obliterated during contact metamorphism, much of this information is derived from studies of other mines within the Goldfield. The overall similarity between the various ironstone lodes throughout the Tennant Creek Goldfield suggest it is unlikely there are significant differences between the various deposits. Where no local information is available geologically reasonable values are determined from the literature.

9.2 Fluid Characteristics

Temperature

Estimates of the temperature of ore deposition in the Tennant Creek Goldfield based on the mineral assemblage, solubility constraints, and by analogy with other styles of mineralisation have ranged widely, e.g. Edwards, 1955 (125° to 500°C); Elliston, 1966 (< 150°C?); Wright, 1969 (low temperature); Wyborn, 1971 (350°C); Large, 1974, 1975 (200° to 300°C); Norris, 1980 (< 250°C). The recrystallisation and deformation accompanying intrusion of the Warrego Granite has meant that primary fluid inclusion evidence of the conditions of mineralisation in the Warrego ironstone lodes has been

destroyed. Throughout the ironstone lodes (as in the sediments), quartz has been recrystallised to an assemblage of equant grains displaying triple point junctions. These grains are transected by trails of secondary fluid inclusions which post-date recrystallisation, and hence intrusion of the Warrego Granite. Limited heating runs on selected inclusions typically homogenise at temperatures less than 150°C which is considerably lower than mineralisation temperatures recorded in other ironstone lodes (see below).

Therefore estimates of the temperatures during lode formation and mineralisation must be determined by analogy with other deposits, chlorite geothermometry and constraints on mineral stability.

Fluid Inclusions: It is only relatively recently that systematic fluid inclusion studies carried out in the goldfield have been able to provided constraints on temperatures of mineralisation, e.g. Nguyen (1987), Horvath (1988), Zaw (1987, 1988), Huston (1989, 1990a, 1990b), Nguyen et al. (1990) and Zaw et al. (1990). Fluid inclusion temperatures obtained from a range of mines (Eldorado, Gecko, Juno, TC8, and White Devil) and barren prospects (Explorers 28, 41, 50, and 141, and Perseverance) suggest temperatures of formation of the ironstone lodes and associated mineralisation are relatively consistent throughout the goldfield, and may therefore also be applied to the Warrego mine.

Zaw (1988) recognises three generations of fluid inclusions within the ironstone lodes:

1. Early, often isolated two or three phase (L-V or L-V-Halite) inclusions that frequently decrepitate above 300°C, that are common in samples from both mineralised and unmineralised ironstone lodes.
2. Multiple arrays of healed microfractures containing two phase (gas and/or vapour-rich) and three phase inclusions (daughter crystals in addition to halite are observed) which are common in the mineralised ironstones and closely related to the gold-rich zones, and
3. Randomly oriented planes of two phase inclusions that cross-cut other generations and are common in both mineralised and unmineralised ironstone lodes.

These characteristic inclusion types have been confirmed in subsequent studies (e.g. Huston, 1990a and 1990b) and have been related to mineral parageneses. Type 1 and 2 inclusions are interpreted as related to ironstone lode formation and Au-Cu-Bi mineralisation respectively, whereas Type 3 are post-mineralisation secondary inclusions.

Overall primary fluid inclusion homogenisation temperatures show a wide range from 180° to >500°C but there is a general concentration in the range 300° to 400°C, and Zaw (1988) suggests it is possible to discriminate between barren and mineralised ironstone lodes on the basis of the homogenisation temperatures (<300°C and >320°C

respectively). Although the information available to date is limited, there also appears to be evidence of temperature differences within the TC8 ironstone lode associated with gold (280–440°C), and copper (240–360°C) mineralisation (Zaw, 1989). The common association of Type 2 inclusions within single healed fractures that homogenise to both liquid and vapour, and variable association of halite daughter crystals lead Zaw (1987, 1988) to suggest heterogeneous trapping resulted from the unmixing of a gas-rich phase during upward migration of a metal-bearing brine. Huston (1990a) has subsequently identified zonation within the Gecko K-44 orebody of vapour-rich, high-temperature (>400°C) inclusions in the core of the body, and fluid-rich, cooler (<400°C) inclusions at the lode margins.

Although Nguyen (1987) and Nguyen et al. (1990) determined an overall similarity of temperature and salinity of White Devil mineralisation to other fluid inclusion studies at Tennant Creek, their interpretation that ironstone lode formation was associated with hotter and more saline fluids than subsequent economic mineralisation differs from the other interpretations, and is contradicted by recent fluid inclusion evidence from White Devil (Huston, 1989, 1980b). Although there has been no resolution of these differences, Huston, (1989) and Wedekind et al. (1990) suggested that the paragenesis of the barren mineralisation was insufficiently constrained.

Bismuth Sulphosalt Stability Relationships: Estimates of temperature derived from the assemblage of bismuth sulphosalts in the Warrego and Juno mines suggest they formed in the range 300° to 400°C (Chapter Six). The exsolution of gladite within pekoite observed in the Juno mine may indicate segregation during slow cooling below 300°C, suggesting that temperatures of formation were above this temperature (Large, 1974; Mumme and Watts, 1976), and similarly the observation of the assemblage chalcopyrite-wittichenite, and occurrence of tellurides in the Warrego mine indicate temperatures below 396°C and 350°C respectively (Sugaki, 1981; Afifi, 1988a).

Sulphur Isotope Geothermometry: Bismuthinite-chalcopyrite mineral pairs from the Warrego mine yield temperatures that are considered to reflect the temperature of recrystallisation during contact metamorphism. However, the possible preservation of primary temperatures within the central gold pod in the range 300° to 400°C may be indicated (Chapter Eight).

Salinity

Estimates of fluid salinity through the measurement of freezing point depression of fluid inclusions suggest that the solutions responsible for ironstone lode formation and mineralisation in the Tennant Creek Goldfield although variable, were of high salinity with most determinations falling in the range 15–25 equivalent weight % NaCl (e.g. Nguyen, 1987; Zaw, 1987,1988; Horvath, 1988; Huston, 1989, 1990a, 1990b; Nguyen et al., 1990 and Zaw et al., 1990). These determinations are further reinforced by the

common observation of halite daughter crystals within fluid inclusions in all of the above studies which indicate salinities >26 equiv. wt % NaCl. There is also a general overlap in the salinity range of both the barren and mineralised ironstone lodes that suggests both the ironstone lode formation and overprinting of economic mineralisation were associated with highly saline fluids.

pH

Estimates of the pH of the fluids involved in the formation of ironstone lodes and associated mineralisation are constrained by the pH buffering provided by the gangue mineral assemblage. Although potassic feldspar is a common constituent of the unaltered Warramunga Group sediments (Large, 1974), within alteration zones beneath and adjacent to the ironstone lodes it is totally replaced by sericite which is in turn replaced by chlorite in the core of the alteration zone. The reaction of feldspar to sericite is controlled by two variables namely pH and the K^+ content of the fluid, i.e.

$$\underset{\text{K-spar}}{KAlSi_3O_8} + 2H^+ + 6H_2O \Leftrightarrow \underset{\text{sericite}}{KAl_3Si_3O_{10}(OH)_2} + 2K^+ + \underset{\text{quartz}}{6SiO_2} \qquad (1)$$

Because there is no information available on the chemistry of the fluids, it is necessary to make assumptions based on other ore forming systems. Sodium and potassium are typically the dominant cations in solution, and assuming a geologically reasonable Na/K ratio of 10 (e.g. Ellis, 1979; Roedder, 1979; Weissberg et al., 1979; Henley et al., 1984), a concentration of K^+ in the saline fluids of ~0·5*m* is suggested. Using the thermochemical data compiled in Appendix G, the pH of a solution buffered by the sericite-K feldspar reaction may be calculated to provide an upper limit on the pH of the solutions. Similarly because the reaction of sericite to kaolinite is controlled by the same parameters as reaction (1), i.e.

$$\underset{\text{sericite}}{2KAl_3Si_3O_{10}(OH)_2} + 2H^+ + 3H_2O \Leftrightarrow \underset{\text{kaolinite}}{3Al_2Si_2O_5(OH)_4} + 2K^+ \qquad (2)$$

and kaolinite is absent from the alteration mineral assemblage, this reaction may be used to constrain the lower pH limit of the fluid (e.g. Crerar and Barnes, 1976; Barnes, 1979).

Figure 9.1 illustrates the variation in the pH of these reaction boundaries with temperature and $\sum K^+$ and hence the possible range in pH of a solution buffered by sericite. The effect of temperature on the position of these boundaries is minimal, but an order of magnitude variation in $\sum K^+$ changes the boundary position by 1 pH unit. Although there is a wide variability in the measured Na/K ratio from fluid inclusions from ore deposits (Roedder, 1979), and direct measurement from active geothermal systems (e.g Ellis, 1979; Weissberg et al., 1979; Henley et al., 1984), the ratio tends to

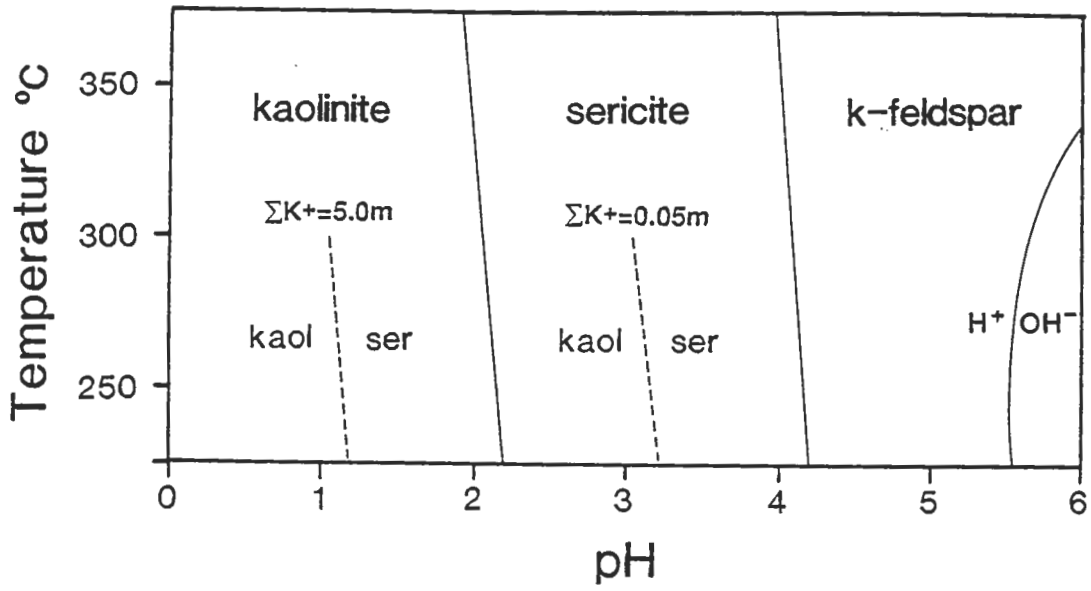

Figure 9.1 — Constraints imposed on pH of a fluid in equilibrium with kaolinite, sericite, and K-feldspar with $\Sigma K^+ = 0.5$ *m*. Variation in the kaolinite/sericite boundary with $\Sigma K^+ = 0.05$ *m* and 5.0 *m* is illustrated by the dashed lines. Thermodynamic data for this and subsequent diagrams is tabulated in Appendix G.

cluster between 5 and 12. Based on the observed temperature dependence of Na/K ratio (Ellis and Mahon, 1967) this range in the Na/K ratio indicates temperatures between 250° and 400°C which correlates well with the generally accepted range of temperatures for hydrothermal mineralisation. This relatively consistent relationship of Na/K ratio with temperature suggests that the estimate of the ratio for the Tennant Creek hydrothermal solutions is unlikely to be significantly different from that suggested here, and therefore the selection of a solution pH in the range of 3 to 4 is likely to be reasonable.

The separation of the ironstone lode formation and mineralisation into two stages on the basis fluid inclusion, stable isotope and petrographic evidence raises the question of how fluid conditions varied between these two stages. Ironstone lode formation seems to have occurred at slightly lower temperatures but mineral assemblages are not significantly different. Sericitisation of feldspars in the sediments followed by pervasive chloritisation characterises alteration accompanying ironstone lode formation, while the growth of coarse bladed muscovite and magnesian chlorite are characteristic of gold pod mineralogy. It therefore seems unlikely pH conditions were dramatically different during the two stages of mineralisation.

Although the reaction between sericite and chlorite would appear more appropriate in constraining pH relations during ironstone formation and mineralisation, the non-stoichiometry of chlorite and general absence of thermodynamic data for this mineral make meaningful predictions on prevailing conditions tenuous. Additional uncertainty is also introduced into calculations involving only end-member chlorite compositions which also require additional assumptions on fluid composition (e.g. ΣMg^{2+} or ΣFe^{2+}) i.e.

$$\underset{\text{sericite}}{2KAl_3Si_3O_{10}(OH)_2} + \underset{\text{quartz}}{3SiO_2} + 15Mg^{2+} + 24H_2O \Leftrightarrow \underset{\text{Mg chlorite}}{3Mg_5Al_2Si_3O_{10}(OH)_8} + 28H^+ + 2K^+ \qquad (3)$$

Pressure

Regardless of the age of mineralisation (Chapter Two), the depth of formation of the Tennant Creek ironstone lodes is constrained to depths of at least 2 to 5 km. The consistent Rb/Sr isochron age of 1810 Ma from muscovite associated with mineralisation in several of the mines (Black, 1984) suggests a minimum depth of 3000 m based on estimates of the thickness of the Warramunga Group sediments above the Black Eye Member, plus Hatches Creek Group sediments and volcanics below the 1813±5 Ma Treasure Volcanics (Le Messurier et al., in press; Blake and Page, 1988). If as Wall and Valenta (1990) suggest, mineralisation accompanied reactivation of Warramunga Group structures during folding of the Tomkinson Group, depths in excess of 7 km are possible. Alternatively if the 1810 Ma age represents resetting by a subsequent metamorphic event, ironstone lode formation and mineralisation is likely to have accompanied folding and granite intrusion some 60 Ma earlier. Although a minimum thickness of less than 2000 m of overlying Warramunga Group sediments is suggested (Le Messurier et al., in press), a further unknown thickness has been eroded during uplift and folding and it is likely depths of formation were significantly greater. Based on these depth estimates pressures in the order of 0·5 to 1 kb seem likely.

Minimum depth estimates from the Tm-NaCl of salt crystals using the data of Bodnar et al. (1985) for the Juno, Eldorado and Gecko mines (Zaw, 1987; Horvath, 1988; Huston, 1990b) range between 700m and nearly 1500m, well short of the predicted depths of mineralisation. However, correction for presence of gases (CO_2 and N_2) in the fluid is likely to significantly alter these estimates (Zaw, 1988; Huston, 1990b).

Sulphur Content

Large (1974, 1975) suggested that the general lack of sulphides in the Juno lode, combined with the high selenium to sulphur ratio observed in the bismuth sulphosalts and the orebody as a whole was the result of deposition from a fluid with a relatively low

total sulphur content ($\Sigma S \leq 10^{-3}m$). Similarly the oxidised nature of the Warramunga Group, and general absence of sulphides (detrital or diagenetic) within the sediment pile is likely to limit the amount of sulphur available in any model of ironstone lode formation which involves convective leaching from the sediments. However, not all of the Tennant Creek ironstone lodes are characterised by low sulphur contents; although mines in the south-east of the goldfield (Golden Forty, Nobles Nob, Juno, and Eldorado) may be characterised as sulphide-poor, those in the central and north-western parts of the goldfield (Peko, Argo, TC8, Ivanhoe, Gecko, White Devil and Warrego) are characterised by high sulphide contents and therefore either the physicochemical conditions in each mine control the relative ratios and abundance of sulphur and selenium, or the differences are more fundamental and are related to the source (see below).

To evaluate the probable sulphur content of the Tennant Creek ore fluids a series of $\log fS_2$ vs. $\log fO_2$ diagrams have been constructed over the probable mineralisation temperature range i.e. 250°C to 350°C (Fig. 9.2). Assumptions regarding the composition of the fluid or the physical conditions during mineralisation used in the construction of these diagrams are minimal, pressure is assumed to be on the vapour-water equilibrium curve, temperature of deposition between 250° and 350°C, and a pH of 3. The pH of the solution controls only the position of the H_2S/HSO_4^- predominance boundary and ΣS contours in the HSO_4^- stability field and therefore is not an important consideration for the mineral assemblage in the Warrego mine (see Fig. 9.2). Changing the selection of pH by one unit will move the position of the H_2S/HSO_4^- boundary by half a log fO_2 unit which is insufficient to influence ΣS in the area of interest.

The best control on the range of possible fS_2 and fO_2 is provided by the apparent equilibrium mineral assemblage associated with economic mineralisation i.e. magnetite - chalcopyrite - bismuthinite ± pyrite ± pyrrhotite. The stability range of this assemblage decreases with increasing temperature (stippled areas in Fig. 9.2). The coexistence of pyrrhotite and bismuthinite constrains the temperature to ~300°C as both above and below this temperature native bismuth rather than bismuthinite is stable with pyrrhotite. The suggestion that high selenium contents stabilise the complex bismuth minerals observed in the Juno mine (Mumme, 1976), may indicate the field of bismuthinite stability is enhanced by the presence of selenium although the generally low selenium content of bismuthinite from Warrego mine suggests that such effects are likely to be minimal.

Therefore constraints provided by the equilibrium mineral assemblage of magnetite–chalcopyrite–bismuthinite ± pyrite ± pyrrhotite restrict the total sulphur content of the fluid between $10^{-2}m$ and $10^{-3}m$, a range that is essentially the same as that observed for many massive sulphide deposits (e.g. Skinner and Barton, 1973). Because the sulphide-poor deposits do not contain pyrrhotite it is not possible to constrain the

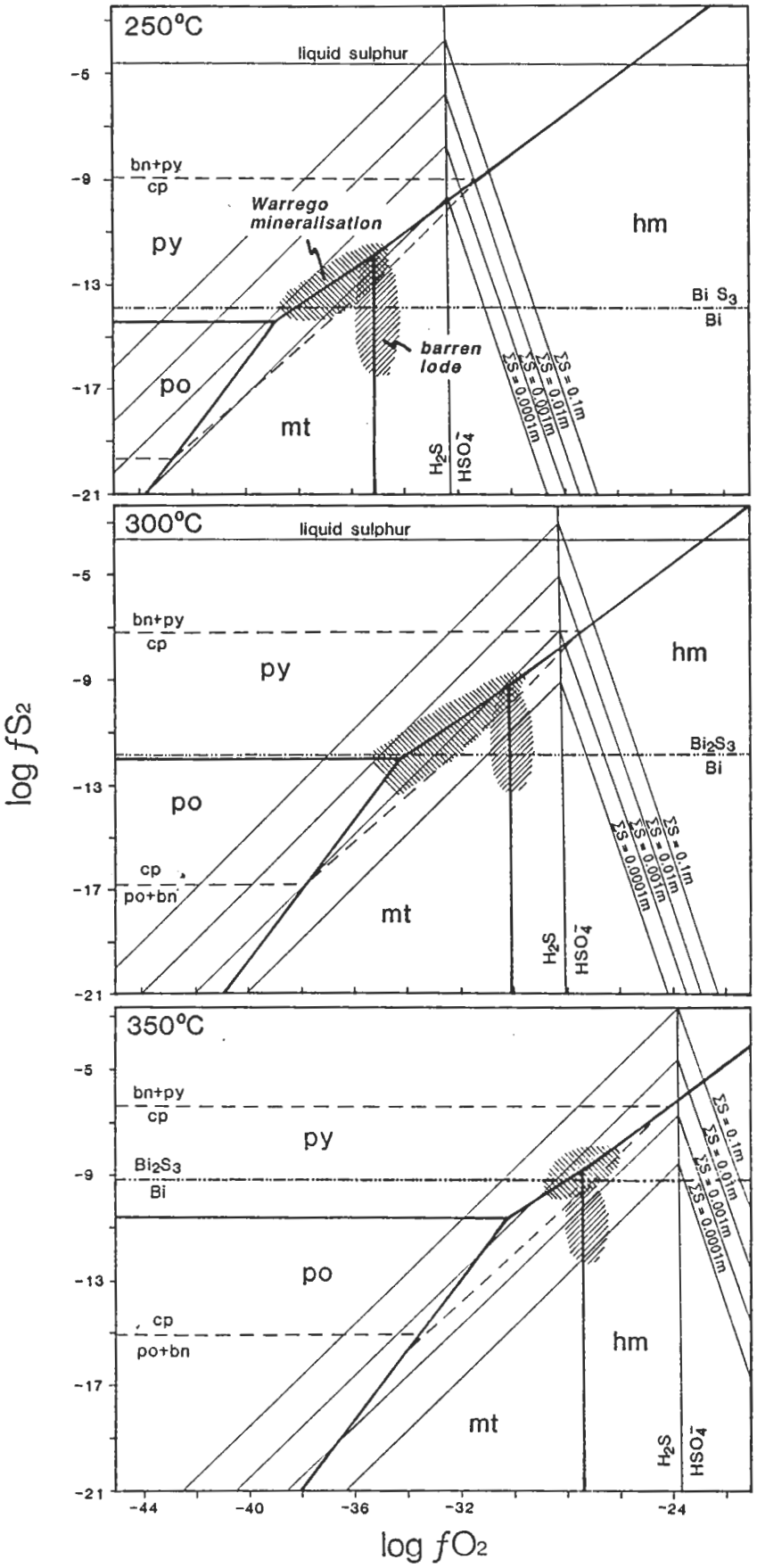

Figure 9.2 — Log fS_2–log fO_2 diagrams at 250°C, 300°C and 350°C showing contours of sulphur content for solutions in equilibrium with pyrite, pyrrhotite, magnetite, hematite, chalcopyrite, bornite, bismuthinite and native bismuth. The fields indicate the suggested range of fluid compositions associated with ironstone lode formation and economic mineralisation. pH = 3.

temperature as at Warrego (and other pyrrhotite-bearing lodes), and therefore ΣS may range from $10^{-4}m$ at 250°C to $10^{-2}m$ at 350°C (Fig. 9.2). However the high temperatures indicated for economic mineralisation in all orebodies suggest that the ΣS content of the fluid was similar to that suggested for Warrego.

The relatively simple mineralogy of the barren and pre-mineralisation ironstone lodes (magnetite/hematite-chlorite-quartz) makes it difficult to constrain the conditions of their formation. However, assuming conditions were at of near the magnetite-hematite buffer and that the fluid inclusion temperatures measured in the barren systems reflect the formation temperatures of the ironstone lodes in general, the sulphur content of the solutions are likely to be lower than those of mineralisation by at least an order of magnitude. At a temperature of 250°C the ΣS of the fluid is likely to have been $<10^{-4}m$ but would increase at higher temperatures. The general absence of sulphides associated with ironstone lode formation is incompatible with the the high ΣS_{fluid} indicated by modelling at higher temperatures. Therefore modelling would support the fluid inclusion evidence that late-stage economic mineralisation was associated with higher temperatures.

9.3 Chlorite as an Indicator of Mineralisation Conditions

Observations of systematic chlorite compositional variation with both intensive and extensive variables are well documented in natural systems. Most studies of chlorite compositional variation within a specific environment, suggest unquantified empirical relationships, the most common being trends of increasing Fe content of chlorite with temperature, e.g. Albee (1962), Cathelineau and Nieva (1985), Shikazono and Kawahata (1987), and Yau et al. (1988); increasing stability of Mg chlorite with rising water/rock ratios, e.g. Slack and Coad (1989), and vice versa Andrews et al. (1986); the association of Mg-rich chlorite with conditions of high fO_2, e.g. Bryndzia and Scott (1983, 1987a, b), Shikazono and Kawahata (1987), and Wilde, et al. (1990), and high ΣS, e.g. McLeod and Stanton (1984), Bryndzia and Scott (1987), Shikazono and Kawahata (1987), and Kalogeropoulos and Scott (1988); control on the Si content of chlorite by the fluid pH, e.g. McLeod and Stanton (1984); and the availability of iron and magnesium in solution Walshe and Solomon (1981) and Shikazono and Kawahata (1987).

Several authors have recently made use of the solid solution exchange reactions observed in chlorite minerals to model conditions of mineral formation in a predictive sense. Rather than simply suggesting possible paths of fluid evolution, actual physical and chemical parameters are calculated and have the potential to greatly assist in understanding the processes of ore formation; especially in cases where, for any number of reasons, the mineral assemblage is not amenable for the determination of parameters such as temperature, fO_2, and fS_2. However, these 'models' are not a

universal panacea, their application may be limited by particular mineral assemblages with reliability hampered by the relative lack of thermodynamic data on chlorite end-members, and assumptions in the distribution and mixing of cations within the crystal structure. Also as these models are based on electron microprobe analyses, where ferric iron and water content are not determined, assumptions are required in normalising probe data to a chemical formula. Because all calculations of the variables controlling chlorite composition are based on normalised probe data, it is appropriate to reiterate Lairds' (1988) comments on this matter,

"Because of problems [in estimating the mineral formula]*it seems prudent not to place too much emphasis on small changes in chlorite composition."*

The abundance of chlorite, lack of fluid inclusions, and the relatively simple mineral assemblage of the Warrego system make the determination of physical and chemical conditions of ore formation through chlorite modelling particularly attractive. The increasing body of data on the physicochemical conditions of mineralisation for other Tennant Creek ironstone lodes (e.g. Zaw et al.,1990), together with mineralogical, and stable isotopic constraints observed at Warrego may be used to test the relative accuracy of the chlorite modelling. Three models are considered:

Chlorite Geothermometer (Cathelineau and Nieva)

The chlorite geothermometer of Cathelineau and Nieva (1985), is based on the observed temperature dependence of chlorite chemistry for samples collected from the active Los Azufres geothermal system. Strong correlation between well temperature and Al^{IV} (r = 0.87), Fe^{VI} (r = 0.70), and octahedral vacancy (r = -0.82) of chlorite were observed for this system. Similar though less significant correlations were also obtained for the Larderello and Salton Sea geothermal systems, and the Mount Lyell copper deposit. The geothermometer is a simple linear function relating the tetrahedral Al content of chlorite to temperature:

$$T°C = 212\ Al^{IV} + 18$$

Kranidiotis and MacLean (1987), and Slack and Coad (1989) have applied the geothermometer to the Phelps Dodge and Kidd Creek volcanogenic massive sulphide deposits respectively. Kranidiotis and MacLean (1987) suggest the determined temperature for the chlorites (290°C) from Phelps Dodge were reasonable to somewhat low compared to theoretical estimates for their genetic model, and indicated the geothermometer could be improved with further calibration. Both studies applied a correction factor to the value of Al^{IV} to account for the observed co-variation of Al^{IV} and $Fe^{\#}$ such that,

$$Al^{IV}_{corrected} = Al^{IV}_{sample} \pm 0.7\ Fe/(Fe+Mg)$$

where 0.7 is the slope of the best fit line through the chlorite data plotted on an Al^{IV} vs. $Fe^{\#}$ plot.

Restrictions on the application of the geothermometer appear to be relatively limited although Cathelineau and Nieva (1985) caution indiscriminate application of the geothermometer as parameters other than temperature may explain variations in chlorite composition. The assumption of negligible ferric iron in calculating structural formulae, appears to be born out by studies where ferric and ferrous iron contents have been determined, e.g. Deer et al., 1962; and Foster, 1962. Kranidiotis and MacLean (1987) suggest there may be a significant pressure effect on Al^{IV}/Si substitution and recommend the geothermometer should only be used for chlorites that formed in low pressure environments, and were not recrystallised during metamorphism. These restrictions are of possible significance in the Warrego situation where depths of formation were probably of the order of several kilometres, and contact metamorphism has overprinted the mineralisation.

Sulphur and Oxygen Fugacity Determination (Bryndzia and Scott)

Bryndzia and Scott (1987a,) experimentally evaluated the relative controls of fS_2 and fO_2 on systematic variations in the iron content of chlorites of variable bulk composition. Their conclusions were that equilibrium Fe/(Fe+Mg) ratios in chlorite run products were a function of the ambient fS_2 and fO_2 conditions, and were independent of bulk charge compositions. The iron component in chlorite reacts with either sulphur or oxygen to leave chlorite that is enriched in Mg, e.g.

$$Fe_5Al_2Si_3O_{10}(OH)_8 \text{ (in Fe-Mg chlorite)} + 2{\cdot}5S_2 \Leftrightarrow Al_2SiO_5 + FeS \text{ (in pyrrhotite)} + 2SiO_2 + 2{\cdot}5O_2 + 4H_2O$$

and

$$Fe_5Al_2Si_3O_{10}(OH)_8 \text{ (in Fe-Mg chlorite)} + {}^5/_6O_2 \Leftrightarrow Al_2SiO_5 + {}^5/_3Fe3O4 + 2SiO_2 + 4H_2O$$

Using an ideal ionic solution model involving random mixing of Si and Al over six octahedral sites to calculate the chamosite ($Fe_5Al_2Si_3O_{10}(OH)_8$) component in chlorite, and their experimentally determined free energy data for this species, it is possible to calculate fS_2 and fO_2 for a given pressure and temperature.

Because the experiments were carried out in the temperature and pressures interval of 575–625°C and 2·0 to 6·0 kb, this model is directly applicable to medium and high grade metamorphic terrains containing the requisite mineral assemblage, where chlorite does not contain appreciable ferric iron, e.g. Bryndzia and Scott (1987a,

b). However, direct extrapolation of free energy data to the lower temperature and pressure conditions associated with ironstone lode formation and mineralisation is problematical, especially in view of Kranidiotis' suggestion that the non-conformity of Bryndzia and Scott's experimental data to the Al^{IV} vs temperature geothermometer of Cathelineau and Nieva (1985) may be due to the effect of pressure on Al^{IV}/Si substitution.

General principles of increasing chlorite $Fe^{\#}$ through oxidation and sulphidation determined from their experimental work led Bryndzia and Scott (1983) to suggest the chlorite zonation to increasingly magnesian compositions observed in the Juno ironstone lode was compatible with a trend of increasing fO_2; at odds with the zonation model of Large (1974, 1975) which was supported by Walshe (1986). Uncertainty in the extrapolation of thermodynamic data to lower temperatures and pressures suggest this model is not directly applicable to the Tennant Creek situation.

A variation on Bryndzia and Scott's (1987) model has been applied to the Hunt mine by Neall and Phillips (1987); in addition to the chamosite end-member of Bryndzia and Scott (1987a,b), the model uses two magnesian end-members $Mg_6Si_4O_{10}(OH)_8$ and $Mg_5Al_2Si_3O_{10}(OH)_8$ which correspond to Walshe's (1986) components 1 and 2 respectively. In their model ferrous iron mixes randomly on five of the six octahedral sites, while Mg and Al mix on all six sites. Mixing on the four tetrahedral sites is ignored.

Of the four isothermal, univariant mass action relationships used in this model to calculate fO_2 and fS_2, two involving magnetite rather than pyrrhotite, are applicable to the Tennant Creek ironstone lodes:

$$Mg_5Al_2Si_3O_{10}(OH)_8 + 3Fe_3O_4 + {}^{10}/_3SiO_2 + {}^{10}/_3H_2O \Leftrightarrow Fe_5Al_2Si_3O_{10}(OH)_8 + {}^{5}/_6Mg_6Si_4O_{10}(OH)_8 + {}^{5}/_6O_{2(g)}$$

$$Mg_5Al_2Si_3O_{10}(OH)_8 + {}^{5}/_2Fe_3O_4 + {}^{10}/_3SiO_2 + 5H_2S_{(aq)} \Leftrightarrow Fe_5Al_2Si_3O_{10}(OH)_8 + {}^{5}/_6Mg_6Si_4O_{10}(OH)_8 + {}^{5}/_2FeS_2 + {}^{5}/_3H_2O_{(l)}$$

The results determined are dependent on the applicability of the ionic solution model, experimental and theoretical determinations of logK for the reactions (taken from Walshe and Solomon, 1981), and assumptions regarding the pressure and temperature. Similar to the models Cathelineau and Nieva (1985) and Bryndzia and Scott (1987), ferric iron is assumed to be negligible in the calculation of structural formulae from probe analyses. Because this approach is essentially a cut down version of the Walshe (1986) model and uses thermodynamic data determined by Walshe and Solomon (1981) there is little difference in the predicted log fO_2 and log fH_2S between the models and therefore this approach will not be considered further.

Six Component Chlorite Solid Solution Model (Walshe)

The most ambitious chlorite model is that of Walshe and Solomon (1981) and Walshe (1986); this model calculates temperature, fO_2, fS_2, and H_2S content of the fluid during chlorite formation at a given pressure. In this model, the nonstoichiometry of chlorite is approximated by six thermodynamic components for which thermodynamic data have been estimated using compositional constraints provided by natural geothermal systems and well studied mineral deposits. The modelling of activity-composition relationships differs from that of Bryndzia and Scott (1987) in that the mixing of Si and Al in tetrahedral sites is considered in addition to the octahedral sites.

Two geothermometers have been calibrated:

$$2Mg_5Al_2Si_3O_{10}(OH)_8 + {}^{14}/_{3}SiO_2 + {}^{8}/_{3}H_2O \Leftrightarrow Al_4Si_4O_{10}(OH)_8 + {}^{10}/_{6}Mg_6Si_4O_{10}(OH)_8$$

and,

$$Mg_5Al_2Si_3O_{10}(OH)_8 + {}^{5}/_{7}Fe^{2+}{}_5Fe^{3+}{}_2Si_3O_{10}(OH)_8 + {}^{3}/_{7}Fe^{2+}Al_2Si_3O_{10}(OH)_8 + {}^{25}/_{21}SiO_2 \Leftrightarrow {}^{10}/_{7}Fe^{2+}{}_4Fe^{3+}Al_2Si_3O_{11}(OH)_7 + {}^{5}/_{6}Mg_6Si_4O_{10}(OH)_8 + {}^{5}/_{21}H_2O_{(l)}$$

which together with constraints provided by the Gibbs-Duhem equation allow calculation of the temperature of formation, and the ferric iron and water contents of chlorite coexisting with quartz and an aqueous phase at a known (or assumed) pressure, from probe data. The fO_2 may then be calculated from,

$$Fe^{2+}{}_5Al_2Si_3O_{10}(OH)_8 + {}^{1}/_{4}O_{2(g)} \Leftrightarrow Fe^{2+}{}_4Fe^{3+}Al_2Si_3O_{11}(OH)_7 + {}^{1}/_{2}H_2O_{(l)}$$

and similarly, fS_2 may be calculated where quartz and chlorite coexist with an iron sulphide. This then allows calculation of the H_2S content of the fluid.

Again as with the model of Bryndzia and Scott (1987a), the accuracy of solution mixing model, and the approximation of thermodynamic properties for the chlorite end-members are significant limiting factors in the accuracy of this model. Because the model determines water and ferric iron contents, assumptions regarding the ferric iron content used in the above models are not required.

The six-component chlorite model has been applied to several ore deposits, e.g. Walshe and Solomon (1981), Green et al. (1981), and Walshe (1986), but its recent application in the Tennant Creek area is of particular interest. Investigations of the mineralisation at White Devil mine (Nguyen, 1987, and Nguyen et al., 1990) and Eldorado mine (Horvath, 1988), using the chlorite model have produced temperatures

that are compatible with fluid inclusion results, while predictions of fO_2 and fS_2 are generally consistent with the observed mineral assemblages and trends in fluid evolution suggested by mineral parageneses and stable isotopes.

Predictions of the Conditions of Chlorite Formation

Before the application of any one of these models to the Warrego chlorite data, the factors limiting their use must be considered. Foremost in these models is the assumption of an equilibrium mineral assemblage involving chlorite, quartz and an alumino-silicate. Although chlorite coexists with muscovite in the immediate vicinity of the gold pod, chlorite is the dominant (and commonly only) silicate mineral associated with alteration of the sediments and ore parageneses. Within the altered sediments surrounding the ironstone lodes, quartz dissolution and removal from the system is obvious, and within the lode quartz is rarely associated with chlorite suggesting assumptions of quartz equilibrium used in the models of Walshe (1986), Bryndzia and Scott (1987a), and Neall and Phillips (1987) are not fulfilled.

This problem was evident in the non-solution of a significant proportion of chlorite analyses using the chlorite model of Walshe (1986). It was however, possible to apply a correction, such that analyses that would not solve at $aSiO_2 = 1$, were calculated at gradually reducing $aSiO_2$ until magnetite or hematite just reach saturation or become slightly undersaturated. The geothermometer of Cathelineau and Nieva (1985) does not specify a particular mineral assemblage, but chlorites from the Los Azufres geothermal system coexist with alumino-silicates (kaolinite, illite, or epidote) and compositions lie on the Al-saturated side of the chlorite solid solution field in Al-Mg-Fe space (Kranidiotis and MacLean, 1987). Compared to the chlorite solid solution field of Kranidiotis and MacLean (1987), the Warrego (and other Tennant Creek deposits) fall below the Al-saturation boundary suggesting temperatures determined by this geothermometer may be suspect.

Another common assumption in the chlorite models is that the ferric iron content of chlorite is relatively insignificant and can be ignored in the calculation of structural formulae. In Chapter Six, the ferric iron content of chlorite was approximated for Warrego and other Tennant Creek ironstone lode chlorites based on the relative depletion of octahedrally coordinated iron versus tetrahedrally coordinated iron. The results suggested that for TC8, Juno, Explorer 28, and the magnetite-chlorite assemblage at Warrego, that ferric iron contents exceeded 5% of total iron (Fig. 6.6), and therefore assumptions of insignificant ferric iron may not be appropriate.

The assumptions made regarding ideal solid solution mixing between chlorite end-members cannot be evaluated at this stage due to the relative lack of thermodynamic data on chlorite end-members. However the different approaches to modelling chlorite solid solution by Walshe (1986) which includes mixing of Si and Al

in tetrahedral and octahedral sites, and that of Bryndzia and Scott (1987a) and Neall and Phillips (1987) which only consider mixing on tetrahedral sites do not appear to be significant (Bryndzia and Scott, 1987a).

Temperature

Temperatures of chlorite formation were calculated for samples from the Warrego and Explorer 28 ironstone lodes using the geothermometers of Cathelineau and Nieva (1985), and Walshe (1986). The temperature ranges determined by the two geothermometers show a general correlation (Fig. 9.3), although there is a tendency in the Warrego samples for the geothermometer of Cathelineau and Nieva (1985) to predict a narrower range of temperatures that overlap with the higher end of the range predicted by the geothermometer of Walshe (1986). The majority of the Warrego temperatures from both models fall in the range 300°C to 350°C. Both geothermometers suggest similar temperature ranges for the magnetite-chlorite and magnetite-sulphide populations although both suggest a slightly higher temperature range for the magnetite-sulphide assemblage. The Explorer 28 probe analyses (and possibly also Juno), show a well defined trend of increasing $Fe^{\#}$ with Al^{IV} (reverse of the trend in Fig. 6.2), for which Kranidiotis and MacLean (1987) suggested a correction factor should be applied to the geothermometer of Cathelineau and Nieva (1985). The effect of this correction to the Explorer 28 data is to increase both the magnitude and spread of the calculated temperature range, such that temperatures no longer overlap, but are well in excess of the range predicted by the Walshe (1986). The corrected temperatures also exceed the range predicted for Warrego. The narrow range in Si contents of the Warrego chlorites and complete lack of correlation between Al^{IV} and $Fe^{\#}$ suggest it is not appropriate to apply the correction factor for these samples.

The range in temperature of chlorite formation predicted by the two geothermometers for Warrego are in accord with temperatures determined for other Tennant Creek ironstone lodes by other means described above. The range of fluid inclusion temperatures reported for the mineralised zones of Juno, TC8, Eldorado and Gecko ironstone lodes (Zaw et al., 1990) range from 230° to 440°C with a mode of 320°C in both gold-rich and copper-rich ore. This distribution mirrors the temperature distribution observed for chlorite temperatures from Warrego. In contrast Zaw et al. (1990) report fluid inclusion homogenisation temperatures in the range 200° to 250°C with a mode at 220°C for barren parts of the ironstone lodes; the barren Explorer 28 ironstone lode gives chlorite temperatures well in excess of this range.

To directly compare the results provided by the two chlorite geothermometers with alternative techniques of temperature determination, chlorites were analysed and temperatures calculated for a single gold-rich sample from the Juno mine (R27787 — Large, 1974), for which fluid inclusion homogenisation temperatures in quartz are also

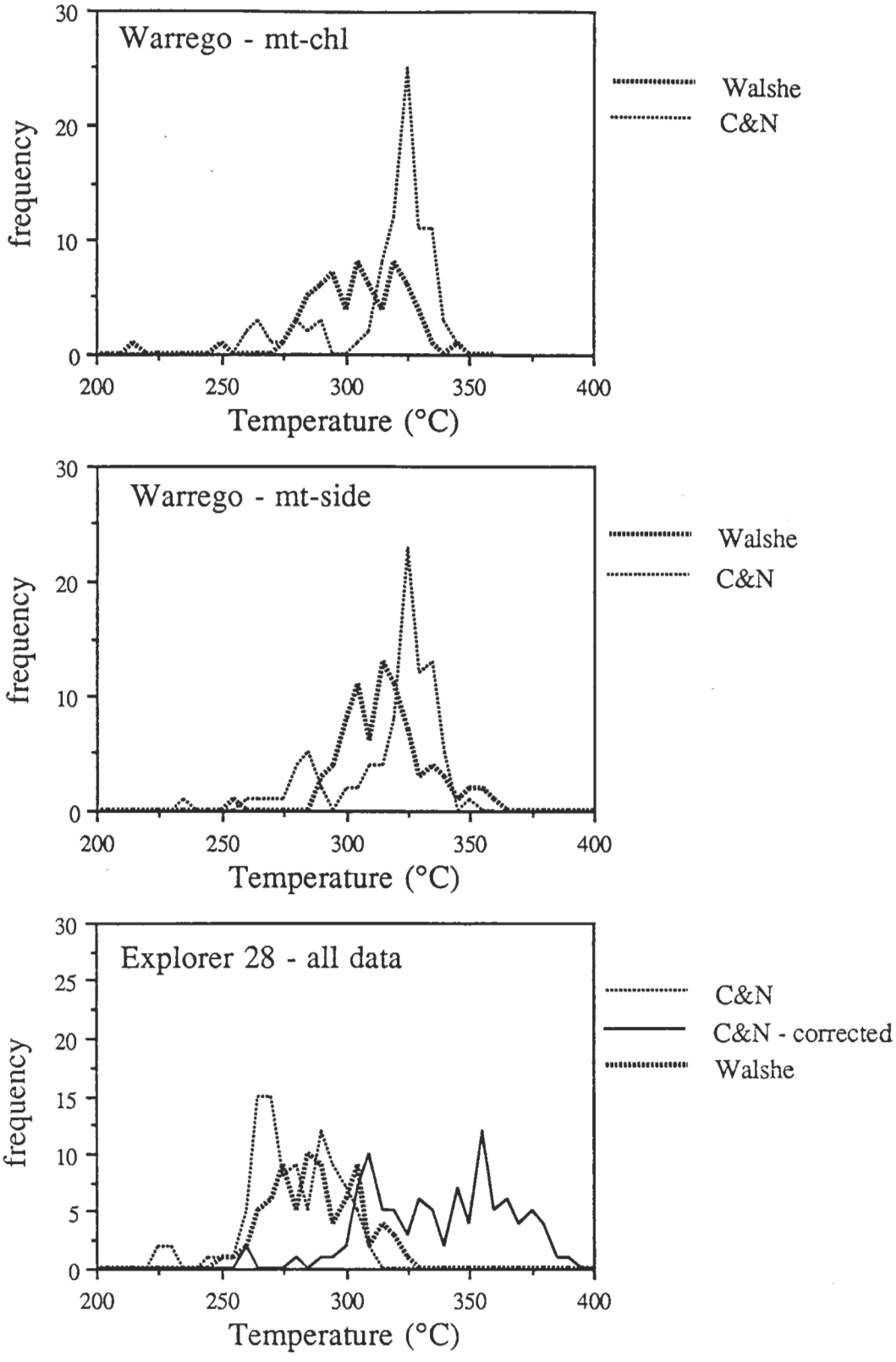

Figure 9.3 —Frequency diagrams comparing the range in temperature predicted by the chlorite geothermometers of Cathelineau and Nieva (1985), and Walshe (1986) for the magnetite-chlorite and magnetite-sulphide assemblages of the Warrego mine and the Explorer 28 prospect.

available (Zaw, 1987). To date, this is the only sample from a Tennant Creek ironstone lode for which this data is available. The results of this comparison are illustrated in Figure 9.4, and show that although there is good correlation in the temperature estimates between geothermometers (225–275°C), they are significantly lower than fluid inclusion estimates from the same sample. Application of the correction factor of Kranidiotis and MacLean (1987) to the Cathelineau and Nieva (1985) geothermometer increases the observed temperature range such that it overlaps with the low end of the fluid inclusion temperature range (300–350°C). Note that the fluid inclusion temperature range includes primary (300–375°C), secondary (100–175°C), and possible leaked inclusions(>400°C). The significance of these results is not presently understood and will require further comparison of the geothermometers with fluid inclusion evidence. The chlorite temperatures calculated for Juno are low compared to Warrego and it is uncertain if this difference is related to the Juno sample only, or that the chlorite geothermometers are underestimating actual temperatures of formation. Temperatures determined for the Explorer 28 prospect fall within the range of fluid inclusion temperatures measured for this and other barren deposits (Huston, 1990b), although falling at the high end of the range. The close overlap of the Warrego temperature data with those determined from fluid inclusions from other mineralised ironstone lodes, and predictions based on mineral assemblage and sulphur isotopes at Warrego tend to suggest the Warrego chlorite temperatures are probably a good estimate of actual temperatures.

Estimation of fO_2 and fS_2

The chlorite model of Walshe (1986) calculates the fO_2 and fS_2 conditions at the determined temperature of formation and the results are illustrated in Figure 9.5. Although the magnetite-chlorite and magnetite sulphide assemblages show a large degree of overlap, on average the general relationship between the two groups suggests that chlorites from the magnetite-sulphide assemblage formed at slightly higher temperature and fS_2 , and lower fO_2 and conditions. The Explorer 28 population overlaps with the bulk of the magnetite-chlorite analyses but extends to lower temperatures, fO_2, and fS_2. The predictions of the model that iron-rich chlorites denote high temperatures while magnesian chlorites indicate relatively oxidised conditions is in accord with empirical evidence (e.g. Albee, 1962; Bryndzia and Scott, 1983, 1987a,b; Cathelineau and Nieva, 1985; Shikazono and Kawahata, 1987; Yau et al., 1988; Wilde, et al., 1990). The range of fO_2 and fS_2 predicted by the chlorite model overlaps exactly with the mineralisation field in Figure 9.2 (300°C), and although none of the chlorites measured in the Warrego mine (with the exception of the late-stage post mineralisation forms not considered in this modelling), suggest equilibrium with pyrrhotite, the magnetite-sulphide assemblage

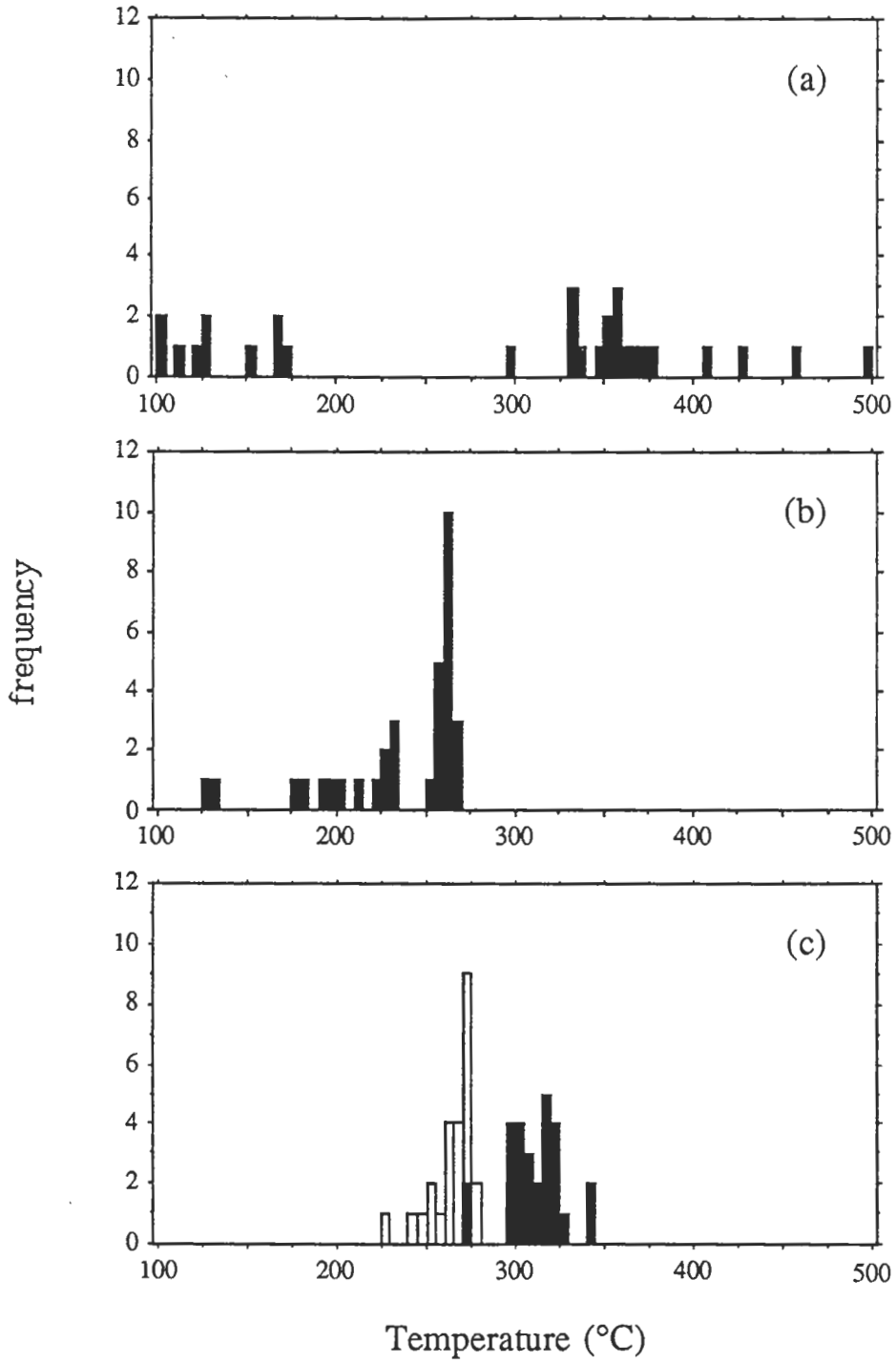

Figure 9.4 — Histogram comparing the range in temperature predicted by (a) fluid inclusions in quartz (Zaw, 1987), and the chlorite geothermometers of (b) Walshe (1986), and (c) Cathelineau and Nieva (1985), for corrected (filled symbol) and uncorrected (open symbol) data.

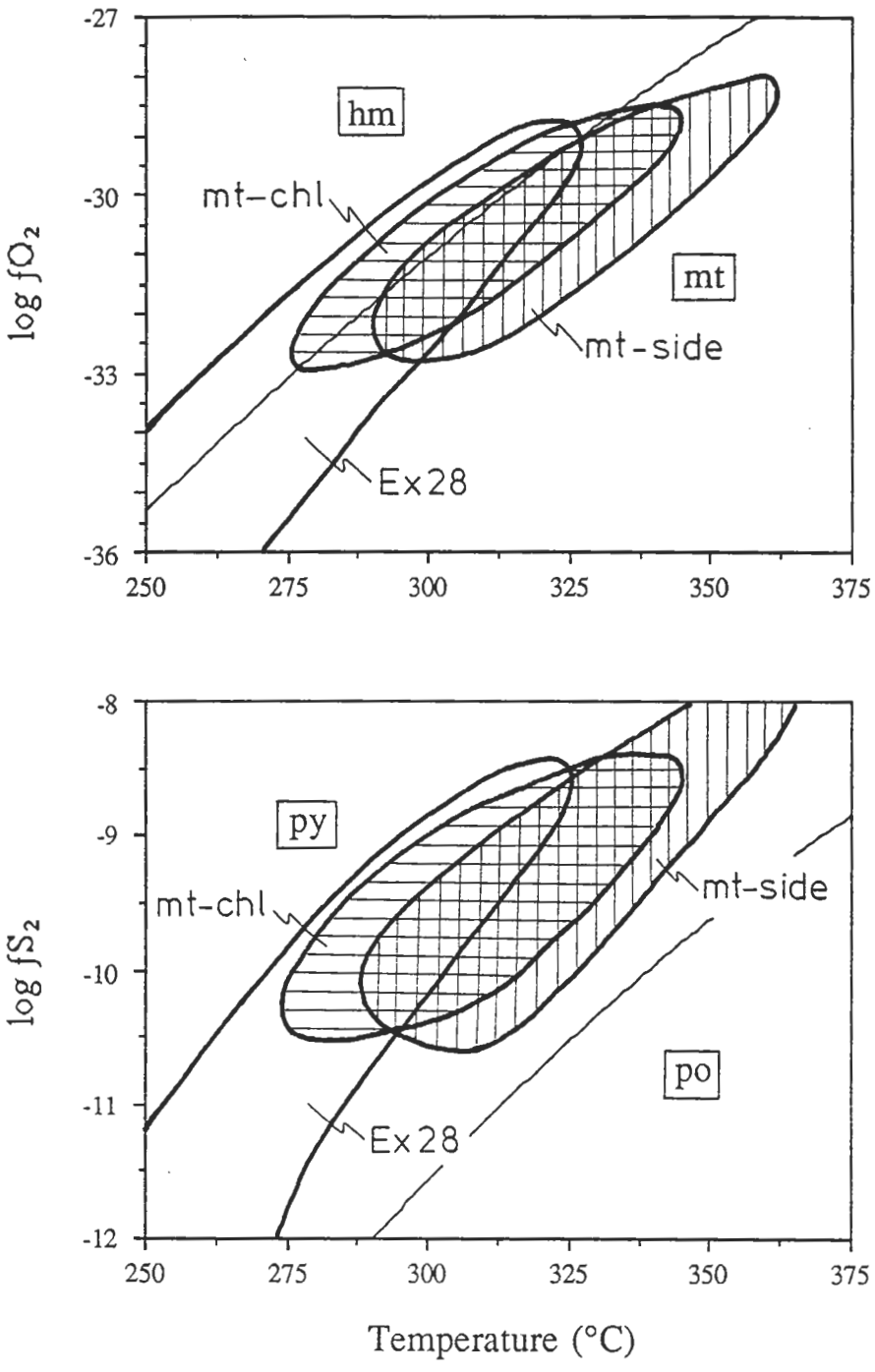

Figure 9.5 — Log fO_2–T and fS_2–T diagrams illustrating the range of fluid compositions in equilibrium with chlorites from the magnetite-chlorite and magnetite-sulphide assemblages of the Warrego mine and Explorer 28 prospect calculated by the Chlorite Model of Walshe (1986).

indicate conditions that were further removed from the magnetite-hematite buffer than the magnetite-chlorite assemblage.

Predictions that many of the Explorer 28 chlorites are in equilibrium with hematite are born out by the strong hematite alteration of the magnetite lode, and although there has not been any exhaustive examination of the petrography at Explorer 28, the magnetite lode has undergone strong deformation associated with quartz veining and alteration of magnetite to hematite suggesting that the lower temperature hematite-stable chlorites represent the late-stage alteration of the lode (Appendix H).

9.4 Variation of Physicochemical Conditions

Estimates of the conditions of mineralisation in the Warrego mine are made assuming an overall equilibrium mineral assemblage, when petrologic and geochemical examinations of the system indicate mineral zonation patterns that apparently form in response to physicochemical gradients. Two potential indicators of variability during ore deposition are the $\delta^{34}S$ and Se/S ratio of sulphide minerals which are both sensitive to changes in temperature, fO_2 and pH of the fluids during mineralisation.

$\delta^{34}S$

The determined value of $\delta^{34}S$ for a particular sulphide mineral is not only a function of the bond strength of the mineral and temperature at which it formed, but is also strongly dependant on the pH and fO_2 conditions prevailing during mineralisation (Ohmoto, 1972; Ohmoto and Rye, 1979). $\delta^{34}S_{H2S}$ varies markedly in response to changes in the relative proportions of oxidised and reduced sulphur species in solution, which are in turn influenced by temperature, pH, and fO_2. Therefore changes in the physicochemical conditions during mineralisation will be reflected in the $\delta^{34}S$ values determined for equilibrium sulphide assemblages.

Three general regions may be defined in terms of T–fO_2–pH space where characteristic patterns of ^{34}S variation are predicted (Fig. 9.6). Under relatively high temperature, low fO_2 and pH conditions (H_2S dominant), $\delta^{34}S$ of the sulphide minerals will be relatively constant, and minerals such as chalcopyrite where fractionation of ^{34}S relative to H_2S is negligible (Kajiwara and Krouse, 1971; Ohmoto and Rye, 1979) will directly reflect $\delta^{34}S_{fluid}$. In contrast under conditions of relatively low temperature and high fO_2 and pH ($SO_4^=$ dominant), $\delta^{34}S$ will also be relatively constant, but up to 20‰ lighter than $\delta^{34}S_{fluid}$. Mineralisation conditions in the immediate vicinity of the $SO_4^=/H_2S$ boundary will produce significant variations in the $\delta^{34}S$ of equilibrium sulphides for only minor fluctuations in physicochemical conditions (Fig. 9.6).

The well defined isotopic zonation in the Warrego mine shows a consistent pattern in which highest grades of mineralisation are correlated with lowest values of $\delta^{34}S$. The

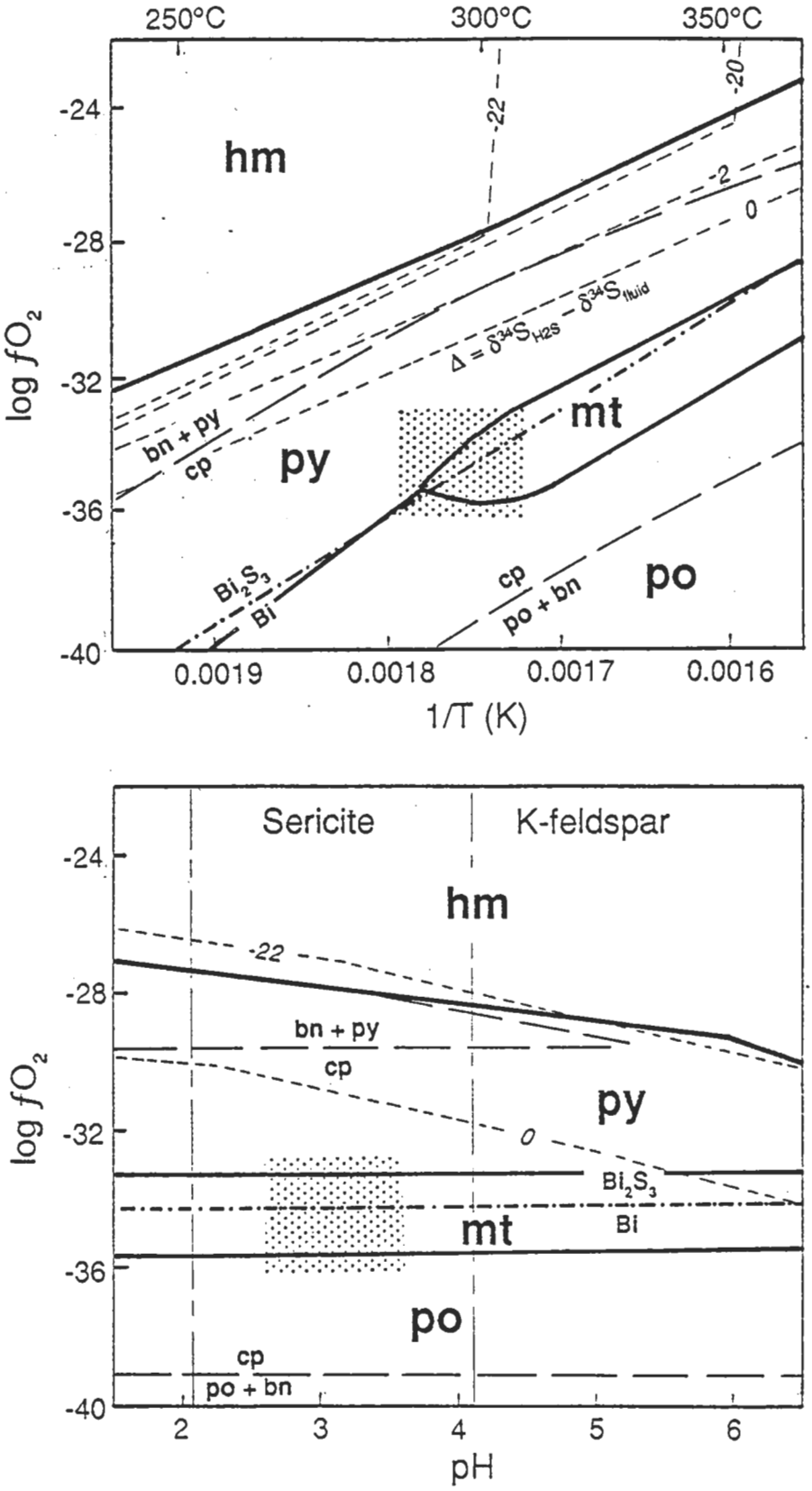

Figure 9.6 — Log fO_2–T and log fO_2-pH diagrams showing deviation of $\delta^{34}S_{cp}$ from $\delta^{34}S_{fluid}$ under equilibrium conditions. Mineral boundaries are for logΣS = –2.5m, mK$^+$ = 0.5 m, mNa$^+$ = 4.5, mCa^{2+} = 0.1 and mCl$^-$ = 5.0 m. Log fO_2–pH diagram is calculated for T = 300°C. Log fO_2–T diagram is calculated for pH = 3. The box represents mineralisation fluid conditions as defined in Figure 9.2.

outward increase in $\delta^{34}S$, albeit small, apparently signifies proximity to the boundary between oxidised and reduced sulphur species. However, the same isotopic zonation pattern from a core ~1‰ to the margin ~4‰ is observed in all four of the mine sections studied, irrespective of the grade or style of mineralisation. Copper mineralisation in the core of 8340N (3–4% Cu, <5g/t Au) has the same isotopic signature as gold-rich ore in section 8140N (>10 g/t Au, <1% Cu). These results are inconsistent with the evolution of a single ore fluid in the vicinity of the sulphate/sulphide boundary. Regardless of the control on gold and copper deposition, be it temperature, pH, fO_2, if both mineralisation styles were derived from the same fluid, one must have evolved relative to the other and should be evident in the isotopic composition of the sulphides. It is therefore suggested that the zonation pattern results from the overprinting of copper mineralisation by the gold pod assemblage. Interaction of a relatively light $\delta^{34}S$, gold-rich fluid with pre-existing copper orebody ~4‰ would be expected to produce the mixed (zoned) signature observed.

Selenium/Sulphur Ratio

In a manner analogous to sulphur isotopes, the solubility of selenium, and the stability of its complexes in solution is subject to physicochemical controls (temperature, pH, and fO_2) which influence the $\Sigma Se/\Sigma S$ of the hydrothermal fluid (Rosenfeld and Beath, 1964; Loftus-Hills and Solomon, 1967; Yamamoto, 1976; Auclair et al., 1987; Soler, 1987). Calculation of the variation in the ratio of S and Se with changing conditions allows construction of contours that are directly analogous with the variation of $\delta^{34}S_{H2S}$, although the boundary between oxidised and reduced selenium species occurs at higher fO_2 values than the equivalent sulphur species (Yamamoto, 1976; Shikazono, 1978). At relatively low pH and fO_2, i.e. within the predominance region of reduced aqueous selenium species, Se/S is low (log (Se/S) < ~–6), whereas the predominance region of oxidised aqueous selenium species at relatively high fO_2 and pH, Se/S is relatively high (log (Se/S) > ~–3). In both regions ratios are relatively constant. The transition zone between these two areas is marked by closely spaced Se/S contours suggesting that significant variations in Se/S may result from relatively minor changes in $\log fO_2$ and pH.

However, high selenium contents of sulphide minerals does not necessarily imply selenium is more soluble, or that less sulphur was available, because at higher temperatures more selenium can be incorporated into the structure of a particular sulphide mineral (Yamamoto, 1976). This is evident in the actively depositing hydrothermal vents on the East Pacific Rise (Auclair et al., 1987). Sulphides within the chimneys are buffered from seawater and formed at high temperature under relatively reduced conditions, yet display high Se/S (~0·003) compared to sulphides formed in the outer chimney environment where cooler and relatively oxidised fluid have low Se/S

(~0·00001). Selenium is also preferentially concentrated in some minerals, Rosenfeld and Beath (1964) indicate that selenium shows relative enrichment in sulphide minerals such that galena > chalcopyrite > sphalerite > pyrite. This sequence is the reverse of the relative fractionation of ^{34}S in sulphide minerals and suggests that selenium will show preferential concentration in sulphide minerals with weaker bond strengths. Therefore the high selenium content of bismuth-rich ores is in accord with the observed similarity in fractionation factors for ^{34}S in bismuthinite and galena (Ohmoto and Rye, 1979; Bente, 1982).

Variation in the selenium content of bismuthinite forms one of the best examples of zonation within the central gold pod (Chapter Six). The highest Se/S values occur within the gold-rich zone (0·3) and decrease across the magnetite-sulphide zone to background sedimentary ratios in the quartz-magnetite zone (0·00001). If the Se/S content in the bismuthinite directly reflects fluid compositions, the changing ratio of Se to S might be interpreted as the reduction of a fluid at the boundary between the stability fields of oxidised and reduced aqueous selenium complexes. However, it is suggested that this trend reflects the high temperatures of mineral deposition in association with the crystallisation of a bismuth-rich assemblage that is likely to concentrate selenium relative to sulphur.

Discussion

Both $\delta^{34}S$ and Se/S show a well developed zonation pattern in the Warrego orebody in which the highest gold grades in a section are correlated with low $\delta^{34}S$ and high Se/S. This pattern is repeated in other mines in the Tennant Creek area; e.g. Juno for both $\delta^{34}S$ and Se/S (Large, 1974,1975), and in $\delta^{34}S$ at Gecko and White Devil (Huston, 1989)[1]. In each example gold-rich mineralisation is associated with the low $\delta^{34}S$ values, where the overall range in values between gold- and copper-rich is generally less than 4‰. Although it seems somewhat fortuitous, each of the four mines studied displays the same pattern and general range in isotope values regardless of mineralogy, mineralisation style, or size.

Huston (1989) has suggested the sulphur isotope zonation is compatible with the reduction of an oxidised fluid by reaction with the magnetite lode, however the copper orebodies at Warrego contain abundant marcasite after pyrrhotite, and White Devil contains arsenopyrite (Huston, 1990b) and marcasite (after pyrrhotite?) (Nguyen, 1987; Nguyen et al., 1990) which are incompatible with this model. These mineral assemblages suggest that the sulphides were precipitated under reduced conditions and therefore $\delta^{34}S$ determined for chalcopyrite = $\delta^{34}S_{fluid}$. This is not only compatible with mineralogy in Warrego and White Devil, but also reflects the undifferentiated igneous source signature (0±5‰) common to virtually all pre-1·7 Ga sulphide mineral deposits

[1] No data on the selenium content of these mines has been reported.

(e.g. Eastoe, 1990). An oxidised environment of mineralisation implies a source isotope signature in the range 10 to 20‰, a range more characteristic of Phanerozoic mineralisation than that of the Early Proterozoic (e.g. Franklin et al., 1981; Eastoe, 1990).

Although the overprinting of copper by later gold mineralisation at Warrego is suggested, evidence of this in the other deposits is tenuous to say the least and it does not appear to be possible to apply a general model that satisfies each of the four deposits.

9.5 Metal Solubility

Using the constraints on the physicochemical conditions during ironstone lode formation and mineralisation outlined in the preceding section, it is possible to calculate the solubility of the various metals and minerals in solution using theoretical and experimentally derived data. Although this provides only a simplistic approximation of the actual conditions at the time of formation, these calculations are extremely useful in understanding the evolution of the system and identifying important controls in metal zonation and deposition. Because of the relative uncertainty in the conditions of ore formation, and inexact nature of thermodynamic data, activity coefficients of the dissolved components in solution have not been considered in this modelling.

The temperature and salinity of the solution determined from fluid inclusions, together with the mineral assemblage magnetite-chalcopyrite-pyrite-pyrrhotite-sericite-bismuthinite combine to restrict the conditions of mineralisation to a relatively small physicochemical range in terms of pH, temperature and $\log fO_2$ as illustrated in Figure 9.6.

Iron

Clearly any effort to understand the formation of the Tennant Creek ironstone lodes, must consider the probable controls of iron solubility in hydrothermal solutions. The stability relationships of the Fe–S–O system are well constrained in terms of fO_2, T, pH, and ΣS (e.g. Barnes and Kullerud, 1961), and experimentally derived data on the solubility of iron in this system is sufficient to model its variation in hydrothermal solutions. With the exception of very abnormal, highly oxidising hydrothermal systems, ferrous iron predominates over ferric in solution (Barnes, 1979), and chloride complexes appear to be the most important (Chou and Eugster, 1977; Crerar et al. 1978, Wood et al., 1987, McKibben and Williams, 1989). Thio- (Crerar and Barnes, 1976; Seward, 1977), and hydroxy- (Seward, 1977; Tremaine et al., 1977) species appear to be of little significance under the conditions of interest.

Figure 9.7 illustrates the solubility of iron in terms of the probable conditions of mineralisation as defined in Figure 9.6. The high solubility of iron indicated by these diagrams agrees with experimental (Whitney et al., 1985; Hemley et al., 1986) and fluid

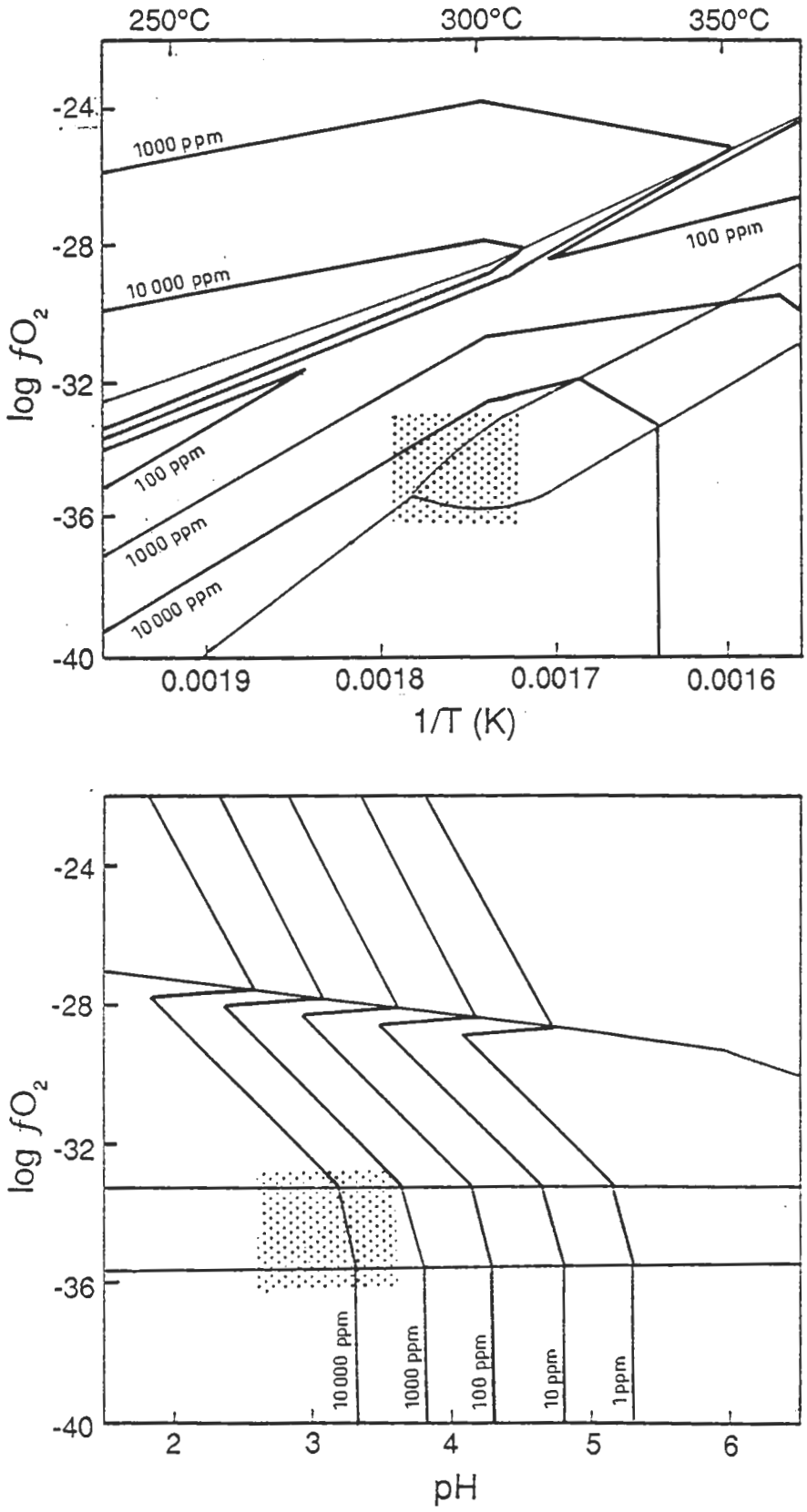

Figure 9.7 — The concentration of iron in solution in equilibrium with the mineral assemblages as defined in Figure 9.6.

inclusion (Kwak et al., 1986) evidence of iron solubility in high temperature and saline hydrothermal systems. Under the proposed conditions of mineralisation in the Warrego mine, iron complexes are relatively stable in solution and fluctuations in the pH of the fluid appears to exert the greatest control on magnetite solubility. Large fluctuations in the temperature and $\log fO_2$ of the solution are apparently ruled out by the relatively restricted stability of magnetite.

The conditions of ironstone lode formation are suggested to have been lower temperature with lower sulphur content in the fluid, and therefore the conditions depicted in Figure 9.7 are inappropriate to model this mineralisation stage. The result of changing these parameters will be to reduce the stability field of pyrite such that coexisting hematite and magnetite is compatible, and total iron solubility is reduced. However, the most effective control on deposition of iron from solution will be through increasing pH and to a lesser extent an increase in fO_2.

Copper

The solubility of copper under the probable conditions of mineralisation at Tennant Creek has been calculated as the cuprous chloride complex (Crerar and Barnes, 1978). The calculated solubility of copper chloride is illustrated in Figure 9.8, and suggests that Cu concentrations in solution are of the order of ~100 ppm. An order of magnitude change in the solubility of copper can be achieved through a 1 unit increase in pH, or a drop in temperature in the order of 20–30°C. Changes in the fO_2 of solution are unlikely to have any effect unless conditions are at or near the HSO_4^-/H_2S predominance boundary where solubility contours are very close together.

Gold

The solubility of gold has recently been discussed by Huston and Large (1989) in which they define a switchover line between predominantly bisulphide and chloride transport of gold. They suggest that in relatively oxidised, high temperature systems (e.g. Tennant Creek and porphyry copper deposits) gold will be transported in solution as a chloride complex, while in moderate to low temperature, low salinity deposits gold transport occurs as the bisulphide species. Figure 9.9 illustrates the relative solubility of the $Au(HS)_2^-$ and $AuCl_2^-$, and clearly demonstrates the dominance of the chloride ligand under the inferred conditions of Warrego mineralisation. However, similar to copper, contour intervals are relatively widely spaced and deposition through destabilisation of gold complexes in solution is only likely to occur with a significant decrease in fO_2 accompanied by increasing pH and/or decreasing temperature.

The importance of other gold complexes in hydrothermal fluids cannot at present be evaluated due to the absence of thermodynamic data although several potential ligands are suggested in the literature e.g. $Au_2S_2^=$, $Au(CN)_2^-$ and AuHS (Seward, 1990).

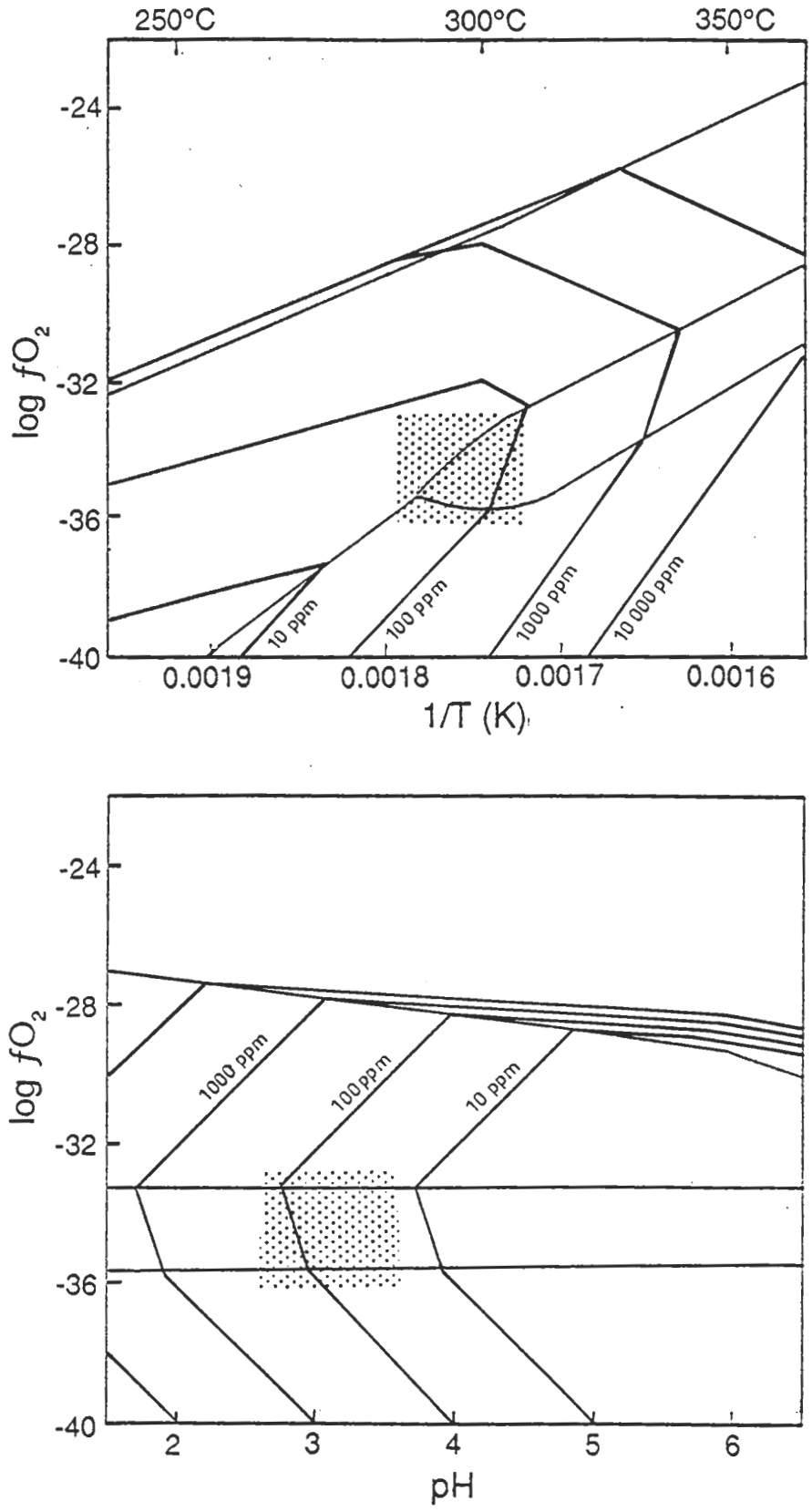

Figure 9.8 — The concentration of copper in solution in equilibrium with the mineral assemblages as defined in Figure 9.6.

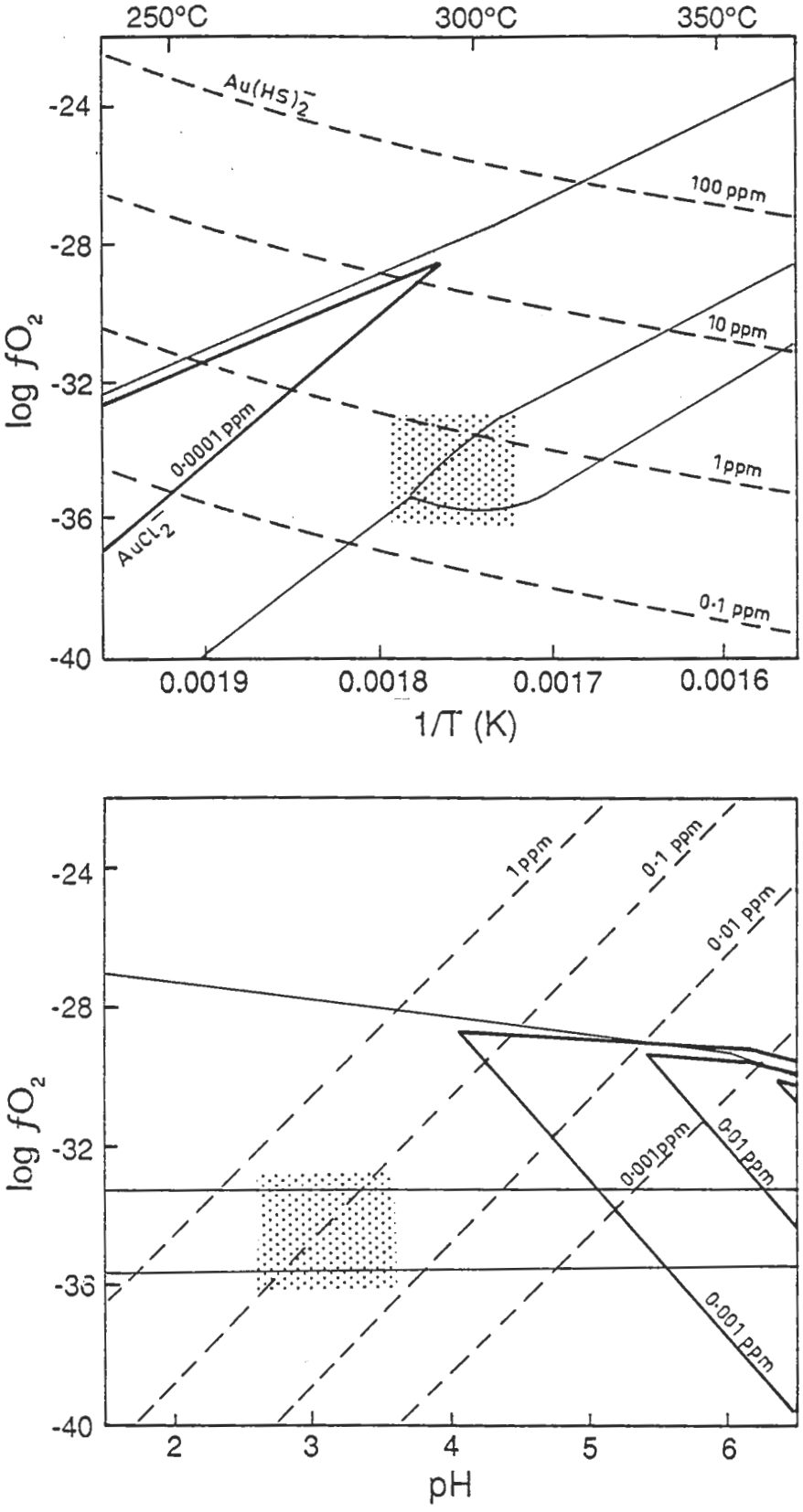

Figure 9.9 — The concentration of gold in solution in equilibrium with the mineral assemblages as defined in Figure 9.6.

Selenium is another possible gold complex in the Tennant Creek environment; Seward (1990) suggests that the stability of gold-halide complexes increase down the periodic table with increasing ionic radius and polarisability, such that AuI_2^- is ten orders of magnitude more stable than $AuCl_2^-$. Assuming similar behaviour for Group VIA elements, selenium and tellurium appear to be attractive candidates to form gold complexes where they form significant components in the ore fluid. Although tellurides are rare in the Warrego mine, seleniferous bismuth sulphosalts spatially associated with gold mineralisation are abundant. Again there is no thermodynamic data available to assess the potential of selenium as a significant transporter of gold in solution.

9.6 Quartz Solubility

Quartz is an important component in the mineral zonation patterns observed in Warrego and many of the other mineralised ironstone lodes where quartz-magnetite forms a barren outer shell to the lode. The sympathetic distribution of quartz-magnetite relative to the overall metal zonation patterns suggest that a major portion of the quartz has been deposited in response to the same physicochemical conditions associated with economic mineralisation.

To better constrain the probable style of silica deposition in the Warrego ironstone lode, the relationship of quartz to the overall zonation of the ironstone body and chemistry of mineralising solutions is considered. Quartz is virtually absent from the zones of stringer mineralisation and intense chloritisation in the footwall of the Warrego lode; it is only a minor phase associated with gold pod mineralisation, but increases in abundance through the copper mineralisation (<20%), and becomes dominant in the quartz-magnetite zone proper.

Quartz mineralisation is divided into two stages based on the paragenesis in the ironstone lode; an early phase associated with ironstone lode formation and a later stage related to mineralisation. Quartz associated with ironstone lode formation is observed as the complex, often colloform, intergrowth of magnetite and quartz at the outer margins of the lode. These textures indicate deposition of quartz (and magnetite), from solutions supersaturated with respect to quartz. Rock alteration by acidic solutions during ironstone lode formation are likely to promote such conditions (Fournier, 1985), and the evidence of extensive quartz leaching from the altered rocks adjacent to the lodes is probably indicative of such conditions. Deposition of quartz and magnetite from solution may be related to dilution through mixing with fluids in the sediment pile. Although difficult to quantify, the enveloping nature of the quartz-magnetite zone about the mineralised core in the Warrego and Peko mines can be interpreted as the 'reaction front' between the mineralising solutions and adjacent fluids in the sediment pile (Chapter Six).

The often knife-sharp boundaries against adjacent wallrocks imply a channelway for fluid flow that draws fluids into it from the margins rather than the pervasive

movement of fluids into the adjacent sediments where broad alteration haloes and disseminated mineralisation would be expected. Conditions across such a mixing zone might initially be expected to have a steep temperature gradient — conditions ideal to promote the deposition of quartz and amorphous silica from solutions saturated or supersaturated with respect to silica. The common association of colloform magnetite with quartz in the lodes (Chapter Six), supports a model involving initial deposition of quartz as amorphous silica because temperature and pH are also likely to have controlled the deposition of amorphous iron oxides. The formation of a fairly continuous quartz-magnetite shell is likely to have acted as a cap that effectively seals the system from further fluid ingress and therefore stabilised the physicochemical environment preventing the further deposition of amorphous iron oxides and silica..

Quartz associated with mineralisation is spatially associated with primary quartz-magnetite, but typically occurs as cross-cutting veins. At the temperatures and pressures likely at the time of mineralisation (300–400°C, 0·5–1.5 kbar) quartz is highly soluble, and solubility will be further enhanced by the high salinity (Fournier, 1983) and low pH (Kamiya et al., 1974; Weres et al., 1982) of solutions. The increasing abundance of quartz towards the margins of the lode implies a physical and/or chemical gradient for which the most likely components are temperature, pressure, and possibly also pH and salinity. Temperature would probably be controlled by dilution as changes in temperature resulting from cooling on the geothermal gradient will be no more than a few degrees over the distances involved (<100 m), and conduction to the cooler host rocks is also likely to be negligible.

The pH of solutions will also be controlled by dilution, and reaction with the wallrocks (including the lode), but as there is no evidence for a pH gradient in the mineral zonation of the Warrego mine it is unlikely pH has played a role in the deposition of silica. Other deposits in the Tennant Creek field show mineral zonation of muscovite-chlorite-talc-dolomite, e.g. Juno mine (Large, 1974,1975), TC8 mine (Large et al., 1988), and Argo mine (Mead, 1986), which has been attributed to a pH gradient through the lodes (Large, 1974, 1975) . Significantly both Juno and Argo mines contain only minor quartz in their gangue mineral assemblage, and thus despite a probable gradient of increasing pH across the lodes, there has been little deposition of quartz associated with it. Therefore it is unlikely that pH is an important parameter controlling the deposition of quartz in the Tennant Creek ironstone lodes.

Another possible control on the deposition of silica is through the reduction of pressure which again is unlikely to result from normal crustal gradients, but more likely to result from fluid assisted fracturing of the rocks. It is suggested that much of the quartz is deposited as a result of reductions in pressure associated with fracturing of the lode.

9.7 Fluid Unmixing

In all of the fluid inclusion studies undertaken to date in the Tennant Creek goldfield, one characteristic of the inclusions associated with mineralisation stands out. That is, the coexistence of variably filled inclusions (inclusions homogenise to liquid or vapour), with erratic salinities (Zaw, 1987, 1988; Huston, 1989, 1990a, b; Zaw et al., 1990). These results have been interpreted to suggest heterogeneous trapping of multiphase fluids in which a gas-rich phase (e.g. CO_2, N_2) has been exsolved from the metal bearing brine, or mixing of two fluids, one gas-rich and the other salt-rich (Zaw, 1988). Because of the wide range in salinities (~30 wt. % NaCl equiv.), Zaw (1988) suggested boiling or simple cooling trends (increasing salinity with cooling and constant salinity with cooling respectively), were incompatible with the available data. Zaw (1988) suggests the unmixing may result from the the transition from lithostatic to hydrostatic pressures and that this was likely to contribute to the deposition of gold.

The close association of fluid inclusion evidence of heterogeneous trapping with gold mineralisation in four of the mines in the Tennant Creek area (Juno, TC8, Gecko, and White Devil) strongly supports the premise that this relationship is not purely fortuitous, but related to ironstone lode formation and mineralisation. It is suggested that fracturing of the ironstone lode associated with the introduction of mineralisation resulted in a drop in pressure and evolution of the gas-rich phase.

9.8 Discussion of Conditions of Ore Formation

The probable conditions of ore formation at Warrego and other Tennant Creek ironstone lodes seem to be relatively well constrained. The process of ironstone lode formation and mineralisation is separated into two distinct events, i.e. ironstone lode formation followed by economic mineralisation. However, the relationship between the gold pods and copper orebodies does not appear to signify a simple model of fluid evolution resulting from interaction with the lode.

The character of mineralisation in the copper orebodies and the gold pods is distinctive, and apparently contradictory in their relationships and mineral assemblages. The copper orebodies contain pyrrhotite and iron-rich chlorite that signify higher temperatures and sulphur contents compared to the magnesian-rich chlorite gold pod assemblage. Although hematite appears to be no more, or less prevalent in either the gold or copper mineralisation at Warrego, and there is no evidence of a direct spatial association of hematite and gold (Plate XI), the chlorite model suggests that fluid conditions were close to (or straddled) the magnetite-hematite buffer similar to the interpretations of Wall and Valenta (1990) and Huston (1990b). However, the evolution of a fluid from at or near hematite stability in the gold pod, to pyrrhotite stable through reaction with the magnetite lode is patently untenable. Similarly the relationship of the overall gold pod assemblage with the surrounding halo of barren quartz magnetite (Fig.

5.7) appear to overprint the more pervasive copper mineralisation style observed in the upper copper orebodies. In addition, the pyrrhotite mineralisation in the copper orebodies has been oxidised by some late stage event that is considered part of the overall mineralisation because the pyrite/marcasite assemblage (after pyrrhotite) has been overgrown by pyrite.

Thus the relationship between the copper orebodies and gold pods at Warrego suggest an overprint of a reduced copper-rich assemblage by later, relatively oxidised, gold pod-style mineralisation. The evolution from copper to gold appears to be related to an increase in fO_2 as is observed in the oxidation of pyrrhotite, and mineral associations suggesting relatively oxidised conditions, e.g. elevated U (Wilde et al., 1990). However, fO_2 conditions associated with gold mineralisation is not considered to have crossed the boundary from the predominance field of reduced to oxidised sulphur species.

The mineral solubility diagrams (Figs. 9.7 to 9.9) calculated for iron, copper and gold do not define conditions where mineral deposition is likely to be achieved rapidly through relatively small changes in the conditions of temperature, fO_2 and/or pH. In each case, to produce an order of magnitude drop in metal solubility, an increase in pH by one unit, a drop in temperature of up to 100°C, or a decrease in fO_2 by up to 4 units is required. Although the relative magnitude of changes in chemistry, temperature or pressure required to produce the zonation documented in the lode is unknown, the overall range in sulphur isotope ratios (mixing or no mixing) is small and the significant variation in physicochemical conditions required to promote metal deposition does not appear to have occurred.

The intimate association of gold mineralisation with the ironstone lodes indicate the deposition of gold is linked to a 'reaction' between the lode and mineralising solutions. In virtually all of the documented mines at Tennant Creek, gold is concentrated at the base of the ironstone lode where mineralisation may either wrap around the lode as at TC8 (Wedekind et al., 1990) and many of the smaller near-surface mines (Ivanac, 1954), or may spread through the lode following fractures. Mineralisation fills open space veins within the immediate footwall and fractures in the lode and there is little evidence of alteration or fluid interaction with the lode or adjacent sediments (Chapter Six).

The ironstone lode is obviously the factor controlling mineralisation within the Warramunga Group, having acted as either a chemical or structural trap. Chemical models relating gold deposition to various reactions between the fluid and the lode (e.g. Wedekind et al., 1990; Wall, and Valenta, 1990; Huston, 1990b) can define appropriate changes in the chemistry of the system to promote gold deposition from solution, but the lack of obvious alteration suggesting reaction between the lode and the fluids suggest that it is the physical properties of the lodes that has localised mineralisation. The

ironstone lode represents a rigid block within the relatively ductile chloritic alteration halo, and deformation associated with mineralisation has fractured and brecciated the lode. Pressure release associated with such fracturing is suggested to result in the observed heterogeneous fluid inclusion population, and is likely to have promoted mineral deposition.

The efficiency of boiling as a mechanism of metal deposition is well documented in the epithermal environment (e.g. Drummond and Ohmoto, 1985; Reed, and Spycher, 1986; Spycher and Reed, 1989). Boiling will induce an abrupt decrease in temperature, increase in pH (through CO_2 exsolution), and destabilise sulphides and perturb the oxidation state (H_2S exsolution). Various mineral assemblages may be established depending on the saturation or non-saturation of a particular metal in solution. Where all metals in solution are saturated, Drummond and Ohmoto (1985) predict the following paragenesis in response to boiling:

magnetite $\Rightarrow$ sphalerite $\Rightarrow$ silver $\Rightarrow$ gold (as a chloride)

$\Rightarrow$ chalcopyrite (if $\sum Cu > \sum Fe$)

Such a mechanism might explain the general absence of chalcopyrite associated with the gold pods, although undersaturation in zinc (which is plausible because of its extremely high solubilities in the Tennant Creek fluids) and silver is required. Similarly the general absence of quartz with mineralisation may be explained by its markedly different behaviour compared to metals during boiling. The weight ratio of quartz to metal deposited varies from 1 at 350°C to ~ 30 at 200°C (Drummond and Ohmoto, 1985).

Thus boiling or volatile exsolution associated with mineralisation in Tennant Creek ore deposits is consistent with petrographic relationships, but sequential deposition of native metals and sulphides may at least in part explain some of the zonation patterns observed in the orebodies.

Chapter Ten

SUMMARY AND MODEL OF FORMATION

10.1 Introduction

In this chapter an attempt is made to draw together the results presented in the preceding chapters and to provide a model for the formation of, and controls on, mineralisation in the Warrego ironstone lode. Through a better understanding of the Warrego system it is hoped further exploration in the Tennant Creek goldfield can be better targeted, and the results obtained in drilling of prospects better interpreted.

10.2 Depositional Environment

The sediments of the Black Eye Member of the Warramunga Group in the vicinity of the Warrego mine do not appear to differ significantly from those observed elsewhere in the goldfield. The immature, poorly sorted greywack-shale observed in the mine sequence appears on average to be finer grained than similar sequences in the southeast of the goldfield (lacking the coarse greywacke units evident there), and this relationship is consistent with interpretations of a sedimentary basin deepening to the west with sediments sourced from the east (e.g. Crohn and Oldershaw, 1965; Norris, 1980; Edwards, 1987; Rattenbury 1990b). The quartz and quartz-feldspar porphyries observed in the Warrego sequence can similarly be linked to the stratigraphic porphyry units in the central and southeastern part of the goldfield, and their recent reinterpretation as shallow intrusions into wet unlithified sediments (McPhie, 1990) is consistent with observations of the textures within the porphyry and its contact relationships with the sediments at Warrego.

The Warrego porphyries are chemically very similar to the sediments, early granites, and porphyries elsewhere in the goldfield (Duncan, 1970; Wyborn et al., 1987; Blake and Page 1988; Stoltz 1990) and a close affinity between them is inferred. Trace element chemistry defines two sediment populations within the Warrego sequence. The total lack of mixing between them and the preservation of magmatic fractionation trends indicate two distinct volcanic sources for the sediments, with sediment deposition occurring as instantaneous events associated with slumping of recently erupted volcanic material into the basin.

An overall interpretation of the geological setting of the Warramunga Group is of a central igneous core (Tennant Creek Granite) surrounded by time equivalent subaerial to shallow marine sediments and volcanics (Bernborough Formation) which grade laterally into deeper water volcanogenic marine sediments (Warramunga Group). The sediments are derived from massive submarine slumping of the proximal volcanic apron, and have been intruded by porphyry sills while still wet and unlithified.

10.3 Time Constraints

Limited Rb/Sr, U/Pb, and Sm/Nd dating in the Tennant Creek Inlier (Black, 1977, 1984; Black and McCulloch, 1984; Blake and Page, 1988; Page 1988) is barely sufficient to constrain the relative time-frame for deposition, deformation and mineralisation of the Warramunga Group. Deposition of the Warramunga Group (~1870 Ma) appears to have been consanguineous with intrusion of the Tennant Creek Granite, which probably represents a sub-volcanic source for the volcanism and volcanic-derived sediments in the basin. This period of granite intrusion, basin formation and associated deformation is related to the Barramundi Orogeny, a northern Australia-wide orogenetic event (Etheridge et al., 1987).

The general localisation of ironstone lodes within the plane of cleavage, and the conflicting timing relationships between the two indicate that ironstone lode formation accompanied folding of the Warramunga Group during the Barramundi Orogeny (Rattenbury, 1989b). Economic mineralisation has consistently been dated at 1810 Ma (Black, 1977, 1984), which would indicate a considerable hiatus between the formation of the ironstone lodes and the subsequent introduction of economic mineralisation. However, the recording of a similar reset Rb/Sr age from the Tennant Creek Granite (Black, 1977, 1984) suggests that the 1810 Ma event is not restricted to mineralisation, but represents a major tectonothermal event throughout the goldfield. Because this time frame coincides with volcanism in the overlying Hatches Creek Group, Wall and Valenta (1990) have suggested that this event is related to reactivation of Barramundi structures during the regional folding of the younger rocks.

However, unlike Wall and Valenta (1990), rather than the reactivation of Barramundi structures corresponding to the time of mineralisation, it is suggested that this is a subsequent event that has reset primary mineralisation ages; especially in the highly susceptible hydrothermally altered rocks. The strong evidence for a link between folding of the Warramunga Group and ironstone lode formation together with fluid inclusion and stable isotopic evidence that the fluids associated with this and subsequent mineralisation were very similar, suggests that the two events were temporally related and preceded the subsequent tectonothermal event.

Stoltz (1990) has suggested that the anomalous trace element chemistry and close proximity of the Warrego Granite to mineralisation make it the most likely source for metals and hydrothermal fluids at Warrego mine. Although the Rb/Sr age of the Warrego Granite is considerably younger than the mineralisation age, he states there is sufficient doubt in the reliability of this age for his proposal to be considered further.

However, there is abundant evidence from within the Warrego mine that the intrusion of the Warrego Granite has post-dated mineralisation and therefore cannot be related paragenetically to either ironstone lode formation or mineralisation. Key observations confirming this relationship include:

1. Porphyroblasts of biotite, cordierite and andalusite that have grown in response to contact metamorphism associated with the intrusion of the Warrego Granite are essentially static, i.e. they overgrow the cleavage foliation which has clearly controlled the orientation and localisation of the ironstone lode.
2. The distribution of the contact metamorphic mineral assemblages (especially andalusite) is restricted to areas of hydrothermal alteration where obviously the modified bulk chemistry of the rocks is favourable for the growth of metamorphic minerals. The existence of pre-existing chlorite (→ cordierite and biotite) and intense chlorite-muscovite (→ andalusite) alteration assemblages was therefore an essential precursor to the contact metamorphic mineral growth.
3. Quartz in both the sediments and the ironstone lodes have been recrystallised by the contact metamorphism.
4. The ~1690 Ma event is real. Localised resetting of Rb/Sr and Pb/Pb ages within and adjacent to the Warrego ironstone lode (Black, 1977, 1984; Dean et al., 1988) to those determined for the Warrego Granite suggests that the two events are related.
5. A young age for the Warrego Granite (<1810Ma.) is supported by stratigraphic relationships. The Warrego Granite intrudes the Tomkinson Creek Beds which are considered the equivalent of the Hatches Creek Group.
6. Stable isotopes determinations from chlorite, quartz and muscovite (D/H and $^{18}O/^{16}O$), define two distinct alteration types. Alteration associated with ironstone lode formation and mineralisation has an ambiguous signature that might include seawater, metamorphic water or formation water as the source of the hydrothermal fluids. However, barren quartz-muscovite-K feldspar 'greisen' veins which cross-cut the ironstone lode and mineralisation have an unmistakable magmatic signature. Furthermore, isotopic temperatures determined from these veins are higher than those determined for alteration, consistent with a direct magmatic link.

Certainly there is a need for further age dating to more closely constrain the ages of volcanism, granite intrusion, and mineralisation. Without precise U-Pb age determin-

ations the unequivocal establishment of timing relationships is unlikely (see Section 10.11).

10.4 Shape and Orientation of the Ironstone Lodes

The Warrego ironstone lodes are generally ellipsoidal in shape forming flattened pipes that plunge 45° to the southeast. The ironstone lodes are localised at or near the lower contact of the east dipping quartz porphyry, and as such represent a relatively rare example among Tennant Creek ironstone lodes where the attitude is sub-parallel to, rather than cross-cutting of, the stratigraphy. Overall the ironstone lode is transgressive of the stratigraphy and an epigenetic paragenesis is indicated. The quartz porphyry/ sediment contact is suggested as the controlling factor in the localisation of the lode.

The unusual plunging attitude of the ironstone lode, and exceptional orientation of bedding and cleavage in the Warrego area when compared to the rest of the goldfield, suggest that the orientation of the lode and immediately surrounding sediments has been modified from the typical regional attitudes. It is possible to restore the ironstone lode to an attitude such that it is horizontal, and aligned east-west with the footwall alteration zone localised at the base of the lode via a simple 90° rotation. Bedding and cleavage are also restored to a regional orientation by this rotation. It is suggested that the intrusion of the Warrego Granite has resulted in the rotation of a block of adjacent sediments to produce the unusual attitude observed today.

A marked lineation defined by the north and south extensions of the No. 3 and No. 1 orebodies respectively, parallels the cleavage orientation, and corresponds to an apparent offset in the lower contact of the quartz porphyry. The interpretation of a reverse fault in this position is consistent with either faulting of the porphyry during folding, or late-stage movement associated with intrusion of the Warrego Granite and movement on the Footwall Fault. It is therefore possible to suggest a model whereby the offset between the lodes was (a) controlled by a pre-existing structure, or (b) the subsequent offset of a once continuous lode. Because there is no evidence of fragmentation of the lodes in the proposed position of faulting, stringer mineralisation wraps around the lower No.1 ironstone lode, and the lodes are joined by a narrow neck of massive magnetite, a model where the formation of the ironstone lode was localised by an already offset porphyry is preferred. The development of this fault is suggested to have localised hydrothermal fluid flow during ironstone lode formation. Subsequent minor reactivation of the fault during rotation and flattening of the ironstone lode during intrusion of the Warrego Granite is also indicated.

10.5 Alteration

Alteration of the sediments adjacent to the ironstone lodes has been examined in some detail in an attempt to clarify the process of ironstone lode formation, and to indicate some wider target that may be of assistance to mineral exploration. Major and trace element analyses of samples from the lode and adjacent sediments define an outer alteration halo that is consistent with the chloritisation of the sediment through the breakdown and replacement of feldspar and muscovite. This zone is defined by depletion in mobile elements such as Ba and K, and the addition of Fe and Mg. Comparison of more strongly altered examples from this zone with the least altered sediments suggest modest volume increases, which is compatible with the observation of quartz, chalcopyrite, magnetite, and chlorite veining. The margins of this outer alteration zone corresponds to the Footwall Fault in the west, and the footwall contact of the quartz porphyry in the east. Although the hangingwall contact of the porphyry is strongly altered, the intervening porphyry and overlying sediments are not altered beyond mild chloritisation of the matrix.

The width of an inner intense alteration zone varies from less than a metre in the hangingwall of the ironstone lode, to 40 m in the immediate footwall of the gold pods. This narrow margin of intense alteration may contain greater than 90% magnetite and chlorite, but is still recognised as altered sediment by the coherent ratios of immobile trace elements compared to unaltered sediment. Calculated volume changes associated with this alteration are minimal; falling within normal sedimentary variation, and near isovolumetric replacement of the sediment is indicated. Similarly in the stringer zone in the immediate footwall of the gold pod, calculated volume changes are small (~25%) and only minor open space filling is implied.

Within the ironstone lode immobile trace elements are generally at, or near their detection limits and coherent behaviour cannot be demonstrated. However, one sample from the gold pod showed immobile trace element abundances that were intermediate between the sediment and general ironstone values. Calculated volume changes are significant with an increase of the order of 70%. This result is consistent with strong brecciation of the ironstone lode associated with the introduction of economic mineralisation, yet the coherent behaviour of immobile trace elements still support a near isovolumetric replacement model for the formation of the ironstone lode.

While barren magnetite stringers in the footwall (assumed to be related to ironstone lode formation), show textures consistent with at least partial replacement of the sediment, mineralised stringers comprising magnetite, chlorite, and muscovite are seen to occupy fractures within the sediment without significant adjacent alteration. This observation is consistent with textures in the magnetite-sulphide and quartz-magnetite zones, where mineralisation has occurred by open space infilling and is associated with a significant volume increase. Thus the process of ironstone lode formation appears to

have occurred in large part through isovolumetric replacement, while economic mineralisation occurs as open space filling of the lode. Modelling of trace element behaviour indicates that lode formation cannot occur totally by replacement, and either some mobility of the immobile trace elements and/or open space filling is required.

Oxygen and hydrogen isotope analysis of chlorites from the sediments surrounding the Warrego and Explorer 28 ironstone lodes failed to detect an enhanced alteration halo surrounding the lode, as has been evidenced in alteration studies of other ore deposit types, e.g. Criss et al. (1985). Strong depletion in δD and $\delta^{18}O$ is recorded only in the most intensely altered sediment adjacent to the ironstone lode and therefore provides no greater target for exploration than existed previously.

However, because the oxygen and hydrogen isotopic determinations are largely made from pure mineral separates of a single hydrothermal alteration mineral (i.e. chlorite), each analysis may be taken to reflect the ratio of the fluid. Significantly two zones are delineated; an internal depleted zone corresponding to the most intensely altered rocks immediately adjacent to the ironstone lode, and a broader outer zone where there is pervasive chloritisation of the sediments. Therefore two fluids are implied, one 'exotic' and related to ironstone lode formation, while the other is more widespread in extent, and probably related to regional alteration. The mixing of these two fluids could therefore be extremely important in controlling the deposition of iron oxides to form the ironstone lode.

10.6 Zonation within the Ironstone Lode

In spite of the rotation and contact metamorphism of the ironstone lodes, many primary zonation features are preserved without significant modification. In many respects the central gold pod at Warrego duplicates mineralogical and trace element zonation patterns identified in the Juno mine (Large, 1974, 1975). At Warrego the zonation is asymmetrical, reflecting the acute angle between the footwall, and the orientation of cleavage and stringer mineralisation. Metals in the Warrego gold pods show the same zonation from gold to bismuth to copper, but rather than the partially overlapping shells observed at Juno, the Warrego ore zones completely overlap. Although high-grade gold mineralisation forms a central core surrounded by a high-grade bismuth zone similar to Juno, the copper ore is considerably more extensive, and marginal to the gold pods is enriched in gold. Trace element zonation across the gold pod is complicated by the channelised flow of hydrothermal fluids within the ironstone lode, but generally there is the same bismuth sulphosalt zonation as observed at Juno with decreasing selenium and increasing lead with distance from the footwall. Gangue mineral zonation from chlorite-muscovite in the gold pod through minor chlorite associated with the magnetite-sulphide assemblage to quartz in the outer quartz magnetite zone does not show the same evolution to talc and dolomite assemblages observed in Juno.

Although the relationship of the gold pods to the rest of the ironstone lode appears to be transitional, e.g. elevated gold in adjacent chalcopyrite mineralisation and decreasing gold fineness, in detail the transition from the gold pod mineralisation to magnetite sulphide is abrupt and an overprinting relationship is suggested. Strong development of a quartz magnetite zone surrounding the gold pods, oxidation of pyrrhotite in the magnetite-sulphide assemblage, different chlorite compositions in the two assemblages and sulphur isotopic zonation that is apparently derived from mixing all suggest that the gold pod mineralisation is a relatively late-stage overprint of copper-rich mineralisation.

10.7 Constraints on Mineralisation Conditions

Much of the information regarding physical conditions of mineralisation at Warrego comes from fluid inclusion studies of other Tennant Creek ironstone lodes (Zaw, 1987, 1988; Huston, 1989, 1990a, 1990b; Zaw et al., 1990). Consistent results between the mines suggest that ironstone lode formation was associated with moderate temperature (~250°C), saline fluids (15 to >25 equiv. wt. % NaCl), while economic mineralisation was associated with high temperature (>300°C) saline fluids (15 to >25 equiv. wt. % NaCl). These results are compatible with mineralogic relationships within the Warrego ironstone lode, possible primary sulphur isotope temperatures, and application of chlorite geothermometers. Fluid inclusion relationships in all samples associated with economic mineralisation throughout the goldfield consistently indicate heterogeneous trapping which has been suggested as resulting from the exsolution of a gas-rich phase from a saline brine (Zaw, 1987).

Chemical constraints on mineralisation provided by the mineral assemblage magnetite–chalcopyrite–bismuthinite–sericite–pyrrhotite, and the chlorite model (Walshe, 1986), suggest that ironstone lode formation occurred under conditions of $\Sigma S \sim 0{\cdot}0001m$, $\log fO_2 = -34$ to -36, $\log fS_2 = -12$ to -14 and pH = 3 to 4, while economic mineralisation occurred under conditions of $\Sigma S \sim 0{\cdot}003m$, $\log fO_2 = -30$ to -34, $\log fS_2 = -9$ to -12 and pH ~ 3. Under these conditions, the calculated solubilities of the metals gold, copper, and iron are high, and metal complexes in solution are relatively stable. Significant fluctuations in pH, fO_2 and temperature are required to cause an order of magnitude change in the concentration of metals in solution.

Although elegant equations may be written to produce the desired shifts in chemical conditions likely to promote metal deposition, e.g. Wedekind et al. (1990) and Huston (1990b), these models are far from robust and fail to account for the single most important feature of gold mineralisation at Tennant Creek. Bonanza gold mineralisation is localised in fractures at the immediate footwall contact of the ironstone lode where there is little or no evidence of fluid reaction with the magnetite. It is suggested here that

the fluid unmixing observed in fluid inclusions from all of the mines studied to date is not merely fortuitous, but is related to the competency contrast between the ironstone lode and adjacent sediments. Brittle fracturing of the ironstone lode during deformation is likely to have resulted in instantaneous pressure release, gas separation, and metal deposition in a manner akin to boiling in epithermal systems.

10.8 Source of Metals and Fluids

Many different sources for the ore components and fluids at Tennant Creek have been suggested during the history of investigation: (a) magmatic sources in the form of the mafic intrusives (Whittle, 1966; Dunnet and Harding, 1967) and granites (Woolnough, 1936; Ivanac, 1954; Crohn and Oldershaw, 1965; Stoltz, 1990) and (b) leaching of metals from the sediments (Elliston, 1966; Large 1974, 1975). Possible indicators that may assist in the interpretation of the metal and fluid source are lead isotopes and stable isotopes (sulphur, oxygen, and hydrogen). Additional data pertaining to the dimensions of the system may also be provided through the modelling of trace element abundances in the host rocks and the solubility of metals in solution.

Lead Isotopes

A collaborative study between the University of Tasmania, C.S.I.R.O. and Geopeko was undertaken to characterise the lead isotopic signature of barren and mineralised ironstone lodes at Tennant Creek for possible application in exploration (Gulson et al., 1988). The initial results of this programme were promising with the mineralised ironstone lodes (Juno, Peko, Argo, Gecko, and Orlando) displaying a very limited range in $^{208}Pb/^{204}Pb$ and $^{206}Pb/^{204}Pb$. However, problems with the general application of this technique were encountered with the Warrego ironstone lode for which only a small proportion of the samples display the ore signature (Fig. 10.1), and the general inability of the technique to distinguish between ironstone lodes containing economic, and sub-economic concentrations of ore mineralisation.

Despite this outcome, the results of this (Gulson et al., 1988), and subsequent studies (Dean et al., 1988), may be used to gain an insight into the process of ironstone lode formation and possible sources of the ore components. The isotopic homogeneity displayed by the mineralised ore deposits is characteristic of ore deposits in general, and is commonly taken to indicate the existence of a large, long acting hydrothermal system in which any isotopic variation in the source region has been homogenised during solution, transport, and deposition (Gulson, 1986). Although isotopic inhomogeneity may indicate a relatively small hydrothermal system, the extreme variation in the

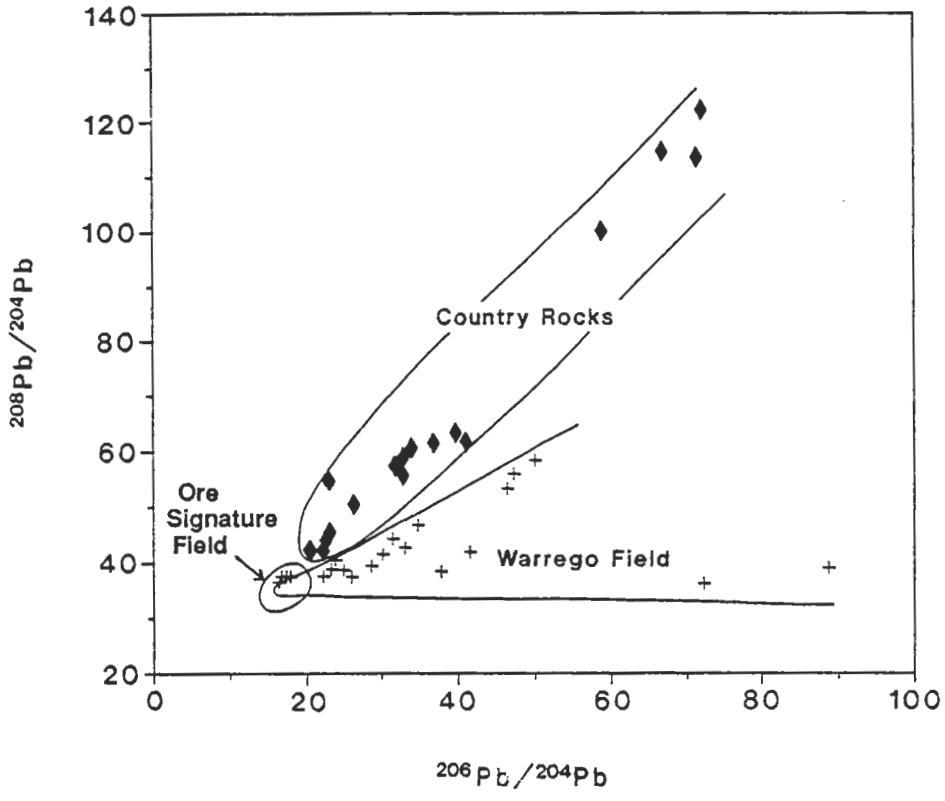

Figure 10.1 — Lead isotope data for Tennant Creek ironstone lodes and country rocks on a thorium derived lead isotope plot of $^{208}Pb/^{204}Pb$ vs $^{206}Pb/^{204}Pb$. The Warrego field (+) shows minor overlap with the tight ore signature field, but is dominated by strong shifts related to radiogenic decay of uranium and thorium. The country rock field is derived from analyses of Warramunga Group sediments, porphyries and granites (diamonds). The range observed in barren ironstone lodes overlaps with the country rock range. (Data from Gulson et al., 1988.)

Warrego samples appears to be related to the lead content of the lodes (Gulson et al., 1988). The Warrego ironstone lode is lead-poor compared to the other mineralised lodes (<40 ppm compared to >300 ppm in analysed samples), and therefore radiogenic decay (since the time of mineralisation), of ^{232}Th and ^{238}U to ^{208}Pb and ^{206}Pb respectively, has affected the overall isotopic ratios of the lode. In contrast, the other relatively lead-rich lodes contain insignificant radiogenic lead compared to the total, and isotopic ratios are unaffected.

The country rock data illustrated in Figure 10.1 define a linear array which is consistent with radiogenic decay (and hence age) of rocks that contained variable absolute contents of U, Th, and Pb, but a similar (~crustal) Th/U ratio (Gulson et al., 1988). This range overlaps with that of the barren ironstone lodes and is taken to indicate that they were formed from relatively small sized hydrothermal systems that preserved the isotopic variation of the source rock. The intersection of the source rock array with the ore signature may be interpreted as evidence of a genetic affiliation (Gulson, 1986), and implies lead in the Tennant Creek mineralised systems is derived through leaching of the Warramunga Group. However, because the country rock array includes samples from the porphyry and the Tennant Creek Granite, a magmatic source cannot be ruled out.

Stable Isotopes

Sulphur: The use of sulphur isotopes to characterise the source of sulphur must be used with caution in view of the considerable fractionation that may occur between the fluid and mineral depending on the chemical conditions (Ohmoto, 1972; Ohmoto and Rye, 1979). In the case of Warrego, the sulphur isotopic signature falls within a very narrow range that is close to zero, and as mineralisation is interpreted to have occurred under relatively reduced conditions, fractionation between the fluid and sulphide minerals will have been minimal. The suggestion that the isotopic zonation observed in the Warrego ore results from mixing does not alter this interpretation markedly, the two fluids do not appear to have been significantly different from each other, and therefore a similar sulphur source is implicated.

Narrow ranges in the isotopic composition at or near 0‰ indicate a magmatic sulphur source which is compatible with most pre 1.7 Ga sulphur isotope data (Eastoe et al., 1990). The magmatic source may imply sulphur derived directly from a de-volatilising melt, but more likely represents leaching of sulphur from detrital magmatic sulphides in the sediment pile. Although sulphides within the Warramunga Group sediments are rare, modelling (see below) suggests that even at very low contents there would be sufficient sulphur available through leaching of the sediments.

Oxygen and Hydrogen Isotopes: The isotopic composition of the ore fluid was discussed in Chapter Eight where it was suggested that the total database for the Tennant

Creek ironstone lodes indicated they were formed through the circulation of formation waters. The observed separation of barren from mineralised ironstone lodes is suggested to have resulted from the mixing of the fluid with a magmatic or metamorphic component, or more likely, the higher temperatures (~100°C) associated with the economic mineralisation.

Not only are the barren and mineralised ironstone lodes separated from each other in terms of oxygen and hydrogen isotopes, but also individual mines are distinctive; Juno, Argo and TC8 mines all have higher δD and $\delta^{18}O$ values than the Warrego mine. Within a given sedimentary basin, the isotopic composition of the hottest and most saline fluids also have the highest $\delta^{18}O$ values (Taylor, 1979), which may indicate different physicochemical conditions were associated with the formation of these deposits. This observation is supported by differences in gangue and ore mineralogy observed within these deposits. Warrego displays a relatively simple gangue zonation compared to the other deposits where talc and/or carbonate alteration halos surrounding the lodes are an important component.

Trace Element Abundances

To evaluate the possible contribution of trace and minor elements via leaching of the Warramunga Group sediments, the abundance of gold, copper, bismuth, silver, and iron in the Warrego and Juno orebodies is compared with values measured (or likely) in the host sediments (Table IX). The Warrego and Juno orebodies were selected because of their contrasting sizes and mineralisation styles, and their relatively complete production records. The gold-rich and copper-poor Juno orebody was virtually mined out, and therefore production figures should reasonably represent the true metal content of the lode. Similarly, ore reserve figures for unmined mineralisation together with production figures for the gold- and copper-rich Warrego mine should also provide a reasonable estimate of total element abundances.

Table IX — Trace and major element contents of Warrego and Juno mines, and the Warramunga Group sediments.

	WARREGO (g)	JUNO (g)	W. GP SEDS (g/t)
Au	$5{\cdot}75 \times 10^{7}$	$2{\cdot}4 \times 10^{7}$	$2{\cdot}0 \times 10^{-3}$
Cu	$1{\cdot}84 \times 10^{11}$	$1{\cdot}5 \times 10^{9}$	10
Bi	$2{\cdot}2 \times 10^{10}$	$2{\cdot}3 \times 10^{9}$	0·5
Ag	$-3{\cdot}0 \times 10^{6}$	0·05	
S	$2{\cdot}0 \times 10^{11}$	$2{\cdot}0 \times 10^{9}$	7
Fe	$6{\cdot}7 \times 10^{12}$	$7{\cdot}2 \times 10^{11}$	$1{\cdot}4 \times 10^{4}$

Elemental abundances in the two orebodies were determined from production and reserve figures for Au, Cu, Bi, and Ag; the S content is that required to balance Cu and Bi as chalcopyrite and bismuthinite (guanajuatite for Juno) respectively, plus an assumption that pyrite constitutes 10% of the sulphide ore. Iron was calculated from the approximate mass of ironstone lode hosting each orebody in which magnetite constitutes ~50% of the total volume. Abundances of trace metals in sediments adjacent to the Warrego ironstone lodes are (with the exception of Cu) below their detection limits (see Appendix C), and values for Bi and Ag used in this analysis are average sediment abundances taken from Heinrichs et al. (1980), and Vincent and Frueth (1972) respectively. Several low level gold analyses ranging from below detection (<0.001 ppm) to a high of 0.069 ppm are available for relatively unaltered Warramunga Group sediments (Large and Robinson, 1987, and this study). This range is similar to that recorded for greywacke by Boyle (1979) and an average value of 0.002 ppm has been used in this modelling. A similar value has been reported for Warramunga Group sediments by Stoltz (1990). The calculated iron content of the Warramunga Group sediments assumes that the only source of iron available for leaching by hydrothermal fluids is the disseminated magnetite which typically constitutes 2–3 volume per cent.

All analyses of the sulphur content of Warramunga Group sediments are essentially at or below the limit of detection by XRF analysis (e.g. Wyborn, 1971; Large, 1974; Mead, 1986), and therefore provide only an approximation of the upper limit of sulphur concentration. While sulphur contents reported for sedimentary rocks are typically in the order of several hundred ppm (e.g. Rose et al., 1979), the abundance of magnetite within the Warramunga Group without sulphides or associated sulphidation suggests average sulphur contents are likely to be much lower than the sediment norm. The value selected for sulphur in Table IX was chosen to maintain the proportions of copper and sulphur as chalcopyrite.

Table IX and Figure 10.2 illustrate that both inter-element ratios, and the enrichment of major and trace elements in the two ore bodies relative to the sediments differ markedly. Such variation may be controlled by any number of factors including the relative concentrations of these elements in the source rocks, processes of metal mobilisation into solution, saturation or non-saturation of the element in solution, and efficiency of metal deposition, e.g. Huston and Large, 1987. However, the suggestion that gold and bismuth mineralisation at Warrego is a late-stage overprint of pre-existing copper mineralisation may explain some of the differences in relative metal abundances in the two mines. Although production records and ore reserve calculations for the Warrego mine do not distinguish between the gold pod proper and the gold-rich magnetite-sulphide ore marginal to it, the overall dimensions of the central gold pod at

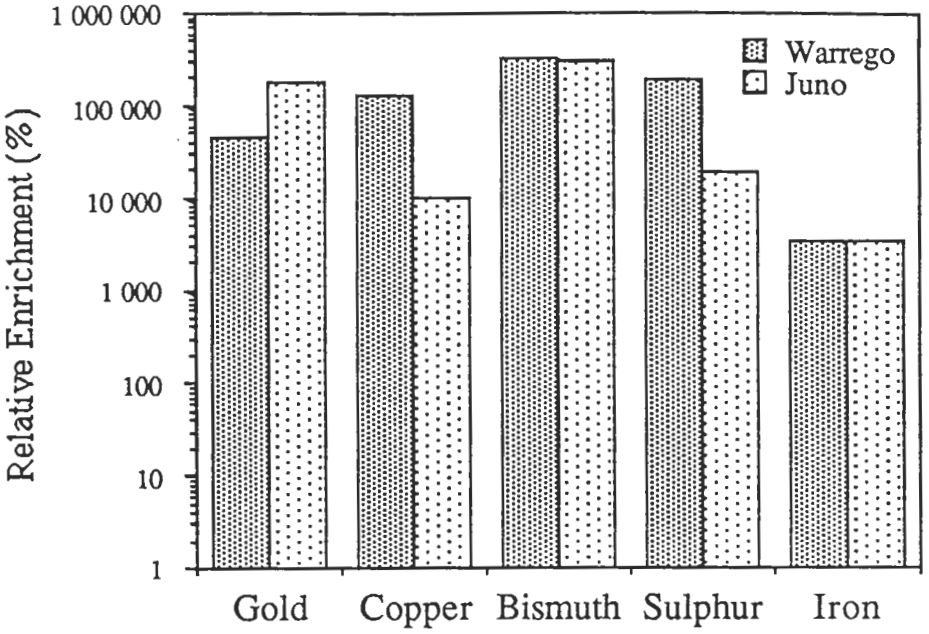

Figure 10.2 — Relative enrichment of the Warrego and Juno ironstone lodes in selected major and trace elements compared to the Warramunga Group sediments.

Warrego is similar to those of the Juno lode, and it is suggested that the two are more comparable. Re-evaluation of the Warrego ore resource to maximise gold production following the fall in copper price in 1975 resulted in a proven resource of 474,000 t @ 31·12 g/t Au, 2·22% Cu, and 0·57% Bi (Le Messurier and Bujtor, 1975, unpublished company report), which while still reflecting the gold-rich copper ore adjacent to the gold pods, shows a trend to the gold-rich compositions of the Juno mine.

If all the elements constituting the mineralisation in the ironstone lodes were sourced via leaching of the Warramunga Group sediments, the minimum volume of rock that must have been leached to produce the observed abundances in the Warrego and Juno ore bodies may be readily calculated. Estimates as to the efficiency of the leaching and deposition of metals in hydrothermal systems are varied ranging from 50% (e.g. Kerrich and Fryer, 1979) to 0·01% (Cumming et al., 1982). The minimum volume of rock required to produce the metal contents of the Warrego and Juno mines (i.e. 100% efficiency of leaching and deposition) is presented in Table X, and the volume of rock required for 10% efficiency is illustrated in Figure 10.3 as a cone of leaching beneath the lode.

It is apparent in both orebodies that the volume of rock required to produce the ironstone lode is significantly less than that for the mineralisation. However, as is illustrated below, even under the high iron solubility conditions calculated, a significantly larger volume of rock is required to produce the fluid required for ironstone lode formation.

Table X — Calculated minimum volume of sediments (km^3) leached at 100% efficiency to produce Warrego and Juno orebodies.

	WARREGO	JUNO
Au	2·4	1·1
Cu	7·0	0.1
Bi	16·0	1.7
Ag	–	0.02
S	0·2	0·002
Fe	0.16	0.02

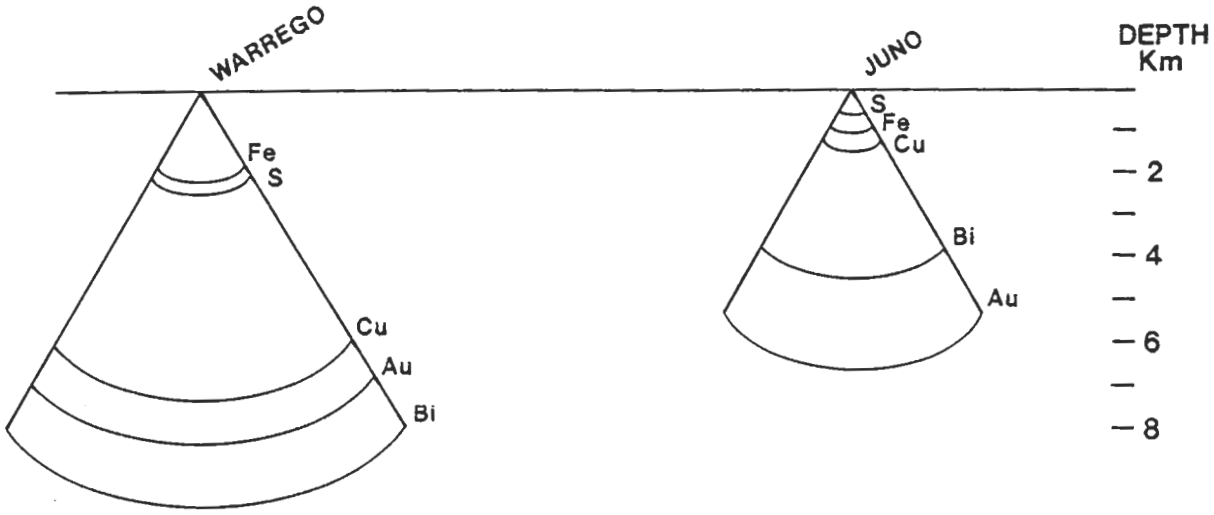

Figure 10.3 — Leaching cone models to illustrate the relative volumes of Warramunga Group sediments that must have been leached to produce the ironstone lodes and economic mineralisation observed in the Warrego and Juno orebodies. Leaching in this model assumes 10% efficiency.

Hydrothermal Fluids and Source Volumes

Similar to the method used above to determine the dimensions of the hydrothermal system, modelling using the known metal content of the lodes, calculated metal solubilities (Chapter Nine), and an assumed rock porosity of 20% may be used to determine source volumes. The assumption regarding the pre-metamorphic porosity of the Warramunga Group sediments seems valid based on the measured porosities in sedimentary basins up to depths of 5 km (Hanor, 1979). The calculated mass of fluid required to transport key metals constituting the Warrego ironstone lodes and likely volume of the source rocks presented in Table XI assumes 100% efficiency of transport and deposition and that the fluids under consideration are formation waters. Fluids derived from metamorphic devolatilisation (~2 wt. % H_2O in metasediments), or evolved during magma crystallisation would require considerably larger volumes of source rock.

Comparison of these results with those calculated from the trace metal abundances in the sediments reveal a close similarity in calculated source volume for gold and copper, but quite dissimilar values for iron. The correlation of the gold and copper values are encouraging, they suggest that the calculated solubilities for these metals are reasonable estimates of the actual conditions, but in the case of iron, either the solubility has been radically underestimated, or is too low to totally leach the sediments with the calculated volume of fluid. The absence of extensively leached zones immediately beneath the ironstone lodes as evidenced in drilling or magnetometer surveys is in accord with the latter interpretation.

Using Elders Rule (Elder, 1977; Cathles, 1981), it has also been possible to determine the volume of an intrusion that would be required to circulate the calculated mass of hydrothermal fluid (Table XI). Elders Rule states that the total mass of hydrothermal fluid circulated is approximately equal to the mass of the heat source and therefore using iron as an example, an intrusion with the dimensions 200 x 700 x 600 m would be required to circulate the hydrothermal fluid. Although this is only a minimum estimate, these dimensions are similar to those of the porphyry in the immediate mine environment.

Discussion

Despite rigourous examination of the potential source of metals contained within the ironstone lodes, because the Warramunga Group sediments are largely derived from the reworking of recently erupted volcanic material, it is virtually impossible to distinguish between source models involving leaching of the sediments and/or a direct magmatic contribution. However, because oxygen and hydrogen isotope studies of the Warrego and other Tennant Creek ironstone lodes suggest that the hydrothermal fluids are formation waters (± a magmatic component), a leaching model is preferred. In addition, because there is little difference between the isotopic signature of the fluids involved in

Table XI — Constraints on the mass of fluid and volume of sediments within the Warrego hydrothermal system.

	Metals in Warrego mine (g)	Concentration in solution (ppm)	Minimum mass of fluid required to transport (g)	Volume of sediment required to source fluid (km^3)*	Volume of heat source required to circulate hydrothermal fluid (km^3)**
Au	5.75×10^7	0.1	5.75×10^{14}	2.87	0.22
Cu	1.84×10^{11}	100	1.84×10^{15}	9.20	0.69
Fe	6.70×10^{12}	10,000	6.70×10^{14}	3.35	0.25

* The volume of sediment required to produce the mass of water has been calculated assuming a rock porosity of 20%.
** Assumes the heat source is granite with a density of 2.65 g/cc.

ironstone lode formation and mineralisation, the fluids in these two stages are considered to be essentially the same, and an evolutionary model from lode formation to mineralisation is preferred.

The variable lead isotope signature of individual barren ironstone lodes probably reflects local compositional variation within the Warramunga Group whereas, the mineralised systems display an overall similarity that suggests a much larger system in which compositional variations have been homogenised. These results are compatible with an evolutionary model where the localised mobilisation and concentration of formation waters results in the formation of the ironstone lode. It seems likely that this stage is associated with early folding of the Warramunga Group that was probably initiated by granite intrusion.

The trend to higher temperatures during economic mineralisation, suggests that the fluids have been heated; the establishment of large scale hydrothermal convection cells associated with the intrusion of granite higher into the stratigraphy would seem to be the most likely mechanism by which this has occurred. Not only would the granites act as a heat engine increasing the temperature, expanding the hydrothermal system and possibly changing the chemistry of the fluids, intrusion is likely to have fractured and 'opened' the lodes through the reactivation of the structures that originally localised the ironstone lodes.

Calculations of the volume of sediment required to produce either the metals that make up the Warrego ironstone lode, or the fluid that transported them, suggest that at 100% efficiency with sequential extraction (i.e iron, then copper, then gold/bismuth), at least 16 km^3 is required. However, because leaching, transport and deposition is unlikely to have been this efficient, and an expanding system seem probable, source

volumes in the order of hundreds of cubic kilometres are required. Expressed as a leaching cone below the ironstone lode,160 km3 (Bi in Figure 10.3) would require a cone that has a height of 8 km and a radius of approximately 4.5 km.

This result is significant because estimates of the minimum depth to basement range from only 1.2 km based on seismic interpretation at Warrego (Finlayson, 1981) to approximately 5 km interpreted by gravity modelling (D. Leaman, 1989, unpublished report). These studies suggest that there is insufficient thickness of Warramunga Group sediments below the ironstone lodes to account for the volumes of rock required.

Either the expanding hydrothermal solutions have tapped metals from the granitic? basement or the hydrothermal systems are considerably broader than they are deep. Rattenbury (1990b) has interpreted a major south-over-north thrust system at the base of the Warramunga Group, with anticlinal structures propagated from upward curving blind splinter thrusts. These structures would obviously constitute important conduits for concentrated fluid flow, and would provide access to considerably larger volumes of rock than occurring immediately below the ironstone lode. Thus metals and fluids may have been derived from over a broad area but to relatively shallow depths. This proposal is consistent with observations in the southwest of the Tennant Creek goldfield where mineralised deposits (i.e. Noble's Nob, Juno, Eldorado, Golden Forty, Peko, and Argo mines appear to be relatively evenly spaced at 6 km intervals.

10.9 Model for Ironstone Lode Formation and Mineralisation

The formation of the ironstone lodes and associated mineralisation at Tennant Creek has been much debated throughout the history of the goldfield, but generally an epigenetic origin of the ironstone lodes is accepted. An alternative model involving diapiric remobilisation of syngenetic mineralisation through deformation of unlithified seafloor iron oxide accumulations has been proposed as a mechanism of ironstone lode formation, e.g. Norris (1980) and Main and O'Neil (unpublished manuscript). However, because the ironstone lodes cross-cut the stratigraphy, stringer zones are frequently observed beneath the lodes, and mineral textures indicate hydrothermal replacement of the sediment by chlorite and magnetite, an epigenetic model of formation is preferred.

Variations on the epigenetic model regarding the number of stages, mechanisms of ironstone lode formation, controls on the deposition of economic mineralisation, and sources of fluids and metals are numerous. The localisation of all economic mineralisation within cracks and fractures within the ironstone lodes and complete absence of ore constituents within the unfractured lode support a two stage model of lode formation and mineralisation which is now generally accepted, e.g. Wedekind et al. (1990), Huston, (1990b), and Wall and Valenta (1990), although as indicated above, the

relative time frame is still problematical. An evolutionary model is preferred as opposed to one involving distinct time breaks between stages.

Ironstone Lode Formation

The localisation of ironstone lodes within the Tennant Creek goldfield reflects both structural and stratigraphic controls as has been reported by Ivanac (1954), Large (1974, 1975), Rattenbury (1988, 1989, 1990a, 1990b) and Wedekind et al. (1990). Although many of the ironstone lodes show no direct evidence of localisation within shear or fault zones, all show alignment within the plane of cleavage, and a structural control on their orientation and shape is strongly evident. Blind thrusts at depth are likely to be the locus for the concentration of hydrothermal fluid flow into anticlinal sites (Rattenbury, 1988).

The stratigraphic level at which ironstone lode formation occurs appears to be related to particular horizons being favoured for replacement and ironstone lode formation (e.g. Ivanac, 1954; Large, 1974, 1975; Wedekind et al., 1990). In the central and southeastern part of the goldfield, there is a well defined association of the ironstone lodes and a hematitic banded iron formation (hematite shale), with most of the lodes localised at one of at least three distinct horizons of hematite shale (Rattenbury, 1988). The ironstone lodes typically occur at the level of the hematite shale, but are transgressive of it, and there is evidence within Juno and TC8 mines that the hematite shale may be traced as partially replaced blocks into the ironstone lodes (Large, 1974, 1990). These relationships suggest that the hematite shale has in some way acted as a chemical trap (Wedekind et al., 1990), with deposition of magnetite and/or hematite deposition promoted by the oxidation of iron-saturated solutions.

The chemical trap may have acted either through the physical reaction of hydrothermal solutions with the hematite shale, e.g.

$$Fe_2O_3 + FeCl_2 + H_2O \Leftrightarrow Fe_3O_4 + 2Cl^- + 2H^+$$

or via the mixing of the Fe-saturated brines with local oxidised waters, e.g.

$$3FeCl_2 + {}^1/_2O_2 + 3H_2O \Leftrightarrow Fe_3O_4 + 6H^+ + 6Cl^-$$

or

$$2FeCl_2 + {}^1/_2O_2 + 2H_2O \Leftrightarrow Fe_2O_3 + 4H^+ + 4Cl^-$$

Because of the hematite shales relatively small volume, and the tendency of the ironstone lodes to be transgressive of this unit, the first model is intuitively unacceptable. If this was the mechanism by which the ironstone lodes formed, stratiform bodies that grade laterally into the hematite shale with an overall volume that is little different from the hematite shale might be expected. Examples of stratiform chemical traps with features similar to those described above include the sulphidation of banded iron formations (e.g.

similar to those described above include the sulphidation of banded iron formations (e.g. Phillips et al., 1984) and the preferential replacement of carbonate units in skarn deposits (e.g. Einaudi et al., 1981; Meinert, 1982).

Stolz (1990) has measured $Fe_2O_3/(Fe_3O_4+FeO)$ of the sediments and the porphyry, and suggests that sedimentary rock samples collected above the porphyry are consistently more oxidised than the porphyry and the rocks beneath it. Therefore, there is the possibility that the hematite shale is merely indicative of a broader package of oxidised rocks, and it is this whole unit that has localised ironstone lode formation. The hematite shale itself may have acted as the catalyst for the deposition of iron oxides from solution. Because hematite shale units occur above and below the porphyry (Rattenbury, 1988), multiple repetitions of the oxidised horizons throughout the Warramunga Group stratigraphy might be expected.

There is little textural evidence of mineralogical reactions controlling ironstone deposition, i.e. the predominantly quartz-feldspar composition of the sediment pile is not by itself likely to control magnetite deposition, a more realistic scenario is one where fluids in equilibrium with the more oxidised rock packages mix with and oxidise rising hydrothermal solution, promoting supersaturation in iron and causing its deposition. This model is in accord with observations made in this study regarding the different isotopic signature of chlorites from sediments and the lode. The sediments are progressively chloritised by the rising hydrothermal brines and mixing with cooler and more oxidised fluids at the edge of the system progressively promotes the deposition of magnetite from solution.

On a localised scale within the oxidised sediment package, the composition of the sediments also appears to have exerted some control on the localisation of the ironstone lodes (e.g. Ivanac, 1954; Whittle, 1966; Wyborn, 1971; Norris, 1980). Many of the ironstone lodes examined in these studies (including Nobles Nob and Golden Forty mines) were localised in finer grained argillaceous units with the lodes observed to terminate against over- and underlying coarse sandstone units. Two possible explanations for this observation might be that the finer grained sediments are more strongly cleaved and fractured than the massive coarser sediments allowing greater fluid access, and/or a higher argillaceous component would be more susceptible to chlorite alteration.

The Warrego ironstone lode is one of the largest in the goldfield and is unusual because it occurs at or near the lower contact of the quartz porphyry where there is no evidence for the former presence of a hematite shale unit that may have catalysed iron oxide deposition, or indicated a more oxidised package of rocks. However, the localisation of the lode beneath the porphyry and its immediate contact of hornfelsed sediments suggest that they have acted as an impermeable barrier and controlled fluid flow. Compared to the chloritic sediments, the porphyry has a relatively unaltered core

which supports this interpretation and also precludes the porphyry itself from having been the heat source that promoted hydrothermal circulation.

Deformation of the relatively rigid porphyry is likely to have occurred in large part through reverse faulting rather than the folding observed in the sediments, and it is in such a fault position that the Warrego ironstone lodes appear to have formed. The fault is interpreted to have provided a conduit for hydrothermal fluid flow, with the pre-existing displacement of the porphyry responsible for the apparent offset in the No. 1 and No. 3 orebodies (Fig. 10.5). The fault possibly tapped a deeper structure, and channelled hydrothermal fluid flow to the quartz porphyry where the relative impermeability of this unit "choked" the flow forcing lateral migration. Mixing of these fluids with local cooler and more oxidised fluids is invoked to explain the precipitation of magnetite from solution.

The relative rarity of ironstones lodes at what is a near-continuous horizon with a strike length in excess of 60 km suggests that the conditions at Warrego were somewhat specialised, but because there is a general lack of information regarding the porphyry contact elsewhere in the goldfield, it is difficult to present a definitive explanation as to the nature of the factors controlling mineralisation at Warrego. The large size of the ironstone lode does indicate a large hydrothermal system.

A model of ironstone lode formation requires strongly channelised fluid flow in order to explain the absence of a pervasive geochemical or stable isotopic alteration halo surrounding the Warrego and other ironstone lodes. Lateral fluid flow immediately below the porphyry was possibly localised in bedding parallel shears which may in part reflect the original character of the sediment. Observations of apparently stratigraphic bands of strong alteration well removed from the ironstone lode, are contrasted with relatively unaltered sediments immediately adjacent to the lode. These relationships suggest that similar to observations elsewhere in the goldfield, some sedimentary units have been more amenable to replacement than others.

The abundance of textures that indicate replacement of sediment by chlorite and magnetite on both a hand specimen and thin section scale support the replacement model of ironstone lode formation proposed by Large (1974, 1975). Trace element modelling of the alteration process further supports this model, suggesting near-isovolumetric replacement has occurred in the transition from sediment to massive chlorite-magnetite in the most altered sediments. The typical trace element signature of the lode itself suggests that the process of ironstone lode formation cannot have occurred by replacement alone and some increase in volume and/or mobility of 'immobile elements' is required.

The knife-sharp lode boundaries characteristic of the Tennant Creek orebodies also suggest a 'replacement front' style of formation in a manner that is perhaps analogous with the formation of roll front uranium deposits (e.g. Nash et al., 1981) where in this case, the reaction front occurs between relatively reduced (magnetite-stable) fluids and

relatively oxidised sediments and/or pore fluids. The sharp boundaries characteristic of these deposits contrasts with other sediments- or volcanic-hosted replacement deposits where a strong tectonic control is evident, e.g. Eulera mine (de Roo, 1989) and the Reward prospect (Beams and Hartley, 1990) are characterised by an irregular outer breccia zone of partially replaced host rocks. Thus relatively passive fluid infiltration following favourable sediment horizons is preferred for the Warrego and other Tennant Creek deposits.

A model involving the early formation of a relatively massive outer shell of magnetite is preferred to explain the development of the outer quartz-magnetite zone, characteristic of the Warrego and many other ironstone lodes, where it is suggested subsequent fracturing of this outer shell has promoted quartz and magnetite deposition into open spaces in response to the associated release in pressure, e.g. Fournier (1986). A rim to core replacement model is consistent with the observation of an inner core of brecciated altered sediments at the base of the Peko ironstone lode (Fig. 10.4) and provides a plane (or planes) of weakness within the core that localises deformation associated with the subsequent introduction of economic mineralisation (see Fig. 10.5).

It is suggested that pervasive chloritisation of the sediments through alteration and veining throughout the core allows the growth of Type IA magnetite, through the formation of a homogeneous chloritic medium. Random nucleation on pre-existing magnetite (or other phases) and rapid growth of crystals via fluid diffusion through the chlorite seems the most likely mechanism to produce the spherulitic textures. Under such conditions it may be possible to directly crystallise magnetite in a bladed or colloform habit that is not typical of 'normal' equilibrium conditions. Frater (1983) records the occurrence of spherical and nodular structures consisting of annular aggregates of fine quartz, chlorite, magnetite, and pyrite that are superimposed on tuffs and chlorite altered rocks up to 1 km from the Golden Grove orebody and their origin was similarly attributed to initially restricted crystal nucleation followed by supersaturated precipitation and rapid crystal growth in an isotropic medium.

The fluids associated with ironstone lode formation are difficult to characterise in view of the strong overprint associated with the subsequent introduction of economic mineralisation. However, fluid inclusion and stable isotope studies suggest that the fluids were of moderate temperature (~250°C), high salinity (15–25 equiv. wt% NaCl) and were probably derived from formation waters. The absence of evaporitic sequences within the Warramunga Groups suggests that the high salinities were derived through processes such as membrane filtration (e.g. De Sitter, 1947).

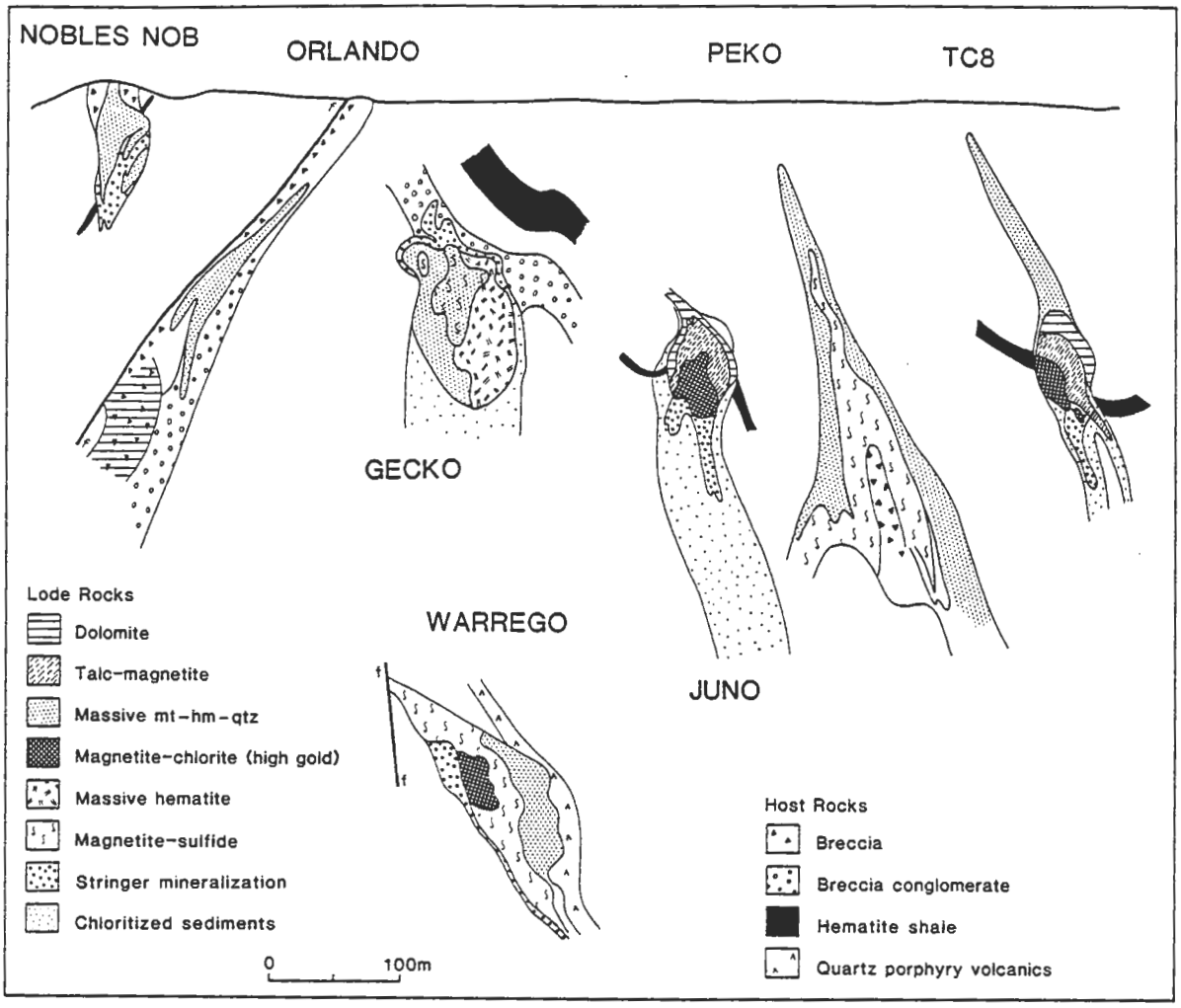

Figure 10.4 — Typical cross sections of selected mines from the Tennant Creek goldfield illustrating the relative size and depth relationships.

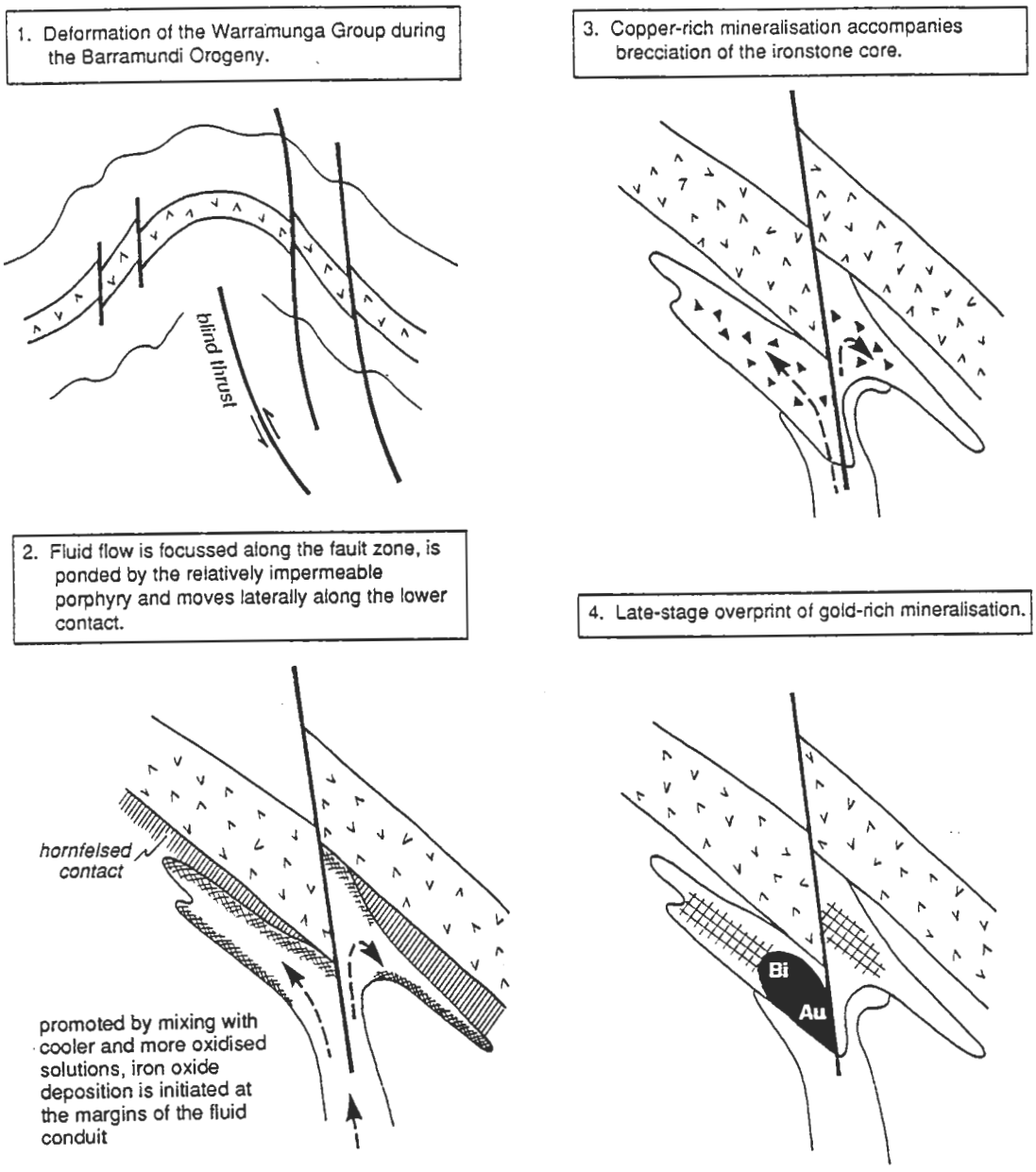

Figure 10.5 — Cartoon illustrating (1) the suggested faulting of the quartz porphyry during folding; (2) the control of the relatively impermeable quartz porphyry on fluid flow and ironstone lode localisation; (3) the introduction of copper mineralisation into the brecciated core of the ironstone lode; and (4) pervasive local overprinting of the copper ore in the form of the gold pods, and lateral alteration effects observed as mixing of sulphur isotopic ratios and oxidation of pyrrhotite.

Economic Mineralisation

The introduction of economic mineralisation was associated with extensive fracturing and brecciation of the Warrego ironstone lode, and the bulk of the mineralisation is localised within its core. Because of the general similarity of the fluids (i.e. salinity and isotopic composition), the two stages of lode formation and mineralisation are suggested to represent an evolving system in which an expanding hydrothermal system taps deeper and hotter fluids which are more reduced and have a lower pH. In view of the high temperatures associated with economic mineralisation, it seems likely that this event was directly related to the intrusion of granite rocks at depth, and the development of hydrothermal systems surrounding it. The role of the intrusion as anything other than a heat engine for the system cannot be evaluated at this stage, but certainly isotopic studies and the 'magmatic' trace element associations (e.g. Mo, W, and Bi) may indicate a direct magmatic component. This model of an expanding hydrothermal system is also compatible with observed lead isotope and trace element mobility calculations. These suggest that small systems which preserve local source rock heterogeneity are associated with ironstone lode formation, while larger systems which homogenise source rock variation are related to economic mineralisation.

Two styles of economic mineralisation are recognised within the Warrego ironstone lodes: in the upper lode, mineralisation is characterised by a sulphide-dominant mineral assemblage where predominantly chalcopyrite fills the fractured lode without alteration or replacement of the adjacent magnetite. A distinctive mineral assemblage associated with the chalcopyrite comprises pyrite, marcasite/pyrite (after pyrrhotite), carrollite, bismuth sulphosalts, paracostibite/famatinite and gold. This assemblage appears to be relatively constant in its distribution throughout the upper lode. The second mineralisation style is that of the gold pods which comprise a sulphide-poor mineral assemblage dominated by the gangue minerals chlorite and muscovite and characterised by extremely rich intersections of gold and bismuth mineralisation. The gold pods display a well developed zonation in gangue mineralogy, bismuth sulphosalt chemistry and metal zonation across the ironstone lode that suggests changing physicochemical conditions of ore deposition across the lode. The gold pods proper are relatively restricted in their areal extent and are surrounded by extensive haloes of barren quartz-magnetite.

These two styles of mineralisation are observed separately elsewhere in the goldfield, but the Warrego ironstone lode is apparently the only example where both styles coexist. The mineralogy and general zonation of a copper-rich brecciated ironstone core surrounded by an outer rim of relatively barren quartz-magnetite is characteristic of the Peko mine, whereas the gold pod with its distinctive gangue mineral assemblage, well developed zonation in trace element chemistry and high grades of gold and bismuth, is directly analogous with the gold pod style of mineralisation observed in the Juno

mine. Although the Juno mine contains almost two orders of magnitude less copper than Warrego, the well defined zonation sequence includes an outer envelope of weak copper mineralisation (Large, 1974, 1975), which might be considered consistent with the overall zonation pattern within the Warrego mine from the gold pods to copper mineralisation. Similarly the copper ore marginal to the gold pods appears to be transitional to the copper orebodies being enriched in gold, and displaying intermediate gold fineness values compared to the gold pod and copper orebody gold mineralisation. However, in detail several observations are incompatible with a model in which the mineralisation in the Warrego mine represents a single zoned ore system. Clear evidence that the gold mineralisation is a late-stage event that overprints copper mineralisation is provided in the following observations.

1. Chlorite compositions in the two assemblages are distinct, gold pod mineralisation is associated with magnesian chlorite (similar to gold pod mineralisation elsewhere in the goldfield), whereas copper-rich mineralisation is characterised by relatively iron-rich chlorite compositions. Modelling of chlorite chemistry suggests that the conditions of formation for copper orebodies were more reduced, relatively sulphur rich, and higher temperature than those in the gold pod. None of these differences are compatible with the expected evolution of a fluid interacting with a large magnetite body. In addition, trends in chlorite composition reported at Juno mine show increasing magnesium compositions from core to the lode margins.
2. Although both gold and copper orebodies show a well developed zonation in sulphur isotopes with $\delta^{34}S$ increasing from areas of high-grade mineralisation to low-grade mineralisation at the margins of the ironstone lode, both styles show exactly the same range. If mineralisation has occurred through the sequential deposition of gold and then copper from a single event in response to changing physicochemical conditions, the isotopic zonation should reflect this with the isotopic composition of the copper ore at least the same as that of the copper mineralisation in the gold pod.
3. Pyrrhotite in the copper orebody has been oxidised to a pyrite/marcasite mineral assemblage during the mineralisation event as is evidenced by the overgrowth of this assemblage by pyrite. A late-stage (pre-Warrego Granite), relatively oxidising, mineralisation event is indicated.
4. The gold pods are surrounded by an envelope of barren quartz-magnetite which is considerably more extensive than that developed in the copper orebodies, and the overall relationship suggests that the quartz-magnetite has overprinted the copper mineralisation.

These features are incompatible with a single-stage process of economic mineralisation, and it is suggested that they are consistent with a different paragenesis for the two styles of mineralisation. Although mineral, trace element and isotopic zonation is preserved, the sulphide mineral assemblage has been extensively recrystallised and

locally remobilised by intrusion of the Warrego Granite. Thus important information as to the physical and chemical conditions of mineralisation that might be provided by fluid inclusions is not available. The variation in chlorite chemistry between the two mineralisation styles appears to indicate fluid conditions associated with gold mineralisation were more oxidised, and somewhat lower in temperature than those associated with copper mineralisation. The introduction of the gold-rich mineralisation is believed to have locally remobilised copper ore, mixed isotopically with the pre-existing assemblage, and oxidised pyrrhotite within the lode to a pyrite/marcasite assemblage.

The evolution of the Warrego hydrothermal system from an ironstone lode forming event to the introduction of economic mineralisation is believed to result from the expansion of the hydrothermal system tapping deeper, hotter, more reduced fluids from within the Warramunga Group. The presence of large fault systems at depth is considered important for the concentration of fluids from the large area required to concentrate metals. Extensive fracturing of the lode must have accompanied mineralisation and it is suggested that this played an important role in promoting mineral deposition through pressure release and associated phase separation. While the difference between the barren and mineralised systems might be attributed to the overall size of the hydrothermal system (possibly related to the absence or presence of a large structure at depth), the difference between the gold and copper mineralisation is not easily explained. The more oxidised, late, gold-bearing fluids may have been derived through mixing with an additional fluid, or be the consequence of a retrograding hydrothermal system.

10.10 Comparison with Other Deposits

Ironstone Lodes

The Tennant Creek ironstone lodes and their associated gold, copper and bismuth mineralisation are apparently unique on a world scale. However, elements of both the ironstone lodes and economic mineralisation are observed in numerous deposits. Iron-rich replacement bodies are not uncommon in a number of environments of which the most significant are:

Magmatic Iron Deposits: There are a number of examples of cross-cutting pipe- and plug-shaped magnetite deposits where a close association with alkalic volcanics and intrusions, and high apatite contents have lead to their characterisation as magnetite intrusions and flows (e.g. Park, 1961; Kisvarsanyi and Procter, 1967; Snyder, 1969; Frutos, 1975; Henriques and Martin, 1978; Forster and Jafarzadeh, 1984; Kisvarsanyi, 1988; Meyer, 1988). Alternate hydrothermal models for the formation of these deposits still involve direct magmatic contributions through the rapid dehydration of sub-volcanic

plutons that produce an iron- and phosphorous-enriched volatile phase from which magnetite and hematite sublimate (Hildebrand, 1986).

Panno and Hood (1983) attribute a replacement origin for part of the Pilot Knob deposit in southeastern Missouri where in a manner similar to the model described for the Warrego deposit, the relative permeability and porosity of a rock type has controlled the localisation of iron mineralisation. Here the unwelded upper and lower portions of of an ash flow tuff have been extensively replaced, whereas the welded core is only sparsely mineralised. Massive magnetite ore at the base of the replacement ore is attributed to magmatic injection, and although no genetic relationship between the two ore types is discussed, a magmatic hydrothermal origin is implied from the association.

In all of the above examples the close proximity of the iron-rich lodes to volcanic or intrusive rocks is interpreted to imply a direct magmatic relationship. This interpretation is frequently supported by additional evidence such as fluid inclusions and stable isotopes. However, the Tennant Creek ironstone lodes differ from these deposits in three key areas:

1. Although present, phosphorus is only a trace component in the lodes.
2. The presence of stringer alteration zones below many of the lodes rule out an intrusive origin.
3. There is no direct spatial relationship between the ironstone lodes and intrusive rocks that are obviously related to ironstone lode formation.

Skarn Deposits: Although the volcanic sediment-hosted ironstone lodes at Tennant Creek fail the most basic definition of skarn deposits i.e. the metasomatic replacement of dominantly carbonate rocks by Ca-Fe-Mg-Mn silicates (Einaudi et al., 1981), there are a number of parallels which suggest some similarities in their paragenesis. Mineralised skarn deposits typically form in two stages; an early contact metamorphic event in which rocks adjacent to a cooling pluton are recrystallised and metasomatised by Fe- and Mg-rich fluids (not observed at Tennant Creek), which is then followed by a retrograde hydrothermal event in which meteoric fluids are entrained into what was formerly a magmatic hydrothermal system. The initial stage is considered to have been an important factor in the subsequent concentration of economic mineralisation because the calc-hornfelses generated in this early stage are brittle and easily fractured (Einaudi et al., 1981).

Economic mineralisation is typically associated with the retrograde event (Einaudi et al., 1981; Meinert, 1982). Unlike the initial pervasive, broad-front alteration accompanying skarn formation, later retrograde alteration is typically fracture controlled and is restricted to relatively narrow transgressive zones (Einaudi et al., 1981; Meinert, 1982). This event frequently extends beyond the immediate pluton environment, and thus, it may be difficult to establish a direct paragenetic link between the alteration/ mineralisation and a pluton. Similarly, although carbonate-rich rocks are still the

dominant host rocks, examples of massive alteration/replacement of sediments and volcanics are also documented (e.g. Einaudi et al., 1981). However, even in these examples, the skarns typically develop at lithological contacts with carbonate rocks.

Analogies with the Tennant Creek ironstone lodes are obvious, chlorite and magnetite are typical constituents of the retrograde mineral assemblage and pipe-like and stratiform massive replacement bodies may form where rock type is conducive (typically carbonates) or where brecciation and faulting has provided a conduit for hydrothermal fluids (Meinert,1982). Similar also is the fact that the Fe skarns show a considerable size range 2–300 Mt, and may, or may not be associated with other metals. Typically where sulphide mineralisation does occur, this retrograde mineralisation is structurally controlled, overprinting the late-prograde Fe-skarn development (Einaudi et al., 1981) and the sulphide mineralisation may exhibit zonation, e.g. Meinert (1982), documents an example where breccia pipes show vertical and lateral zonation from copper to zinc to lead.

Hydrothermal Iron Deposits: A single example from the literature that appears to be directly analogous with the model developed here for the Tennant Creek ironstone lodes is that of the hard iron ores of central Michigan (Canon, 1976). Distinctive massive magnetite bodies are interpreted to have formed where the upper jasperlite unit of the Negaunee Iron Formation has oxidised iron-bearing metamorphic fluids and caused the deposition of iron. The fluids were generated in the lower parts of the iron formation and concentrated at the sites of deposition along structurally or stratigraphically controlled channelways.

The similarity of this model to that proposed for the Tennant Creek ironstone lodes suggests that similar examples should be relatively common in the geological record i.e. wherever fluids that have equilibrated with relatively reduced (magnetite), iron-rich source rock encounter a more oxidised stratigraphic package or fluid, ironstone lodes might be expected to form. One possible explanation for their lack of documentation may be that because of their relatively small mass, they are not by themselves economic, and therefore have not attracted the attention of researchers.

Economic Mineralisation

The economic mineral assemblage overprinting the ironstone lodes (Au–Cu–Bi ± Se ± Pb ± U ± Co ± Mo ± W) is by itself not particularly distinctive, and once again is commonly associated with magmatic-type deposits, especially skarns (e.g. Einaudi et al., 1981; McQueen and Larson, 1985; Brown and Nesbitt, 1987; Cameron and Garmoe, 1987; Meinert, 1990). However, in varying proportions, this mineral assemblage is not uncommon of a variety of hydrothermal deposits where a magmatic component is not evident. Volcanogenic massive sulphide deposits may contain many of the 'exotic' trace element constituents listed above (e.g. Thorpe et al., 1976; Pringle and

Thorpe, 1980; Carlon and Bleeker, 1988; Huston and Large, 1988, 1989). Very similar trace element enrichment to that observed in the Tennant Creek orebodies is exhibited by the Starra volcanogenic copper-bearing oxide deposits, where seafloor exhalation of ore fluids very similar to those at Tennant Creek is suggested to have produced the Au–Cu iron oxide mineralisation (Davidson, 1990; Davidson et al., 1990).

Similar analogies might be drawn between the Tennant Creek mineralisation and other Proterozoic mineralisation styles which include the Olympic Dam Cu–U–Au–Ag–REE (Roberts and Hudson, 1983; Oreskes and Einaudi, 1990), Coronation Hill Au–PGM–U (Wyborn, 1990), and unconformity-related U–Au deposits (Wilde et al., 1990) where many parallels are evident. These deposits are characterised by oxidised, saline and low pH fluids, and are associated with strong chlorite-muscovite and iron-oxide alteration. The solubility of U, Cu, PGE, Au and REE in oxidised fluids (Huston and Large, 1989; Wyborn et al., 1989; Wilde et al., 1990) suggests that there is a link between these deposit types and the relatively oxidised sediments hosting them. The oxidation state of the fluid forming these deposits appears to control the relative levels of trace element enrichment, highly oxidised (hematite stable) deposits are characterised by high U, REE and PGE contents (Coronation Hill, unconformity-related U deposits, Olympic Dam?), while relatively reduced (magnetite/hematite stable) deposits have lower levels of these trace elements (Starra and Tennant Creek). The higher temperatures in these latter deposits is suggested as responsible for the elevated Bi, Mo and W contents observed.

Thus the two stages of mineralisation observed at Tennant Creek characterised by ironstone lode formation and the overprint of Au–Cu–Bi mineralisation are individually not exceptional, and in fact might be considered characteristic of their tectonic setting and chemistry of the host rocks. However, the juxtaposition of the two is somewhat unique: the suggestion that the dominant control on mineralisation is the relative competency of the ironstone lodes and their tendency to brittle deformation compared to the ductile character of the sediments suggests that the search for a Tennant Creek analogue should concentrate on an oxidised ore environment where suitable dilational structures are developed to promote mineral deposition.

10.11 Areas for Further Research

This thesis appears to have posed more questions than appear to have been answered as to the process of mineralisation at Tennant Creek and the Warrego orebody in particular. Areas for further research include:

1. To better constrain the timing relationships of mineralisation, volcanism and granite intrusion. Precise ion microprobe zircon dating should resolve the relationship of these events and assist in the evaluation of potential genetic links. The documentation of hydrothermal overgrowths on zircons at Warrego, may provide a means of accurately dating mineralisation provided examples with sufficiently wide rims can be located. D. Compston at the Australian National University is currently investigating the use of ion microprobe zircon age dating at Tennant Creek.
2. Further oxygen and hydrogen isotope studies are required of the Tennant Creek ironstone lodes (both mineralised and unmineralised), to confirm and clarify the interpretations regarding fluid source and temperatures of mineralisation. More precise geothermometry of ironstone samples will be achieved through the development of improved mineral separation and the ability to measure oxygen isotopic ratios in magnetite. Continuing studies of stable isotope systematics of Tennant Creek mineralisation are being carried out at the University of Tasmania.
3. Fluid inclusion studies have broadly characterised the characteristics of hydrothermal fluids associated with ironstone lode formation and economic mineralisation. However, further detailed research into the differences between the gold-rich and copper-rich styles of mineralisation is required. Zaw (1989) noted temperature differences between these two styles of economic mineralisation in a preliminary investigation of the TC8 deposit and continuation of this work is required.
4. Detailed documentation of the petrography of mineral phases within ironstone lodes that have not undergone contact metamorphism may elucidate the paragenesis of the lodes. Work of this nature is being carried out at the Australian University by J. Walshe and R. Skirrow as part of a detailed evaluation of the chlorite model.
5. A more detailed approach than that attempted here, into thermodynamic modelling of the mineralisation events at Tennant Creek may provide greater insights into the mineralisation process and importance of various observations. Computer simulation of the complex processes of fluid mixing, boiling and reaction with host rocks are now possible, e.g. Spycher and Reed (1989) and application of these programmes to simulate Tennant Creek mineralisation are currently being attempted.
6. The majority of the studies recommended here are currently in progress, or will hopefully commence shortly. We can therefore expect further developments into the understanding of the enigmatic Tennant Creek mineralisation styles in the near future.